frontiers | Research Topics

Ecology and molecular biology of bloom-forming cyanobacteria

Edited by
Petra M. Visser, Robert Michael McKay and George S. Bullerjahn

Published in
Frontiers in Microbiology

ISSN 1664-8714
ISBN 978-2-8325-4204-0
DOI 10.3389/978-2-8325-4204-0

About Frontiers

Frontiers is more than just an open access publisher of scholarly articles: it is a pioneering approach to the world of academia, radically improving the way scholarly research is managed. The grand vision of Frontiers is a world where all people have an equal opportunity to seek, share and generate knowledge. Frontiers provides immediate and permanent online open access to all its publications, but this alone is not enough to realize our grand goals.

Frontiers journal series

The Frontiers journal series is a multi-tier and interdisciplinary set of open-access, online journals, promising a paradigm shift from the current review, selection and dissemination processes in academic publishing. All Frontiers journals are driven by researchers for researchers; therefore, they constitute a service to the scholarly community. At the same time, the *Frontiers journal series* operates on a revolutionary invention, the tiered publishing system, initially addressing specific communities of scholars, and gradually climbing up to broader public understanding, thus serving the interests of the lay society, too.

Dedication to quality

Each Frontiers article is a landmark of the highest quality, thanks to genuinely collaborative interactions between authors and review editors, who include some of the world's best academicians. Research must be certified by peers before entering a stream of knowledge that may eventually reach the public - and shape society; therefore, Frontiers only applies the most rigorous and unbiased reviews. Frontiers revolutionizes research publishing by freely delivering the most outstanding research, evaluated with no bias from both the academic and social point of view. By applying the most advanced information technologies, Frontiers is catapulting scholarly publishing into a new generation.

What are Frontiers Research Topics?

Frontiers Research Topics are very popular trademarks of the *Frontiers journals series*: they are collections of at least ten articles, all centered on a particular subject. With their unique mix of varied contributions from Original Research to Review Articles, Frontiers Research Topics unify the most influential researchers, the latest key findings and historical advances in a hot research area.

Find out more on how to host your own Frontiers Research Topic or contribute to one as an author by contacting the Frontiers editorial office: frontiersin.org/about/contact

Ecology and molecular biology of bloom-forming cyanobacteria

Topic editors

Petra M. Visser — University of Amsterdam, Netherlands

Robert Michael McKay — University of Windsor, Canada

George S. Bullerjahn — Bowling Green State University, United States

Citation

Visser, P. M., McKay, R. M., Bullerjahn, G. S., eds. (2024). *Ecology and molecular biology of bloom-forming cyanobacteria*. Lausanne: Frontiers Media SA.

doi: 10.3389/978-2-8325-4204-0

Table of contents

frontiers | Frontiers in Microbiology

TYPE Editorial
PUBLISHED 12 December 2023
DOI 10.3389/fmicb.2023.1346581

OPEN ACCESS

EDITED AND REVIEWED BY
Michael Rappe,
University of Hawaii at Manoa, United States

*CORRESPONDENCE
George S. Bullerjahn
bullerj@bgsu.edu

RECEIVED 29 November 2023
ACCEPTED 05 December 2023
PUBLISHED 12 December 2023

CITATION
Bullerjahn GS, McKay RML and Visser PM (2023) Editorial: Ecology and molecular biology of bloom-forming cyanobacteria.
Front. Microbiol. 14:1346581.
doi: 10.3389/fmicb.2023.1346581

Editorial: Ecology and molecular biology of bloom-forming cyanobacteria

George S. Bullerjahn[1]*, R. Michael L. McKay[2] and Petra M. Visser[3]

[1]Department of Biology and Great Lakes Center for Fresh Waters and Human Health, Bowling Green State University, Bowling Green, OH, United States, [2]Great Lakes Institute for Environmental Research, University of Windsor, Windsor, ON, Canada, [3]Department of Freshwater and Marine Ecology, Institute for Biodiversity and Ecosystem Dynamics, University of Amsterdam, Amsterdam, Netherlands

KEYWORDS

cyanobacteria, cyanotoxins, microcystins, secondary metabolites, harmful algal blooms

Editorial on the Research Topic
Ecology and molecular biology of bloom-forming cyanobacteria

Given the worldwide expansion of cyanobacterial harmful algal blooms (cHABs), this Research Topic seeks to highlight the threats that bloom events pose to environmental and human health. As many studies link severity of cHABs to a warming climate and changing precipitation patterns, such events are expected to grow, with cHABs increasing in distribution, duration and frequency, contributing to unbalanced and degraded ecosystems. Addressing this global concern, research is aimed at understanding the environmental factors contributing to bloom formation and decline, toxin and metabolite synthesis, bloom ecology, and cHAB mitigation. This Research Topics collection of papers, largely drawn from contributions to the 12th International Conference on Toxic Cyanobacteria, aims to showcase the state of the science related to cHABs, which may point to potential solutions to this growing threat to our freshwater resources.

Several papers contributed to the Research Topic addressed community structure and the ecology of blooms. Whereas colonial *Microcystis* has become synonymous with blooms, there is increased recognition of community diversity between bloom locations and even within a bloom itself. In part, this is attributed to more widespread adoption of metabarcoding and genomics approaches as evidenced by each of the studies highlighted here. Beyond methodological advances, community structure often reflects environmental gradients to which communities are exposed. One such gradient is the fluvial-lacustrine continuum. Surveying bloom-forming regions of the Laurentian Great Lakes, Crevecoeur et al. identified a clear shift in dominance of the cyanobacterial communities between river and lake, yet also noted strong connectivity and dispersal of taxa within the system as a whole. Elsewhere, seasonality can play a role in shaping community structure. In Florida's Lake Okeechobee, Lefler et al. showed that cyanobacterial communities within the lake are significantly different between the wet and dry seasons. Also noted from this study was that the dominant cyanobacterial bloom formers in this lake maintain distinct bacterial associations that may confer competitive advantages across spatial and temporal scales.

In many cases, underlying environmental gradients are nutrients, the parameter conventionally recognized as dominant in the "bottom-up" control of cHABs. The important role of nutrients in shaping community structure was assessed in several of the contributing articles. Chen et al. frame the role of nutrients in a management framework, noting that closed-lake management practices adopted to control nutrient loading in the Taihu Basin

River Network were successful at mitigating blooms of *Microcystis*. Using a metagenomic approach to compare the taxonomic and functional structure of the bacterioplankton community between open and closed lakes, differences were detected at fine taxonomic resolution (genus and species), but not extending to functional genes maintained by keystone taxa. In another managed system, Feng et al. assessed seasonal variability of microbial community composition in a subtropical reservoir following completion of a multi-year ecological restoration project aimed to reduce nutrient loading from adjacent tributaries. Their study showed negligible variability in community structure related to seasonality; however, the surveys showed enrichment of cyanobacterial communities in benthic samples pointing to possible internal loading as a nutrient source. Finally, Kim et al. examined microbial community structure and the presence of cyanotoxins in aerosols generated from wind-driven wave action in South Korea's Nakdong River. There is increased recognition of the potential threat of aerosols as a vector for cyanotoxin exposure, a concern reinforced by this study that showed toxigenic *Microcystis* to be one of the dominant genera in the aerosol microbiome.

Three articles in this Research Topic investigated diverse aspects of natural control of cyanobacterial blooms, ranging from the role of cyanophages and chytrids on cyanobacteria and the viral influence on phytoplankton community dynamics. McKindles et al. focused on understanding the diversity and role of cyanophages in bloom control in Sandusky Bay, revealing the molecular characterization of *Planktothrix* specific cyanophages. Transcriptomic analysis revealed only low levels of viral gene expression despite the highly abundant cyanophages over the course of multiple years. The study also aimed to design monitoring methods for bloom lysis events, where potentially toxins are being released. Wagner et al. explored the dynamics of chytrid (*Rhizophydium* sp.) infections in *Planktothrix agardhii* blooms, with modified environmental conditions in mesocosms to explore infection prevalence. The results identified temperature and water flow as crucial factors in chytrid prevalence. The study provides valuable insights into control measures to reduce blooms. Lastly, Peng et al. investigated viral influences on phytoplankton community succession in the Three Gorges Reservoir, emphasizing the multiple roles viruses play in summer bloom dynamics. The viral lysis of eukaryotes and increase of nutrients due to the lysis of bacterioplankton appeared to be beneficial for the success of cyanobacteria. Together, these studies provide comprehensive insights into the complex interactions shaping cyanobacterial blooms, offering valuable knowledge for developing effective control strategies and safeguarding water ecosystems.

Concluding the Research Topic, three papers present data on metabolites that include both the synthesis of the common cyanotoxin, microcystin, as well as other products that arise in concert with bloom events. Extending prior work on the temperature dependence of microcystin accumulation in *Microcystis* sp. at lower temperatures, Roy et al. showed that a wild type *Microcystis* toxin-producing strain, has a growth advantage over its Δ*mcyB* (nontoxic) mutant strain at both low (20°C) and high temperature (30 and 35°C), and that cellular quotas of soluble microcystins are lower at higher temperature. However, higher temperature yields a shift in the intracellular toxin pool. This paper helps provide a better understanding of the role of microcystins in adaptation of *Microcystis* sp. to long-term and diel temperature shifts.

The papers by Zhou et al. and Lee et al. examined other metabolites and factors associated with blooms that may also affect environmental and human health. Zhou et al. have studied exudates of *Microcystis aeruginosa* that can be inhibitory to aquatic life, and in this paper, they employed LC/MS to characterize exudates from non-toxic and toxic *Microcystis* strains during exponential and stationary phases of growth. Whereas the toxin-producing strain produced a higher diversity of exudate compounds, the non-toxic strain produced higher concentrations of potentially ecotoxic metabolites. This work demonstrated that even non-toxic bloom formers can produce compounds that degrade ecosystem health. The paper by Lee et al. raises awareness of both disinfection byproducts by water treatment of cHABs, and of potential pathogens (*Legionella* sp.) and antibiotic resistance genes associated by blooms. Evidently, bloom biomass may afford multiple threats to health which extend past the well-known consequences of microcystin exposure.

Author contributions

GB: Writing – review & editing. RM: Writing – review & editing. PV: Writing – review & editing.

Funding

The author(s) declare that no financial support was received for the research, authorship, and/or publication of this article.

Acknowledgments

The Editors thank the timely reviews provided by the authors' peers.

Conflict of interest

The authors declare that the research was conducted in the absence of any commercial or financial relationships that could be construed as a potential conflict of interest.

The author(s) declared that they were an editorial board member of Frontiers, at the time of submission. This had no impact on the peer review process and the final decision.

Publisher's note

frontiers | Frontiers in Microbiology

TYPE Original Research
PUBLISHED 19 January 2023
DOI 10.3389/fmicb.2022.1075621

OPEN ACCESS

EDITED BY
Jin Zhou,
Tsinghua University,
China

REVIEWED BY
Mohammed Loudiki,
Cadi Ayyad University,
Morocco
Benjamin Kramer,
Stony Brook University,
United States

*CORRESPONDENCE
Xuexiu Chang
xchang@uwindsor.ca

SPECIALTY SECTION
This article was submitted to Aquatic Microbiology, a section of the journal Frontiers in Microbiology

RECEIVED 20 October 2022
ACCEPTED 29 November 2022
PUBLISHED 19 January 2023

CITATION
Zhou Y, Xu J, MacIsaac HJ, McKay RM, Xu R, Pei Y, Zi Y, Li J, Qian Y and Chang X (2023) Comparative metabolomic analysis of exudates of microcystin-producing and microcystin-free *Microcystis aeruginosa* strains. *Front. Microbiol.* 13:1075621. doi: 10.3389/fmicb.2022.1075621

Comparative metabolomic analysis of exudates of microcystin-producing and microcystin-free *Microcystis aeruginosa* strains

Yuan Zhou[1,2], Jun Xu[1], Hugh J. MacIsaac[1,3], Robert Michael McKay[3], Runbing Xu[1], Ying Pei[4], Yuanyan Zi[1,3], Jiaojiao Li[1], Yu Qian[1] and Xuexiu Chang[3,4]*

[1]School of Ecology and Environmental Science, Yunnan University, Kunming, China, [2]Department of Ecology and Environment of Yunnan Province, Kunming Ecology and Environment Monitoring Station, Kunming, China, [3]Great Lakes Institute for Environmental Research, University of Windsor, Windsor, ON, Canada, [4]College of Agronomy and Life Sciences, Kunming University, Kunming, China

Cyanobacterial harmful algal blooms (cHABs) dominated by *Microcystis aeruginosa* threaten the ecological integrity and beneficial uses of lakes globally. In addition to producing hepatotoxic microcystins (MC), *M. aeruginosa* exudates (MaE) contain various compounds with demonstrated toxicity to aquatic biota. Previously, we found that the ecotoxicity of MaE differed between MC-producing and MC-free strains at exponential (E-phase) and stationary (S-phase) growth phases. However, the components in these exudates and their specific harmful effects were unclear. In this study, we performed untargeted metabolomics based on liquid chromatography-mass spectrometry to reveal the constituents in MaE of a MC-producing and a MC-free strain at both E-phase and S-phase. A total of 409 metabolites were identified and quantified based on their relative abundance. These compounds included lipids, organoheterocyclic compounds, organic acid, benzenoids and organic oxygen compounds. Multivariate analysis revealed that strains and growth phases significantly influenced the metabolite profile. The MC-producing strain had greater total metabolites abundance than the MC-free strain at S-phase, whereas the MC-free strain released higher concentrations of benzenoids, lipids, organic oxygen, organic nitrogen and organoheterocyclic compounds than the MC-producing strain at E-phase. Total metabolites had higher abundance in S-phase than in E- phase in both strains. Analysis of differential metabolites (DMs) and pathways suggest that lipids metabolism and biosynthesis of secondary metabolites were more tightly coupled to growth phases than to strains. Abundance of some toxic lipids and benzenoids DMs were significantly higher in the MC-free strain than the MC-producing one. This study builds on the understanding of MaE chemicals and their biotoxicity, and adds to evidence that non-MC-producing strains of cyanobacteria may also pose a threat to ecosystem health.

KEYWORDS

Microcystis aeruginosa, untargeted metabolomics, growth phase, differential metabolites, cyanobacterial harmful algal blooms

Introduction

Cyanobacterial harmful algal blooms (cHABs)- often dominated by *Microcystis* spp. are increasing in frequency and severity globally, with further increases predicted coincident with climate change (Harke et al., 2016; Paerl et al., 2016; Huisman et al., 2018; Ho et al., 2019). Cyanobacteria are renowned for their negative impacts on aquatic ecosystems, largely owing to the noxious and harmful, secondary metabolites that they produce and release upon cell lysis (Carmichael and Boyer, 2016; Janssen, 2018; Jones et al., 2021). The ecotoxic effects of cHABs directly and indirectly impact other bacterioplankton, phytoplankton, and zooplankton (Zhang et al., 2009; Chen et al., 2016; Ger et al., 2016; Dias et al., 2017; Wang et al., 2017; Wituszynski et al., 2017; Xu et al., 2019). Toxic effects are also reported in animals and humans (Carmichael and Boyer, 2016; Papadimitriou et al., 2018; Zi et al., 2018; Breinlinger et al., 2021; Cai et al., 2022).

While more than 5,000 studies have been published on production and toxicity of microcystins (MCs; Janssen, 2018), cyanobacteria also produce a wide range of other organic compounds that vary in concentration and toxicity (e.g., aeruginosin, anabaenopeptin, cyanopeptolin, microginin, microviridin, aerucyclamide and retinoic acids; Janssen, 2018; Huang and Zimba, 2019; Yeung et al., 2020). Research on these other toxic compounds of cyanobacteria has been far more limited than that on MCs (Ma et al., 2015; Racine et al., 2019; Jones et al., 2021).

Microcystis strains may be characterized as 'Microcystin-producing' (MC-producing strain) or 'Microcystin-free' (MC-free strain; Davis et al., 2009). It is known that MC-producing strains often coexist with MC-free strains in nature, and their proportions change seasonally (Kurmayer and Kutzenberger, 2003; Lorena et al., 2004; Hu et al., 2016; Islam and Beardall, 2017; Fernanda et al., 2019). Moreover, previous laboratory research suggests that both MC-producing and MC-free strains can be harmful-eliciting damage to mitochondrial function by altering the membrane potential-and that the latter strain may be more toxic than the former (Xu, 2021). Histopathological observations indicate that both MC-free and MC-producing *Microcystis aeruginosa* induce liver cellular impairments in medaka fish, possibly in association with toxic metabolites (Manach et al., 2018). However, information on other toxic metabolites of MC-free strains is lacking.

Microcystis aeruginosa is one of the most common *Microcystis* species (Harke et al., 2016). Exudates produced and released by *M. aeruginosa* (MaE) have a greater impact on other organisms than extracts (derived from freeze–thaw treatment or lyophilization) prepared from cultures. For example, MaE have higher, more estrogenic potential than extracts from cells (Sychrova et al., 2012). The aquatic plant *Potamogeton malaianus* was significantly more sensitive to MaE than to extracts (Zheng et al., 2013). Likewise, compared to extracts, MaE had a stronger effect on the structure of the biofilm microbial community on leaves of *Vallisneria natans* (Jiang et al., 2019). MaE also has adverse effects on aquatic animals, such as estrogenic effects in *Daphnia magna* (Xu et al., 2019), and embryonic heart failure and neurotoxicity to early-life stages in fish (Zi et al., 2018; Cai et al., 2022).The synthesis and release of MaE can be influenced by many factors, including different growth stages. Typical growth phases of cyanobacteria include lag, exponential, stationary and decline phases, and toxicity may vary by phase. For example, MaE from exponential growth phase (E-phase) cultures disrupted photosynthesis and induced oxidative stress in submerged macrophytes (Xu et al., 2015), and inhibited growth of green algae and diatoms much more than MaE from stationary growth phase (S-phase) cultures (Wang et al., 2017). Notably, MaE obtained from S-phase cultures had a stronger effect on the mitochondrial membrane potential of *D. magna* than that of E-phase (Xu, 2021).

We hypothesize that MaE contains metabolites whose concentration and toxicity are influenced by strain-type and culture growth phases. We used untargeted metabolomics based on liquid chromatography-mass spectrometry (LC–MS) to identify metabolites coupled with multivariate data analyses to compare metabolome profiles of MaE of MC-producing and MC-free strains in cultures at both E-phase and S-phase (Rinschen et al., 2019; Chen et al., 2020; Zhang et al., 2021). The study was designed to identify, classify and compare the differential metabolites and potentially harmful compounds in the E and S-phase MaE of MC-producing and MC-free strains. We also performed Kyoto Encyclopedia of Genes and Genomes (KEGG) classification on these exudates to identify potential biosynthetic pathways.

Materials and methods

Strains cultivation

Microcystis aeruginosa, MC-producing (FACHB-905) and MC-free (FACHB-526) strains were provided by the Freshwater Algae Culture Collection of the Institute of Hydrobiology (FACHB-Collection) at the Chinese Academy of Sciences. The two strains originated from Dianchi Lake in Kunming and Dong-hu Lake in Wuhan, respectively. Both Dianchi and Donghu are eutrophic lakes heavily impacted by cHABs (Liu et al., 2016; Yan et al., 2017; Li et al., 2019). Strains were grown in a modified

HGZ-145 medium at 25 ± 1°C at 50 μmol quanta m^{-2} s^{-1}, with a 12:12 h light–dark cycle, and gently mixed twice daily by hand (Xu, 2021). Strains were cultured in 1,000 ml of nutrient solution in 2,000 ml Erlenmeyer flasks with six biological replicates. Initial inoculation density was 2.0×10^6 cells/ml. One milliliter of each culture was collected under aseptic conditions daily in order to develop a growth curve and identify cell growth phase based on cell density. Culture approaches adopted principles of sterile technique and routine microscopic examination to verify the low abundance of heterotrophic microbiome (Fernanda et al., 2019; Pound et al., 2021).

Experimental design and sample collection

Microcystis aeruginosa cells were counted daily using a hemocytometer and an optical microscope (Olympus, BX51, Japan). E-phase and S-phase cultures of both strains were harvested on days 3 and 35 for MaE analysis.

To obtain MaE, cultures were clarified by centrifugation at 6,000 × *g* for 10 min following which supernatant was filtered through a 0.22 μm glass fiber filter (MiLiMo separation technology limited company, Shanghai, China). After filtration, MaE was flash-frozen using liquid nitrogen, and all samples stored at −80°C for subsequent metabolomics analysis (Pinu et al., 2018). We found the cells remained intact under the microscope at two growth stages, and no turbidity was observed in extracellular exudate during centrifugation.

Hereafter, we refer to MaE of the MC-producing strain collected at E- and S-phases as MCE and MCS, respectively, while that of the MC-free strain are MCFE and MCFS, respectively.

LC–MS analysis

To a lyophilized 1 ml exudates sample, we added 500 μl acetonitrile: methanol: H_2O (2:2:1, containing isotopically-labelled internal standard mixture), following which we vortexed for 30 s, sonicated for 10 min in an ice-water bath, and incubated for 1 h at −40°C to precipitate proteins. The sample was then clarified by centrifugation at 10,000 × *g* for 15 min at 4°C. The quality control (QC) sample was prepared by mixing an equal aliquot of the supernatants from all the samples. During the pre-treatment process, samples were added with three isotopically-labelled internal standards (HPLC purity, Sigma Aldrich) in each of the positive and negative ion modes for repeatability and availability.

Supernatant was analyzed by Ultra High Pressure Liquid Chromatography (UHPLC)-Orbitrap MS (Thermo Fisher Scientific, MA, USA). UHPLC separation was performed using ACQUITY UPLC BEH amide column (2.1 mm × 100 mm, 1.7 μm). The mobile phase consisted of 25 mmol/l ammonium acetate and ammonia hydroxide in water (phase A) and acetonitrile (phase B). The auto-sampler temperature was 4°C, and the injection volume was 3 μl. Q Exactive mass spectrometer (Thermo, Massachusetts, USA) was used to acquire MS/MS spectra on information-dependent acquisition (IDA) mode in the control of the acquisition software (Xcalibur, Thermo), and acquisition from m/z 100 to 1,100. At different collision energy (10/30/60 NCE), the MS/MS spectra of QC samples were obtained off the top 10 precursor ions.

Data processing

The acquired raw data were converted to the mzXML format using ProteoWizard and processed. After raw data pre-processing, peak detection, extraction, alignment and integration, metabolites were annotated by an in-house database (Biotree database, Biotechnology Co., Ltd., Shanghai, China). The database was built with available commercial standard compounds and existing public mass spectrometry databases, including HMDB[1], MoNA[2] and METLIN.[3] Metabolites were identified by strict criteria steps (Liang et al., 2020; Shen et al., 2020), including comparison of accurate mass (m/z, ±10 ppm), MS/MS spectra similarity score (considers both fragments and intensities), and isotope distribution. The identification of compounds met the level 1and 2 according to the Metabolomics Standards Initiative (Alexandra et al., 2016; Viant et al., 2017).

Quantitative analysis and relative concentration were calculated by the internal standard normalization for peak area method (Sun et al., 2019). Metabolites were quantified by the internal standard with the lowest RSD value. Positive and negative ion mode metabolites were quantitative separately. Retention time and abundance of internal standard in QC and blank samples were stable. The data acquisition stability and accuracy of the method meet the requirements of metabolomic studies (Supplementary Figure S3; Broadhurst et al., 2018). Metabolite peaks present in <50% of group samples were removed from the subsequent analysis, and missing values were imputed with the minimal peak value of the metabolomics dataset (Sun et al., 2019; Liu et al., 2021).

Statistical analysis

Student's *t*-test was used to compare growth rate of the two strains. Data were analyzed usingGraphPad Prism 8.0 (GraphPad Software, Inc., San Diego, CA). Principal component analysis (PCA) and orthogonal partial least squares discriminant analysis (OPLS-DA) were used to visualize the differences between and within groups. PCA and OPLS-DA were performed using

1 https://hmdb.ca

2 https://mona.fiehnlab.ucdavis.edu/

3 https://metlin.scripps.edu/

SIMCA14.1 (Sartorius AG, Gottingen, Germany). Differential metabolites (DMs) were determined by variable importance in projection (VIP) from the OPLS-DA model and fold change (FC; VIP score ≥ 1, absolute Log2FC ≥ 1; Wang et al., 2020; Zhang et al., 2021). Hierarchical cluster analysis, Venn and volcano maps were produced using R version 3.6.3 (pheatmap package, VennDiagram, ggpubr, ggthemes packages). The Kyoto Encyclopedia of Genes and Genomes (KEGG) database (organism-dependent:[4] *M. aeruginosa*) was used to search metabolic pathways. DMs pathways were analyzed according to the type of KEGG pathway.

4 www.kegg.jp/kegg

Results

Growth of MC-producing and MC-free strains

Growth curves demonstrate that MC-producing and MC-free strains had the same growth rate and similar cell density from day 1 to 10 (Figure 1A). The growth rate of the MC-free strain started to decrease after day 11. By day 35 and cultures in stationary phase, the MC-producing strain achieved a greater cell density than the MC-free strain cultures ($P<0.05$). Cell density of the MC-producing and MC-free strains at E-phase (day 3) were 4.12×10^6 cells/mL and 4.11×10^6 cells/mL, respectively, and 3.42×10^7 cells/mL and 1.87×10^7 cells/mL at S-phase (day 35).

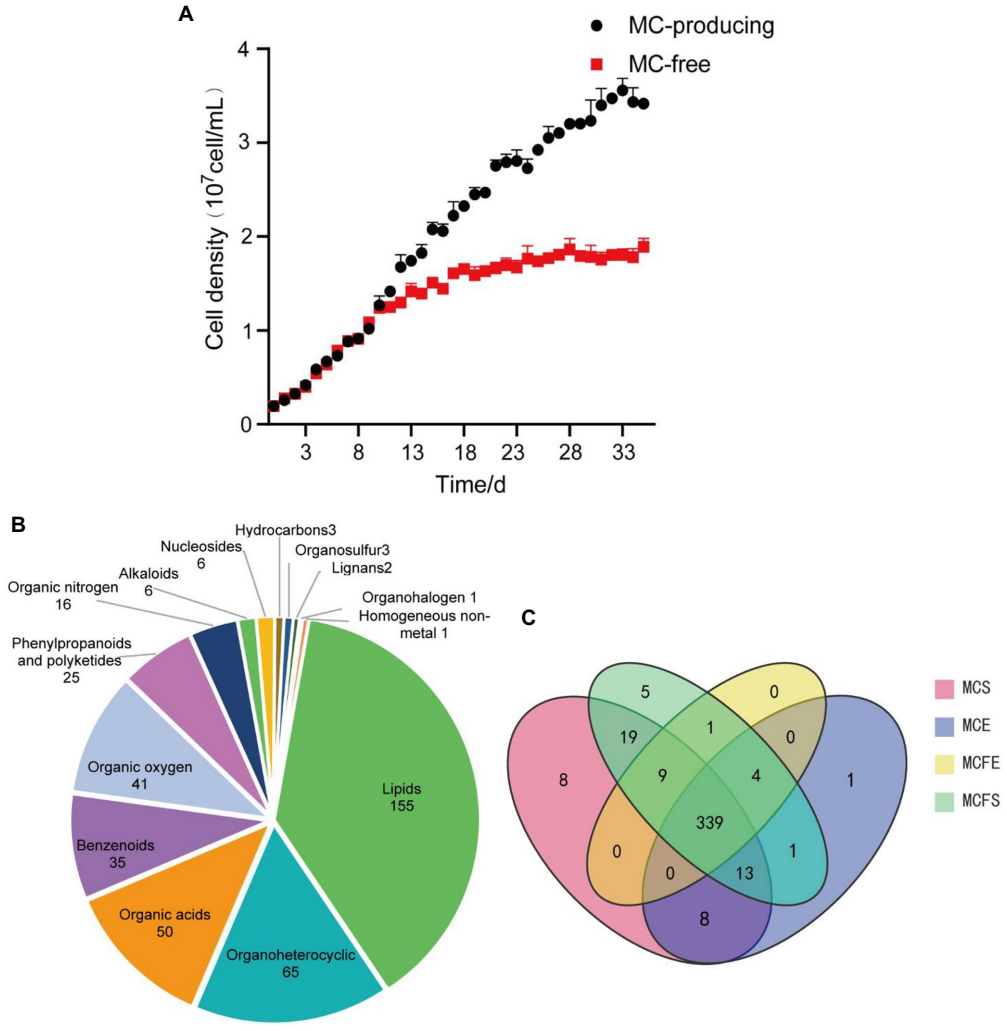

FIGURE 1
Growth curves of the MC strain and MC-free strain, data are presented as means±standard deviation (n=6; **A**). Pie diagram showing classification of 409 total metabolites identified in MaE **(B)**; Venn diagram of metabolites distribution in four groups, with numbers representing metabolites in common **(C)**. MCE, MC-producing strain at exponential phase; MCFE, MC-free strain at exponential phase; MCS, MC-producing strain at stationary phase; MCFS, MC-free strain at stationary phase.

Metabolite classification and profiling

In total, 409 metabolites were identified among the four MaE groups. These metabolites were grouped into 14 categories at the superclass level with Chemical Taxonomy of HMDB (Figure 1A), mainly including lipids, organoheterocyclic compounds, organic acid, benzenoids, organic oxygen, phenylpropanoids, organic nitrogen, alkaloids, nucleosides, hydrocarbons, organosulfur, lignans, organohalogen compounds and homogeneous non-metals. Detailed information on these metabolites is highlighted in Supplementary Table S1.

The majority (339) of these compounds overlapped in the four groups, indicating that 83% of the metabolites were common (Figure 1B). The relative concentrations of metabolites in MaE in the four groups are presented in Table 1. In terms of total metabolite relative concentrations, the MC-free strain was 10.9% higher than that of the MC-producing strain at E-phase. The accumulation of some metabolites such as benzenoids, hydrocarbons, lipids, nucleosides, organic oxygen and organoheterocyclic compounds were higher in the MC-free strain than in the MC-producing strain at E-phase. However, at S-phase, total metabolites of the MC-producing strain were 24.7% higher than that of the MC-free strain, mainly owing to the higher content of lipids, organic acids, organic oxygen and organoheterocyclic compounds. Total metabolites relative concentration of MaE was higher in S-phase than in E-phase in both strains.

We identified 50 pathways in the KEGG database for the 409 MaE metabolites in the four groups (Figure 2). These metabolites were involved in lipid pathways (such as metabolism of glycerophospholipid, glycerolipid, fatty acid, biosynthesis of unsaturated fatty acids), carbohydrate metabolism (such as pentose phosphate pathway, starch and sucrose metabolism, citrate cycle), amino acid synthesis (such as histidine metabolism, glycine, serine and threonine metabolism, phenylalanine, tyrosine and tryptophan biosynthesis, valine, leucine and isoleucine biosynthesis, arginine and proline metabolism), and secondary metabolites pathways (such as benzoate degradation *via* CoA ligation, folate biosynthesis, carotenoid biosynthesis, terpenoid backbone biosynthesis, nicotinate and nicotinamide metabolism, cyanoamino acid metabolism).

TABLE 1 Relative concentration of metabolites in MaE.

Biochemical categories	Relative concentration index			
	MCE	MCFE	MCS	MCFS
Alkaloids	8.38	6.77	8.59	9.36
Benzenoids	34.2	35.82	44.98	48.58
Hydrocarbons	0.27	0.3	0.29	0.27
Lignans	0.59×10^{-4}	0.45×10^{-4}	0.072	0.023
Lipids	25.2	29.07	67.47	45.56
Nucleosides	0.02	0.05	2.2	0.79
Organic acids	6.99	6.81	19.64	11.89
Organic nitrogen	1.69	1.8	2.54	1.77
Organic oxygen	38.55	48	47.18	40.73
Organoheterocyclic	7.88	8.19	22.45	14.31
Organosulfur	0.019	0.017	0.21	0.024
Phenylpropanoids	1.13	1.09	2.96	2.01
Total	124.3	137.9	218.6	175.3

MCE, MC-producing strain at exponential phase; MCFE, MC-free strain at exponential phase; MCS, MC-producing strain at stationary phase; MCFS, MC-free strain at stationary phase.

Multivariate statistical analysis of metabolites

Principal component analysis (PCA) of metabolites from different strains and growth phases revealed that the first and second principal components PC [1] and PC [2] explained 34.3 and 15.2% of total variation, respectively (Figure 3A). PCA results demonstrated that metabolites of the two strains overlapped almost completely during E-phase, but were clearly separated during S-phase, indicating metabolic shifts during growth in both strains. Variation between replicates was greater for S-phase cultures than that observed with E-phase cultures.

Hierarchical cluster analysis (HCA) revealed differences in metabolite profiling between strains and growth phases (Figure 3B). Regardless of strain, metabolites from E-phase and S-phase clustered together, indicating greater homogeneity among growth phases than among strains. Further, most metabolites exhibited higher relative concentrations in stationary than exponential growth phase.

The orthogonal partial least squares discriminant analysis (OPLS-DA) was performed to reveal the differential metabolites (DMs) for the different strains at the same phase and the same strain at different phases (Supplementary Figure S1). Values of R^2Y and Q^2 from the permutation test for the OPLS-DA model were higher than their original values, indicating good quality of each supervised model without overfitting (Supplementary Figure S2).

Differential metabolites identification and analysis

DMs of different strains in the same growth phase

There were 10 DMs in exponential cultures MCFE vs. MCE (5 each up-regulated and down-regulated, Figure 4A), and 38 DMs in stationary cultures MCFS vs. MCS (10 up-regulated and 28 down-regulated, Figure 4B). Thus, the total number of DMs at exponential phase was much less than that at stationary phase. Four DMs of different strains at same growth phase overlapped, including 7-ketocholesterol, choline, sinapyl alcohol and [8]-Dehydrogingerdione. 7-ketocholesterol and sinapyl alcohol in the MC-free strain were significantly higher than those of the MC-producing strain at both growth phases.

DMs with similar variation trends in concentration were positioned closer together on the HCA heat map (Figure 5). In

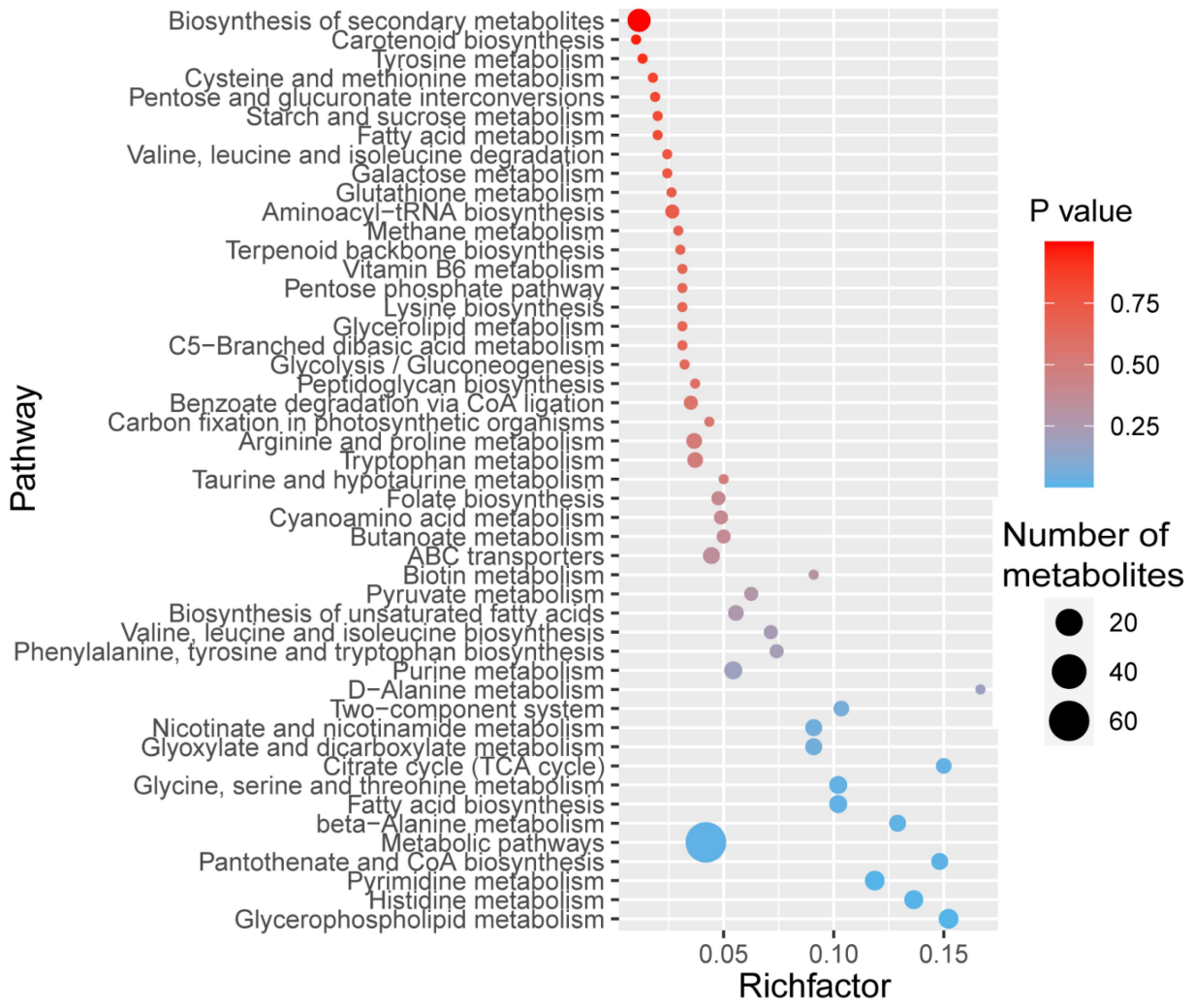

FIGURE 2
Bubble diagram showing KEGG pathway annotation covered by 409 metabolites. The x-axis indicates the scale of the "Rich factor" (the ratio of the number of metabolites in the corresponding pathway to the total metabolites annotated by the pathway detection) of the pathway in topological analysis, while the y-axis presents individual pathways. The color of the bubble indicates the *p* value of enrichment analysis with darker colors having a lower p value and greater enrichment. Size of the bubble is proportional to the number of metabolites in this pathway.

terms of clustering between groups, the similarity of the two strains in E-phase was greater than that in S-phase. Relative concentration of most DMs in stationary phase was higher than that in E-phase for both strains.

DMs of same strain in different growth phases

There were 50 DMs in MCS vs. MCE (45 up-regulated and 5 down-regulated, Figure 4C), and 36 DMs in MCFS vs. MCFE (33 up-regulated and 3 down-regulated, Figure 4D). The total number of DMs of the MC-producing strain were greater than those of the MC-free strain. Growth phase significantly affected metabolites, as most lipids, organoheterocyclic compounds, benzenoids, organic acids, phenylpropanoids and nucleosides were significantly up-regulated in the S-phase. Secondary metabolites, such as flavonoids, phenylpropanoids, benzene and substituted derivatives, indoles and lactones were significantly up-regulated in S-phase cultures. Nine DMs overlapped and displayed the same change trend, that was up-regulated during the S-phase for both strains, including 1,3,5-trihydroxybenzene, 2-hydroxyethanesulfonate, 3-hydroxyanthranilic acid, adenine, adenosine, kynurenic acid, mesna, pyrrole-2-carboxylic acid and sinapyl alcohol. We putatively identify these overlapped metabolites as key growth phase-related metabolites of *M. aeruginosa*. Detailed information on DMs is provided in Supplementary Table S2.

Metabolic pathway analysis of DMs

DMs pathway of different strains in the same growth phase

Differential metabolites were linked to metabolic pathways in the KEGG database. In the MCFE vs. MCE group, DMs

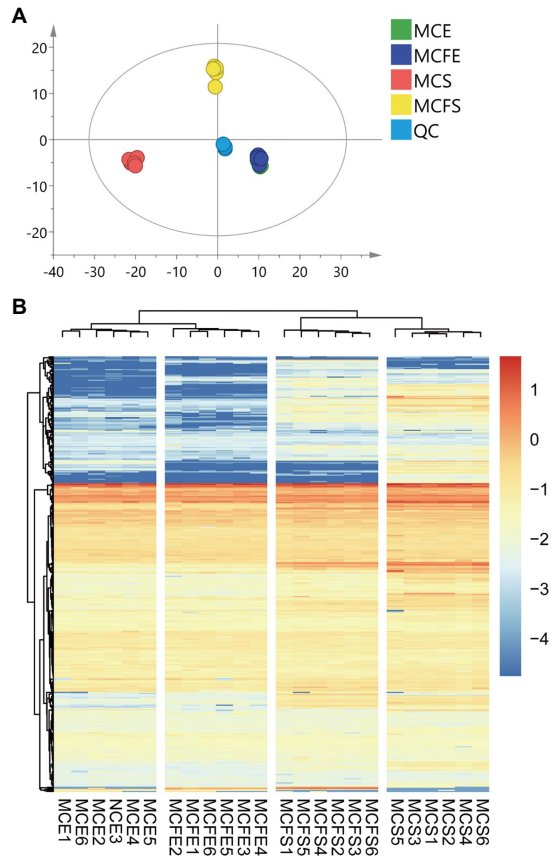

FIGURE 3
Principal component analysis (PCA) of metabolic profiles in all samples, with six replicates per treatment **(A)**; Cluster heatmap of metabolite content in different samples **(B)**. The x-axis represents six replicate cultures of each of the four treatment groups, the y-axis represents individual metabolites of the groups. Color blocks represent the relative concentration of metabolites at the corresponding positions. MCE, MC-producing strain at exponential phase; MCFE, MC-free strain at exponential phase; MCS, MC-producing strain at stationary phase; MCFS, MC-free strain at stationary phase.

mapped to six pathways (Figure 6A), including biosynthesis of secondary metabolites, glycine, serine and threonine metabolism, glycerophospholipid metabolism, ABC transporters and aromatic amino acid biosynthesis. In the MCFS vs. MCS comparison, DMs were mapped to 13 pathways (Figure 6B), including pyrimidine metabolism, purine metabolism, lipids and amino acid metabolisms, and benzoate degradation *via* CoA ligation.

DMs pathway of same strain in the different growth phases

In the MCS vs. MCE group, DMs mapped into 22 pathways (Figure 6C), including biosynthesis of secondary metabolites, amino acid metabolism, pyrimidine and purine metabolism and lipid metabolites. In the MCFS vs. MCFE group, the DMs were mapped to 11 pathways (Figure 6D), including biosynthesis of secondary metabolites, amino acid metabolism, purine metabolism, folate biosynthesis, lipid metabolism and benzoate degradation *via* CoA ligation.

At different growth phases, the MC-producing strain had 11 more DMs pathways than the MC-free strain. These pathways were mainly involved in lipids and amino acid metabolism. To further highlight the changes in the metabolic pathway induced during growth stage and strain, a metabolic pathway map was generated based on the DMs (Figure 7). DMs pathways were mainly focused on lipids biosynthesis and their downstream pathways, biosynthesis of secondary metabolites, and amino acids biosynthesis pathways.

Discussion

Cyanobacteria produce many more potentially harmful metabolites aside from the classic toxins such as microcystins (Huang and Zimba, 2019; Ferreira et al., 2021). In this study, we found that exudate mixtures of *M. aeruginosa* contain a large number of lipids, organoheterocyclics, organic acids, benzenoids, organic oxygen compounds, phenylpropanoids and organic nitrogen metabolites. Amongst lipid and organoheterocyclics compounds detected were a number whose toxicologic effects have been established (Table 2). Some organic oxygen compounds, such as carbonyl compounds and ethers, are also toxic. For example, carbonyl compounds were potential mutagens and carcinogens (Vilma et al., 2006), and ethers had antibacterial activity and neurotoxic characteristics (Suyama et al., 2010). Alkaloids (harmala and tropane alkaloids) have pharmacological and therapeutic effective (Moloudizargari et al., 2013; Kathrin and Oliver, 2019). Zi et al. (2022) screened nine neurotoxic compounds, including lysoPC (16:0), 2-acetyl-1-alkyl-sn-glycero-3phosphocholine, egonol glucoside, polyoxyethylene monoricinoleate, and phytosphingosin from MaE by using machine learning and molecular docking methods. Toxic effects of MaE on organisms are likely to result from the combined effect of these mixtures (Dias et al., 2017; Manach et al., 2018).

We observed an orchestrated elevation of some differential metabolites (DMs) in a MC-free strain compared with a MC-producing strain, including 7-ketocholesterol, sinapyl alcohol, myristoleic acid and diethyl phthalic acid. Xu (2021) revealed that MaE was toxic to mitochondrial membranes in *D. magna*, and the MC-free strain was more toxic to mitochondrial membrane than a MC-producing strain, and toxicity effects were stronger in S-phase than E-phase cultures. Additionally, metabolic pathways associated with benzenoids biosynthesis (e.g., phenylalaine biosynthesis,benzoate degradation *via* CoA ligation) were significantly up-regulated in the MC-free strain (Table 1; Figure 7). We suspect that these chemicals in the MC-free strain are linked to mitochondrial membrane damage. 7-Ketocholesterol can activate apoptosis, autophagy and induced mitochondrial damage (Gabriella et al., 2006; Lee et al., 2007; Ghzaiel et al., 2021), in turn causing

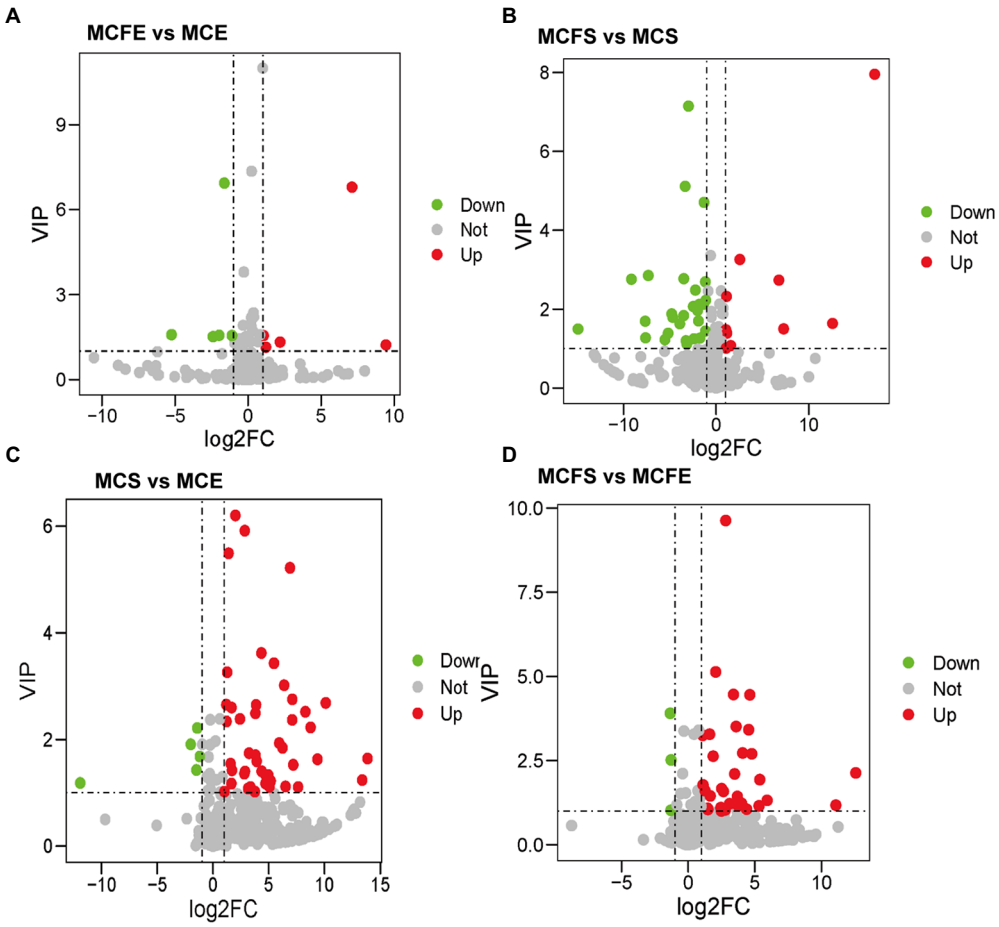

FIGURE 4
Differential metabolites in pairwise comparison among four MaE groups: volcano plots of differential metabolites in MCFE vs. MCE **(A)**; MCFS vs. MCS **(B)**; MCS vs. MCE **(C)**; MCFS vs. MCFE **(D)**. MCE, MC-producing strain at exponential phase; MCFE, MC-free strain at exponential phase; MCS, MC-producing strain at stationary phase; MCFS, MC-free strain at stationary phase.

cellular damage *via* multiple stress-response pathways (Anderson et al., 2020). Sinapyl alcohol exhibited significant cytotoxic activities against human tumor cell lines (Zou et al., 2006; Lee et al., 2015). Myristoleic acid as one of the cytotoxic components, induces mixed cell death of apoptosis and necrosis in LNCaP cells (Kazuhiro et al., 2001). Diethyl phthalic acid belongs to the group of phthalates which are widely applied as plasticizers and solvents in the chemical industry. Phthalates can be endocrine disrupting chemicals and they exhibit both toxicity and bioaccumulation (Sun et al., 2012). Phthalates are also produced by marine algae, with abundance varying among species (Chen, 2004; Namikoshi et al., 2006).

Despite the same culture conditions and initial cells density, MC-producing cultures accumulated more cells and higher concentrations of most primary and secondary metabolites than the MC-free cultures at S-phase (Table 1). Compared to the E-phase, both strains in S-phase had higher numbers and abundance of differential metabolites (DMs) of lipid, organoheterocyclic compounds and benzenoids compounds, indicating that growth phase significantly affects metabolites more than strain type. The dynamic accumulation of metabolites is largely determined by growth processes, as is variation in secondary metabolites (Zhang et al., 2021; Guo et al., 2022). Results of the analysis of DMs and pathways suggest that lipid metabolism and biosynthesis of some amino acids correlate more closely with growth phase than by strain (Figure 6), suggesting that some secondary metabolites—such as alkaloids, sulfide and benzenoids derived from tyrosine metabolism, taurine and hypotaurine metabolism and phenylalaine metabolism, respectively—accumulated during the S-phase (Tiago et al., 2017; Cao et al., 2020). An understanding of the metabolites accumulated in MaE and the dynamic changes in metabolites during exponential and stationary growth phases is essential for assessing the toxicity of compounds and would also provide a basis for subsequent research on *M. aeruginosa* of MC-producing and MC-free strains. *Microcystis* colony formations and other ecological factors, could differ between laboratory and field conditions (Xiao et al., 2018), thus we propose further attention be given to cyanobacterial compounds in relation to biotic and abiotic factors in the field. At the same time, we propose that water quality monitoring guidance consider the different growth stages that may occur in

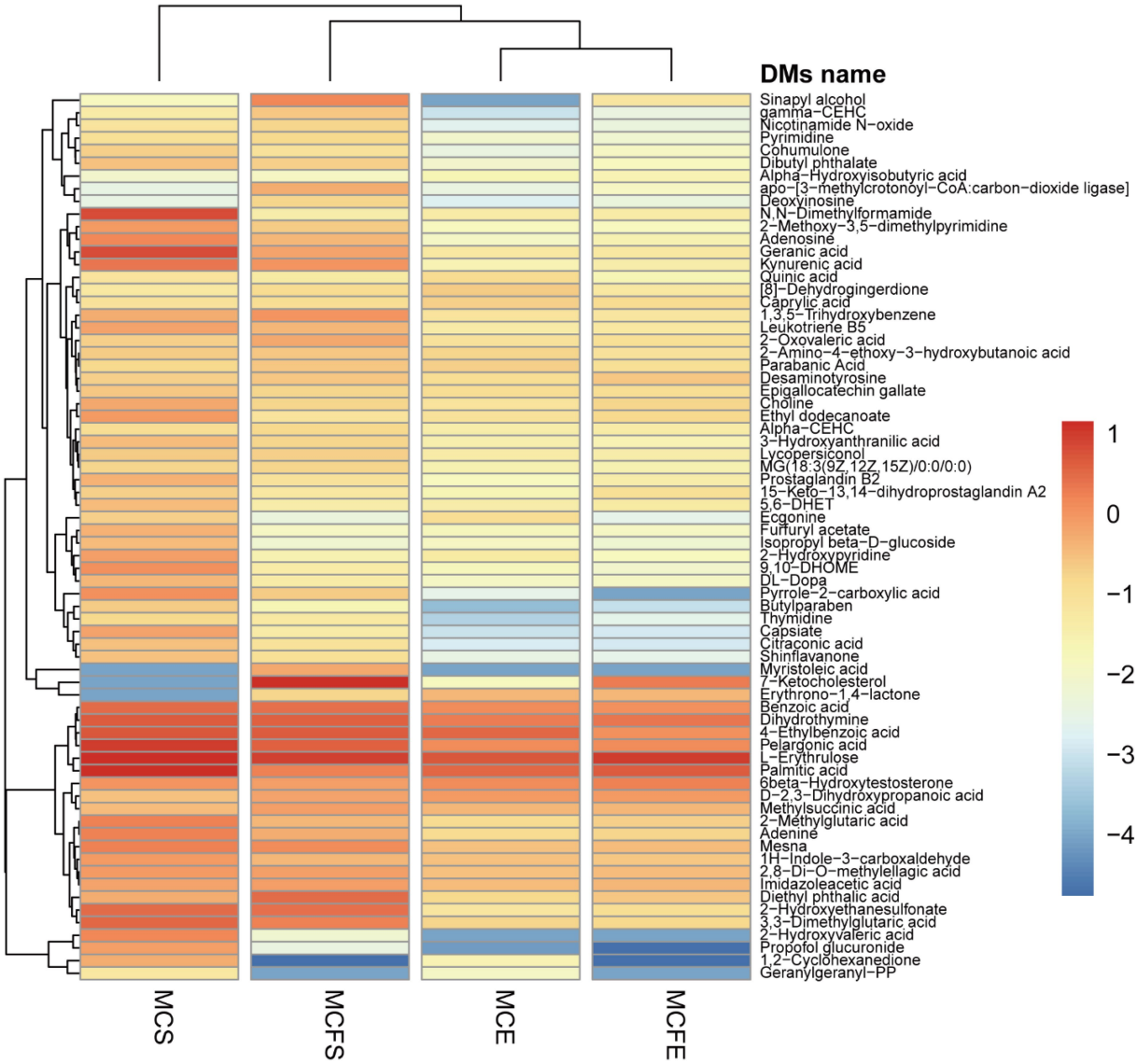

FIGURE 5
Heatmap for differential metabolites based upon hierarchical clustering of the four groups. The *x*-axis represents the four experimental groups, the *y*-axis the differential metabolites. The color blocks represent the relative concentration of metabolites at the corresponding positions. MCE, MC-producing strain at exponential phase; MCFE, MC-free strain at exponential phase; MCS, MC-producing strain at stationary phase; MCFS, MC-free strain at stationary phase.

cyanobacterial blooms as well as potential ecological risks associated with MC-free strains and the toxic compounds that they produce.

Conclusion

Microcystis aeruginosa exudates (MaE) contain a large number of lipids, organoheterocyclics compounds, organic acids, benzenoids, organic oxygen compounds, phenylpropanoids and organic nitrogen metabolites. Clear distinctions existed between metabolites of different growth phases, which clearly exceeded differences amongst strains. Some metabolites such as benzenoids, lipids, organic oxygen and organoheterocyclic compounds were higher in the MC-free strain than the MC-producing strain at E-phase. The MC-producing strain reached higher cell density and accumulated more total metabolites than the MC-free strain at S-phase. Some metabolites with known cytotoxicity, apoptosis-inducing effects, neurotoxicity and reproductive toxicity were detected in both strains. This study expands awareness of the metabolites and toxicity of *M. aeruginosa* at different growth phases and across strains, and adds to growing recognition that cyanobacteria can produce numerous compounds with potentially harmful effects on aquatic life.

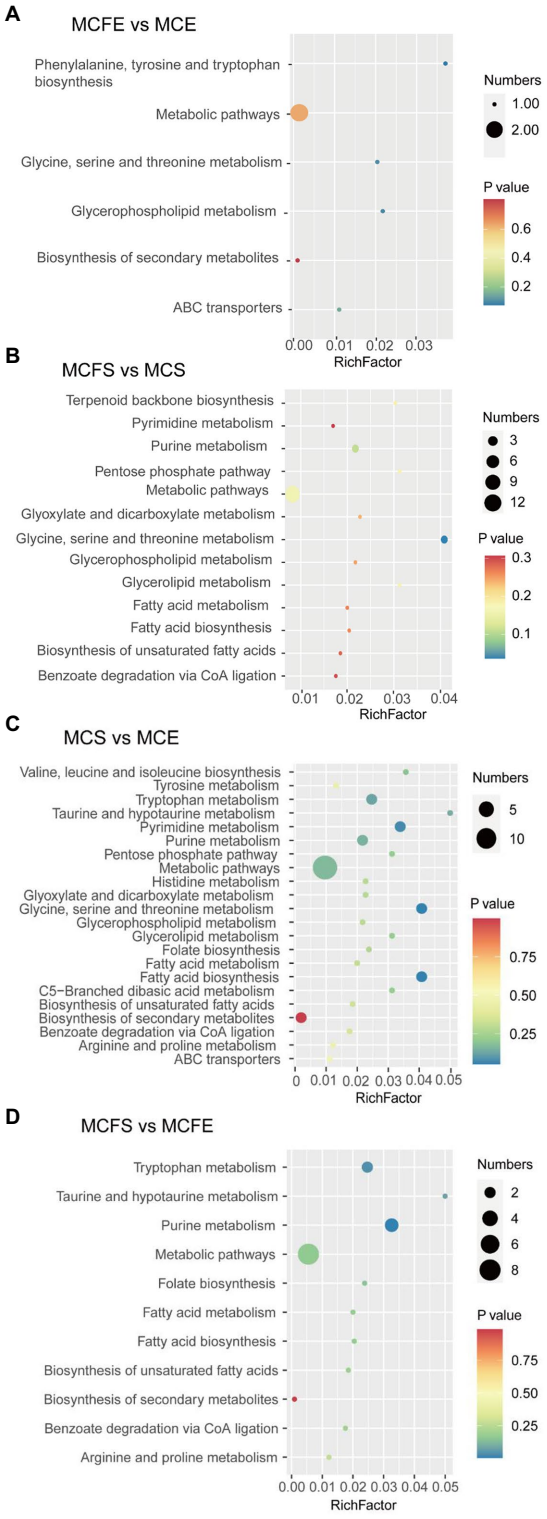

FIGURE 6
Bubble diagram of KEGG pathway annotation covered by differential metabolites. The x-axis indicates the scale of the "Rich factor" (the ratio of the number of differential metabolites in the corresponding pathway to the total metabolites annotated by the pathway detection), while the y-axis presents individual pathways identified. The color of the bubble indicates the p value of enrichment analysis with darker colors having a lower value and more significant enrichment. Size of the bubble is proportional to the number of metabolites in this pathway. Bubble diagrams of MCFE vs. MCE **(A)**; MCFS vs. MCS **(B)**; MCS vs. MCE **(C)**; MCFS vs. MCFE **(D)**. MCE, MC-producing strain at exponential phase; MCFE, MC-free strain at exponential phase; MCS, MC-producing strain at stationary phase; MCFS, MC-free strain at stationary phase.

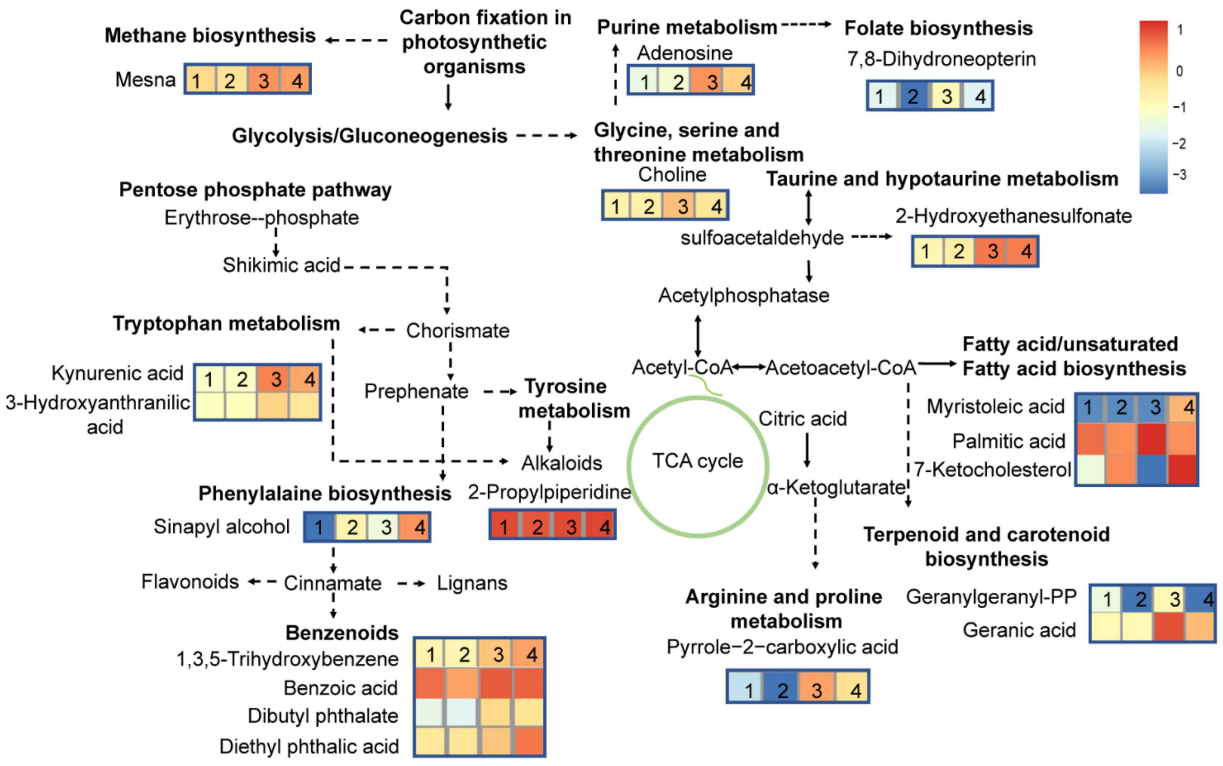

FIGURE 7
Differential metabolites pathways in MC-producing and MC-free strains harvested at exponential- and stationary-growth phases. The numbers 1, 2, 3, and 4 represent MCE, MCFE, MCS, MCFS, respectively. MCE, MC-producing strain at exponential phase; MCFE, MC-free strain at exponential phase; MCS, MC-producing strain at stationary phase; MCFS, MC-free strain at stationary phase.

TABLE 2 Main compounds identified and their toxicologic effects.

Name	Target	Toxicity type	Mode of action	References
Pelargonic acid	Broadleaf and grass weeds	Growth inhibition	-	Webber and Shrefler (2006)
Goyaglycoside	Cancer cells	Cytotoxicity	-	Wang et al. (2012)
Phloroglucinol	Pathogenic fungi, bacteria	Growth inhibition	-	Haas and Keel (2003); Abdel-Ghany et al. (2016)
Geranic acid	Phytopathogen	Antifungal	-	Mi et al. (2014)
Gingerol	Mammary carcinoma	Growth inhibition	Apoptosis	Bernard et al. (2017)
Phyto-sphingosine	Watermelon Fusarium oxysporum	Growth inhibition	-	Li et al. (2020)
	CNE-2 cells	Cytotoxicity	Mitochondria-mediated apoptosis	Li et al. (2022)
3-Amino-1,4-dimethyl-5H-pyrido[4,3-b] indole	Rat Splenocytes	Cytotoxicity	Apoptosis and Necrosis	Hashimoto et al. (2004)
Nicotine	Nerve, blood vessel	Neurotoxicity, atherosclerotic lesions	Autonomic imbalance, endothelial dysfunction and coronary blood flow dysregulation	Adamopoulos et al. (2008)
3-Hydro-xyanthranilic acid	THP-1 and U937 cells		Apoptosis	Morita et al. (2001)
Palmitic acid	Multiple myeloma cells	Growth inhibition	Apoptosis	Nagata et al. (2015)

Data availability statement

We have registered an account on Metabolightes website (MTBLS6603). The metabolite data is being uploaded for validation.

Author contributions

XC and HM designed the study. JX, YZh, YP, and YZi collected samples and conducted the experiments. YZh analyzed and interpreted the data. XC, HM, RM,

RX, YQ, and JL revised the manuscript. All authors contributed to the article and approved the submitted version.

Funding

This research was supported by funds from the National Natural Science Foundation of China (NSFC)—Yunnan Joint Key Grant (No. U1902202), Yunnan Provincial Science and Technology Department grants (2019FA043; 2018BC002; and 202101AU070078), and Great Lakes Fishery Commission (2020_MAC_440940).

Conflict of interest

The authors declare that the research was conducted in the absence of any commercial or financial relationships that could be construed as a potential conflict of interest.

Publisher's note

Supplementary material

The Supplementary material for this article can be found online at: https://www.frontiersin.org/articles/10.3389/fmicb.2022.1075621/full#supplementary-material

References

Abdel-Ghany, S. E., Day, I., Heuberger, A. L., Broeckling, C. D., and Reddy, A. S. (2016). Production of phloroglucinol, a platform chemical, in Arabidopsis using a bacterial gene. *Sci. Rep.* 6:38483. doi: 10.1038/srep38483

Adamopoulos, D., van de Borne, P., and Argacha, J. F. (2008). New insights into the sympathetic, endothelial and coronary effects of nicotine. *Clin. Exp. Pharmacol. Physiol.* 35, 458–463. doi: 10.1111/j.1440-1681.2008.04896.x

Alexandra, C. S., Simona, G. C., Codreanu, S. G., Stacy, D. S., and John, A. M. (2016). Untargeted metabolomics strategies-challenges and emerging directions. *J. Am. Soc. Mass Spectrom.* 27, 1897–1905. doi: 10.1007/s13361-016-1469-y

Anderson, A., Campo, A., Fulton, E., Corwin, A., Jerome, W. G. 3rd, and O'Connor, M. S. (2020). 7-Ketocholesterol in disease and aging. *Redox Biol.* 29:101380. doi: 10.1016/j.redox.2019.101380

Bernard, M. M., McConnery, J. R., and Hoskin, D. W. (2017). [10]-Gingerol, a major phenolic constituent of ginger root, induces cell cycle arrest and apoptosis in triple-negative breast cancer cells. *Exp. Mol. Pathol.* 102, 370–376. doi: 10.1016/j.yexmp.2017.03.006

Breinlinger, S., Phillips, T. J., Haram, B. N., Mares, J., Martinez Yerena, J., Hrouzek, P., et al. (2021). Hunting the eagle killer: a cyanobacterial neurotoxin causes vacuolar myelinopathy. *Science* 371:1355. doi: 10.1126/science.aax9050

Broadhurst, D., Goodacre, R., Reinke, S. N., Kuligowski, J., Wilson, I. D., and Lewis, M. R. (2018). Guidelines and considerations for the use of system suitability and quality control samples in mass spectrometry assays applied in untargeted clinical metabolomic studies. *Metabolomics* 14:72. doi: 10.1007/s11306-018-1367-3

Cai, W., MacIsaac, H. J., Xu, R., Zhang, J., Pan, X., Chang, X., et al. (2022). Abnormal neurobehavior in fish early life stages after exposure to cyanobacterial exudates. *Ecotoxicol. Environ. Saf.* 245:114119. doi: 10.1016/j.ecoenv.2022.114119

Cao, M., Gao, M., Suastegui, M., Mei, Y., and Shao, Z. (2020). Building microbial factories for the production of aromatic amino acid pathway derivatives: from commodity chemicals to plant-sourced natural products. *Metab. Eng.* 58, 94–132. doi: 10.1016/j.ymben.2019.08.008

Carmichael, W. W., and Boyer, G. L. (2016). Health impacts from cyanobacteria harmful algae blooms: implications for the north American Great Lakes. *Harmful Algae* 54, 194–212. doi: 10.1016/j.hal.2016.02.002

Chen, C. (2004). Biosynthesis of di-(2-ethylhexyl) phthalate (DEHP) and di-*n*-butyl phthalate (DBP) from red alga—*Bangia atropurpurea*. *Water Res.* 38, 1014–1018. doi: 10.1016/j.watres.2003.11.029

Chen, L., Chen, J., Zhang, X., and Xie, P. (2016). A review of reproductive toxicity of microcystins. *J. Hazard Mater.* 301, 381–399. doi: 10.1016/j.jhazmat.2015.08.041

Chen, S., Liu, H., Zhao, X., Li, X., Shan, W., Wang, X., et al. (2020). Non-targeted metabolomics analysis reveals dynamic changes of volatile and non-volatile metabolites during oolong tea manufacture. *Food Res. Int.* 128:108778. doi: 10.1016/j.foodres.2019.108778

Davis, T. W., Berry, D. L., Boyer, G. L., and Gobler, C. J. (2009). The effects of temperature and nutrients on the growth and dynamics of toxic and non-toxic strains of Microcystis during cyanobacteria blooms. *Harmful Algae* 8, 715–725. doi: 10.1016/j.hal.2009.02.004

Dias, F., Antunes, J. T., Ribeiro, T., Azevedo, J., Vasconcelos, V., and Leao, P. N. (2017). Cyanobacterial allelochemicals but not cyanobacterial cells markedly reduce microbial community diversity. *Front. Microbiol.* 8:1495. doi: 10.3389/fmicb.2017.01495

Fernanda, R., Ana, B. F. P., Fungyi, C., Giovani, C. V., Dário, E. K., Janaina, R., et al. (2019). Different ecophysiological and structural strategies of toxic and non-toxic *Microcystis aeruginosa* (cyanobacteria) strains assessed under culture conditions. *Algal Res.* 41:101548. doi: 10.1016/j.algal.2019.101548

Ferreira, L., Morais, J., Preto, M., Silva, R., Urbatzka, R., Vasconcelos, V., et al. (2021). Uncovering the bioactive potential of a cyanobacterial natural products library aided by untargeted metabolomics. *Mar. Drugs* 19:633. doi: 10.3390/md19110633

Gabriella, L., Barbara, V., Barbara, S., Veronica, V., and Paola, G. (2006). Early involvement of ROS overproduction in apoptosis induced by 7-ketocholesterol. *Antioxid. Redox Signal.* 8, 375–380. doi: 10.1089/ars.2006.8.375

Ger, K. A., Urrutia-Cordero, P., Frost, P. C., Hansson, L. A., Sarnelle, O., Wilson, A. E., et al. (2016). The interaction between cyanobacteria and zooplankton in a more eutrophic world. *Harmful Algae* 54, 128–144. doi: 10.1016/j.hal.2015.12.005

Ghzaiel, I., Sassi, K., Zarrouk, A., Nury, T., Ksila, M., Leoni, V., et al. (2021). 7-Ketocholesterol: effects on viral infections and hypothetical contribution in COVID-19. *J. Steroid Biochem. Mol. Biol.* 212:105939. doi: 10.1016/j.jsbmb.2021.105939

Guo, J., Wu, Y., Jiang, M., Wu, C., and Wang, G. (2022). An LC–MS-based metabolomic approach provides insights into the metabolite profiles of *Ginkgo biloba* L. at different developmental stages and in various organs. *Food Res. Int.* 159:111644. doi: 10.1016/j.foodres.2022.111644

Haas, D., and Keel, C. (2003). Regulation of antibiotic production in root-colonizing *Peudomonas* spp. and relevance for biological control of plant disease. *Annu. Rev. Phytopathol.* 41, 117–153. doi: 10.1146/annurev.phyto.41.052002.095656

Harke, M. J., Steffen, M. M., Gobler, C. J., Otten, T. G., Wilhelm, S. W., and Wood, S. A. (2016). A review of the global ecology, genomics, and biogeography of the toxic cyanobacterium. *Microcystis spp. Harmful Algae.* 54, 4–20. doi: 10.1016/j.hal.2015.12.007

Hashimoto, T., Sano, T., Ito, W., Kanazawa, K., Danno, G., and Ashida, H. (2004). 3-Amino-1,4-dimethyl-5H-pyrido[4,3-b] indole induces apoptosis and necrosis with activation of different caspases in rat splenocytes. *Biosci. Biotechnol. Biochem.* 68, 964–967. doi: 10.1271/bbb.68.964

Ho, J. C., Michalak, A. M., and Pahlevan, N. (2019). Widespread global increase in intense lake phytoplankton blooms since the 1980s. *Nature* 574, 667–670. doi: 10.1038/s41586-019-1648-7

Hu, L., Shan, K., Lin, L., Shen, W., Huang, L., Gan, N., et al. (2016). Multi-year assessment of toxic genotypes and microcystin concentration in northern Lake Taihu, China. *Toxins* 8:23. doi: 10.3390/toxins8010023

Huang, I. S., and Zimba, P. V. (2019). Cyanobacterial bioactive metabolites-a review of their chemistry and biology. *Harmful Algae* 86, 139–209. doi: 10.1016/j.hal.2019.05.001

Huisman, J., Codd, G. A., Paerl, H. W., Ibelings, B. W., Verspagen, J. M. H., and Visser, P. M. (2018). Cyanobacterial blooms. *Nat. Rev. Microbiol.* 16, 471–483. doi: 10.1038/s41579-018-0040-1

Islam, M. A., and Beardall, J. (2017). Growth and photosynthetic characteristics of toxic and non-toxic strains of the cyanobacteria *Microcystis aeruginosa* and *Anabaena circinalis* in relation to light. *Microorganisms* 5:45. doi: 10.3390/microorganisms5030045

Janssen, E. M. (2018). Cyanobacterial peptides beyond microcystins—a review on co-occurrence, toxicity, and challenges for risk assessment. *Water Res.* 151, 488–499. doi: 10.1016/j.watres.2018.12.048

Jiang, M., Zhou, Y., Wang, N., Xu, L., Zheng, Z., and Zhang, J. (2019). Allelopathic effects of harmful algal extracts and exudates on biofilms on leaves of *Vallisneria natans*. *Sci. Total Environ.* 655, 823–830. doi: 10.1016/j.scitotenv.2018.11.296

Jones, M. R., Pinto, E., Torres, M. A., Dörr, F., Mazur-Marzec, H., Szubert, K., et al. (2021). CyanoMetDB, a comprehensive public database of secondary metabolites from cyanobacteria. *Water Res.* 196:117017. doi: 10.1016/j.watres.2021.117017

Kathrin, L., and Oliver, K. (2019). Tropane alkaloids: chemistry, pharmacology, biosynthesis and production. *Molecules* 24:796. doi: 10.3390/molecules24040796

Kazuhiro, I., and Naoya, O., Shigeyuki,U., Hironao, S., Kosaku, H., and Hirano, K. (2001). Myristoleic acid, a cytotoxic component in the extract from *Serenoa repens*, induces apoptosis and necrosis in human prostatic LN CaP cells. *Prostate* 47, 59–65.doi: 10.1002/pros.1047

Kurmayer, R., and Kutzenberger, T. (2003). Application of real-time PCR for quantification of microcystin genotypes in a population of the toxic cyanobacterium *Microcystis* sp. *Appl. Environ. Microbiol.* 69, 6723–6730. doi: 10.1128/AEM.69.11.6723–6730.2003

Lee, C., Park, W., Han, E., and Bang, H. (2007). Differential modulation of 7-ketocholesterol toxicity against PC12 cells by calmodulin antagonists and Ca^{2+} channel blockers. *Neurochem. Res.* 32, 87–98. doi: 10.1007/s11064-006-9230-8

Lee, C., Yen, M., Hwang, T., Yang, J., Peng, C., Chen, C., et al. (2015). Anti-inflammatory and cytotoxic components from *Dichrocephala integrifolia*. *Phytochemistry* 12, 237–242. doi: 10.1016/j.phytol.2015.04.012

Li, X., Janssen, A., Klein, J., Kroeze, C., Strokal, M., Ma, L., et al. (2019). Modeling nutrients in Lake Dianchi (China) and its watershed. *Agric. Water Manag.* 212, 48–59. doi: 10.1016/j.agwat.2018.08.023

Li, C., Tian, Q., Rahman, M., and Wu, F. (2020). Effect of anti-fungal compound phytosphingosine in wheat root exudates on the rhizosphere soil microbial community of watermelon. *Plant Soil* 456, 223–240. doi: 10.1007/s11104-020-04702-1

Li, J., Wen, J., Sun, C., Zhou, Y., Xu, J., Macisaac, H. J., et al. (2022). Phytosphingosine-induced cell apoptosis via mitochondria-mediated pathway. *Toxicology* 482:153370. doi: 10.1016/j.tox.2022.153370

Liang, L., Rasmussen, M. H., Piening, B., Shen, X., Chen, S., Rost, H., et al. (2020). Metabolic dynamics and prediction of gestational age and time to delivery in pregnant women. *Cells* 181, 1680–1692.e15. doi: 10.1016/j.cell.2020.05.002

Liu, Q., Li, B., Li, Y., Wei, Y., Huang, B., Liang, J., et al. (2021). Altered faecal microbiome and metabolome in IgG4-related sclerosing cholangitis and primary sclerosing cholangitis. *Gut* 71, 899–909. doi: 10.1136/gutjnl-2020-323565

Liu, J., Luo, X., Zhang, N., and Wu, Y. (2016). Phosphorus released from sediment of Dianchi Lake and its effect on growth of *Microcystis aeruginosa*. *Environ. Sci. Pollut. Res.* 23, 16321–16328. doi: 10.1007/s11356-016-6816-9

Lorena, V., Jutta, F., Rainer, K., Michael, H., Elke, D., Jiri, K., et al. (2004). Distribution of microcystin-producing and non-microcystin-producing *Microcystis* sp. in European freshwater bodies: detection of microcystins and microcystin genes in individual colonies. *Syst. Appl. Microbiol.* 27, 592–602. doi: 10.1078/0723202041748163

Ma, Z., Fang, T., Thring, R. W., Li, Y., Yu, H., Zhou, Q., et al. (2015). Toxic and non-toxic strains of *Microcystis aeruginosa* induce temperature dependent allelopathy toward growth and photosynthesis of *Chlorella vulgaris*. *Harmful Algae* 48, 21–29. doi: 10.1016/j.hal.2015.07.002

Manach, S. L., Sotton, B., Huet, H., Duval, C., Paris, A., Marie, A., et al. (2018). Physiological effects caused by microcystin-producing and non-microcystin producing *Microcystis aeruginosa* on medaka fish: a proteomic and metabolomic study on liver. *Environ. Pollut.* 234, 523–537. doi: 10.1016/j.envpol.2017.11.011

Mi, J., Becher, D., Lubuta, P., Dany, S., Tusch, K., Schewe, H., et al. (2014). *De novo* production of the monoterpenoid geranic acid by metabolically engineered *pseudomonas putida*. *Microb. Cell Factories* 13:170. doi: 10.1186/s12934-014-0170-8

Moloudizargari, M., Mikaili, P., Aghajanshakeri, S., Asghari, M. H., and Shayegh, J. (2013). Pharmacological and therapeutic effects of *Peganum harmala* and its main alkaloids. *Pharmacogn. Rev.* 7, 199–212. doi: 10.4103/0973-7847.120524

Morita, T., Saito, K., Takemura, M., Maekawa, N., Fujigaki, S., Fujii, H., et al. (2001). 3-Hydroxyanthranilic acid, an L-tryptophan metabolite, induces apoptosis in monocyte-derived cells stimulated by interferon-γ. *Ann. Clin. Biochem.* 38, 242–251. doi: 10.1258/0004563011900461

Nagata, Y., Ishizaki, I., Michihiko, W., Yoshimi, I., Md Amir, H., Kazunori, O., et al. (2015). Palmitic acid, verified by lipid profiling using secondary ion mass spectrometry, demonstrates anti-multiple myeloma activity. *Leuk. Res.* 39, 638–645. doi: 10.1016/j.leukres.2015.02.011

Namikoshi, M., Fujiwara, T., Nishikawa, T., and Ukai, K. (2006). Natural abundance ^{14}C content of Dibutyl phthalate (DBP) from three marine algae. *Mar. Drugs* 4, 290–297. doi: 10.3390/md404290

Paerl, H. W., Gardner, W. S., Havens, K. E., Joyner, A. R., McCarthy, M. J., Newell, S. E., et al. (2016). Mitigating cyanobacterial harmful algal blooms in aquatic ecosystems impacted by climate change and anthropogenic nutrients. *Harmful Algae* 54, 213–222. doi: 10.1016/j.hal.2015.09.009

Papadimitriou, T., Katsiapi, M., Vlachopoulos, K., Christopoulos, A., Laspidou, C., Moustaka-Gouni, M., et al. (2018). Cyanotoxins as the "common suspects" for the Dalmatian pelican (*Pelecanus crispus*) deaths in a Mediterranean reconstructed reservoir. *Environ. Pollut.* 234, 779–787. doi: 10.1016/j.envpol.2017.12.022

Pinu, F. R., Villas-Boas, S. G., and Aggio, R. (2018). Analysis of intracellular metabolites from microorganisms: quenching and extraction protocols. *Metabolites* 7:53. doi: 10.3390/metabo7040053

Pound, H. L., Martin, R. M., Sheik, C. S., Steffen, M. M., Newell, S. E., Dick, G. J., et al. (2021). Environmental studies of Cyanobacterial harmful algal blooms should include interactions with the dynamic microbiome. *Environ. Sci. Technol.* 55, 12776–12779. doi: 10.1021/acs.est.1c04207

Racine, M., Saleem, A., and Pick, F. R. (2019). Metabolome variation between strains of *Microcystis aeruginosa* by untargeted mass spectrometry. *Toxins* 11:723. doi: 10.3390/toxins11120723

Rinschen, M. M., Ivanisevic, J., Giera, M., and Siuzdak, G. (2019). Identification of bioactive metabolites using activity metabolomics. *Nat. Rev. Mol. Cell Biol.* 20, 353–367. doi: 10.1038/s41580-019-0108-4

Shen, B., Yi, X., Sun, Y., Bi, X., Du, J., Zhang, C., et al. (2020). Proteomic and Metabolomic characterization of COVID-19 patient sera. *Cells* 182, 59–72.e15. doi: 10.1016/j.cell.2020.05.032

Sun, Y., Kumiko, T., Toshiyuki, H., Takeshi, S., and Masaaki, K. (2012). Diethyl phthalate enhances apoptosis induced by serum deprivation in PC12 cells. *Basic Clin. Pharmacol. Toxicol.* 111, 113–119. doi: 10.1111/j.1742-7843.2012.00869.x

Sun, X., Lyu, G., Luan, Y., Yang, H., and Zhao, Z. (2019). Metabolomic study of the soybean pastes fermented by the single species *Penicillium glabrum* GQ1-3 and *Aspergillus oryzae* HGPA20. *Food Chem.* 295, 622–629. doi: 10.1016/j.foodchem.2019.05.162

Suyama, T. L., Cao, Z., Murray, T. F., and Gerwick, W. H. (2010). Ichthyotoxic brominated diphenyl ethers from a mixed assemblage of a red alga and cyanobacterium: structure clarification and biological properties. *Toxicon* 55, 204–210. doi: 10.1016/j.toxicon.2009.07.020

Sychrova, E., Stepankova, T., Novakova, K., Blaha, L., Giesy, J. P., and Hilscherova, K. (2012). Estrogenic activity in extracts and exudates of cyanobacteria and green algae. *Environ. Int.* 39, 134–140. doi: 10.1016/j.envint.2011.10.004

Tiago, O., Maicon, N., Ivan, R. C., Diego, N. F., Vinícius, J. S., Mauricio, F., et al. (2017). Plant secondary metabolites and its dynamical systems of induction in response to environmental factors: a review. *Afr. J. Agric. Res.* 12, 71–84. doi: 10.5897/AJAR2016.11677

Viant, M. R., Kurland, I. J., Jones, M. R., and Dunn, W. B. (2017). How close are we to complete annotation of metabolomes? *Curr. Opin. Chem. Biol.* 36, 64–69. doi: 10.1016/j.cbpa.2017.01.001

Vilma, M., Márcia, C., Eliane, T., Gislaine, V., Miguel, C. A., Pedro, A., et al. (2006). Determination of 11 low-molecular-weight carbonyl compounds in marine algae by high-performance liquid chromatography. *J. Chromatogr. Sci.* 44, 233–238. doi: 10.1093/chromsci/44.5.233

Wang, Y., Liang, X., Li, Y., Fan, Y., Li, Y., Cao, Y., et al. (2020). Changes in metabolome and nutritional quality of *Lycium barbarum* fruits from three typical growing areas of China as revealed by widely targeted metabolomics. *Metabolites* 10:46. doi: 10.3390/metabo10020046

Wang, X., Sun, W., Cao, J., Qu, H., Bi, X., and Zhao, Y. (2012). Structures of new triterpenoids and cytotoxicity activities of the isolated major compounds from the fruit of *Momordica charantia* L. *J. Agric. Food Chem.* 60, 3927–3933. doi: 10.1021/jf204208y

Wang, L., Zi, J., Xu, R., Hilt, S., Hou, X., and Chang, X. (2017). Allelopathic effects of *Microcystis aeruginosa* on green algae and a diatom: evidence from exudates addition and co-culturing. *Harmful Algae* 61, 56–62. doi: 10.1016/j.hal.2016.11.010

Webber, C. L., and Shrefler, J. W. (2006). Pelargonic acid weed control parameters. Poster session abstracts, 103rd annual international conference of the American Society for Horticultural Science new Orleans, Louisiana. *Hort Science* 41:4. doi: 10.21273/hortsci.41.4

Wituszynski, D. M., Hu, C., Zhang, F., Chaffin, J. D., Lee, J., Ludsin, S. A., et al. (2017). Microcystin in Lake Erie fish: risk to human health and relationship to cyanobacterial blooms. *J.Great Lakes Res.* 43, 1084–1090. doi: 10.1016/j.jglr.2017.08.006

Xiao, M., Li, M., and Reynolds, C. S. (2018). Colony formation in the cyanobacterium *Microcystis*. *Biol. Rev.* 93, 1399–1420. doi: 10.1111/brv.12401

Xu, J. (2021). Toxicities of *Microcystis aeruginosa* at different growth phases on *Daphnia magna* and the correlation between effects and metabolites. Master degree. Yunnan: Yunnan University.

Xu, R., Hilt, S., Pei, Y., Yin, L., Wang, X., and Chang, X. (2015). Growth phase-dependent allelopathic effects of cyanobacterial exudates on *Potamogeton crispus* L. seedlings. *Hydrobiologia* 767, 137–149. doi: 10.1007/s10750-015-2489-5

Xu, R., Jiang, Y., MacIsaac, H. J., Chen, L., Li, J., Chang, X., et al. (2019). Blooming cyanobacteria alter water flea reproduction via exudates of estrogen analogues. *Sci. Total Environ.* 696:133909. doi: 10.1016/j.scitotenv.2019.133909

Yan, Q., Stegen, J. C., Yu, Y., Deng, Y., Li, X., Wu, S., et al. (2017). Nearly a decade-long repeatable seasonal diversity patterns of bacterioplankton communities in the eutrophic Lake Donghu (Wuhan, China). *Mol. Ecol.* 26, 3839–3850. doi: 10.1111/mec.14151

Yeung, K., Zhou, G., Klára, H., Giesy, J. P., and Leung, K. (2020). Current understanding of potential ecological risks of retinoic acids and their metabolites in aquatic environments. *Environ. Int.* 136:105464. doi: 10.1016/j.envint.2020.105464

Zhang, D., Xie, P., Liu, Y., and Qiu, T. (2009). Transfer, distribution and bioaccumulation of microcystins in the aquatic food web in Lake Taihu, China, with potential risks to human health. *Sci. Total Environ.* 407, 2191–2199. doi: 10.1016/j.scitotenv.2008.12.039

Zhang, B., Zhang, X., Yan, L., Kang, Z., Tan, H., Jia, D., et al. (2021). Different maturities drive proteomic and metabolomic changes in Chinese black truffle. *Food Chem.* 342:128233. doi: 10.1016/j.foodchem.2020.128233

Zheng, G., Xu, R., Chang, X., Hilt, S., and Wu, C. (2013). Cyanobacteria can allelopathically inhibit submerged macrophytes: effects of *Microcystis aeruginosa* extracts and exudates on *Potamogeton malaianus*. *Aquat. Bot.* 109, 1–7. doi: 10.1016/j.aquabot.2013.02.004

Zi, Y., Barker, J. R., MacIsaac, H. J., Zhang, R., Gras, R., Chiang, Y., et al. (2022). Identification of neurotoxic compounds in cyanobacteria exudate mixtures. *Sci. Total Environ.* 857:159257. doi: 10.1016/j.scitotenv.2022.159257

Zi, J., Pan, X., MacIsaac, H. J., Yang, J., Xu, R., Chen, S., et al. (2018). Cyanobacteria blooms induce embryonic heart failure in an endangered fish species. *Aquat. Toxicol.* 194, 78–85. doi: 10.1016/j.aquatox.2017.11.007

Zou, H., Dong, S., Zhou, C., Hu, L., Wu, Y., Li, H., et al. (2006). Design, synthesis, and SAR analysis of cytotoxic sinapyl alcohol derivatives. *Bioorg. Med. Chem.* 14, 2060–2071. doi: 10.1016/j.bmc.2005.10.056

frontiers | Frontiers in Microbiology

TYPE Original Research
PUBLISHED 09 February 2023
DOI 10.3389/fmicb.2023.1073753

OPEN ACCESS

EDITED BY
David A. Walsh,
Concordia University,
Canada

REVIEWED BY
Veljo Kisand,
University of Tartu,
Estonia
Olga Maria Perez-Carrascal,
Montreal University,
Canada

*CORRESPONDENCE
Sophie Crevecoeur
✉ Sophie.crevecoeur@ec.gc.ca

SPECIALTY SECTION
This article was submitted to Aquatic Microbiology, a section of the journal Frontiers in Microbiology

RECEIVED 18 October 2022
ACCEPTED 16 January 2023
PUBLISHED 09 February 2023

CITATION
Crevecoeur S, Edge TA, Watson LC, Watson SB, Greer CW, Ciborowski JH, Diep N, Dove A, Drouillard KG, Frenken T, McKay RM, Zastepa A and Comte J (2023) Spatio-temporal connectivity of the aquatic microbiome associated with cyanobacterial blooms along a Great Lake riverine-lacustrine continuum. *Front. Microbiol.* 14:1073753. doi: 10.3389/fmicb.2023.1073753

Spatio-temporal connectivity of the aquatic microbiome associated with cyanobacterial blooms along a Great Lake riverine-lacustrine continuum

Sophie Crevecoeur[1]*, Thomas A. Edge[2], Linet Cynthia Watson[1], Susan B. Watson[3], Charles W. Greer[4], Jan J. H. Ciborowski[5,6], Ngan Diep[7], Alice Dove[1], Kenneth G. Drouillard[8], Thijs Frenken[8,9], Robert Michael McKay[8,10], Arthur Zastepa[1] and Jérôme Comte[11,12]

[1]Watershed Hydrology and Ecology Research Division, Environment and Climate Change Canada, Burlington, ON, Canada, [2]Department of Biology, McMaster University, Hamilton, ON, Canada, [3]Department of Biology, Trent University, Peterborough, ON, Canada, [4]Energy, Mining and Environment, National Research Council of Canada, Montreal, QC, Canada, [5]Department of Integrative Biology, University of Windsor, Windsor, ON, Canada, [6]Department of Biological Sciences University of Calgary, Calgary, AB, Canada, [7]Ontario Ministry of the Environment, Conservation and Parks, Environmental Monitoring and Reporting Branch, Etobicoke, ON, Canada, [8]Great Lakes Institute for Environmental Research, University of Windsor, Windsor, ON, Canada, [9]Cluster Nature & Society, HAS University of Applied Sciences, s-Hertogenbosch, Netherlands, [10]Great Lakes Center for Fresh Waters and Human Health, Bowling Green State University, Bowling Green, OH, United States, [11]Centre Eau Terre Environnement, Institut National de la Recherche Scientifique, Quebec City, QC, Canada, [12]Groupe de Recherche Interuniversitaire en Limnologie et en Environnement Aquatique (GRIL), Université de Montréal, Montreal, QC, Canada

Lake Erie is subject to recurring events of cyanobacterial harmful algal blooms (cHABs), but measures of nutrients and total phytoplankton biomass seem to be poor predictors of cHABs when taken individually. A more integrated approach at the watershed scale may improve our understanding of the conditions that lead to bloom formation, such as assessing the physico-chemical and biological factors that influence the lake microbial community, as well as identifying the linkages between Lake Erie and the surrounding watershed. Within the scope of the Government of Canada's Genomics Research and Development Initiative (GRDI) Ecobiomics project, we used high-throughput sequencing of the 16S rRNA gene to characterize the spatio-temporal variability of the aquatic microbiome in the Thames River–Lake St. Clair-Detroit River–Lake Erie aquatic corridor. We found that the aquatic microbiome was structured along the flow path and influenced mainly by higher nutrient concentrations in the Thames River, and higher temperature and pH downstream in Lake St. Clair and Lake Erie. The same dominant bacterial phyla were detected along the water continuum, changing only in relative abundance. At finer taxonomical level, however, there was a clear shift in the cyanobacterial community, with *Planktothrix* dominating in the Thames River and *Microcystis* and *Synechococcus* in Lake St. Clair and Lake Erie. Mantel correlations highlighted the importance of geographic distance in shaping the microbial community structure. The fact that a high proportion of microbial sequences found in the Western Basin of Lake Erie were also identified in the Thames River, indicated a high degree of connectivity and dispersal within the system, where mass effect induced by passive transport play an important role in microbial community assembly. Nevertheless, some cyanobacterial amplicon sequence variants (ASVs) related to *Microcystis*, representing less than 0.1% of relative abundance in the upstream Thames River, became dominant in Lake St. Clair and Erie, suggesting selection of those ASVs based on the lake conditions. Their extremely low relative abundances in the Thames suggest additional sources are likely to contribute to the rapid development of summer and fall blooms in the Western Basin of Lake

Erie. Collectively, these results, which can be applied to other watersheds, improve our understanding of the factors influencing aquatic microbial community assembly and provide new perspectives on how to better understand the occurrence of cHABs in Lake Erie and elsewhere.

KEYWORDS

aquatic microbiome, cyanobacteria, Lake Erie watershed, harmful algal blooms, genetic connectivity

1. Introduction

Cyanobacterial harmful algal blooms (cHABs) represent a major threat to waterbodies worldwide and are increasing in frequency, magnitude, and duration (Taranu et al., 2015; Huisman et al., 2018; Ho et al., 2019). cHABs are a major concern for lake management because, beside greatly impairing water quality for recreational and fisheries purposes, compromising the safety of drinking water, they can also produce toxins and secondary metabolites (Paerl and Otten, 2013) that may cause fatalities or serious health issues for humans and animals in contact with the contaminated water (Carmichael, 2001; Martínez Hernández et al., 2009; Backer et al., 2013). Therefore, identifying the principal factors that cause and mitigate cHABs is a high priority need for assessing ecosystems current and future health.

Nutrient loads, especially phosphorus (P), have been identified as the main cause of cyanobacterial blooms in most inland waters (Downing et al., 2001; Stumpf et al., 2012; Michalak et al., 2013; Scavia et al., 2014). However, there is increasing evidence that abiotic factors alone do not explain and predict the occurrence of cHABs (Paerl et al., 2016; Woodhouse et al., 2016). Indeed, a decrease in external P loading to impaired waterbodies does not always result in the disappearance of cHABs, and often results in hysteresis with recurrent outbreaks of these blooms (Berthold and Campbell, 2021). Intense eutrophication often results in a regime shift and legacy of nutrient-rich sediments, which can act as an internal source and continue to fuel blooms despite efforts to reduce external loading (Matisoff et al., 2016). Nutrient stoichiometry (e.g., N:P) can also plays a role in bloom size, composition and toxin content, and low N:P ratios in eutrophic lakes have been associated with increased toxin concentration in blooms (Zastepa et al., 2017). While the idea of dual nutrient management is gaining traction (Paerl et al., 2016), a recent provocative claim that P-only management will lead to more toxin production (Hellweger et al., 2022), has been challenged for not taking into account *in situ* lake processes and responses of phytoplankton communities (Huisman et al., 2022; Stow et al., 2022).

Lake Erie has experienced multiple cHAB events during the last few decades and still suffers from human impact despite the implementation of remediation action plans (Watson et al., 2016). Severe eutrophication of Lake Erie dates back to the 1950s, and the lake experienced major lake-wide blooms in the 1960s and 1970s (Allinger and Reavie, 2013). These were dominated by eukaryotic algae (notably diatoms, chlorophytes, and dinoflagellates) together with N-fixing (*Aphanizomenon* and *Dolichospermum*) and non N-fixing cyanobacteria (notably *Planktothrix*, *Microcystis*, and *Pseudanabaena*; Munawar et al., 2008; Allinger and Reavie, 2013). High external point-source inputs of P were identified as the primary cause of these events, and in 1972, a binational effort was established under the Canada-USA Great Lakes Water Quality Agreement (GLWQA), which successfully reduced loading to meet phosphorus reduction targets and resulted in a significant decline in Lake Erie blooms (Scavia et al., 2014). However, since the mid 1990's, there has been a significant increase in diffuse loading - notably of highly bioavailable forms of P and N. Furthermore, lake-wide colonization by dreissenid mussels has, despite increasing water transparency, radically altered the nearshore-offshore nutrient exchange by excreting and enhancing P input directly around the substrate they colonized (Watson et al., 2016). These factors have been linked with a resurgence of blooms, and shift in dominance toward toxin-producing cHABs – notably, species of non-diazotrophic *Microcystis* and *Planktothrix* (Davis et al., 2014; Harke et al., 2016; Davenport et al., 2019), and diazotrophs such as *Dolichospermum* (Michalak et al., 2013). However, modeling and forecasting still lead to substantial uncertainties related to cHABS extent and variability in Lake Erie (Obenour et al., 2014), which suggests that the functioning of the ecosystem as a whole is not well understood and that an integrated approach is needed to understand how the lake ecosystem will respond to future changes.

The 'lake as a microcosm' (Forbes, 1887) is a fundamental concept in limnology, which contributes to our understanding of in-lake biological and physico-chemical interactions. However, this is an overly simplistic representation of lakes (and many other waterbodies), which are in fact integrated within watersheds and are thus influenced by large-scale processes such as climate perturbations (Adrian et al., 2009), hydrology (Martin and Soranno, 2006), and land-use allocation (Walsh et al., 2003). The connection between the lake and watershed processes means that management action on land and/or in tributaries will have repercussions on the downstream lake ecosystem. For example, nutrient loads from Lake Erie's watershed directly and indirectly impact in-lake nutrient concentrations (Maccoux et al., 2016), that have the potential to support cHABs (Guo et al., 2021). However, the role(s) of microbial communities in mediating drainage inputs - and how they affect downstream events of cHAB - are poorly understood. Therefore, there is a need to assess the spatio-temporal variability of the aquatic microbial communities (i.e., aquatic microbiome) within the Lake Erie watershed in order to better understand the biological and ecological contexts underlying cHAB occurrences. Additionally, the role of the co-occurring microbes is often overlooked when studying cHABs (Mou et al., 2013; Pound et al., 2021), despite their key involvement in carbon and nutrient cycling (Falkowski et al., 2008), and in bloom and toxin degradation (Shao et al., 2014; Dziga et al., 2019; Salter et al., 2021).

In this study, we took an integrated approach and used high-throughput sequencing of the 16S rRNA gene to characterize spatio-temporal variation of the aquatic microbiome in Lake Erie and its connectivity with watershed components from the upstream Huron-Erie corridor, focusing on the Canadian side. We also examined the structure of the cyanobacterial community to gain insight on the

factors influencing the development of cHABs. Watershed integration involved sampling the Thames River, Lake St. Clair, Detroit River, and Lake Erie, which altogether represent a more than 500 km long hydrological continuum spanning a strong environmental gradient, reflecting land use. The Thames River transports elevated concentrations of nutrients, draining 6,000 km^2 of agricultural land in southwestern Ontario (Leach, 1980). Amongst Canadian tributaries to Lake St. Clair and Lake Erie, the Thames has the highest discharge and is the largest contributor of P (Maccoux et al., 2016; Kao et al., 2022). With this framework, we aim to uncover the spatial and environmental factors shaping the microbial community within Lake Erie watershed, and assess the role of selection or dispersion and passive transport of cells from upstream to downstream. We hypothesized that, despite the extended geographic distance and gradient in environmental variables, upstream watershed input can be an important source of recruitment for Lake Erie's microbial and cyanobacterial communities.

2. Methods

2.1. Study sites and physicochemical variables

A total of 285 water samples (93 in the Upper Thames River, 47 in the Lower Thames, 70 in Lake St. Clair, 14 in the Detroit River, and 61 in Lake Erie) were collected between January 2016 and October 2019 (sampling frequency detailed in Supplementary Table S1). Samples were taken repeatedly at the same sites over the years and seasons encompassing different systems defined as the Upper and Lower Thames River, Lake St. Clair, Detroit River, and the Western, Central and Eastern basins of Lake Erie (Figure 1). Surface samples were collected in triplicate using a Niskin bottle in a rosette configuration for Lake Erie, a Van Dorn bottle for Lake St. Clair and the Detroit River, and from the shore or from a bridge with a pole holding sterile bottles for the Thames River. All samples were kept in a cooler on ice and filtered within 24 h on board the Canadian Coast Guard Ship (CCGS) *Limnos* for Lake Erie and in the lab for the other systems. Temperature (Temp), specific conductivity (Cond), pH, and dissolved oxygen (DO) were measured at each site with a SBE 25plus Sealogger (Seabird) on board the CCGS Limnos, and with a Quatro Pro (YSI Inc.) in Lake St. Clair, Detroit and Thames Rivers. Water samples for total phosphorus (TP), total dissolved phosphorus (TDP), total nitrogen (TN), total dissolved nitrogen (TDN), and particulate organic carbon (POC), were submitted to Environment and Climate Change Canada's National Laboratory for Analytical Testing (NLET, Burlington, Ontario) and prepared following their Standard Operating Procedures for filtration and preservation. Chlorophyll a (chl*a*) concentrations were determined spectrophotometrically after extraction in acetone following the NLET method (NLET, 1997; Table 1).

Estimates of mean daily discharge from 2016 to 2019 were calculated from data available from the Water Survey of Canada[1] for the Thames River and from the U.S. National Water Information System[2] for the Maumee, Sandusky, St. Clair, and Detroit Rivers.

1 https://wateroffice.ec.gc.ca/

2 https://waterdata.usgs.gov/nwis

2.2. DNA sampling and amplicon sequencing processing

From 250 to 300 ml of water for DNA extraction was filtered in triplicate through 0.2 µm Polyethersulfone filters (Fisher Scientific) and stored at −80°C until further processing. All genomic procedures were carried out following a standard approach for genomic research conducted by the government of Canada (Edge et al., 2020). DNA was extracted using the Qiagen DNAEasy PowerSoil DNA isolation kits following instructions from the manufacturer. The V4–V5 hypervariable regions of the 16S rRNA gene were amplified with primers 515F (GTGCCAGCMGCCGCGGTAA) and 926R (CCGYCAATTYMTTTRAGTTT). Libraries were prepared in the Energy, Mining and Environment Biotechnology Research Center of the National Research Council of Canada (Montreal, Quebec). All triplicate samples were sequenced on an Illumina MiSeq platform at the National Research Council (Saskatoon, Saskatchewan). The 16S rRNA gene sequences were analyzed in R Core Team (2018) following the dada2 pipeline (Callahan et al., 2016), using the high-performance computing environment of Shared Services Canada in Dorval, Quebec (Edge et al., 2020). First, non-biological sequences of the primers were removed with cutadapt (Martin, 2012). Then, for each sequencing plate, raw read quality profiles were assessed and the low-quality bases at the end of the read were trimmed with a truncQ score of 11, as suggested for large datasets. Sequences with a maximum expected error (maxEE) greater than 2 were removed and high-quality sequences were merged in an amplicon sequence variant (ASV) table. Chimeras were removed with the 'removeBimeraDenovo' command and taxonomy was assigned with the Silva database version 128 released in 2016 (Yilmaz et al., 2014). Additionally, a Barcode of Life Data System (BOLD) reference database that was developed using sequences of cyanobacterial and algal cultures, was used to classify sequences belonging to the Cyanobacteria phylum (Ivanova et al., 2019). Sequences corresponding to Archaea, Chloroplasts, and Eukaryotes were removed from the ASV table and identical sequences that only varied in length were collapsed with the 'collapseNoMismatch' command in dada2. The ASV table was rarefied a hundred times at 10,000 reads per sample with the 'rarefy_even_depth' command available in the package phyloseq version 1.36.0 (McMurdie and Holmes, 2013), and the average read counts of the 100 tables was used for downstream analyses. This process discarded 383 ASVs out of 68,230 and 50 samples, which when taking into account the number of samples that were collected and sequenced in triplicate, represented a loss of only 9 biological samples.

2.3. Statistical analyses

Dispersion plots for visualizing variation across systems, seasons, and years were generated with the 'betadisper' function available in the R package vegan version 2.6.2 (Oksanen et al., 2019). Non metric multidimensional scaling (NMDS) was generated using the command 'metaMDS' available in the R package vegan (Oksanen et al., 2019) and based on Bray-Curtis distances on the squared-root ASV table. To examine how environmental variables correlated with the community ordination, we selected the environmental variables measured in all systems (i.e., Cond, pH, temperature, TP, TDP, TN, TDN, POC, and chl*a*) based on the following: a matrix of Spearman correlations among all environmental variables was calculated and those with high correlation ($\rho > 0.8$ and $p < 0.01$) with more than one other variable were

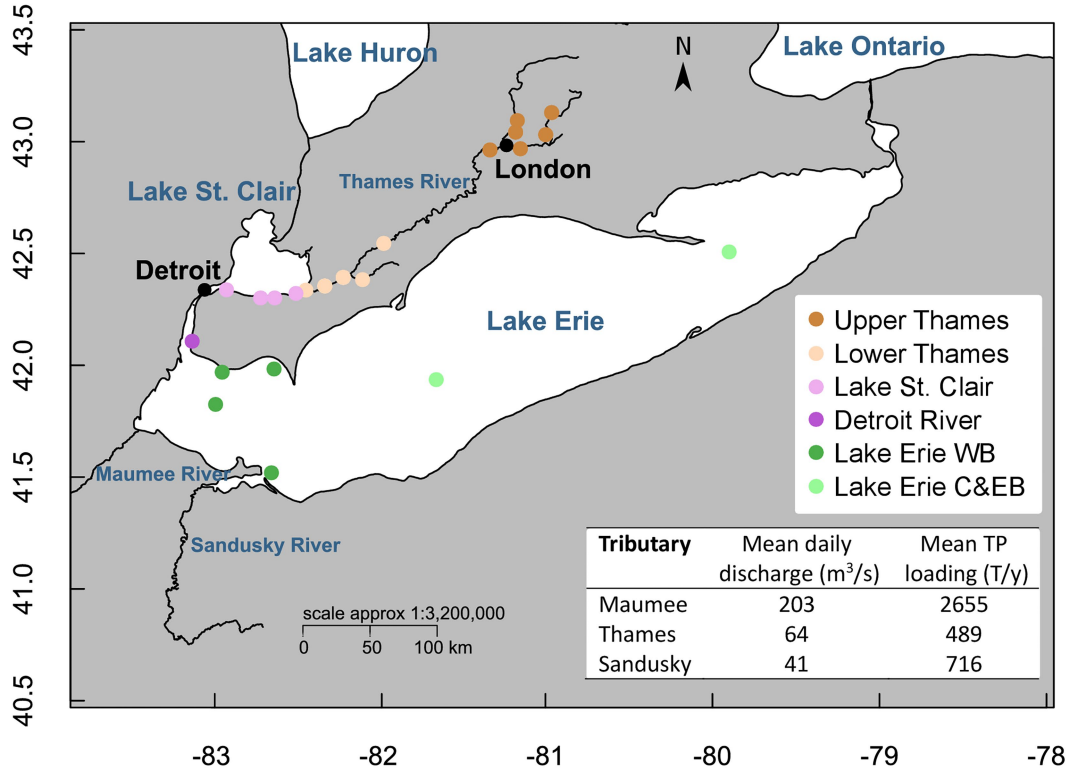

FIGURE 1
Location of the sampling sites colored by systems (Upper and Lower Thames Rivers, Lake St. Clair, Detroit River and Lake Erie). Map created with R using the open-access databases "worldHires" (https://www.evl.uic.edu/pape/data/WDB/) and river line downloaded from the Government of Canada Open Data Portal (http://open.canada.ca/en/open-data) and the National Weather service (https://www.weather.gov/gis/Rivers). Estimates of mean daily discharge from 2016 to 2019 were calculated from data available from the Water Survey of Canada (https://wateroffice.ec.gc.ca/) for the Thames River and from the U.S. National Water Information System (https://waterdata.usgs.gov/nwis) for the Maumee and Sandusky Rivers. Estimates of mean TP loads from 2016 to 2019 were calculated from the data available from ErieStat (https://www.blueaccounting.org/).

removed. Hence, TDP and TN were removed for downstream analyses. The remaining environmental variables were projected onto the NMDS ordination using envfit function available in package vegan (Oksanen et al., 2019). Significant differences in microbial community composition as a function of the system sampled or the season were tested with PERMANOVA (Adonis function in package vegan) with 999 permutations.

Mantel correlations were used to assess correlations between geographic distances and structure of the microbial and cyanobacterial communities. Community matrices were first Hellinger transformed with the decostand command in vegan and then detrended (Borcard et al., 2018). Distances between each sampling site coordinate were calculated with the 'pointDistance' function available in R package raster version 3.6.3 (Hijmans, 2020) while accounting for the flow direction (from the most upstream to the most downstream site). Additionally, a variation partitioning analysis was employed to disentangle the proportion of variation observed in the microbial community that was due solely to environmental variables or spatial variability. This analysis was performed using the 'varpart' function and by transforming geographic coordinates into principal coordinates of neighbor matrices (PCNM) with the 'pcnm' function (both are available in the R package vegan; Oksanen et al., 2019). PCNM allows for the detection of any type of spatial patterns and is not restricted to linear ones (Borcard and Legendre, 2002). For this analysis, only environmental variables that were measured in all systems were used (Cond, pH, temperature, TP, TDP, and TDN), and samples containing missing data were removed (Table 1). All environmental variables and PCNMs were selected with the forward.sel function in the adespatial version 0.3.19 package (Dray et al., 2018) prior to being included in the variation partitioning analysis. Consequently, the analysis was performed on 231 samples (85 from the Upper Thames, 40 from the Lower Thames, 38 from Lake St. Clair, 12 from Detroit River, and 56 from Lake Erie).

Stacked bar plots of the microbial and cyanobacterial community composition, merged as a function of the system to improve plot clarity, were drawn with ggplot2 version 3.3.6 (Wickham, 2016). Sparse Correlations for Compositional data (SparCC) at the phylum level between the relative abundance of cyanobacterial and the most abundant bacterial groups, were produced with the sparcc command in the package SpiecEasi version 1.1.2 (Kurtz et al., 2022). Shared taxa across seasons and systems were represented with and upset plot from the UpSetR package version 1.4.0 (Gehlenborg, 2019).

A phylogenetic analysis of the 15 most abundant cyanobacterial ASVs was performed with sequences from the BOLD database (Ivanova et al., 2019) and from GenBank release 239 (Benson et al., 2018). Two Escherichia coli 16S sequences were used as outgroup (accession number HG917881 and HF584705). Sequences were first aligned with MUSCLE algorithm available in the software mega11. The best molecular model was tested with mega and a consensus neighbor-joining tree was then built, based on 1,000 trees, with associated bootstrap values using the best fit model Kimura 2 with gamma parameter.

TABLE 1 Average (SD in brackets) of the environmental variables for each ecosystem and across seasons: pH, temperature (Temp), dissolved oxygen (DO), conductivity (Cond), total phosphorus (TP), total dissolved phosphorus (TDP), total nitrogen (TN), total dissolved nitrogen (TDN), chlorophyll a (Chla).

System	Season	pH	Temp (°C)	DO (mgL^{-1})	Chla (μgL^{-1})	Cond (μScm^{-1})	TP (μgL^{-1})	TDP (μgL^{-1})	TN (mgL^{-1})	TDN (mgL^{-1})
Upper Thames	Winter	8.2 (0.2)	2.9 (1.8)	-	1.9 (1.1)	479 (168)	151 (144)	112 (103)	-	9 (1.8)
	Spring	8.2 (0.2)	12.3 (7.3)	-	18.7 (7.8)	593 (115)	93 (38)	51 (30)	7.9 (1)	7.4 (1.7)
	Summer	8.3 (0.3)	21.2 (2.7)	-	11.6 (20.9)	707 (113)	90 (60)	49 (32)	4.9 (2.2)	5.5 (2.5)
	Fall	8.3 (0.3)	15.2 (2.5)	-	100.1 (203)	679 (137)	159 (136)	41 (27)	5.3 (1.2)	4.5 (1.6)
Lower Thames	Winter	8.2 (0.1)	2.5 (1.9)	-	1.1 (0)	576 (86)	188 (99)	88 (26)	-	7.9 (0.8)
	Spring	8.2 (0.3)	15.1 (6.7)	-	48.7 (41.7)	589 (110)	242 (174)	66 (50)	7.4 (0.3)	6.1 (1)
	Summer	8.1 (0.3)	23.3 (2.4)	-	7.6 (7.5)	676 (108)	127 (91)	44 (27)	4.9 (1.2)	4.1 (1.3)
	Fall	8.4 (0.3)	15.9 (3)	-	16.6 (7.8)	696 (61)	103 (36)	32 (17)	3.8 (0.6)	3.4 (0.8)
Lake St. Clair	Winter	⊗	⊗	⊗	⊗	⊗	⊗	⊗	⊗	⊗
	Spring	8.2 (0.3)	19.6 (2.6)	9.9 (–)	15.3 (18.4)	356 (157)	57 (65)	23 (37)	2.7 (2.6)	2.6 (2.5)
	Summer	8.5 (0.4)	23.2 (2.6)	7 (1.1)	10.5 (8.5)	326 (156)	40 (26)	10 (14)	1.3 (1.4)	1.1 (1.3)
	Fall	7.9 (0.5)	17.2 (3.7)	3.8 (0.9)	6 (8.1)	288 (89)	71 (88)	28 (43)	0.7 (0.4)	0.5 (0.3)
Detroit River	Winter	⊗	⊗	⊗	⊗	⊗	⊗	⊗	⊗	⊗
	Spring	8.1 (–)	17.6 (–)	10 (–)	1.4 (–)	194 (–)	11 (–)	2 (–)	0.6 (–)	0.6 (–)
	Summer	8.6 (0.5)	22.3 (2.2)	8.2 (1.5)	1.9 (1.5)	217 (16)	14 (2)	4 (2)	0.6 (0.1)	0.5 (0.1)
	Fall	8.3 (0.2)	18 (0.8)	5.5 (–)	1.5 (0)	201 (2)	18 (12)	6 (5)	0.4 (–)	0.4 (–)
Lake Erie WB	Winter	-	-	-	-	-	-	-	-	-
	Spring	8.2 (0.1)	11.8 (5)	10.4 (1.1)	2.3 (1)	260 (26)	24 (23)	8 (9)	1.3 (0.6)	0.8 (0.7)
	Summer	8.6 (0.3)	23.6 (1.5)	8.1 (0.9)	6.1 (6.1)	231 (26)	18 (9)	6 (9)	0.5 (0.1)	0.4 (0.1)
	Fall	8.4 (0.3)	19.9 (1.1)	8.2 (1.2)	5.2 (3.3)	228 (19)	19 (10)	6 (4)	0.4 (0.1)	0.3 (0.1)
Lake Erie C&EB	Winter	8.2 (–)	-1 (–)	-	1 (–)	215 (–)	15 (–)	10 (–)	0.4 (–)	0.4 (–)
	Spring	8.3 (0.2)	6.7 (1.6)	-	2.9 (3.4)	284 (15)	13 (6)	5 (2)	0.4 (0.1)	0.3 (0.1)
	Summer	8.6 (0.1)	23 (1.4)	-	1.9 (1.7)	272 (5)	7 (2)	3 (0.6)	0.4 (0.1)	0.3 (0.1)
	Fall	8 (0.1)	18.9 (0.6)	-	6.2 (4.3)	274 (5)	19 (13)	6 (4)	0.4 (0)	0.3 (0)

Absence of value is either because the data was not measured for the sample (–) or because the sample was not taken (⊗).

Generalized additive models (GAMs) were used to assess the relationship between the proportion (from 0 to 1) of cyanobacterial genera relative abundance (arcsine and squared-root transformed) and the following environmental variables: temperature, pH, log-transformed TP, TDP, TN, TDN, and the ratio between TN and TP. GAMs have the advantage of mixing linear model terms with a smoothed and flexible model term and are therefore best suited for non-linear relationships because they can fit non-linear models to data (Hastie and Tibshirani, 1990). GAMs where constructed in R using the gam function in the mgcv version 1.8.36 package (Wood, 2011) and drawn with ggplot2.

3. Results

3.1. Physico-chemical parameters

The pH level tended to be highest during the summer in Lake St. Clair and Lake Erie (Table 1), and reached a maximum value of 10 in the Western Basin during the summer of 2017. Temperature and DO were more variable across seasons than systems, and temperature was, on average, the highest in Lake Erie surface water during the summer. There was a gradient of decreasing Cond and nutrient concentrations along the water continuum. In particular, the Thames River had higher average TP compared to the rest of the sampled systems, especially in winter for the Upper Thames and in spring for the Lower Thames (Table 1). The highest TP concentration was measured in January 2018 at the most upstream site of the Thames River, reaching 519 μgL^{-1}. TP decreased downstream in Lake St. Clair and averaged below 25 μgL^{-1} in Lake Erie, even in the Western Basin, which experiences annual cyanobacterial blooms and normally corresponds to a mesotrophic state. However, a brief peak of 79.3 μgL^{-1} TP was measured during spring 2017 in the Western Erie Basin. In fact, the average TP concentration in the Western Basin was only marginally higher than observed in the two other basins during the sampling period. A similar trend was observed for TDP, where concentrations were on average higher in the Thames River than in the rest of the aquatic continuum. No TN data were collected in the Thames River from 2016 to 2018, so reported values are only based on 2019 sampling. This showed a clear gradient of decreasing TN and TDN concentrations from the Thames River to Lake St. Clair and Lake Erie, where concentrations were on average one order of magnitude lower than in the Thames River (Table 1).

Chl*a*, which can be used as a proxy for algal biomass, was on average higher in the Thames River and Lake St. Clair during the spring, and decreased in summer and fall in all systems. Maximum levels of chl*a* were found in the Upper Thames River during the fall. In Lake Erie, chl*a*

levels were on average always higher in the Western Basin compared to the Central and Eastern basin.

3.2. Microbial and cyanobacterial community structure and composition

The bio-informatics analysis recovered 67,847 ASVs present in 276 samples (85 in the Upper Thames, 55 in the Lower Thames, 62 in Lake St. Clair, 14 in Detroit River, and 60 in Lake Erie). Since there was a strong overlap among the centroids for the 4 years in dispersion plots (Supplementary Figure S1A), all further analyses were performed using the collated data for the 4 years.

Microbial community composition was significantly different among the different systems (PERMANOVA $R^2 = 0.21$, $p < 0.01$) and presented a longitudinal dissimilarity gradient along the hydrological continuum, as pointed out by two different multivariate ordinations (Figure 2A; Supplementary Figure S1B). Samples from the same system were more similar to each other with dissimilarity increasing from the Upper Thames River to Lake Erie's Western Basin. The Central and Eastern Basins marginally clustered with the rest of the Lake Erie samples (Figure 2A). Cond, pH, Temp, POC, TP, and TDN were significantly correlated with the community spatial structuring ($p < 0.01$ for all variables). Our analyses indicated that the Thames River microbial community was influenced by higher nutrient concentrations, while those of Lake St. Clair and Lake Erie appeared to be mediated by higher pH, Cond, and temperature. Across the whole aquatic continuum, the microbial community showed distinct patterns across seasons (PERMANOVA $R^2 = 0.15$, $p < 0.01$), although there seemed to be more overlapping across season than system, for example, between summer and fall (Figure 2B; Supplementary Figure S1C).

The microbial and cyanobacterial communities showed the same type of spatial patterns, as inferred by the Mantel correlations, which suggested that both were significantly correlated with spatial extent. Both communities showed the highest positive and significant spatial autocorrelation across samples that were less than 7 km apart (Table 2). Spatial autocorrelation stayed positive and mostly significant for samples within a geographic distance of less than 79 km, suggesting that within this distance, communities were more similar to each other than by chance. Beyond this ~79 km radius, the Mantel r became negative, indicating that beyond this distance, communities were more distinct from each other than by chance. Variance partitioning analysis was used to disentangle the influence of spatial vs. environmental variables. Environmental variables that were measured in every system (TDN, Cond, Temp, TDP, pH, TP) and the 12 PCNM axes representing the spatial variation were selected by the forward selection as significant explaining factors ($p < 0.01$ for each variable) for the variation partitioning analysis. This analysis explained 35% of the microbial community composition, and attributed 24% ($p < 0.01$) of the variance in microbial community to the environmental and 23% ($p < 0.01$) to the spatial variables, with a 12% intersection between the two. This indicates that 12% ($p < 0.01$) of the variation was solely due to the measured environmental variable and 11% ($p < 0.01$) solely to the geographic location. Sixty-five percent of the variation was left unexplained.

The following proportions of phyla, genera, and ASVs represent average relative abundances of the 4 years of sampling with the standard deviation in parentheses. The phylum Proteobacteria dominated the Upper Thames River, representing 53% (9%) of the winter microbial community, and then decreasing in relative abundance through the water continuum as observed in each season (Figure 3A). A similar trend was observed for the Bacteriodetes, whereas the Actinobacteria and Cyanobacteria seemed to follow the opposite trend and increased in relative abundance from the Upper Thames River to Lake Erie. Cyanobacteria were further observed to be more abundant during summer and fall than in winter and spring. Here, the different cyanobacterial genera were classified using the BOLD database constructed with species representing a diverse array of cyanobacteria (Ivanova et al., 2019). Taxonomic assignment remained problematic for sequences corresponding to the genera *Anabaena*, *Aphanizomenon*, and *Dolichospermum*, which were then classified as the *Anabaena-Aphanizomenon-Dolichospermum* complex (AAD complex). During winter, the relative abundance of cyanobacteria was very low and only reached 0.3% of the microbial community in Lake Erie (only one winter sample available) and was mostly composed of *Synechococcus* and the AAD complex (60 and 40% of the cyanobacterial community, respectively; Figure 3B), while *Planktothrix* was dominant in the Upper and Lower Thames River (50% and 65% of the cyanobacterial community, respectively). In spring, the relative abundance of cyanobacteria reached a maximum of 1.4% (2%) in the Lower Thames River (Figure 3A), and was mostly composed of a mix between the genera *Planktothrix* and *Synechococcus* along the entire water continuum (Figure 3B). In summer, cyanobacterial relative abundance increased in the whole water continuum, reaching up to 17% (11%) in the Western Basin of Lake Erie (Figure 3A), and was mostly composed of the genera *Synechoccocus* and *Microcystis*, which increased in relative abundance from the Upper Thames River to the Western Basin of Lake Erie. At this season, *Synechoccocus* represented 57% of the cyanobacterial community in Lake St. Clair, 40% in the Detroit River, 50% in the Western Basin of Lake Erie, and 68% in Lake Erie Central and Eastern Basin, while *Microcystis* was the second most abundant genus with 25% of the cyanobacterial community in Lake St. Clair, 39% in the Detroit River, and 23% in Lake Erie Western Basin (Figure 3B). *Microcystis* was poorly represented in the central and eastern basin of Lake Erie, which were mostly dominated by *Synechococcus*. In contrast, *Planktothrix* was the most abundant cyanobacterial genus in the Upper Thames River, reaching 55% of the cyanobacterial community. During the fall, the cyanobacterial community stayed relatively abundant reaching 18% (14%) of the Lake Erie's Western Basin, with *Microcystis* as the dominant cyanobacterial genus (*ca.* 45% of the cyanobacterial community), while *Pseudanabaena* dominated in the Central and Eastern Basins. *Planktothrix* was dominant in Lake St. Clair composing 32% of the cyanobacterial community.

3.3. Microbial connectivity within the watershed

The genetic connectivity was assessed amongst part of the system that were closely connected from upstream and downstream, and because of their poor connection with the rest of the water continuum, notably highlighted by the NMDS analysis (Figure 2A), Lake Erie's Central and Eastern Basins were removed from subsequent analyses.

The highest number of ASVs was found in the Thames River, followed by Lake St. Clair (including the Detroit River) and Lake Erie (Western Basin; Figure 4). In each system, the number of ASVs was the

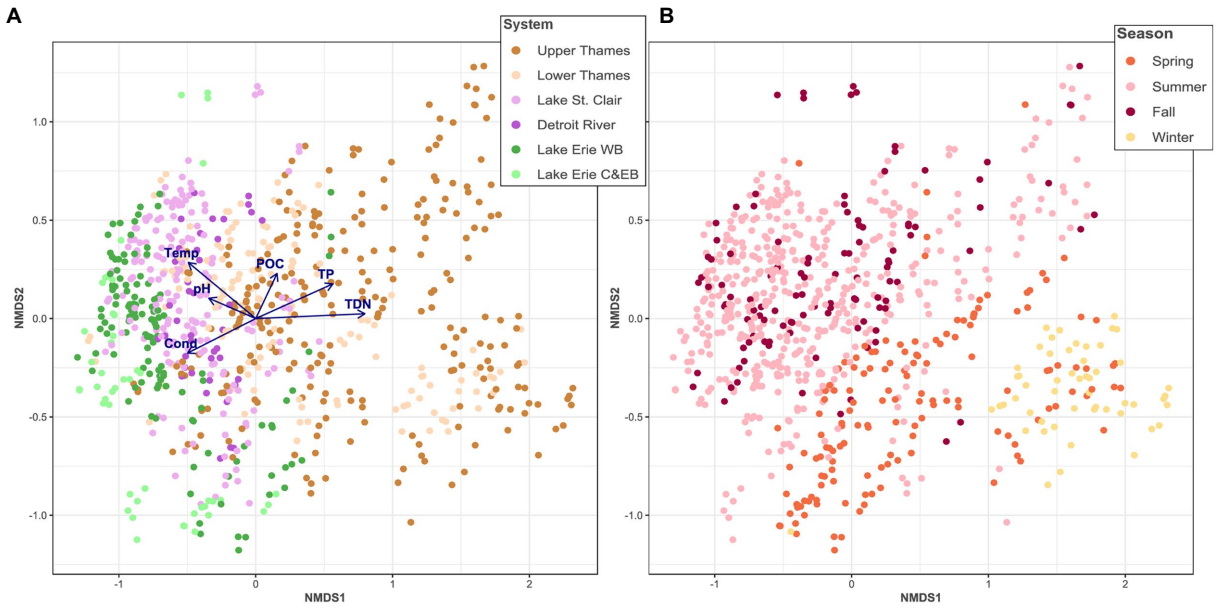

FIGURE 2
Non-metric multidimensional scaling (NMDS) of the microbial community based on Bray-Curtis distance, colored as a function of the system sampled overlaid with the significantly correlated environmental variables **(A)** and colored as a function of the season **(B)**. WB stands for Western Basin and C&EB for Central and Eastern Basin, respectively.

TABLE 2 Mantel *r* value for the whole microbial and cyanobacterial community as a function of the geographic distances with corresponding value of p <0.05 (*), < 0.01 (**) and<0.001 (***).

Distance (km)	Mantel *r*	
	Microbial community	Cyanobacterial community
7	0.13***	0.14***
22	−0.001	−0.002
36	0.02*	0.02**
50	0.05**	0.06**
65	0.03**	0.03**
79	0.007	−0.0002
94	−0.03**	−0.03**
108	−0.08**	−0.09**
123	−0.05**	−0.01

highest during the summer, but overall, few were shared among systems and seasons. The data showed a 'core microbiome' of 287 ASVs shared across all systems and seasons, which represented less than 1% of all the 67,847 ASVs identified. The relative abundance of this 'core microbiome' varied from 10% of the community during the winter in the Upper Thames, to 77% during the spring in the Detroit River, and was composed of the same dominant phyla identified in Figure 3. Amongst those, the proportion of the cyanobacterial phyla in this core was from 0.04% of the microbial community during the winter in both Upper and Lower Thames, to 13% of the community during the fall in the Lower Thames. During spring and summer, the greatest number of ASVs were unique to the Thames River system and not found elsewhere along the water continuum. A smaller number of ASVs seemed to be specific to downstream Lake Erie Western Basin, and this number was the highest during spring (1823). The summer community in Lake Erie's Western Basin had more ASVs in common with the summer community of Lake St. Clair and the Thames River or the fall community of Lake Erie than with the Western Basin of Lake Erie spring community.

The composition of the microbial community in Lake Erie's Western Basin was highly connected to the rest of the watershed in terms of a high proportions of the reads (Figure 5A). A smaller proportion of ASVs (Figure 5B) in Lake Erie's Western Basin were also detected in the upstream systems. The same pattern was observed for the cyanobacterial community (Figures 5C,D). In all seasons, the Thames River contributed the highest proportion of reads in the Western Basin of Lake Erie for both the whole microbial and the cyanobacterial community followed by Lake St. Clair and Lake Erie, while the contribution of the Detroit River was minimal. On the other hand, the greatest proportion of the bacterial and cyanobacterial ASV, at least in spring and fall, were first and only identified in the Lake Erie's Western Basin.

Genetic connectivity within the watershed was further explored for the 15 most abundant cyanobacterial ASVs using a phylogenetic analysis. Those ASVs clustered with the genera *Microcystis*, *Gloeocapsa*, *Planktothrix*, *Aphanizomenon*, *Anathece* and *Synechococcus* (Figure 6A). Three ASVs (# 2, 5, and 10), clustering with representative of the genus *Microcystis*, seemed to dominate in different parts of the aquatic continuum and at different times (Figure 6B), and could generally be detected along the water continuum. During summer, ASV 2 started to become dominant in Lake St. Clair and reached 3.4% (3.8%) of the microbial community, followed by 3.7% (3.2%) in the Detroit River and 2.2% (2.5%) in Lake Erie's Western Basin, it only accounted for less than 0.01% of relative abundance in the Upper Thames River. On the other hand, the other two ASVs clustering with *Microcystis* (ASV 5 and 10) seemed to become more abundant in Lake Erie during the fall, reaching 5% (8.3%) and 1.8% (1.4%) of the microbial community, respectively, but stayed in lower relative abundance in Lake St. Clair. ASV 12 clustered

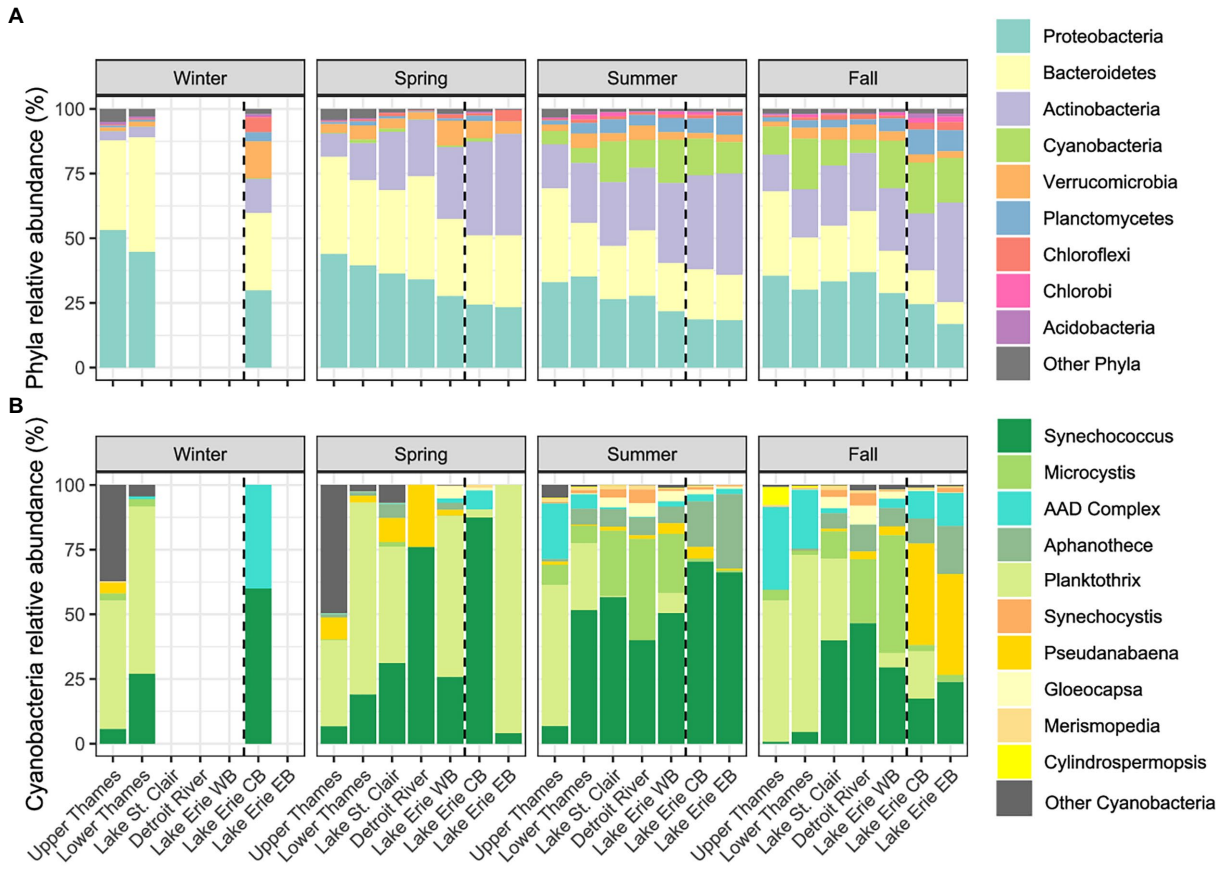

FIGURE 3
Relative abundances of the main microbial phyla expressed as % of the microbial community **(A)** and cyanobacterial genera expressed as % of the cyanobacterial community **(B)** along the water continuum and as a function of the different seasons. The Western Basin (WB) is separated by a dotted line from CB for the Central Basin (CB) and Eastern Basin (EB). Not all systems were sampled during winter (for sampling frequency see Supplementary Table 1).

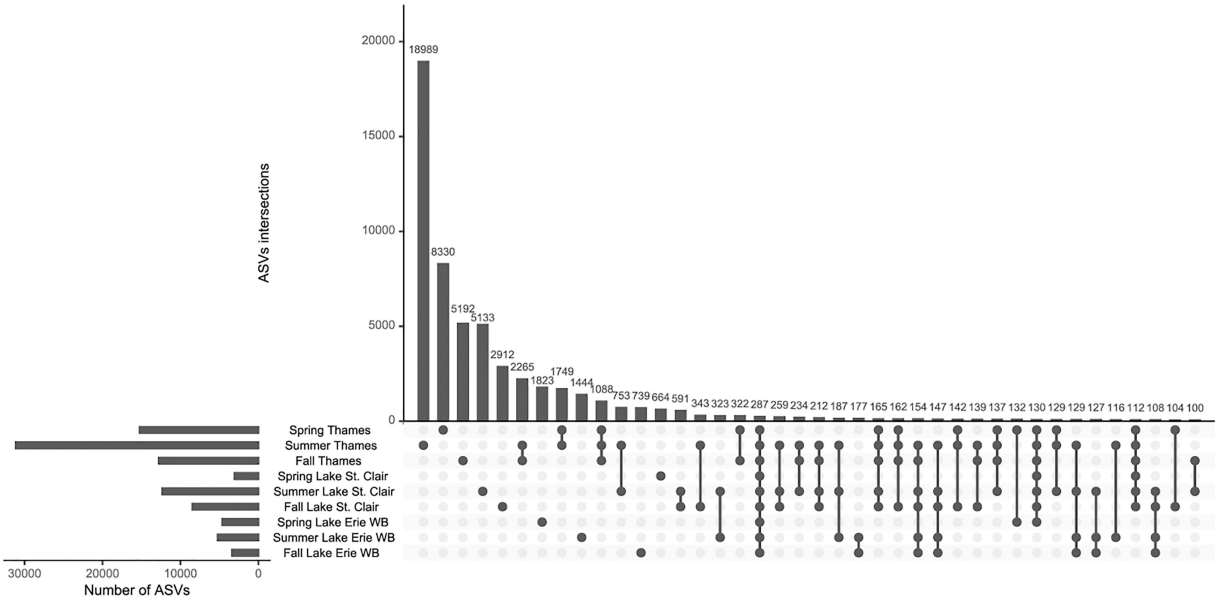

FIGURE 4
Intersection of ASVs across systems and seasons. Horizontal bars indicate the total number of ASVs for each system at each season and vertical bars represent the number of ASVs in the category designated by the dot below. Detroit River samples were lumped with Lake St. Clair samples and winter samples were removed due to lack of system represented. Only intersections of more than 100 ASVs are shown.

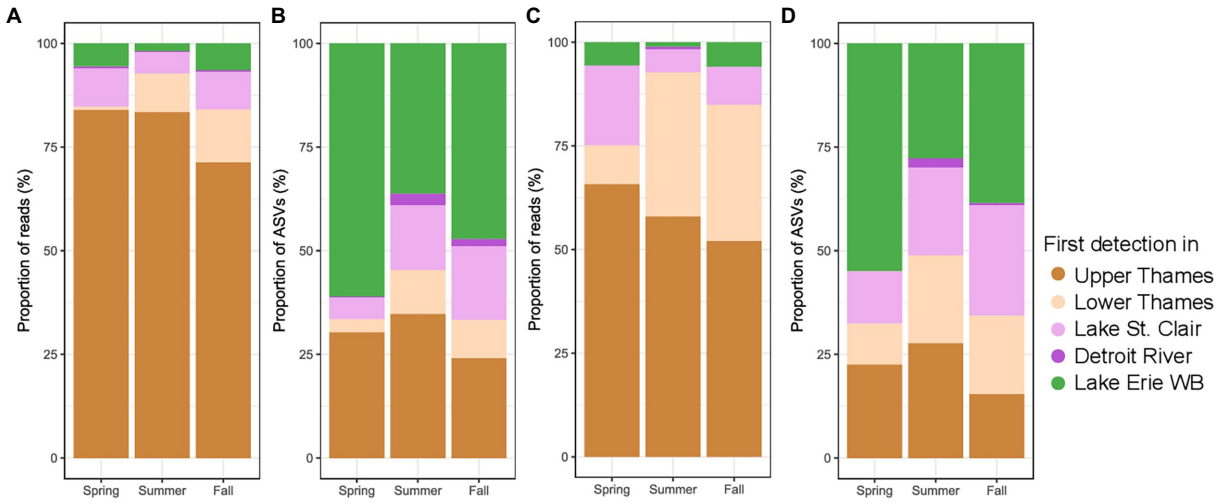

FIGURE 5
Proportion microbial reads **(A)** and ASVs **(B)**, as well as Cyanobacterial reads **(C)** and ASVs **(D)** in the Lake Erie Western basin at different season, classified as a function of the most upstream system they were first detected in (WB stands for Western Basin). Winter samples were removed due to lack of system represented.

with the culture representative[3] identified as *Gloeocapsa*, which peaked in relative abundance in the Western Basin during summer but represented only 0.5% (0.7%) of the microbial community. The next cluster in the phylogenetic tree contained two ASVs of the genus *Planktothrix* (ASV 1 and 3) that both dominated in the Thames River during summer and fall, especially ASV 1 which accounted for 9.9% (10.3%) of the microbial community in the Lower Thames River during fall. ASV 4 clustered closely with the sequence of the culture representative *Aphanizomenon flos-aquae* that was more abundant in the Thames River, reaching 4.4% (7.6%) of relative abundance in the Lower Thames during the fall. This ASV was also present in Lake St. Clair and Erie, although in lower relative abundance. Finally, the last cluster of the phylogenetic tree gathered sequences of 6 different ASVs clustering with the genus *Synechococcus* and two with the genus *Anathece*, both genera belonging to the Order Synechococcales. Those ASVs started to become more abundant in Lake St. Clair, followed by the Detroit River, and Lake Erie during summer and fall, and some were not detectable at all in the Upper Thames River (ASVs 7, 15 and 6).

3.4. Influence of environmental variables on cyanobacterial dynamic

Because of the non-linear nature of the relationships, Generalized Additive Models (GAMs) were used to test those correlations, and, although all the relationships presented here were significant ($p < 0.01$), the explanatory power of the R^2 remained relatively low (from 0.02 to 0.47), and no clear pattern was observed between the set of selected environmental variables and the relative abundance of dominant Cyanobacteria (*Microcystis*, *Synechococcus*, and *Planktothrix*). Compared to *Planktothrix*, both *Microcystis* and *Synechoccocus* genera seemed to peak at lower nutrient (N and P) concentrations which corresponded to concentrations found in Lake Erie in comparison to the Thames River (Supplementary Figure S2). It was noteworthy that across all sites, the relative abundance of both *Microcystis* and *Synechoccocus* tended to decrease as nutrient concentrations increased. Although significant and positively correlated, temperature had an extremely low R^2 for *Microcystis* ($R^2 = 0.02$) compared to *Synechococcus* ($R^2 = 0.3$). No clear relationship was observed between cyanobacterial relative abundance and pH. Finally, the relative abundance of *Microcystis* seemed to peak at a TN/TP mass ratio ≥ 30, which generally corresponds to the multi-annual average TN/TP mass ratio (35) of Lake Erie's Western Basin, while the other systems had higher average TN/TP mass ratio values (Central and Eastern Basin of Lake Erie = 47, Lake St. Clair = 40, Detroit River = 41, Lower Thames = 48, and Upper Thames = 80). However, no clear trend was observed between *Synechoccocus* or *Planktothrix* relative abundances and nutrient mass ratios.

4. Discussion

Here we showed how geographic distance and seasonal variations, as well as environmental variables, are shaping the microbial communities in the Thames River–Lake St. Clair-Lake Erie continuum, and found a high degree of connectivity between upstream and downstream systems, despite the extended geographic distance. We found support for our hypothesis that upstream watershed can be a source of recruitment for Lake Erie's microbial and cyanobacterial communities, though stronger for microbial than cyanobacterial communities, and not excluding other tributaries or sediments as more proximal sources of microbial communities. Overall, our results provide support for the importance of watersheds (and associated land use activities) as a major influence for Lake Erie's communities.

The Thames River–Lake Erie continuum represents a strong gradient of environmental conditions reflecting change in land use and urbanization. Amongst Canadian tributaries to Lake St. Clair and western Lake Erie, the Thames River contributes greatest to P loading consistent with elevated discharge draining a watershed dominated by

3 http://www.boldsystems.org/

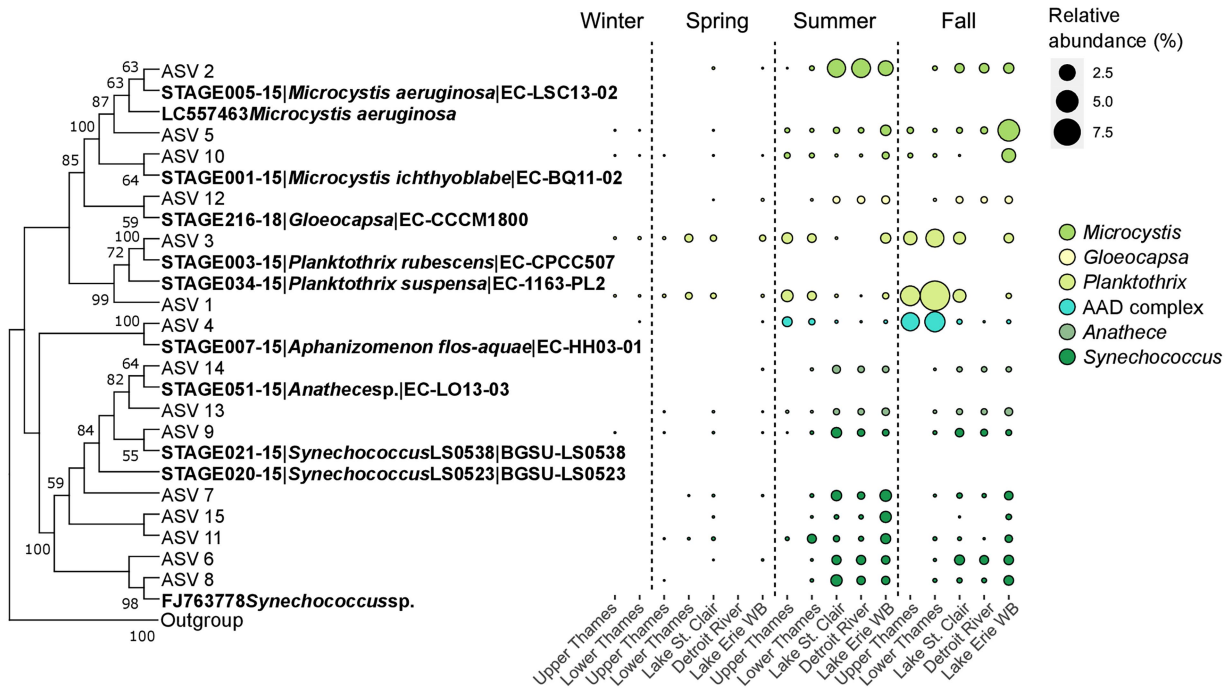

FIGURE 6
Neighbor-joining bootstrapped phylogenetic tree of the 15 most abundant cyanobacterial ASVs with sequences from culture representative of the BOLD reference database and sequences downloaded from GenBank with only bootstrap values above 50% from the 1,000 replicated trees indicated at the nodes of branches **(A)**. Corresponding relative abundance in % of the microbial community of the single ASVs along the water continuum and across season colored based on their genera **(B)**. WB stands for Western Basin.

row crop agriculture (Van Rossum and Norouzi, 2021; Kao et al., 2022). Amongst all tributaries discharging into Lake Erie, the Thames River ranks 3rd behind the Maumee and Sandusky Rivers in contributing TP and SRP to Lake Erie (Maccoux et al., 2016; Figure 1). Although the largest annual hydrological loads to Lake St. Clair come from the St. Clair River (average 2016–2019 discharge of 6,122 m^3/s), which flows directly from Lake Huron, the Thames River has a disproportionate effect on the TP load, to the extent that P reduction in the Thames River basin will be more effective in reducing the P export from Lake St. Clair than from the equivalent in-flow Sydenham or Clinton Rivers (Bocaniov et al., 2019). Lake St. Clair has a water residence time of ~9 days, and due to it shallow depth, is subjected to frequent vertical mixing, yet nutrient loads from its tributaries are not homogeneously mixed and vary seasonally and spatially (Bocaniov et al., 2019). Lake St. Clair has also been shown to be a sink for nutrients retaining up to 20% of the TP load (Bocaniov et al., 2019; Scavia et al., 2019), but altogether with loads from Canada and the US still contributes up to 41% of the annual TP load to Lake Erie's Western Basin *via* the Detroit River (average 2016–2019 discharge of 6,383 m^3/s), which is the second in importance after the Maumee River which contributes up to 48% (Scavia et al., 2016).

4.1. Microbial and cyanobacterial community structure and composition

We observed longitudinal and seasonal changes in the aquatic microbiome within the Lake Erie watershed from the Upper Thames River to Lake St. Clair and Lake Erie. We observed a low relative abundance of cyanobacteria in winter and spring, followed by an increase in their relative abundance during summer and fall which is similar to observations elsewhere when cyanobacterial blooms tend to occur due to higher temperature optima and preference for strong stratification (Paerl and Huisman, 2009). Nevertheless, PERMANOVA analyses suggested that the spatial pattern was more influential than the seasonal pattern on the microbial community structure. While part of the same water continuum, the aquatic systems sampled here represents a gradient of environmental conditions and trophic status, with the Thames River draining nutrients from its predominantly agricultural watershed, which are gradually diluted downstream in Lake St. Clair and Erie. Lake Erie itself represents a longitudinal gradient in trophic status where its Western Basin is mesoeutrophic while the Central and Eastern Basins trend to oligomesotrophic (Dove and Chapra, 2015). The spatial directional pattern observed for the microbial community composition has already been observed in previous meta-community studies on boreal inland waters (Ruiz-Gonzalez et al., 2015), Arctic systems (Crump et al., 2012; Comte et al., 2018), and across the Great Lakes (Rozmarynowycz et al., 2019; Paver et al., 2020). Those studies, together with our findings on the most important tributary on the Canadian side, highlighted the importance of hydrological processes in shaping the microbial community structure in aquatic continuums.

The mantel correlations showed that, for both microbial and cyanobacterial communities, the highest spatial autocorrelation occurred within a radius of 7 km (Table 2). At a wider spatial scale, within a 79 km radius, communities remained more similar than by chance, indicating a certain degree of selection of the microbial community within similar types of system. This radius matches the limit of each system sampled (Upper and Lower Thames, Lake St. Clair, Detroit River and Lake Erie's Western Basin), where the greatest distance between two samples of a similar system was 54 km between the two most distant Lower Thames samples. Beyond 79 km, a distance-decay

pattern started to appear, which indicate dispersal limitation and system filtering as observed in other aquatic ecosystems (Logares et al., 2018). Even within Lake Erie, where despite having the shortest residence time of all the Great Lakes (ca 2.7 years; Quinn, 1992), there was a distinction in the microbial and cyanobacterial community structure between the Western Basin and the rest of the lake, probably driven by the difference in trophic status and hydrology. Collectively, the results indicated that both microbial and cyanobacterial community structures were significantly correlated with the spatial distances and that, beyond a threshold of 79 km which also corresponded to samples within the same system, communities switched from being more similar to more dissimilar than by chance.

Environmental variables including conductivity, temperature, pH, particulate organic matter and nutrients (TP and TDN) have been identified as variables which significantly influenced microbial community structure. Water chemistry parameters often shape aquatic system due to their direct impact on microbial metabolism. Nutrients, and by extension, trophic status, have a prime effect on microbial community structure (Lindström, 2000) and diversity, with higher richness associated with more eutrophic lakes (Kiersztyn et al., 2019), yet richness tends to decrease with N fertilization (Schulhof et al., 2020). As an integrator of landscape properties, pH is often identified as one of the main factors influencing microbial community structure (Lindström et al., 2005; Fierer and Jackson, 2006; Logue and Lindström, 2008; Niño-García et al., 2016). However, variance partitioning analysis of our data indicated that environmental variables *per se* only explained 12% of the variation observed within the microbial community, and this proportion reached 35% when accounting for both environmental and spatial patterns. This relatively low explanatory power is not uncommon when investigating factors that influence aquatic microbiomes (Marmen et al., 2020), and highlights the importance of examining other factors that can play key roles in microbial community assembly, for example, by including a more complete characterization of the hydrological properties of the systems, including the lag time (Lindström et al., 2005; Marmen et al., 2020), and taking into account the biotic interactions with co-occurring microbes or with higher and lower trophic levels (Louca et al., 2016).

The rest of the aquatic microbiome community interacts extensively with cyanobacteria, notably through mutualistic interactions (Eiler and Bertilsson, 2004; Woodhouse et al., 2016; Berg et al., 2018), toxin degradation (Mou et al., 2013), or predation (Rashidan and Bird, 2001); and bloom events may create a disturbance to this microbiome (Berry et al., 2017). The typical dominant freshwater bacterial phyla, i.e., Proteobacteria, Bacteroidetes, Actinobacteria, and Verrucomicrobia, are often found associated with cyanobacterial blooms (Eiler and Bertilsson, 2004; Bagatini et al., 2014; Tromas et al., 2017; Li et al., 2020), while Proteobacteria have been associated with two strains of cultured cyanobacteria (*Microcystis* and *Cylindrospermopsis*; Bagatini et al., 2014). However, in our case, Proteobacteria's relative abundance was weakly and negatively correlated with cyanobacteria's (SparCC $\rho = -0.05$, $p < 0.01$), and Proteobacteria were found in higher relative abundance in the Thames River compared to the downstream systems. Zhu et al. (2019) also noticed a significant negative correlation between the two phyla relative abundances, suggesting a potential competitive interaction. Negative correlations have been observed between cyanobacteria and Actinobacteria's relative abundances (Ghai et al., 2014; Matson et al., 2020), with Actinobacteria occurrence being associated with less eutrophic systems (Haukka et al., 2006), although actinobacterial clades were abundant in eutrophic Lake Taihu (Tang et al., 2017). Yet, some taxa affiliated with the Actinobacteria phylum co-occur with cyanobacterial blooms (Woodhouse et al., 2016) or having the relative abundance of certain clade strongly correlated, either positively or negatively, to bloom occurrence (Berry et al., 2017). In our case, Actinobacteria's relative abundance was positively correlated with cyanobacteria's (SparCC $\rho = 0.4$, $p < 0.01$) and were found in higher relative abundances in the downstream Lakes St. Clair and Erie. Some taxa belonging to the Verrucomicrobia have been shown to display a higher diversity in the presence of cyanobacteria (Parveen et al., 2013) and are known to degrade algal polysaccharides and organic matter (Bagatini et al., 2014; Woodhouse et al., 2016). However, in our dataset, there was no significant relationship between relative abundances of Verrucomicrobia and Cyanobacteria. Bacteroidetes have also been shown to increase in absolute and relative abundance during or after a cyanobacterial bloom, especially the Sphingobacteria and Flavobacteria classes (Newton et al., 2011; Bagatini et al., 2014). However, we observed a weak but negative correlation between Bacteroidetes and Cyanobacteria's relative abundances (SparCC $\rho = -0.07$, $p < 0.01$), which suggests that other factors not investigated in this study are important. In contrast, the relative abundance of Planctomycetes and Cyanobacteria were positively correlated (SparCC $\rho = 0.5$, $p < 0.01$), consistent with other reported associations between Planctomycetes and phytoplankton blooms (Eiler and Bertilsson, 2004). Because of their involvement in nutrient cycling, the aquatic microbiome is likely to play a crucial role in bloom occurrence and duration, and it has already been highlighted that the rest of the aquatic microbiome could be a better predictor of cHAB events than environmental factors (Tromas et al., 2017). More studies are needed to explore those interactions in further detail, notably by including eukaryotic microbes, and unveiling the mechanisms underlying these interactions.

Microscopy and molecular tools have been found to identify the same predominant taxa of cyanobacteria, with the exception of pico-cyanobacteria which are underestimated by microscopy (MacKeigan et al., 2022). Here, molecular tools allowed detection of *Synechococcus* as one of the dominant genera of cyanobacteria in Lake Erie's watershed, along with *Microcystis*, *Planktothrix*, and *Aphanizomenon*, which were already identified in Lake Erie using microscopy (Millie et al., 2009; Chaffin et al., 2011; Allinger and Reavie, 2013; Davis et al., 2015). Other studies based on meta-barcoding results also identified *Microcystis*, *Planktothrix*, *Synechococcus*, *Aphanizomenon*, and *Dolichospermum* as dominant genera of cyanobacteria in river mouths (Sandusky and Maumee) and in the Western and Central Basins of Lake Erie (Berry et al., 2017; Salk et al., 2018; Jankowiak et al., 2019; Rozmarynowycz et al., 2019; Matson et al., 2020). *Synechoccocus* and *Microcystis* were found to co-occur as dominant genera in Lake St. Clair, Detroit River, and Lake Erie (Figure 3B), and this co-occurrence was already observed in Lake Erie (Berry et al., 2017; Rozmarynowycz et al., 2019) and in Lake Taihu (Ye et al., 2011). *Synechococcus* also initiated the 2014 cyanobacterial bloom in the Western Basin of Lake Erie and stayed abundant until the end of the bloom (Berry et al., 2017). In the Thames River, sequences corresponding to the genera *Planktothrix* and *Aphanizomenon* were found in high relative abundances (Figure 6B). To date, very few blooms have been reported in the Thames River, although there is increasing evidence that the river experiences recurrent blooms (Crevecoeur, Molina and Watson, pers. communication, Supplementary Figure S3). A bloom reported in the lower portion of the river around Chatham and identified by microscopy was dominated by *Aphanizomenon flos aquae* and *Planktothrix agardhii* (McKay et al., 2020), which is consistent at the genus level with what we found in our genomic data from 2016 to 2019. However, our data also suggest the

presence of ASVs clustering with *Planktothrix rubescens* and *P. suspensa* (Figure 6A). As a comparison, *Plantkothrix* has also been reported as abundant on the US side of Lake Erie, specifically in the Sandusky Bay (Davis et al., 2015; Salk et al., 2018; Jankowiak et al., 2019). These observations suggest that *Microcystis* and *Synechococcus* might be well adapted to lake conditions and *Planktothrix* to more turbid river-type conditions. Our data also highlight the existence of complex assemblages of different strains of cyanobacteria that successively dominate the water continuum through space and time. Further investigation is needed to determine if these different strains and ASVs respond in the same way to environment triggers for toxin production.

4.2. Microbial connectivity within the watershed

While the connectivity between Lake Erie and its tributaries has been clearly identified in terms of P loading (Maccoux et al., 2016), the connectivity of the aquatic microbiome and the contribution of riverine Bacteria to the lake microbiome remain uncertain. The Thames River holds a high proportion of microbial taxa that were only identified in the upstream river but not in any of the downstream systems (Figure 4). Lake St. Clair appeared to act as a filter and is also influenced by other sources not taken into account here, such as the upstream Huron corridor. In summer and fall, there were more taxa shared between Lake Erie and the rest of the watershed than between Lake Erie in the spring. This highlights the seasonal succession and change in aquatic microbial community.

Within a watershed, the most commonly observed patterns of microbial community assembly are mass effect, i.e., massive advection of numerically dominant microbes by passive transport, and species sorting (Lindström and Bergström, 2004; Zhao et al., 2021). In our case, the majority of microbial reads found in the Western Basin of Lake Erie were likewise identified from the Thames River (Figure 5). This observation allows to unveil the impact of dispersal within the watershed in general, but this does not rule out other sources, notably amongst other more proximal tributaries, or with higher discharge, and/or the sediment, as ASVs can be shared across multiple watersheds (Urycki et al., 2022). Other studies have classified reads and ASVs as a function of the system in which they were first detected (Crump et al., 2012; Ruiz-Gonzalez et al., 2015; Matson et al., 2020), and our data clearly indicated that mass effect played an important role in the downstream microbial community assemblage. This phenomenon is prevalent when dispersion is high due to elevated levels of connectivity between the upstream river community and the downstream lake (Adams et al., 2014; Ruiz-Gonzalez et al., 2015). However, in lake systems, where water flow generally decreases and residence time increases, species sorting occurs (Zhao et al., 2021). Indeed, our data showed that certain cyanobacterial ASVs, mainly ASVs 2, 5 and 10, clustering with *Microcystis* isolates, were found in low relative abundance in the Upper Thames River, but became dominant in the Western Basin of Lake Erie (Figure 6), suggesting the lake conditions were selecting these cyanobacterial ASVs to become dominant. This genetic connectivity between upstream and downstream has already been highlighted for microcystin producers such as *Microcystis*, *Planktothrix*, and *Anabaena* in Lake Erie, Lake St. Clair, and Lake Ontario based on the *mcyA* gene responsible for microcystin production (Davis et al., 2014). Our data suggest that this connectivity extends beyond the Great Lakes to the upstream tributaries, and also across different seasons. As to whether Lake Erie *Microcystis*-dominated harmful blooms are seeded from the river, based on our data it seems unlikely that the Thames River is the sole source for those *Microcystis* ASVs given the extremely low relative abundance in which they were recovered. Additional sources likely contribute to the rapid development of summer and fall blooms in the Western Basin of Lake Erie, for example, recruitment from the sediment (Kitchens et al., 2018), or other tributaries (Maumee, Sandusky, and St. Clair Rivers), which still need to be investigated as both evidences supporting (Bridgeman et al., 2012) or refuting (Kutovaya et al., 2012) riverine seeding from the Maumee River have been documented.

4.3. Influence of environmental and spatial patterns

In our study, no clear pattern was observed between cyanobacteria relative abundance and nutrient concentrations, although our results suggested that *Planktothrix* relative abundance peaked at higher N and P concentrations than *Microcystis* and *Synechococcus* (Supplementary Figure S2). *Planktothrix* also dominated in an experiment with nutrients (N, P) addition while, under the same conditions, *Microcystis* decreased in relative abundance (Jankowiak et al., 2019). A similar observation was made by Harke et al. (2016) based on shipboard incubations of samples collected from a bloom site on Lake Erie's Western Basin. These authors found that *Microcystis* abundance significantly decreased with P enrichment, while *Planktothrix* and *Dolichospermum* (formerly *Anabaena*) dominated samples collected from the high P environment near the mouth of the Maumee River. On the other hand, *Planktothrix* dominance has also been observed in the Sandusky river plume, where it's capacity to accumulate N through cyanophycin compounds provided a competitive advantage under N limiting conditions (Hampel et al., 2019).

Microcystis seems to be more efficient at scavenging P, giving it an advantage to dominate at lower nutrient concentrations (Gobler et al., 2016; Harke et al., 2016), but it is also more adapted to stable water conditions because of its ability to regulate its buoyancy (Dokulil and Teubner, 2000). In contrast, *Synechococcus* is generally dominant in oligotrophic lakes (Ruber et al., 2016). It has been argued that the ability of some cyanobacteria to fix N provides a competitive edge in eutrophic systems with low N:P ratios (Smith, 1983), however this tenet has been debated (Downing et al., 2001). Our data showed generally negative correlations between N concentrations and the relative abundance of some non-diazotroph genera like *Microcystis* and *Synechococcus*, which showed higher relative abundances at lower N:P ratios (Supplementary Figure S2). These genera could be complemented by the presence of diazotrophic cyanobacteria and Proteobacteria (Davis et al., 2015; Li et al., 2020). Therefore, the presence, for instance, of N2-fixing *Aphanizomenon* and *Cylindrospermopsis* along the water continuum, could play a role in promoting the growth of *Microcystis* and *Synechococcus*. More investigations are needed to address those questions but molecular tools have the potential to provide more insight into the role of the entire microbiome, often overlooked in early studies.

Increasing temperature and longer warmer periods likely to happen due to climate change will also have an effect on cHABS, because a more stable thermocline and reduction in epilimnion mixing can lead to better light competition outcomes for cyanobacteria due to their ability to adjust their buoyancy. For instance, when nutrient concentrations are high enough to sustain bloom formation, climatic variables may become

crucial for predicting bloom onset and duration, as was observed by Zhang et al. (2012), who found that increasing temperature, hours of sunshine, and reduction of wind speed in Lake Taihu lead to earlier onset and longer bloom duration. However, Taihu is a subtropical lake, and because Lake Erie has a temperate climate, the variables influencing its microbiome might be very different. Since our study was conducted across different seasons, we were likely to identify an effect of temperature. The relationship was positive and significant for *Microcystis*, *Synechoccocus*, and *Plantkothrix*, but the R^2 of the GAMs were very low for *Microcystis* and *Planktothrix* (0.02 and 0.11, respectively); hence it is difficult to draw conclusions regarding the link between cyanobacteria relative abundance and temperature. However, climate projections predict that Lake Erie will have longer and more stable periods of stratification, which are likely to lead to increasing frequency and worsening impact of cHABs (Paerl and Huisman, 2008).

5. Conclusion

Here we used an integrated approach at the watershed scale to better understand the biological and ecological context shaping Lake Erie's microbiome, with a special focus on the cyanobacterial community given Lake Erie's long history of harmful algal blooms. This study showed how spatial and temporal variations, as well as environmental variables, are shaping the microbial communities in the Thames River–Lake St. Clair-Lake Erie continuum. In terms of community composition, gradual changes along the water continuum were observed for the whole microbial community. On a finer taxonomical level, distinct communities of cyanobacteria developed in the Thames River, mostly dominated by *Planktothrix*, compared to Lake St. Clair and Lake Erie, which were dominated by *Microcystis* and *Synechococcus*, notably during the summer. The high proportion of microbial reads shared between the Thames River and the Western Basin of Lake Erie suggested a high degree of connectivity and dispersal within the watershed in general, which probably extend to other tributaries, and where mass effect seemed to be an important driver of microbial community assembly. Nevertheless, distance-decay patterns of the Mantel correlations indicated some selection pressure within similar systems as it was notably observed for some cyanobacterial ASVs related to *Microcystis*. Despite being found in low relative abundance in the upstream river, *Microcystis* ASVs were selected by the conditions in the Western basin of Lake Erie, where they became progressively dominant. Genetic characterization of the community also showed that the dominant genera of cyanobacteria in Lake Erie watershed (*Microcystis*, *Synechococcus*, *Planktothrix*) were in fact composed of an assemblage of different ASVs becoming dominant at different times. These data further suggested that the two most abundant cyanobacterial genera in Lake St. Clair and Lake Erie, *Microcystis* and *Synechococcus*, stayed relatively abundant even at lower N and P concentrations than *Planktothrix*, which dominated in the higher nutrient regimes of the Thames River. Overall, there was still a large proportion of the variation observed in the microbial community structure that was not explained by spatial and environmental factors, demonstrating the importance of unexplored drivers of microbial and cyanobacterial community structure such as biotic interactions and hydrodynamics. The high connectivity and level of dispersion between the upstream, riverine and Lake Erie microbial and cyanobacterial communities highlight the need for watershed scale management to improve the water quality conditions in Lake St. Clair and the Western Basin of Lake Erie.

6. Data availability statement

The datasets presented in this study can be found in online repositories. The names of the repository/repositories and accession number(s) can be found at: https://www.ncbi.nlm.nih.gov/genbank/, PRJNA877648.

Author contributions

SC, TE, SW, and JC designed study. SC, TE, LW, JC, ND, AD, KD, TF, RM, AZ, and JC collected data. SC and JC analyzed sequencing data, performed statistical analyses, and conceived of the manuscript. SC, TE, LW, SW, CG, and JC supervised the project and performed research. SC took the lead in writing the manuscript with help in editing and correcting from all the other authors. All authors contributed to the article and approved the submitted version.

Funding

This study was funded under the Canada's Genomics Research and Development Initiative (GRDI) & Great Lake Protection Initiative (GLPI), and also supported by grants from the Natural Sciences and Engineering Research Council of Canada (NSERC) (RGPIN-2019-03943; RGPIN-2020-06874), the Great Lakes Center for Fresh Waters and Human Health supported by NIEHS (1P01ES02328939–01), and NSF (OCE-1840715).

Acknowledgments

We would like to thank Sean Backus, Marianne Racine, Anqi Liang, Maria Molina, Carly Charon, and Julianne Radford for their invaluable help in the field and laboratory, Sylvie Sanschagrin for preparing all the DNA libraries, and Tracie Greenberg for assistance with acquiring hydrological data. We also thank the Editor and two reviewers for their constructive comments on the manuscript.

Conflict of interest

The authors declare that the research was conducted in the absence of any commercial or financial relationships that could be construed as a potential conflict of interest.

Publisher's note

Supplementary material

The Supplementary material for this article can be found online at: https://www.frontiersin.org/articles/10.3389/fmicb.2023.1073753/full#supplementary-material

References

Adams, H. E., Crump, B. C., and Kling, G. W. (2014). Metacommunity dynamics of bacteria in an arctic lake: the impact of species sorting and mass effects on bacterial production and biogeography. *Front. Microbiol.* 5:82. doi: 10.3389/fmicb.2014.00082

Adrian, R., O'Reilly, C. M., Zagarese, H., Baines, S. B., Hessen, D. O., Keller, W., et al. (2009). Lakes as sentinels of climate change. *Limnol. Oceanogr.* 54, 2283–2297. doi: 10.4319/lo.2009.54.6_part_2.2283

Allinger, L. E., and Reavie, E. D. (2013). The ecological history of Lake Erie as recorded by the phytoplankton community. *J. Great Lakes Res.* 39, 365–382. doi: 10.1016/j.jglr.2013.06.014

Backer, L. C., Landsberg, J. H., Miller, M., Keel, K., and Taylor, T. K. (2013). Canine cyanotoxin poisonings in the United States (1920s-2012): review of suspected and confirmed cases from three data sources. *Toxins* 5, 1597–1628. doi: 10.3390/toxins5091597

Bagatini, I. L., Eiler, A., Bertilsson, S., Klaveness, D., Tessarolli, L. P., and Vieira, A. A. H. (2014). Host-specificity and dynamics in bacterial communities associated with bloom-forming freshwater phytoplankton. *PLoS One* 9:e85950. doi: 10.1371/journal.pone.0085950

Benson, D. A., Cavanaugh, M., Clark, K., Karsch-Mizrachi, I., Ostell, J., Pruitt, K. D., et al. (2018). GenBank. *Nucleic Acids Res.* 46, D41–D47. doi: 10.1093/nar/gkx1094

Berg, C., Dupont, C. L., Asplund-Samuelsson, J., Celepli, N. A., Eiler, A., Allen, A. E., et al. (2018). Dissection of microbial community functions during a cyanobacterial bloom in the Baltic Sea via metatranscriptomics. *Front. Mar. Sci.* 5:55. doi: 10.3389/fmars.2018.00055

Berry, M. A., Davis, T. W., Cory, R. M., Duhaime, M. B., Johengen, T. H., Kling, G. W., et al. (2017). Cyanobacterial harmful algal blooms are a biological disturbance to Western Lake Erie bacterial communities. *Environ. Microbiol.* 19, 1149–1162. doi: 10.1111/1462-2920.13640

Berthold, M., and Campbell, D. A. (2021). Restoration, conservation and phytoplankton hysteresis. *Conserv. Physiol.* 9:coab062. doi: 10.1093/conphys/coab062

Bocaniov, S. A., Van Cappellen, P., and Scavia, D. (2019). On the role of a large shallow lake (Lake St. Clair, USA-Canada) in modulating phosphorus loads to Lake Erie. *Water Resour. Res.* 55, 10548–10564. doi: 10.1029/2019wr025019

Borcard, D., Gillet, F., and Legendre, P. (2018). "Spatial analysis of ecological data" in *In Numerical Ecology with R* (Springer), 299–367.

Borcard, D., and Legendre, P. (2002). All-scale spatial analysis of ecological data by means of principal coordinates of neighbour matrices. *Ecol. Model.* 153, 51–68. doi: 10.1016/S0304-3800(01)00501-4

Bridgeman, T. B., Chaffin, J. D., Kane, D. D., Conroy, J. D., Panek, S. E., and Armenio, P. M. (2012). From river to lake: phosphorus partitioning and algal community compositional changes in Western Lake Erie. *J. Great Lakes Res.* 38, 90–97. doi: 10.1016/j.jglr.2011.09.010

Callahan, B. J., McMurdie, P. J., Rosen, M. J., Han, A. W., Johnson, A. J., and Holmes, S. P. (2016). DADA2: high-resolution sample inference from Illumina amplicon data. *Nat. Methods* 13, 581–583. doi: 10.1038/nmeth.3869

Carmichael, W. W. (2001). Health effects of toxin-producing cyanobacteria: "the CyanoHABs". *Hum. Ecol. Risk. Assess.* 7, 1393–1407. doi: 10.1080/20018091095087

Chaffin, J. D., Bridgeman, T. B., Heckathorn, S. A., and Mishra, S. (2011). Assessment of *Microcystis* growth rate potential and nutrient status across a trophic gradient in western Lake Erie. *J. Great Lakes Res.* 37, 92–100. doi: 10.1016/j.jglr.2010.11.016

Comte, J., Culley, A. I., Lovejoy, C., and Vincent, W. F. (2018). Microbial connectivity and sorting in a high Arctic watershed. *ISME J.* 12, 2988–3000. doi: 10.1038/s41396-018-0236-4

Crump, B. C., Amaral-Zettler, L. A., and Kling, G. W. (2012). Microbial diversity in arctic freshwaters is structured by inoculation of microbes from soils. *ISME J.* 6, 1629–1639. doi: 10.1038/ismej.2012.9

Davenport, E. J., Neudeck, M. J., Matson, P. G., Bullerjahn, G. S., Davis, T. W., Wilhelm, S. W., et al. (2019). Metatranscriptomic analyses of diel metabolic functions during a Microcystis bloom in Western Lake Erie (United States). *Front. Microbiol.* 10:2081. doi: 10.3389/fmicb.2019.02081

Davis, T. W., Bullerjahn, G. S., Tuttle, T., McKay, R. M., and Watson, S. B. (2015). Effects of increasing nitrogen and phosphorus concentrations on phytoplankton community growth and toxicity during *Planktothrix* blooms in Sandusky Bay, Lake Erie. *Environ. Sci. Technol.* 49, 7197–7207. doi: 10.1021/acs.est.5b00799

Davis, T. W., Watson, S. B., Rozmarynowycz, M. J., Ciborowski, J. J., McKay, R. M., and Bullerjahn, G. S. (2014). Phylogenies of microcystin-producing cyanobacteria in the lower Laurentian Great Lakes suggest extensive genetic connectivity. *PLoS One* 9:e106093. doi: 10.1371/journal.pone.0106093

Dokulil, M. T., and Teubner, K. (2000). Cyanobacterial dominance in lakes. *Hydrobiologia* 438, 1–12. doi: 10.1023/A:1004155810302

Dove, A., and Chapra, S. C. (2015). Long-term trends of nutrients and trophic response variables for the Great Lakes. *Limnol. Oceanogr.* 60, 696–721. doi: 10.1002/lno.10055

Downing, J. A., Watson, S. B., and McCauley, E. (2001). Predicting cyanobacteria dominance in lakes. *Can. J. Fish. Aquat. Sci.* 58, 1905–1908. doi: 10.1139/f01-143

Dray, S., Blanchet, G., Borcard, D., Guenard, G., Jombart, T., Larocque, G., et al. (2018). *adespatial: Multivariate Multiscale Spatial Analysis*. R package version 0.3-8.

Dziga, D., Kokocinski, M., Barylski, J., Nowicki, G., Maksylewicz, A., Antosiak, A., et al. (2019). Correlation between specific groups of heterotrophic bacteria and microcystin biodegradation in freshwater bodies of Central Europe. *FEMS Microbiol. Ecol.* 95:fiz162. doi: 10.1093/femsec/fiz162

Edge, T. A., Baird, D. J., Bilodeau, G., Gagné, N., Greer, C., Konkin, D., et al. (2020). The Ecobiomics project: advancing metagenomics assessment of soil health and freshwater quality in Canada. *Sci. Total Environ.* 710:135906. doi: 10.1016/j.scitotenv.2019.135906

Eiler, A., and Bertilsson, S. (2004). Composition of freshwater bacterial communities associated with cyanobacterial blooms in four Swedish lakes. *Environ. Microbiol.* 6, 1228–1243. doi: 10.1111/j.1462-2920.2004.00657.x

Falkowski, P. G., Fenchel, T., and Delong, E. F. (2008). The microbial engines that drive earth's biogeochemical cycles. *Science* 320, 1034–1039. doi: 10.1126/science.1153213

Fierer, N., and Jackson, R. B. (2006). The diversity and biogeography of soil bacterial communities. *Proc. Natl. Acad. Sci. U. S. A.* 103, 626–631. doi: 10.1073/pnas.0507535103

Forbes, S. A. (1887). "The Lake as a microcosm" in *Bulletin of the Peoria Scientific Association*. ed. Edward Hine & Co. (Peoria, IL: the association), 77–87.

Gehlenborg, N. (2019). *UpSetR: A More Scalable Alternative to Venn and Euler Diagrams for Visualizing Intersecting Sets.* R package version 1.4.0.

Ghai, R., Mizuno, C. M., Picazo, A., Camacho, A., and Rodriguez-Valera, F. (2014). Key roles for freshwater actinobacteria revealed by deep metagenomic sequencing. *Mol. Ecol.* 23, 6073–6090. doi: 10.1111/mec.12985

Gobler, C. J., Burkholder, J. M., Davis, T. W., Harke, M. J., Johengen, T., Stow, C. A., et al. (2016). The dual role of nitrogen supply in controlling the growth and toxicity of cyanobacterial blooms. *Harmful Algae* 54, 87–97. doi: 10.1016/j.hal.2016.01.010

Guo, T., Johnson, L. T., LaBarge, G. A., Penn, C. J., Stumpf, R. P., Baker, D. B., et al. (2021). Less agricultural phosphorus applied in 2019 led to less dissolved phosphorus transported to Lake Erie. *Environ. Sci. Technol.* 55, 283–291. doi: 10.1021/acs.est.0c03495

Hampel, J. J., McCarthy, M. J., Neudeck, M., Bullerjahn, G. S., McKay, R. M. L., and Newell, S. E. (2019). Ammonium recycling supports toxic *Planktothrix* blooms in Sandusky Bay, Lake Erie: evidence from stable isotope and metatranscriptome data. *Harmful Algae* 81, 42–52. doi: 10.1016/j.hal.2018.11.011

Harke, M. J., Davis, T. W., Watson, S. B., and Gobler, C. J. (2016). Nutrient-controlled niche differentiation of Western Lake Erie cyanobacterial populations revealed via metatranscriptomic surveys. *Environ. Sci. Technol.* 50, 604–615. doi: 10.1021/acs.est.5b03931

Hastie, T. J., and Tibshirani, R. J. (1990). *Generalized Additive Models*. Boca Raton, FL: CRC press.

Haukka, K., Kolmonen, E., Hyder, R., Hietala, J., Vakkilainen, K., Kairesalo, T., et al. (2006). Effect of nutrient loading on bacterioplankton community composition in lake mesocosms. *Microb. Ecol.* 51, 137–146. doi: 10.1007/s00248-005-0049-7

Hellweger, F. L., Martin, R. M., Eigemann, F., Smith, D. J., Dick, G. J., and Wilhelm, S. W. (2022). Models predict planned phosphorus load reduction will make Lake Erie more toxic. *Science* 376, 1001–1005. doi: 10.1126/science.abm6791

Hijmans, R. J. (2020). *Raster: Geographic data analysis and Modeling*. R package version 3.5-15.

Ho, J. C., Michalak, A. M., and Pahlevan, N. (2019). Widespread global increase in intense lake phytoplankton blooms since the 1980s. *Nature* 574, 667–670. doi: 10.1038/s41586-019-1648-7

Huisman, J., Codd, G. A., Paerl, H. W., Ibelings, B. W., Verspagen, J. M. H., and Visser, P. M. (2018). Cyanobacterial blooms. *Nat. Rev. Microbiol.* 16, 471–483. doi: 10.1038/s41579-018-0040-1

Huisman, J., Dittmann, E., Fastner, J., Schuurmans, J. M., Scott, J. T., Van de Waal, D. B., et al. (2022). Comment on "models predict planned phosphorus load reduction will make Lake Erie more toxic". *Science* 378:eadd9959. doi: 10.1126/science.add9959

Ivanova, N. V., Watson, L. C., Comte, J., Bessonov, K., Abrahamyan, A., Davis, T. W., et al. (2019). Rapid assessment of phytoplankton assemblages using next generation sequencing – barcode of life database: a widely applicable toolkit to monitor biodiversity and harmful algal blooms (HABs). bioRxiv, 873034. doi: 10.1101/2019.12.11.873034.

Jankowiak, J., Hattenrath-Lehmann, T., Kramer, B. J., Ladds, M., and Gobler, C. J. (2019). Deciphering the effects of nitrogen, phosphorus, and temperature on cyanobacterial bloom intensification, diversity, and toxicity in western Lake Erie. *Limno. Oceanogr.* 64, 1347–1370. doi: 10.1002/lno.11120

Kao, N., Mohamed, M., Sorichetti, R. J., Niederkorn, A., Van Cappellen, P., and Parsons, C. T. (2022). Phosphorus retention and transformation in a dammed reservoir of the Thames River, Ontario: impacts on phosphorus load and speciation. *J. Great Lakes Res.* 48, 84–96. doi: 10.1016/j.jglr.2021.11.008

Kiersztyn, B., Chróst, R., Kaliński, T., Siuda, W., Bukowska, A., Kowalczyk, G., et al. (2019). Structural and functional microbial diversity along a eutrophication gradient of interconnected lakes undergoing anthropopressure. *Sci. Rep.* 9:11144. doi: 10.1038/s41598-019-47577-8

Kitchens, C. M., Johengen, T. H., and Davis, T. W. (2018). Establishing spatial and temporal patterns in *Microcystis* sediment seed stock viability and their relationship to

subsequent bloom development in Western Lake Erie. *PLoS One* 13:e0206821. doi: 10.1371/journal.pone.0206821

Kurtz, Z., Mueller, C., Miraldi, E., and Bonneau, R. (2022). *SpiecEasi: Sparse Inverse Covariance for Ecological Statistical Inference.* R Package Version 1.1.2.

Kutovaya, O. A., McKay, R. M. L., Beall, B. F. N., Wilhelm, S. W., Kane, D. D., Chaffin, J. D., et al. (2012). Evidence against fluvial seeding of recurrent toxic blooms of *Microcystis* spp. in Lake Erie's western basin. *Harmful Algae* 15, 71–77. doi: 10.1016/j.hal.2011.11.007

Leach, J. H. (1980). Limnological sampling intensity in Lake St. Clair in relation to distribution of water masses. *J. Great Lakes Res.* 6, 141–145. doi: 10.1016/S0380-1330(80)72092-0

Li, H., Barber, M., Lu, J., and Goel, R. (2020). Microbial community successions and their dynamic functions during harmful cyanobacterial blooms in a freshwater lake. *Water Res.* 185:116292. doi: 10.1016/j.watres.2020.116292

Lindström, E. S. (2000). Bacterioplankton Community Composition in Five Lakes Differing in Trophic Status and Humic Content. *Microb. Ecol.* 40, 104–113. doi: 10.1007/s002480000036

Lindström, E. S., and Bergström, A.-K. (2004). Influence of inlet bacteria on bacterioplankton assemblage composition in lakes of different hydraulic retention time. *Limnol. Oceanogr.* 49, 125–136. doi: 10.4319/lo.2004.49.1.0125

Lindström, E. S., Kamst-Van Agterveld, M. P., and Zwart, G. (2005). Distribution of typical freshwater bacterial groups is associated with pH, temperature, and lake water retention time. *Appl. Environ. Microbiol.* 71, 8201–8206. doi: 10.1128/aem.71.12.8201-8206.2005

Logares, R., Tesson, S. V. M., Canbäck, B., Pontarp, M., Hedlund, K., and Rengefors, K. (2018). Contrasting prevalence of selection and drift in the community structuring of bacteria and microbial eukaryotes. *Environ. Microbiol.* 20, 2231–2240. doi: 10.1111/1462-2920.14265

Logue, J. B., and Lindström, E. S. (2008). Biogeography of bacterioplankton in inland waters. *Freshw. Rev.* 1:116. doi: 10.1608/FRJ-1.1.9

Louca, S., Parfrey, L. W., and Doebeli, M. (2016). Decoupling function and taxonomy in the global ocean microbiome. *Science* 353, 1272–1277. doi: 10.1126/science.aaf4507

Maccoux, M. J., Dove, A., Backus, S. M., and Dolan, D. M. (2016). Total and soluble reactive phosphorus loadings to Lake Erie: a detailed accounting by year, basin, country, and tributary. *J. Great Lakes Res.* 42, 1151–1165. doi: 10.1016/j.jglr.2016.08.005

MacKeigan, P. W., Garner, R. E., Monchamp, M. È., Walsh, D. A., Onana, V. E., Kraemer, S. A., et al. (2022). Comparing microscopy and DNA metabarcoding techniques for identifying cyanobacteria assemblages across hundreds of lakes. *Harmful Algae* 113:102187. doi: 10.1016/j.hal.2022.102187

Marmen, S., Blank, L., Al-Ashhab, A., Malik, A., Ganzert, L., Lalzar, M., et al. (2020). The role of land use types and water chemical properties in structuring the microbiomes of a connected lake system. *Front. Microbiol.* 11:89. doi: 10.3389/fmicb.2020.00089

Martin, M. (2012). Cutadapt removes adapter sequences from high-throughput sequencing reads. *Bioinformat. Action* 17, 10–12. doi: 10.14806/ej.17.1.200

Martin, S. L., and Soranno, P. A. (2006). Lake landscape position: relationships to hydrologic connectivity and landscape features. *Limnol. Oceanogr.* 51, 801–814. doi: 10.4319/lo.2006.51.2.0801

Martínez Hernández, J., López-Rodas, V., and Costas, E. (2009). Microcystins from tap water could be a risk factor for liver and colorectal cancer: a risk intensified by global change. *Med. Hypotheses* 72, 539–540. doi: 10.1016/j.mehy.2008.11.041

Matisoff, G., Kaltenberg, E. M., Steely, R. L., Hummel, S. K., Seo, J., Gibbons, K. J., et al. (2016). Internal loading of phosphorus in western Lake Erie. *J. Great Lakes Res.* 42, 775–788. doi: 10.1016/j.jglr.2016.04.004

Matson, P. G., Boyer, G. L., Bridgeman, T. B., Bullerjahn, G. S., Kane, D. D., McKay, R. M. L., et al. (2020). Physical drivers facilitating a toxigenic cyanobacterial bloom in a major Great Lakes tributary. *Limnol. Oceanogr.* 65, 2866–2882. doi: 10.1002/lno.11558

McKay, R. M., Frenken, T., Diep, N., Cody, W. R., Crevecoeur, S., Dove, A., et al. (2020). Bloom announcement: an early autumn cyanobacterial bloom co-dominated by *Aphanizomenon flos-aquae* and *Planktothrix agardhii* in an agriculturally-influenced Great Lakes tributary (Thames River, Ontario, Canada). *Data Brief* 30:105585. doi: 10.1016/j.dib.2020.105585

McMurdie, P. J., and Holmes, S. (2013). Phyloseq: an R package for reproducible interactive analysis and graphics of microbiome census data. *PLoS One* 8:e61217. doi: 10.1371/journal.pone.0061217

Michalak, A. M., Anderson, E. J., Beletsky, D., Boland, S., Bosch, N. S., Bridgeman, T. B., et al. (2013). Record-setting algal bloom in Lake Erie caused by agricultural and meteorological trends consistent with expected future conditions. *Proc. Natl. Acad. Sci. U. S. A.* 110, 6448–6452. doi: 10.1073/pnas.1216006110

Millie, D. F., Fahnenstiel, G. L., Bressie, J. D., Pigg, R. J., Rediske, R. R., Klarer, D. M., et al. (2009). Late-summer phytoplankton in western Lake Erie (Laurentian Great Lakes): bloom distributions, toxicity, and environmental influences. *Aquat. Ecol.* 43, 915–934. doi: 10.1007/s10452-009-9238-7

Mou, X., Lu, X., Jacob, J., Sun, S., and Heath, R. (2013). Metagenomic identification of bacterioplankton taxa and pathways involved in microcystin degradation in Lake Erie. *PLoS One* 8:e61890. doi: 10.1371/journal.pone.0061890

Munawar, M., Munawar, I. F., Fitzpatrick, M., Niblock, H., Bowen, K., and Lorimer, J. (2008). *Checking the Pulse of Lake Erie*. East Lansing, MI: Michigan State University Press.

Newton, R. J., Jones, S. E., Eiler, A., McMahon, K. D., and Bertilsson, S. (2011). A guide to the natural history of freshwater lake bacteria. *Microbiol. Mol. Biol. Rev.* 75, 14–49. doi: 10.1128/mmbr.00028-10

Niño-García, J. P., Ruiz-González, C., and del Giorgio, P. A. (2016). Interactions between hydrology and water chemistry shape bacterioplankton biogeography across boreal freshwater networks. *ISME J.* 10, 1755–1766. doi: 10.1038/ismej.2015.226

NLET (National Laboratory for Environmental Testing). (1997). Schedule of Services. Environment and Climate Change Canada, C.C.f.I.W.; NLET (National Laboratory for Environmental Testing): Burlington, ON, Canada.

Obenour, D. R., Gronewold, A. D., Stow, C. A., and Scavia, D. (2014). Using a Bayesian hierarchical model to improve Lake Erie cyanobacteria bloom forecasts. *Water Resour. Res.* 50, 7847–7860. doi: 10.1002/2014WR015616

Oksanen, J., Blanchet, F.G., Friendly, M., Kindt, R., Legendre, P., McGlinn, D., et al. (2019). *Vegan: Community Ecology Package.* R Package Version 2.5-6.

Paerl, H. W., and Huisman, J. (2008). Blooms like it hot. *Science* 320, 57–58. doi: 10.1126/science.1155398

Paerl, H. W., and Huisman, J. (2009). Climate change: a catalyst for global expansion of harmful cyanobacterial blooms. *Environ. Microbiol. Rep.* 1, 27–37. doi: 10.1111/j.1758-2229.2008.00004.x

Paerl, H. W., and Otten, T. G. (2013). Harmful cyanobacterial blooms: causes, consequences, and controls. *Microb. Ecol.* 65, 995–1010. doi: 10.1007/s00248-012-0159-y

Paerl, H. W., Scott, J. T., McCarthy, M. J., Newell, S. E., Gardner, W. S., Havens, K. E., et al. (2016). It takes two to tango: when and where dual nutrient (N & P) reductions are needed to protect lakes and downstream ecosystems. *Environ. Sci. Technol.* 50, 10805–10813. doi: 10.1021/acs.est.6b02575

Parveen, B., Mary, I., Vellet, A., Ravet, V., and Debroas, D. (2013). Temporal dynamics and phylogenetic diversity of free-living and particle-associated Verrucomicrobia communities in relation to environmental variables in a mesotrophic lake. *FEMS Microbiol. Ecol.* 83, 189–201. doi: 10.1111/j.1574-6941.2012.01469.x

Paver, S. F., Newton, R. J., and Coleman, M. L. (2020). Microbial communities of the Laurentian Great Lakes reflect connectivity and local biogeochemistry. *Environ. Microbiol.* 22, 433–446. doi: 10.1111/1462-2920.14862

Pound, H. L., Martin, R. M., Sheik, C. S., Steffen, M. M., Newell, S. E., Dick, G. J., et al. (2021). Environmental ctudies of cyanobacterial harmful algal blooms should include interactions with the dynamic microbiome. *Environ. Sci. Technol.* 55, 12776–12779. doi: 10.1021/acs.est.1c04207

Quinn, F. H. (1992). Hydraulic residence times for the Laurentian Great Lakes. *J. Great Lakes Res.* 18, 22–28. doi: 10.1016/S0380-1330(92)71271-4

R Core Team (2018). *R: A Language and Environment for Statistical Computing*. R Foundation for Statistical Computing, Vienna, Austria.

Rashidan, K. K., and Bird, D. F. (2001). Role of predatory bacteria in the termination of a cyanobacterial bloom. *Microb. Ecol.* 41, 97–105. doi: 10.1007/s002480000074

Rozmarynowycz, M. J., Beall, B. F. N., Bullerjahn, G. S., Small, G. E., Sterner, R. W., Brovold, S. S., et al. (2019). Transitions in microbial communities along a 1600 km freshwater trophic gradient. *J. Great Lakes Res.* 45, 263–276. doi: 10.1016/j.jglr.2019.01.004

Ruber, J., Bauer, F. R., Millard, A. D., Raeder, U., Geist, J., and Zwirglmaier, K. (2016). Synechococcus diversity along a trophic gradient in the Osterseen Lake District, Bavaria. *Microbiology* 162, 2053–2063. doi: 10.1099/mic.0.000389

Ruiz-Gonzalez, C., Nino-Garcia, J. P., and del Giorgio, P. A. (2015). Terrestrial origin of bacterial communities in complex boreal freshwater networks. *Ecol. Lett.* 18, 1198–1206. doi: 10.1111/ele.12499

Salk, K. R., Bullerjahn, G. S., McKay, R. M. L., Chaffin, J. D., and Ostrom, N. E. (2018). Nitrogen cycling in Sandusky Bay, Lake Erie: oscillations between strong and weak export and implications for harmful algal blooms. *Biogeosciences* 15, 2891–2907. doi: 10.5194/bg-15-2891-2018

Salter, C., VanMensel, D., Reid, T., Birbeck, J., Westrick, J., Mundle, S. O. C., et al. (2021). Investigating the microbial dynamics of microcystin-LR degradation in Lake Erie sand. *Chemosphere* 272:129873. doi: 10.1016/j.chemosphere.2021.129873

Scavia, D., Bocaniov, S. A., Dagnew, A., Long, C., and Wang, Y.-C. (2019). St. Clair-Detroit River system: phosphorus mass balance and implications for Lake Erie load reduction, monitoring, and climate change. *J. Great Lakes Res.* 45, 40–49. doi: 10.1016/j.jglr.2018.11.008

Scavia, D., David Allan, J., Arend, K. K., Bartell, S., Beletsky, D., Bosch, N. S., et al. (2014). Assessing and addressing the re-eutrophication of Lake Erie: central basin hypoxia. *J. Great Lakes Res.* 40, 226–246. doi: 10.1016/j.jglr.2014.02.004

Scavia, D., DePinto, J. V., and Bertani, I. (2016). A multi-model approach to evaluating target phosphorus loads for Lake Erie. *J. Great Lakes Res.* 42, 1139–1150. doi: 10.1016/j.jglr.2016.09.007

Schulhof, M. A., Allen, A. E., Allen, E. E., Mladenov, N., McCrow, J. P., Jones, N. T., et al. (2020). Sierra Nevada mountain lake microbial communities are structured by temperature, resources and geographic location. *Mol. Ecol.* 29, 2080–2093. doi: 10.1111/mec.15469

Shao, K., Zhang, L., Wang, Y., Yao, X., Tang, X., Qin, B., et al. (2014). The responses of the taxa composition of particle-attached bacterial community to the decomposition of *Microcystis* blooms. *Sci. Total Environ.* 488-489, 236–242. doi: 10.1016/j.scitotenv.2014.04.101

Smith, V. H. (1983). Low nitrogen to phosphorus ratios favor dominance by blue-green algae in lake phytoplankton. *Science* 221, 669–671. doi: 10.1126/science.221.4611.669

Stow, C. A., Stumpf, R. P., Rowe, M. D., Johnson, L. T., Carrick, H. J., and Yerubandi, R. (2022). Model assumptions limit implications for nitrogen and phosphorus management. *J. Great Lakes Res.* 48, 1735–1737. doi: 10.1016/j.jglr.2022.09.003

Stumpf, R. P., Wynne, T. T., Baker, D. B., and Fahnenstiel, G. L. (2012). Interannual variability of cyanobacterial blooms in Lake Erie. *PLoS One* 7:e42444. doi: 10.1371/journal.pone.0042444

Tang, X., Chao, J., Gong, Y., Wang, Y., Wilhelm, S. W., and Gao, G. (2017). Spatiotemporal dynamics of bacterial community composition in large shallow eutrophic Lake Taihu: high overlap between free-living and particle-attached assemblages. *Limnol. Oceanogr.* 62, 1366–1382. doi: 10.1002/lno.10502

Taranu, Z. E., Gregory-Eaves, I., Leavitt, P. R., Bunting, L., Buchaca, T., Catalan, J., et al. (2015). Acceleration of cyanobacterial dominance in north temperate-subarctic lakes during the Anthropocene. *Ecol. Lett.* 18, 375–384. doi: 10.1111/ele.12420

Tromas, N., Fortin, N., Bedrani, L., Terrat, Y., Cardoso, P., Bird, D., et al. (2017). Characterising and predicting cyanobacterial blooms in an 8-year amplicon sequencing time course. *ISME J.* 11, 1746–1763. doi: 10.1038/ismej.2017.58

Urycki, D. R., Bassiouni, M., Good, S. P., Crump, B. C., and Li, B. (2022). The streamwater microbiome encodes hydrologic data across scales. *Sci. Total Environ.* 849:157911. doi: 10.1016/j.scitotenv.2022.157911

Van Rossum, T., and Norouzi, Y. (2021). Quantifying phosphorous loadings in the Thames River in Canada. *Water Cycle* 2, 44–50. doi: 10.1016/j.watcyc.2021.06.002

Walsh, S. E., Soranno, P. A., and Rutledge, D. T. (2003). Lakes, wetlands, and streams as predictors of land use/cover distribution. *Environ. Manag.* 31, 198–214. doi: 10.1007/s00267-002-2833-1

Watson, S. B., Miller, C., Arhonditsis, G., Boyer, G. L., Carmichael, W., Charlton, M. N., et al. (2016). The re-eutrophication of Lake Erie: harmful algal blooms and hypoxia. *Harmful Algae* 56, 44–66. doi: 10.1016/j.hal.2016.04.010

Wickham, H. (2016). *ggplot2: Elegant Graphics for Data Analysis*. New-York: Springer-Verlag.

Wood, S. N. (2011). Fast stable restricted maximum likelihood and marginal likelihood estimation of semiparametric generalized linear models. J. R. *Stat. Soc. Series B. Stat. Methodol.* 73, 3–36. doi: 10.1111/j.1467-9868.2010.00749.x

Woodhouse, J. N., Kinsela, A. S., Collins, R. N., Bowling, L. C., Honeyman, G. L., Holliday, J. K., et al. (2016). Microbial communities reflect temporal changes in cyanobacterial composition in a shallow ephemeral freshwater lake. *ISME J.* 10, 1337–1351. doi: 10.1038/ismej.2015.218

Ye, W., Tan, J., Liu, X., Lin, S., Pan, J., Li, D., et al. (2011). Temporal variability of cyanobacterial populations in the water and sediment samples of Lake Taihu as determined by DGGE and real-time PCR. *Harmful Algae* 10, 472–479. doi: 10.1016/j.hal.2011.03.002

Yilmaz, P., Parfrey, L. W., Yarza, P., Gerken, J., Pruesse, E., Quast, C., et al. (2014). The SILVA and "all-species living tree project (LTP)" taxonomic frameworks. *Nucl. Acids Res.* 42, D643–D648. doi: 10.1093/nar/gkt1209

Zastepa, A., Watson, S. B., Kling, H., and Kotak, B. (2017). Spatial and temporal patterns in microcystin toxins in Lake of the Woods surface waters. *Lake Reserv. Manag.* 33, 433–443. doi: 10.1080/10402381.2017.1384415

Zhang, M., Duan, H., Shi, X., Yu, Y., and Kong, F. (2012). Contributions of meteorology to the phenology of cyanobacterial blooms: implications for future climate change. *Water Res.* 46, 442–452. doi: 10.1016/j.watres.2011.11.013

Zhao, J., Peng, W., Ding, M., Nie, M., and Huang, G. (2021). Effect of water chemistry, land use patterns, and geographic distances on the spatial distribution of bacterioplankton communities in an anthropogenically disturbed riverine ecosystem. *Front. Microbiol.* 12:633993. doi: 10.3389/fmicb.2021.633993

Zhu, C., Zhang, J., Nawaz, M. Z., Mahboob, S., Al-Ghanim, K. A., Khan, I. A., et al. (2019). Seasonal succession and spatial distribution of bacterial community structure in a eutrophic freshwater Lake, Lake Taihu. *Sci. Total Environ.* 669, 29–40. doi: 10.1016/j.scitotenv.2019.03.087

frontiers | Frontiers in Microbiology

TYPE Original Research
PUBLISHED 14 February 2023
DOI 10.3389/fmicb.2023.1091818

OPEN ACCESS

EDITED BY
Robert Michael McKay,
University of Windsor,
Canada

REVIEWED BY
Lijuan Ren,
Jinan University,
China
Emily Varga,
University of Windsor,
Canada

*CORRESPONDENCE
Linshen Xie
✉ xlins2000@126.com
Lei Sun
✉ sunlei@genemind.com

†These authors share first authorship

SPECIALTY SECTION
This article was submitted to Aquatic Microbiology, a section of the journal Frontiers in Microbiology

RECEIVED 07 November 2022
ACCEPTED 09 January 2023
PUBLISHED 14 February 2023

CITATION
Feng J, Zhou L, Zhao X, Chen J, Li Z, Liu Y, Ou L, Xie Z, Wang M, Yin X, Zhang X, Li Y, Luo M, Zeng L, Yan Q, Xie L and Sun L (2023) Evaluation of environmental factors and microbial community structure in an important drinking-water reservoir across seasons. *Front. Microbiol.* 14:1091818. doi: 10.3389/fmicb.2023.1091818

Evaluation of environmental factors and microbial community structure in an important drinking-water reservoir across seasons

Jie Feng[1†], Letian Zhou[2†], Xiaochao Zhao[2†], Jianyi Chen[1], Zhi Li[1], Yongfeng Liu[2], Lei Ou[1], Zixin Xie[1], Miao Wang[2], Xue Yin[1], Xin Zhang[2], Yan Li[2], Mingjie Luo[2], Lidong Zeng[2], Qin Yan[2], Linshen Xie[1*] and Lei Sun[2*]

[1]State Environmental Protection Key Laboratory of Drinking Water Source Management and Technology, Shenzhen Academy of Environmental Sciences, Shenzhen, China, [2]GeneMind Biosciences Company Limited, Shenzhen, China

The composition of microbial communities varies in water and sediments, and changes in environmental factors have major effects on microbiomes. Here, we characterized variations in microbial communities and physicochemical factors at two sites in a large subtropical drinking water reservoir in southern China. The microbiomes of all sites, including the diversity and abundance of microbial species, were determined *via* metagenomics, and the relationships between microbiomes and physicochemical factors were determined *via* redundancy analysis. The dominant species in sediment and water samples differed; *Dinobryon* sp. LO226KS and *Dinobryon divergens* were dominant in sediment samples, whereas Candidatus *Fonsibacter ubiquis* and *Microcystis elabens* were dominant in water. The diversity was also significantly different in microbial alpha diversity between water and sediment habitats ($p<0.01$). The trophic level index (TLI) was the major factor affecting the microbial community in water samples; *Mycolicibacterium litorale* and *Mycolicibacterium phlei* were significantly positively related to TLI. Furthermore, we also studied the distribution of algal toxin-encoding genes and antibiotic-resistant genes (ARGs) in the reservoir. It found that water samples contained more phycotoxin genes, with the cylindrospermopsin gene cluster most abundant. We found three genera highly related to cylindrospermopsin and explored a new cyanobacteria *Aphanocapsa montana* that may produce cylindrospermopsin based on the correlation through network analysis. The multidrug resistance gene was the most abundant ARG, while the relationship between ARGs and bacteria in sediment samples was more complicated than in water. The results of this study enhance our understanding of the effects of environmental factors on microbiomes. In conclusion, research on the properties, including profiles of algal toxin-encoding genes and ARGs, and microbial communities can aid water quality monitoring and conservation.

KEYWORDS

metagoenomics, trophic level index (TLI), cylindrospermopsins (CYNs), subtropical drinking water source, multidrug resistance genes

1. Introduction

Reservoirs are essential for managing imbalances in the supply and demand for water resources (Wu et al., 2021). In recent decades, the release of pollutants from river tributaries (e.g., sewage discharge) has stimulated the accumulation of nutrients and algal growth, leading to eutrophication and reductions in water quality (Wurtsbaugh et al., 2019). Blooms of algae, such as cyanobacteria, in reservoirs occur frequently, and this poses a threat to the safety of drinking water sources and induces major economic losses (Paerl, 2018). The size, frequency, and duration of harmful algal blooms are increasing, which has been driven in part by human activities, such as habitat degradation and global climate change (Sakamoto et al., 2021). Harmful algal blooms pose considerable threats to water quality and drinking water security because they are difficult to predict; gauging the deleterious effects of the toxins produced by algae during such blooms is also a grand challenge (Park et al., 2021). Harmful algal blooms affect the composition of microbial communities and various aspects of the reservoir environment (Park et al., 2021). Several challenges are associated with studying the ecotoxicology of reservoirs because they are natural sinks for contaminants derived from atmospheric fallout (Wiesner-Friedman et al., 2021). Reservoirs can also provide a favorable environment for the reproduction of microorganisms serving as a bioreactor. Thus, it is important to characterize the composition of microbial communities in reservoirs.

Yantian Reservoir was built in 1976 (22°40′3″N, 114°9′48″E; altitude 83 m). It lies in a medium-sized subtropical basin at the junction of the Shenzhen and Dongguan regions of the South China Basin. The reservoir draws water from the Shima River Basin, a tributary of the Dongjiang River in the tropical and subtropical regions of Guangdong. The reservoir has an area of 25.6 km^2 and a storage capacity of 8.99 million m^3; it provides potable water for residents of the Pearl River Delta (Wang et al., 2019). The reservoir provides drinking water for 1.3 million people and supplies 350,000 m^3 of water per day. It also plays an important role in flood control. Nutrient concentrations in adjacent inflow rivers have increased because of the rapid development of township corporations over the last few decades (Wang et al., 2019). The reservoir's waters are vulnerable to eutrophication and algal blooms, and the aquatic ecosystem is deteriorating into simplified food networks with inferior water quality (Wang et al., 2019). Given this situation, a 10-km^2 restoration project was initiated in 2015 to remove excess nutrients and inhibit algal blooms in the eutrophic bay of the reservoir, which involved stocking fish and increasing areal coverage of submerged vegetation (Wang et al., 2019). Planting submerged hydrophytes and stocking herbivorous, planktivorous, and molluscivorous fish enhanced water quality by stabilizing plankton micro-ecosystems and reducing the content of nutrients. Although ecological restoration measures of this pilot project have been completed, the water quality and composition of microbial communities in this reservoir have not yet been evaluated. Given that Yantian Reservoir is the most important water supply for the urban population in the Pearl River Delta and several ecological restoration projects have been carried out, the water quality and structure of microbial communities of the reservoir require evaluation.

Surface water is the primary source of potable water, and the quality of surface water has considerable human health implications (Long and Luo, 2020). Algal toxins, antibiotic-resistant genes (ARGs), and 2-methylisoborneol pose major health risks (Van Dolah, 2000). The abundance of antibiotic-resistant bacteria (ARB) has increased in recent years because of the widespread use of antibiotics. The ARGs contained in ARB have become recognized environmental pollutants. The uptake of ARGs by pathogens and the development of antibiotic resistance pose threats to human health. Given that the long-term storage of water in reservoirs increases the retention and accumulation of ARGs (Dang et al., 2020), studies of the distribution and diffusion of ARGs in reservoirs are required to control ARG pollution and mitigate health risks.

Diverse types of organisms are essential for maintaining the stability of freshwater ecosystems. Microbial communities are affected by various environmental factors, and the relationships between microbial communities and environmental factors are indicators of the function and structure of aquatic ecosystems (Mucha et al., 2004; Boucher et al., 2006; Pound et al., 2021). However, changes in microbial communities in water sources are complicated by upstream water input and reservoir function (Jiang et al., 2021). For example, microbes can affect the Earth's energy fluxes and diverse biogeochemical cycling pathways in lakes and reservoirs (Sjöstedt et al., 2012; Penn et al., 2014; Savvichev et al., 2018; Bobkov et al., 2021). Next-generation sequencing (NGS), bioinformatics, and functional genomic studies have revealed a high diversity of microorganisms in lakes and reservoirs (Qin et al., 2016). Previous studies have also revealed high similarity in the predominant microorganisms in various water ecosystems; however, the abundances of these microorganisms likely vary with water quality (Jiang et al., 2021). The abundances of dominant species have also been shown to vary with depth and among sampling locations (Chien et al., 2009). Here, we used metagenomic sequencing to assess the variation in the composition of microbial communities in Yantian Reservoir. We also characterized the distribution of algal toxins and ARGs in Yantian Reservoir to provide information that could aid water quality monitoring efforts.

2. Materials and methods

2.1. Collection of water and sediment samples

Water samples were collected weekly from October 2020 to January 2021 in a subtropical drinking water reservoir in southern China (Supplementary Figure S1). Samples were collected from two sites: the center of the reservoir (KZ) and the water intake (QSK). Water samples were collected using 3-L brown glass bottles at a depth of 0.5 m. They were then taken to the laboratory and maintained at 4°C. All samples were filtered *via* a 0.45-μm polycarbonate membrane (Collins, Shanghai, China) prior to chemical analysis. Sediments were sampled following the methods described in a previous study (He et al., 2015), and the sampling frequency was twice a month from October 2020 to December 2020.

2.2. Water physicochemical properties

Measurements were taken on the following parameters: water temperature, pH, dissolved oxygen (DO), transparency, permanganate index (PI), ammonia nitrogen (NH3.N), total nitrogen (TN), total phosphorus (TP), and chlorophyll *a* (Elser et al., 2007). Measurements of water quality parameters were taken following national standard specifications (Water quality—Determination of pH—Electrode method HJ1147-2020, Water quality—Determination of dissolved

oxygen—Electrochemical probe method HJ 506-2009, Seville disc method, Water quality-Determination of permanganate index GB/T 11892-1989, Water quality—Determination of ammonia nitrogen—Salicylic acid spectrophotometry HJ 536-2009, Water quality-Determination of total nitrogen-Alkaline potassium persulfate digestion UV spectrophotometric method HJ 636-2012, Water quality-Determination of total phosphorus-Ammonium molybdate spectrophotometric method GB/T 11893-1989, and Water quality—Determination of chlorophyll *a*—Spectrophotometric method SL88-2012). The tropic level index (TLI) of water samples was calculated using TN, TP, permanganate index, transparency, and chlorophyll *a* indicators and equations from a previous study (Ding et al., 2021). There were five trophic levels in the lake: hypereutrophic (TLI > 70), middle eutrophic (60 < TLI ≤ 70), mesotrophic (30 ≤ TLI ≤ 50), and oligotrophic (TLI < 30).

2.3. DNA extraction and library sequencing

DNA was extracted from membrane filters and frozen sediment samples by the FastDNA® SPIN Kit for Soil (MP Biomedicals, United States) according to the manufacturer's protocols. The NanoDrop One instrument (Thermo Fisher Scientific, United States) was used to determine DNA concentrations and purity. Shotgun metagenomic sequencing of the DNA library was carried out concurrently. In brief, 30 micrograms of DNA was processed to build a library, which was then sequenced using the GeneLab M sequencing platform.

2.4. Bioinformatics analysis

A total of 26 samples were sequenced (Supplementary Table S1) and annotated to a database of freshwater algae in China[1] withmore than 200 freshwater algal genomes to characterize the composition of freshwater algae in Yantian Reservoir. This database was used to identify algal taxa in our samples. Reads that could not be mapped to the freshwater algae genome were aligned to the reference database Kraken2. The Chao1, ACE, Shannon, and Simpson indices (Edwards et al., 2001) were computed using the vegan package in R. Principal component analysis (PCA) was carried out using the FactoMineR package in R. Pearson correlation coefficients were calculated to evaluate correlations among variables. The pheatmap package in R was used to build a correlation heatmap. The vegan, FactoMineR, and pheatmap packages were all implemented in R. Differential abundance analysis was performed using the DESeq2 Bioconductor package (v.1.36.0) in R with default parameters. Significant species were identified using the following criteria: $p < 0.05$ and fold change >2 or <1/2. All samples were integrated into the global network according to the count data. Species that were present in all samples (total number greater than 50,000) were subjected to correlation analyses. Correlations were considered significant using the following criteria: Spearman correlation coefficients ($R > 0.6$) and ($p < 0.01$). Networks were visualized using Cytoscape software. Sequences of the 10 most dominant species with $\log_2$ (fold change) > 1 and $p < 0.05$ were obtained from NCBI. Clean reads were aligned to these genes using Bowtie2 v2.4.5 to confirm their presence in our samples [at least 18 and 34 reads were aligned in sediment samples ($n = 9$) and water samples ($n = 17$), respectively]. Kyoto Encyclopedia of Genes and Genomes (KEGG) analysis of these genes was conducted by aligning them against the KEGG database using DIAMOND software. A diagram of the results of the KEGG pathway analysis was made using the ggplot2 package in R.

2.5. ARG-like and algal toxin gene abundance calculations

The abundance of ARGs was calculated by ARGs-OAP v2.0 (Yin et al., 2018) based on the sequencing reads. For algal toxins, 16 common algal toxin gene clusters were selected (Supplementary Table S2) to calculate the abundance. The heatmap was drawn by standardizing the read counts of the algal toxin gene cluster as log10 (value*1000000 + 0.001).

2.6. Correlation networks

A transboundary symbiosis network consisting of the algal toxin genes or ARG and genus was established to assess species' coexistence in different habitats and regions. We focused on the ones in all samples to reduce rare absolute abundance (SAV) in the data set. Robust correlations with Spearman's correlation coefficients (p) >0.8 or <−0.8 and $p < 0.001$ were used to construct networks, which have been extensively used in the literature and are comparable across studies (Delgado-Baquerizo et al., 2020). The Gephi interactive platform[2] was used to visualize the network.

3. Results

3.1. Physicochemical properties of samples

The physicochemical characteristics of the water samples were determined (Table 1). Temperature and TLI ranged from 17.4 to 26.5°C and from 48.56 to 58.63 in QSK and from 16.8 to 24.8°C and from 48.12 to 51.77 in KZ, respectively. The TLI and temperature were higher in most of the QSK samples than in the KZ samples (e.g., on November 3 and 23). The pH ranged from 7.89 to 8.74 in QSK and from 7.79 to 9.45 in KZ. The difference in pH between QSK and KZ samples was small. Over the study period, TLI and chlorophyll *a* increased (>20), and the Secchi disc depth gradually decreased (<0.5 m). Generally, differences in the physicochemical properties of samples among months were not pronounced. Because Shenzhen features a subtropical to tropical oceanic climate, temperature differences between October 20 and January 21 are not substantial. High temperatures are more conducive to the reproduction of algae and bacteria, which poses major risks to drinking water safety. The TLI values of QSK samples were higher than those of KZ samples at the same sampling times, indicating that algae and bacteria were more abundant in QSK than in KZ.

1 http://www.fwalagedb.com/

2 https://gephi.org

TABLE 1 Value of environmental variables measured in the samples of water.

	Sample name	Temperature of water (°C)	pH	Dissolved oxygen (mg/L)	Permanganate index (mg/L)	Ammonia nitrogen (mg/L)	Total nitrogen (mg/L)	Total phosphorus (mg/L)	Secchi disc depth (M)	Chlorophyl a (μg/L)	TLI	Eutropher
KZ	W_KZ201103	24.80	7.97	7.85	1.40	0.02	1.07	0.06	0.51	31	49.32	Mesotropher
	W_KZ201116	24.30	8.01	7.99	2.60	0.03	1.04	0.07	0.47	12	50.27	Light eutropher
	W_KZ201123	22.50	8.33	8.14	2.10	0.03	1.11	0.05	0.41	28	51.34	Light eutropher
	W_KZ201130	22.90	8.05	8.93	1.30	0.05	1.09	0.07	0.48	22	48.71	Mesotropher
	W_KZ201207	20.10	8.30	9.48	1.80	0.04	1.24	0.07	0.45	24	51.17	Light eutropher
	W_KZ201214	20.00	8.59	9.90	2.20	0.03	1.24	0.04	0.49	32	50.97	Light eutropher
	W_KZ201229	20.80	9.45	11.76	2.30	0.04	1.16	0.04	0.56	14	48.12	Mesotropher
	W_KZ210104	16.80	8.74	11.61	2.60	0.03	1.20	0.05	0.52	28	51.77	light eutropher
QSK	W_QSK201020	26.50	8.74	9.71	3.30	0.02	0.80	0.14	0.35	45	57.63	Light eutropher
	W_QSK201103	25.70	8.00	7.99	1.90	0.01	0.96	0.09	0.45	36	52.60	Light eutropher
	W_QSK201116	24.30	7.89	7.90	3.30	0.02	0.90	0.08	0.47	20	52.88	light eutropher
	W_QSK201123	22.50	8.52	8.23	2.30	0.01	0.94	0.09	0.43	26	52.69	Light eutropher
	W_QSK201130	23.00	8.01	8.82	1.30	0.05	1.11	0.10	0.45	13	48.56	Mesotropher
	W_QSK201207	19.80	8.52	9.58	1.90	0.02	1.18	0.10	0.43	28	52.98	light eutropher
	W_QSK201229	19.10	8.54	9.78	2.20	0.03	1.12	0.05	0.53	14	48.68	Mesotropher
	W_QSK210104	17.40	8.62	10.75	2.70	0.04	1.23	0.05	0.55	16	50.21	Light eutropher
	T-test (*p* value)	0.19	0.70	0.37	0.36	0.18	0.01	0.01	0.26	0.85	0.17	

10.3389/fmicb.2023.1091818

3.2. Microbial community composition and diversity

The microbial communities in sediment and water samples differed (Figure 1A; MRPP: Chance corrected within-group agreement A: 0.4801; observed delta 0.1902 and expected delta 0.3659; significance of delta: 0.001). No differences were observed in samples collected at different times and sampling sites (Figure 1B). Shannon alpha diversity values did not differ among sediment samples from different sites nor water samples from different sites (Figure 1C). The alpha diversity of the sediment samples was significantly higher than that of the water samples ($p < 0.01$, Wilcoxon rank-sum test). No significant differences were observed in the alpha diversity of KZ and QSK in sediment or water samples (Table 2). Pearson correlation coefficients revealed weak correlations between sediment and water samples in alpha diversity; however, intra-group correlations were high (Supplementary Figure S2). Sample origin (water vs. sediment) had a greater effect on microbial alpha diversity than sampling time or the sampling site. This might stem from the stable climate of Shenzhen, which experiences little variation in water temperatures (21.91 ± 2.89; Table 1). Seasonal shifts did not significantly decrease or increase water temperature; seasonal variation thus did not affect microbial alpha diversity. Algae can influence water quality; we thus analyzed algal alpha diversity. The alpha diversity of algae was greater in sediment samples than in water samples (Supplementary Table S3). The diversity of algae was greater in the QSK than in the KZ. We found that TLI was higher in QSK than in KZ. In conclusion, obvious differences in microbial communities were observed between sediment and water samples. Although sampling location and time did not substantially affect algal alpha diversity, the algal alpha diversity of QSK was higher than that of KZ.

3.3. Variation in microbial abundance

The relative abundances of microbes were calculated at the species level (Figure 2). Overall, the composition of microbial communities in sediment and water samples differed significantly. The dominant species in the sediment samples were *Dinobryon* sp_LO226KS, *Dinobryon*

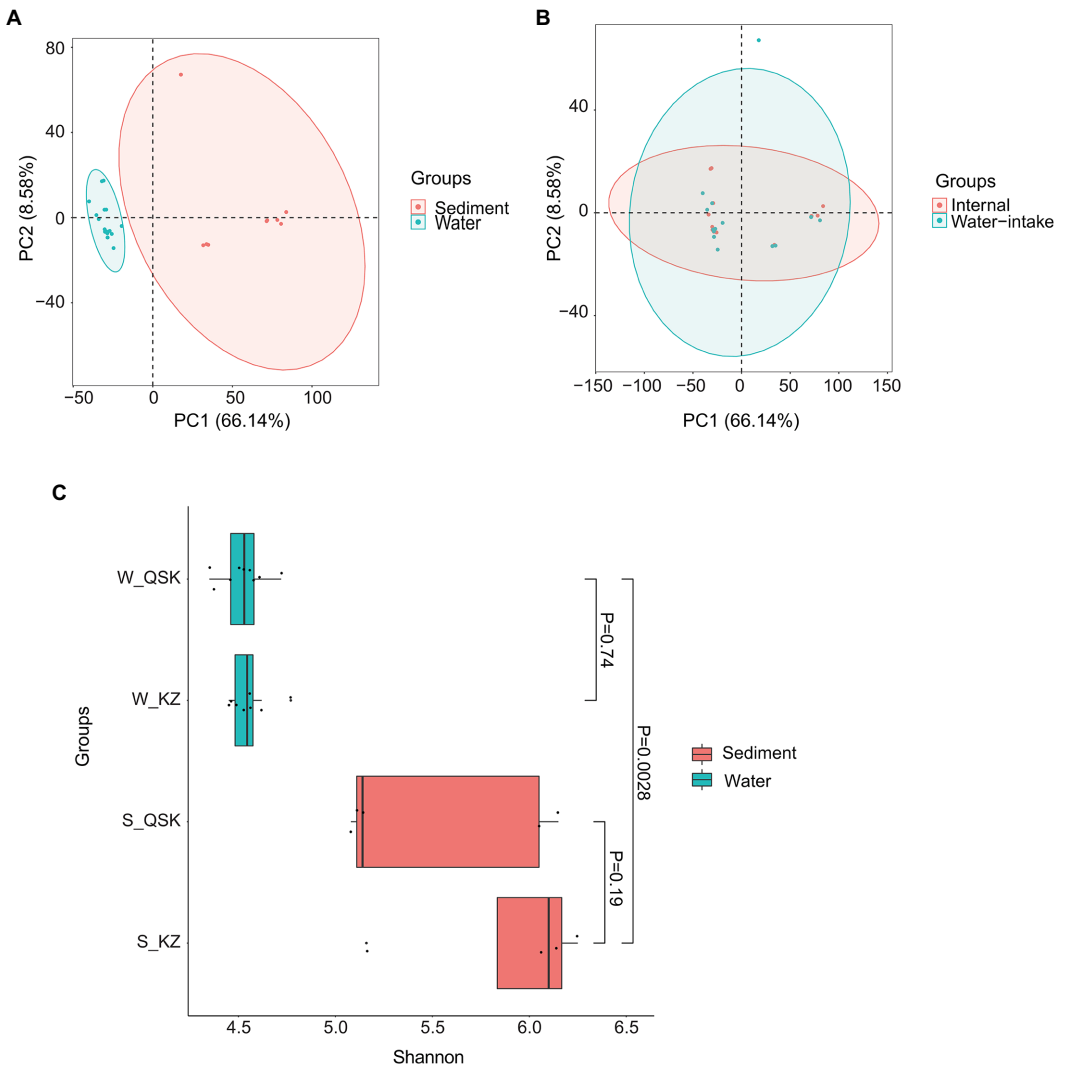

FIGURE 1
PCA and alpha diversity of sediment samples and water samples. **(A)** PCA of all samples, **(B)** PCA of water samples; **(C)** Shannon index of water and sediment samples.

10.3389/fmicb.2023.1091818

TABLE 2 Relative abundance and diversity of all species community.

Sample name	Observed_species	Chao1	ACE	Shannon	Simpson
W_QSK201020	4,304	4,594	4,452	4.35	0.07
W_QSK201207	4,439	4,708	4,610	4.61	0.05
W_QSK201116	4,351	4,617	4,489	4.46	0.07
W_QSK201123	4,386	4,671	4,547	4.53	0.06
W_QSK201103	4,333	4,586	4,466	4.58	0.05
W_KZ210104	4,304	4,552	4,441	4.77	0.03
W_KZ201123	4,384	4,677	4,533	4.62	0.05
W_KZ201207	4,418	4,835	4,603	4.56	0.06
W_QSK201214	4,366	4,644	4,526	4.72	0.05
W_KZ201214	4,392	4,665	4,543	4.46	0.06
W_KZ201116	4,360	4,635	4,508	4.45	0.07
W_QSK210104	4,351	4,678	4,504	4.56	0.04
W_KZ201103	4,340	4,562	4,472	4.56	0.05
W_KZ201130	4,336	4,655	4,472	4.53	0.06
W_QSK201229	4,338	4,576	4,480	4.37	0.07
W_QSK201130	4,355	4,630	4,505	4.50	0.06
W_KZ201229	4,311	4,568	4,447	4.49	0.07
S_KZ201130	4,597	5,241	4,917	6.25	0.01
S_QSK201020	4,267	4,522	4,415	5.11	0.06
S_KZ201229	4,562	5,025	4,829	6.06	0.01
S_QSK201130	4,352	4,643	4,507	5.08	0.04
S_KZ201214	4,450	4,875	4,660	5.16	0.03
S_QSK201103	4,396	4,733	4,587	5.14	0.04
S_QSK201229	4,526	5,034	4,794	6.15	0.01
S_QSK201214	4,501	4,874	4,705	6.05	0.01
S_KZ201103	4,545	5,117	4,837	6.14	0.01

Shannon, Simpson: diversity indice. ACE, Chao: community richness indice.

divergens, *Chara braunii*, and *Mallomonas annulata*. *Candidatus Fonsibacter ubiquis*, *Pseudanabaena yagii*, *Chara braunii*, and *Microcystis elabens* were dominant species in water samples. Based on reads, more bacteria were detected in water samples. For example, *Candidatus Fonsibacter ubiquis* and *Candidatus Nanopelagicus limne* were only identified in water samples. Little variation was observed in the composition of the microbial community under different trophic levels; variation in TLI among samples was also low (mesotrophic 48.68 ± 0.43 and light eutrophic 52.23 ± 2.05). A total of 14 of the 20 most abundant species were algae. The abundances of the 20 most abundant algae were determined. The average relative abundance of algae was higher in water samples than in sediment samples (DESeq2, $p < 0.05$; Supplementary Figure S3). *Chara braunii* and *Euglena gracilis* were dominant in water samples, whereas *Haematococcus lacustris* and *Snowella* sp. were dominant in sediment samples. These findings reinforce that the composition of microbial communities differed in sediment and water samples.

Benthic cyanobacteria can be a nuisance because of their potent toxins, as well as tastes and odours they can impart to the water. The dominant taxa of benthic cyanobacteria have changed little over time (Supplementary Figure S4), suggesting that seasonal change had less impact on these taxa in Yantian Reservoir. Additionally, all sediment samples exhibited a similar dominating genera *Oscillatoria, Cyanobium*, *Leptolyngbya*, and *Microcystis*.

Differences in the abundances of species between water and sediment were determined. Significant differences in the abundance of species were detected for 2,411 species (Supplementary Table S4). The average abundance of most species was greater in water samples than in sediment samples (61.47%). We focused on species with high abundance and with significant differences in abundance between water and sediment samples. *Snowella* sp., *Comamonadaceae bacterium* B1, and *Scenedesmus* sp. PABB004 best met these criteria in sediment samples; *Candidatus Fonsibacter ubiquis*, *Candidatus Nanopelagicus limnes,* and *Limnohabitans* sp. 103DPR2 best met these criteria in water samples. We conducted KEGG analysis to characterize functional differences between water and sediment samples (Supplementary Figure S5). Differences in KEGG pathways were observed between water and sediment. The main KEGG pathways in the water samples were related to photosynthesis and pigment synthesis, whereas, in sediments, the main KEGG pathways were related to flagella formation. *Candidatus Fonsibacter ubiquis* and *Candidatus Nanopelagicus limnes* were dominant in water samples, and *Snowella* sp. was dominant in sediment samples. These findings suggest that sediment and water samples might mutually affect each other. Therefore, we constructed a network based on

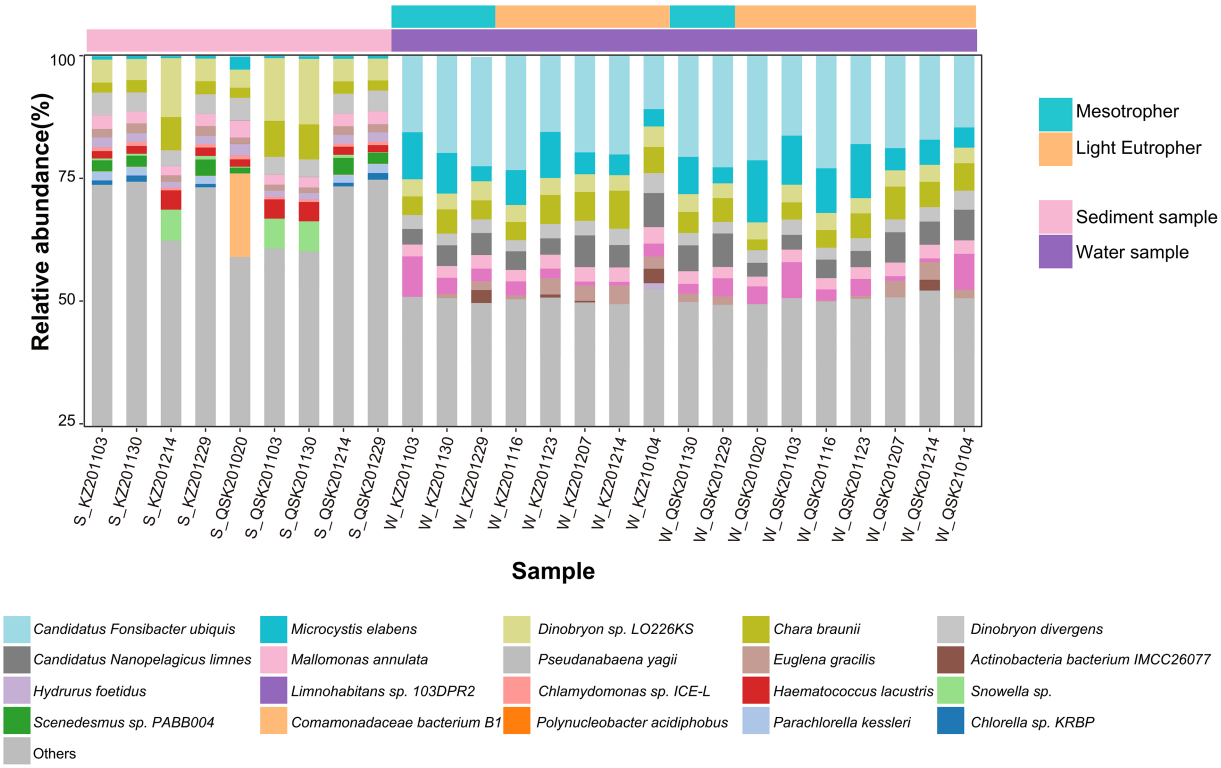

FIGURE 2
Histogram of relative abundances at the species level. The 20 most abundant species are shown, and "Other" indicates species with relative abundances less than 0.6% across all samples.

abundance differences and correlation coefficients (Figure 3). In the network analysis of dominant species, we found that *Pseudanabaena* sp. ABRG5.3 occupies a key position in the entire network, *Pseudanabaena* sp. ABRG5.3 is positively correlated with numerous species in water samples and negatively correlated with *Scenedesmus* sp. PABB004, and *Scenedesmus* sp. PABB004 is a key specie in the sediment samples and positively correlated with species in sediment samples, such as *Snowella* sp. These findings indicate that the abundances of dominant species in water and sediment samples mutually influence each other.

3.4. Effect of water physicochemical factors on microbial communities

TLI is widely used to evaluate the magnitude of eutrophication of rivers, reservoirs, and lakes in China (Ding et al., 2021). We found that changes in the TLI in KZ were similar to changes in the Shannon index; exceptions to this general pattern were only observed at two time points (2020-11-03 and 2020-12-29; Figure 4). This suggests that TLI might be a key environmental factor affecting species diversity. The relative abundance of *Microcystis elabens* gradually decreased over time, consistent with the changing trend of water temperature. RDA was performed to identify the key environmental factors affecting microbial diversity. The amount of variation in the data explained by RDA1 and RDA2 was similar (Figure 5). The long length of the arrow for TLI indicates that it was most strongly correlated with microbial communities, followed by temperature and DO. Temperature and TLI were nearly perpendicular to each other, meaning they were not correlated. The angle between DO and TLI was less than $\pi/2$, which suggests that they might be weakly positively correlated. The relationship between water physicochemical factors and species was explored. The number of species that were strongly positively correlated with temperature and TLI was greater than the number of species that were negatively correlated with temperature and TLI (Figure 6). The abundances of *Mycolicibacterium litorale* and *Mycolicibacterium phlei* were significantly positively correlated ($p < 0.01$), and alpha-proteobacterium HIMB59 was significantly negatively correlated with TLI ($p < 0.001$). We also analyzed correlations of these species with other environmental factors to provide information for follow-up studies (Supplementary Figure S6). Species were significantly positively or negatively correlated with TP and PI. By contrast, only species significantly negatively correlated with ammonia-N and TN could be found. This might indicate that ammonia-N negatively affects biodiversity.

3.5. Algal toxin gene clusters

The relative abundances of algal toxin gene clusters were identified from reservoir samples. Three classes of five algal toxin gene clusters were detected, and the abundances of these gene clusters were higher in water samples than in sediment samples (Supplementary Table S2 and Supplementary Figure S7). The abundances of algal toxin gene clusters were highest in November 2020. The relative abundance of cylindrospermopsin (CYN) gene clusters was the highest among all algal toxin gene clusters and comprised 98% of mapping reads. Two CYN gene clusters *EU140798.1* and *JN873921.1* were found to be prevalent among all the water samples and they were strongly correlated with

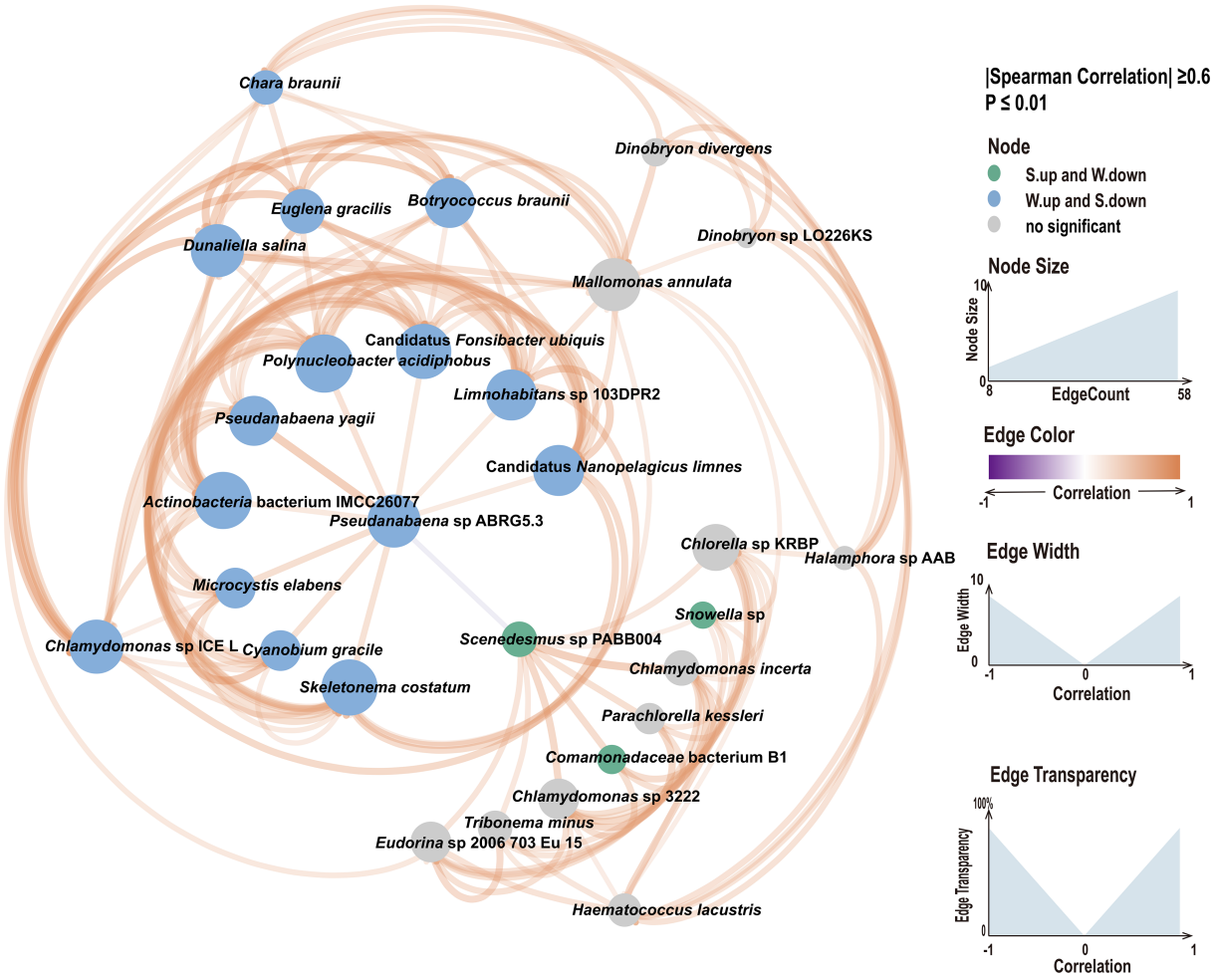

FIGURE 3
Network analysis of dominant species with significant differences among samples. The thickness and thinness of the lines indicate strong and weak correlations, respectively. Orange lines indicate positive correlations, and gray lines indicate negative correlations. Blue circles indicate taxa with higher abundances in water samples, and green circles indicate taxa with higher abundances in sediment samples.

three genera, including *Cylindrospermopsis*, *Raphidiopsis* and *Aphanocapsa* (Figure 7 up). The absolute abundances of these three genera and algal toxins were calculated to analyze the likely source species of algal toxins (Figure 7 down). It revealed the changes in the abundance of *Raphidiopsis curvata, Cylindrospermopsis raciborskii, Cylindrospermopsis curvispora*, and *Cylindrospermopsis* sp. CR12 were consistent with the changes in the abundance of the two CYN gene clusters. The sample W_KZ201214 had the highest abundance of gene cluster. Few studies have indicated that *Aphanocapsa montana* contains the algal toxin gene cluster *EU140798.1* while a sequence similar to the algal toxin gene cluster *EU140798.1* was found to be present in the genome of *A. montana* (Supplementary Table S5). The TLI of these samples was also high, except the sample W_KZ201130, suggesting that a high TLI might promote algal growth and lead to a rise in the abundance of algal toxin genes in water.

3.6. Abundances of ARGs

In recent years, a growing number of reservoir-related studies have examined ARGs (Li et al., 2015; Dang et al., 2020). In the present investigation, the distribution of ARGs in sediment and water samples was similar (Supplementary Figure S8). The three most abundant types of ARG genes—multidrug resistance (MDR), macrolide-lincosamide-streptogramin, and beta-lactam ARGs—accounted for over 70.5% of all ARGs. More than 95% of all the ARGs were derived from Proteobacteria, Actinobacteria, and Firmicutes. The relative abundance of ARGs carried by Firmicutes was 4.11% lower in water samples than in sediment samples; the relative abundance of ARGs from Actinobacteria was 20.54% higher in water samples than in sediment samples. Multidrug (−0.36%) and beta-lactam (+0.22%) ARGs were the most common Actinobacteria-derived ARGs. The multidrug-resistant bacteria were mainly in the family Enterobacteriaceae (relative abundance over 53%). To explore the potential hosts of ARGs, we investigated the correlation between ARGs and bacterial genera. The results indicated that the network relationship in sediment samples was far more complex than in water (Figure 8). Under the same screening criteria, there were more interspecies connections in the sediment samples, and more species and ARG types were present. *Polynucleobacter* in sediment samples was positively correlated with multiple multidrug resistance genes such as *mdtB* and *mdtC*. Likewise, *Paenalcaligenes* in water samples was positively associated with multiple drug-resistance genes.

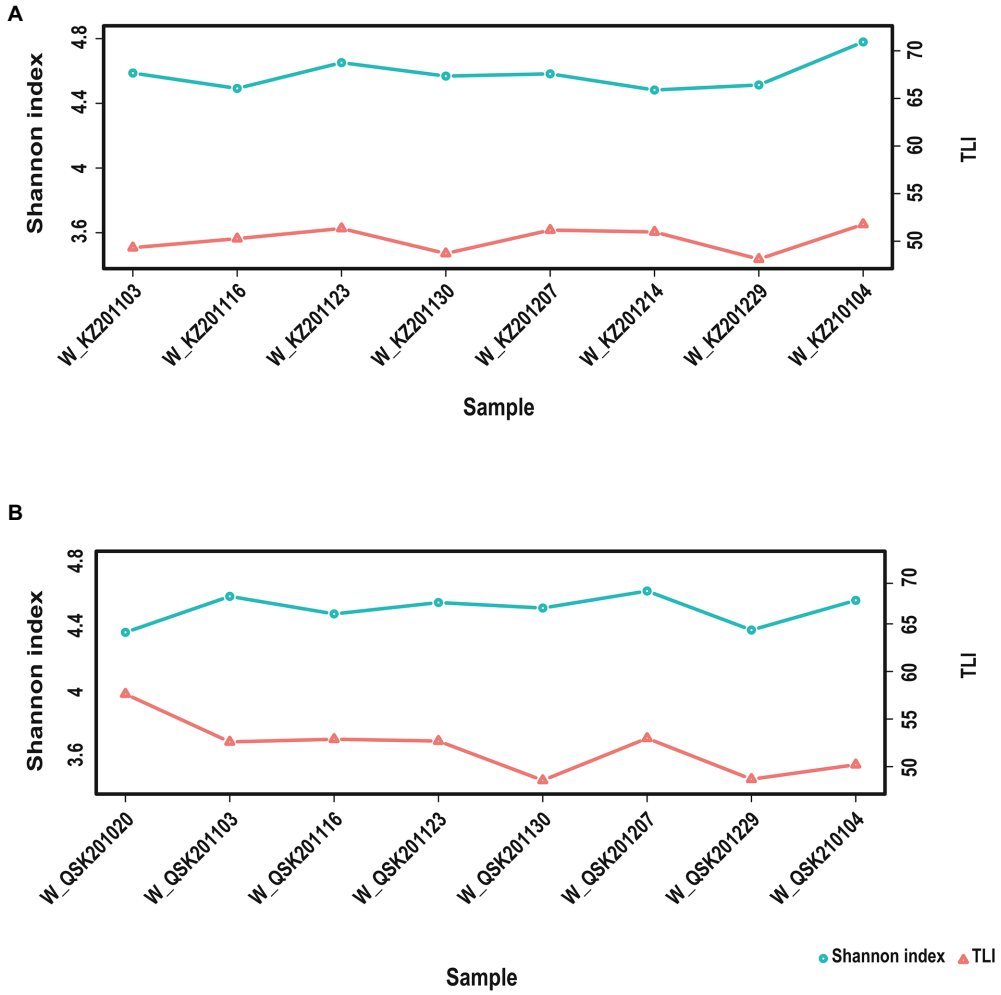

FIGURE 4
Relationships between TLI and the Shannon index. **(A)** KZ samples, **(B)** QSK samples.

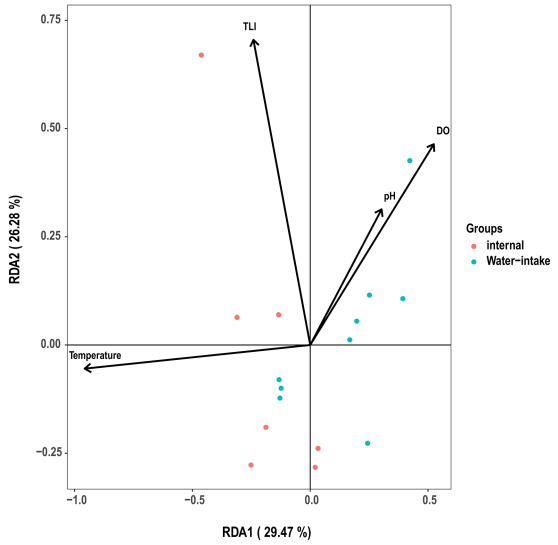

FIGURE 5
Redundancy analysis ordination diagram of all communities and environmental variables. Circles correspond to samples.

4. Discussion

Clarifying associations between microbial communities and water quality is essential for enhancing the understanding of reservoir characteristics. In this study, the structure of microbial communities was explored through continuous monitoring of the water and sediment of drinking water reservoirs at two locations in southern China over a 4-month period. We found that the dominant species in sediment samples and water samples differed, which is consistent with the results of previous studies (Yang et al., 2012; El Najjar et al., 2020; Nwosu et al., 2021). We also found that the composition of microbial communities in the reservoir was not significantly affected by seasonal factors, which might stem from the lack of variation in the water temperature of Yantian Reservoir among seasons. On the one hand, a relatively stable water temperature can facilitate the study of the effects of other environmental factors, such as TLI, TP, and TN on the composition of microbial communities in reservoirs. On the other hand, the growth of many microorganisms is enhanced when reservoir water temperatures are maintained above 18°C, increasing the health risks posed by algal toxins and ARGs. MDR genes were the most abundant ARGs in water and sediment samples. Algal toxin genes were more abundant in water samples than in sediment samples.

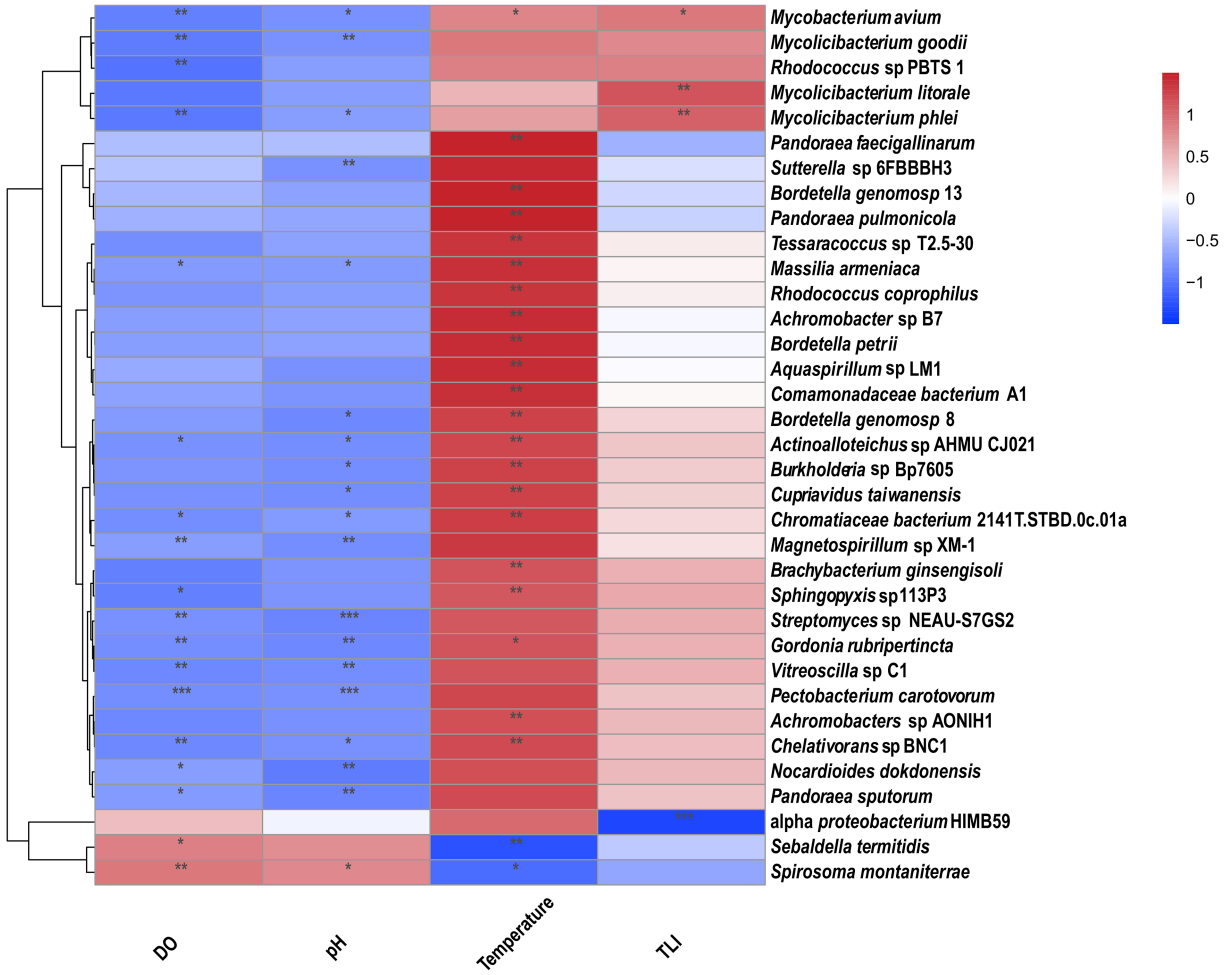

FIGURE 6
Correlation heatmap for microbes and environmental factors. The magnitude of the *R*-values is shown in the color gradient. *$p \leq 0.05$, **$p \leq 0.01$, and ***$p \leq 0.001$.

A four-year ecological restoration project was initiated at Yantian Reservoir in October 2014, and completed in December 2017. During this period, a 10,000-m^2 ecological restoration area was constructed to reduce nutrient loading and mitigate the consequences of eutrophication and to provide food and habitat for fish and mollusks (Wang et al., 2019). Fish were harvested to maintain system stability. Despite project completion, changes in water quality and the composition of microbial communities following the partial restoration of Yantian Reservoir have not been investigated. This study details the results of data collected over several years on the microbial communities in this reservoir, as well as various environmental factors. No pre-ecological restoration project samples were obtained; thus, no comparisons before and after ecological restoration are possible. However, data were obtained on the water quality and composition of microbial communities in Yantian Reservoir 4 years after ecological restoration measures had been completed. These data are essential for evaluating the effects of the ecological restoration project on water quality.

Water quality is a major environmental priority for modern society (Alcamo, 2019). Regular water quality monitoring is essential for ensuring the safety of drinking water, an adequate food supply, and the health of human populations. Basic field kits with multiple sensors, fluorescence, spectrophotometric, and microscopic-based mobile technologies have been used to characterize the composition of microbial communities and estimate water quality. These can be used to detect microbes (bacterial concentrations) and chemicals (Grossi et al., 2013), fecal coliforms, pathogenic parasites, heavy metals, and pesticides (Acharya et al., 2020). However, these methods only provide preliminary insights into the composition of microbial communities in water. NGS permits more comprehensive characterizations of the water microbiome. Metagenomic approaches permit real-time quantification of microbial hazards in sewage (Aarestrup and Woolhouse, 2020). Therefore, the use of metagenomic techniques for monitoring water quality merits further study. The excessive growth of cyanobacteria because of eutrophication is becoming increasingly widespread, leading to deterioration in water quality (Huisman et al., 2018). The health threats posed by algal toxins have raised concerns among health organizations and water authorities (Van Dolah, 2000). Microcystin, a well-known algal toxin, might be associated with developing irritant reactions, hepatic diseases, and the progression of tumors (Tamele and Vasconcelos, 2020). CYN can impair the liver, heart, kidney, and thymus (Terao et al., 1994) by inhibiting protein synthesis (Froscio et al., 2008) and glutathione metabolism (Runnegar et al., 1995).

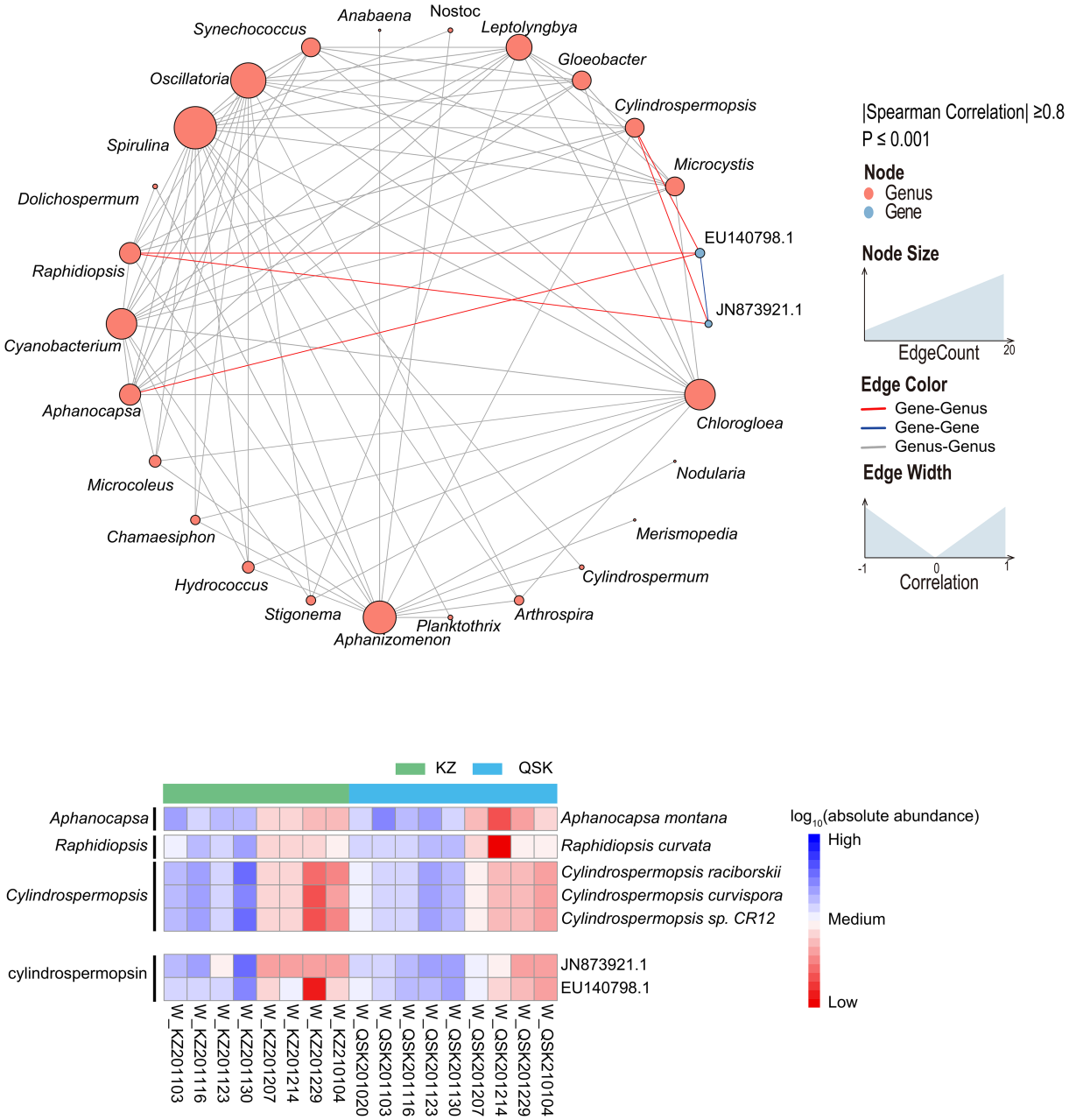

FIGURE 7
Cross-genus co-occurrence network of phycotoxin gene clusters in water samples. Network analysis coloring based on taxonomic genus preference. Associations indicated a significant (p<0.001), scored as positive (spearman's p>0.8). The size of each node is proportional to the SAV degree; the thickness of the connection between two nodes is proportional to the value of the Spearman correlation coefficient. Heatmap of the relative abundances of algal toxin gene clusters in all samples.

CYN is also a potential carcinogen that inhibits pyrimidine nucleotide synthesis (Reisner et al., 2004) and induces DNA strand breakage (Bazin et al., 2012). Although we detected algal toxin gene clusters, such as CYN and microcystin, in Yantian Reservoir in this study, the association between algal toxins and species could not be accurately quantified because we did not attempt to detect chemical substances in the samples. In future studies, we plan to monitor the relationships between phycotoxins and algal species.

In this study, species from genera, *Cyanobium*, *Leptolyngbya*, *Microcystis*, and *Oscillatoria* predominated in all sediment samples. Species of these four genera are reported to produce algal toxins (Frazão et al., 2010) and benthic cyanobacteria can cause taste and odour concerns in the water (Frazão et al., 2010; Casero et al., 2019; Entfellner et al., 2022). Thus, monitoring benthic cyanobacteria should be added to monitoring programs advocating drinking water safety (Izaguirre et al., 2007; Gaget et al., 2017, 2020).

Although the health risks posed by ARGs are a worldwide concern, research in this field is lacking (Hu et al., 2021). Increases in the abundance of ARGs in reservoirs affect the safety of drinking water and the efficacy of clinical antibiotics therapy (Ghai et al., 2014; Nnadozie and Odume, 2019; Dang et al., 2020). Previous studies of reservoirs in eastern China have revealed that high

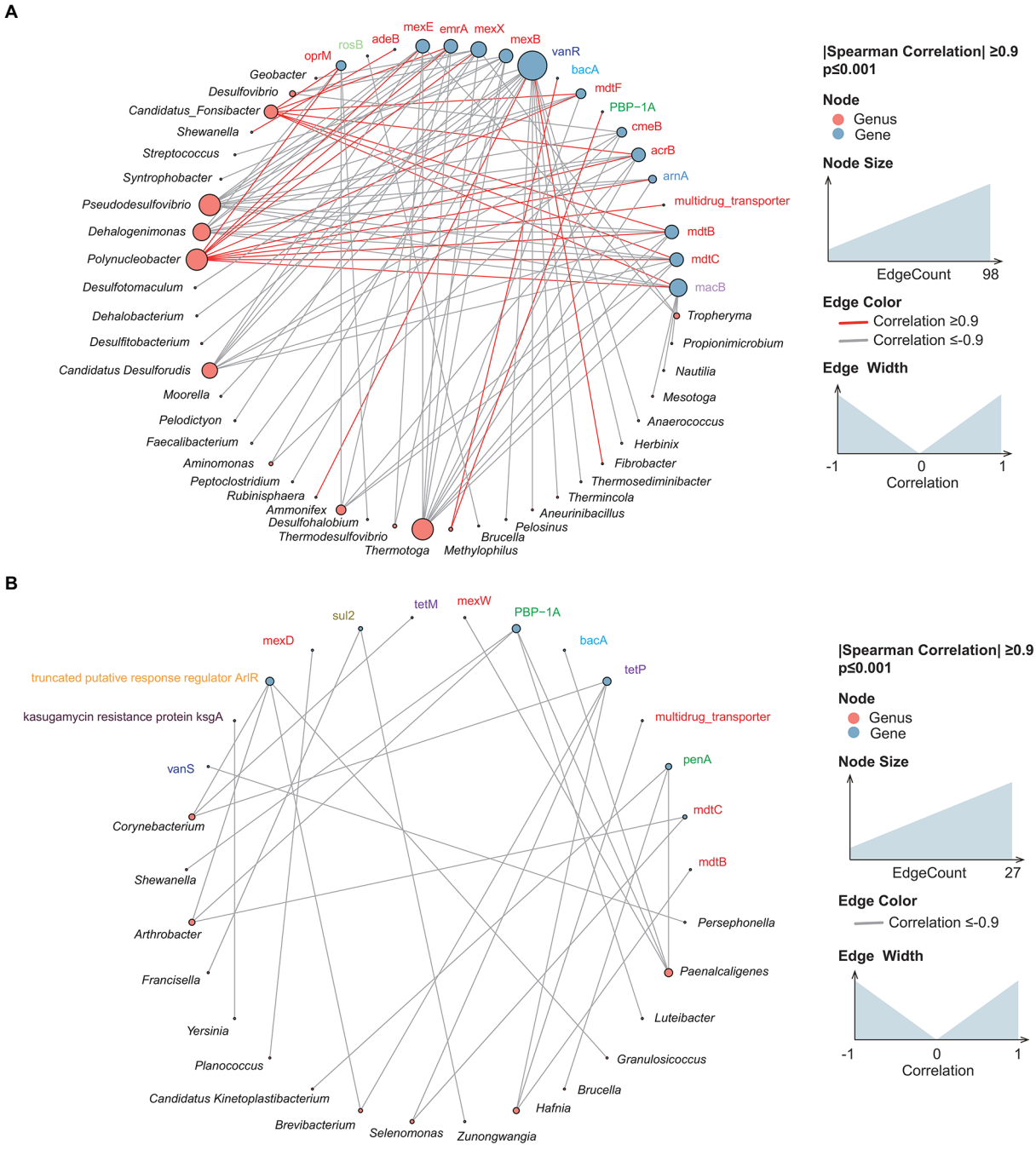

FIGURE 8
Cross-genus co-occurrence network of ARGs in samples. Network analysis coloring based on taxonomic genus preference. Associations indicated a significant (p<0.001), scored as positive (spearman's p>0.9 or p<−0.9). The size of each node is proportional to the SAV degree; the thickness of the connection between two nodes is proportional to the value of the Spearman correlation coefficient. **(A)** Sediment samples; **(B)** water samples.

concentrations of ARGs can be detected in the water after being transported over long distances (Hu et al., 2018; Hu and Lin, 2018). We also identified ARGs in Yantian Reservoir, and the most abundant ARGs were MDR genes, which is consistent with the results of a previous study of Danjiangkou Reservoir (Dang et al., 2020). Firmicutes, which are dominant intestinal microorganisms, were the second largest source of ARGs of all microbial phyla in Yantian Reservoir; their presence in large numbers indicates that the water quality of Yantian Reservoir poses serious human health risks. The problem of drug resistance in MDR pathogens has attracted clinical attention because these pathogens result in increased morbidity and mortality, especially in immunocompromised populations (Catalano et al., 2022). Enterobacteriaceae was the primary source of MDR genes in a previous study (Dang et al., 2020). The occurrence and spread of multidrug-resistant Enterobacteriaceae pose public health threats because available treatment options are limited, and the development of new antimicrobial agents is historically slow (Cerceo et al., 2016; Chen et al., 2019). The widespread occurrence of MDR genes in reservoirs poses major threats to human health.

5. Conclusion

Metagenomic approaches were used to characterize the composition of microbial communities and environmental factors in water and sediment samples in Yantian Reservoir across seasons at two different locations. Seasonal changes and sampling location did not have major effects on the composition of microorganisms in Yantian Reservoir; however, sample origin (water vs. sediment) had a substantial effect on the composition of microorganisms. The distribution of algal toxins and ARGs was analyzed as were the source species of algal toxins. The distribution of algal toxins and ARGs in Yantian Reservoir was also studied, and then based on correlation analysis, the potential sources species of algal toxins and ARGs were identified. This study revealed a new potential source of cyanotoxins through the colonial cyanophyte *Aphanocapsa montana*. The study also found that TLI is a key factor affecting the composition of microbes in Yantian Reservoir and identified the species most strongly correlated with TLI.

Data availability statement

The datasets presented in this study can be found in online repositories. The names of the repository/repositories and accession number(s) can be found in the article/Supplementary material.

Author contributions

LS and LX conceived and designed the research, reviewed and revised the manuscript. JF and XZhao wrote the manuscript. YLiu and QY reviewed and revised the manuscript. JC, ZL, and LO performed the sample preparation. YLi and ML took charge of library construction and sequencing. LZho, LZen, and MW supported data mining and figure drawing. ZX and XY designed the database. All authors read and approved the final version of the manuscript.

Funding

This work was supported by the Shenzhen Science and Technology Program: KCXFZ20201221173007020.

Acknowledgments

We thank Liwen Bianji (Edanz; www.liwenbianji.cn) for editing the language of a draft of this manuscript.

Conflict of interest

LS, LZho, YLiu, XZhao, MW, XZhan, YLi, ML, LZen, and QY were employed by GeneMind Biosciences Company Limited. JF, JC, ZL, LO, ZX, XY, and LX were employed by the State Environmental Protection Key Laboratory of Drinking Water Source.

Publisher's note

All claims expressed in this article are solely those of the authors and do not necessarily represent those of their affiliated organizations, or those of the publisher, the editors and the reviewers. Any product that may be evaluated in this article, or claim that may be made by its manufacturer, is not guaranteed or endorsed by the publisher.

Supplementary material

The Supplementary material for this article can be found online at: https://www.frontiersin.org/articles/10.3389/fmicb.2023.1091818/full#supplementary-material

References

Aarestrup, F. M., and Woolhouse, M. E. J. S. (2020). Using sewage for surveillance of antimicrobial resistance. *Science* 367, 630–632. doi: 10.1126/science.aba3432

Acharya, K., Blackburn, A., Mohammed, J., Haile, A. T., Hiruy, A. M., and Werner, D. J. W. R. (2020). Metagenomic water quality monitoring with a portable laboratory. *Water Res.* 184:116112. doi: 10.1016/j.watres.2020.116112

Alcamo, J. (2019). Water quality and its interlinkages with the Sustainable Development Goals. *Curr. Opin. Environ. Sustain.* 36, 126–140. doi: 10.1016/j.cosust.2018.11.005

Bazin, E., Huet, S., Jarry, G., Hégarat, L. L., Munday, J. S., Humpage, A. R., et al. (2012). Cytotoxic and genotoxic effects of cylindrospermopsin in mice treated by gavage or intraperitoneal injection. *Environ. Toxicol.* 27, 277–284. doi: 10.1002/tox.20640

Bobkov, Y. V., Walker Iii, W. B., and Cattaneo, A. M. J. S. R. (2021). Altered functional properties of the codling moth Orco mutagenized in the intracellular loop-3. *Sci. Rep.* 11:3893. doi: 10.1038/s41598-021-83024-3

Boucher, D., Jardillier, L., and Debroas, D. J. F. M. E. (2006). Succession of bacterial community composition over two consecutive years in two aquatic systems: a natural lake and a lake-reservoir. *FEMS Microbiol. Ecol.* 55, 79–97. doi: 10.1111/j.1574-6941.2005.00011.x

Casero, K. C., Velázquez, D., Medina-Cobo, M., Quesada, A., and Cirés, S. (2019). Unmasking the identity of toxigenic cyanobacteria driving a multi-toxin bloom by high-throughput sequencing of cyanotoxins genes and 16S rRNA metabarcoding. *Science of the Total Environment* 665, 367–378.

Catalano, A., Iacopetta, D., Ceramella, J., Scumaci, D., Giuzio, F., Saturnino, C., et al. (2022). Multidrug resistance (MDR): a widespread phenomenon in pharmacological therapies. *Molecules* 27:616. doi: 10.3390/molecules27030616

Cerceo, E., Deitelzweig, S. B., Sherman, B. M., and Amin, A. N. J. M. D. R. (2016). Multidrug-resistant gram-negative bacterial infections in the hospital setting: overview, implications for clinical practice, and emerging treatment options. *Microb. Drug Resist.* 22, 412–431. doi: 10.1089/mdr.2015.0220

Chen, Y., Su, J.-Q., Zhang, J., Li, P., Chen, H., Zhang, B., et al. (2019). High-throughput profiling of antibiotic resistance gene dynamic in a drinking water river-reservoir system. *Water Res.* 149, 179–189. doi: 10.1016/j.watres.2018.11.007

Chien, Y., Wu, S., and Wu, J. J. (2009). Identification of physical parameters controlling the dominance of algal species in a subtropical reservoir. *Water Sci. Technol.* 60, 1779–1786. doi: 10.2166/wst.2009.541

Dang, C., Xia, Y., Zheng, M., Liu, T., Liu, W., Chen, Q., et al. (2020). Metagenomic insights into the profile of antibiotic resistomes in a large drinking water reservoir. *Environ. Int.* 136:105449. doi: 10.1016/j.envint.2019.105449

Delgado-Baquerizo, M., Reich, P. B., Trivedi, C., Eldridge, D. J., and Singh, B. K. (2020). Multiple elements of soil biodiversity drive ecosystem functions across biomes. *Nat. Ecol. Evol.* 4, 210–220. doi: 10.1038/s41559-019-1084-y

Ding, Y., Zhao, J., Peng, W., Zhang, J., Chen, Q., Fu, Y., et al. (2021). Stochastic trophic level index model: A new method for evaluating eutrophication state. *J. Environ. Manag.* 280:111826. doi: 10.1016/j.jenvman.2020.111826

Edwards, M. L., Lilley, A. K., Timms-Wilson, T. H., Thompson, I. P., and Cooper, I. J. F. M. E. (2001). Characterisation of the culturable heterotrophic bacterial community in a small eutrophic lake (Priest Pot). *FEMS Microbiol. Ecol.* 35, 295–304. doi: 10.1111/j.1574-6941.2001.tb00815.x

El Najjar, P., Pfaffl, M., Ouaini, N., Abdel Nour, A., and El Azzi, D. (2020). Water and sediment microbiota diversity in response to temporal variation at the outlet of the Ibrahim River (Lebanon). *Environ. Monit. Assess.* 192, 1–11. doi: 10.1007/s10661-020-8139-z

Elser, J. J., Bracken, M. E., Cleland, E. E., Gruner, D. S., Harpole, W. S., Hillebrand, J. T., et al. (2007). Global analysis of nitrogen and phosphorus limitation of primary producers in freshwater, marine and terrestrial ecosystems. *Ecology Letters* 10, 1135–1142.

Entfellner, E., Li, R., Jiang, Y., Ru, J., Blom, J., Deng, L., et al. (2022). Toxic/Bioactive Peptide Synthesis Genes Rearranged by Insertion Sequence Elements Among the Bloom-Forming Cyanobacteria Planktothrix. *Frontiers in Microbiology* 13.

Frazão, B., Martins, R., and Vasconcelos, V. (2010). Are known cyanotoxins involved in the toxicity of picoplanktonic and filamentous North Atlantic marine cyanobacteria?. *Marine Drugs* 8, 1908–1919.

Froscio, S., Humpage, A., Wickramasinghe, W., Shaw, G., and Falconer, I. J. T. (2008). Interaction of the cyanobacterial toxin cylindrospermopsin with the eukaryotic protein synthesis system. *Toxicon* 51, 191–198. doi: 10.1016/j.toxicon.2007.09.001

Gaget, V., Humpage, A. R., Huang, Q., Monis, P., and Brookes, J. D. (2017). Benthic cyanobacteria: A source of cylindrospermopsin and microcystin in Australian drinking water reservoirs. *Water Research* 124, 454–464.

Gaget, V., Hobson, P., Keulen, A., Newton, K., Monis, P., Humpage, A., et al. (2020). Toolbox for the sampling and monitoring of benthic cyanobacteria. *Water Research* 169:115222.

Ghai, R., Mizuno, C. M., Picazo, A., Camacho, A., and Rodriguez-Valera, F. J. M. E. (2014). Key roles for freshwater A ctinobacteria revealed by deep metagenomic sequencing. *Mol. Ecol.* 23, 6073–6090. doi: 10.1111/mec.12985

Grossi, M., Lazzarini, R., Lanzoni, M., Pompei, A., Matteuzzi, D., and Riccò, B. J. I. S. J. (2013). A portable sensor with disposable electrodes for water bacterial quality assessment. *IEEE Sensors J.* 13, 1775–1782. doi: 10.1109/JSEN.2013.2243142

He, T., Lu, Y., Cui, Y., Luo, Y., Wang, M., Meng, W., et al. (2015). Detecting gradual and abrupt changes in water quality time series in response to regional payment programs for watershed services in an agricultural area. *J. Hydrol.* 525, 457–471. doi: 10.1016/j.jhydrol.2015.04.005

Hu, Y., Jiang, L., Sun, X., Wu, J., Ma, L., Zhou, Y., et al. (2021). Risk assessment of antibiotic resistance genes in the drinking water system. *Sci. Total Environ.* 800:149650. doi: 10.1016/j.scitotenv.2021.149650

Hu, Y., Jiang, L., Zhang, T., Jin, L., Han, Q., Zhang, D., et al. (2018). Occurrence and removal of sulfonamide antibiotics and antibiotic resistance genes in conventional and advanced drinking water treatment processes. *J. Hazard. Mater.* 360, 364–372. doi: 10.1016/j.jhazmat.2018.08.012

Hu, Y., and Lin, P. (2018). Probabilistic prediction of maximum tensile loads in soil nails. Advances in Civil Engineering 2018.

Huisman, J., Codd, G. A., Paerl, H. W., Ibelings, B. W., Verspagen, J. M., and Visser, P. M. J. N. R. M. (2018). Cyanobacterial blooms. *Nat. Rev. Microbiol.* 16, 471–483. doi: 10.1038/s41579-018-0040-1

Izaguirre, G., Jungblut, M.-D., and Neilan, B. A. (2007). Benthic cyanobacteria (Oscillatoriaceae) that produce microcystin-LR, isolated from four reservoirs in southern California. *Water Research* 41, 492–498.

Jiang, T., Sun, S., Chen, Y., Qian, Y., Guo, J., Dai, R., et al. (2021). Microbial diversity characteristics and the influence of environmental factors in a large drinking-water source. *Sci. Total Environ.* 769:144698. doi: 10.1016/j.scitotenv.2020.144698

Li, X.-Z., Plésiat, P., and Nikaido, H. J. C. M. R. (2015). The challenge of efflux-mediated antibiotic resistance in Gram-negative bacteria. *Clin. Microbiol. Rev.* 28, 337–418. doi: 10.1128/CMR.00117-14

Long, J., and Luo, K. J. E. P. (2020). Elements in surface and well water from the central North China plain: enrichment patterns, origins, and health risk assessment. *Environ. Pollut.* 258:113725. doi: 10.1016/j.envpol.2019.113725

Mucha, A. P., Vasconcelos, M. T. S., and Bordalo, A. (2004). Vertical distribution of the macrobenthic community and its relationships to trace metals and natural sediment characteristics in the lower Douro estuary, Portugal. *Estuar. Coast. Shelf Sci.* 59, 663–673. doi: 10.1016/j.ecss.2003.11.010

Nnadozie, C. F., and Odume, O. N. (2019). Freshwater environments as reservoirs of antibiotic resistant bacteria and their role in the dissemination of antibiotic resistance genes. *Environ. Pollut.* 254:113067. doi: 10.1016/j.envpol.2019.113067

Nwosu, E. C., Roeser, P., Yang, S., Ganzert, L., Dellwig, O., Pinkerneil, S., et al. (2021). From water into sediment—tracing freshwater cyanobacteria via DNA analyses. *Microorganisms* 9:1778. doi: 10.3390/microorganisms9081778

Paerl, H. W. (2018). Mitigating toxic planktonic cyanobacterial blooms in aquatic ecosystems facing increasing anthropogenic and climatic pressures. *Toxins* 10:76. doi: 10.3390/toxins10020076

Park, Y., Lee, H. K., Shin, J.-K., Chon, K., Kim, S., Cho, K. H., et al. (2021). A machine learning approach for early warning of cyanobacterial bloom outbreaks in a freshwater reservoir. *J. Environ. Manag.* 288:112415. doi: 10.1016/j.jenvman.2021.112415

Penn, K., Wang, J., Fernando, S. C., and Thompson, J. R. (2014). Secondary metabolite gene expression and interplay of bacterial functions in a tropical freshwater cyanobacterial bloom. *ISME J.* 8, 1866–1878. doi: 10.1038/ismej.2014.27

Pound, H. L., Martin, R. M., Sheik, C. S., Steffen, M. M., Newell, S. E., Dick, G. J., et al. (2021). Environmental studies of cyanobacterial harmful algal blooms should include interactions with the dynamic microbiome. *Environ. Sci. Technol.* 55, 12776–12779. doi: 10.1021/acs.est.1c04207

Qin, S., Liu, Y., Wang, X., Xu, Y., Shi, Y., Zhang, R., et al. (2016). Light-activated artificial synapses based on graphene hybrid phototransistors: IEEE, 1–2.

Reisner, M., Carmeli, S., Werman, M., and Sukenik, A. (2004). The cyanobacterial toxin cylindrospermopsin inhibits pyrimidine nucleotide synthesis and alters cholesterol distribution in mice. *Toxicol. Sci.* 82, 620–627. doi: 10.1093/toxsci/kfh267

Runnegar, M. T., Kong, S.-M., Zhong, Y.-Z., and Lu, S. C. (1995). Inhibition of reduced glutathione synthesis by cyanobacterial alkaloid cylindrospermopsin in cultured rat hepatocytes. *Biochem. Pharmacol.* 49, 219–225. doi: 10.1016/S0006-2952(94)00466-8

Sakamoto, S., Lim, W. A., Lu, D., Dai, X., Orlova, T., and Iwataki, M. (2021). Harmful algal blooms and associated fisheries damage in East Asia: current status and trends in China, Japan, Korea and Russia. *Harmful Algae* 102:101787. doi: 10.1016/j.hal.2020.101787

Savvichev, A. S., Babenko, V. V., Lunina, O. N., Letarova, M. A., Boldyreva, D. I., Veslopolova, E. F., et al. (2018). Sharp water column stratification with an extremely dense microbial population in a small meromictic lake, Trekhtzvetnoe. *Environ. Microbiol.* 20, 3784–3797. doi: 10.1111/1462-2920.14384

Sjöstedt, J., Koch-Schmidt, P., Pontarp, M., Canbäck, B., Tunlid, A., Lundberg, P., et al. (2012). Recruitment of members from the rare biosphere of marine bacterioplankton communities after an environmental disturbance. *Appl. Environ. Microbiol.* 78, 1361–1369. doi: 10.1128/AEM.05542-11

Tamele, I. J., and Vasconcelos, V. J. T. (2020). Microcystin incidence in the drinking water of mozambique: Challenges for public health protection. *Toxins* 12:368. doi: 10.3390/toxins12060368

Terao, K., Ohmori, S., Igarashi, K., Ohtani, I., Watanabe, M., Harada, K., et al. (1994). Electron microscopic studies on experimental poisoning in mice induced by cylindrospermopsin isolated from blue-green alga Umezakia natans. *Toxicon* 32, 833–843. doi: 10.1016/0041-0101(94)90008-6

Van Dolah, F. M. (2000). Marine algal toxins: origins, health effects, and their increased occurrence. *Environ. Health Perspect.* 108, 133–141. doi: 10.1289/ehp.00108s1133

Wang, S., Wang, L., Zheng, Y., Chen, Z.-B., Yang, Y., Lin, H.-J., et al. (2019). Application of mass-balance modelling to assess the effects of ecological restoration on energy flows in a subtropical reservoir, China. *Sci. Total Environ.* 664, 780–792. doi: 10.1016/j.scitotenv.2019.01.334

Wiesner-Friedman, C., Beattie, R. E., Stewart, J. R., Hristova, K. R., and Serre, M. L. J. E. S. (2021). Microbial find, inform, and test model for identifying spatially distributed contamination sources: framework foundation and demonstration of ruminant bacteroides abundance in river sediments. *Environ. Sci. Technol.* 55, 10451–10461. doi: 10.1021/acs.est.1c01602

Wu, T., Zhu, G., Zhu, M., Xu, H., Yang, J., and Zhao, X. (2021). Effects of algae proliferation and density current on the vertical distribution of odor compounds in drinking water reservoirs in summer. *Environ. Pollut.* 288:117683. doi: 10.1016/j.envpol.2021.117683

Wurtsbaugh, W. A., Paerl, H. W., and Dodds, W. K. (2019). Nutrients, eutrophication and harmful algal blooms along the freshwater to marine continuum. *Wiley Interdiscip. Rev. Water* 6:e1373. doi: 10.1002/wat2.1373

Yang, J., Yu, X., Liu, L., Zhang, W., and Guo, P. (2012). Algae community and trophic state of subtropical reservoirs in Southeast Fujian, China. *Environ. Sci. Pollut. Res.* 19, 1432–1442. doi: 10.1007/s11356-011-0683-1

Yin, X., Jiang, X.-T., Chai, B., Li, L., Yang, Y., Cole, J. R., et al. (2018). ARGs-OAP v2. 0 with an expanded SARG database and Hidden Markov Models for enhancement characterization and quantification of antibiotic resistance genes in environmental metagenomes. *Bioinformatics* 34, 2263–2270. doi: 10.1093/bioinformatics/bty053

frontiers | Frontiers in Microbiology

TYPE Original Research
PUBLISHED 08 March 2023
DOI 10.3389/fmicb.2023.1112590

OPEN ACCESS

EDITED BY
George S. Bullerjahn,
Bowling Green State University,
United States

REVIEWED BY
Jiaojiao Li,
Yunnan University,
China
Casey Michael Godwin,
University of Michigan,
United States

*CORRESPONDENCE
Mingjun Liao
✉ lmj1112@163.com

SPECIALTY SECTION
This article was submitted to Aquatic Microbiology, a section of the journal Frontiers in Microbiology

RECEIVED 30 November 2022
ACCEPTED 13 February 2023
PUBLISHED 08 March 2023

CITATION
Peng K, Jiao Y, Gao J, Xiong W, Zhao Y, Yang S and Liao M (2023) Viruses may facilitate the cyanobacterial blooming during summer bloom succession in Xiangxi Bay of Three Gorges Reservoir, China. *Front. Microbiol.* 14:1112590. doi: 10.3389/fmicb.2023.1112590

Viruses may facilitate the cyanobacterial blooming during summer bloom succession in Xiangxi Bay of Three Gorges Reservoir, China

Kaida Peng[1,2], Yiying Jiao[2], Jian Gao[2], Wen Xiong[2], Yijun Zhao[2], Shao Yang[1] and Mingjun Liao[2]*

[1]School of Life Sciences, Central China Normal University, Wuhan, Hubei, China, [2]Hubei Key Laboratory of Ecological Restoration for River-Lakes and Algal Utilization, School of Civil and Environmental Engineering, Hubei University of Technology, Wuhan, Hubei, China

The occurrence of cyanobacterial blooms in summer are frequently accompanied by the succession of phytoplankton communities in freshwater. However, little is known regarding the roles of viruses in the succession, such as in huge reservoirs. Here, we investigated the viral infection characteristics of phytoplankton and bacterioplankton during the summer bloom succession in Xiangxi Bay of Three Gorges Reservoir, China. The results indicated that three distinct bloom stages and two successions were observed. From cyanobacteria and diatom codominance to cyanobacteria dominance, the first succession involved different phyla and led to a *Microcystis* bloom. From *Microcystis* dominance to *Microcystis* and *Anabaena* codominance, the second succession was different Cyanophyta genera and resulted in the persistence of cyanobacterial bloom. The structural equation model (SEM) showed that the virus had positive influence on the phytoplankton community. Through the Spearman's correlation and redundancy analysis (RDA), we speculated that both the increase of viral lysis in the eukaryotic community and the increase of lysogeny in cyanobacteria may contributed to the first succession and *Microcystis* blooms. In addition, the nutrients supplied by the lysis of bacterioplankton might benefit the second succession of different cyanobacterial genera and sustain the dominance of cyanobacteria. Based on hierarchical partitioning method, the viral variables still have a marked effect on the dynamics of phytoplankton community, although the environmental attributes were the major factors. Our findings suggested that viruses played multiple potential roles in summer bloom succession and may help the blooms success of cyanobacteria in Xiangxi Bay. Under the background of increasingly serious cyanobacterial blooms worldwide, our study may have great ecological and environmental significance for understanding the population succession in phytoplankton and controlling the cyanobacterial blooms.

KEYWORDS

viruses, lysis, lysogeny, succession, cyanobacterial bloom, Three Gorges Reservoir

1. Introduction

Cyanobacterial blooms have increased in frequency around the world in recent decades (Huisman et al., 2018) and are likely to become more severe as a consequence of eutrophication, rising CO_2 levels and accelerating global warming (Verspagen et al., 2014; Chapra et al., 2017). Moreover, cyanobacterial blooms can cause major problems, such as toxin production, hypoxia generation, and food web disruption, leading to the loss of ecosystem services (Verspagen et al., 2014; Chapra et al., 2017). However, some mechanisms underlying the ecological success of cyanobacteria remain unclear, which makes it difficult to deal with cyanobacterial blooms (Wilhelm et al., 2020).

In summer, cyanobacterial communities occur widely in freshwater by displacing eukaryotic algae, which generally includes diatom and green algae (Ke et al., 2008; Zepernick et al., 2021). In addition, the succession of phytoplankton among different cyanobacterial genera also occurs frequently (Moustaka-Gouni et al., 2006; Chun et al., 2020; Tanvir et al., 2021). Various factors, including nutrients, predation, temperature, light, pH, antibiotics, and water turbulence, have been found to influence these successions and the ecological success of cyanobacteria (Steffen et al., 2015; Reavie et al., 2016; Huisman et al., 2018; Wang et al., 2021; Xu et al., 2021; Zepernick et al., 2021). Given the complexity of cyanobacterial blooms, the drivers of cyanobacterial dominance and succession are still being explored (Wang et al., 2021).

Cases in past decades have shown that viruses are becoming more pronounced in phytoplankton community regulation (Suttle et al., 1990; Fuhrman, 1999; Brussaard, 2004; Knowles et al., 2016; Pound et al., 2020). As suggested by negative frequency-dependent selection, the "Kill-the-Winner" (KtW) model of lytic infection predicts that abundant prokaryotic types will be exposed to strong viral pressure for maintaining high prokaryotic richness (Winter et al., 2010). Many studies on phytoplankton blooms showed direct viral control and provided empirical support for the KtW model (Bratbak et al., 1993; Hewson et al., 2001; Baudoux et al., 2006). Under a modified KtW model, Pound et al. (2020) found that viruses may suppress the competition of eukaryotic community and allow for the cyanobacterial bloom. Recently, infection strategy of the "Piggyback-the-Winner" (PtW) model has been proposed in which lysogeny predominates at high microbial abundance and growth rates (Silveira and Rohwer, 2016). Several studies also supported the PtW model (Knowles et al., 2016; Coutinho et al., 2017). However, these different viral infection strategies could be favored depending on environmental conditions (Bongiorni et al., 2005; Payet and Suttle, 2013). Viral lysis and lysogenic infection also contribute to bacterioplankton community. Similar to phytoplankton, high viral lysis pressure will apply to dominant and fast-growing bacteria, which has been confirmed to have a major impact on bacterial diversity and the community structure, i.e., the "Kill-the-Winner" model (Winter et al., 2010). Besides, lysogeny also has been previously hypothesized to be a preferable survival strategy for both the virus and bacterioplankton (Paul, 2008). Notably, viral lysis predominantly channels particulate organic carbon and nutrients away from higher trophic levels, which was called "viral shunt" (Wilhelm and Suttle, 1999). Nutrients released by viral lysis of heterotrophic bacteria can be efficiently remineralized and transferred to phytoplankton (Weinbauer et al., 2011; Shelford and Suttle, 2018). Currently, the accumulated scientific evidence about the role of viruses is growing fast, but the information about the roles of viruses in bloom succession is still limited.

Cyanobacterial bloom succession has occurred frequently in several tributaries of the Three Gorges Reservoir (TGR), the world's largest hydroelectric power project, since the initial water impounding in 2003 (Zhou et al., 2019). And the summer phytoplankton population succession in Xiangxi Bay of TGR in 2010 was in order as follows: diatom, green algae, cyanobacteria, and the main factors of were water temperature, water stability, and mixed layer depth (Fang et al., 2013). It also has been revealed that nutrients, temperature, light, and hydrodynamic regimes are the key environmental factors affecting the outbreaking and succession of blooms (Fang et al., 2013; Yang et al., 2022). As for viruses in reservoirs, Kopylov and Zabotkina (2021) investigated the distribution of viruses, the frequency of visibly infected cells of heterotrophic bacteria and autotrophic picocyanobacteria and their virus-induced mortality in six reservoirs along the Volga. The viral infection rate of picocyanobacteria in mesoeutrophic reservoir was higher than that in mesotrophic reservoir (Kopylov et al., 2010). Although a large number of reservoirs have been built worldwide, there have been very few studies on the ecological effects of viruses in these manipulated aquatic ecosystems in-depth, especially when the bloom occurs.

In the present study, we investigated the viral lysis and lysogeny of phytoplankton and bacterioplankton in the Xiangxi Bay (the largest tributary of the TGR, China) during a bloom succession event from July 18 to August 29. The abiotic environmental factors were also monitored to compare how they differ from the effects of viral factors during bloom succession. The results revealed that viruses played multiple potential roles in summer bloom succession in Xiangxi Bay of TGR and may facilitate the bloom success of cyanobacteria. These findings provide a foundation for further understanding phytoplankton succession and controlling the cyanobacterial blooms.

2. Materials and methods

2.1. Sampling and physicochemical variables

Xiangxi Bay is the largest tributary close to the Three Gorges Dam in Hubei Province, China. The main stream of Xiangxi Bay is 94 km with a basin area of 3,099 km^2. The study site is located in the middle reaches of Xiangxi Bay (Figure 1), which is affected not only by the main stream of the TGR but also a typical bloom area (Yang et al., 2018).

To monitor viral and environmental parameter variations in summer blooms, water samples at 0.2 m below the water surface were collected at 10 am every 2 days from July 18th to August 29th, 2017. The total nitrogen (TN), total phosphorous (TP), PO_4^{3-}, permanganate index (COD_{Mn}), dissolved silicate (D-Si), chlorophyll *a* (Chl-*a*), and water temperature (*T*) were determined as described by Nwankwegu et al. (2020). One liter of water samples were fixed with Lugol's iodine solution (2% final concentration) and allowed to settle for 48 h. Phytoplankton species were identified according to Paerl et al. (2015).

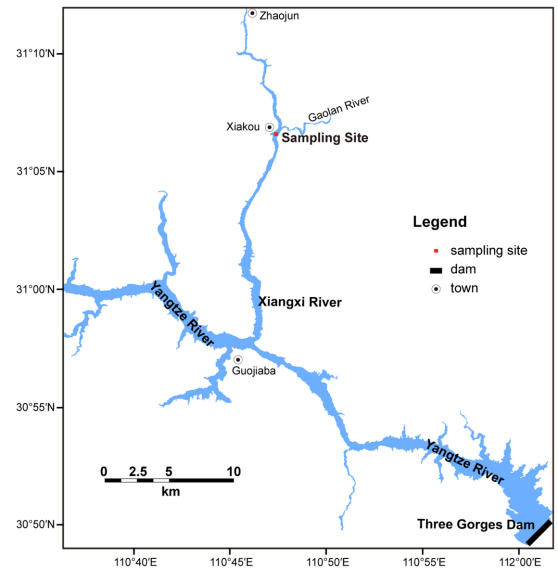

FIGURE 1
Location of the sampling site in Xiangxi Bay of Three Gorges Reservoir.

For the counting of microbial abundances, 5 mL of water samples were firstly fixed with 25% glutaraldehyde to a final concentration of 0.5% for 15–30 min at 4°C, then the samples were flash frozen and stored at −80°C until analysis. Ten liters water samples were collected and put into a polyethylene pot, and then the viral lysis and lysogenic fraction experiments were carried out within 1 h.

2.2. Microbial abundances

Viruses and bacterioplankton were counted simultaneously by epifluorescence microscopy (Steele et al., 2007). Briefly, 1 mL sub-samples from the glutaraldehyde-fixed samples vacuum-filtered onto an Anodisc 25 mm 0.02-μm filter (Whatman, Middlesex, United Kingdom) for epifluorescence microscopy. When necessary for accurate enumeration, samples were diluted with 0.02 μm-filtered water prior to filtration. The filter was stained for 15 min with SYBR green I solution (1:400) in the dark. After being dried, the filter was placed on a glass slide and mounted with an antifade mounting solution. For each filter, a minimum of 200 bacteria and 200 viruses were counted in random fields of view. Analyses were performed under 1,000 × magnification with an epifluorescence microscope (Leica DMR, Wetzlar, Germany) equipped with a 100 W high-pressure mercury lamp and using light filters for blue excitation (450–490 nm wide bandpass).

Phytoplankton was analyzed without staining, but by using their natural autofluorescence. Briefly, 2 ml water samples were filtered onto 0.22 μm pore size cellulose acetate layer sheets (Xinya, Shanghai, China). Then, phytoplankton were counted by their orange and red autofluorescence (that is, Chl *a*, present in all phytoplankton; Parésys et al., 2005) under blue excitation light (450–490 nm wide bandpass) using a Leica DMR microscope. To obtain reliable estimates of abundance of phytoplankton, at least 200 phytoplankton were counted in random fields per sample under a 200 × magnification.

2.3. Viral lysis rate

Phytoplankton community is controlled by viral induced lysis of phytoplankton directly and also influenced by the viral induced lysis of bacterioplankton indirectly (Weinbauer et al., 2011; Biggs et al., 2021). The modified dilution approach was used to determine the viral induced mortality on both phytoplankton and bacterioplankton (Parvathi et al., 2014; Tsai et al., 2015a). First, sampling water was gently passed through a 200 μm mesh, 0.2 μm membrane (Pall, Dreieich, Germany), and a 30 kDa tangential flow filtration system (Sartorius Stedim Biotech, Göttingen, Germany) to create mesoplankton-free whole water, grazer-free water, and virus-free water, respectively. Then, the mesoplankton-free whole water was mixed with 0.2 μm diluent or 30 kDa ultrafiltrate in proportions of 100, 70, 40, and 20%, to gradually decrease the mortality impact with increasing dilution. All experiments were performed in triplicate in 0.5 L clear polycarbonate bottles. After preparation of the two parallel dilution series, a 3 ml subsample was taken for phytoplankton and bacterioplankton enumeration as specified in section 2.2. And the bottles were incubated for 24 h *in situ*. After the 24-h incubation, a second phytoplankton and bacterioplankton count was executed. Apparent phytoplankton and bacterioplankton growth rates (μ, d^{-1}) of 0.2 μm and 30 kDa diluent series (i.e., 100, 70, 40, and 20%) are calculated from the changes in abundance during the incubation using the equation:

$$\mu = \ln\left(P_t / P_0\right) / t$$

where P_t and P_0 are the final and initial measured phytoplankton and bacterioplankton abundance, respectively, and t is the duration of the experiment.

Linear regression analysis of apparent growth rates against fraction of water is applied to each of the dilution experimental series (0.2 μm and 30 kDa diluent series). The grazing rates of phytoplankton and bacterioplankton were estimated from the regression coefficient of the apparent growth rate for the 0.2 μm series, whereas the combined rate of viral induced lysis and grazing was estimated from the regression for the 30 kDa series. Viral mortality of phytoplankton and bacterioplankton were determined from the corresponding significant difference between the two regression coefficients of 0.2 μm and 30 kDa series (as tested by analysis of covariance; Kimmance et al., 2007).

2.4. The percent of lysogeny

Lysogeny in particular is assumed to be a beneficial life strategy for both hosts and viruses under unfavorable conditions (Weinbauer et al., 2003). The lysogenic fractions of phytoplankton and bacterioplankton were determined using the mitomycin C method (Williamson et al., 2002). One hundred milliliters of mesoplankton-free whole water (the sampling water filtered with 200 μm mesh) was filtered through a 0.2 μm filter (Pall, Dreieich, Germany) using a 47 mm filtration apparatus to reduce the volume to approximately 5 ml. Then, 100 ml of virus-free water (the sampling water filtered with 30 kDa membrane) was added back to the remaining 5 ml of the 0.2 μm filtered sample, and the volume was once again reduced to

approximately 5 ml through filtration. The filtration and resuspension processes were repeated three times. Subsequently, virus-reduced samples were either added to a final concentration of 1 μg/mL mitomycin C (Sigma-Aldrich, St. Louis, United States) or left untreated as controls. All samples were incubated at room temperature in the dark for 24 h and counted using the method as described in section 2.2 to obtain the abundances of phytoplankton and bacterioplankton after 24 h. The frequency of lysogenic cells (FLC) of phytoplankton and bacterioplankton were calculated according to the following equation:

$$FLC = \frac{(C_{24} - T_{24})}{C_{24}} \times 100\%$$

where, C_{24} and T_{24} are the number of phytoplankton or bacterioplankton enumerated in the control and induced samples at 24 h, respectively.

2.5. Statistical analysis

The taxonomic compositions of the phytoplankton communities were analyzed at the species level (for these with relative abundance >1%) and visualized using the R (v4.2.2) package "ggplot2". To display the succession of phytoplankton community composition, hierarchical cluster analysis (HCA) and principal coordinate analysis (PCoA) were carried out using Bray–Curtis distance based on the relative abundance matrices of phytoplankton species. Permutational multivariate ANOVA (PERMANOVA, $n = 999$) was then used to examine the statistical significance of differences among the bloom stages (Anderson, 2001). According to the bloom stages defined by HCA, a box plot of viral lysis rate and the percent of lysogeny was constructed and one way ANOVA was performed to test the difference among the bloom stages.

To understand the relationship between viral factors and phytoplankton community succession, the structural equation modeling (SEM) was used to test the pathway that the virus changed the phytoplankton community. All variables were transformed by log10 $(x+1)$ before SEM and we determined the latent variables first. To support a conclusion that virus shaped the blooms succession (i.e., the change of phytoplankton community), the latent variable "Phytoplankton" was determined as a proxy for phytoplankton community change. As for other latent variables which have close relation with latent variable phytoplankton community, we concluded as "Virus", "Nutrient", and "Physical factor" in our study. We next chose the observed variables to each latent variable. Spearman's correlation analysis was performed to examine the relationships among all variables, and variables were filtered with high correlation to simplify the modeling. Then, we took the most likely paths in consideration and checked the suitability of the estimated parameters. The SEM was finally established after the remove of some observed variables. And the SEM fitness was examined on the basis of a non-significant chi-square (χ^2) test ($p > 0.05$), the comparative fit index (CFI > 0.95), and the root mean square error of approximation (RMSEA < 0.05; Jonsson and Wardle, 2010; Shen et al., 2019).

Spearman's correlation analysis was also used to identify the correlations between the phytoplankton community and viral factors (including viral abundance, viral-induced lysis rate of phytoplankton, viral-induced lysis rate of bacterioplankton, frequency of lysogenic phytoplankton, and frequency of lysogenic bacterioplankton) using the R package "psych". As for phytoplankton community, relevant indicators include abundance of different species of phytoplankton, Shannon Wiener index, PCo1 (principal component score in axis 1 of PCoA) and PCo2 (principal component score in axis 2 of PCoA). Only statistically significant correlations ($p < 0.05$) are shown. Due to the result of the longest gradient lengths obtained by detrended correspondence analysis (DCA) were <3, we further performed redundancy analysis (RDA) to examine the effect of environmental factors (including viral factors) on the succession of summer blooms using "vegan" package of the statistical language R. Hellinger transformation of phytoplankton abundance was carried out before performing RDA to minimize the effect of zeroes in the community data, and environmental factors were transformed with log10 $(x+1)$ to approximate a normal distribution. To obtain the parsimonious model, environmental variables were selected by calculating variance inflation factors, and environmental variables with variance inflation factors >8 were removed. Then, a Monte Carlo test (999 permutations) based on the RDA was used to assess the significance of RDA model and each selected variable ($p < 0.05$; Brener-Raffalli et al., 2018; Hao et al., 2020). And we further determined the explanation effect of each selected environmental factor on the RDA results based on the hierarchical partitioning method using the "rdacca.hp" package in R (Lai et al., 2022).

3. Results

3.1. Dynamics of bloom characteristics

According to the HCA (Figure 2) and PCoA (Figure 3), three significant ($p < 0.05$) summer bloom stages were observed: Bloom I (18th July—30th July), Bloom II (30th July—17th August), and Bloom III (17th August—29th August). There was an increasing trend in the mean concentrations of Chl *a*, which were 23.27, 29.18, and 45.50 μg/L, respectively (Table 1). Both *Microcystis* sp. (Cyanophyta) and *Melosira granulata* var. *angustissima* (Bacillariophyta) were dominant in Bloom I. However, only *Microcystis* sp. dominated in Bloom II. *Microcystis* sp. and *Anabaena circinalis* (Cyanophyta) were the main species in Bloom III. Corresponding to the three stages, there were two successions, including the first succession from eukaryotic algae to cyanobacteria (Bloom I–Bloom II) and the second succession among different cyanobacterial genera (Bloom II–Bloom III).

There was an increase in the abundance of viruses and a decrease of bacterioplankton along the bloom succession (Table 1). For the abiotic characteristics (Table 1), the TN concentrations were 1.78, 1.77, and 1.26 mg/L, respectively, which decreased markedly in Bloom III. The TP concentration decreased gradually with succession proceeded and was 0.12, 0.11, and 0.10 mg/L along the three bloom stages. The concentrations of PO_4^{3-} and D-Si first decreased and then increased. In addition, the average water temperature first increased slightly and then decreased to 28.00, 28.52, and 26.50°C, respectively. Temporal variation of environmental characteristics in the summer bloom succession was shown in Supplementary Table S1.

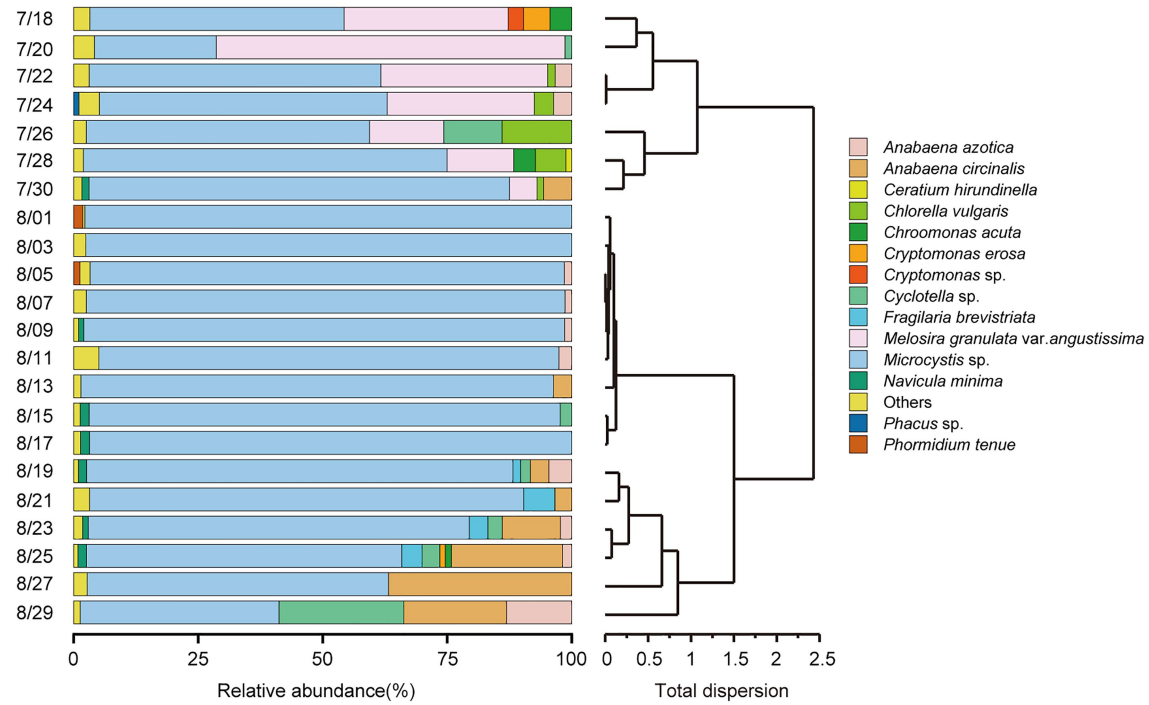

FIGURE 2
Temporal trends in phytoplankton community composition at the species level (relative abundance of >1%) and hierarchical cluster analysis (HCA) were applied to identify the succession of phytoplankton compositional change based on Bray–Curtis dissimilarity matrices.

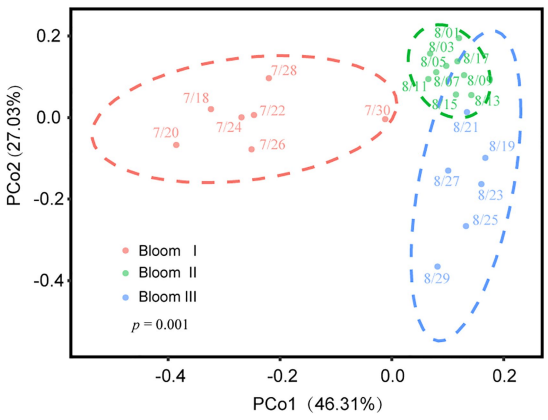

FIGURE 3
Variation in beta diversity visualized using principal coordinate analysis (PCoA). Different color regions represented the 95% bootstrapped confidence ellipses of each bloom stage. The PERMANOVA test determined that phytoplankton communities diverged significantly in these three stages (p=0.001).

3.2. Viral lysis and lysogeny

To assess influence of viruses on phytoplankton community, we quantified the viral lysis to the mortality of phytoplankton and bacterioplankton by conducting 22 modified dilution assays during the summer blooms (see Supplementary Table S2 for details). And prophage induction by mitomycin C was also applied to quantify the percent of lysogenic phytoplankton and bacterioplankton (see Supplementary Table S2 for details).

The viral lysis rates of phytoplankton and bacterioplankton in the three bloom stages were significantly different ($p < 0.05$; Figure 4). The viral lysis rate of phytoplankton (VLP) in Bloom I, II, and III first decreased and then increased (Figure 4A). The mean VLP was the highest (0.251 d^{-1}) in Bloom I and the lowest (0.124 d^{-1}) in Bloom II. The viral lysis rate of bacterioplankton (VLB) increased gradually during the summer blooms and reached up to 0.312 d^{-1} in Bloom III (Figure 4C).

The frequency of lysogenic phytoplankton and bacterioplankton in the three bloom stages were also significantly different ($p < 0.05$; Figure 4). The frequency of lysogenic phytoplankton (FLP) first increased and then decreased, with the highest mean FLP (38.52%) in Bloom II (Figure 4B). The frequency of lysogenic bacterioplankton (FLB) were observed to decrease gradually from Bloom I to Bloom III (Figure 4D).

3.3. Effects of viruses on phytoplankton community succession

A structural equation model was successfully established ($\chi^2 = 0.719$, $p = 0.698$, CFI = 1.0, GFI = 0.987, RMSEA = 0; Figure 5). In the final SEM, Shannon Wiener index was used to model the latent variable "Phytoplankton" as a proxy for phytoplankton community change. The SEM analysis showed that Virus, Nutrient, and Physical factor all had influence on the phytoplankton diversity, and Virus and Nutrient had higher path coefficient than Physical factor. In latent variable "Virus", VLP was the only important factor, and VLB, FLP,

TABLE 1 Mean (±SD) microbial and environmental characteristics of the summer bloom succession in Xiangxi Bay from 18th July to 29th August 2017.

	Bloom I mean±SD	Bloom II mean±SD	Bloom III mean±SD
Viral abundance (10^7 VLPs/mL)	0.29 ± 0.10	0.67 ± 0.79	0.71 ± 0.32
Bacterial abundance (10^6 cells/mL)	1.90 ± 0.80	1.43 ± 0.47	1.45 ± 0.43
Phytoplankton abundance (10^6 cells/L)	4.84 ± 2.42	26.62 ± 51.88	8.36 ± 6.56
Bacillariophyta (10^6 cells/L)	1.73 ± 1.77	0.15 ± 0.13	0.58 ± 0.54
Dinoflagellata (10^6 cells/L)	0.03 ± 0.04	0.02 ± 0.02	0.01 ± 0.01
Cyanophyta (10^6 cells/L)	2.67 ± 1.18	26.41 ± 51.73	7.63 ± 6.01
Euglenophyta (10^6 cells/L)	0.01 ± 0.01	0.00	0.00
Chlorophyta (10^6 cells/L)	0.28 ± 0.44	0.03 ± 0.02	0.02 ± 0.02
Cryptophyta (10^6 cells/L)	0.13 ± 0.13	0.02 ± 0.02	0.07 ± 0.07
TN (mg/L)	1.78 ± 0.24	1.77 ± 0.49	1.26 ± 0.53
TP (mg/L)	0.12 ± 0.14	0.11 ± 0.07	0.10 ± 0.03
COD_{Mn} (mg/L)	2.13 ± 0.22	2.09 ± 1.66	2.54 ± 0.41
PO_4^{3-} (mg/L)	0.006 ± 0.003	0.001 ± 0.001	0.004 ± 0.001
D-Si (mg/L)	8.42 ± 5.66	4.93 ± 1.14	5.10 ± 0.25
Temperature (°C)	28.00 ± 0.50	28.52 ± 0.81	26.50 ± 0.37
Chl *a* (μg/L)	23.27 ± 9.47	29.18 ± 36.92	45.50 ± 21.44

VLPs, virus like particles; TN, total nitrogen; TP, total phosphorus; D-Si, dissolved silicate; and Chl *a*, chlorophyll *a*.

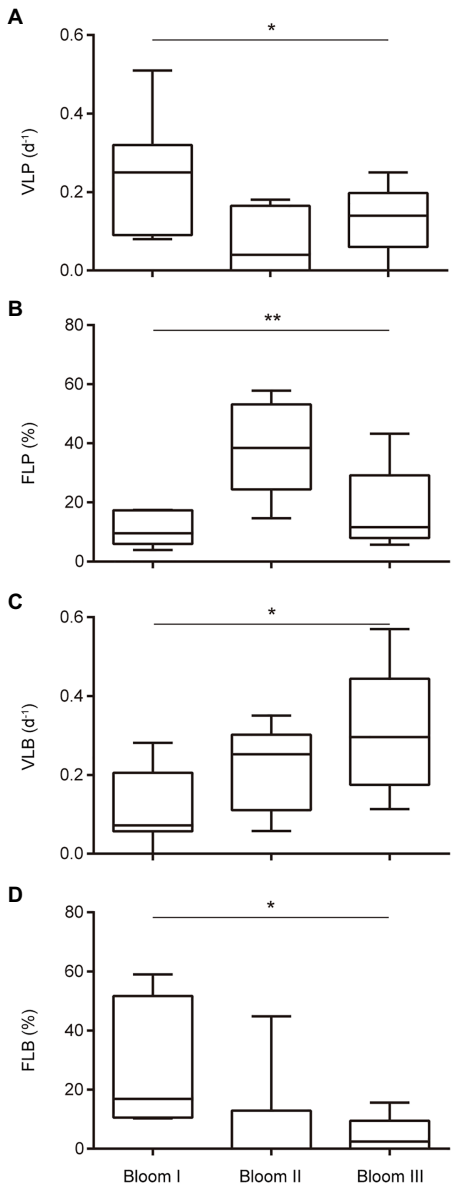

FIGURE 4
Boxplot of the viral-induced lysis rate of phytoplankton (VLP) **(A)**, viral-induced lysis rate of bacterioplankton (VLB) **(C)**, frequency of lysogenic phytoplankton (FLP) **(B)**, and frequency of lysogenic bacterioplankton (FLB) **(D)** in three bloom stages. * and ** indicate significant differences among the three stages at $p < 0.05$ and $p < 0.01$, respectively.

and FLB were deleted in SEM adjustments. Besides, TN and N:P were important to model the latent variable "Nutrient", and PO_4^{3-}, COD_{Mn}, D-Si were also deleted in SEM adjustments. Similarly, *T* was the only important factor to model the latent variable "Physical factor".

The Spearman rank correlation analysis also showed strongly association between viral infection characteristics and phytoplankton community composition. Specifically, there was significant positive correlation between the VLP and Bacillariophyta, Euglenophyta as well as Chlorophyta ($p < 0.05$; Figure 6). PCoA results for the phytoplankton communities are shown in Figure 3. As the indexes of phytoplankton community structure, the first PCoA axis (PCo1) explained 46.31% of the total variance, and the second was 27.03%. And both the Shannon index of phytoplankton community and the values of axis 2 (PCo2) of PCoA exhibited significant correlations with the FLP ($p < 0.05$). The FLB had a significant negative correlation with the values of axis 1 (PCo1) of PCoA ($p < 0.05$).

Redundancy analysis was another method to explore the importance of viruses to the phytoplankton community. Monte Carlo test revealed that the RDA model was significant ($p < 0.01$), and also showed that the explanatory variables (TN, T, PO_4^{3-}, VA, VLP, VLB, and FLP) selected by variance inflation factors were contributed significantly ($p < 0.05$) to the RDA model (Table 2). The first two axes of the RDA (Figure 7) explained 32.05 and 19.22% of the variation in the data, respectively. This variation was closely related to the viral factors. For example, the eukaryotic algae, such as *M. granulata* var. *angustissima*, *Chlorella vulgaris*, *Chroomonas acuta*, *Cryptomonas erosa*, and *Cryptomonas* sp., were positively correlated with the VLP and were negatively correlated with the FLP (Figure 7). Besides, a positive relationship of the VLB, VA with *A. circinalis*, *Anabaena azotica*, and *Fragilaria brevistriata* were found (Figure 7). Hierarchical partitioning analysis demonstrated that viral factors (VA, VLP, VLB,

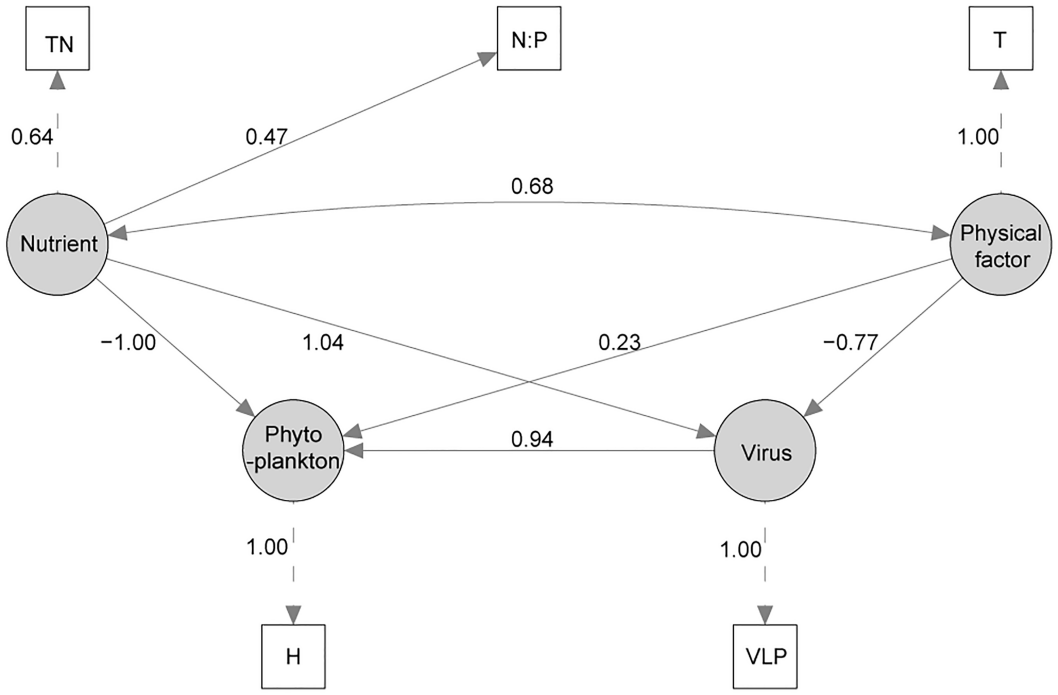

FIGURE 5
The structural equation model (SEM) of the effects of virus, nutrient, and physical variable on phytoplankton community. Measured variables are indicated with rectangles, latent (unmeasured) variables with ovals. Numbers beside each arrow indicate the standardized path coefficient. (TN, total nitrogen; N:P, TN/TP ratio; *T*, water temperature; VLP, viral-induced lysis rate of phytoplankton; H, Shannon Wiener index).

and FLP) had obvious effect on the phytoplankton composition among the seven selected significant explanatory variables (Table 2) included in RDA model [total R^2 (adj) = 0.433], which was lower than that independently explained by environmental factors (i.e., PO_4^{3-}, TN, and T).

4. Discussion

In the present study, three stages of summer bloom succession were observed (Figures 2, 3; Table 1) and this phenomenon occurs frequently in Xiangxi Bay of the TGR (Fang et al., 2013). Both phyto- and bacterioplankton lytic and lysogenic infection characteristics were significantly different in these three stages (Figure 4) and may have influenced the succession of summer blooms by different ways from the analysis of SEM, Spearman rank correlation, RDA, and Hierarchical partitioning (Table 2; Figures 5–7). And these effects of viruses in summer bloom succession may further have helped the success of cyanobacterial bloom.

To explore the causation between virus and the phytoplankton community succession, the biodiversity of Shannon Wiener index (H) was used as the observed variable of phytoplankton in SEM. The path coefficient between H and latent variable "phytoplankton" was 1.0, which showed that the SEM could explain the most of the variation of H. Nutrient, virus, and physical factor are the factors influence the H, but Nutrient and Virus are more important. Many other studies also have shown that nutrient was more important than climate change for phytoplankton community change (Yan et al., 2019; Zhang et al., 2021). As for virus, VLP was the only important factor and showed positive influence on H, which is similar to the "Kill-the-Winner" (KtW) model for maintaining high prokaryotic richness (Winter et al., 2010). Besides, VLP may be suppressed under a higher temperature for the adaption of virus to the adverse environment (Tsai et al., 2015b; Stough et al., 2017), which was also reflected in SEM (Figure 5). And there are reports with similar feature that nutrient had positive influence to VLP (Kopylov et al., 2010; Payet and Suttle, 2013). Overall, the established SEM has high credibility, and results showed that virus had obvious influence on phytoplankton diversity.

From Bloom I to Bloom II, the first successional shift was from cyanobacteria-diatom (*Microcystis* sp. and *M. granulata* var. *angustissima* codominance) to cyanobacteria (*Microcystis* sp. dominance) blooms, which can be described as the succession of different phyla. The roles of viral infection may include photosynthetic eukaryotic community suppression and cyanobacterial enhancement, and they were both likely to be work positively for the first succession and helped the success of cyanobacterial bloom.

In our speculation that the suppression of photosynthetic eukaryotic community in the first succession, the VLP was higher in Bloom I (Figure 4A) and also exhibited significant positive relationships with eukaryotic algal species (Figures 6, 7), which showed the potential control of eukaryotic community. Kopylov et al. (2010) found that mesoeutrophic reservoir have higher viral-induced mortality than mesotrophic one. In our study, water with high nutrient levels in Bloom I may contribute to result of the higher VLP. In Lake Taihu, Pound et al. (2020) also observed that the viral lysis may suppresses the eukaryotic community during the *Microcystis* bloom and regarded that the virus-mediated transition from diatoms to cyanobacteria could be explained within the

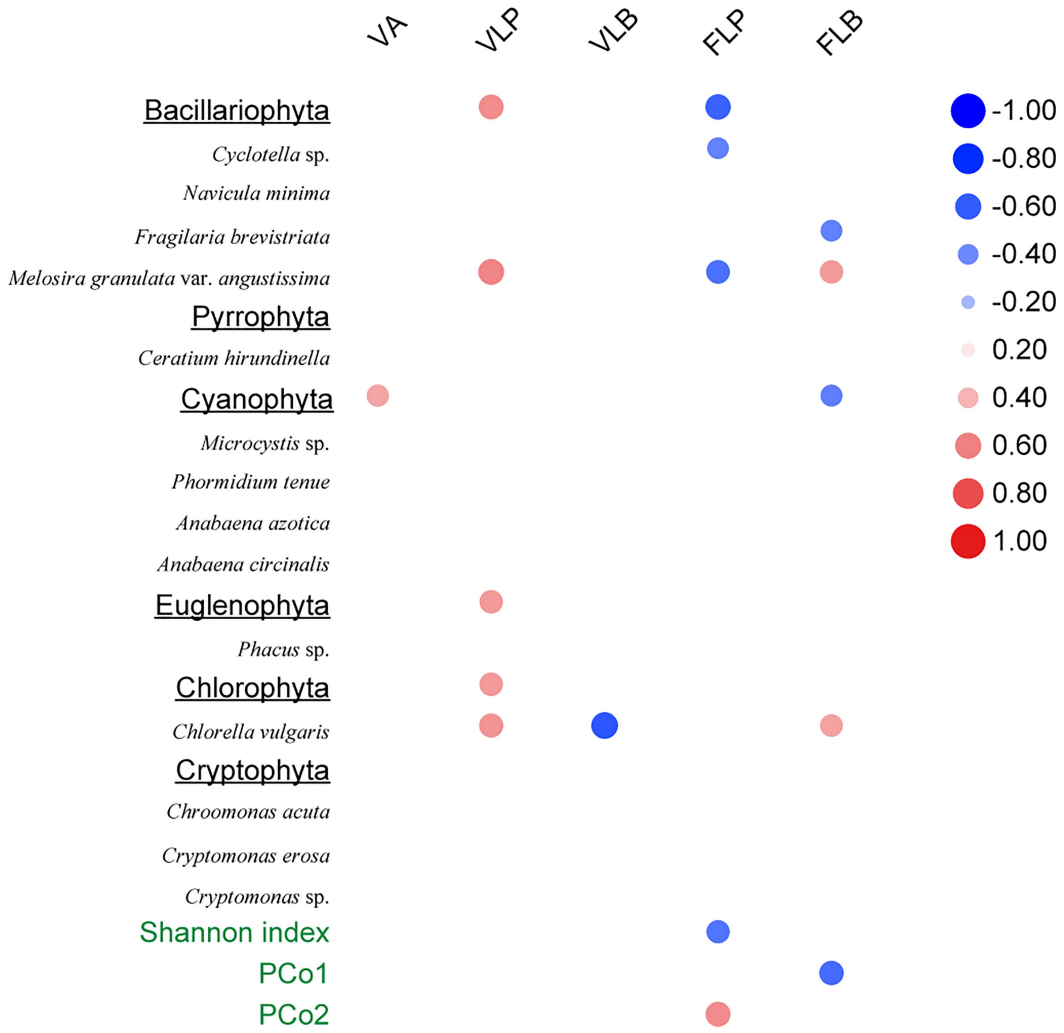

FIGURE 6
Spearman rank correlations between viral-related variables and the phytoplankton community composition. Only statistically significant (p<0.05) correlations are shown. Right column data represent correlation coefficient.

TABLE 2 Percentage and significance of the seven selected explanatory variables to the summer phytoplankton community composition change.

Variables	Individual importance	I. Perc (%)[a]	p value[b]
TN	0.0580	13.39	0.0290
PO_4^{3-}	0.2097	48.43	0.0001
T	0.0724	16.72	0.0001
VA	0.0143	3.30	0.0229
VLP	0.0294	6.79	0.0447
VLB	0.0060	1.39	0.0491
FLP	0.0432	9.98	0.0191
Total	0.433	100	

[a]Individual effects as a proportion of total corrected R^2.
[b]p value for the permutation test based on 999 randomizations.

context of a modified version of the KtW model. However, different from the relatively stable hydrological conditions in Lake Taihu, the hydrological conditions in Xiangxi Bay were much more complex due to the reservoir operation (Xu et al., 2011). These hydrodynamic changes shaped the abiotic environments significantly and affected the algal bloom in Xiangxi Bay (Yang et al., 2018). Unavoidably, the hydrodynamic conditions (including tide, thermal stratification, flow velocity changes, and water vertical mixing) can strongly affect the virus-host interactions (Auguet et al., 2005; Barros et al., 2010; Säwström and Pollard, 2012; Chen et al., 2019). Although hydrodynamic conditions in Xiangxi Bay are susceptible to human manipulation and may affect viral infection, there was still obvious viral lysis suppression on eukaryotic algal community in Xiangxi Bay, which is similar to the role of viruses in Lake Taihu (Pound et al., 2020). The summer hydrodynamic conditions in Xiangxi Bay (including stable stratification, low surface mixing layer depth, and velocity) that created similar with shallow lakes may contributed to this result (Zhao et al., 2012; Yang et al., 2018). However, it is regrettable that potential effect of hydrodynamic changes on the bloom dynamics cannot be discussed due to the lack of monitoring data. In addition, silicon limitation has been found to facilitate the viral infection and mortality of marine diatoms in marine environments (Kranzler

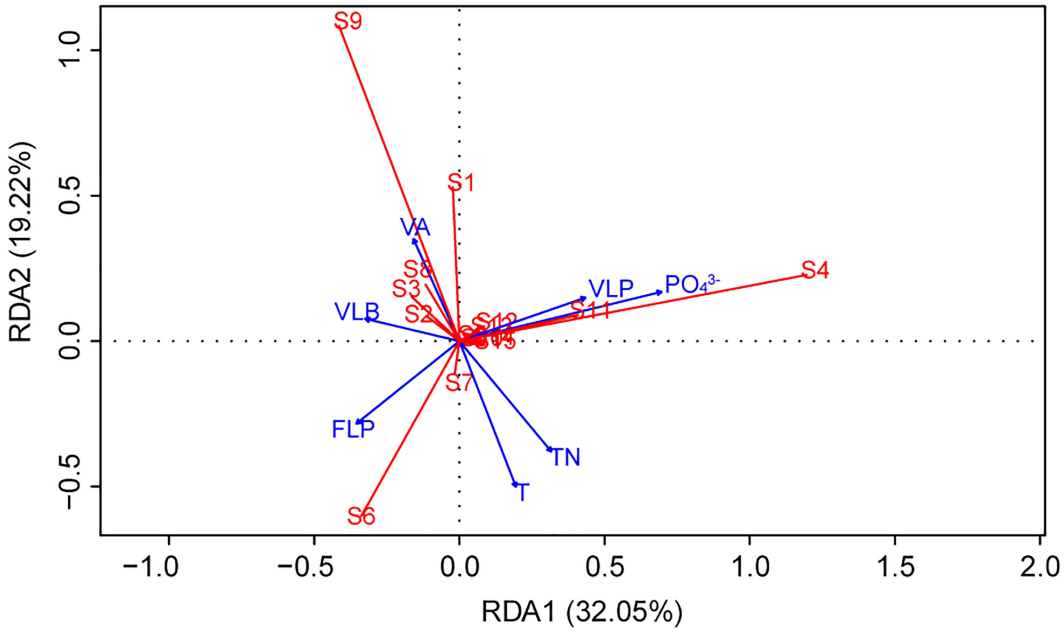

FIGURE 7
Redundancy analysis (RDA) ordination plot describing the phytoplankton community composition (response variables, in red) in relation to viral and environmental variables (explanatory variables, in blue). (S1, *Cyclotella* sp.; S2, *Navicula minima*; S3, *Fragilaria brevistriata*; S4, *Melosira granulata* var. *angustissima*; S5, *Ceratium hirundinella*; S6, *Microcystis* sp.; S7, *Phormidium tenue*; S8, *Anabaena azotica*; S9, *Anabaena circinalis*; S10, *Phacus* sp.; S11, *Chlorella vulgaris*; S12, *Chroomonas acuta*; S13, *Cryptomonas erosa*; S14, *Cryptomonas* sp.; and S15, Others).

et al., 2019). And silicate concentration was significantly reduced in the first bloom succession (Table 1), which may also act as the constraining nutrient that causes the collapse of diatoms and provides opportunities for the later cyanobacterial bloom.

As for cyanobacterial enhancement, there was an increasing abundance of *Microcystis* sp. during the first succession (Table 1) and the highest FLP in *Microcystis* bloom (Figure 4B). The infection characteristic of FLP may also have influenced the phytoplankton composition. Specifically, the Shannon diversity index of the phytoplankton community decreased with increasing FLP (Figure 6). The second component in the PCoA, which captured the second-most amount of variance in the phytoplankton communities (Figure 6), showed a positive correlation with FLP. Previous studies have shown that *Microcystis* can resist viral lysis through high number of restriction modification systems (Zhao et al., 2018), and may also minimize losses by forming a lysogenic state (Stough et al., 2017). Knowles et al. (2016) found that the viral densities were more consistent with temperate than lytic life cycles with increasing microbial abundance and growth rates, which was the infection strategy of the PtW model. The potential for *Microcystis* to resist viral lysis and increase dominance by forming a lysogenic state could be another important factor that allows for cyanobacterial dominance and the first succession.

From Bloom II to Bloom III, the second succession was the bloom of different cyanobacterial genera (*Microcystis* sp. dominance to *Microcystis* sp. and *A. circinalis* codominance). VLB, which has significant contribution in RDA model (Table 2), showed a positive relationship with different species (e.g., *A. circinalis* and *A. azotica*; Figure 7). Nutrients released by viral lysis of heterotrophic bacteria may help the second succession and contribute to the continued success of cyanobacterial bloom. And indeed, there exist a decline of bacterioplankton along the succession (Supplementary Table S1) and an increase of PO_4^{3-} in Bloom III (Table 1). In Bloom II and III, TN/TP ratios were 16.1 and 12.6, respectively. And there was the lowest TN in Bloom III (Table 1). Tian et al. (2012) also found the decrease of nitrate in summer bloom of *Anabaena* in Xiangxi Bay and N limitation was considered as an important cause. Besides, the heterocytes existed in the morphological features of *Anabaena* in Bloom III during the phytoplankton species identification, which is a typical characteristic for nitrogen fixation (Golden and Yoon, 1998). And there was a high concentration of TN in Bloom I, which *Anabaena* was not dominant during this period. Hence, there was high possibility of N limitation in Bloom III, which may cause the replacement of non-N_2-fixing *Microcystis* sp. by N_2-fixing *A. circinalis*. Previous studies showed a competitive advantage of *Microcystis* at low P concentrations because of its ability to rapidly uptake and store inorganic P, which also caused P deficiency to other coexisting phytoplankton species in Bloom II (Wan et al., 2019). During the second succession, the PO_4^{3-} concentration in Xiangxi Bay was still low, but an increase in Bloom III (Table 1), which might be caused by the increase of the VLB, and may help the growth of N_2-fixing species. Importantly, N_2 fixation, a metabolically expensive process, is controlled by P availability (Wang et al., 2018). Vanderhoef et al. (1974) found the increased algal growth and nitrogen fixation are correlated with higher phosphate concentrations. Weinbauer et al. (2011) found that the abundant regenerative nutrients required for *Synechococcus* growth were adequately provided due to the viral lysis of heterotrophic bacteria. Tsai (2020) emphasized the importance of the viral shunt of bacteria and quantified the P nutrient released by the viral lysis to be approximately 597.6 ng P L^{-1} d^{-1} in coastal waters.

From Bloom II to Bloom III, the VLB followed a rising trend, the average size increasing from 0.211 to 0.312 d^{-1} (Figure 4), which may also contribute to the increase of PO_4^{3-} concentration from 0.001 mg/L in Bloom II to 0.004 mg/L in Bloom III (Table 1) and finally help the growth of N_2-fixing species.

This study found that the variation of phytoplankton communities during summer bloom successions was closely associated with the changes in abiotic environmental factors (i.e., T, TN, and PO_4^{3-}) and viral factors (i.e., VA, VLP, FLP, and VLB; Table 2; Figures 6, 7). Hierarchical partitioning method has been widely used to estimate the individual importance of each explanatory variable (Li et al., 2022; Pecuchet et al., 2022). Based on the hierarchical partitioning analysis, the viral variables still have a marked effect on the dynamics of phytoplankton community, although the environmental attributes were the major factors (Table 2). Studies on the estimate of the viral lysis in bloom succession are scarce, so the importance of viruses compared to other factors remain uncertain. However, our results quantified the size of the viral infection characteristics of phytoplankton and bacterioplankton, and showed that viruses may play an important role in summer bloom succession (Figures 5–7). Moreover, our findings were consistent with other studies which showed that viruses were important in bloom control (Jacquet et al., 2002; Du et al., 2020). In general, viruses may play vital roles in phytoplankton community regulation, but these roles may be ignored. And our results highlighted the need for understanding viral infection dynamics in realistic environmental contexts to better predict their biogeochemical consequences (Mojica et al., 2016; Zimmerman et al., 2020).

5. Conclusion

The roles of viruses in cyanobacterial blooms and taxa succession have yet to be well elucidated in aquatic ecosystems, including the world largest hydropower reservoir, TGR. In this study, viral infection characteristics monitoring during the summer bloom successions was conducted to determine the effects of viruses on cyanobacterial bloom in Xiangxi Bay of TGR. The main conclusions were drawn as follows:

1. Viruses may promote the cyanobacterial blooms and work by multiple and complex ways, including the enhanced lysis of eukaryotic community, the increase of lysogeny in cyanobacteria, and the nutrients supplied from the lysis of bacterioplankton.
2. Multiple potential roles of viruses were found during the bloom succession, highlighting the complexity of viral regulation in helping the summer cyanobacteria bloom success in Xiangxi Bay. Neither the KtW model nor the PtW model can fully explain the roles of viruses in summer bloom succession of Xiangxi Bay. The theoretical framework of virus-host interaction may need further modification.

Data availability statement

The original contributions presented in the study are included in the article/Supplementary material, further inquiries can be directed to the corresponding author.

Author contributions

ML, YZ, and SY conceived and designed the study. YJ and JG performed the analyses. YJ provided the additional sample material. ML, YZ, and WX contributed to the project administration. KP analyzed the results and wrote the manuscript, which was edited and approved by all authors. All authors contributed to the article and approved the submitted version.

Funding

This work was supported by the National Natural Science Foundation of China (No. 51579092) and the National Key Basic Research Program of China (No. 2016YFC0401702).

Conflict of interest

The authors declare that the research was conducted in the absence of any commercial or financial relationships that could be construed as a potential conflict of interest.

Publisher's note

All claims expressed in this article are solely those of the authors and do not necessarily represent those of their affiliated organizations, or those of the publisher, the editors and the reviewers. Any product that may be evaluated in this article, or claim that may be made by its manufacturer, is not guaranteed or endorsed by the publisher.

Supplementary material

The Supplementary material for this article can be found online at: https://www.frontiersin.org/articles/10.3389/fmicb.2023.1112590/full#supplementary-material

References

Anderson, M. J. (2001). A new method for non-parametric multivariate analysis of variance. *Austral. Ecol.* 26, 32–46. doi: 10.1111/j.1442-9993.2001.01070.pp.x

Auguet, J. C., Montanié, H., Delmas, D., Hartmann, H. J., and Huet, V. (2005). Dynamic of virioplankton abundance and its environmental control in the Charente estuary (France). *Microb. Ecol.* 50, 337–349. doi: 10.1007/s00248-005-0183-2

Barros, N., Farjalla, V. F., Soares, M. C., Melo, R. C. N., and Roland, F. (2010). Virus-bacterium coupling driven by both turbidity and hydrodynamics in an Amazonian floodplain lake. *Appl. Environ. Microbiol.* 76, 7194–7201. doi: 10.1128/AEM.01161-10

Baudoux, A. C., Noordeloos, A., Veldhuis, M., and Brussaard, C. (2006). Virally induced mortality of *Phaeocystis globosa* during two spring blooms in temperate coastal waters. *Aquat. Microb. Ecol.* 44, 207–217. doi: 10.3354/ame044207

Biggs, T. E. G., Huisman, J., and Brussaard, C. P. D. (2021). Viral lysis modifies seasonal phytoplankton dynamics and carbon flow in the Southern Ocean. *ISME J.* 15, 3615–3622. doi: 10.1038/s41396-021-01033-6

Bongiorni, L., Magagnini, M., Armeni, M., Noble, R., and Danovaro, R. (2005). Viral production, decay rates, and life strategies along a trophic gradient in the North Adriatic Sea. *Appl. Environ. Microbiol.* 71, 6644–6650. doi: 10.1128/AEM.71.11.6644-6650.2005

Bratbak, G., Egge, J. K., and Heldal, M. (1993). Viral mortality of the marine alga *Emiliania huxleyi* (Haptophyceae) and termination of algal blooms. *Mar. Ecol. Prog. Ser.* 93, 39–48. doi: 10.3354/meps093039

Brener-Raffalli, K., Clerissi, C., Vidal-Dupiol, J., Adjeroud, M., Bonhomme, F., Pratlong, M., et al. (2018). Thermal regime and host clade, rather than geography, drive *Symbiodinium* and bacterial assemblages in the scleractinian coral *Pocillopora damicornis sensu lato*. *Microbiome* 6:39. doi: 10.1186/s40168-018-0423-6

Brussaard, C. P. (2004). Viral control of phytoplankton populations--a review. *J. Eukaryot. Microbiol.* 51, 125–138. doi: 10.1111/j.1550-7408.2004.tb00537.x

Chapra, S. C., Boehlert, B., Fant, C., Bierman, V. J., Henderson, J., Mills, D., et al. (2017). Climate change impacts on harmful algal blooms in U.S. freshwaters: a screening-level assessment. *Environ. Sci. Technol.* 51, 8933–8943. doi: 10.1021/acs.est.7b01498

Chen, X., Wei, W., Wang, J., Li, H., Sun, J., Ma, R., et al. (2019). Tide driven microbial dynamics through virus-host interactions in the estuarine ecosystem. *Water Res.* 160, 118–129. doi: 10.1016/j.watres.2019.05.051

Chun, S., Cui, Y., Lee, J. J., Choi, I., Oh, H., and Ahn, C. (2020). Network analysis reveals succession of *Microcystis* genotypes accompanying distinctive microbial modules with recurrent patterns. *Water Res.* 170:115326. doi: 10.1016/j.watres.2019.115326

Coutinho, F. H., Silveira, C. B., Gregoracci, G. B., Thompson, C. C., Edwards, R. A., Brussaard, C. P. D., et al. (2017). Marine viruses discovered via metagenomics shed light on viral strategies throughout the oceans. *Nat. Commun.* 8:15955. doi: 10.1038/ncomms15955

Du, X., Cai, Z., Zuo, P., Meng, F., Zhu, J., and Zhou, J. (2020). Temporal variability of virioplankton during a *Gymnodinium catenatum* algal bloom. *Microorganisms* 8:107. doi: 10.3390/microorganisms8010107

Fang, L., Liu, D., Yang, Z., Ao, X., Hu, X., and Tian, Z. (2013). Succession of phytoplankton in Xiangxi Bay of three-gorge reservoir in summer and its causes. *J. Ecol. Rural Environ.* 29, 234–240.

Fuhrman, J. A. (1999). Marine viruses and their biogeochemical and ecological effects. *Nature* 399, 541–548. doi: 10.1038/21119

Golden, J. W., and Yoon, H. (1998). Heterocyst formation in anabaena. *Curr. Opin. Microbiol.* 1, 623–629. doi: 10.1016/S1369-5274(98)80106-9

Hao, B., Wu, H., Zhen, W., Jo, H., Cai, Y., Jeppesen, E., et al. (2020). Warming effects on periphyton community and abundance in different seasons are influenced by nutrient state and plant type: a shallow lake mesocosm study. *Front. Plant Sci.* 11:404. doi: 10.3389/fpls.2020.00404

Hewson, I., O'Neil, J. M., and Dennison, W. C. (2001). Virus-like particles associated with *Lyngbya majuscula* (Cyanophyta; Oscillatoriacea) bloom decline in Moreton Bay. *Aust. Aquat. Microb. Ecol.* 25, 207–213. doi: 10.3354/ame025207

Huisman, J., Codd, G. A., Paerl, H. W., Ibelings, B. W., Verspagen, J. M. H., and Visser, P. M. (2018). Cyanobacterial blooms. *Nat. Rev. Microbiol.* 16, 471–483. doi: 10.1038/s41579-018-0040-1

Jacquet, S., Heldal, M., Iglesias, R. D., Larsen, A., Wilson, W., and Bratbak, G. (2002). Flow cytometric analysis of an *Emiliana huxleyi* bloom terminated by viral infection. *Aquat. Microb. Ecol.* 27, 111–124. doi: 10.3354/ame027111

Jonsson, M., and Wardle, D. A. (2010). Structural equation modelling reveals plant-community drivers of carbon storage in boreal forest ecosystems. *Biol. Lett.* 6, 116–119. doi: 10.1098/rsbl.2009.0613

Ke, Z., Xie, P., and Guo, L. (2008). Controlling factors of spring-summer phytoplankton succession in Lake Taihu (Meiliang Bay, China). *Hydrobiologia* 607, 41–49. doi: 10.1007/s10750-008-9365-5

Kimmance, S. A., Wilson, W. H., and Archer, S. D. (2007). Modified dilution technique to estimate viral versus grazing mortality of phytoplankton: limitations associated with method sensitivity in natural waters. *Aquat. Microb. Ecol.* 49, 207–222. doi: 10.3354/ame01136

Knowles, B., Silveira, C. B., Bailey, B. A., Barott, K., Cantu, V. A., Cobián-Güemes, A. G., et al. (2016). Lytic to temperate switching of viral communities. *Nature* 531, 466–470. doi: 10.1038/nature17193

Kopylov, A. I., Kosolapov, D. B., Zabotkina, E. A., and Straskrabova, V. (2010). Distribution of picocyanobacteria and virioplankton in mesotrophic and eutrophic reservoirs: the role of viruses in mortality of picocyanobacteria. *Biol. Bull.* 37, 565–573. doi: 10.1134/S1062359010060038

Kopylov, A. I., and Zabotkina, E. A. (2021). Virioplankton as an important component of plankton in the Volga reservoirs. *Biosyst. Divers.* 29, 151–159. doi: 10.15421/012120

Kranzler, C. F., Krause, J. W., Brzezinski, M. A., Edwards, B. R., Biggs, W. P., Maniscalco, M., et al. (2019). Silicon limitation facilitates virus infection and mortality of marine diatoms. *Nat. Microbiol.* 4, 1790–1797. doi: 10.1038/s41564-019-0502-x

Lai, J., Zou, Y., Zhang, J., and Peres Neto, P. R. (2022). Generalizing hierarchical and variation partitioning in multiple regression and canonical analyses using the rdacca.hp R package. *Methods Ecol. Evol.* 13, 782–788. doi: 10.1111/2041-210X.13800

Li, X., Wang, J., Lin, J., Yin, W., Shi, Y. Y., Wang, L., et al. (2022). Hysteresis analysis reveals dissolved carbon concentration—discharge relationships during and between storm events. *Water Res.* 226:119220. doi: 10.1016/j.watres.2022.119220

Mojica, K. D., Huisman, J., Wilhelm, S. W., and Brussaard, C. P. (2016). Latitudinal variation in virus-induced mortality of phytoplankton across the North Atlantic Ocean. *ISME J.* 10, 500–513. doi: 10.1038/ismej.2015.130

Moustaka-Gouni, M., Vardaka, E., Michaloudi, E., Kormas, K. A., Tryfon, E., Mihalatou, H., et al. (2006). Plankton food web structure in a eutrophic polymictic lake with a history of toxic cyanobacterial blooms. *Limnol. Oceanogr.* 51, 715–727. doi: 10.4319/lo.2006.51.1_part_2.0715

Nwankwegu, A. S., Li, Y., Huang, Y., Wei, J., Norgbey, E., Lai, Q., et al. (2020). Nutrient addition bioassay and phytoplankton community structure monitored during autumn in Xiangxi Bay of three gorges reservoir, China. *Chemosphere* 247:125960. doi: 10.1016/j.chemosphere.2020.125960

Paerl, H. W., Xu, H., Hall, N. S., Rossignol, K. L., Joyner, A. R., Zhu, G., et al. (2015). Nutrient limitation dynamics examined on a multi-annual scale in Lake Taihu, China: implications for controlling eutrophication and harmful algal blooms. *J. Freshw. Ecol.* 30, 5–24. doi: 10.1080/02705060.2014.994047

Parésys, G., Rigart, C., Rousseau, B., Wong, A. W. M., Fan, F., Barbier, J. P., et al. (2005). Quantitative and qualitative evaluation of phytoplankton communities by trichromatic chlorophyll fluorescence excitation with special focus on cyanobacteria. *Water Res.* 39, 911–921. doi: 10.1016/j.watres.2004.12.005

Parvathi, A., Zhong, X., Pradeep Ram, A. S., and Jacquet, S. (2014). Dynamics of auto- and heterotrophic picoplankton and associated viruses in Lake Geneva. *Hydrol. Earth Syst. Sci.* 18, 1073–1087. doi: 10.5194/hess-18-1073-2014

Paul, J. H. (2008). Prophages in marine bacteria: dangerous molecular time bombs or the key to survival in the seas? *ISME J.* 2, 579–589. doi: 10.1038/ismej.2008.35

Payet, J. P., and Suttle, C. A. (2013). To kill or not to kill: the balance between lytic and lysogenic viral infection is driven by trophic status. *Limnol. Oceanogr.* 58, 465–474. doi: 10.4319/lo.2013.58.2.0465

Pecuchet, L., Jørgensen, L. L., Dolgov, A. V., Eriksen, E., Husson, B., Skern Mauritzen, M., et al. (2022). Spatio-temporal turnover and drivers of bentho-demersal community and food web structure in a high-latitude marine ecosystem. *Divers. Distrib.* 28, 2503–2520. doi: 10.1111/ddi.13580

Pound, H. L., Gann, E. R., Tang, X., Krausfeldt, L. E., Huff, M., Staton, M. E., et al. (2020). The "neglected viruses" of Taihu: abundant transcripts for viruses infecting eukaryotes and their potential role in phytoplankton succession. *Front. Microbiol.* 11:338. doi: 10.3389/fmicb.2020.00338

Reavie, E. D., Cai, M., Twiss, M. R., Carrick, H. J., Davis, T. W., Johengen, T. H., et al. (2016). Winter-spring diatom production in Lake Erie is an important driver of summer hypoxia. *J. Great Lakes Res.* 42, 608–618. doi: 10.1016/j.jglr.2016.02.013

Säwström, C., and Pollard, P. (2012). Environmental influences on virus-host interactions in an Australian subtropical reservoir. *Environ. Microbiol. Rep.* 4, 72–81. doi: 10.1111/j.1758-2229.2011.00303.x

Shelford, E. J., and Suttle, C. A. (2018). Virus-mediated transfer of nitrogen from heterotrophic bacteria to phytoplankton. *Biogeosciences* 15, 809–819. doi: 10.5194/bg-15-809-2018

Shen, H., Dong, S., Li, S., Xiao, J., Han, Y., Yang, M., et al. (2019). Grazing enhances plant photosynthetic capacity by altering soil nitrogen in alpine grasslands on the Qinghai-Tibetan plateau. *Agric. Ecosyst. Environ.* 280, 161–168. doi: 10.1016/j.agee.2019.04.029

Silveira, C. B., and Rohwer, F. L. (2016). Piggyback-the-winner in host-associated microbial communities. *Npj Biofilms Microb.* 2:16010. doi: 10.1038/npjbiofilms.2016.10

Steele, J. A., Hewson, I., Schwalbach, M. S., Patel, A., Fuhrman, J. A., and Noble, R. T. (2007). Virus and prokaryote enumeration from planktonic aquatic environments by epifluorescence microscopy with SYBR Green I. *Nat. Protoc.* 2, 269–276. doi: 10.1038/nprot.2007.6

Steffen, M. M., Belisle, B. S., Watson, S. B., Boyer, G. L., Bourbonniere, R. A., and Wilhelm, S. W. (2015). Metatranscriptomic evidence for co-occurring top-down and bottom-up controls on toxic cyanobacterial communities. *Appl. Environ. Microbiol.* 81, 3268–3276. doi: 10.1128/AEM.04101-14

Stough, J. M. A., Tang, X., Krausfeldt, L. E., Steffen, M. M., Gao, G., Boyer, G. L., et al. (2017). Molecular prediction of lytic vs lysogenic states for *Microcystis* phage: Metatranscriptomic evidence of lysogeny during large bloom events. *PLoS One* 12:e184146:e0184146. doi: 10.1371/journal.pone.0184146

Suttle, C. A., Chan, A. M., and Cottrell, M. T. (1990). Infection of phytoplankton by viruses and reduction of primary productivity. *Nature* 347, 467–469. doi: 10.1038/347467a0

Tanvir, R. U., Hu, Z., Zhang, Y., and Lu, J. (2021). Cyanobacterial community succession and associated cyanotoxin production in hypereutrophic and eutrophic freshwaters. *Environ. Pollut.* 290:118056. doi: 10.1016/j.envpol.2021.118056

Tian, Z., Liu, D., Yang, Z., Fang, X., Yao, X., and Fang, L. (2012). Cyanobacterial bloom in Xiangxi Bay, three gorges reservoir. *China Environ. Sci.* 32, 2083–2089. doi: 10.3969/j.issn.1000-6923.2012.11.023

Tsai, A. (2020). Effects of bacteria-virus interaction on *Synechococcus* spp. growth in the coastal waters. *Terr. Atmos. Ocean. Sci.* 31, 691–696. doi: 10.3319/TAO.2020.08.13.01

Tsai, A., Gong, G., Huang, Y. W., and Chao, C. F. (2015a). Estimates of bacterioplankton and *Synechococcus* spp. mortality from nanoflagellate grazing and viral lysis in the subtropical Danshui River estuary. *Estuar. Coast. Shelf Sci.* 153, 54–61. doi: 10.1016/j.ecss.2014.11.032

Tsai, A., Gong, G., and Shiau, W. (2015b). Viral lysis and nanoflagellate grazing on prokaryotes: effects of short-term warming in a coastal subtropical marine system. *Hydrobiologia* 751, 43–54. doi: 10.1007/s10750-014-2170-4

Vanderhoef, L. N., Huang, C. Y., and Musil, R. (1974). Nitrogen fixation (acetylene reduction) by phytoplankton in Green Bay, Lake Michigan, in relation to nutrient concentrations1. *Limnol. Oceanogr.* 19, 119–125. doi: 10.4319/lo.1974.19.1.0119

Verspagen, J. M., Van de Waal, D. B., Finke, J. F., Visser, P. M., Van Donk, E., and Huisman, J. (2014). Rising CO_2 levels will intensify phytoplankton blooms in eutrophic and hypertrophic lakes. *PLoS One* 9:e104325. doi: 10.1371/journal.pone.0104325

Wan, L., Chen, X., Deng, Q., Yang, L., Li, X., Zhang, J., et al. (2019). Phosphorus strategy in bloom-forming cyanobacteria (*Dolichospermum* and *Microcystis*) and its role in their succession. *Harmful Algae* 84, 46–55. doi: 10.1016/j.hal.2019.02.007

Wang, Z., Akbar, S., Sun, Y., Gu, L., Zhang, L., Lyu, K., et al. (2021). Cyanobacterial dominance and succession: factors, mechanisms, predictions, and managements. *J. Environ. Manag.* 297:113281. doi: 10.1016/j.jenvman.2021.113281

Wang, S., Xiao, J., Wan, L., Zhou, Z., Wang, Z., Song, C., et al. (2018). Mutual dependence of nitrogen and phosphorus as key nutrient elements: one facilitates *Dolichospermum flos-aquae* to overcome the limitations of the other. *Environ. Sci. Technol.* 52, 5653–5661. doi: 10.1021/acs.est.7b04992

Weinbauer, M. G., Bonilla-Findji, O., Chan, A. M., Dolan, J. R., Short, S. M., Simek, K., et al. (2011). *Synechococcus* growth in the ocean may depend on the lysis of heterotrophic bacteria. *J. Plankton Res.* 33, 1465–1476. doi: 10.1093/plankt/fbr041

Weinbauer, M. G., Brettar, I., and Höfle, M. G. (2003). Lysogeny and virus-induced mortality of bacterioplankton in surface, deep, and anoxic marine waters. *Limnol. Oceanogr.* 48, 1457–1465. doi: 10.4319/lo.2003.48.4.1457

Wilhelm, S. W., Bullerjahn, G. S., and McKay, R. (2020). The complicated and confusing ecology of *Microcystis* blooms. *MBio* 11, e520–e529. doi: 10.1128/mBio.00529-20

Wilhelm, S. W., and Suttle, C. A. (1999). Viruses and nutrient cycles in the sea. *Bioscience* 49, 781–788. doi: 10.2307/1313569

Williamson, S. J., Houchin, L. A., McDaniel, L., and Paul, J. H. (2002). Seasonal variation in lysogeny as depicted by prophage induction in Tampa Bay, Florida. *Appl. Environ. Microbiol.* 68, 4307–4314. doi: 10.1128/AEM.68.9.4307

Winter, C., Bouvier, T., Weinbauer, M. G., and Thingstad, T. F. (2010). Trade-offs between competition and defense specialists among unicellular planktonic organisms: the "killing the winner" hypothesis revisited. *Microbiol. Mol. Biol. R.* 74, 42–57. doi: 10.1128/MMBR.00034-09

Xu, S., Jiang, Y., Liu, Y., and Zhang, J. (2021). Antibiotic-accelerated cyanobacterial growth and aquatic community succession towards the formation of cyanobacterial bloom in eutrophic lake water. *Environ. Pollut.* 290:118057. doi: 10.1016/j.envpol.2021.118057

Xu, Y., Zhang, M., Wang, L., Kong, L., and Cai, Q. (2011). Changes in water types under the regulated mode of water level in three gorges reservoir. *China. Q. Int.* 244, 272–279. doi: 10.1016/j.quaint.2011.01.019

Yan, D., Xu, H., Yang, M., Lan, J., Hou, W., Wang, F., et al. (2019). Responses of cyanobacteria to climate and human activities at Lake Chenghai over the past 100 years. *Ecol. Indic.* 104, 755–763. doi: 10.1016/j.ecolind.2019.03.019

Yang, Z., Wei, C., Liu, D., Lin, Q., Huang, Y., Wang, C., et al. (2022). The influence of hydraulic characteristics on algal bloom in three gorges reservoir, China: a combination of cultural experiments and field monitoring. *Water Res.* 211:118030. doi: 10.1016/j.watres.2021.118030

Yang, Z., Xu, P., Liu, D., Ma, J., Ji, D., and Cui, Y. (2018). Hydrodynamic mechanisms underlying periodic algal blooms in the tributary bay of a subtropical reservoir. *Ecol. Eng.* 120, 6–13. doi: 10.1016/j.ecoleng.2018.05.003

Zepernick, B. N., Gann, E. R., Martin, R. M., Pound, H. L., Krausfeldt, L. E., Chaffin, J. D., et al. (2021). Elevated pH conditions associated with *Microcystis* spp. blooms decrease viability of the cultured diatom *Fragilaria crotonensis* and natural diatoms in Lake Erie. *Front. Microbiol.* 12:598736. doi: 10.3389/fmicb.2021.598736

Zhang, H., Huo, S., Yeager, K. M., and Wu, F. (2021). Sedimentary DNA record of eukaryotic algal and cyanobacterial communities in a shallow lake driven by human activities and climate change. *Sci. Total Environ.* 753:141985. doi: 10.1016/j.scitotenv.2020.141985

Zhao, L., Song, Y., Li, L., Gan, N., Brand, J. J., and Song, L. (2018). The highly heterogeneous methylated genomes and diverse restriction-modification systems of bloom-forming *Microcystis*. *Harmful Algae* 75, 87–93. doi: 10.1016/j.hal.2018.04.005

Zhao, Q., Sun, J., and Zhu, G. (2012). Simulation and exploration of the mechanisms underlying the spatiotemporal distribution of surface mixed layer depth in a large shallow lake. *Adv. Atmos. Sci.* 29, 1360–1373. doi: 10.1007/s00376-012-1262-1

Zhou, B., Shang, M., Zhang, S., Feng, L., Liu, X., Wu, L., et al. (2019). Remote examination of the seasonal succession of phytoplankton assemblages from time-varying trends. *J. Environ. Manag.* 246, 687–694. doi: 10.1016/j.jenvman.2019.06.035

Zimmerman, A. E., Howard-Varona, C., Needham, D. M., John, S. G., Worden, A. Z., Sullivan, M. B., et al. (2020). Metabolic and biogeochemical consequences of viral infection in aquatic ecosystems. *Nat. Rev. Microbiol.* 18, 21–34. doi: 10.1038/s41579-019-0270-x

frontiers | Frontiers in Microbiology

TYPE Original Research
PUBLISHED 19 May 2023
DOI 10.3389/fmicb.2023.1181341

OPEN ACCESS

EDITED BY
Robert Michael McKay,
University of Windsor, Canada

REVIEWED BY
Lijuan Ren,
Jinan University, China
Yuanyan Zi,
Yunnan University, China

*CORRESPONDENCE
Shuqing An
✉ anshq@nju.edu.cn

†These authors share first authorship

RECEIVED 07 March 2023
ACCEPTED 09 May 2023
PUBLISHED 19 May 2023

CITATION
Chen J, Zhang T, Sun L, Liu Y, Li D, Leng X and An S (2023) Abundance trade-offs and dominant taxa maintain the stability of the bacterioplankton community underlying *Microcystis* blooms.
Front. Microbiol. 14:1181341.
doi: 10.3389/fmicb.2023.1181341

Abundance trade-offs and dominant taxa maintain the stability of the bacterioplankton community underlying *Microcystis* blooms

Jun Chen[1,2†], Tiange Zhang[1,2†], Lingyan Sun[1,2], Yan Liu[1,2], Dianpeng Li[1,2], Xin Leng[1,2] and Shuqing An[1,2*]

[1]School of Life Science and Institute of Wetland Ecology, Nanjing University, Nanjing, China, [2]Nanjing University Ecology Research Institute of Changshu (NJUecoRICH), Changshu, China

Microcystis blooms are an intractable global environmental problem that pollute water and compromise ecosystem functioning. Closed-lake management practices keep lakes free of sewage and harmful algae invasions and have succeeded in controlling local *Microcystis* blooms; however, there is little understanding of how the bacterioplankton communities associated with *Microcystis* have changed. Here, based on metagenomic sequencing, the phyla, genera, functional genes and metabolic functions of the bacterioplankton communities were compared between open lakes (underlying *Microcystis* blooms) and closed lakes (no *Microcystis* blooms). Water properties and zooplankton density were investigated and measured as factors influencing blooms. The results showed that (1) the water quality of closed lakes was improved, and the nitrogen and phosphorus concentrations were significantly reduced. (2) The stability of open vs. closed-managed lakes differed notably at the species and genus levels ($p<0.01$), but no significant variations were identified at the phylum and functional genes levels ($p>0.05$). (3) The relative abundance of *Microcystis* (Cyanobacteria) increased dramatically in the open lakes (proportions from 1.44 to 41.76%), whereas the relative abundance of several other dominant genera of Cyanobacteria experienced a trade-off and decreased with increasing *Microcystis* relative abundance. (4) The main functions of the bacterioplankton communities were primarily related to dominant genera of Proteobacteria and had no significant relationship with *Microcystis*. Overall, the closed-lake management practices significantly reduced nutrients and prevented *Microcystis* blooms, but the taxonomic and functional structures of bacterioplankton communities remained stable overall.

KEYWORDS

abundance trade-offs, bacterioplankton, *Microcystis*, closed-lake management, dominant taxa

1. Introduction

Over the past decades, there has been a rise in the frequency and distribution of cyanobacterial blooms worldwide (Paerl, 2014; Almanza et al., 2019), and the extensive propagation and decay of algae has reduced the dissolved oxygen content of water, compromising ecosystem health (O'Boyle et al., 2016; Zhao et al., 2019). In particular, the public has become

aware of *Microcystis*, a genus of Cyanobacteria synonymous with harmful algal blooms (HABs). For example, a drinking water crisis caused by toxic *Microcystis aeruginosa* led directly to 2 million people unable to safely access municipal water for more than a week in May 2007 in Wuxi, Jiangsu Province, China (Qin et al., 2010). In August 2014, more than 400,000 people were subject to a 'do not drink advisory' for nearly 48 h because of contamination by microcystins in Toledo, Ohio, United States (Steffen et al., 2017). Since that time, numerous investigations and experiments have analysed the organic matter and genotypic structure of *Microcystis* and cyanobacteria blooms (Chen et al., 2018), long-term bloom changes (Zhang M. et al., 2021), and environmental driving forces of blooms (Zhang J. et al., 2021). However, cyanobacterial blooms are a largely unresolved global environmental problem (Ho et al., 2019; Wilhelm et al., 2020).

Wetland construction provides essential protection and management of many small shallow lakes through sewage discharge control and aquaculture implementation to improve water quality (Zhu et al., 2014) and tourism development control to enhance biodiversity (Li et al., 2010). For instance, by building sluices to isolate lakes from rivers, small lakes in Taihu National Wetland Park were constructed to prevent periodic local cyanobacterial outbreaks (Wang et al., 2020). Similarly, in a study of closed-lake management practices, Xiao et al. (2019) studied the Donghu Lake area (Wuhan, China), which is closed off by tunnel construction, based on 16S rRNA gene sequencing and found that Cyanobacteria abundance in the closed lake area was much lower than that in open lake areas. This represents a new perspective that closed-lake management practices may be a powerful precautionary strategy for preventing HABs. In contrast, Wang et al. (2020) compared the bacterioplankton communities in 3 types of closed ponds based on 16S rRNA gene sequencing and found that slight eutrophication in closed ponds led to an increase in Cyanobacteria. To further investigate the ecological effects of closed-lake management practices, it is necessary to consider changes in both cyanobacteria and *Microcystis* (Berg et al., 2018), as well as responses to the associated planktonic microbiome (Shi et al., 2010; Pound et al., 2021).

Recently, high-throughput sequencing has been used to explore the dynamics of the bacterial community (Chen et al., 2018), also to examine the consequences of cyanobacterial blooms on both the cyanosphere and the wider bacterioplankton community. Louati et al. (2016) surveyed a recreational lake and found that changes in the composition of cyanobacterial species led to significant changes in the bacterial communities associated with bloom-forming freshwater cyanobacteria. Similarly, Shen et al. (2019) compared lakes with different nutrient states and found that the functional structure of the bacterioplankton community was significantly different from that of other communities dominated by Cyanobacteria. Liu et al. (2019) also found that the biomass of Cyanobacteria during a bloom strongly affected the community composition of microeukaryotic plankton in a reservoir. In contrast, an enclosure experiment showed that aquatic bacterial communities were resilient and therefore generally stable in the face of disturbance (Shade et al., 2011). Although these 16S rRNA gene sequencing methods are useful, they have limitations in terms of identifying species. It is necessary to implement metagenomic methods for further analysis, which are better suited for identifying both species and functional genes (Shen et al., 2019; Yancey et al., 2022).

Here, we used metagenomic analysis to compare the taxonomic and functional structure of bacterioplankton communities of open lakes (*Microcystis* blooms) and artificially closed lakes (no *Microcystis* blooms) along the Wangyu River. The study reinforced the ecological effects of closed-lake management practices on controlling nutrient loading and mitigating *Microcystis* blooms.

2. Methods

2.1. Study area and sampling

The Wangyu River (31°39′N, 120°38′E), a major tributary of Taihu Lake, is used to divert water from the Yangtze River. In the Taihu Basin river network, the open lakes, which are connected to the river, are subject to direct influence from the water diversion project's navigation and fisheries efforts. On the other hand, the closed lakes were formed as a part of a wetland development initiative and are not directly connected to the river. Hence, we have selected 2 closed lakes with the same closed-lake management and 2 adjacent open lakes for our research. Sites at 3 locations away from immediate influence of large aquatic plants were selected for sampling in each lake (Figure 1).

In July 2021, cyanobacterial blooms continued to occur in the open lakes for a month but did not occur in the closed lakes. At each sampling site, surface water (<0.5 m) was collected using a 5 L water harvester. Using individual filter units (Nalgene, United States), 1 L water was passed through 47 mm, 0.22 μm hydrophilic nylon membranes (Merck Millipore, Germany), which were then separately packed into centrifuge tubes and stored on dry ice (−80°C) for metagenomic sequencing. In addition, 100 mL of surface water was collected using sterile bottles (3 replicates), and approximately 1 mL of dilute sulphuric acid was added to acidify the water to a pH < 2 and stored away from light for nutrient analysis.

Zooplankton collection involved two methods: the protozoan and rotiferan samples were placed in plastic bottles to which 1 L of surface water with 5 mL Lugol solution was added; the cladoceran and copepod samples were collected by passing 20 L of surface water through a 64 um mesh diameter plankton net and 5 mL formaldehyde solution was added for fixation.

2.2. Biotic and abiotic factor analysis

Temperature, oxidation–reduction potential (ORP), pH, salinity, dissolved oxygen (DO) and electrical conductivity (EC) were measured in the field with an AP-800 handheld metre (Aquaread, United Kingdom). Total phosphorus (TP), labile phosphate (labile P), total nitrogen (TN), total oxidised nitrogen (TON) and ammonium nitrogen (ammonium N) were analysed using an auto discrete analyser Cleverchem-200 (DeChem-Tech, Germany). Chemical oxygen demand (COD) was analysed using TNT-821 kits and a DR-3900 instrument (HACH, United States). The zooplankton species were identified using a 1 mL counting plate under an optical microscope at 100–400 × magnification.

2.3. Metagenomic analysis

Microbial community genomic DNA was extracted from the freshwater samples using the FastDNA® SPIN Kit (Omega Bio-Tek,

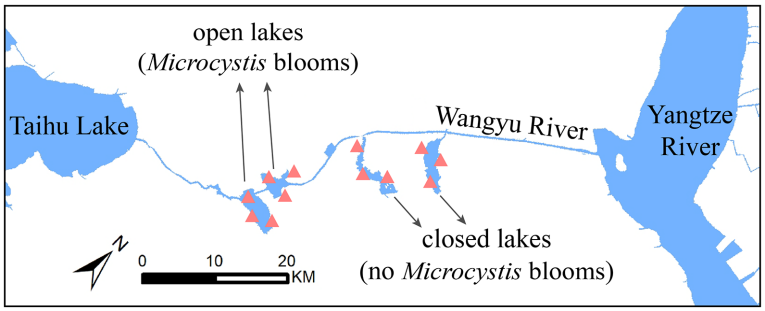

FIGURE 1
Map of sampling stations. A total of 12 stations were set up, including in open lakes (Chaohu Lake and Ehu Lake) and closed lakes (Shanghu National Wetland Park and Nanhu Provincial Wetland Park).

Norcross, GA, United States) following the manufacturer's instructions. The DNA extract was checked on a 1% agarose gel, and DNA concentration and purity were determined with a NanoDrop 2000 UV–vis spectrophotometer (Thermo Scientific, Wilmington, DE, United States; Zheng et al., 2022). On an Illumina Genome Analyser IIx, metagenome sequencing was performed and yielded >8 GB per library (>50 M reads, 150 bp paired-end reads, insert size = 500 bp). Quality trimming was performed in Fastp v0.20.0, and reads <20 bp were discarded. After filtering, we used Multiple Megahit v1.1.2 (Li et al., 2015) to assemble the metagenomics data. CD-HIT software (Fu et al., 2012) was used to cluster a nonredundant gene catalogue (90% identity, 90% coverage). The taxonomic annotation and functional analysis were performed based on the NR (Non-Redundant Protein Sequence Database) and KEGG (Kyoto Encyclopedia of Genes and Genomes), respectively.

2.4. Statistical analysis

The bacterioplankton community stability was evaluated by average variation degree (AVD), which is calculated using the deviation degree from the mean of the normally distributed relative abundance of species (genus, phylum or functional gene) between open and closed lakes. Lower AVD value indicates higher bacterioplankton community stability (Xun et al., 2021).

The variance inflation factor (VIF) was used to filter the autocorrelated environmental factors, and these factors were filtered several times until the VIF values corresponding to the selected environmental factors were all less than 10. Nonmetric multidimensional scaling analyses (NMDS) were used to reduce and rank species and functions to directly characterise the degree of differences between sampling stations. Distance-based redundancy analysis (db-RDA) used Bray–Curtis distance calculations to analyse the relationship between species or functions and environmental factors. The Wilcoxon rank-sum test was used to analyse the species/function differences between the two groups of samples. Correlation network analysis was calculated to construct the correlation network of species and function.

Statistical analyses were performed in R 4.0.3 and Python 3.11. Origin 2021 was used to create figures. The geographic and connectivity variables were calculated in ArcGIS 10.8.

3. Results

3.1. Diversity and stability of bacterioplankton communities

To determine the differences in the bacterioplankton communities between the open and closed lakes, we first aimed to determine the taxonomic and functional diversity of the bacterioplankton communities through metagenomic sequencing. A total of 650.07 million high-quality sequence reads with an average length of 126 bp were obtained from 12 sampling sites. A total of 4,487 distinct bacterioplankton taxa were detected across all sampling sites, covering 53 phyla, 1,509 genera and 511 families. The majority of bacterioplankton reads belonged to Cyanobacteria, Proteobacteria and Actinobacteria, accounting for 48.53%, 19.81%, and 19.04% of the total bacterioplankton reads, respectively (Figure 2A). The dominant genera were *Microcystis* (32.58% of reads), *Actinomycetes* (7.29% of reads), *Clavibacter* (5.39% of reads), *Prochlorothrix* (3.51% of reads), and *Acidimicrobium* (3.00% of reads; Figure 2A).

There were 6,695 KEGG orthologues, and 70.77% of the sequences belonged to the metabolism group. In the metabolism group, the "global and overview maps" subgroup accounted for 39.83% of the reads, representing metabolic pathways, biosynthesis of secondary metabolites, amongst others. In addition, amino acid metabolism, carbohydrate metabolism and energy metabolism were the main metabolism types, accounting for 11.00%, 10.70%, and 9.53% of the reads, respectively (Figure 2B).

In general, there were no noteworthy discrepancies observed in the stability of the two lake types at the phylum and functional genes levels ($p > 0.05$), as depicted in Figures 2E,F. There was a significant discrepancy observed at the species and genus levels ($p < 0.01$), with closed lakes exhibiting lower ASV indices and higher stability (Figures 2C,D).

3.2. Comparison of taxonomic and functional structures of bacterioplankton communities between open and closed lakes

To compare the community structure differences from the perspective of taxonomy and function, the components with the

10.3389/fmicb.2023.1181341

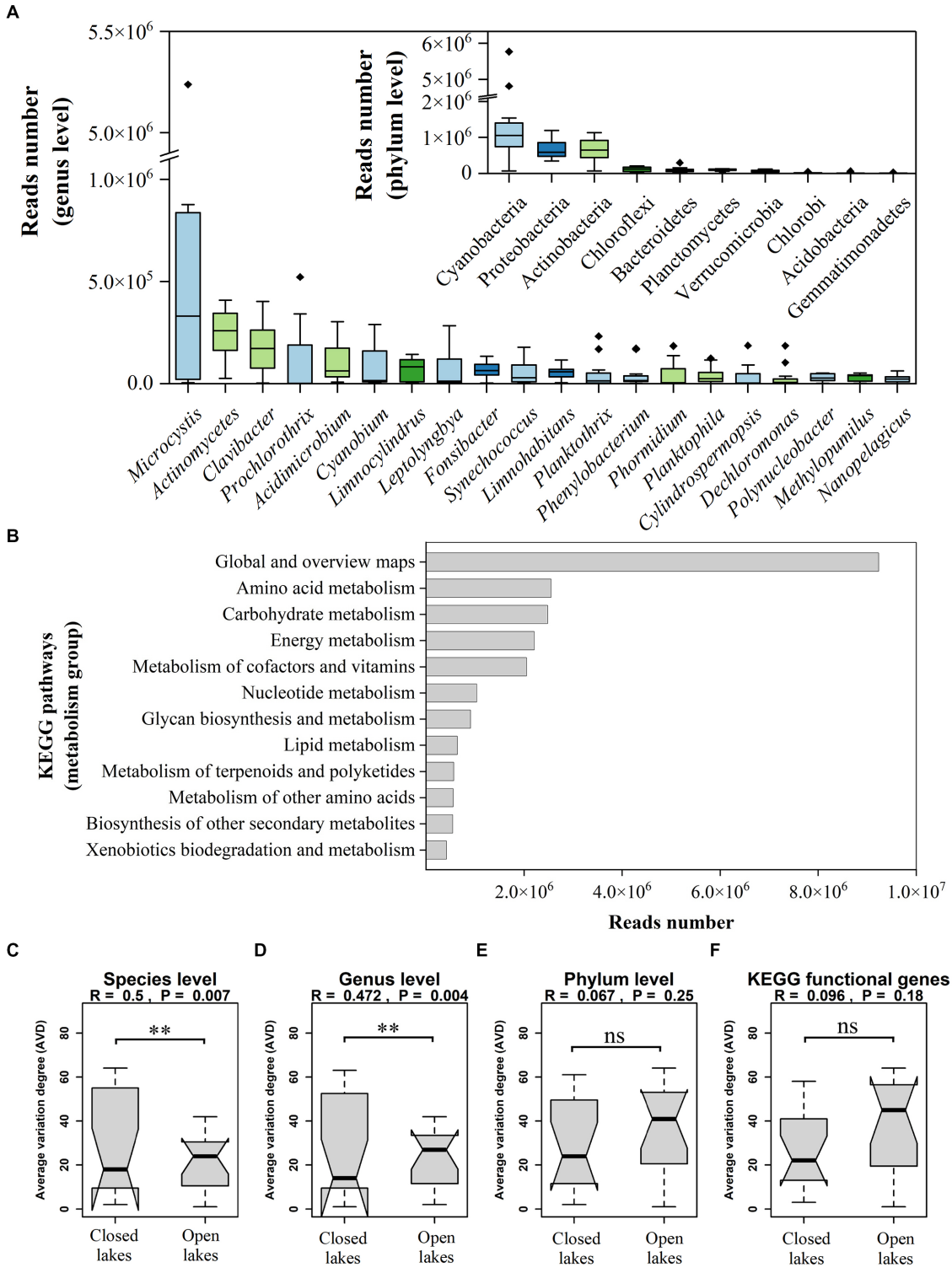

FIGURE 2
(A) Genus and phylum relative abundance variation box plot for the most abundant genera and phyla as determined by read relative abundance. Genera are coloured by their respective phylum. **(B)** The relative abundance of metabolic functional genes in the KEGG database. **(C–F)** Comparison of the stability at different taxonomic and functional levels.

largest proportion were selected, and their significance was tested. In addition, the similarity pattern of all sample communities was visually displayed by NMDS analyses (Figure 3). The bacterioplankton community structures of the open and closed lakes showed little difference at the phylum level or at a functional gene level (Figures 3A,D) but showed obvious differentiation at the genus and species levels (Figures 3B,C). At the phylum level, the relative abundances of the top 4 phyla, such as Cyanobacteria and

10.3389/fmicb.2023.1181341

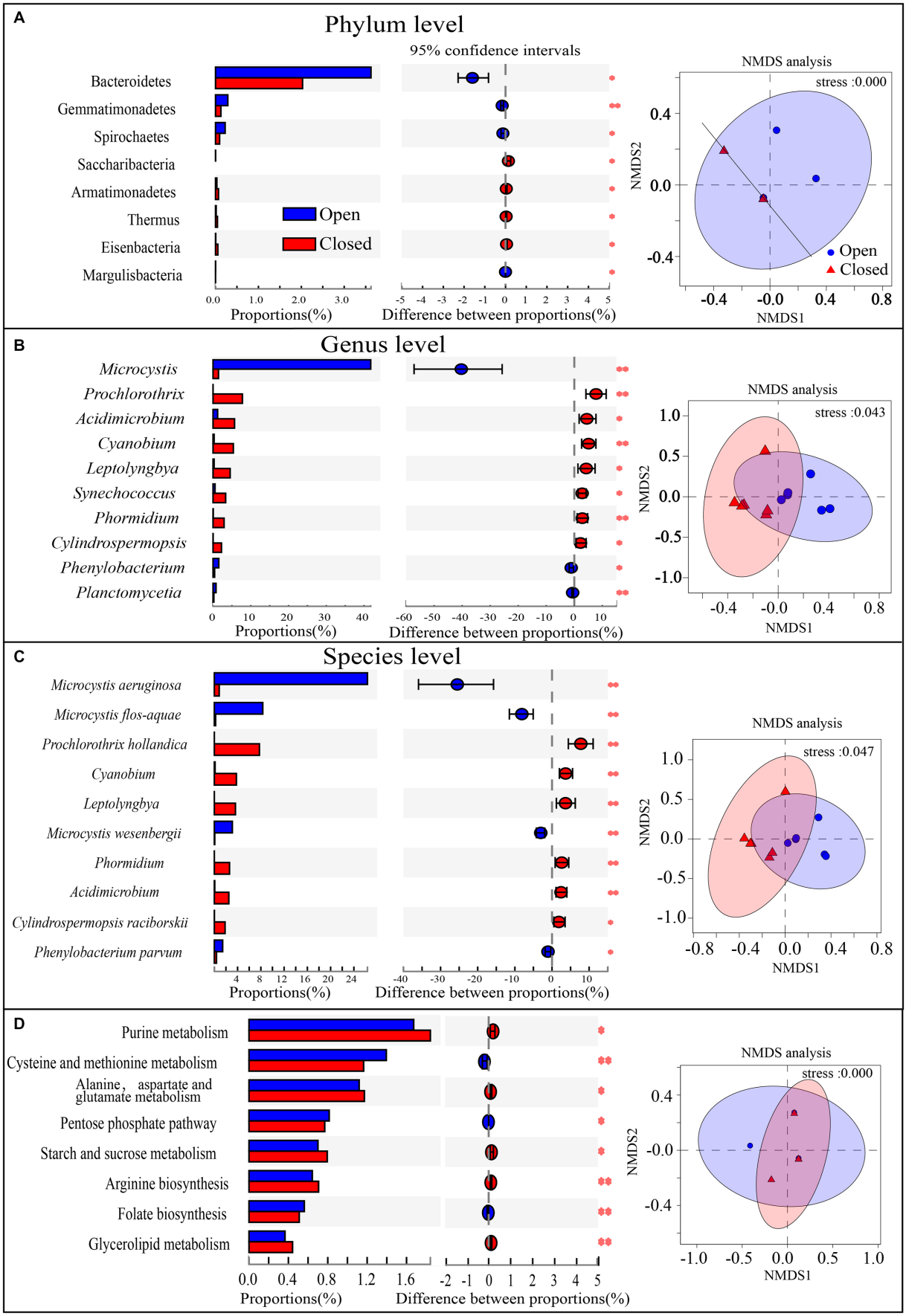

FIGURE 3
(A–D) Species relative abundance or KEGG functional gene relative abundance comparison and significance test between the open lake group and closed lake group, 0.01<*P*≤ 0.05 *, 0.001<*P*≤ 0.01 **, *P*≤ 0.001 ***. In addition, NMDS analyses were added, and the 95% confidence intervals are shown.

Proteobacteria, did not differ significantly between the open and closed lakes (Figure 3A). Only the relative abundance of Bacteroides showed fluctuations, and the NMDS pattern showed that the phylum-level community structures at most sampling stations were very similar (Figure 3A). At the same time, the functional gene patterns were not significantly different between the open and closed lakes, with little difference in the dominant functional genes (Figure 3D).

At the genus level, *Microcystis* was highly abundant in open lakes (proportion = 41.76%) and directly accounted for the differentiation in community taxonomic structures; in contrast, other genera of Cyanobacteria, such as *Prochlorothrix*, *Cyanobium* and *Leptolyngbya*, occurred at significantly higher proportions in the closed lakes (Figure 3B). Furthermore, at the species level, Figure 3C shows that the key cyanobacterial bloom species were *Microcystis aeruginosa*, *Microcystis flos-aquae* and *Microcystis wesenbergii*, whilst *Microcystis aeruginosa* accounted for the primary differences in the communities between the open and closed lakes. In addition, the genus *Acidimicrobium* of Actinobacteria was significantly more abundant ($p < 0.01$) in the closed lakes than in the open lakes (Figure 3B), and *Acidimicrobium* also contributed more to functional genes in the closed lakes than in the open lakes (Figure 4B).

3.3. Dominant taxa driving functional differences in bacterioplankton communities

Metagenomic approaches allow structural and functional correlations to be analysed at different levels (Figure 4), reflecting how species composition drives functional composition. At the genus and phylum levels, the species contributions to different functional genes were approximately the same, but there was a significant difference between the open and closed lakes (Figures 4A,B). At the phylum level, the top three phyla with the highest relative abundance (Figure 2A), Cyanobacteria, Proteobacteria and Actinobacteria, were primarily responsible for the metabolic functions of the bacterioplankton communities (Figure 4A). At the genus level, the dominant genera had different responses to the different lake types: *Microcystis*, the most abundant genus, contributed significantly more to the metabolic functions in the open lakes; the contribution of *Prochlorothrix*, *Cyanobium*, and *Leptolyngbya* of Cyanobacteria to metabolic functions decreased significantly in the open lakes and the other genera were not obviously responsive to lake type (Figure 4B).

Figure 4C shows the correlations between the bacterioplankton phyla and metabolic functional genes: Cyanobacteria and Chlorobi were positively correlated with the dominant functional genes (Spearman correlation coefficients > 0.601, $p < 0.05$), and Bacteroidetes were only positively correlated with carbon metabolism (Spearman correlation coefficients =0.587, $p < 0.05$). However, Actinobacteria generally had strong negative associations with these dominant functional genes (Figure 4C). Figure 4D shows the correlations between the dominant genera and dominant functional genes: both *Limnohabitans* and *Polynucleobacter* of Proteobacteria had strong positive associations with the dominant functional genes (Spearman correlation coefficients >0.615, $p < 0.05$), especially carbon metabolism (Spearman correlation coefficients > 0.776, $p < 0.01$) and oxidative phosphorylation (Spearman correlation coefficients > 0.748, $p < 0.01$).

3.4. Correlations between bacterioplankton communities and biotic or abiotic factors

In general, the closed lakes demonstrated significantly lower levels of nitrogen and phosphorus compared to the open lakes, as evidenced by a noticeable reduction across TP, labile P, TN and TON (Figure 5E; Supplementary Figure 2). At the same time, the density of zooplankton did not vary between open and closed lakes.

As mediators of the effects of closed-lake management practices on bacterioplankton, water properties and zooplankton density were used to explain community differences (Figure 5). In the db-RDA models (Figures 5A–C), although the current 8 biotic and abiotic indicators only explained 38.77% to 47.26% of the variation in bacterioplankton community structures, they did reflect the community differences between the open and closed lakes. At different taxonomic levels, there were correlations between zooplankton density and bacterioplankton community structures. For example, Cladocera and Rotifera were correlated with the genera of the bacterioplankton community structure ($R^2 = 0.539$, $p < 0.05$; $R^2 = 0.503$, $p < 0.05$).

On the other hand, the water properties affected the community structures of the bacterioplankton communities (Figures 5A–C). For example, salinity directly affected the bacterioplankton community structure at the species level ($R^2 = 0.512$, $p < 0.05$) and KEGG functional genes ($R^2 = 0.543$, $p < 0.05$). In contrast, although biotic and abiotic indicators can affect the bacterioplankton community taxonomic structures, they did not further significantly affect the functional gene structures (Figure 5D); for example, salinity and Cladocera had no significant effect on the functional gene structures ($R^2 = 0.275$, $p = 0.239$; $R^2 = 0.493$, $p < 0.05$).

4. Discussion

Although the relationship between cyanobacterial blooms and the bacterial community has been frequently investigated in previous studies (Chen et al., 2018; Liu et al., 2019), few studies have investigated the taxonomic and functional structures of bacterioplankton communities based on metagenomic sequencing. In this study, to assess the ecological effects of closed-lake management practices, the taxonomic and functional structures of bacterioplankton communities were compared; furthermore, correlations between species and function were revealed and the main taxa that drove community taxonomic and functional structures were identified.

Our study found strong associations between *Microcystis* and 4 major community metabolic functions (Figure 4B), but there was no significant association between *Microcystis* and functional genes (Figure 4D). At the same time, two genera of Proteobacteria accounted for the most abundant functional genes (Figure 4D), and Steffen et al. (2012) also found that metabolic functional genes were mainly related to Proteobacteria in Taihu Lake. Does this suggest that *Polynucleobacter* and *Limnohabitans* of Proteobacteria have a more dominant influence on maintaining the stability of functional gene structure compared to *Microcystis*? The concept of keystone taxa has helped in understanding the changes in community function; keystone taxa determine the main function of a community regardless of their abundance (Banerjee et al., 2018). For example, Chen et al. (2018) found that although *Microcystis* occurred at the highest proportion in the lake, Proteobacteria were

10.3389/fmicb.2023.1181341

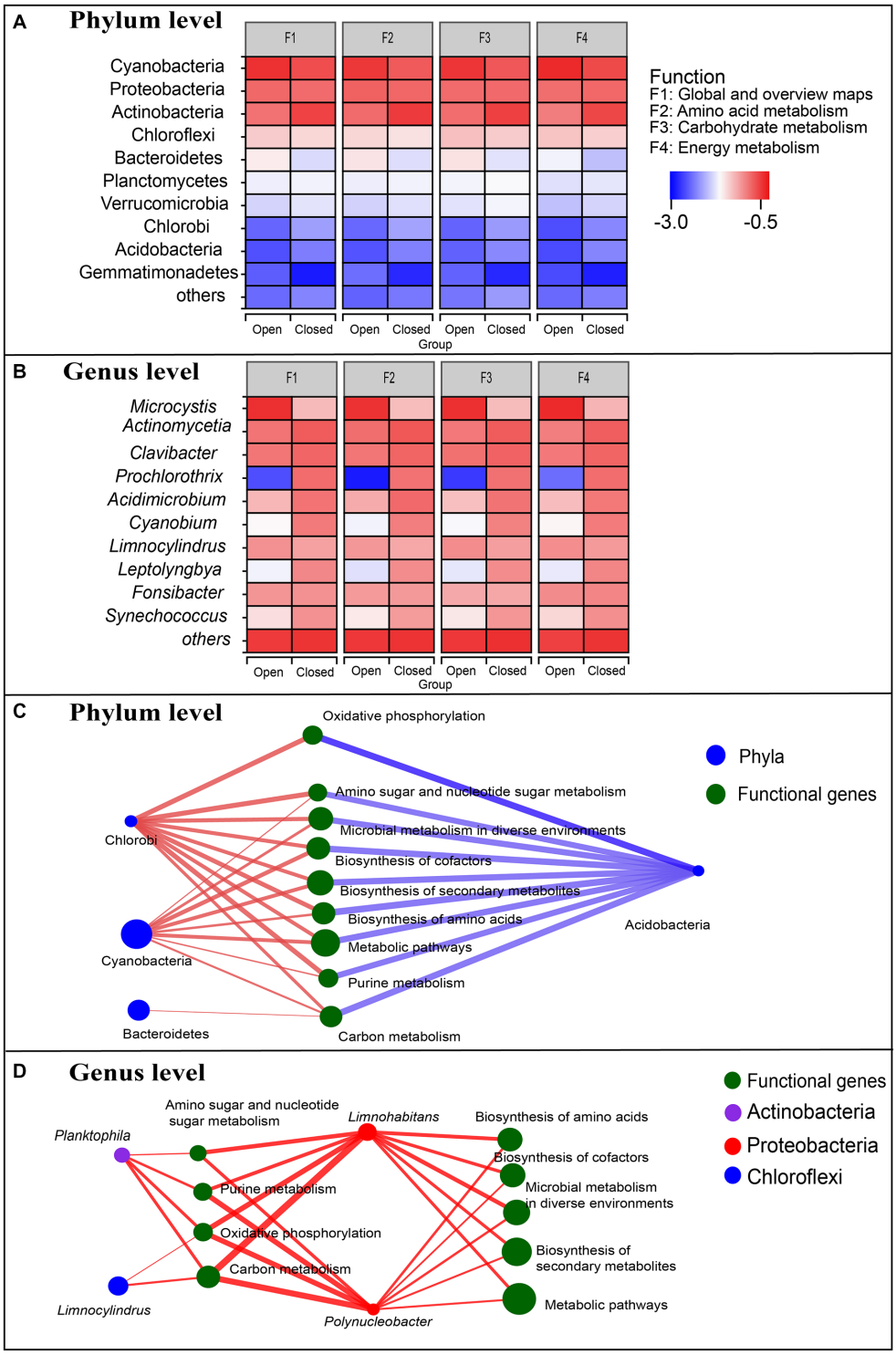

FIGURE 4
(A,B) Comparison of species contributions to metabolic functions between open and closed lakes. Red indicates the highest contribution, and blue indicates the lowest contribution. **(C,D)** Correlation networks between species and functions of the bacterioplankton communities. Larger nodes indicate a higher relative abundance of species or functional genes. The red lines indicate positive and negative correlations, and the blue lines indicate negative correlations.

associated with metabolic functional genes. Similarly here, the *Microcystis* with the greatest relative abundance had no significant correlation with major functional genes (Figure 4D). Thus, compared with the dominant taxa, keystone taxa may also be a contributor to the relatively conserved functional structure.

On the other hand, Cyanobacteria were dominant in this study, mainly driving aerobic respiration, nitrogen assimilation, nitrogen mineralisation, assimilatory sulphate reduction and other metabolic pathways (Figure 4C), whilst Actinobacteria and Proteobacteria potentially mediated these metabolic processes (Shen et al., 2019).

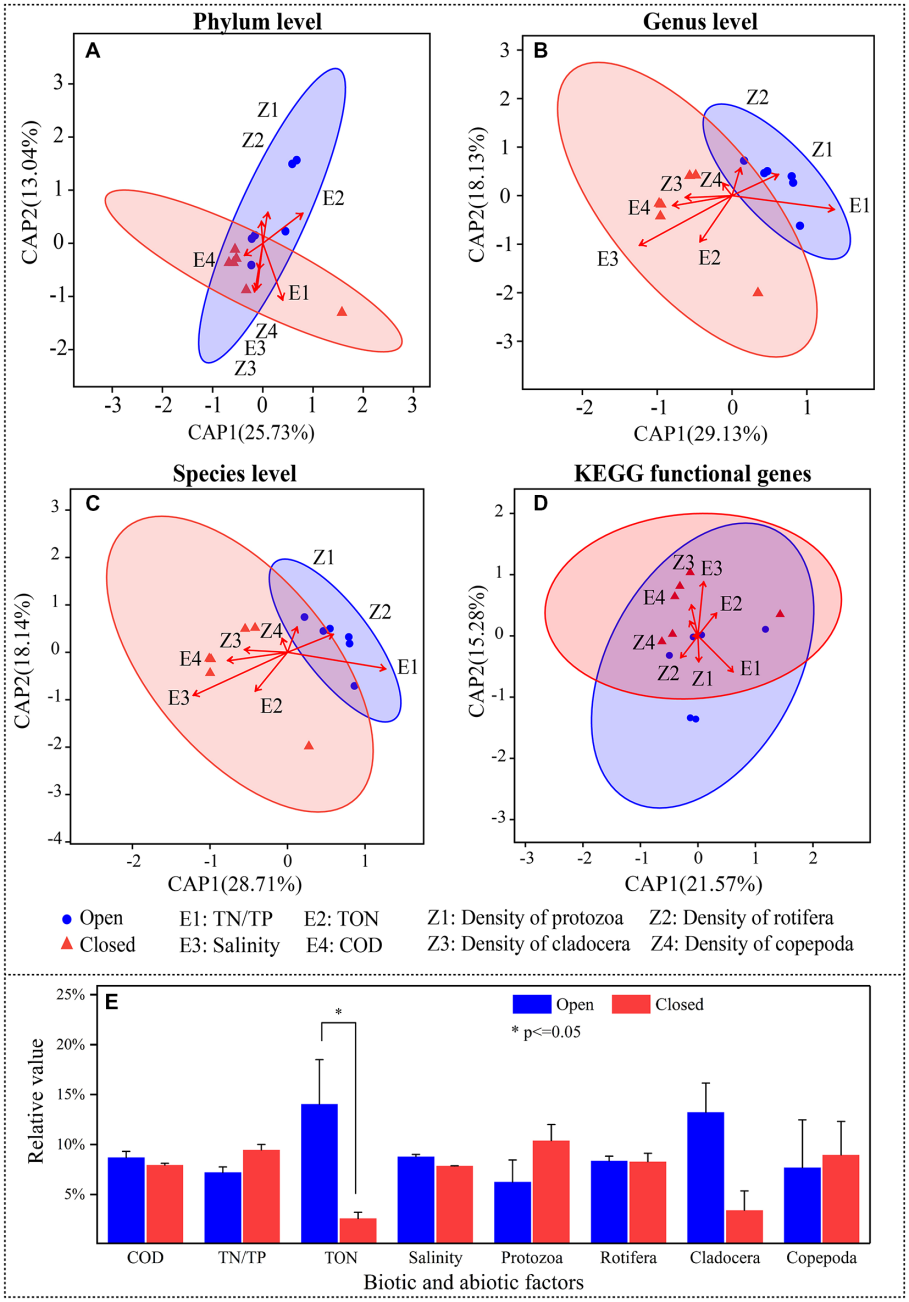

FIGURE 5
(A–D) Distance-based redundancy analysis (db-RDA) with 95% confidence intervals showing the relationships between bacterioplankton species relative abundance or KEGG functional gene relative abundance (response variables) and biotic or abiotic factors (explanatory variables).
(E) Comparison of biotic or abiotic factors between the open and closed lakes, in which zooplankton densities were selected.

Although Cyanobacteria are not directly involved in many functions, the cyanosphere is critical to the associated heterotrophic bacterial communities. For instance, Shi et al. (2010) stressed that the bacteria in the cyanosphere were likely specifically related to Cyanobacteria. Subsequently, Xie et al. (2016) sequenced a stable community in the laboratory and found a mutually beneficial relationship between the bacteria and *Microcystis*: all heterotrophic bacteria were dependent upon *Microcystis* for carbon and energy, whilst *Microcystis* was dependent upon the heterotrophic bacteria for the vitamin B-12 required for its growth. Furthermore, Smith et al. (2021) isolated single *Microcystis* colonies via droplet encapsulation and found that differences between *Microcystis* strains may impact community composition of the *Microcystis* phycosphere.

In our study, despite significant cyanobacterial blooms in the open lakes, there was no significant difference in cyanobacterial relative abundance between the open and closed lakes (Figure 3A). Specifically, although the relative abundance of *Microcystis* was extremely high in the open lakes, the relative abundance of the other dominant Cyanobacteria genera was significantly reduced (Figure 3B). One possible reason for this result was that the members of Cyanobacteria share a very similar niche (Zhao et al., 2016). Similarly, during a cyanobacterial bloom in the Baltic Sea, Berg et al. (2018) stressed the

exceptionally strong biotic driving forces of cyanobacterial blooms on associated microbial communities, but the post-bloom microbial community still re-established a comparable status in terms of diversity to that of the pre-bloom status. In addition, the functional structures of Cyanobacteria did not differ generally between the open and closed lakes (Figure 4A), abundance trade-off may had resulted in a functional structure trade-off in the phylum of Cyanobacteria (Figure 4B). Consistent with these findings of a functional structure trade-off, Steffen et al. (2012) compared the microplanktonic communities amongst Lake Erie (North America), Taihu Lake (China), and Grand Lake St. Marys (United States) and found that despite the variation in the phylogenetic assignments of the bloom-associated organisms, the functional potential remained relatively constant between systems. Our results are consistent with those of previous studies that have found bacterioplankton community structures to be resistant to cyanobacterial blooms.

Unlike Xiao et al. (2019), who found that resource and predator factors play an important role in changes in bacterioplankton communities in Donghu Lake, there were no obvious ecological driving forces of bacterioplankton communities in this study. Specifically, although significantly higher levels of TON were associated with *Microcystis*, the changes in overall community structure were not well explained by biotic and abiotic factors. One possible explanation is that zooplankton have experienced many coevolutionary adaptations; for example, *Daphnia* may feed on *Microcystis*, whilst *Microcystis* may intoxicate *Daphnia* (DeMott et al., 2001; Lemaire et al., 2012), and *Daphnia* have a limited ability to graze on cyanobacterial blooms (DeMott et al., 2001). Furthermore, the hydrological connectivity of the open lake may have played a direct role in the accelerated proliferation of invasive algae (Zhang et al., 2022), thereby impeding or concealing the influential impact of zooplankton.

However, the relationship between zooplankton and cyanobacteria varies widely (Huisman et al., 2018). During a cyanobacterial bloom in open lakes, Jiang et al. (2016) revealed the rapid evolution of tolerance in two cladoceran grazers (*Daphnia pulex* and *Simocephalus vetulus*) to toxic *Microcystis*, and Sadler and von Elert (2014) showed that cladoceran daphnia can successfully inhibit bloom formation. Consistent with this information, Xiao et al. (2019) found that closed-lake management practices resulted in a significant increase in cladoceran species, and cladocerans, as mainly predators, had a significant positive association with bacterioplankton. In general, water quality and zooplankton abundance are not a good explanation for cyanobacterial blooms. On the other hand, a recent study in the Wangyu River based on the ASV structure in eDNA metabarcoding analysis showed that the *Microcystis* in the Wangyu River were different from those in Taihu Lake and the Yangtze River and might act as a potential source of *Microcystis* (Zhang et al., 2022). eDNA metabarcoding can be a powerful tool to reveal habitat-specific biodiversity in lentic systems (Westfall et al., 2020), and the combination of metagenomic sequencing and eDNA metabarcoding can help to more comprehensively reveal the causes of differences in community structure.

5. Conclusion

Our findings support the concept that bacterioplankton community structures are resistant to cyanobacterial blooms. In open lakes, *Microcystis* blooms were accompanied by significant reductions in the proportions of several other Cyanobacteria genera, showing a proportional trade-off amongst Cyanobacteria. At the same time, different species contributions to metabolic functions also showed similar trade-offs, which had important implications for higher levels of stability and resistance. On the other hand, both this trade-off and the presence of dominant taxa reflect community stability, suggesting that although closed-lake management practices improve water quality, the focus of success in controlling cyanobacterial blooms is to cut off the biological invasion pathway. Our study further suggests that there are some dominant taxa associated with many important community functions and provides a reference for controlling cyanobacterial blooms and monitoring and managing lakes. This study highlights the importance of closed-lake management practices in controlling cyanobacterial blooms.

Data availability statement

The original contributions presented in the study are publicly available. This data can be found at: https://www.ncbi.nlm.nih.gov/bioproject; PRJNA948163.

Author contributions

JC: study design, data and sample collection, sample measurement, and writing—original draft. TZ and YL: assisting sample collection and measurement. LS and DL: assisting sample collection. XL: manuscript revision. SA: study design and manuscript revision. All authors contributed to the article and approved the submitted version.

Funding

For support, we thank Forestry Science and Technology Innovation and Promotion Project of Jiangsu Province (LYKJ [2022]02, LYKJ-Chanshu [2021]1) and the Fundamental Research Funds for the Central Universities (0211-14380166).

Conflict of interest

The authors declare that the research was conducted in the absence of any commercial or financial relationships that could be construed as a potential conflict of interest.

Publisher's note

Supplementary material

The Supplementary material for this article can be found online at: https://www.frontiersin.org/articles/10.3389/fmicb.2023.1181341/full#supplementary-material

References

Almanza, V., Pedreros, P., Dail Laughinghouse, H., Félez, J., Parra, O., Azócar, M., et al. (2019). Association between trophic state, watershed use, and blooms of cyanobacteria in south-Central Chile. *Limnologica* 75, 30–41. doi: 10.1016/j.limno.2018.11.004

Banerjee, S., Schlaeppi, K., and van der Heijden, M. G. A. (2018). Keystone taxa as drivers of microbiome structure and functioning. *Nat. Rev. Microbiol.* 16, 567–576. doi: 10.1038/s41579-018-0024-1

Berg, C., Dupont, C. L., Asplund-Samuelsson, J., Celepli, N. A., Eiler, A., Allen, A. E., et al. (2018). Dissection of microbial community functions during a cyanobacterial bloom in the Baltic Sea via Metatranscriptomics. *Front. Mar. Sci.* 5. doi: 10.3389/fmars.2018.00055

Chen, Z., Zhang, J., Li, R., Tian, F., Shen, Y., Xie, X., et al. (2018). Metatranscriptomics analysis of cyanobacterial aggregates during cyanobacterial bloom period in Lake Taihu, China. *Environ. Sci. Pollut. Res. Int.* 25, 4811–4825. doi: 10.1007/s11356-017-0733-4

DeMott, W. R., Gulati, R. D., and Van Donk, E. (2001). Daphnia food limitation in three hypereutrophic Dutch lakes: evidence for exclusion of large-bodied species by interfering filaments of cyanobacteria. *Limnol. Oceanogr.* 46, 2054–2060. doi: 10.4319/lo.2001.46.8.2054

Fu, L., Niu, B., Zhu, Z., Wu, S., and Li, W. (2012). CD-HIT: accelerated for clustering the next-generation sequencing data. *Bioinformatics* 28, 3150–3152. doi: 10.1093/bioinformatics/bts565

Ho, J. C., Michalak, A. M., and Pahlevan, N. (2019). Widespread global increase in intense lake phytoplankton blooms since the 1980s. *Nature* 574, 667–670. doi: 10.1038/s41586-019-1648-7

Huisman, J., Codd, G. A., Paerl, H. W., Ibelings, B. W., Verspagen, J. M. H., and Visser, P. M. (2018). Cyanobacterial blooms. *Nat. Rev. Microbiol.* 16, 471–483. doi: 10.1038/s41579-018-0040-1

Jiang, X., Gao, H., Zhang, L., Liang, H., and Zhu, X. (2016). Rapid evolution of tolerance to toxic Microcystis in two cladoceran grazers. *Sci. Rep.* 6:25319. doi: 10.1038/srep25319

Lemaire, V., Brusciotti, S., van Gremberghe, I., Vyverman, W., Vanoverbeke, J., and De Meester, L. (2012). Genotype x genotype interactions between the toxic cyanobacterium *Microcystis* and its grazer, the waterflea Daphnia. *Evol. Appl.* 5, 168–182. doi: 10.1111/j.1752-4571.2011.00225.x

Li, D., Liu, C. M., Luo, R., Sadakane, K., and Lam, T. W. (2015). MEGAHIT: an ultra-fast single-node solution for large and complex metagenomics assembly via succinct de Bruijn graph. *Bioinformatics* 31, 1674–1676. doi: 10.1093/bioinformatics/btv033

Li, Y., Liu, H., Zheng, N., and Cao, X. (2010). Analysis of trophic status and its influence factors of different water body types in Xixi National Wetland Park, China. *Procedia Environ. Sci.* 2, 768–780. doi: 10.1016/j.proenv.2010.10.088

Liu, L., Chen, H., Liu, M., Yang, J. R., Xiao, P., Wilkinson, D. M., et al. (2019). Response of the eukaryotic plankton community to the cyanobacterial biomass cycle over 6 years in two subtropical reservoirs. *ISME J.* 13, 2196–2208. doi: 10.1038/s41396-019-0417-9

Louati, I., Pascault, N., Debroas, D., Bernard, C., Humbert, J. F., and Leloup, J. (2016). Structural diversity of bacterial communities associated with bloom-forming freshwater Cyanobacteria differs according to the cyanobacterial genus (vol 10, e0140614, 2015). *PLoS One* 11:e0146866. doi: 10.1371/journal.pone.0146866

O'Boyle, S., McDermott, G., Silke, J., and Cusack, C. (2016). Potential impact of an exceptional bloom of Karenia mikimotoi on dissolved oxygen levels in waters off western Ireland. *Harmful Algae* 53, 77–85. doi: 10.1016/j.hal.2015.11.014

Paerl, H. W. (2014). Mitigating harmful cyanobacterial blooms in a human- and climatically-impacted world. *Life* 4, 988–1012. doi: 10.3390/life4040988

Pound, H. L., Martin, R. M., Sheik, C. S., Steffen, M. M., Newell, S. E., Dick, G. J., et al. (2021). Environmental studies of cyanobacterial harmful algal blooms should include interactions with the dynamic microbiome. *Environ. Sci. Technol.* 55, 12776–12779. doi: 10.1021/acs.est.1c04207

Qin, B., Zhu, G., Gao, G., Zhang, Y., Li, W., Paerl, H. W., et al. (2010). A drinking water crisis in Lake Taihu, China: linkage to climatic variability and Lake management. *Environ. Manag.* 45, 105–112. doi: 10.1007/s00267-009-9393-6

Sadler, T., and von Elert, E. (2014). Physiological interaction of Daphnia and *Microcystis* with regard to cyanobacterial secondary metabolites. *Aquat. Toxicol.* 156, 96–105. doi: 10.1016/j.aquatox.2014.08.003

Shade, A., Read, J. S., Welkie, D. G., Kratz, T. K., Wu, C. H., and McMahon, K. D. (2011). Resistance, resilience and recovery: aquatic bacterial dynamics after water column disturbance. *Environ. Microbiol.* 13, 2752–2767. doi: 10.1111/j.1462-2920.2011.02546.x

Shen, M., Li, Q., Ren, M., Lin, Y., Wang, J., Chen, L., et al. (2019). Trophic status is associated with community structure and metabolic potential of planktonic microbiota in Plateau Lakes. *Front. Microbiol.* 10:2560. doi: 10.3389/fmicb.2019.02560

Shi, L. M., Cai, Y. F., Wang, X. Y., Li, P. F., Yu, Y., and Kong, F. X. (2010). Community structure of Bacteria associated with *Microcystis* colonies from cyanobacterial blooms. *J. Freshwater Ecol.* 25, 193–203. doi: 10.1080/02705060.2010.9665068

Smith, D. J., Tan, J. Y., Powers, M. A., Lin, X. N., Davis, T. W., and Dick, G. J. (2021). Individual Microcystis colonies harbour distinct bacterial communities that differ by Microcystis oligotype and with time. *Environ. Microbiol.* 23, 3020–3036. doi: 10.1111/1462-2920.15514

Steffen, M. M., Davis, T. W., McKay, R. M. L., Bullerjahn, G. S., Krausfeldt, L. E., Stough, J. M. A., et al. (2017). Ecophysiological examination of the Lake Erie Microcystis bloom in 2014: linkages between biology and the water supply shutdown of Toledo, OH. *Environ. Sci. Technol.* 51, 6745–6755. doi: 10.1021/acs.est.7b00856

Steffen, M. M., Li, Z., Effler, T. C., Hauser, L. J., Boyer, G. L., and Wilhelm, S. W. (2012). Comparative metagenomics of toxic freshwater cyanobacteria bloom communities on two continents. *PLoS One* 7:e44002. doi: 10.1371/journal.pone.0044002

Wang, B., Zheng, X., Zhang, H., Xiao, F., Gu, H., Zhang, K., et al. (2020). Bacterial community responses to tourism development in the Xixi National Wetland Park, China. *Sci. Total Environ.* 720:137570. doi: 10.1016/j.scitotenv.2020.137570

Westfall, K. M., Therriault, T. W., and Abbott, C. L. (2020). A new approach to molecular biosurveillance of invasive species using DNA metabarcoding. *Glob. Chang. Biol.* 26, 1012–1022. doi: 10.1111/gcb.14886

Wilhelm, S. W., Bullerjahn, G. S., and McKay, R. M. L. (2020). The complicated and confusing ecology of Microcystis blooms. *MBio* 11, e00529–e00520. doi: 10.1128/mBio.00529-20

Xiao, F., Bi, Y., Li, X., Huang, J., Yu, Y., Xie, Z., et al. (2019). The impact of anthropogenic disturbance on Bacterioplankton communities during the construction of Donghu tunnel (Wuhan, China). *Microb. Ecol.* 77, 277–287. doi: 10.1007/s00248-018-1222-0

Xie, M., Ren, M., Yang, C., Yi, H., Li, Z., Li, T., et al. (2016). Metagenomic analysis reveals symbiotic relationship among Bacteria in Microcystis-dominated community. *Front. Microbiol.* 7. doi: 10.3389/fmicb.2016.00056

Xun, W., Liu, Y., Li, W., Ren, Y., Xiong, W., Xu, Z., et al. (2021). Specialized metabolic functions of keystone taxa sustain soil microbiome stability. *Microbiome* 9:35. doi: 10.1186/s40168-020-00985-9

Yancey, C. E., Smith, D. J., Uyl, P. A. D., Mohamed, O. G., Yu, F., Ruberg, S. A., et al. (2022). Metagenomic and Metatranscriptomic insights into population diversity of *Microcystis* blooms: spatial and temporal dynamics of *mcy* genotypes, including a partial operon that can be abundant and expressed. *Appl. Environ. Microbiol.* 88, e0246421–e0202421. doi: 10.1128/aem.02464-21

Zhang, J., Nawaz, M. Z., Zhu, D., Yan, W., Alghamdi, H. A., and Lu, Z. (2021). Diversity, seasonal succession and host specificity of bacteria associated with cyanobacterial aggregates in a freshwater lake. *Environ. Technol. Innov.* 24:101988. doi: 10.1016/j.eti.2021.101988

Zhang, M., Shi, X., Yang, Z., and Chen, K. (2021). Characteristics and driving factors of the long-term shifts between *Microcystis* and *Dolichospermum* in Lake Taihu and Lake Chaohu. *J Lake Sci* 33, 1051–1061. doi: 10.18307/2021.0408

Zhang, L., Yang, J., Zhang, Y., Shi, J., Yu, H., and Zhang, X. (2022). eDNA biomonitoring revealed the ecological effects of water diversion projects between Yangtze River and tai Lake. *Water Res.* 210:117994. doi: 10.1016/j.watres.2021.117994

Zhao, C. S., Shao, N. F., Yang, S. T., Ren, H., Ge, Y. R., Feng, P., et al. (2019). Predicting cyanobacteria bloom occurrence in lakes and reservoirs before blooms occur. *Sci. Total Environ.* 670, 837–848. doi: 10.1016/j.scitotenv.2019.03.161

Zhao, D., Shen, F., Zeng, J., Huang, R., Yu, Z., and Wu, Q. L. (2016). Network analysis reveals seasonal variation of co-occurrence correlations between Cyanobacteria and other bacterioplankton. *Sci. Total Environ.* 573, 817–825. doi: 10.1016/j.scitotenv.2016.08.150

Zheng, F., Zhang, T., Yin, S., Qin, G., Chen, J., Zhang, J., et al. (2022). Comparison and interpretation of freshwater bacterial structure and interactions with organic to nutrient imbalances in restored wetlands. *Front. Microbiol.* 13:946537. doi: 10.3389/fmicb.2022.946537

Zhu, W., Zhou, J., Lan, T., and Wang, Q. (2014). Analysis of phytoplankton community structure characteristics of Suzhou Taihu Lake Wetland Park. *J. Saf. Environ.* 14, 273–277. doi: 10.13637/j.issn.1009-6094.2014.02.056

frontiers | Frontiers in Microbiology

TYPE Original Research
PUBLISHED 19 June 2023
DOI 10.3389/fmicb.2023.1197394

OPEN ACCESS

EDITED BY
Michaela M. Salcher,
Biology Centre of the Czech Academy of Sciences, Czechia

REVIEWED BY
Alena S. Gsell,
Netherlands Institute of Ecology (NIOO-KNAW), Netherlands
Maiko Kagami,
Yokohama National University, Japan

*CORRESPONDENCE
George S. Bullerjahn
✉ bullerj@bgsu.edu

RECEIVED 31 March 2023
ACCEPTED 31 May 2023
PUBLISHED 19 June 2023

CITATION
Wagner RS, McKindles KM and Bullerjahn GS (2023) Effects of water movement and temperature on *Rhizophydium* infection of *Planktothrix* in a shallow hypereutrophic lake.
Front. Microbiol. 14:1197394.
doi: 10.3389/fmicb.2023.1197394

Effects of water movement and temperature on *Rhizophydium* infection of *Planktothrix* in a shallow hypereutrophic lake

Ryan S. Wagner[1,2], Katelyn M. McKindles[2,3] and George S. Bullerjahn[1,2]*

[1]Department of Biology, Bowling Green State University, Bowling Green, OH, United States, [2]Great Lakes Center for Fresh Waters and Human Health, Bowling Green State University, Bowling Green, OH, United States, [3]Ecology and Evolutionary Biology, College of Literature, Science, and the Arts, University of Michigan, Ypsilanti, MI, United States

Grand Lake St. Marys (GLSM) is a popular recreational lake located in western Ohio, United States, generating nearly $150 million in annual revenue. However, recurring algal blooms dominated by *Planktothrix agardhii*, which can produce harmful microcystin toxins, have raised concerns about water safety and negatively impacted the local economy. *Planktothrix agardhii* is host to a number of parasites and pathogens, including an obligate fungal parasite in the Chytridiomycota (chytrids). In this study, we investigated the potential of these chytrid (*Rhizophydium* sp.) to infect *P. agardhii* blooms in the environment by modifying certain environmental conditions thought to limit infection prevalence in the wild. With a focus on temperature and water mixing, mesocosms were designed to either increase or decrease water flow compared to the control (water outside the mesocosm). In the control and water circulation mesocosms, infections were found infrequently and were found on less than 0.75% of the *Planktothrix* population. On the other hand, by decreasing the water flow to stagnation, chytrid infections were more frequent (found in nearly 3x as many samples) and more prevalent, reaching a maximum infection rate of 4.12%. In addition, qPCR coupled with 16S–18S sequencing was utilized to confirm the genetic presence of both host and parasite, as well as to better understand the effect of water circulation on the community composition. Statistical analysis of the data confirmed that chytrid infection was dependent on water temperature, with infections predominantly occurring between 19°C and 23°C. Additionally, water turbulence can significantly reduce the infectivity of chytrids, as infections were mostly found in stagnant mesocosms. Further, decreasing the water circulation promoted the growth of the cyanobacterial population, while increasing water agitation promoted the growth of green algae (Chlorophyta). This study starts to explore the environmental factors that affect chytrid pathogenesis which can provide valuable insights into controlling measures to reduce the prevalence of harmful algal blooms and improve water quality in GLSM and similarly affected waterbodies.

KEYWORDS

Chytridiomycota, *Planktothrix agardhii*, harmful algal blooms, food web, microcystin, mesocosms

1. Introduction

Cyanobacterial blooms are increasing with global climate and land use changes. As a result of large-scale land development and conversion to agriculture, nutrient loading into our waters has increased the size and duration of cyanobacterial harmful algal blooms (cHABS; Paerl and Barnard, 2020; Paerl et al., 2020). Furthermore, climate change has altered weather patterns, creating longer growing periods that, when coupled with increases in temperatures, favor cHABs (Paerl and Huisman, 2008). cHABs are of concern due to their ability to produce toxic compounds, known as cyanotoxins. These toxic metabolites have led to disruptions in drinking water and recreational uses (Bullerjahn et al., 2016). Understanding the mechanisms by which blooms form, are sustained, and decline are of great importance if bloom events are to be mitigated in the future.

Planktothrix is a cHAB species that is more competitive at lower light intensities and over a broader range of growth temperatures than other dominant cHAB species (Foy et al., 1976; Post et al., 1985). *Planktothrix*, with the help of gas vesicles, can adjust their buoyancy in the water column, allowing them to self-shade (Oberhaus et al., 2007) and are a filamentous cyanobacterium that is nutritionally inadequate (Schwarzenberger et al., 2020) to many zooplankton, meaning grazing pressures may be low. It is also adapt at nutrient acquisition by excreting alkaline phosphatases, allowing for the use of dissolved organic phosphorus when phosphate is depleted (Feuillade et al., 1990; Schwarzenberger et al., 2020), and is an excellent scavenger of nitrogen (Hampel et al., 2019). Thus, *Planktothrix* is ideally adapted to thriving under changes in light, temperature, and nutrient availability.

Whereas mechanisms of bloom decline involve both physical and biological drivers, fungal parasitism has received less attention in controlling cyanobacterial blooms compared to physicochemical factors and zooplankton (Sommer et al., 1986; Kagami et al., 2007). Chytridiomycota, often referred to as chytrids, is a phylum of fungi that can be aquatic parasites of phytoplankton. Chytrid infections during epidemics in freshwater environments may exceed 90% of host species (Kagami et al., 2006; Gsell et al., 2013b), particularly for hosts within the *Bacillariophyceae*. Parasitic chytrid infections within the *Cyanophyta* are less frequently linked to epidemics, but can still cause significant mortality largely because every infection leads to the death of the host (Rasconi et al., 2012; Gerphagnon et al., 2017; McKindles et al., 2021a,b). Parasitic chytrids are of great importance because they are involved in most trophic links within aquatic food webs and can contribute significantly to the transfer of carbon and energy between trophic levels through trophic upgrading of nutritionally important molecules (Amundsen et al., 2009; Miki et al., 2011; Gerphagnon et al., 2019). This transfer of carbon and energy has been observed with the bloom-forming cyanobacterium *Planktothrix* and its chytrid parasite (Frenken et al., 2018), and in other host-chytrid systems (Agha et al., 2016). Moreover, chytrids have the potential to regulate host populations, maintain host genetic diversity, and affect community structure (Sønstebø and Rohrlack, 2011; Kagami et al., 2014; Kyle et al., 2015). This host–parasite relationship has likely driven an evolutionary genetic response of the host population to chytrid infection, leading to strain specific susceptibility and the resistance to different chytrid isolates (McKindles et al., 2021a, 2023).

Temperature has a large effect on the rate of chytrid infection, both requiring an optimal temperature in which the host is viable and susceptible to infection, and an optimal temperature for the chytrid parasite to infect. To test this relationship, multiple isolates of *Planktothrix agardhii* and its parasite were obtained from the local water body Sandusky Bay, Lake Erie, United States (McKindles et al., 2021a). Sandusky Bay has a mean of 24°C during the cHAB season, so chytrid infection prevalence on *P. agardhii* was tested under laboratory conditions at temperatures ranging from 17.1°C–30.1°C and found the optimal temperature for infection was 21.7°C (McKindles et al., 2021b). Another study from cold water systems (average temperature of 8.47°C and 6.30°C) in Norway found also peak infection on *Planktothrix rubescens* at 21°C, which was the highest tested temperature (Rohrlack et al., 2015). While each of these study systems have different temperature ranges, they both had a similar infection thermal range, and both noted that there is a potential for thermal refuges to exist where *Planktothrix* can grow without any significant pressure from chytrid pathogenesis.

Chytrid zoospores are relatively small (2–6 μm) but have flagellated tails that can propel them through the water column in search of a host (Sime-Ngando, 2012). It has also been thought that chytrids seek out host through chemotaxis of chemicals released through photosynthesis. Phytoplankton release molecules creating a phycosphere to protect them or to aid in gathering resources (Bell and Mitchell, 1972). Reduced turbulence facilitates the development and establishment of the phycosphere, enabling the attraction of chemotropic organisms. In another host–parasite interaction, specifically the diatom (*Coscinodiscus granii*) and the parasitoid nanoflagellate (*Pirsonia diadema*), it was shown that water turbulence led to endemic infections, which effectively prevented the development of the host diatom (Kühn and Hofmann, 1999). They also noted that turbulent mixing could increase the chances of a parasite contacting the host, but that the contact time decreased along with that turbulent mixing (Kühn and Hofmann, 1999). *Planktothrix* and chytrid interactions have also been shown to have a negative relationship between turbulent mixing and infectivity (McKindles et al., 2021b). Additionally, *Planktothrix* can alter its buoyancy within the water column to allow optimal light and nutrient conditions. This ability to move throughout the water column coupled with water turbulence makes for an environment which chytrids may be unable to locate the hosts, despite being chemotactic.

In the light of global climate change there have been many studies focusing on the interplay of nutrient loading and temperature on the formation of cyanobacterial harmful algal blooms (cHABs). Fungal parasitism is an overlooked mechanism that can have effects on bloom food web dynamics, as well as control the diversity of cyanobacterial species (Gerphagnon et al., 2015). The goals of this study are to examine how environmental conditions can control and drive fungal parasitism in a natural setting, examining factors influencing endemic chytrid/*Planktothrix* interactions in a large, temperate freshwater reservoir.

2. Materials and methods

2.1. Large scale batch infection of Chytridiomycota on *Planktothrix agardhii*

2.1.1. *Planktothrix* and chytrid maintenance and culturing conditions

To establish if Chytridiomycota infections on *Planktothrix agardhii* could be scaled up for mesocosm testing and to test the effects

of water agitation on chytrid infection rates, preliminary experimentation was performed in lab in 15 L glass carboys. *P. agardhii* isolate 1,031 was grown as a unialgal, non-axenic batch culture (McKindles et al., 2021a). *Rhizophydiales* sp. isolate C02 were maintained on a variety of host strains to ensure no adaptations were developed before inoculation. Host and chytrid cultures were maintained in a Caron plant growth chamber (Marietta OH, United States), set at 22°C and 12:12 h light:dark cycles with cool fluorescent lights set to 15 µmol photons m^{-2} s^{-1}. Cultures were maintained in Jaworski's Medium (JM; Culture Collection of Algae and Protozoa).

2.1.2. Large scale batch cultures

Two 15 L glass carboys were filled with 10 L of sterilized JM and set within a growth box that contained a halo bulb (Sylvania FP24/841/HO/ECO) that gives off approximately 100 µmol photons m^{-2} s^{-1} of cool white light. To lower the light intensity, a mesh filter was placed between the light and the carboy until the irradiance was approximately 10 µmol photons m^{-2} s^{-1} at the surface. The experiments occurred at room temperature (20°C–22°C). One carboy was kept stagnant, while the other had a small submersible water pump (Mountain Ark, Eagle UT, United States) attached to tubing to introduce water turbulence, which was estimated to have a circulation rate of 240 L h^{-1}. Stagnant water carboy was treated as the control, as this experiment was testing the effect of water movement on infection on a large scale which previously had an inhibitory effect on infection prevalence in smaller lab cultures. *Planktothrix* was added to each carboy at an initial concentration of 100 filaments mL^{-1} which were allowed to grow and acclimate for 7 days. During this same time, the *Rhizophydiales* sp. isolate C02 (McKindles et al., 2021a) was infected on each host to familiarize the chytrid to its new host. After the week, the host was quantified as a measure of filaments mL^{-1} and the chytrid was quantified as a measure of infected filaments mL^{-1}, where infected filaments contained one or more visible sporangia at either terminus (Gsell et al., 2013a; McKindles et al., 2021a). Additionally, to assess the densities of chytrids, sporangia per filament were counted and then used as a proxy for parasite density. The chytrid culture was added to the glass jar to reach an initial infection prevalence of 10% infected filaments.

Sample collection occurred right after chytrid introduction and continued approximately every 2 days for 20 days. Water samples were collected through a neoprene tube (Tygon S3 E-3603) to minimize disturbance of the culture and allowed for depth specific sampling, which included the settled population at the bottom of the jar and the suspended population toward the top of the vessel. Sample analysis included infection prevalence and both total and dissolved microcystin production, as described below.

2.2. Amplification of chytrid infection on *Planktothrix* sp. in mesocosms

2.2.1. Grand Lake Saint Marys study site

Grand Lake St. Marys (GLSM) is a reservoir located in western Ohio and is utilized for recreation, boating, fishing, and swimming. It has a mean depth of 1.6 m, a surface area of 5,000 ha, it is hypereutrophic, and has a long East to West wind fetch of 16 km (Figure 1; Welch et al., 2017). GLSM is known for its large blooms of *Anabaena, Aphanizomenon, Microcystis,* and *Planktothrix* with summer chlorophyll and total phosphorus (TP) averaging >100 µg L^{-1} (Hoorman et al., 2008; Filbrun et al., 2013; Steffen et al., 2014; Welch et al., 2017). Mesocosms were installed at the dock on the Lake Campus of Wright State University (lat/lon 40.543889, −84.507778). The dock is set into a manmade cove and was surrounded by the Wright State campus on the west side and the east side a farm field. The only access to the lake was from the south.

2.2.2. Mesocosm design

A total of six mesocosms were installed off the dock. Each mesocosm is a 1.8 m × 28 cm (110 L volume) diameter clear polycarbonate cylinder open at the top and bottom and imbedded in the bottom sediment (Supplementary Figure 1). The mesocosms were filled with the natural community present in the water column at the start of the experiment. A cage was installed above the top opening to protect them from falling debris. The mesocosms were split into two treatments; three mesocosms had solar-powered water pumps to maintain water circulation at a rate of 240 L h^{-1}, and the other three were left stagnant. Each week the mesocosms were assayed using a YSI EXO2 sonde to measure physiochemical parameters. Samples were taken from the top and bottom of each of the mesocosms for microscopy for infections, DNA extraction, chlorophyll extraction, microcystin concentration via ELISA, and nutrient analysis. After the sampling on 24 September 2021, the mesocosms were pulled from the sediment and replaced on the same site to allow for nutrient replenishment and to reset the physiochemical properties back to ambient fall weather lake conditions. This was done by lifting each of the mesocosms out of the sediment and allowing time for the sediment cloud to dissipate then resubmerging them into the water and setting them in the sediment. Additionally, samples were collected by Silvia Newell and Stephen Jacquemin in the open waters of the lake to provide a broader community analysis sites are indicated on Figure 1.

Samples for analysis were also collected outside of the mesocosms for use as a control to determine the impact the mesocosms were having on the general water quality parameters, and the measurements within each mesocosm were used to compare the differences between replicates and treatments. All measurements were taken both inside the mesocosms and immediately outside.

2.3. Sample processing and analysis

2.3.1. Chytrid infection prevalence

Prevalence was calculated using a Sedgewick-Rafter counting cell. Each sample was counted under 100× magnification using the grids on the Sedgewick-Rafter as a reference. Samples were counted to 300 filaments or 15–1 µL grid squares with a minimum of 5 squares counted. Long filaments that were partially in the field of view were also counted by moving the microscope slide until the end of the filament was found. Prevalence was calculated by dividing the number of infected filaments over the total number of filaments inspected. Infection was determined by counting *P. agardhii* filaments with 1 or more sporangia attached to either terminus since infections only occur on the filament ends and infections are lethal (McKindles et al., 2021a,b). Prevalence of infection was reported as a percent infection of the total filaments mL^{-1}.

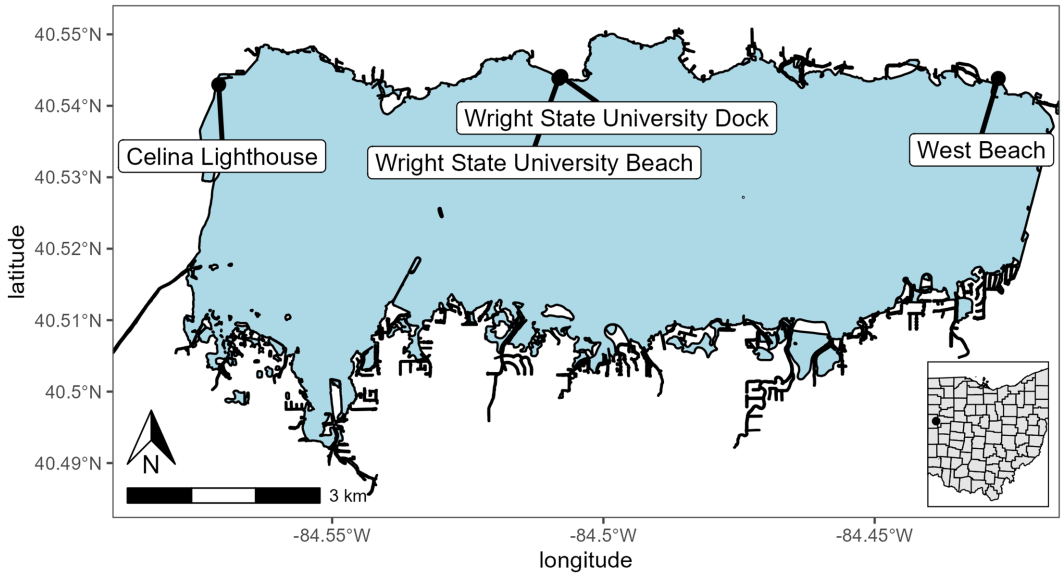

FIGURE 1
Sampling and mesocosm location for Grand Lake Saint Marys. The inset map shows the location of the lake in Ohio. Sites were Celina Lighthouse (40.54296079 and−84.57090855), Wright State University Beach and dock (40.54383316 and−84.50821996; 40.544115 and−84.507835, respectively), and west beach (40.54383316 and−84.42721725).

2.3.2. Particulate and dissolved microcystin toxin analysis

Microcystin samples were collected for both particulate and dissolved fractions during the duration of the experiment. The dissolved fraction was filtered through a 0.2 µm PTFE filter into glass vials and samples were frozen at −20°C until processed. The concentrations of particulate and dissolved microcystin toxins were measured using the Ohio EPA-approved Abraxis Microcystins-ADDA ELISA immunoassay (Abraxis LLC; Warminster, PA; EPA Method 546).

2.3.3. DNA extraction, sequencing, and qPCR

DNA was taken at each time point at both the top (0.5 m) and bottom (1 m) depths. 200 mL of water was filtered through a 0.22 µm Sterivex filter (Millipore) on site and then stored in lab at −80°C until extraction. Samples from the 1 m depth at each time point were then extracted using a DNeasy PowerWater Kit (Qiagen, Germantown, MD, United States). Sample filter cartridges were cut open using a pipe cutter and the filter was removed prior to extraction per the manufacturer's instructions. Each sample was quantified using a NanoDrop one microvolume UV-Vis spectrophotometer (Thermo Fisher Scientific, Waltham, MA, United States) to determine if the samples were appropriate for amplification and sequencing. Samples that had a concentration of at least 20 ng µL^{-1} were selected for further analysis and stored at −80°C. Samples were sent to HudsonAlpha Discovery Life Sciences (Hudson, AL, United States) for sequencing. Amplicon sequencing and QC was performed by HudsonAlpha Discovery Life Sciences using an Illumina MiSeq V3 with 600 cycle flow cells and up to 15Gb/25 M reads.

Real-time PCR was performed as outlined in McKindles et al. (2021b). In brief, the same volume of each extracted sample and 400 nM of each primer were run with PowerUp SYBR Green Master Mix (Thermo Fisher Scientific, Waltham, MA, United States) as described in McKindles et al. (2021b). Each sample was run under the same conditions multiple times using the different primer sets, as each reaction was a singleplex run. After an initial activation step at 50°C for 2 min and a denaturing step at 95°C for 2 min, 40 cycles were performed as follows: 15 s at 95°C, 30 s at 55°C and 60 s at 72°C. The efficiency of the rpoC1 primer set is 97.1% and the efficiency of the chytrid ITS primer set is 91.5% as described in McKindles et al. (2021b).

2.3.4. Chlorophyll-a extraction

Chlorophyll-a was measured following filtration onto 0.2 µm polycarbonate membranes (Millipore) and extraction with Dimethyl sulfoxide (DMSO) at room temperature. After a 30 s sonification, each sample was left to extract overnight, followed by a centrifugation and measurement by fluorometry on a Turner TD-700 fluorometer (Turner Designs, Sunnyvale, CA) calibrated with a solid standard.

2.3.5. Nutrient analysis

Nutrient samples were taken as whole water for total nutrients and filtered through a 0.22 µm Sterivex filter (Millipore) which was used as part of the DNA extraction protocol for the dissolved fraction. Both filtrate and whole water samples were sent for nutrient analysis. Nutrients were analyzed by analytical services on a SEAL AA3 autoanalyzer at The Ohio State University Stone Laboratory.

2.4. Molecular taxonomy

2.4.1. 16S and 18S rRNA taxonomic assessment

Communities were analyzed targeting the 16S V3–V4 region and 18S V9 region. Amplicon sequence libraries were constructed using

the dual index approach and the FASTQ files, along with the QC were then retrieved for further analysis.

Sequences from both 16S and 18S were processed using RStudio version 2022.07.2 working on R version 4.2.2 (2022-10-31). The DADA 2 pipeline (Callahan et al., 2016) was used for filtering, trimming, and taxonomic identification. Following DADA 2, sequences were added to the phyloseq package for further analysis. In short, samples were analyzed for quality of base calls for each sample in the forward and reverse directions. These QC scores were used to then trim sequencing to a QC threshold of 28. After trimming the primers and low-quality base calls, a DADA 2 error rate model was constructed then the sequences were dereplicated and finally the DADA 2 sequence error correction algorithm was applied to the sequences. These sequences were then merged using a 25-base pair and 12-base pair overlap with no mismatching bases for 16S and 18S, respectively. After merging, a sequence table was created, and chimeras were removed. Lastly, the sequence table was then assigned taxonomy using three separate sequence reference databases for 16S and one for 18S (Silva version 138.1, RDP trainset 16, GreenGenes version 13.8, and PR2 version 4.14.1). Following taxonomic assignment alpha diversity plots were constructed and relative abundance graphs were made to look at the community composition and relative abundance of taxa in each sample and treatment type. Finally, two beta diversity plots were constructed using Bray distances with both PCoA and NMDS methods.

2.5. Statistical analysis

Data analysis was done using RStudio version 2022.07.2 working on R version 4.2.2 (2022-10-31). Furthermore packages: Tidyverse (version 1.3.2), DADA2 (version 1.26.0), Vegan (version 2.6-4), phyloseq (version 1.42.0), and stats (version 4.2.2) were used for all data processing, statistical analysis, and graphing. Statistical significance was measured using two-way ANOVA and multiple pairwise comparisons were coupled with Tukey's *post hoc*. Community relative abundances were compared using ADONIS and was corrected using the Benjamini Hochberg protocol.

3. Results

3.1. Large scale batch culture of chytrid infections on a toxin producing *Planktothrix agardhii*

For the batch culture trial, a microcystin toxin-producing *Planktothrix agardhii* strain (strain designation 1,031) was used, and infected with chytrid isolate C2. A water pump was used to simulate natural water movement. The water circulation batch culture infection prevalence was 0–1.5% while the stagnant batch culture ranging from 1.20% to 83% (Figure 2A). Sporangia were counted as a proxy for chytrid abundances which were significantly different between the two

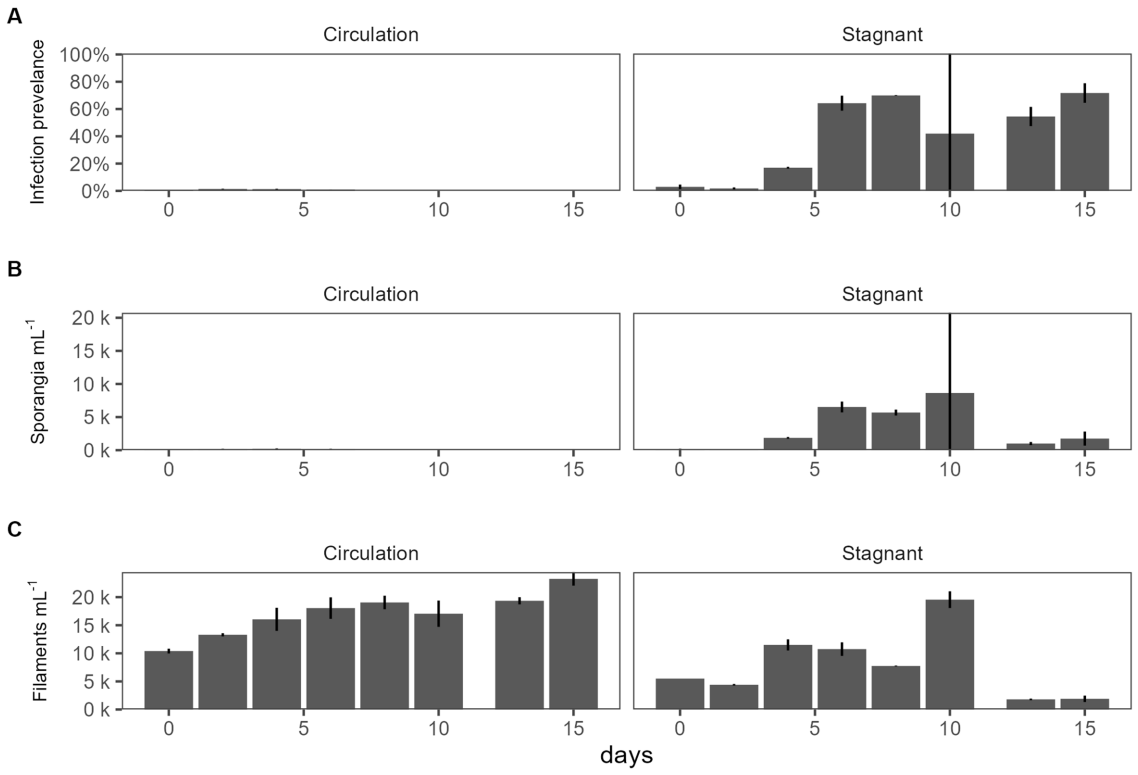

FIGURE 2
The effect of water circulation on chytrid isolate C2 pathogenesis on a toxin producing *Planktothrix agardhii* 1031. Batch culture experiment comparing water circulation and stagnant cultures. **(A)** Chytrid infection prevalence measured as percent of infected *Planktothrix* filaments over the total number of *Planktothrix agardhii* filaments. **(B)** Estimated number of sporangia. **(C)** Estimated number of total *Planktothrix agardhii* filaments. Error bars indicate standard deviation.

cultures ($p = 1.03E-02$; Figure 2B). There was no significant difference between the top and the bottom of the batch culture (Supplementary Figure 2). Infection prevalence were significantly different between the stagnant and the water circulation ($p = 1.15E-06$; Supplementary Table 1). Because a microcystin producing *P. agardhii* strain was used, the dissolved fraction of toxin was tested to assess if chytrid infection increased toxin release in large cultures. Dissolved microcystin concentrations were consistently below 1 μg L^{-1} and concentrations between the water circulation and stagnant batch cultures were significantly different ($p = 2.87E-03$; Supplementary Table 1). Looking at microcystin per filament of *Planktothrix* revealed differences between the two treatments ($p = 1.05E-08$; Supplementary Table 1) and throughout the experiment ($p = 2.47E-06$).

3.2. Physiochemical data for GLSM

To better understand the environment in which chytrid infections would occur, physiochemical data was collected within each mesocosm tube as well as in the cove waters for a period of 8 weeks, from 27 August 2021 to 22 October 2021. During this time, water temperatures ranged from 14.24°C to 27.83°C and had averages of 20.9°C ± 4.21°C, 20.7°C ± 4.24°C, and 20.7°C ± 4.18°C for control, stagnant, and circulation treatments, respectively (Figure 3A). Furthermore, over the 8-week period, temperatures were between 20°C and 22°C for about 25% of the time. The pH ranged 8.52–10.77 with stagnant water having the greatest fluctuations during the experiment (Figure 3B). Conductivity ranged 295.00–491.10 μS cm^{-1}, again with the stagnant water mesocosms having the greatest range (Figure 3C). Lastly, Secchi disk measurements as a proxy for light attenuation had an average of 21 cm for all mesocosms during the experiment and ranged from 10 to 62 cm with the highest depth values taken in the water circulation mesocosms. During peak chlorophyll-a measurements, the stagnant water mesocosms developed a film of cyanobacteria, which decreased Secchi disk measurements for these samples (Supplementary Figure 4).

3.3. Nutrients

Nutrient samples were obtained throughout the experiment at the control site and in the mesocosms to track nutrient availability to the community. Nutrient concentrations during the experimental period were 4.09–33.05 μmol L^{-1} for total phosphorus and 138.24–694.16 μmol L^{-1} for total nitrogen (Figures 4H,F). Treatments had large differences between the replicate mesocosms causing high standard deviation (Supplementary Table 1). Interestingly, stagnant mesocosms had large spikes in ammonium, dissolved reactive phosphorus and total kjeldahl nitrogen (Figures 4A,B,E) while the water circulation treatment had large spikes of nitrate and nitrite early in the experiment (Figures 4C,D). These spikes could be caused by changes in pH and changes in dissolved oxygen (Supplementary Figure 5). Additionally, the spikes in the water circulation mesocosms could be caused by the circulation which could allow for nutrient resuspension. Total phosphorus and total

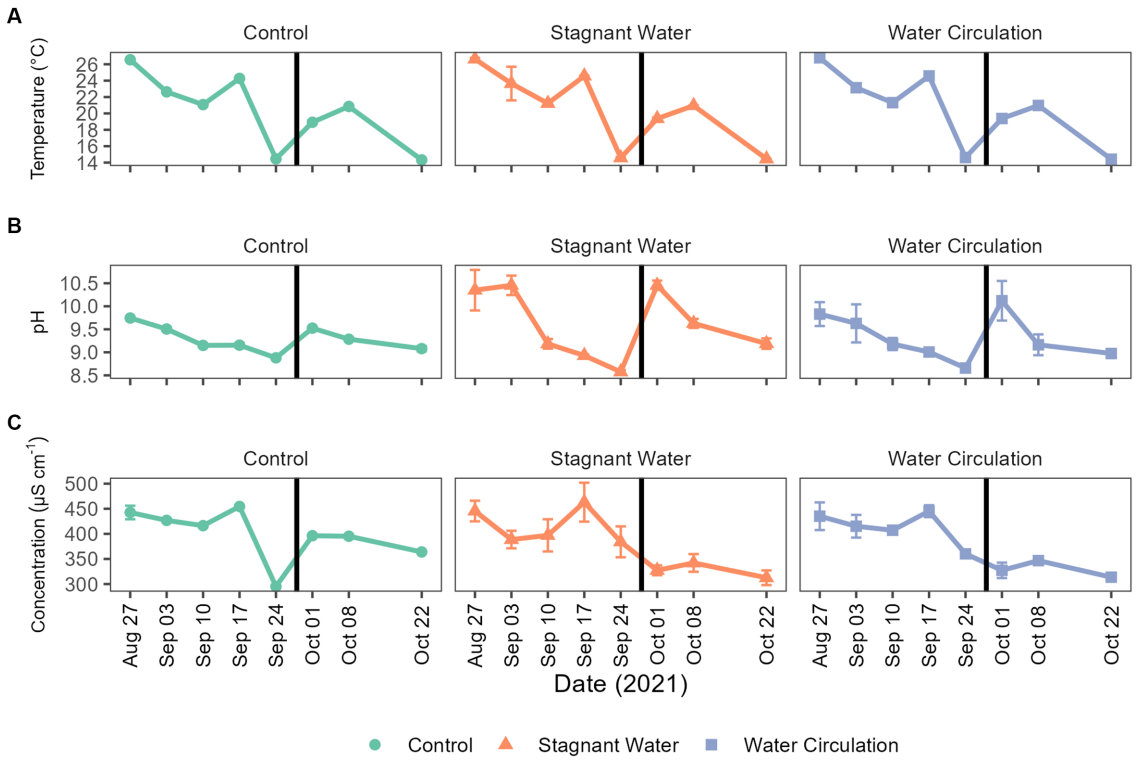

FIGURE 3
Abiotic parameters for Grand Lake Saint Marys and the mesocosms. **(A)** Temperature, **(B)** pH, and **(C)** conductivity measurements taken weekly. The black vertical line between 24 September 2021 and 01 October 2021 indicate the mesocosm reset point. Error bars indicate standard deviation.

nitrogen were significantly different between the treatments ($p = 6.40E-06$ and $p = 2.92E-02$ respectively). There were some differences between other individual nutrients during the experiment, see Supplementary Table 2. Furthermore, the spikes seen at date 24 September 2021, and leading up to that time correspond to a period when dissolved oxygen was low in both treatments with an average of $2.54 \pm 1.36\,mg\,L^{-1}$ and $1.60 \pm 0.36\,mg\,L^{-1}$ for stagnant and water circulation, respectively, on 24 September 2021 (Supplementary Table 3).

3.4. Chlorophyll-a analysis

Chlorophyll-a concentrations have been used as a proxy of productivity within a water body. Extractive chlorophyll concentration ranged from 24.77 to $896.5\,\mu g\,L^{-1}$ and had an average of $356.6 \pm 62.23\,\mu g\,L^{-1}$, $376.5 \pm 236.8\,\mu g\,L^{-1}$, and $347.2 \pm 304.9\,\mu g/L\,L^{-1}$ for control, stagnant water, and water circulation, respectively (Figure 5). This high standard deviation is due to a large amount of variability between the six mesocosms and there was a cold spell where air temperatures dropped from 28.3°C to 13.4°C during the day and at night it went from 13.9°C to 7.8°C which caused the mesocosms to drop from an average of 24.53°C to 14.58°C across both mesocosm treatments and the control (Figure 3A). Stagnant mesocosm concentrations were significantly higher than the water circulation ($p = 4.57E-09$) and the control treatment ($p = 3.76E-02$) but water circulation was not significantly different from the control ($p = 6.33E-02$; Supplementary Table 4). There was a noticeable decline in chlorophyll during the beginning part of the experiment, with an increase on 01 October 2021, when the mesocosms were reset, and a subsequent decline for the rest of the experiment until the mesocosms were removed on 22 October 2021.

3.5. Microcystin toxin concentrations

Microcystin toxin concentrations were measured during the experiment to look for the potential increase in the dissolved fraction as a response to increasing cell breakage from chytrid infections. The World Health Organization (WHO) has set a recreation exposure guideline to 10 and $1.5\,\mu g\,L^{-1}$ for drinking water. Both particulate and dissolved were measured by mixing the three mesocosms for each treatment into one sample for analysis. Dissolved concentration averaged $0.58 \pm 0.32\,\mu g\,L^{-1}$ and particulate concentrations averaged $4.87 \pm 2.86\,\mu g\,L^{-1}$. All samples from the particulate fraction were diluted 10-fold (Figure 6). Two-way ANOVA resulted in significant differences between all treatments and dates in particulate fraction ($p = 7.79E-08$ and $p = 5.90E-06$, respectively). The dissolved fraction was not significant between treatments and dates ($p = 3.98E-01$ and $p = 3.97E-01$, respectively). While particulate toxins were significantly different total toxins (both particulate and dissolved) was

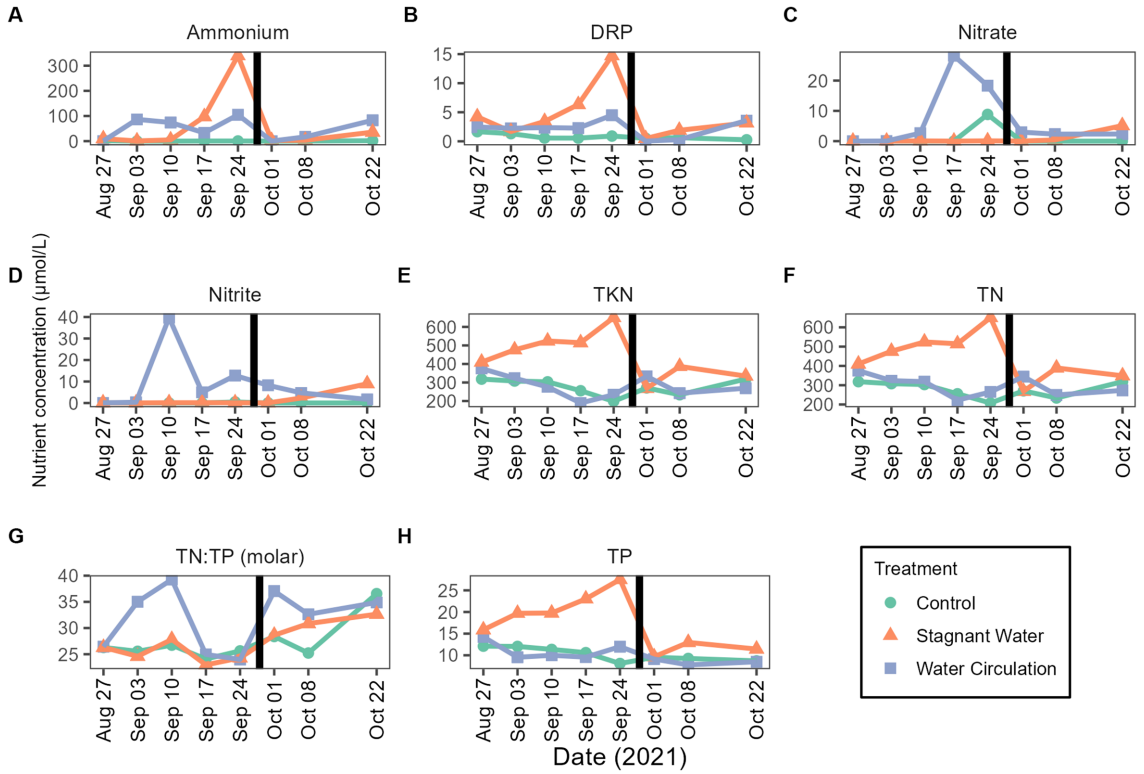

FIGURE 4
Mesocosms nutrient concentrations from 27 August 2021 to 22 October 2021. **(A)** Ammonium, **(B)** dissolved reactive phosphorus (DRP), **(C)** nitrate, **(D)** nitrite, **(E)** total kjeldahl nitrogen (TKN), **(F)** total nitrogen (TN), **(G)** TN:TP ratios as molar mass, and **(H)** total phosphorus (TP). The black vertical line between 24 September 2021 and 01 October 2021 indicate the mesocosm reset point. Please see Supplementary Table 3 for the complete data set (with standard deviations).

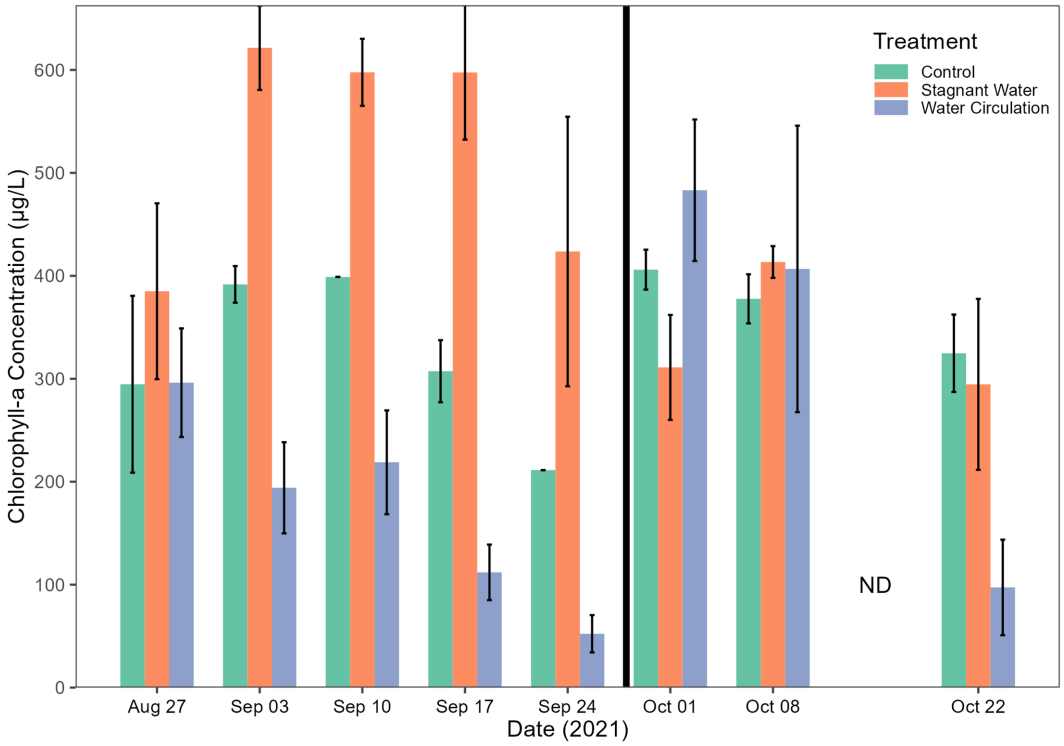

FIGURE 5
Chlorophyll-a concentrations. Error bars indicate standard deviation. The black vertical line between 24 September 2021 and 01 October 2021 indicate the mesocosm reset point.

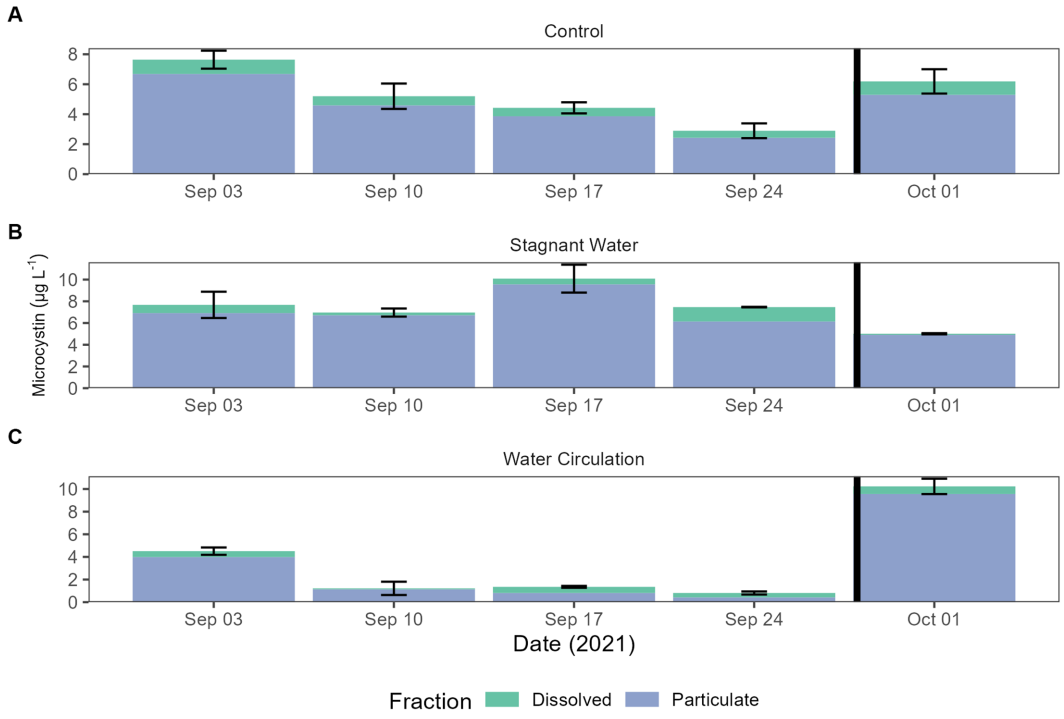

FIGURE 6
Microcystin concentrations for both total and dissolved. Error bars indicate standard deviation. **(A)** Control (cove water just outside mesocosm placement), **(B)** stagnant water mesocosms, and **(C)** water circulation mesocosms. The black vertical line between 24 September 2021 and 01 October 2021 indicate the mesocosm reset point.

not significantly different between treatments and dates (Supplementary Table 5).

3.6. Microscopy infection counts

Infection prevalence was quantified using microscopy for the duration of the experiment. Infections reached a max of 4.12% infection with an average of 0.27% ± 0.76% over all samples and dates (Figure 7). There were infections in 25% of the samples examined (n = 112), with more infections occurring in the stagnant samples vs. the other two treatment types. There were trends within the data that suggest that 9.1–9.4 and 10.3–10.6 pH, 19°C–23°C, and 316–412 µS cm^{-1} were ideal for infections but due to the low number of samples with infections we could not statistically show significance. Furthermore, there was a significant difference between infections in the three treatment groups ($p = 8.85E-07$, Supplementary Table 6) with the stagnant treatment being different from both the control ($p = 1.05E-03$) and water circulation treatment ($p = 1.72E-06$; Supplementary Table 7). There was no statistical difference in infections between the control and the water circulation treatment ($p = 9.94E-01$). Temperatures between 19°C and 23°C had the highest percent of the counted filaments infected (Figure 7) and infections within this range were significantly higher than outside of the range ($p = 1.52E-05$; Supplementary Table 8). Samples were taken at both top and bottom of each mesocosm and the control with no apparent difference between the two depths, as was seen as the *in vitro* experiments.

3.7. Community analysis

3.7.1. 16S

In addition to the mesocosms, three sites (designated "open water") were added along the north shore of GLSM for community analysis: West beach, Wright State University beach, and the lighthouse near the Celina water treatment plant intake (Figure 1). Phylum level relative abundance revealed that the stagnant water mesocosms and the open water sites were dominated by Cyanobacteria, apart from the Celina lighthouse (Figure 8). On the other hand, the water circulation mesocosms had less cyanobacteria over the course of this experiment and had higher abundances of Proteobacteria and Bacteroidota than all other treatments (Figure 8). Furthermore, the control for the mesocosms showed higher abundance of Verrucomicrobiota than the mesocosms, and less cyanobacteria than the open water and stagnant water mesocosms (Figure 8). Similar relative abundances and community composition were found between the water circulation treatment, control, and the Celina lighthouse. More specifically, the cyanobacteria were almost exclusively dominated by *Planktothrix agardhii* in all treatments including the open water samples. While many treatments were dominated by *Planktothrix agardhii* there were a few other cyanobacteria worth noting: *Cylindrospermopsis raciborskii* (1.2%–2.0%), *Aphanizomenon gracile* (1.3%–7.4%), *Dolichospermum circinale* (1%–1.4%), and *Limnothrix* (1.3%; Supplementary Figure 6). Additional information regarding the alpha and beta diversities of the 16S and 18S community is in Supplementary material.

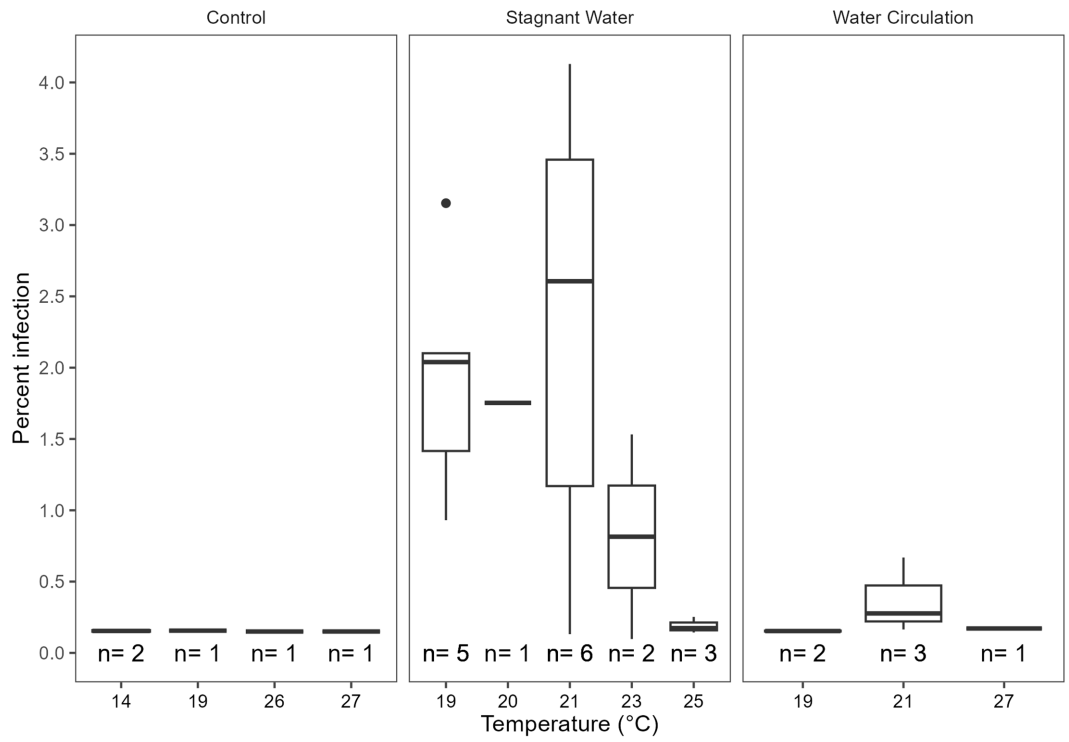

FIGURE 7
Calculated percent of infection at a given temperature separated by the treatment type control being the cove outside the mesocosms, stagnant the stagnant mesocosms, and the water circulation being the treatments with a water pump circulating water. The number of samples that had at least one identified chytrid infection within a temperature range are displayed as (*n*).

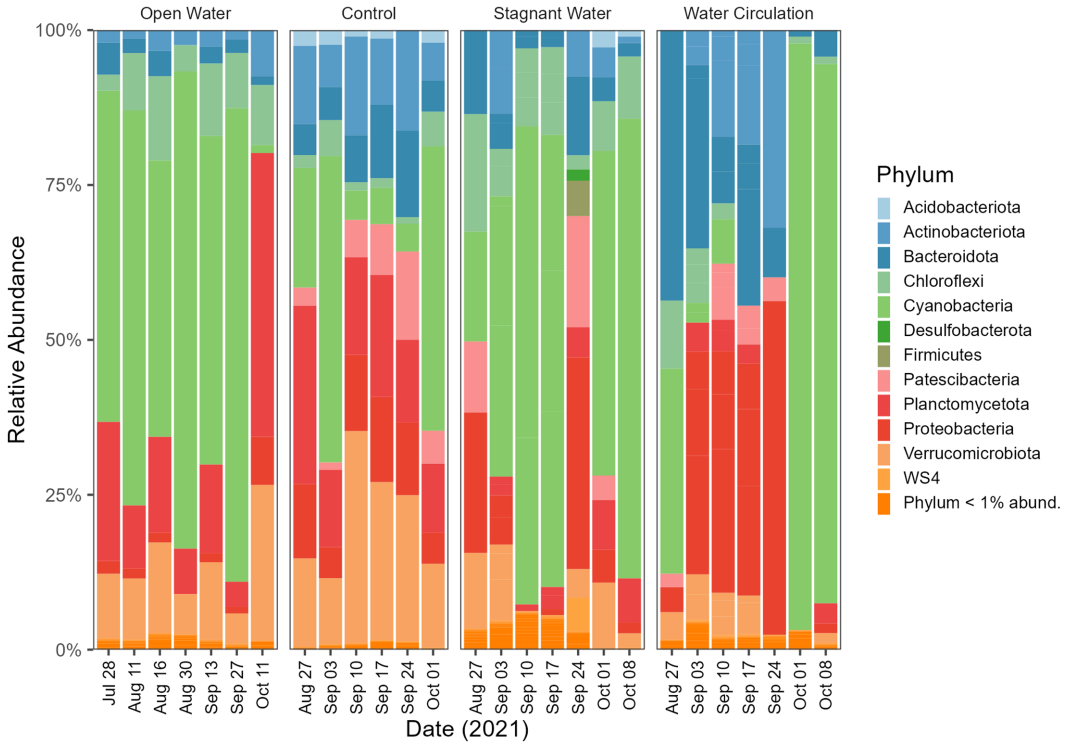

FIGURE 8
Bacterioplankton community composition at the phylum level. Open water is sites sampled outside of the cove where the mesocosms were installed. Control is within the cove next to the mesocosms. Stagnant water are mesocosms with no water circulation and the water circulation are mesocosms with a water pump moving water at 240 Lh^{-1}. Each treatment except for open water were sampled in triplicate and then pooled by date for community analysis.

3.7.2. 18S

The division level relative abundance data that was collected in this study highlights some differences between the eukaryotic communities of the different mesocosm treatments. Ciliophora and Fungi dominated the stagnant mesocosms with 8.8% and 12.4% relative abundance respectively, whereas Chlorophyta was more prevalent in the water circulation mesocosms with 14.9% relative abundance (Figure 9). The open water and control samples, on the other hand, were both dominated by Metazoa, with 19.7% and 8.5%, respectively (Figure 9). Furthermore, the specific genera of fungi that were identified in the control, open water, and stagnant mesocosms provide additional insight into the microbial communities present in each treatment. The domination of *Rhizidium*, *Rhizophydium*, and *Rhyzophidiales_X* (Supplementary Figure 7) in the control, open water, and stagnant mesocosms, respectively, could be due to the high abundance of *P. agardhii* as these genera have several species known to be parasitic on the cyanobacterial host. Additionally, there are several groups of ciliates (Ciliophora) that are known to consume *P. agardhii* including the species *Urotricha, Vorticella* and *Coleps* (Supplementary Figure 8). All three of the taxa listed here were found in abundances between 1% and 70% of the total ciliate abundances.

3.7.3. Quantitative PCR

Quantitative polymerase chain reaction (qPCR) was used to confirm microscopic trends in the abundances of chytrids (*Rhizophydiales*) and *Planktothrix* during this experiment. A total of 100 samples were tested for the genetic signatures for both *Planktothrix* and *Rhizophydiales*; of those samples, 86% of them detected *Rhizophydiales* and 100% of them detected *Planktothrix* (Figures 10A–C). Regardless of treatment, both chytrid and *Planktothrix* abundances mirrored each other with some occasional lag time (Figures 10A–C). There was statistical difference in abundances of chytrid ($p = 2.99E-02$) *Planktothrix* genetic signatures ($p = 9.54E-03$) between all the treatments including the open water samples (Supplementary Table 9). Pairwise analysis showed that *Planktothrix* was statistically different in the mesocosms vs. the control samples (Supplementary Table 10), but *Planktothrix* abundances between the mesocosm treatments were not significantly different (Supplementary Table 10). Chytrid abundances were only significantly different between the water circulation and stagnant water treatments ($p = 3.65E-02$; Supplementary Table 10).

4. Discussion

4.1. Large scale batch culture experiments

In vitro batch cultures were utilized to help predict the dynamics of *in situ* mesocosm experiments by controlling for all factors except for water agitation. Agitation using a water pump maintained similar levels of biomass between the stagnant and water circulation carboy and indicated that water movement could significantly reduce chytrid

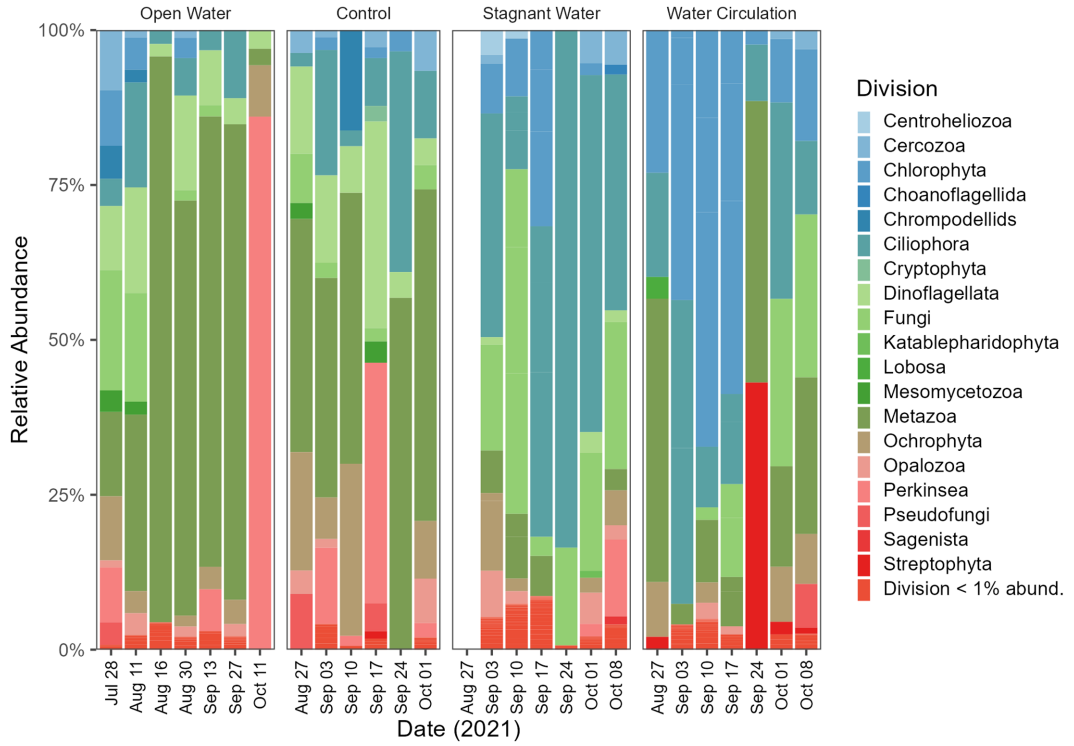

FIGURE 9
Eukaryotic community composition at the Division level. Open water is sites sampled outside of the cove where the mesocosms were installed. Control is within the cove next to the mesocosms. Stagnant water are mesocosms with no water circulation and the water circulation are mesocosms with a water pump moving water at 240 Lh^{-1}. Each treatment except for open water were sampled in triplicate and then pooled by date for community analysis.

infections on *P. agardhii* (Figure 2). Additionally, *Planktothrix* growth under moving water and stagnant water conditions are different. In batch culture water movement increased the growth rate of *Planktothrix*. This could be due to the introduction of CO_2 from the movement on the surface layer of water or from the lack of parasite infectability. This confirmed previous work that suggested water agitation would reduce chytrid infections in the wild, either by preventing zoospores from finding their host through signal disruption or by preventing swarming and attachment (McKindles et al., 2021a,b).

The presence of microcystin, a toxin of great concern, was also evaluated, as it was previously suggested that chytrid infection could cause the cells to release high concentrations of microcystin into the dissolved fraction. However, the batch culture experiment showed that even when the chytrid infection prevalence reached 40%–60%, there was almost no detectable dissolved microcystin presence (0.06 to 0.6 $\mu g L^{-1}$). Therefore, chytrid infections may not have a significant impact on microcystin production by *Planktothrix*, which support data in another recent study (Agha et al., 2022).

4.2. Grand Lake St. Marys mesocosms

The main goal of this work was to build upon previous studies looking at the environmental effects on chytrid infection on *Planktothrix agardhii* within the context of a real environment. The mesocosms were accessing an environment without amendment. Most studies have been conducted in laboratory-controlled conditions, which are important to get an estimation of what is possible, but *in situ* studies like the one conducted here can confirm lab observations and identify other potential factors that may constrain or maximize chytrid pathogenesis. Our 16S and 18S community analysis showed a population shift following installation of the mesocosms. GLSM has a dominant *Planktothrix* bloom through many months of the year (Steffen et al., 2014), meaning it would be an ideal study location.

Physiochemical measurements during the sampling period indicated that both temperature and conductivity were well suited for chytrid pathogenesis as found in previous studies (McKindles et al., 2021b). In lab studies using local to Ohio isolates of both host and parasite indicated that infections were most prominent at 0.226–0.426 mS cm^{-1} (McKindles et al., 2021b), which was consistent with the conductivity range of our study site at GLSM (0.246–0.491 mS cm^{-1}; Figure 3). Temperature was also indicated to have a significant effect on infection prevalence, with an optimal infection temperature of 21°C (McKindles et al., 2021b). Similarly, our mesocosm had the highest precent of infections between 19°C and 22°C (Figure 7). During the sampling period, the mesocosm were exposed to a wide range of water temperatures, from 14°C to 28°C (Figure 3). Infections could occasionally be identified at these extreme temperatures, but they were infrequent and not at a high prevalence (Figure 7), further suggesting the significance of thermal refuges for chytrid infections. Previous work looking at infection dynamics of Chytridiomycota and *Planktothrix* species has identified these thermal refuges in which the

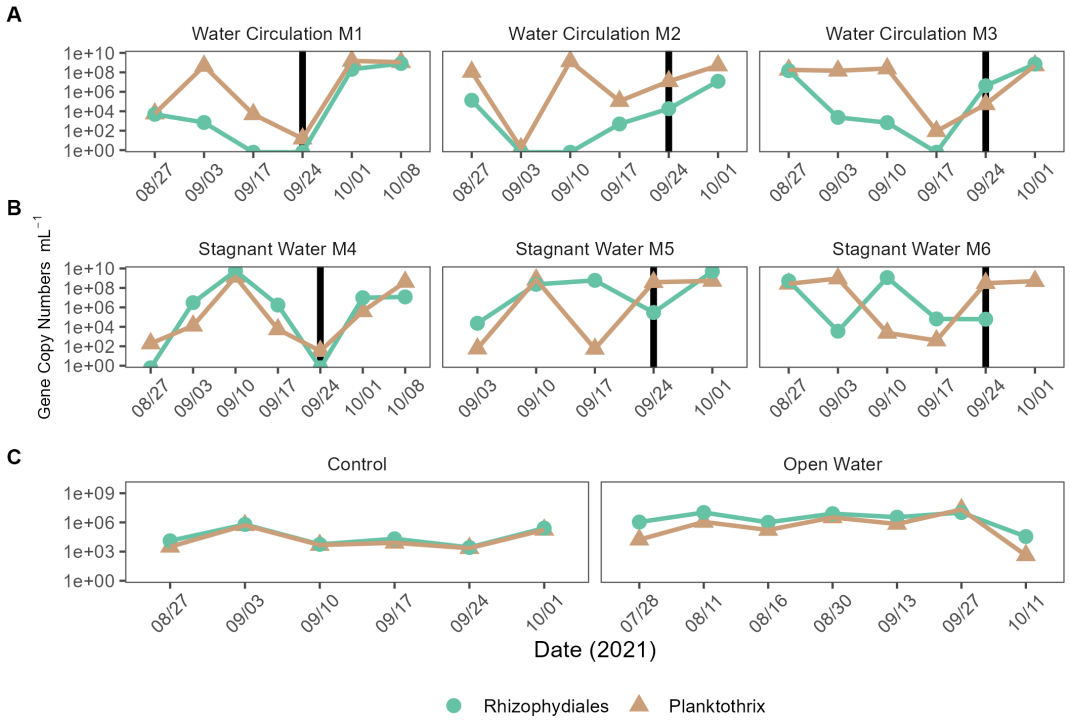

FIGURE 10
qPCR quantification of *Planktothrix agardhii* and the *Planktothrix*-specific chytrid. **(A)** Water circulation mesocosm treatments, **(B)** stagnant water mesocosm treatments, and **(C)** are the controls. The control group consists of two groups the "Control" which is right outside the mesocosm, and "Open Water" are from sites within the lake but outside of the cove where the experiment took place. Vertical lines represent the date where the mesocosms were reset after sampling.

host is able to grow at temperatures which are limiting to the parasite. In controlled laboratory studies, Rohrlack et al. (2015) identified a lower thermal refuge for *Planktothrix rubescens* at temperatures below 11.6°C, while McKindles et al. (2021b) identified an upper thermal refuge for *Planktothrix agardhii* at temperatures above 27.1°C. To date many of the experiments looking into chytrid-host interactions have been laboratory based and have reported infection rates that are not seen in the environment. More real-world experimentation like what is being done here should be done to elucidate what factors are preventing chytrid pathogenesis in the environment.

Nutrients in Grand Lake Saint Marys have been an ongoing topic of concern (Jacquemin et al., 2018). During the 8 weeks that the mesocosms were in total nitrogen in the control ranged from 138.24–694.16 μmol L^{-1} (Figure 4F) and the total phosphorus ranged from 4.091–33.05 μmol L^{-1} (Figure 4H). In the water circulation mesocosms, there was a spike of nitrate (Figures 4C,D) causing a high TN:TP ratio which could have allowed for *Planktotrhix* to be less competitive (Figure 4G). These spikes on 20 September 2021 and leading up to that time correspond to a period when dissolved oxygen was low in both treatments (Supplementary Figure 5). One possible explanation for the increase could be the decreasing temperature or the large rain event that dropped nearly 12.7 cm of rain, reducing phytoplankton production and thus relieving the use of these nutrients causing the spike. Interestingly, stagnant mesocosms had large spikes in ammonium, dissolved reactive phosphorus and total kjeldahl nitrogen (Figures 4A,B,E) this was also during the time when temperatures were low and right after the rain event. Ammonium plays a key role in sustaining *Planktothrix* blooms (Hampel et al., 2019), despite this, chlorophyll-a declined on 24 September 2021 and did not fully recover.

By reducing the water flow and creating a stagnant environment with the untreated mesocosm, both the bioactivity and cyanobacterial toxin production increased. Measurements of chlorophyll-a were used a proxy for bioactivity for each treatment, with significantly higher values in the stagnant water mesocosms compared to the water outside of the mesocosms, which was higher still than the water circulation mesocosm (Figure 5). The increased chlorophyll-a measurements for the stagnant water mesocosms were due to an increase in abundance of cyanobacteria, particularly *Planktothrix* species (Figure 8; Supplementary Figure 6). Due to *Planktothrix* being a fast migrating buoyant cyanobacteria, it is able to take advantage of stable, stagnant water column by adjusting its depth for optimal light conditions (Carey et al., 2012). This increase was also reflected in the increases in microcystin total toxin concentrations (Figure 6). In the batch culture experiment, the stagnant water treatment had a reduced *Planktothrix* carrying capacity, whereas in the mesocosms, *Planktothrix* was more prevalent in the stagnant condition than the water circulation treatments despite having more parasite pressures. This is likely because in the environment the *Planktothrix* community is more diverse than a single strain that is known to be susceptible to infection like in the batch culture. In other studies where they look at mixed populations of both host and parasite they find that mixed cultures leads to a decline in infection prevalence (McKindles et al., 2023). While McKindles et al. utilized smaller benchtop experiments more lab experiments with mixed cultures would likely be necessary to see if non-susceptible

strains of *Planktothrix* present in the stagnant water of the batch culture could then thrive as seen in the environmental mesocosms. While the cyanobacterial population dominated in the stagnant water mesocosms, it was replaced by a Chlorophyta population in the water circulation mesocosm (Figure 8; Supplementary Figure 11), perhaps indicating other environmental factors are involved population shifts besides parasitic pressure.

Within the stagnant water mesocosms, *Planktothrix* proliferated and so did the organisms that could lead to their demise. 18S reads indicated that the stagnant mesocosm was dominated by Ciliophora, Dinoflagellata, and Fungi. Ciliates are an important group of microorganisms in freshwater ecosystems, playing key roles in controlling algal populations and nutrient cycling and can therefore play an important role in mitigating the negative impacts of algal blooms. Many of the taxa within the Ciliophora and Fungi division were ones that have been reported to consume (Filip et al., 2012; Combes et al., 2013; Farthing et al., 2021) or parasitize *Planktothrix* species (Kagami et al., 2007; Agha et al., 2016; Frenken et al., 2017; McKindles et al., 2021a,b). Combined with the measures of diversity provided by the 16S and 18S data, this study reveals the importance of water movement in structuring the phytoplankton population. Overall, water movement suppresses *Planktothrix* dominance, despite the reduction of chytrid parasitism by coexisting *Rhizophydiales*. Combined with the fact that infections were rarest at 23°C and 25°C, the effects of climate change and lake warming may further reduce chytrid success. Consequently, the role of chytrid pathogenesis has limited impact in this system, despite the potential importance of trophic upgrading to grazers in the food web (Gerphagnon et al., 2019).

5. Conclusion

Fungal parasitism is an overlooked mechanism that can have effects on bloom food web dynamics, as well as control the diversity and relative abundances of cyanobacterial species. Chytrid pathogenesis reached a maximum of 4% with infections mostly occurring in the stagnant mesocosm. Temperature coupled with water movement factors limiting or restricting chytrid pathogenesis in temperate lakes. As more systems are receiving anthropogenic nutrient additions, understanding the mechanisms that control bloom severity is of great importance as chytrid pathogenesis also may play an important role in trophic upgrading and nutrient recycling within the ecosystem.

Data availability statement

The datasets presented in this study can be found in online repositories. The names of the repository/repositories and accession number(s) can be found at: https://www.ncbi.nlm.nih.gov/, PRJNA950135.

Author contributions

RW: conceptualization and writing—original draft preparation. RW and KM: methodology, formal analysis, and investigation. RW, KM, and GB: writing—review and editing and supervision. GB: funding acquisition and resources. All authors contributed to the article and approved the submitted version.

Funding

This work was supported by funding from the National Institutes of Health (1P01ES028939-01) and the National Science Foundation (OCE-1840715) awards to the Bowling Green State University Great Lakes Center for Fresh Waters and Human Health.

Acknowledgments

We thank Silvia Newell (Wright State University) and Stephen Jacquemin (Wright State University-Lake Campus) for collecting and providing samples for sequencing analysis. We also thank Wright State University for allowing us to set up our mesocosms alongside their docks. Finally, we thank the Bullerjahn and Ward lab members at BGSU for their assistance with sample processing.

Conflict of interest

The authors declare that the research was conducted in the absence of any commercial or financial relationships that could be construed as a potential conflict of interest.

Publisher's note

Supplementary material

The Supplementary material for this article can be found online at: https://www.frontiersin.org/articles/10.3389/fmicb.2023.1197394/full#supplementary-material

References

Agha, R., Gerphagnon, M., Schampera, C., Rohrlack, T., Fastner, J., and Wolinska, J. (2022). Fate of hepatotoxin microcystin during infection of cyanobacteria by fungal chytrid parasites. *Harmful Algae* 118:102288. doi: 10.1016/j.hal.2022.102288

Agha, R., Saebelfeld, M., Manthey, C., Rohrlack, T., and Wolinska, J. (2016). Chytrid parasitism facilitates trophic transfer between bloom-forming cyanobacteria and zooplankton (Daphnia). *Sci. Rep.* 6:35039. doi: 10.1038/srep35039

Amundsen, P.-A., Lafferty, K. D., Knudsen, R., Primicerio, R., Klemetsen, A., and Kuris, A. M. (2009). Food web topology and parasites in the pelagic zone of a subarctic lake. *J. Anim. Ecol.* 78, 563–572. doi: 10.1111/j.1365-2656.2008.01518.x

Bell, W., and Mitchell, R. (1972). Chemotactic and growth responses of marine bacteria to algal extracellular products. *Biol. Bull.* 143, 265–277. doi: 10.2307/1540052

Bullerjahn, G. S., McKay, R. M., Davis, T. W., Baker, D. B., Boyer, G. L., D'Anglada, L. V., et al. (2016). Global solutions to regional problems: collecting global expertise to address the problem of harmful cyanobacterial blooms. A Lake Erie case study. *Harmful Algae* 54, 223–238. doi: 10.1016/j.hal.2016.01.003

Callahan, B. J., McMurdie, P. J., Rosen, M. J., Han, A. W., Johnson, A. J. A., and Holmes, S. P. (2016). DADA2: high-resolution sample inference from Illumina amplicon data. *Nat. Methods* 13, 581–583. doi: 10.1038/nmeth.3869

Carey, C. C., Ibelings, B. W., Hoffmann, E. P., Hamilton, D. P., and Brookes, J. D. (2012). Eco-physiological adaptations that favour freshwater cyanobacteria in a changing climate. *Water Res.* 46, 1394–1407. doi: 10.1016/j.watres.2011.12.016

Combes, A., Dellinger, M., Cadel-six, S., Amand, S., and Comte, K. (2013). Ciliate Nassula sp. grazing on a microcystin-producing cyanobacterium (*Planktothrix agardhii*): impact on cell growth and in the microcystin fractions. *Aquat. Toxicol.* 126, 435–441. doi: 10.1016/j.aquatox.2012.08.018

Farthing, H. N., Jiang, J., Henwood, A. J., Fenton, A., Garner, T. W. J., Daversa, D. R., et al. (2021). Microbial grazers may aid in controlling infections caused by the aquatic Zoosporic fungus Batrachochytrium dendrobatidis. *Front. Microbiol.* 11:592286. doi: 10.3389/fmicb.2020.592286

Feuillade, J., Feuillade, M., and Blanc, P. (1990). Alkaline phosphatase activity fluctuations and associated factors in a eutrophic lake dominated by *Oscillatoria rubescens*. *Hydrobiologia* 207, 233–240. doi: 10.1007/BF00041461

Filbrun, J. E., Conroy, J. D., and Culver, D. A. (2013). Understanding seasonal phosphorus dynamics to guide effective management of shallow, hypereutrophic grand Lake St. Marys, Ohio. *Lake Reserv Manage* 29, 165–178. doi: 10.1080/10402381.2013.823469

Filip, J., Müller, L., Hillebrand, H., and Moorthi, S. (2012). Nutritional mode and specialization alter protist consumer diversity effects on prey assemblages. *Aquat. Microb. Ecol.* 66, 257–269. doi: 10.3354/ame01573

Foy, R. H., Gibson, C. E., and Smith, R. V. (1976). The influence of daylength, light intensity and temperature on the growth rates of planktonic blue-green algae. *Br. Phycol. J.* 11, 151–163. doi: 10.1080/00071617600650181

Frenken, T., Alacid, E., Berger, S. A., Bourne, E. C., Gerphagnon, M., Grossart, H.-P., et al. (2017). Integrating chytrid fungal parasites into plankton ecology: research gaps and needs: research needs in plankton chytridiomycosis. *Environ. Microbiol.* 19, 3802–3822. doi: 10.1111/1462-2920.13827

Frenken, T., Wierenga, J., Donk, E., Declerck, S. A. J., Senerpont Domis, L. N., Rohrlack, T., et al. (2018). Fungal parasites of a toxic inedible cyanobacterium provide food to zooplankton. *Limnol. Oceanogr.* 63, 2384–2393. doi: 10.1002/lno.10945

Gerphagnon, M., Agha, R., Martin-Creuzburg, D., Bec, A., Perriere, F., Rad-Menéndez, C., et al. (2019). Comparison of sterol and fatty acid profiles of chytrids and their hosts reveals trophic upgrading of nutritionally inadequate phytoplankton by fungal parasites. *Environ. Microbiol.* 21, 949–958. doi: 10.1111/1462-2920.14489

Gerphagnon, M., Colombet, J., Latour, D., and Sime-Ngando, T. (2017). Spatial and temporal changes of parasitic chytrids of cyanobacteria. *Sci. Rep.* 7:6056. doi: 10.1038/s41598-017-06273-1

Gerphagnon, M., Macarthur, D. J., Latour, D., Gachon, C. M. M., van Ogtrop, F., Gleason, F. H., et al. (2015). Microbial players involved in the decline of filamentous and colonial cyanobacterial blooms with a focus on fungal parasitism. *Environ. Microbiol.* 17, 2573–2587. doi: 10.1111/1462-2920.12860

Gsell, A. S., de Senerpont Domis, L. N., van Donk, E., and Ibelings, B. W. (2013a). Temperature alters host genotype-specific susceptibility to Chytrid infection. *PLoS One* 8:e71737. doi: 10.1371/journal.pone.0071737

Gsell, A. S., de Senerpont Domis, L. N., Verhoeven, K. J., van Donk, E., and Ibelings, B. W. (2013b). Chytrid epidemics may increase genetic diversity of a diatom spring-bloom. *ISME J.* 7, 2057–2059. doi: 10.1038/ismej.2013.73

Hampel, J. J., McCarthy, M. J., Neudeck, M., Bullerjahn, G. S., McKay, R. M. L., and Newell, S. E. (2019). Ammonium recycling supports toxic Planktothrix blooms in Sandusky Bay, Lake Erie: evidence from stable isotope and metatranscriptome data. *Harmful Algae* 81, 42–52. doi: 10.1016/j.hal.2018.11.011

Hoorman, J., Hone, T., Sudman, T., Dirksen, T., Iles, J., and Islam, K. R. (2008). Agricultural impacts on Lake and stream water quality in grand Lake St. Marys, Western Ohio. *Water Air Soil Pollut.* 193, 309–322. doi: 10.1007/s11270-008-9692-1

Jacquemin, S. J., Johnson, L. T., Dirksen, T. A., and McGlinch, G. (2018). Changes in water quality of grand Lake St. Marys watershed following implementation of a distressed watershed rules package. *J. Environ. Qual.* 47, 113–120. doi: 10.2134/jeq2017.08.0338

Kagami, M., de Bruin, A., Ibelings, B. W., and Van Donk, E. (2007). Parasitic chytrids: their effects on phytoplankton communities and food-web dynamics. *Hydrobiologia* 578, 113–129. doi: 10.1007/s10750-006-0438-z

Kagami, M., Gurung, T. B., Yoshida, T., and Urabe, J. (2006). To sink or to be lysed? Contrasting fate of two large phytoplankton species in Lake Biwa. *Limnol. Oceanogr.* 51, 2775–2786. doi: 10.4319/lo.2006.51.6.2775

Kagami, M., Miki, T., and Takimoto, G. (2014). Mycoloop: chytrids in aquatic food webs. *Front. Microbiol.* 5:166. doi: 10.3389/fmicb.2014.00166

Kühn, S. F., and Hofmann, M. (1999). Infection of *Coscinodiscus granii* by the parasitoid nanoflagellate Pirsonia diadema: III. Effects of turbulence on the incidence of infection. *J. Plankton Res.* 21, 2323–2340. doi: 10.1093/plankt/21.12.2323

Kyle, M., Haande, S., Ostermaier, V., and Rohrlack, T. (2015). The red queen race between parasitic Chytrids and their host, Planktothrix: a test using a time series reconstructed from sediment DNA. *PLoS One* 10:e0118738. doi: 10.1371/journal.pone.0118738

McKindles, K. M., Jorge, A. N., McKay, R. M., Davis, T. W., and Bullerjahn, G. S. (2021a). Isolation and characterization of Rhizophydiales (Chytridiomycota), obligate parasites of *Planktothrix agardhii* in a Laurentian Great Lakes embayment. *Appl. Environ. Microbiol.* 87, e02308–e02320. doi: 10.1128/AEM.02308-20

McKindles, K. M., Manes, M. A., McKay, R. M., Davis, T. W., and Bullerjahn, G. S. (2021b). Environmental factors affecting chytrid (Chytridiomycota) infection rates on *Planktothrix agardhii*. *J. Plankton Res.* 43, 658–672. doi: 10.1093/plankt/fbab058

McKindles, K. M., McKay, R. M. L., Bullerjahn, G. S., and Frenken, T. (2023). Interactions between chytrids cause variable infection strategies on harmful algal bloom forming species. *Harmful Algae* 122:102381. doi: 10.1016/j.hal.2023.102381

Miki, T., Takimoto, G., and Kagami, M. (2011). Roles of parasitic fungi in aquatic food webs: a theoretical approach. *Freshw. Biol.* 56, 1173–1183. doi: 10.1111/j.1365-2427.2010.02562.x

Oberhaus, L., Briand, J. F., Leboulanger, C., Jacquet, S., and Humbert, J. F. (2007). Comparative effects of the quality and quantity of light and temperature on the growth of Planktothrix agardhii and *P. rubescens* [1]. *J. Phycol.* 43, 1191–1199. doi: 10.1111/j.1529-8817.2007.00414.x

Paerl, H. W., and Barnard, M. A. (2020). Mitigating the global expansion of harmful cyanobacterial blooms: moving targets in a human- and climatically-altered world. *Harmful Algae* 96:101845. doi: 10.1016/j.hal.2020.101845

Paerl, H. W., Havens, K. E., Xu, H., Zhu, G., McCarthy, M. J., Newell, S. E., et al. (2020). Mitigating eutrophication and toxic cyanobacterial blooms in large lakes: the evolution of a dual nutrient (N and P) reduction paradigm. *Hydrobiologia* 847, 4359–4375. doi: 10.1007/s10750-019-04087-y

Paerl, H. W., and Huisman, J. (2008). Blooms Like It Hot. *Science* 320, 57–58. doi: 10.1126/science.1155398

Post, A. F., de Wit, R., and Mur, L. R. (1985). Interactions between temperature and light intensity on growth and photosynthesis of the cyanobacterium *Oscillatoria agardhii*. *J. Plankton Res.* 7, 487–495. doi: 10.1093/plankt/7.4.487

Rasconi, S., Niquil, N., and Sime-Ngando, T. (2012). Phytoplankton chytridiomycosis: community structure and infectivity of fungal parasites in aquatic ecosystems: fungal epidemics in the plankton. *Environ. Microbiol.* 14, 2151–2170. doi: 10.1111/j.1462-2920.2011.02690.x

Rohrlack, T., Haande, S., Molversmyr, Å., and Kyle, M. (2015). Environmental conditions determine the course and outcome of phytoplankton Chytridiomycosis. *PLoS One* 10:e0145559. doi: 10.1371/journal.pone.0145559

Schwarzenberger, A., Kurmayer, R., and Martin-Creuzburg, D. (2020). Toward disentangling the multiple nutritional constraints imposed by Planktothrix: the significance of harmful secondary metabolites and sterol limitation. *Front. Microbiol.* 11:586120. doi: 10.3389/fmicb.2020.586120

Sime-Ngando, T. (2012). Phytoplankton Chytridiomycosis: fungal parasites of phytoplankton and their imprints on the food web dynamics. *Front. Microbiol.* 3:361. doi: 10.3389/fmicb.2012.00361

Sommer, U., Gliwicz, Z., Lampert, W., and Duncan, A. (1986). The PEG-model of seasonal succession of planktonic events in fresh waters. *Archiv. Fur Hydrobiologie* 106, 433–471. doi: 10.1127/archiv-hydrobiol/106/1986/433

Sønstebø, J. H., and Rohrlack, T. (2011). Possible implications of Chytrid parasitism for population subdivision in freshwater Cyanobacteria of the genus Planktothrix. *Appl. Environ. Microbiol.* 77, 1344–1351. doi: 10.1128/AEM.02153-10

Steffen, M. M., Zhu, Z., McKay, R. M. L., Wilhelm, S. W., and Bullerjahn, G. S. (2014). Taxonomic assessment of a toxic cyanobacteria shift in hypereutrophic grand Lake St. Marys (Ohio, USA). *Harmful Algae* 33, 12–18. doi: 10.1016/j.hal.2013.12.008

Welch, E. B., Gibbons, H. L., Brattebo, S. K., and Corson-Rikert, H. A. (2017). Distribution of aluminum and phosphorus fractions following alum treatments in a large shallow lake. *Lake Reserv Manage* 33, 198–204. doi: 10.1080/10402381.2016.1276653

frontiers | Frontiers in Microbiology

TYPE Original Research
PUBLISHED 29 June 2023
DOI 10.3389/fmicb.2023.1199641

OPEN ACCESS

EDITED BY
Ryan Paerl,
North Carolina State University, United States

REVIEWED BY
Maureen Coleman,
The University of Chicago, United States
Sheri Floge,
Wake Forest University, United States

*CORRESPONDENCE
Katelyn M. McKindles
✉ kmckindl@umich.edu

RECEIVED 03 April 2023
ACCEPTED 08 June 2023
PUBLISHED 29 June 2023

CITATION
McKindles KM, Manes M, Neudeck M, McKay RM and Bullerjahn GS (2023) Multi-year molecular quantification and 'omics analysis of *Planktothrix*-specific cyanophage sequences from Sandusky Bay, Lake Erie. *Front. Microbiol.* 14:1199641. doi: 10.3389/fmicb.2023.1199641

Multi-year molecular quantification and 'omics analysis of *Planktothrix*-specific cyanophage sequences from Sandusky Bay, Lake Erie

Katelyn M. McKindles[1,2,3]*, Makayla Manes[4], Michelle Neudeck[3], Robert Michael McKay[2,3] and George S. Bullerjahn[3]

[1]Ecology and Evolutionary Biology, University of Michigan, Ann Arbor, MI, United States, [2]Great Lakes Institute for Environmental Research, University of Windsor, Windsor, ON, Canada, [3]Great Lakes Center for Fresh Waters and Human Health, Bowling Green State University, Bowling Green, OH, United States, [4]Department of Microbiology, The Ohio State University, Columbus, OH, United States

Introduction: *Planktothrix agardhii* is a microcystin-producing cyanobacterium found in Sandusky Bay, a shallow and turbid embayment of Lake Erie. Previous work in other systems has indicated that cyanophages are an important natural control factor of harmful algal blooms. Currently, there are few cyanophages that are known to infect *P. agardhii*, with the best-known being PaV-LD, a tail-less cyanophage isolated from Lake Donghu, China. Presented here is a molecular characterization of Planktothrix specific cyanophages in Sandusky Bay.

Methods and Results: Putative *Planktothrix*-specific viral sequences from metagenomic data from the bay in 2013, 2018, and 2019 were identified by two approaches: homology to known phage PaV-LD, or through matching CRISPR spacer sequences with *Planktothrix* host genomes. Several contigs were identified as having viral signatures, either related to PaV-LD or potentially novel sequences. Transcriptomic data from 2015, 2018, and 2019 were also employed for the further identification of cyanophages, as well as gene expression of select viral sequences. Finally, viral quantification was tested using qPCR in 2015–2019 for PaV-LD like cyanophages to identify the relationship between presence and gene expression of these cyanophages. Notably, while PaV-LD like cyanophages were in high abundance over the course of multiple years (qPCR), transcriptomic analysis revealed only low levels of viral gene expression.

Discussion: This work aims to provide a broader understanding of Planktothrix cyanophage diversity with the goals of teasing apart the role of cyanophages in the control and regulation of harmful algal blooms and designing monitoring methodology for potential toxin-releasing lysis events.

KEYWORDS

cyanophage, *Planktothrix agardhii*, PaV-LD, metagenome, metatranscriptome, qPCR

1. Introduction

Cyanobacterial harmful algal bloom (cHAB) prevalence is increasing worldwide due to a combination of nutrient pollution and climate change (O'Neil et al., 2012; Wurtsbaugh et al., 2019; Gobler 2020). These blooms are of concern due to their ability to impact human health, ecosystem processes, and regional economies. cHABs can produce multiple toxins and secondary

metabolites which have been linked to neurotoxicity, respiratory distress, cancers with prolonged exposure, and death of livestock and pets (Codd et al., 2020; Metcalf et al., 2021; Wang et al., 2021; Mchau et al., 2022). They can grow so dense that they block light penetration in aquatic ecosystems, leading to a reduction in the diversity and abundance of other species (Sunda et al., 2006). Further, cHABs can cause significant economic losses in affected regions by reducing the value of aquatic products, reducing tourism, and reducing home values (Hoagland et al., 2002; Sanseverino et al., 2016; Guillotreau et al., 2021; Heil and Muni-Morgan, 2021; Wolf et al., 2022).

Planktothrix agardhii can form blooms inhabiting eutrophic freshwaters worldwide (Kurmayer et al., 2015). *P. agardhii* is of particular concern in the Laurentian Great Lakes region due to annual recurrence in Sandusky Bay, a drowned river mouth draining into the open waters of Lake Erie (Davis et al., 2015; Hampel et al., 2019). Unlike *Microcystis* which dominates in the western basin of Lake Erie, *Planktothrix* grows at a broader temperature range (Foy et al., 1976; Post et al., 1985), is adapted to lower light levels (Oberhaus et al., 2007) and can scavenge ammonium more effectively (Hampel et al., 2019), all of which allow it to thrive in turbid Sandusky Bay, in which nitrogen can become limiting due to high rates of denitrification (Salk et al., 2018).

Previous work has sought to better understand the dominance of *Planktothrix agardhii* in Sandusky Bay through metagenome and metatranscriptome analysis (Hampel et al., 2019; McKindles et al., 2022). Part of this characterization included an analysis of the host foreign DNA defense response, the CRISPR-cas system, which was used to aid in the identification of viral signatures (McKindles et al., 2022). This study noted that only a small percentage of spacer sequences could be identified as previously isolated cyanophage sequences, indicating the presence of heretofore unexplored viral diversity.

Part of the issue of identification of cyanophages is the lack of available reference sequences due to a low success rate in cyanophage isolation. Currently, there is only one isolated cyanophage that is known to target *P. agardhii*: PaV-LD (Gao et al., 2009). This virus belongs to the Podoviridae and was isolated from Lake Donghu (East Lake), China, with a burst size of 340 viral particles per cell and an incubation period of 6–8 days (Gao et al., 2009). PaV-LD contains a double-stranded DNA genome of 95.3 kbp and approximately 142 open reading frames (Gao et al., 2012a). Notably, the phage does not cause complete lysis of the host in the lab, which could be a combination of viral infection strategies and host defense response. Indeed, infections varied depending on stage of host growth, leading to the hypothesis that infections in stable environments were limited due to more stable cell wall structures and more robust host restriction (Gao et al., 2012b).

Despite these studies, there has been little progress to understand the geographical distribution of related *Planktothrix* specific cyanophages in regions where *Planktothrix*-dominated blooms are common, nor is it well known what kind of cyanophage diversity is found in these same regions. To address this, methodology was utilized similar to Morimoto et al. (2020) to identify novel viral signatures in metagenomic data sets from local *Planktothrix agardhii* CRIPSR-cas spacer sequences and then to utilize metatranscriptomics to confirm viral gene expression. Further, PaV-LD major capsid protein (ORF073) primers were utilized to evaluate PaV-LD-like cyanophage presence over the course of 5 bloom seasons in Sandusky Bay, showcasing the high frequency in which viral signatures can be found over the course of a bloom and the consistency in host to virus gene copy ratio across years in the host assocated fraction.

2. Materials and methods

2.1. Sampling sites and processing

At the southeast region of the western Lake Erie is the shallow (mean depth, 2.6 m), hourglass-shaped Sandusky Bay, which is divided into an outer bay (eastern half) and an inner bay (western half) (Figure 1). In coordination with the Ohio Department of Natural Resources, biweekly water quality surveys of Sandusky Bay were conducted from 2015–2019. In brief, samples were collected during the bloom season (May to October) from three sites between 2015 and 2017 (ODNR4, ODNR1, and EC1163) with the addition of a fourth site, the Edison Bridge, in 2018 and 2019.

Samples were collected in the field from a constant depth of 1 m and biomass was concentrated onto 0.22 µm Sterivex cartridge filters, which were immediately flash-frozen on dry ice. Once in the lab, the filters were stored in a −80°C freezer until nucleic acids were extracted. In addition to sampling for planktonic biomass, physicochemical data were measured at each site using a model 600 QS water quality probe (YSI Inc., Yellow Springs, OH) capturing surface water temperature, dissolved oxygen concentration, and conductivity (Bullerjahn and McKay, 2020a,b).

During the field season of 2018 and 2019, samples were also collected to measure extracellular PaV-LD presence. One liter of unfiltered water was used in the filtration protocol to collect extracellular phage particles as detailed by Haramoto et al. (2005). Briefly, the whole/unfiltered water was split into two 500-ml duplicate portions for each date and prefiltered through a Whatman 4 filter (GE Healthcare Bio-Sciences, Pittsburgh, PA) to remove large particles. A 0.45-µm pore size S-Pak membrane filter (MilliporeSigma, Burlington, MA) was charged with 250 mM $AlCl_3$ and placed on a vacuum filtration apparatus. The filtrate from the first step was passed through the charged S-Pak membrane filter, with the aluminum promoting retention of the cyanophage present in the sample. The filter was washed with 0.5 mM H_2SO_4 to remove remaining aluminum ions prior to phage elution with 10 mM NaOH, and neutralization with 100 × TE buffer [1 M Tris–HCl, 100 mM EDTA (pH 8.0)]. Viral concentrates were stored at −80°C until undergoing DNA extraction.

2.2. DNA and RNA extraction

DNA was extracted from Sterivex cartridge filters with the DNeasy PowerWater Sterivex DNA isolation kit (Qiagen, Germantown, MD) following the manufacturer's instructions. DNA quantity was checked using a Quantus Fluorometer (Promega, Madison, WI) and the associated QuantiFluor ONE dsDNA System kit (Promega), per manufacturer's instructions. RNA was extracted from Sterivex cartridge filters using the Qiagen RNeasy PowerWater Kit by first removing the Sterivex filter from the cartridges under sterile conditions in a laminar flow hood, then following the manufacturer's instructions.

The xanthogenate-SDS extraction method used for viral filtrate DNA extractions was outlined by Tillett and Neilan (2000) to extract the

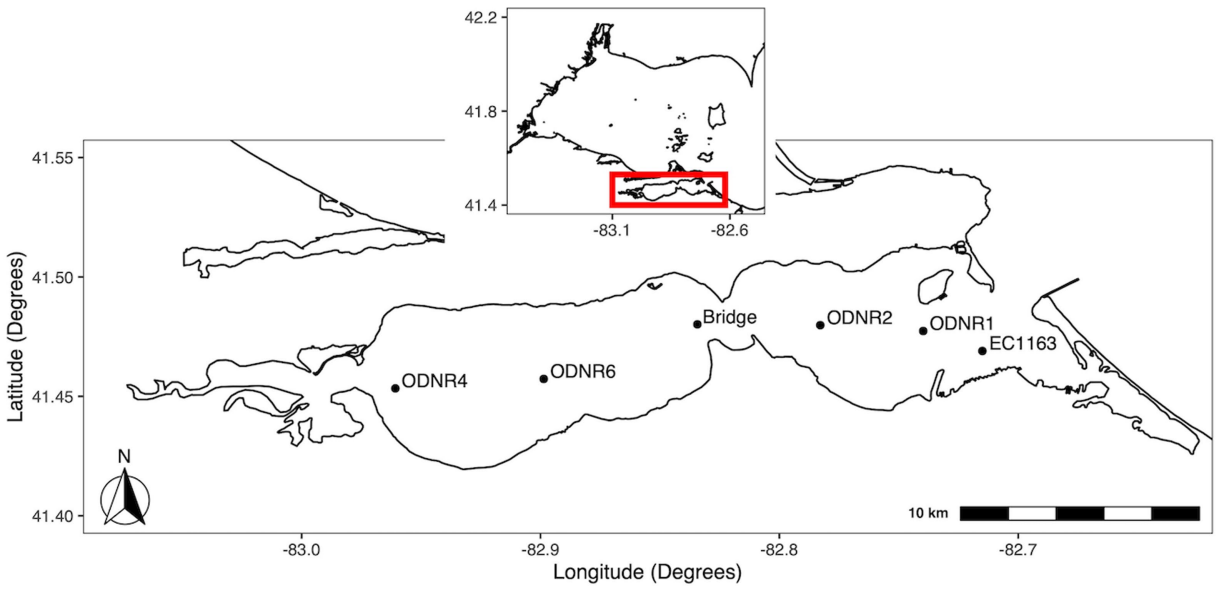

FIGURE 1
Map of sampling locations in Sandusky Bay. The inset shows the location of Sandusky Bay in relation to the western basin of Lake Erie. Sites were chosen to provide representation of the width and depth of the bay. Sites were ODNR4 (41.453333, −82.960767), Edison bridge (41.480156, −82.834328), ODNR1 (41.477367, −82.739783), and EC1163 (41.469000, −82.715000).

DNA from environmental samples containing cyanobacteria and was later modified by Yoshida et al. (2006) for use on *Microcystis* cyanophages. Concentrated viral filtrate (200 µL) was added to 750 µL of XS buffer [1% potassium ethyl xanthogenate, 100 mM Tris–HCl (pH 7.4), 20 mM EDTA (pH 8), 1% sodium dodecyl sulfate, 800 mM ammonium acetate] and incubated at 70°C for 30 min, vortexing every 10 min. After incubation for 30 min on ice, isopropanol was added to each tube to 50% (vol/vol). The tubes were incubated at room temperature for a minimum of 10 min followed by centrifugation to pellet the DNA at 12,000 × *g* for 10 min. DNA was washed with 70% ethanol and then air dried for 24 h before resuspension in TE buffer [10 mM Tris–HCl, 1 mM EDTA (pH 8)]. Once the DNA was extracted, it was stored at −80°C for later use.

2.3. Monitoring of PaV-LD presence by quantitative PCR

Quantification of *Planktothrix agardhii* occurred as described in McKindles et al. (2021). In brief, *Planktothrix agardhii* species-specific primers rpoC1_Plank_F271 and rpoC1_P_agardhii_R472 were used (Churro et al., 2012; Table 1), which have a primer efficiency of 0.971. The g-block standard was also previously described, generating a standard curve range of $38.66–3.866 \times 10^9$ copies μL^{-1}.

To quantify the presence of PaV-LD related cyanophages, primers were generated based on the major capsid protein gene sequence (PaVLD_ORF073R; YP_004957346.1). The capsid gene sequence was uploaded to the primer designer web application (OligoPerfect Primer Designer; Thermo Fisher Scientific, Waltham, MA). Selected primer sets were then analyzed by BLASTn against the nonredundant (nr) database to assess possible spurious hybridization and ensure that the primers were specific to the template, and no other sequences in the nr database could be amplified by the primer sets (Ye et al., 2012). Once tested, the region inclusive of the primer set and extra base pairs in either direction was extracted to create external standards (Supplementary Table S1). External standards were used to determine copy numbers of each qPCR target by creating a 10-fold dilution series of G-block gene fragments (Integrated DNA Technologies, Coralville, IA). G-blocks were diluted to 10 ng μL^{-1} stocks, and the total copy number of G-block fragments was calculated using the formula: number of copies (molecules) = (A ng × 6.0221×10^{23} molecules $mole^{-1}$) / ((N × 660 g $mole^{-1}$) × 1 × 10^9 ng g^{-1}), where A is the amount of amplicon in ng, N is the length of the dsDNA amplicon, and 660 g $mole^{-1}$ is the average mass of 1 bp dsDNA (Prediger, 2013). The range for the PaV-LD capsid standard was $20.56–2.056 \times 10^9$ copies μL^{-1}.

Real-time PCR was performed using 5 µL of each extracted DNA with the PowerUp SYBR Green Master Mix (Thermo Fisher Scientific) and 400 nM of each primer (Table 1). Each sample was amplified under the same conditions multiple times using the different primer sets, as each reaction was a singleplex run. After an initial activation step at 50°C for 2 min and a denaturing step at 95°C for 2 min, 40 cycles were performed as follows: 15 s at 95°C, 30 s at 55°C, and 60 s at 72°C. A melt curve was also performed to ensure a single qPCR product was formed, going from 50°C to 95°C at an increase of 0.5°C per cycle. The program was run on a 4-channel Q Real-Time PCR thermocycler (Quantabio, Beverly, MA) along with the Q-qPCR v1.0.1 software analysis program (Quantabio), which was used to determine the sample concentrations as compared to a standard curve. The efficiency of the PaV-LD major capsid protein primer set is 99.66% (Table 1).

2.4. Metagenome sequences for identification of cyanophage genomes

Two cell faction samples with high viral loads (ODNR4 on June 28, 2017, and ODNR1 on June 26, 2018) were chosen based on qPCR

10.3389/fmicb.2023.1199641

TABLE 1 Primers sets and g-block standards for *Planktothrix agardhii* and PaV-LD.

Target organism	Target gene name	Forward primer (5′-3′)	Reverse primer (5′-3′)	Product size (bp)	Efficiency	Ref.
All *Planktothrix agardhii*	rpoC1	TGTTAAATCCAGGTAACTATGACGGCCTA	GCGTTTTTGTCCCTTAGCAACGG	224	0.971	McKindles et al. (2021), Churro et al. (2012)
PaV-LD	ORF_073RMajor Capsid Protein	GTTAGTCGGATGGGCGAG	CGGGTGGGAGCTAAACCAAT	443	0.9966	This study

quantification of PaV-LD for metagenome sequencing. Samples were sequenced at the University of Michigan Advanced Genomics Core (Ann Arbor, MI) on a NovaSeq 6,000 sequencing system (Illumina, San Diego, CA). Once sequenced, FASTA files were imported into CLC Genomics Workbench v.20.0.2 software (Qiagen, Redwood City, CA) with the default quality settings following Steffen et al. (2017). Failed reads were discarded during import. Paired-end reads for both samples were trimmed for quality prior to being combined for assembly into contigs (minimum length of 2,000 bp) using the CLC Genomics Workbench *de novo* assembly function that also mapped reads back to the generated contigs. Contigs generated from ODNR 4 on June 28, 2017 were denoted with the data set number 140939 while contigs generated from ODNR1 on June 26, 2018 were denoted with the data set number 140938.

To supplement these two samples, metagenome generated contigs were obtained from a SPAdes analysis project (Ga0209229) from JGI Gold Biosample ID Gb0059903, a Sandusky Bay metagenome study dated June 11, 2013.

2.5. Identification of PaV-LD like cyanophage genes

To identify PaV-LD like cyanophage genes, the genomic sequence of PaV-LD (NC_016564) was obtained from NCBI and imported into CLC Genomics Workbench v.20.0.2 software (Qiagen, Redwood City, CA). Gene annotations were extracted using the Extract Annotated Regions 1.4 tool, which was used as a BLASTn database for metagenome generated contigs using standard parameters, except for an increased word size of 50. Positive BLASTn hits were filtered using a Lowest E-value of 0.00, Greatest identity % ≥ 85, and Greatest bit score of ≥1,500. The resulting hit sequences were exported to Geneious Prime (Biomatters Ltd., Auckland, NZ) version 2020.2.3 as a sequence list. Confirmation of relatedness was determined by mapping the contigs to the reference sequence PaV-LD (NC_016564) using Geneious mapper set to Dissolve contigs and re-assemble, Low Sensitivity, and Iterate up to 5 times. The rest of the parameters were kept standard. Regions of mapped coverage were extracted and re-aligned using MUSCLE 3.8.425 to determine percent identity between the viral genes of known function and the contigs. The DNA sequences were translated using the Translate tool and standard genetic code. Protein sequences were re-aligned using the Geneious Alignment tool with Global alignment and Blosum90 cost matrix selected.

2.6. Identification of novel *Planktothrix agardhii* cyanophage contigs

Metagenome generated contigs from 2017 and 2018, along with the downloaded contigs from 2013, were analyzed by BLASTn against Sandusky Bay *P. agardhii* isolate CRISPR spacer sequences as generated in McKindles et al. (2022). BLASTn parameters were modified to accommodate small sequences as follows: Match/Mismatch and Gap Costs were at Match 2, Mismatch 2, Existence 5, and Extension 2, Expectation value was set to 10.0, and Word size set to 25. Contig sequences with multiple hit regions were checked for full *P. agardhii* CRISPR-cas cassettes and were extracted if they contained

novel spacer sequences. These new spacer sequences were added to the spacer sequence database generated previously and are described in Supplementary Table S2. All contigs were then re-analyzed by BLASTn against the newly generated full CRISPR spacer sequence database with the same BLASTn parameters as before. Any hit contigs with CRISPR-cas casettes and/or CRISPR spacer repeat sequence were removed and the remaining contig sequences (71 sequences) were exported as FASTA files for the detection of virus-associated sequences using VirSorter 1.0.3, with the "virome" option (Roux et al., 2015). Suspected prophages (no sequences) and contigs with no viral signatures (47 sequences) were then excluded from further analysis, leaving 24 contig sequences as possible viral sequences. A list of contigs that had CRISPR positive hits but did not pass the VirSorter viral signature analysis can be found in Supplementary Table S3. Several of these contigs were identified as viral homologues against PaV-LD but may not have contained the viral signatures that are searched for using the VirSorter database.

The 24 punitive viral contig sequences were imported in VIPtree (Nishimura et al., 2017) for the generation of a proteomic relatedness tree (generation of genomic similarity scores) and to annotate viral genes with tBLAST function. This tree was used to group similar sequences for in depth analysis of gene function, but given the short length of the viral fragments, may not accurately represent different viral sequences or families.

2.7. Metatranscriptome analysis from Sandusky Bay in 2015, 2018, and 2019

Extracted RNA was sent to Discovery Life Sciences (Huntsville, AL), where the samples were treated to reduce rRNA using TruSeq Stranded Total RNA with Ribo-Zero Plant kit (Illumina, San Diego, CA). RNA was sequenced on an Illumina HiSeq 2,500 platform with paired-end reads of 50 base pairs (2015) or 150 base pairs (2018, 2019).

The metatranscriptome reads were analyzed using the CLC Genomics Workbench v.20.0.2 software (Qiagen, Redwood City, CA). The raw reads were filtered through quality control where failed reads were removed using the CLC Toolbox, remaining reads were trimmed with an ambiguous base limit of 2 and automatic read-through adapter trimming. Reads shorter than 15 bp were discarded. The raw reads were mapped to whole punitive viral contigs generated above, the whole PaV-LD genome (NC_016564), and the whole genome of *Planktothrix agardhii* NIVA-CYA 126/8 (NZ_CM002803) using the RNA-Seq Analysis feature in the CLC Toolbox with a mismatch cost of 2, insertion cost of 3, deletion cost of 3, length fraction of 0.8, a similarity fraction of 0.8, and a maximum number of hits at 10.

2.8. Data availability

Raw read files from ODNR4 on June 28, 2017 (140939), and ODNR1 on June 26, 2018 (140938), were uploaded to the National Center for Biotechnology Information (NCBI) Sequence Read Archive (SRA) under Bioproject accession number PRJNA940836. The *Planktothrix* viral contigs assembled from the metagenome data sets (2017 and 2018) were deposited in the NCBI GenBank Database under accession numbers OQ674116 – OQ674125. Metatranscriptomes from 2015, 2018, and 2019 were also deposited in the NCBI SRA under Bioproject accession numbers PRJNA946791 (2015), PRJNA941812 (2018), and PRJNA945377 (2019).

3. Results

3.1. Monitoring of PaV-LD presence by quantitative PCR

The abundance of *Planktothrix agardhii* in Sandusky Bay was estimated using the single copy housekeeping gene, *rpoC1* (Figure 2). In 2015, *P. agardhii rpoC1* concentrations fluctuated between 186 and 5.76×10^6 gene copies mL^{-1}, with higher average concentrations occurring in the outer bay (EC1163 and ODNR1) compared to the inner bay (ODNR4). All three sites showed a decrease in numbers on August 11, 2015, which rebounded in both EC1163 and ODNR1. In 2016, *P. agardhii* concentrations ranged from 62 to 3.44×10^6 gene copies mL^{-1}. The low end of this range occurred on July 11, 2016, at site EC1163, where abundance of 1.49×10^6 gene copies mL^{-1} dropped rapidly, recovering the next sample date to 2.25×10^4 gene copies mL^{-1}. While not as rapid, ODNR1 also shows a population dip on July 25 and August 3, 2016. 2017 was the most stable year for *P. agardhii* according to genetic quantification. Except for July 31, 2017, at site ODNR4 where the genetic concentration was the lowest for the year at 1.59×10^5 gene copies mL^{-1}, all *P. agardhii* concentrations were above 1.1×10^6 gene copies mL^{-1}. The last trip acquiring genetic information occurred on July 24, 2018, which was correlated with a population decrease at the Edison Bridge, EC1163, and ODNR1, while populations remained high in the inner bay at site ODNR4. ODNR4 in 2018 had a rapid decline in population early in the season, dropping from 4.73×10^6 gene copies mL^{-1} to 1.4×10^4 gene copies mL^{-1} before recovering to 1.58×10^6 gene copies mL^{-1}. These trends in qPCR estimation for 2018 were reflected in the *Planktothrix* biomass cell count data (Supplementary Figure S1). 2019, the final year of molecular quantification in Sandusky Bay as part of this study, was the most distinct. Gene copy numbers started off the season with some of the lowest values recorded at each site, recovering to more typical concentrations by August, and ending the season in September with continually high numbers. Overall, the highest genetic quantification of *P. agardhii* occurred multiple times in 2018 at sites EC1163, ODNR1, and ODNR4, while the lowest numbers occurred primarily at site ODNR 4 in 2015, 2018, and 2019.

Over this period, the presence of PaV-LD and local derivatives of this cyanophage were monitored by testing for the genetic sequence coding for one of the two major capsid proteins (Figure 2). In general, the genetic quantification of the capsid protein mirrored the trends of the host quantification. If the host population declined rapidly, the cyanophage genetic signature also declined. In 2015, the proportion of cyanophage genetic sequence compared to the host genetic sequence ranged from less than 5% (EC1163, August 11, 2015) to almost 3 × more prevalent than its host (June 29, 2015, at ODNR4). In 2016, both ODNR4 and ODNR1 measured lower viral population presence compared with its host, but EC1163 showed increased viral presence mid to late season (July 11, 2016, at 6.9 x more and July 25, 2016, at 2.5 x more). In 2017, cyanophage to host ratios were consistently between 0.23 and 3.29, further indicating that 2017 was a stable year. On July 28, 2018, at the Edison Bridge the first instance of a double-digit virus to host ratio occurred, which was 68 × more

10.3389/fmicb.2023.1199641

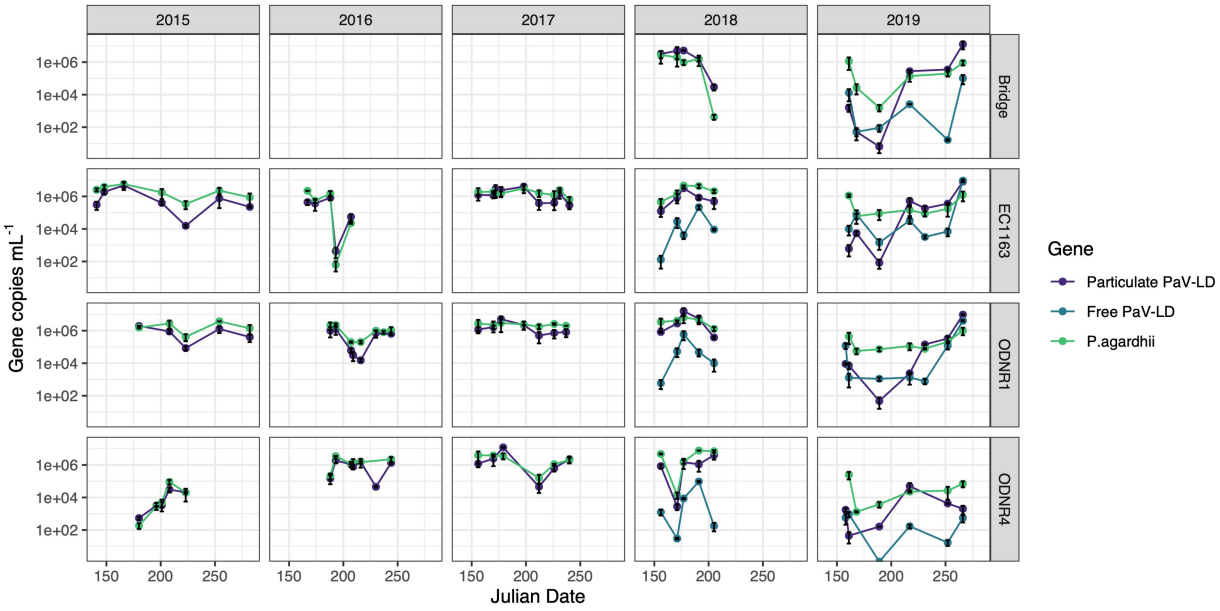

FIGURE 2
Quantitative PCR of PaV-LD like cyanophages and their host, *Planktothrix agardhii*, across five bloom-forming years in Sandusky Bay (Table 1). *Planktothrix agardhii* was quantified using the single copy housekeeping gene, *rpoC1*. PaV-LD like cyanophages were quantified using the major capsid protein gene sequence (PaVLD_ORF073R). Samples were particulate associated (0.22μm filter) or free cyanophage (cation charged filter). Samples were analyzed as biological duplicates and standard deviation is indicated by the black bars.

cyanophage than *P. agardhii*. Otherwise, ratios were more stable, where presence was measured at the lowest at 0.14 and up to 5.33 × more abundant. Finally, in 2019, some of the lowest concentrations of cyanophage genetic signatures were recorded in the early season, which made up only 0.02–1% of the host population concentrations. In mid-season, viral concentrations rebounded, matching the concentration of the host (approximately 1.3 to 3.6 x more virus than host) and ended the season at even higher ratios at the Edison Bridge (13.5 x), EC1163 (6.5 x), and ODNR1 (9.5 x). Given the similar patterns of the cyanophage-host abundance as outlined by this dataset, it becomes clear that these viruses are present and a prevalent component of cyanobacterial harmful algal bloom ecology.

In 2018 and 2019, extracellular PaV-LD quantification of select sites was added by concentrating free cyanophages onto a cation coated filter. In general, this quantification revealed that the free PaV-LD fraction was lower than the host associated fraction (Figure 2). The three sites sampled in 2018 showed a free viral fraction that made up approximately 3 ± 6% of the host associated viral fraction. On the other hand, 2019 was characterized by higher free cyanophage loads in the early season (average 11 times higher than host associated loads), followed by lower free viral percentages the rest of the year (20 ± 30%). Note that both free phage and host associated phage loads increase rapidly at the end of the season.

3.2. Identification of PaV-LD like cyanophage contigs

Metagenome generated contigs were mapped to the only known *Planktothrix agardhii* specific cyanophage, PaV-LD (NC_016564) to determine how related the PaV-LD-like cyanophages may be to the reference. From three metagenomic data sets, 24 contigs were closely related (greatest identity % ≥ 85) to genes from PaV-LD (Figure 3). These alignments can be classified as 100% similar (white regions, Figure 3), or greater than 80% similar (light grey, Figure 3), corresponding to the presence of conserved regions and genes. Discordant regions (Dark grey and black regions, Figure 3) are areas surrounding insertions, deletions, and nucleotide substitutions. These contigs cover several essential PaV-LD sequences, including both capsid proteins, the tail tape measure protein and a highly conserved region including a serine/threonine-protein phosphatase and a protein kinase (Table 2). In particular, the region encompassing both capsid proteins had the most coverage, where one capsid protein (ORF073R) was highly conserved both in nucleotide and amino acid identity, but the other (ORF071R) was only conserved in 3 out of 5 sequence contigs (Table 2).

3.3. Identification of novel *Planktothrix agardhii* cyanophage contigs

To better understand the cyanophage diversity present in Sandusky Bay, CRISPR-cas spacer sequences from previously sequenced *Planktothrix agardhii* genomes were used to identify metagenome contigs that were possible foreign genetic material. Additional curation using viral signatures yielded 24 contigs from 2013 (Ga0209229), 2017 (140939), and 2018 (140938), of lengths ranging from 2,027–24,459 bp (Table 3). The VirSorter Category for each contig is noted, where category 1 contigs are "most confident predictions" (significant enrichment in viral-like genes and at least one hallmark viral gene detected), category 2 contigs are "likely predictions" (either enrichment in viral-like genes or a viral hallmark

10.3389/fmicb.2023.1199641

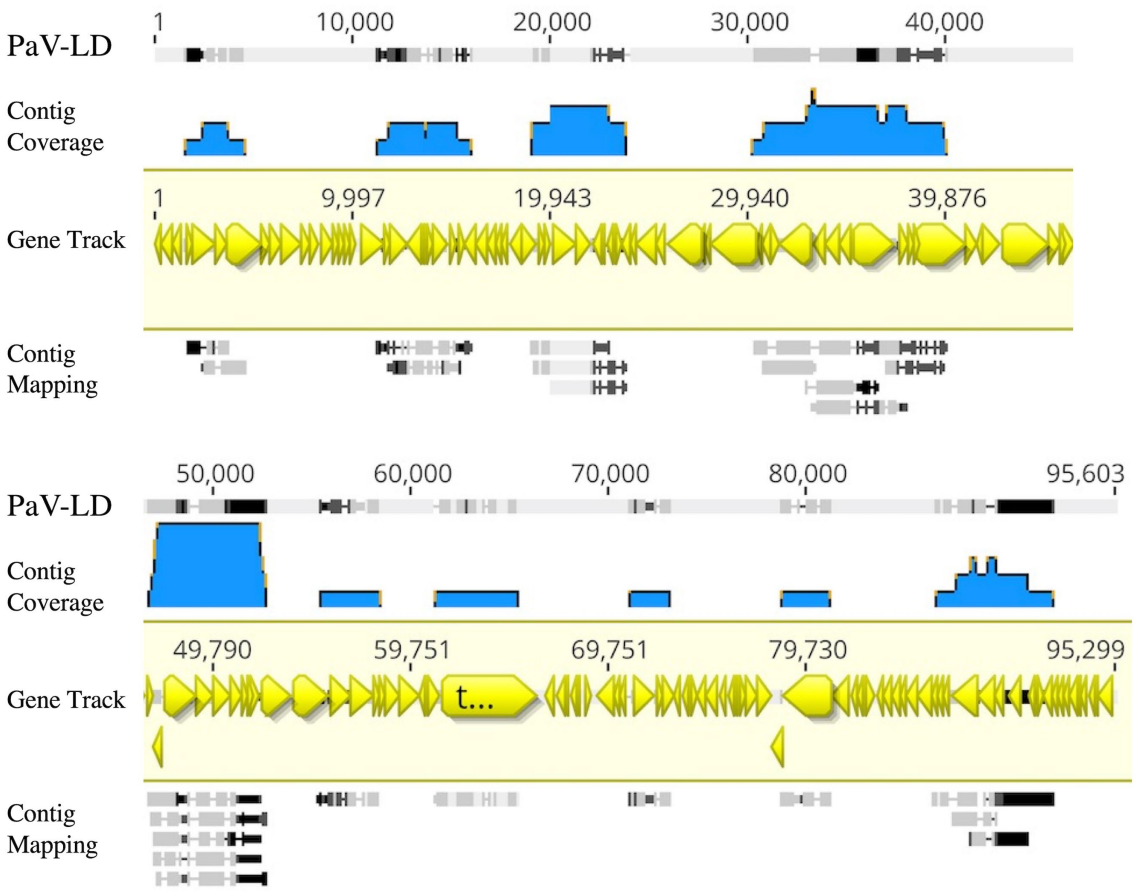

FIGURE 3
Contigs with CRISPR-cas identified viral signatures were aligned with the published genome of PaV-LD. 24 contigs were closely related (greatest identity %≥85). White regions indicate 100% similar, light grey regions indicate greater than 80% similar, while both dark grey and black regions indicate discordant regions (insertions, deletions, and nucleotide substitutions). Reference sequence is highlighted in yellow and includes gene annotations. Coverage is noted using blue.

gene is detected along with other metrics), and category 3 are "possible predictions" (neither a hallmark gene nor enrichment in viral-like genes but significant scores in other metrics) (Roux et al., 2015). VirSorter output includes a GenBank flat file which contains the number and location of genes for each contig, as well as predicted gene product. These annotations along with previous CRISPR spacer sequence alignments were used to determine the number of CRISPR spacer hits and the probable viral gene to which the spacers corresponded. Most of the spacer sequences hit for hypothetical proteins, some of which have a direct PaV-LD ORF associated with them. Others are related to phage clusters as defined by VirSorter. There were several contig sequences that had multiple spacers hit, and a few contigs that had spacers hit for more than one gene. Ga0209229_10034259 had the most CRISPR spacer hits at 19, which were at 4 different regions of the contig alongside each of the 4 genes. Ga0209229_10003398 had the second most hits at 11, which were focused on a single gene, indicating that this spacer sequence was common across 11 different *Planktothrix agardhii* isolates. A list of contigs that had CRISPR positive hits but did not pass the VirSorter viral signature analysis can be found in Supplementary Table S3. These 24 contigs were then used to generate a proteomic viral tree to understand their relationships to one another and to identify novel viral genetic signatures (Figure 4). This analysis identified 6 viral groupings, which mainly represent different gene functionalities. Note that these groupings are not indicative of all new viruses, and may represent different parts of the same virus.

3.3.1. Viral contig group 1 (PaV-LD)

Viral group 1 represents all the metagenome generated viral fragments that cluster on the same proteomic branch as the previously described *Planktothrix agardhii* cyanophage PaV-LD (Table 4). Some of the contigs are highly related to PaV-LD with genomic similarity (S_G) scores above 0.95 or 95%, including Ga0209229_10004734, 140,939_contig_132, and 140,938_contig_201. Additionally, here are a few contigs that are partially related to PaV-LD with S_G scores above 0.75 or 75%, including 140,939_contig_131 and Ga0209229_10008255. Finally, there is a set of 4 contigs that are only loosely related to PaV-LD with S_G scores below 0.75 or 75%, including Ga0209229_10012861, Ga0209229_10034259, Ga0209229_10003398, and Ga0209229_10021454. All the contigs in this group have genes that were originally found in the sequencing of PaV-LD.

The 3 highly similar contigs (Ga0209229_10004734, 140,939_contig_132, and 140,938_contig_201) all encode for the same region of PaV-LD between 47 – 52 kb which includes the genes

TABLE 2 Known PaV-LD annotations that are covered by environmental metagenome generated contigs and their relatedness in nucleotide and amino acid identity.

PaV-LD gene annotation	PaV-LD ORF	Metagenome contig	Nucleotide identity	Amino acid identity
nblA	PaVLD_ORF022L	Ga0209229_10029639	97.58%	92.73%
		Ga0209229_10013247	98.18%	90.91%
Serine/threonine-protein phosphatase	PaVLD_ORF036R	140,939_contig_710	100%	100%
		140,938_contig_91	100%	100%
		Ga0209229_10010503	100%	100%
Protein kinase	PaVLD_ORF037R	140,939_contig_710	99.15%	99.26%
		140,938_contig_91	99.15%	99.26%
		Ga0209229_10010503	99.15%	99.26%
Terminase large subunit	PaVLD_ORF053L	Ga0209229_10001486	91.03%	78.13%
		Ga0209229_10026891	99.00%	97.20%
Portal protein	PaVLD_ORF057R	Ga0209229_10006839	99.35%	99.85%
		Ga0209229_10001486	91.23%	96.08%
Capsid protein	PaVLD_ORF071R	140,938_contig_201	97.05%	98.03%
		140,939_contig_132	97.05%	98.03%
		Ga0209229_10004734	96.98%	97.64%
		140,939_contig_131	89.58%	92.38%
		Ga0209229_10004679	86.15%	89.27%
Capsid protein	PaVLD_ORF073R	Ga0209229_10004734	98.64%	100%
		140,938_contig_201	98.85%	100%
		140,939_contig_132	98.74%	100%
		Ga0209229_10004679	92.77%	99.68%
Virion structural protein	PaVLD_ORF081R	140,938_contig_929	93.32%	85.68%
Tail tape measure protein	PaVLD_ORF088R	Ga0209229_10008835	96.89%	98.75%

PaVLD_ORF070L to PaVLD_ORF077R. This region is mostly hypothetical proteins (6 out of 8 genes) but does include both capsid protein genes (PaVLD_ORF071R and PaVLD_ORF073R). Interestingly, this region of PaV-LD is also covered by the partially related contig 140,939_contig_131 and the contig Ga0209229_10004679, which was not picked up in the VirSorter analysis (Supplementary Table S3). As noted in previous analysis, the capsid protein PaVLD_ORF071R was covered by two distinct groups (Figure 5). The main group, including Ga0209229_10004734, 140,939_contig_132, and 140,938_contig_201, are highly similar to the reference amino acid sequence (~ 97% identity). The other group, including 140,939_contig_131 and Ga0209229_10004679, show a 95% amino acid sequence similarity to each other, but only an 88% amino acid sequence similarity to the reference. Interestingly, while closely related across years, there are some sequence differences between the 2013 data set (Ga0209229) and the 2018 and 2019 metagenomes, which may represent mutations acquired or lost over time.

The remaining contigs line up to other portions of PaV-LD (Table 4). These genes are primarily hypothetical proteins, with the exception of the tail tape measure protein PaVLD_ORF088R found in Ga0209229_10003398. Further, the contig gene hits do not have many conserved domains suggesting function, except for a relative of hypothetical protein PaVLD_ORF116R found in Ga0209229_10021454, which contains a KGG repeat domain indicating a possible function in stress response.

3.3.2. Viral contig group 2

Viral group 2 consists of two approximately identical sequences, Ga0209229_10017258 and Ga0209229_10007918 ($S_G = 1$), which has a weak similarity to PaV-LD at $S_G = 0.2282$. These sequences encode for 5 genes: a DNA modification methylase (Phage_cluster_4886), an uncharacterized Tet_JBP domain-containing protein (Phage_cluster_6254), a nuclease with a partial alignment to PaVLD_ORF098R (Phage_cluster_4886), a hypothetical protein of unknown origin, and a hypothetical protein from *Planktothrix agardhii* (WP_235754195).

3.3.3. Viral contig group 3

Viral group 3 consists of two different groups of three sequences each; Group 3A encompassing 140,939_contig_119, Ga0209229_10002258, and Ga0209229_10001752, while Group 3B includes 140,939_contig_283, 140,938_contig_27, and Ga0209229_10001252. Within subgroups, sequences are highly similar ($S_G = 0.958 \pm 0.026$) and across the two subgroups, they are distantly related ($S_G = 0.725 \pm 0.009$). Despite this lower level of proteomic similarity, the functionality of these sequences are similar across the clades (Supplementary Figure S2). Viral group 3 sequences

TABLE 3 Characterization of environmental metagenome generated contig with viral signatures, including VirSorter confidence category, number of Sandusky Bay *Planktothrix* isolate CRISPR spacers hit to the contig, and the gene annotation of the spacer hit site.

Metagenome contig	VirSorter category	Proteomic viral group	Length (bp)	Number of genes	Genome average coverage	Number of CRISPR spacer hits
140,938_contig_201	1	1	5,399	7	3875.66	2
140,939_contig_131	1	1	5,273	9	1000.5	1
140,939_contig_132	1	1	5,113	8	5066.42	2
Ga0209229_10004734	1	1	5,688	9	N/A	2
Ga0209229_10022288	1	1	2,741	4	N/A	1
Ga0209229_10003398	2	1	6,591	4	N/A	11
Ga0209229_10008255	2	1	4,373	4	N/A	1
Ga0209229_10012861	2	1	3,561	9	N/A	10
Ga0209229_10021454	2	1	2,791	4	N/A	9
Ga0209229_10034259	2	1	2,233	3	N/A	19
Ga0209229_10007918	2	2	4,456	6	N/A	2
Ga0209229_10017258	2	2	3,088	6	N/A	2
Ga0209229_10026795	2	5	2,510	4	N/A	1
140,939_contig_107	2	5	2027	5	7256.96	1
140,939_contig_26474	2	6	2,251	6	8.85	2
140,938_contig_37	3	3	12,452	24	1240.89	2
140,939_contig_119	3	3	7,962	14	1669.29	1
140,939_contig_283	3	3	11,630	23	3013.87	2
Ga0209229_10001252	3	3	10,480	18	N/A	2
Ga0209229_10001752	3	3	8,924	15	N/A	1
Ga0209229_10002258	3	3	7,904	12	N/A	1
140,938_contig_1949	3	4	30,690	42	66.42	9
140,939_contig_345	3	4	46,459	74	194.87	9
Ga0209229_10000210	3	4	22,828	35	N/A	9

Genome coverage not available for Ga0209229 data set. Gene annotation for CRIPSR spacer hits can be found in Supplementary Table S4.

generally encode for hypothetical proteins of unknown origin and hypothetical proteins from various cyanobacterial species (including *Nostoc* sp., *Trichocoleus* sp., and *Oscillatoria* sp.). Notably, these sequences also encode for a set of DNA-binding proteins including a HTH_XRE superfamily protein transcriptional regulator. The additional genes that are unique to subgroup B sequences include a NrdG superfamily protein related to the 7-carboxy-7-deazagunanine synthase QueE found in filamentous cyanobacteria, a PTPS (QueD superfamily) 6-pyruvoyl tetrahydropterin synthase found in some *Oscillatoriaceae*, and a GTP cyclohydrolase I FolE found in some *Nostacales*. These three genes are important in the conversion of GTP into 7-carboxy-7-deazaguanine (CDG) DNA modification.

3.3.4. Viral contig group 4

Viral group 4 consists of three sequences, one contig from each year of metagenome data. These sequences are the largest from these datasets, with the smallest being Ga0209229_10000210 at 22.8 kbp and the largest being 140,939_contig_345 at 46.4 kbp. These three sequences are highly related ($S_G \geq 0.95$) with a common core of ~30 genes, with the greatest difference between them being their size. While the majority of the open reading frames are hypothetical proteins of unknown origin, a few have functional annotations, including genes encoding an M23 family metallopeptidase (Phage_cluster_1627_PFAM-Peptidase_M23), a thymidylate synthase (Phage_cluster_1125_PFAM-Thymidylat_synt), a C39 family peptidase, a DNA polymerase III subunit beta (Phage_cluster_14685_PFAM-DNA_pol3_beta), a DUF5895 domain-containing protein, and a replicative DNA helicase (Phage_cluster_71_PFAM-DnaB_C). One additional functional annotation can be found in 140,938_contig_1949 and 140,939_contig_345 for a sugar kinase/Hsp70/actin family protein. As the longest contig, 140,939_contig_345 also has functional annotations for a DNA-cytosine methylase (DCM) superfamily protein (Phage_cluster_6007), a Nucleoside 2-deoxyribosyltransferase (RCL superfamily), a hypothetical protein which BLASTs to a hypothetical protein found in *Vibrio* phages and AAA family ATPases found in *Planktothrix sp*., a Von Willebrand factor type A (vWFA) superfamily protein found in some cyanobacteria, and three conserved domain of unknown function (DUF) containing proteins (DUF3846, DUF4926, and DUF1825).

3.3.5. Viral contig group 5

Viral group 5 consists of only two short contig sequences, 120939_contig_107 and Ga0209229_10026795, which are quite similar ($S_G = 0.8524$). The similarity between these two sequences is primarily

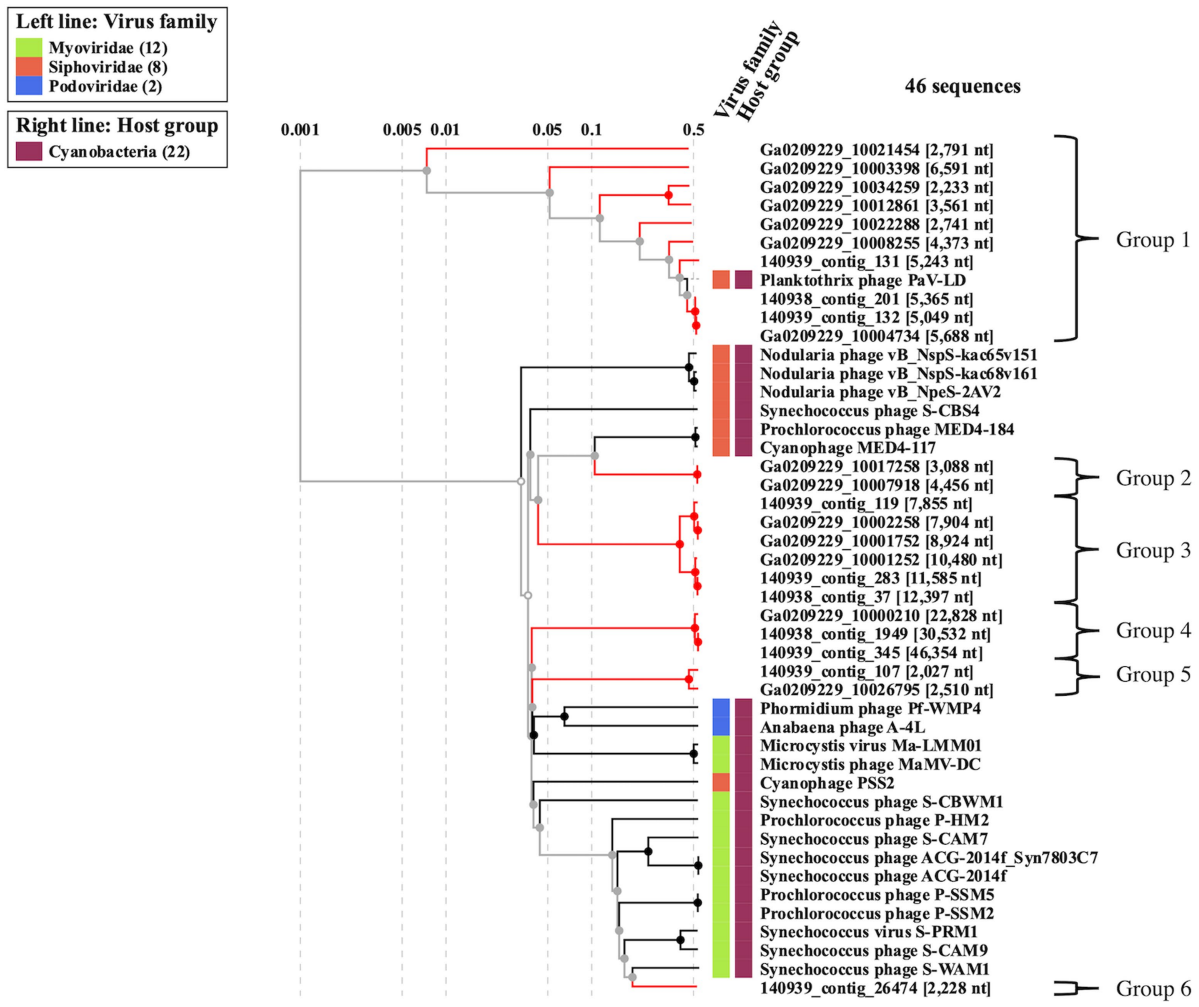

FIGURE 4
Proteomic viral tree (VIPtree) generated from metagenome generated contigs with positive CRISPR-cas spacer hits and viral signatures as identified by VirSorter. These 24 contigs can be placed into one of six proteomic groups, which may represent fragments of novel cyanophage genomes, or different segments of the same virus.

the result of a single large protein common between them, which BLASTp identifies as a hypothetical protein in the *Nostocales* but as a major capsid protein in other cyanobacteria species. Both also contain a Helix-hairpin-helix (HhH_5 superfamily) protein next to the hypothetical/capsid protein. The other open reading frames code for hypothetical proteins.

3.3.6. Viral contig group 6

Viral group 6 consists of a single short contig, 140,939_contig_26474. It contains several hits from the genomic DNA of a freshwater uncultured Caudovirales phage, including a DnaB Replicative DNA helicase, a hypothetical protein, and a T4 gp41 helicase.

3.4. Metatranscriptome analysis from Sandusky Bay in 2015, 2018, and 2019

Samples for metatranscriptome analysis were collected in 2015, 2018, and 2019 during *Planktothrix*-dominated blooms in Sandusky Bay. These data sets were then used to analyze the transcriptomic activity of the cyanophages and foreign DNA identified in this work. All contigs had reads associated with them, but contigs that displayed consistently low Reads Per Kilobase Million (RPKM) compared to *Planktothrix agardhii*, as determined by a viral RPKM consistently less than 10% of the host RPKM, were removed. Only viral groups 1, 3, and 5 had contigs that displayed elevated gene expression (Figure 6).

Viral group 1 was driven by Ga0209229_10004734, 140,939_contig_132, and 140,938_contig_201, the contigs encoding for highly similar capsid proteins as PaV-LD (~97% amino acid similarity). These viruses collectively had peak gene expression on June 26, 2018 with a virus:host RPKM ratio of 0.504 ± 0.097 at ODNR4. They were also seen at elevated expression levels at all three sites in 2015 and 2018 (greater than 0.1, less than the peak of 0.504), but exhibited low expression in 2019. Only one other viral group 1 contig was found to have expression values above the threshold; 140,939_contig_131 within the secondary group encoding the variant major capsid protein of PaV-LD (~88% amino acid similarity). Like the other PaV-LD contigs, 140,939_contig_131 showed elevated expression levels on

10.3389/fmicb.2023.1199641

TABLE 4 Group 1 viral contigs and their genomic similarity to the reference PaV-LD and corresponding alignment to PaV-LD genes.

Group 1 Viral Contig	Genomic Similarity (SG) to PaV-LD	PaV-LD region hits
Ga0209229_10004734	0.9864	PaVLD_ORF070L to PaVLD_ORF077R
140,939_contig_132	0.993	PaVLD_ORF070L to PaVLD_ORF077R
140,938_contig_201	1	PaVLD_ORF070L to PaVLD_ORF077R
140,939_contig_131	0.8672	PaVLD_ORF070L to PaVLD_ORF077R
Ga0209229_10008255	0.7922	PaVLD_ORF078R and PaVLD_ORF079R
Ga0209229_10012861	0.466	PaVLD_ORF023R to PaVLD_ORF025R, PaVLD_ORF027R
Ga0209229_10034259	0.7238	PaVLD_ORF023R to PaVLD_ORF025R, PaVLD_ORF027R
Ga0209229_10003398	0.6411	PaVLD_ORF084R, PaVLD_ORF088R, PaVLD_ORF137L
Ga0209229_10021454	0.4704	PaVLD_ORF111R, PaVLD_ORF114L, PaVLD_ORF116R

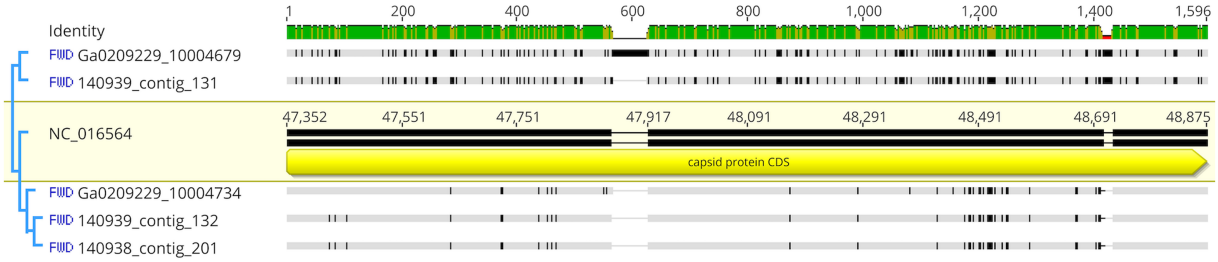

FIGURE 5
Nucleotide comparison of mapped contigs to PaVLD_ORF073R. Reference sequence is highlighted in yellow and includes gene annotations. Black segments in the non-highlighted sequences indicate points of difference, grey segments indicate similar regions. Identity is displayed at the top of the figure. Green sites indicate the same residue across all sequences while yellow sites have 30%–100% identity.

June 26, 2018 (ODNR4) at a virus:host RPKM ratio of 0.102, but peaked on June 8, 2015 (EC1163) at a virus:host RPKM ratio of 0.194.

For viral group 3 contigs, both subgroups saw expression levels above the threshold. Viral group 3A was represented by Ga0209229_10002258 and 140,939_contig_119. Ga0209229_10002258 had higher expression levels more frequently, with virus:host RPKM ratios over 0.1 across 20 site and date combinations. It was most prevalent in June 2018 in the outer bay of Sandusky (ODNR1 and EC1163) at a ratio of 0.46 ± 0.025 and found across all 3 years above the threshold. 140,939_contig_119 had less frequent elevated expression levels, with only 7 site/date combinations above the threshold, limited to the year 2018. Similar to the viral group 1 sequences, this contig peaked on June 26, 2018, at a ratio of 0.426. Viral group 3B was only represented by a single contig: Ga0209229_10001252. Ga0209229_10001252 displayed a similar trend in expression to viral group 3, clade 1 representative Ga0209229_10002258 in that it had quantifiable expression levels in 20 site/date combinations and spanned multiple sites across all 3 years. But unlike the 3A sequence, Ga0209229_10001252 peaked in August 2015, at a RPKM ratio of 0.34. The next highest expression level for this group occurred in June and July of 2018, averaging 0.27 ± 0.033 at sites ODNR4 and EC1163.

The most viral transcript expression was reported from both viral group 5 contigs (Figure 6). In June 2018, across all three sites, these two viral contigs had an average virus:host RPKM ratio of 1.45 ± 0.55, indicating that these genes were expressed approximately 1.5x greater than the host housekeeping gene of the sampled population. These sequences also had elevated expression levels on June 22, 2015 (ODNR) at a ratio of 0.532 ± 0.002, and throughout July 2018 at an average ratio of 0.498 ± 0.122. Interestingly, these sequences are the only ones that show considerable expression levels in 2019, peaking on July 17th (EC1163) at a ratio of 0.344 ± 0.03. In total, these two contigs accounted for 57 site and date combinations where their transcript expression levels were above the threshold.

4. Discussion

Using metagenome and metatranscriptome data sets from the environment combined with *Planktothrix agardhii* isolate genomes from the same region, early work is presented here that identifies possible cyanophage and other foreign DNA associated with *P. agardhii*-dominant cHABs in Sandusky Bay, Lake Erie. Previous work identified the CRISPR-cas systems of Sandusky Bay *P. agardhii* isolates, noting that two of these gene cassettes were common across all isolates and two previously published reference sequences from other geographical regions (McKindles et al., 2022). That same study found that only 14.9% of the CRIPSR spacer sequences from the isolates and reference sequences could be attributed to PaV-LD, indicating that there was a hidden diversity of cyanophages and foreign DNA elements to be uncovered. Using methodology of Morimoto et al. (2019) for the elucidation of novel *Microcystis* cyanophages, some of this hidden diversity was elucidated. In brief, a non-redundant CRISPR-cas spacer sequence was created as a query

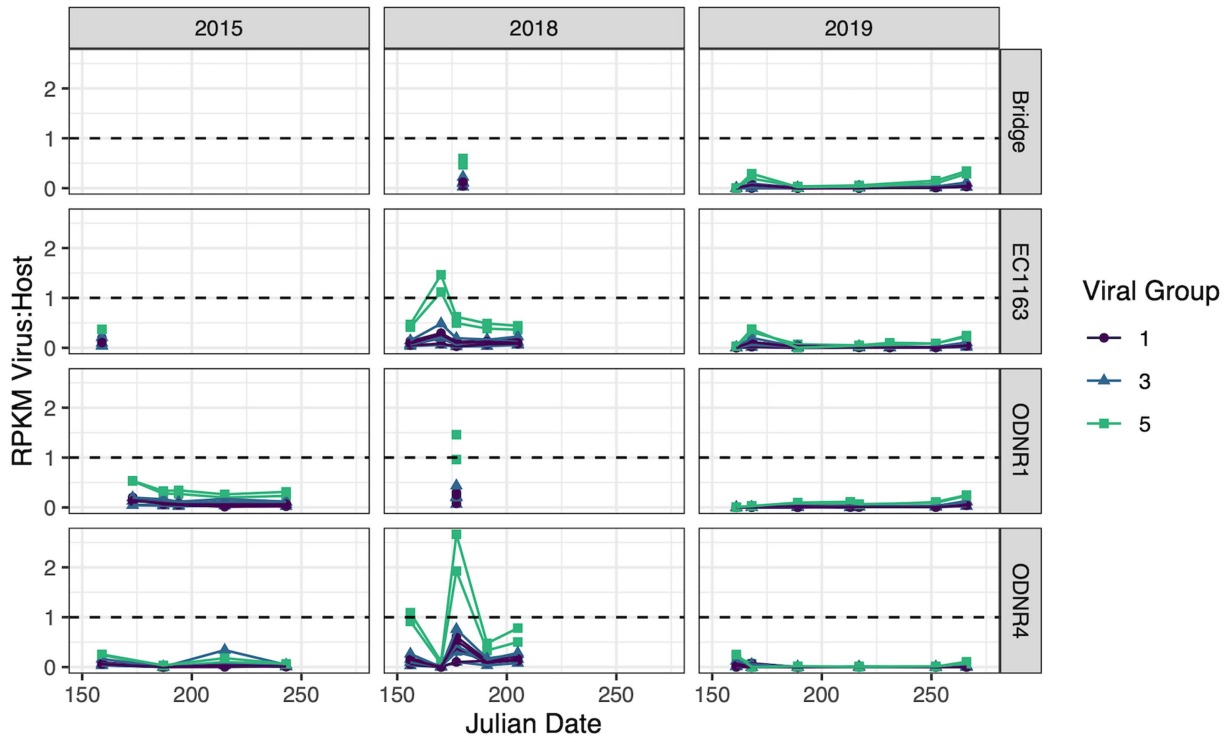

FIGURE 6
Transcripts of putative viral sequences categorized by group and normalized by whole genome expression of *Planktothrix agardhii*. Relative transcript abundance is presented as reads per kilobase of transcript per million mapped reads (RPKM). Viral groups with RPKM consistently less than 10% of the host RPKM were removed. Dashed line represents a viral to host transcript ratio of 1, where higher values indicate an increased likelihood of widespread active infection.

against punitive viral contigs identified using the program VirSorter from environmental metagenomic samples as a method to identify host-virus interactions in the absence of laboratory isolates.

A first analysis using environmental metagenome data sets was to check for local variants of the already characterized *Planktothrix agardhii* cyanophage PaV-LD (Gao et al., 2009, 2012a). Several contigs were able to map to PaV-LD at a greater than 80% sequence similarity (Figure 3), indicating that PaV-LD like cyanophages can be present across geographical regions with region specific variations. While this is not the first study to identify PaV-LD signatures using 'omics data sets, it is the first to confirm the presence of PaV-LD like cyanophages outside of Lake Donghu, China (Gao et al., 2012a). Watkins et al. (2015) discovered PaV-LD signatures in Lake Michigan, another of the Laurentian Great Lakes, but noted that while a BLAST search identified the hits as PaV-LD, they were likely non-species or non-virus specific ABC-transporter homologs. Similarly, Potapov et al. (2022) identified the same ABC-transporter identified as PaV-LD in Lake Baikal from metatranscriptome data but disregarded the presence of PaV-LD as the host cyanobacterium (*Planktothrix agardhii*) was not known to be found in the lake. The analysis presented here was also able to identify partial sequences aligned with this ABC-transporter, but identified it only as part of a larger contig that covered the PaV-LD region inclusive of ORF033R – ORF037R, lending multiple gene support to the contig's identification (Figure 3). Besides this region, contigs inclusive of PaV-LD specific proteins such as the terminase large subunit, the portal protein, both major capsid proteins, and the tail-tape measure protein were identified (Table 2). In particular, the terminase large subunit (TerL) is so specific, it has been used in other studies as a phylogenetic marker for viral relatedness (Jin et al., 2020; Lin et al., 2020). This region was mapped by two related but distinct contigs (Table 2), perhaps denoting the presence of viral evolutionary diversity in response to host diversity. This trend of two related but distinct contigs was also noted in the major capsid proteins (PaV-LD ORF071R and ORF073R; Table 2). PaV-LD has a capsid size of 76 ± 6 nm and is genetically distinct when compared to the major capsid proteins of other cyanophage viral families (Gao et al., 2009, 2012a). Given the conserved regions of these genes between PaV-LD and the local contigs, isolates within this group may have similar characteristics. But the level of conservation was not the same across all contigs (Figure 5), again leading to the hypothesis that there may be evolutionarily related cyanophages present in Sandusky Bay that may be specific to different ecotypes of *Planktothrix agardhii* as a response to host diversity. While some freshwater cyanophage capsid structures have been elucidated by cryoelectron microscopy (Jin et al., 2019; Cui et al., 2021), without isolation, capsid structure and assembly of Sandusky Bay PaV-LD like cyanophages is out of reach.

Besides PaV-LD like cyanophages, the host CRISPR-cas spacer sequences were used to identify novel viral signatures with the idea of enhancing understanding of cyanophage diversity as part of an ecosystem dominated by a freshwater harmful algal bloom. Through this analysis, 5 proteomic groups were identified with potentially novel viral signatures (Figure 4). It should be noted that given the short sequences identified in many of the groups, it is unclear that each

proteomic group represents a different viral family, but that multiple groups may be fragments of the same novel family or that the group identifies common viral genes found across multiple viral families. Despite this caveat, each of the 5 groups presented as part of this study have gene annotations that support the idea that cyanophage diversity is quite large despite the limited number of freshwater cyanophage isolates to date. Group 2 cyanophage contigs (Figure 4) contain a nuclease and DNA methylase genes which are involved in phage DNA replication and can be used to counter bacterial defense systems. Both gene functions can be found in PaV-LD (Gao et al., 2012a) and represent some of the most common phage orthologous groups (POGs; Kristensen et al., 2013). Group 3 cyanophage contigs had a HTH_XRE superfamily gene which may be functionally related to Cro/CI repressors which act as regulators of the lytic and lysogenic life cycle switch, as found in other systems (Wood et al., 1990; Basso et al., 2020; Long et al., 2022). Group 3B cyanophage contigs were longer than group 3A contigs (Figure 4) and had some additional genes that were identified as part of a secondary metabolite cassette. This cassette is important in the conversion of GTP into 7-carboxy-7-deazaguanine (CDG) for the biosynthesis of all 7-deazapurine-containing compounds (also known as pyrrolopyrimidine-containing compounds; McCarty and Bandarian, 2012). While the isolates of *Planktothrix agardhii* from Sandusky Bay have a 6-carboxytetrahydropterin synthase and several different copies of GTP cyclohydrolase I (McKindles et al., 2022), they are not the same as those found in the viral contig, nor does *P. agardhii* have the flanking gene, the 7-carboxy-7-deazagunanine synthase QueE. In *P. agardhii*, these genes are part of a pathway to produce Queuosine (Q), a hypermodified 7-deazaguanosine nucleoside located in the anticodon wobble position of four amino acid-specific tRNAs (Harada and Nishimura, 1972; Reader et al., 2004). In some viruses, 7-deazaguanosine is used during DNA modification to protect against host restriction enzymes (Hutinet et al., 2019). Next, group 4 viral contig sequences were the longest contigs generated from these environmental datasets (Figure 4). This group contains three contigs of variable size, but a core of ~30 genes between them. They have a M23 metallopeptidase gene, like the one encoded in PaV-LD ORF123, which has been shown to have bacteriostatic effects, including growth inhibition and membrane damage (Meng et al., 2022). Additionally, these contigs have an annotation for a thymidylate synthase, which can be found in both freshwater and marine double-stranded DNA viruses (Graziani et al., 2004; Yoshida T. et al., 2008; Huang et al., 2012; Zhang et al., 2020). Thymidylate synthase can be used by phages for catalyzing cyanophage-encoded nucleotide biosynthesis and scavenging of host nucleotides (Graziani et al., 2004; Thompson et al., 2011; Huang et al., 2015). Other genes of note in this groups include a DNA polymerase, helicase, and other enzymes important in the replication of viral genetic material. Despite being the most active viral group (Figure 6), group 5 viral contigs possess only two annotations of note involving a hypothetical capsid protein adjacent to a Helix-hairpin-helix family protein, which is likely related to non-specific DNA binding (Shao and Grishin, 2000). Finally, group 6 consists of only a single contig (Figure 4) which contains genes for a DnaB replicative DNA helicase and a T4 gp41 helicase, both of which are necessary to ensure proper regulation of cyanophage DNA replication initiation and which have been found in Nostoc and marine cyanophages (Dassa et al., 2009; Sullivan et al., 2010; Chénard et al., 2016).

In tandem with the sampling schedule for 'omics datasets, PaV-LD-like cyanophages in the environment were quantified using quantitative PCR methodology. This is the first multi-year data set in which the presence of a freshwater cyanophage was monitored and quantified in the environment. Note that this analysis targets the host-and particle-associated viral fraction, which can include phage particles attached to the host, phage undergoing active lytic infection, and lysogenic and/or integrated cyanophages. This analysis also targets one specific gene, the major capsid protein, using a set of primers designed from the previously published reference sequence (Gao et al., 2012a). Quantification showed that except for a few dates, the genomic copy numbers of PaV-LD-like cyanophages, as determined by the major capsid protein PaV-LD ORF073R, mirror the concentrations of the host genome (Figure 2). Coincident with changes in host abundance, changes in the viral concentration were typically observed. This relationship seems to denote a constant presence of cyanophage which may not affect the duration or intensity of the bloom. Single year quantification of *Microcystis* cyanophages in Singapore showed similar relationships between host cell concentrations and host-associated viral loads between mid-July and early-August, noting that despite the high host-associated load, there was no corresponding high free phage load that would indicate active lytic infections (Zhang et al., 2022). Similarly, despite being a log or two less abundant than its host, *Microcystis*, Ma-LMM01 concentrations in the host cell fraction mirrored host concentrations in a Japanese pond, and high concentrations in the host fraction did not necessarily signal high concentrations in the free phage fraction (Kimura et al., 2012). Both studies suggested that the higher proportion of host-associated viral loads was due to rapid diffusion of free phage and the likelihood that viral progeny may be trapped in host colonies and mucilage. Alternatively, lysogenic genes have been found during *Microcystis* dominated blooms, and the shift between these genes and lytic infections was tied to environmental cues (Stough et al., 2017). Indeed, Ma-LMM01-like cyanophages may utilize lysogeny to replicate during bloom formation in a host that is rapidly growing and can persist at high densities. Given that the viral loads as part of the host-associated fraction in this study were similar to the host concentration, transcriptomics data were assessed to check the gene expression of the viruses. Despite the elevated qPCR quantification of the viral genomes, the transcription levels of these viral genes (Group 1) were not very high (Figure 6). We further analyze this trend with the 2018 and 2019 free phage fraction, noting that in 2018, free cyanophage was less than 10% of the host associated fraction (Figure 2). This may indicate that the viruses could be part of abortive infections, or even undergoing lysogeny. In 2019, free cyanophage concentrations were much higher, particularly in the early season, which may be related to the lower host concentrations found in the bay.

Whereas the transcriptional activity of PaV-LD-like cyanophages was low on most sample dates, the environmental transcriptomic analysis revealed elevated gene expression by group 5 viral contig genes relative to the host housekeeping gene rpoC1, perhaps capturing a viral event occurring throughout Sandusky Bay. Elevated transcriptional activity was found at EC1163 and ODNR4, two sites that are 25 km apart and which represent extreme ends of the embayment (Figure 6). As discussed above, group 5 has an annotation for a hypothetical major capsid protein not seen in any characterized cyanophage before, but since the CRISPR-cas spacer hits for this exact

gene (Table 2), it is likely that this analysis has identified a novel *Planktothrix* cyanophage. Transcriptomics have been utilized to identify viral events before, which particularly focus on the transcript levels of capsid proteins as representative of late action viral genes (virion morphogenesis). The expression of late genes in a lab infection of Ma-LMM01 increased gradually until reaching a peak 6 h later, leading to host lysis (Morimoto et al., 2018). Another study noted that capsid assembly genes were diurnal and typically expressed after dark, which suggests that synchronized lysis of the host occurs during the night (Chen and Zeng, 2020). Unfortunately, due to low sample frequency, many lysis events can be missed, and the nuances of infection dynamics are lost.

While data are presented here with the goal of better understanding the relationship between freshwater cyanophages and their filamentous hosts, there are still many areas that need further research. It has been suggested that cyanophage infections can influence the cyanobacterial composition within a cHAB (Yoshida M. et al., 2008), so future work will examine more in-depth the transcriptomic data to determine if there was a *Planktothrix* shift following the proposed 2018 lysis event. Further, the proposed new viral genetic signatures could be quantified using historical DNA samples from the bay and better resolution of the viral sequences can occur once more metagenomic data sets are obtained. Finally, more research is needed into the triggers that promote cyanophages to become lytic to better inform water treatment plants when a mass lysis event will occur in reservoirs and waterbodies where these cHABs occur.

In conclusion, this study has found that PaV-LD-like cyanophages are a constant presence in *Planktothrix*-dominated cHABs but may not be regularly undergoing lytic infections. It also identified several new viral signatures that may be used to identify novel *Planktothrix*-specific cyanophages in other metagenomic data sets.

Data availability statement

The datasets presented in this study can be found in online repositories. The names of the repository/repositories and accession number(s) can be found in the article/Supplementary material.

Author contributions

KM: conceptualization and writing – original draft preparation. KM and MN: methodology. KM, MM, and MN: formal analysis and investigation. KM, MM, MN, RM, and GB: writing – review and editing. RM and GB: funding acquisition and resources. KM, RM, and GB: supervision. All authors contributed to the article and approved the submitted version.

Funding

This work was supported by funding from the Ohio Department of Natural Resources (GB) and National Institutes of Health (1P01ES028939-01) and National Science Foundation (OCE-1840715) awards to the Bowling Green State University Great Lakes Center for Fresh Waters and Human Health (GB, RM). This work was also supported by funding from the Natural Sciences and Engineering Research Council of Canada, grant RGPN-2019-03943 (RM).

Acknowledgments

The authors thank the Ohio Department of Natural Resources for providing access to boat time for sampling in Sandusky Bay, and the members of the GB, RM, and Davis labs for collecting water samples.

Conflict of interest

The authors declare that the research was conducted in the absence of any commercial or financial relationships that could be construed as a potential conflict of interest.

Publisher's note

Supplementary material

The Supplementary material for this article can be found online at: https://www.frontiersin.org/articles/10.3389/fmicb.2023.1199641/full#supplementary-material

References

Basso, J. T., Ankrah, N. Y., Tuttle, M. J., Grossman, A. S., Sandaa, R. A., and Buchan, A. (2020). Genetically similar temperate phages form coalitions with their shared host that lead to niche-specific fitness effects. *ISME J.* 14, 1688–1700. doi: 10.1038/s41396-020-0637-z

Bullerjahn, G. S., and McKay, R. M.. (2020a). Data from Sandusky Bay, Lake Erie from surveys conducted via Ohio Dept of natural resources watercraft from June to September 2018. Biological and chemical oceanography data management office (BCO-DMO). (version 1) version date 2019-02-07.

Bullerjahn, G. S., and McKay, R. M.. (2020b). *Data from Sandusky Bay, Lake Erie from surveys conducted via Ohio Dept of natural resources watercraft from June to September 2019. Biological and chemical oceanography data management office (BCO-DMO). (version 1) version date 2020-06-09.*

Chen, Y., and Zeng, Q. (2020). Temporal transcriptional patterns of cyanophage genes suggest synchronized infection of cyanobacteria in the oceans. *Microbiome* 8, 1–9. doi: 10.1186/s40168-020-00842-9

Chénard, C., Wirth, J. F., and Suttle, C. A. (2016). Viruses infecting a freshwater filamentous cyanobacterium (Nostoc sp.) encode a functional CRISPR array and a proteobacterial DNA polymerase B. *MBio* 7, e00667–e00616. doi: 10.1128/mBio.00667-16

Churro, C., Pereira, P., Vasconcelos, V., and Valério, E. (2012). Species-specific real-time PCR cell number quantification of the bloom-forming cyanobacterium *Planktothrix agardhii*. *Arch. Microbiol.* 194, 749–757. doi: 10.1007/s00203-012-0809-y

Codd, G. A., Testai, E., Funari, E., and Svirčev, Z. "Cyanobacteria, cyanotoxins, and human health," in *Water Treatment for Purification from Cyanobacteria and Cyanotoxins*, eds A. E. Hiskia, T. M. Triantis, M. G. Antoniou, T. Kaloudis, and D. D. Dionysiou (Hoboken, NJ: Wiley), 37–68.

Cui, N., Yang, F., Zhang, J. T., Sun, H., Chen, Y., Yu, R. C., et al. (2021). Capsid structure of Anabaena Cyanophage A-1 (L). *J. Virol.* 95, e01356–e01321. doi: 10.1128/JVI.01356-21

Dassa, B., London, N., Stoddard, B. L., Schueler-Furman, O., and Pietrokovski, S. (2009). Fractured genes: a novel genomic arrangement involving new split inteins and a new homing endonuclease family. *Nucleic Acids Res.* 37, 2560–2573. doi: 10.1093/nar/gkp095

Davis, T. W., Bullerjahn, G. S., Tuttle, T., McKay, R. M., and Watson, S. B. (2015). Effects of increasing nitrogen and phosphorus concentrations on phytoplankton community growth and toxicity during Planktothrix blooms in Sandusky Bay, Lake Erie. *Environ Sci Technol* 49, 7197–7207. doi: 10.1021/acs.est.5b00799

Foy, R. H., Gibson, C. E., and Smith, R. V. (1976). The influence of daylength, light intensity and temperature on the growth rates of planktonic blue-green algae. *British Phycological Journal* 11, 151–163. doi: 10.1080/00071617600650181

Gao, E. B., Gui, J. F., and Zhang, Q. Y. (2012a). A novel cyanophage with a cyanobacterial nonbleaching protein a gene in the genome. *J. Virol.* 86, 236–245. doi: 10.1128/JVI.06282-11

Gao, E. B., Li, S., and Zhang, Q. (2012b). Analysis of the cyanophage (PaV-LD) infection in host cyanobacteria under different culture conditions. *Acta Hydrobiol. Sin.* 36, 420–425. doi: 10.3724/SP.J.1035.2012.00001

Gao, E. B., Yuan, X. P., Li, R. H., and Zhang, Q. Y. (2009). Isolation of a novel cyanophage infectious to the filamentous cyanobacterium *Planktothrix agardhii* (Cyanophyceae) from Lake Donghu, China. *Aquat. Microb. Ecol.* 54, 163–170. doi: 10.3354/ame01266

Gobler, C. J. (2020). Climate Change and Harmful Algal Blooms: Insights and perspective. *Harmful Algae*. 91:101731. doi: 10.1016/j.hal.2019.101731

Graziani, S., Xia, Y., Gurnon, J. R., Van Etten, J. L., Leduc, D., Skouloubris, S., et al. (2004). Functional analysis of FAD-dependent thymidylate synthase ThyX from *Paramecium bursaria* Chlorella virus-1. *J. Biol. Chem.* 279, 54340–54347. doi: 10.1074/jbc.M409121200

Guillotreau, P., Le Bihan, V., Morineau, B., and Pardo, S. (2021). The vulnerability of shellfish farmers to HAB events: an optimal matching analysis of closure decrees. *Harmful Algae* 101:101968. doi: 10.1016/j.hal.2020.101968

Hampel, J. J., McCarthy, M. J., Neudeck, M., Bullerjahn, G. S., McKay, R. M., and Newell, S. E. (2019). Ammonium recycling supports toxic Planktothrix blooms in Sandusky Bay, Lake Erie: evidence from stable isotope and metatranscriptome data. *Harmful Algae* 81, 42–52. doi: 10.1016/j.hal.2018.11.011

Harada, F., and Nishimura, S. (1972). Possible anticodon sequences of tRNAHis, tRNAAsn, and tRNAAsp from *Escherichia coli*. Universal presence of nucleoside O in the first position of the anticodons of these transfer ribonucleic acid. *Biochemistry* 11, 301–308. doi: 10.1021/bi00752a024

Haramoto, E., Katayama, H., Oguma, K., and Ohgaki, S. (2005). Application of cation-coated filter method to detection of noroviruses, enteroviruses, adenoviruses, and torque Teno viruses in the Tamagawa River in Japan. *Appl. Environ. Microbiol.* 71, 2403–2411. doi: 10.1128/AEM.71.5.2403-2411.2005

Heil, C. A., and Muni-Morgan, A. L. (2021). Florida's harmful algal bloom (HAB) problem: escalating risks to human, environmental and economic health with climate change. *Front. Ecol. Evol.* 9:646080. doi: 10.3389/fevo.2021.646080

Hoagland, P. A., Anderson, D. M., Kaoru, Y., and White, A. W. (2002). The economic effects of harmful algal blooms in the United States: estimates, assessment issues, and information needs. *Estuaries* 25, 819–837. doi: 10.1007/BF02804908

Huang, S., Wang, K., Jiao, N., and Chen, F. (2012). Genome sequences of siphoviruses infecting marine Synechococcus unveil a diverse cyanophage group and extensive phage–host genetic exchanges. *Environ. Microbiol.* 14, 540–558. doi: 10.1111/j.1462-2920.2011.02667.x

Huang, S., Zhang, S., Jiao, N., and Chen, F. (2015). Comparative genomic and phylogenomic analyses reveal a conserved core genome shared by estuarine and oceanic cyanopodoviruses. *PLoS One* 10:e0142962. doi: 10.1371/journal.pone.0142962

Hutinet, G., Kot, W., Cui, L., Hillebrand, R., Balamkundu, S., Gnanakalai, S., et al. (2019). 7-Deazaguanine modifications protect phage DNA from host restriction systems. *Nat. Commun.* 10:5442. doi: 10.1038/s41467-019-13384-y

Jin, M., Cai, L., Ma, R., Zeng, R., Jiao, N., and Zhang, R. (2020). Prevalence of temperate viruses in deep South China Sea and western Pacific Ocean. *Deep-Sea Res. I Oceanogr. Res. Pap.* 166:103403. doi: 10.1016/j.dsr.2020.103403

Jin, H., Jiang, Y. L., Yang, F., Zhang, J. T., Li, W. F., Zhou, K., et al. (2019). Capsid structure of a freshwater cyanophage siphoviridae Mic1. *Structure* 27, 1508–1516.e3. doi: 10.1016/j.str.2019.07.003

Kimura, S., Yoshida, T., Hosoda, N., Honda, T., Kuno, S., Kamiji, R., et al. (2012). Diurnal infection patterns and impact of Microcystis cyanophages in a Japanese pond. *Appl. Environ. Microbiol.* 78, 5805–5811. doi: 10.1128/AEM.00571-12

Kristensen, D. M., Waller, A. S., Yamada, T., Bork, P., Mushegian, A. R., and Koonin, E. V. (2013). Orthologous gene clusters and taxon signature genes for viruses of prokaryotes. *J. Bacteriol.* 195, 941–950. doi: 10.1128/JB.01801-12

Kurmayer, R., Blom, J. F., Deng, L., and Pernthaler, J. (2015). Integrating phylogeny, geographic niche partitioning and secondary metabolite synthesis in bloom-forming Planktothrix. *ISME J.* 9, 909–921. doi: 10.1038/ismej.2014.189

Lin, W., Li, D., Sun, Z., Tong, Y., Yan, X., Wang, C., et al. (2020). A novel freshwater cyanophage vB_MelS-me-ZS1 infecting bloom-forming cyanobacterium *Microcystis elabens*. *Mol. Biol. Rep.* 47, 7979–7989. doi: 10.1007/s11033-020-05876-8

Long, X., Wang, X., Mao, D., Wu, W., and Luo, Y. (2022). A novel XRE-type regulator mediates phage lytic development and multiple host metabolic processes in *Pseudomonas aeruginosa*. Microbiology. *Spectrum* 10, e03511–e03522. doi: 10.1128/spectrum.03511-22

McCarty, R. M., and Bandarian, V. (2012). Biosynthesis of pyrrolopyrimidines. *Bioorg. Chem.* 43, 15–25. doi: 10.1016/j.bioorg.2012.01.001

Mchau, G., Machunda, R., Kimanya, M., Makule, E., Gong, Y., Mpolya, E., et al. (2022). First multiple detection of cyanotoxins in human serum and potential risk for liver cancer after exposure from freshwater of Lake Victoria, Tanzania. *Tanzan. J. Health Res.*:23. doi: 10.1007/s12403-020-00372-7

McKindles, K. M., Manes, M. A., McKay, R. M., Davis, T. W., and Bullerjahn, G. S. (2021). Environmental factors affecting chytrid (Chytridiomycota) infection rates on *Planktothrix agardhii*. *J. Plankton Res.* 43, 658–672. doi: 10.1093/plankt/fbab058

McKindles, K. M., McKay, R. M., and Bullerjahn, G. S. (2022). Genomic comparison of *Planktothrix agardhii* isolates from a Lake Erie embayment. *PLoS One* 17:e0273454. doi: 10.1371/journal.pone.0273454

Meng, L. H., Ke, F., Zhang, Q. Y., and Zhao, Z. (2022). Functional analysis of the endopeptidase and Holin from *Planktothrix agardhii* Cyanophage PaV-LD. *Front. Microbiol.* 13:849492. doi: 10.3389/fmicb.2022.849492

Metcalf, J. S., Tischbein, M., Cox, P. A., and Stommel, E. W. (2021). Cyanotoxins and the nervous system. *Toxins (Basel)* 13:660. doi: 10.3390/toxins13090660

Morimoto, D., Kimura, S., Sako, Y., and Yoshida, T. (2018). Transcriptome analysis of a bloom-forming cyanobacterium *Microcystis aeruginosa* during Ma-LMM01 phage infection. *Front. Microbiol.* 9:2. doi: 10.3389/fmicb.2018.00002

Morimoto, D., Tominaga, K., Nishimura, Y., Yoshida, N., Kimura, S., Sako, Y., and Yoshida, T. (2019). Cooccurrence of broad- and narrow-host-range viruses infection the bloom-forming toxic cyanobacterium Microcystis aeruginosa. *Appl. Environ. Microbiol.* 85, 1–17. doi: 10.1128/AEM.01170-19

Nishimura, Y., Yoshida, T., Kuronishi, M., Uehara, H., Ogata, H., and Goto, S. (2017). ViPTree: the viral proteomic tree server. *Bioinformatics* 33, 2379–2380. doi: 10.1093/bioinformatics/btx157

Oberhaus, L., Briand, J. F., Leboulanger, C., Jacquet, S., and Humbert, J. F. (2007). Comparative effects of the quality and quantity of light and temperature on the growth of Planktothrix agardhii and *P. rubescens* 1. *J. Phycol.* 43, 1191–1199. doi: 10.1111/j.1529-8817.2007.00414.x

O'Neil, J. M., Davis, T. W., Burford, M. A., and Gobler, C. J. (2012). The rise of harmful cyanobacteria blooms: The potential roles of eutrophication and climate change. *Harmful Algae* 14, 313–334. doi : 10.1016/j.hal.2011.10.027

Post, A. F., de Wit, R., and Mur, L. R. (1985). Interactions between temperature and light intensity on growth and photosynthesis of the cyanobacterium Oscillatoria agardhii. *J. Plankton Res.* 7, 487–495. doi: 10.1093/plankt/7.4.487

Potapov, S., Krasnopeev, A., Tikhonova, I., Podlesnaya, G., Gorshkova, A., and Belykh, O. (2022). The viral fraction Metatranscriptomes of Lake Baikal. *Microorganisms* 10:1937. doi: 10.3390/microorganisms10101937

Prediger, E. (2013). Calculations: converting from Nanograms to copy number. Integrated DNA technologies. Available at: https://www.idtdna.com/pages/education/decoded/article/calculations-converting-from-nanograms-to-copy-number)

Reader, J. S., Metzgar, D., Schimmel, P., and de Crécy-Lagard, V. (2004). Identification of four genes necessary for biosynthesis of the modified nucleoside queuosine. *J. Biol. Chem.* 279, 6280–6285. doi: 10.1074/jbc.M310858200

Roux, S., Enault, F., Hurwitz, B. L., and Sullivan, M. B. (2015). VirSorter: mining viral signal from microbial genomic data. *PeerJ* 3:e395. doi: 10.7717/peerj.985

Salk, K. R., Bullerjahn, G. S., McKay, R. M., Chaffin, J. D., and Ostrom, N. E. (2018). Nitrogen cycling in Sandusky Bay, Lake Erie: oscillations between strong and weak export and implications for harmful algal blooms. *Biogeosciences* 15, 2891–2907. doi: 10.5194/bg-15-2891-2018

Sanseverino, I., Conduto, D., Pozzoli, L., Dobricic, S., and Lettieri, T. (2016). *Algal bloom and its economic impact* European Commission, Joint Research Centre Institute for Environment and Sustainability. (European Union: Luxembourg)

Shao, X., and Grishin, N. V. (2000). Common fold in helix–hairpin–helix proteins. *Nucleic Acids Res.* 28, 2643–2650. doi: 10.1093/nar/28.14.2643

Steffen, M. M., Davis, T. W., McKay, R. M., Bullerjahn, G. S., Krausfeldt, L. E., Stough, J. M., et al. (2017). Ecophysiological examination of the Lake Erie Microcystis bloom in 2014: linkages between biology and the water supply shutdown of Toledo, OH. *Environ. Sci. Technol.* 51, 6745–6755. doi: 10.1021/acs.est.7b00856

Stough, J. M., Tang, X., Krausfeldt, L. E., Steffen, M. M., Gao, G., Boyer, G. L., et al. (2017). Molecular prediction of lytic vs lysogenic states for Microcystis phage: metatranscriptomic evidence of lysogeny during large bloom events. *PLoS One* 12:e0184146. doi: 10.1371/journal.pone.0184146

Sullivan, M. B., Huang, K. H., Ignacio-Espinoza, J. C., Berlin, A. M., Kelly, L., Weigele, P. R., et al. (2010). Genomic analysis of oceanic cyanobacterial myoviruses compared with T4-like myoviruses from diverse hosts and environments. *Environ. Microbiol.* 12, 3035–3056. doi: 10.1111/j.1462-2920.2010.02280.x

Sunda, W. G., Graneli, E., and Gobler, C. J. (2006). Positive feedback and the development and persistence of ecosystem disruptive algal blooms 1. *J. Phycol.* 42, 963–974. doi: 10.1111/j.1529-8817.2006.00261.x

Thompson, L. R., Zeng, Q., Kelly, L., Huang, K. H., Singer, A. U., Stubbe, J., et al. (2011). Phage auxiliary metabolic genes and the redirection of cyanobacterial host carbon metabolism. *Proc. Natl. Acad. Sci.* 108, E757–E764. doi: 10.1073/pnas.1102164108

Tillett, D., and Neilan, B. A. (2000). Xanthogenate nucleic acid isolation from cultured and environmental cyanobacteria. *J. Phycol.* 36, 251–258. doi: 10.1046/j.1529-8817.2000.99079.x

Wang, H., Xu, C., Liu, Y., Jeppesen, E., Svenning, J. C., Wu, J., et al. (2021). From unusual suspect to serial killer: cyanotoxins boosted by climate change may jeopardize megafauna. *Innovation (Camb)* 2:100092. doi: 10.1016/j.xinn.2021.100092

Watkins, S. C., Kuehnle, N., Ruggeri, C. A., Malki, K., Bruder, K., Elayyan, J., et al. (2015). Assessment of a metaviromic dataset generated from nearshore Lake Michigan. *Mar. Freshw. Res.* 67, 1700–1708. doi: 10.1071/MF15172

Wolf, D., Gopalakrishnan, S., and Klaiber, H. A. (2022). Staying afloat: the effect of algae contamination on Lake Erie housing prices. *Am. J. Agric. Econ.* 104, 1701–1723. doi: 10.1111/ajae.12285

Wood, H. E., Devine, K. M., and McConnell, D. J. (1990). Characterisation of a repressor gene (xre) and a temperature-sensitive allele from the *Bacillus subtilis* prophage, PBSX. *Gene* 96, 83–88. doi: 10.1016/0378-1119(90)90344-Q

Wurtsbaugh, W. A., Paerl, H. W., and Dodds, W. K. (2019). Nutrients, eutrophication and harmful algal blooms along the freshwater to marine continuum. *Wiley Interdiscip. Rev. Water* 6:e1373. doi: 10.1002/wat2.1373

Ye, J., Coulouris, G., Zaretskaya, I., Cutcutache, I., Rozen, S., and Madden, T. L. (2012). Primer-BLAST: a tool to design target-specific primers for polymerase chain reaction. *BMC bioinformatics* 13:1. doi: 10.1186/1471-2105-13-S6-S1

Yoshida, T., Nagasaki, K., Takashima, Y., Shirai, Y., Tomaru, Y., Takao, Y., et al. (2008). Ma-LMM01 infecting toxic *Microcystis aeruginosa* illuminates diverse cyanophage genome strategies. *J. Bacteriol.* 190, 1762–1772. doi: 10.1128/JB.01534-07

Yoshida, T., Takashima, Y., Tomaru, Y., Shirai, Y., Takao, Y., Hiroishi, S., et al. (2006). Isolation and characterization of a cyanophage infecting the toxic cyanobacterium *Microcystis aeruginosa*. *Appl. Environ. Microbiol.* 72, 1239–1247. doi: 10.1128/AEM.72.2.1239-1247.2006

Yoshida, M., Yoshida, T., Kashima, A., Takashima, Y., Hosoda, N., Nagasaki, K., et al. (2008). Ecological dynamics of the toxic bloom-forming cyanobacterium Microcystis aeruginosa and its cyanophages in freshwater. *Appl. Environ. Microbiol.* 74, 3269–3273. doi: 10.1128/AEM.02240-07

Zhang, D., Te, S. H., He, Y., and Gin, K. Y. (2022). Cyanophage dynamics in a tropical urban freshwater lake. *Ecol. Indic.* 142:109257. doi: 10.1016/j.ecolind.2022.109257

Zhang, D., You, F., He, Y., Te, S. H., and Gin, K. Y. (2020). Isolation and characterization of the first freshwater cyanophage infecting Pseudanabaena. *J. Virol.* 94, e00682–e00620. doi: 10.1128/JVI.00682-20

frontiers | Frontiers in Microbiology

TYPE Original Research
PUBLISHED 13 July 2023
DOI 10.3389/fmicb.2023.1203317

OPEN ACCESS

EDITED BY
Petra M. Visser,
University of Amsterdam, Netherlands

REVIEWED BY
Mickey Rogers,
Pacific Northwest National Laboratory (DOE), United States
Haley Plaas,
University of North Carolina at Chapel Hill, United States

*CORRESPONDENCE
Seungjun Lee
paul5280@pknu.ac.kr
Jae-Ho Shin
jhshin@knu.ac.kr

†These authors share first authorship

RECEIVED 10 April 2023
ACCEPTED 20 June 2023
PUBLISHED 13 July 2023

CITATION
Kim J, Lee G, Han S, Kim M-J, Shin J-H and Lee S (2023) Microbial communities in aerosol generated from cyanobacterial bloom-affected freshwater bodies: an exploratory study in Nakdong River, South Korea.
Front. Microbiol. 14:1203317.
doi: 10.3389/fmicb.2023.1203317

Microbial communities in aerosol generated from cyanobacterial bloom-affected freshwater bodies: an exploratory study in Nakdong River, South Korea

Jinnam Kim[1†], GyuDae Lee[2†], Soyeong Han[1], Min-Ji Kim[2], Jae-Ho Shin[2,3]* and Seungjun Lee[1]*

[1]Major of Food Science & Nutrition, Division of Food Science, College of Fisheries Science, Pukyong National University, Busan, Republic of Korea, [2]Department of Applied Biosciences, Kyungpook National University, Daegu, Republic of Korea, [3]NGS Core Facility, Kyungpook National University, Daegu, Republic of Korea

Toxic blooms of cyanobacteria, which can produce cyanotoxins, are prevalent in freshwater, especially in South Korea. Exposure to cyanotoxins via ingestion, inhalation, and dermal contact may cause severe diseases. Particularly, toxic cyanobacteria and their cyanotoxins can be aerosolized by a bubble-bursting process associated with a wind-driven wave mechanism. A fundamental question remains regarding the aerosolization of toxic cyanobacteria and cyanotoxins emitted from freshwater bodies during bloom seasons. To evaluate the potential health risk of the aerosolization of toxic cyanobacteria and cyanotoxins, the objectives of this study were as follows: 1) to quantify levels of microcystin in the water and air samples, and 2) to monitor microbial communities, including toxic cyanobacteria in the water and air samples. Water samples were collected from five sites in the Nakdong River, South Korea, from August to September 2022. Air samples were collected using an air pump with a mixed cellulose ester membrane filter. Concentrations of total microcystins were measured using enzyme-linked immunosorbent assay. Shotgun metagenomic sequencing was used to investigate microbial communities, including toxic cyanobacteria. Mean concentrations of microcystins were 960μg/L ranging from 0.73 to 5,337μg/L in the water samples and 2.48ng/m^3 ranging from 0.1 to 6.8ng/m^3 in the air samples. In addition, in both the water and air samples, predominant bacteria were *Microcystis* (PCC7914), which has a microcystin-producing gene, and *Cyanobium*. Particularly, abundance of *Microcystis* (PCC7914) comprised more than 1.5% of all bacteria in the air samples. This study demonstrates microbial communities with genes related with microcystin synthesis, antibiotic resistance gene, and virulence factors in aerosols generated from cyanobacterial bloom-affected freshwater body. In summary, aerosolization of toxic cyanobacteria and cyanotoxins is a critical concern as an emerging exposure route for potential risk to environmental and human health.

KEYWORDS

harmful algal blooms, microcystin, *Microcystis*, aerosol, Nakdong River, metagenomics, microbiome

1. Introduction

Events of harmful algal blooms (HABs) caused by cyanobacteria in freshwater (e.g., rivers, lakes, and reservoirs) are a critical issue worldwide (Lu et al., 2020). Climate change may exacerbate the dangers associated with increased occurrence and severity of HABs (Lee et al., 2021). Furthermore, human activities, such as agricultural practice, may create optimal conditions for promoting the growth of toxic cyanobacteria (Hur et al., 2013). Cyanobacteria are a group of oxygenic photosynthetic bacteria widely distributed in freshwater and marine environments (Gonçalves et al., 2016). Cyanobacteria, which do not contain a membrane-bound nucleus, mitochondria, and chloroplasts, are primitive micro-organisms with an intermediate structure between bacteria and plants (Hachicha et al., 2022). Despite formerly being considered algae due to their photosynthetic ability, cyanobacteria are currently classified as bacteria (prokaryotic) (Oren, 2011; Palinska and Surosz, 2014). Several cyanobacteria can produce toxic compounds (known as cyanotoxins) that are problematic when freshwater is used for drinking, agricultural, and recreational purposes (Wood and Dietrich, 2011). Animals and humans can become exposed to cyanotoxins, including anatoxins, cylindrospermopsins, microcystins (MCs), nodularins, and saxitoxins, via inhalation, ingestion, and dermal contact; in particular, MCs are selectively hepatotoxic in fish, birds, and mammals (Dawson, 1998). MC poisoning can cause hepatocyte necrosis and hemorrhage (Bhattacharya et al., 1997). MCs have also been associated with tumor promotion over long-term exposure (Ito et al., 1997). Recent studies focused on human exposure to aerosolized MCs that are significantly related with proinflammatory response in human airway epithelium (Orrell, 2022; Labohá et al., 2023). Both toxic cyanobacteria and MCs either float around the water column or attach to the surface and subsequently enter the atmosphere when they are undulated by the wind or introduced by waves, rainfall, and ship traffic. In a study measuring MC concentrations in the nasal mucosa of residents during a cyanobacterial bloom in a river in Florida, 115 of 121 participants (95.0%) had MC concentrations above the detection limit, with an average concentration of 0.61 + 0.75 μg/L. This result suggests that aerosolization of cyanotoxins is an important pathway for evaluating potential health risk (Schaefer et al., 2020). In addition, in a previous study examining the toxicity of aerosolized MCs to mice, the risk of inhaled MCs was found to be ten times higher than that of orally administered MCs (Benson et al., 2005). Furthermore, in the United Kingdom, respiratory illnesses such as pneumonia have been reported in many people canoeing in reservoirs where *Microcystis* HABs have progressed (Stewart et al., 2006). The results of Sharma et al. (2007) suggest that inhaling cyanotoxins may have worse effects than ingesting cyanotoxins. These studies have emphasized the importance of monitoring cyanotoxins in the air (Olson et al., 2020; Lad et al., 2022; Vigar et al., 2022; Rogers and Stanley, 2023).

The Nakdong River is the longest river in the Republic of Korea (hereafter South Korea), with a total length of 525 km and a watershed area of 23.859 km^2 (Ryu et al., 2016). Water from the Nakdong River has been used as a source of tap water by two metropolitan cities (Daegu and Busan) and several small cities, for recreational activities, and for agricultural purpose (Kim et al., 2021). However, the Nakdong River is afflicted with eutrophication with nitrogen (N) and phosphorus (P), which are critical factors for triggering occurrence of HABs (Kim et al., 2021). Furthermore, since 2012, eight large artificial weirs have been constructed along a 200 km section of the Nakdong River. These weirs reduce the flow velocity and artificially alter the water flow to form stagnant waterbodies, which can lead to the flourishing of cyanobacteria and occurrence of HABs (Choi et al., 2002; Lee et al., 2018; Park et al., 2021). HABs caused by cyanobacteria have occurred frequently in the Nakdong River (Kim et al., 2019). As the Nakdong River is a major source of drinking water, agricultural water, and commercial water, HABs that can produce cyanotoxins pose a serious problem for water use (Park et al., 2021). In particular, cyanobacteria and their toxins may be aerosolized and exposed to people through recreational activities, ship operation, and wind friction (Tesson et al., 2016). However, research on the aerosolization of toxic cyanobacteria and MCs is insufficient in the context of the Nakdong River in South Korea.

Furthermore, eutrophication and HABs can impact the aquatic environment in several ways. Firstly, eutrophication may promote the survival and proliferation of pathogens in aquatic environments (Smith and David, 2009). Recently, it has been proposed that HABs, triggered by eutrophication, could also contribute to the emergence and dissemination of antibiotic resistance genes in aquatic environments (Zhang et al., 2020; Li et al., 2021). Therefore, it is essential to examine the presence of both the pathobiome and the resistome. The concept of pathobiome refers to the collection of host-associated organisms associated with potential health risk (Bass et al., 2019). The resistome refers to all antibiotic resistance genes (ARGs) and their precursors in both pathogenic and nonpathogenic bacteria. The resistome serves as a comprehensive overview of ARGs, accounting for different resistance mechanisms and their potential evolution within microbial communities (Kim and Cha, 2021). In this study, metagenomic analysis was used to examine profiles of microbial communities in water and aerosol samples during HAB events in Nakdong River, South Korea, with quantification of MCs. In addition, the relationship between environmental factors (wind speed, precipitation, air temperature, and humidity) and aerosolization of toxic cyanobacteria and MCs was examined. We aimed to understand the microbial communities, including cyanobacterial community, ARGs, and virulence factors, in aerosols emitted from the Nakdong River during bloom seasons. This study may also provide evidence of potential health risk related to aerosolization of toxic cyanobacteria and cyanotoxins to which humans can be exposed via inhalation.

2. Materials and methods

2.1. Sample collection, meteorological data, and DNA extraction

Water and aerosol samples were collected from the five sites of Nakdong River (Daedong Wharf, Samnakdunchi, Hwawon Amusement Park, Leports Valley, Hapcheon Hakri Reservoir) on August 30 and September 2, 2022. A sterile mixed cellulose ester membrane filter (diameter 37 mm, pore size 0.8 μm, Merck Millipore, Billerica, MA, USA) was used for the aerosol sampling. The filter paper was placed in an aluminum filter holder with a stainless-steel support connected with a silicone tube to a vacuum pump (Model SIP-32 L, Sibata Scientific Technology Ltd., Tokyo, Japan). The flow rate of sampling was adjusted to about 0.02 m^3/min and aerosol samples were collected for a total of 4 h (total volume: 4.8 m^3). To

validate the quality control of aerosol samples, additional aerosol samples were collected in a sterile environment (clean bench) for 8 h. The 16S rRNA and *mcyE* genes were amplified using polymerase chain reaction (PCR) method from extracted DNA of the aerosol samples and the samples of quality control. Gel electrophoresis was performed to confirm microbial contamination.

Water samples (100 mL per hour for 4 h, total volume: 400 mL) were collected from the surface water of the river using a van dorn water sampler (depth: 30 cm, PDNN19080900002, Daihan chemlab, South Korea). For delivering the water and aerosol samples, the samples were kept at 4°C. In addition, meteorological data (i.e., wind speed, precipitation, air temperature and humidity) were obtained by Korea Meteorological Administration (https://www.kma.go.kr/eng/index.jsp).

In the laboratory (Pukyong National University, Busan, South Korea), water samples were filtered with a MultiVac 610-MS-T Multi-Branch Filtration system; each 100 mL water sample was filtered through a sterile 0.22 μm, 47 mm Whatman Nuclepore Hydrophilic Membrane filter (Wilson, 2022). For extracting microbial DNA from the filters (water and aerosol samples), the DNeasy PowerSoil Pro kit (QIAGEN, Germany) was used according to the manufacturer's instructions.

2.2. Measurement of water quality

Water parameters, including conductivity, dissolved oxygen (DO), and pH, were measured using a water quality meter (AZ-8603, AZ Instrument, Taiwan). The biochemical oxygen demand (BOD) value was also examined (Zhao et al., 2019). Concentrations of total nitrogen (N) and total phosphorus (P) were measured using Hach Digital Reactor Block 200 (Hach Co., Loveland, CO, USA) following by Persulfate Digestion Method 10,071, and USEPA PhosVer 3 with Acid Persulfate Digestion Method 8,190, respectively.

MCs were extracted from the air filters and measured according to the previous study (Murby et al., 2016; Swe et al., 2021). Briefly, each sample was conducted with frozen and thawed at three times, and then the samples were applied with sonicating for 1 min and vortexing for 30 s. For measuring levels of MCs in the water samples, US EPA Method 546 was used. Briefly, for cell lysing, the samples were conducted with frozen and thawed at three times. MC concentration was analyzed in triplicate with an enzyme-linked immunosorbent assay (ELISA) kit (PN.520011SAES, Eurofins Abraxis, Warminister, PA, USA) according to the manufacturer's protocol. The detection limit of the kit is 0.016 μg/L (detection range: 0.05 to 5 μg/L). For measuring high concentrations of MCs (more than 5 μg/L) in the water samples, the samples were diluted with double-distilled water and then levels of MCs were re-measured.

2.3. Quantification of MC-producing *Microcystis*

Levels of MC-producing *Microcystis* in water and aerosol samples were quantified with Quantstudio 1 Real-Time PCR system (Applied Biosystems, Foster City, CA, USA) by targeting the *mcyE* gene that encodes *Microcystis*-specific MC production with the set of primers and PCR conditions from a previous study (Sipari et al., 2010). PCR reaction solutions contained TOPreal™ qPCR 2x PreMIX with SYBR green (Enzynomics, Daejeon, South Korea), 10 μM of each primer and the extracted DNA (total volume was 20 μL). The thermal cycling conditions were 50°C for 2 min, 95°C for 10 min, 40 cycles of 95°C for 30 s, and 62°C for 1 min, and by a melting curve stage of 95°C for 15 s and 60°C for 1 min (Lee et al., 2021). The output data were analyzed by associated software (Design and Analysis Software 2.6.0, Applied Biosystems, CA, USA). All experiments were performed in triplicate.

2.4. Library preparation and shotgun metagenomic sequencing

For the aerosol filtered samples, amplification was conducted using REPLI-g Single Cell Kit (Qiagen, Germany) according to manufacturer's protocol to ensure sufficient concentration of DNA. DNA concentration and quality were measured using Qubit™ Flex Fluorometer (Thermo Fisher Scientific, USA) and Nanodrop One spectrophotometer (Thermo Fisher Scientific, USA), respectively. The sequencing library was prepared using the MGIEasy FS DNA Library Prep Kit, Circularization Module, and DNBSEQ-G400RS High-throughput Sequencing Kit PE100 (MGI Tech, China) following the manufacturer's instructions. Shotgun metagenome sequencing was performed at NGS Core facility (Kyungpook National University, Daegu, Korea). The raw sequences were deposited in the National Center for Biotechnology Information (NCBI) SRA dataset under BioProject accession number PRJNA949880 (https://www.ncbi.nlm.nih.gov/bioproject/PRJNA949880).

2.5. Preprocessing of sequencing raw data and taxonomy classification

For trimming low quality sequences of raw reads, Trimmomatic (v.0.39) was performed (Bolger et al., 2014). Reads were scanned with a 50-base wide sliding window, and average quality per base below 28 were trimmed. Using quality filtered reads, taxonomy classification was conducted using Kraken2 (Wood et al., 2019). Custom database was built from NCBI sequences which were include bacterial, fungal, archaeal, and viral genomes. Additional estimation was performed using Bracken to accurately predict the abundance of microbial features at each taxonomic rank based on the resulting output report (Lu et al., 2017).

2.6. Shotgun metagenome assembly and annotation of functional genes

Preprocessed reads from all the samples were merged for co-assembly with MEGAHIT (v1.2.9) (Li et al., 2015). The minimum k-mer was set to 27 and did not add mercy k-mers. We utilized the assembled contigs to carry out two processes: taxa identification of each contigs using Kraken2 and gene prediction. Protein-coding sequences (CDS) were predicted using Prodigal (v2.6.3), and redundant protein sequences with more than 95% identity were clustered using CD-HIT. (v4.8.1) (Li and Godzik, 2006). RPKM (reads per kilobase of exon per million reads mapped) of each predicted gene

was calculated using BBMap (Bushnell, 2014). In case of ARGs, the abundance was calculated by following equation:

$$ARGs\ abundance = \sum_{i}^{n} \frac{N_{i(ARG-Like\ sequence)} \times \frac{L_{reads}}{L_{i(ARG\ reference\ sequence)}}}{N_{16S\ sequence} \times \frac{L_{reads}}{L_{16S\ sequence}}}$$

$N_{i(ARG-Like\ sequence)}$ is the total number of reads which predicted to ARG with CARD reference, $L_{i(ARG\ reference\ sequence)}$ is each read length of predicted ARG, L_{reads} is the average read length of preprocessed raw read, $N_{16S\ sequence}$ is the total number of reads which encoding 16S rRNA gene using SILVA database from Kraken2 custom database. $L_{16S\ sequence}$ is the average length of the 16S rRNA gene sequence in the database (1,080 bp). Gene annotation for functional analysis was done using DIAMOND (v2.0.15.153) (Buchfink et al., 2015). For functional analysis, gene annotation of predicted CDS was carried out using DIAMOND (v2.0.15.153) with parameters set to 70% identity and 80% query coverage. The microcystin biosynthetic gene cluster (BGC0001017: *Microcystis aeruginosa* PCC 7806) was retrieved from the Minimum Information about a Biosynthetic Gene Cluster (MIBiG) database, while the CARD (Alcock et al., 2019) and VFDB (Liu et al., 2022) databases were utilized for resistome and pathobiome analysis, respectively.

2.7. Statistical analysis

Statistical analyses and visualization were processed in R studio (v3.6.3). Importing of microbiome data including taxonomy information, feature table, and metadata was conducted using phyloseq package. Diversity analysis and visualized using vegan and ggplot package, respectively. Bray–curtis dissimilarity was computed for beta diversity analysis and visualized using principal coordinate analysis (PCoA). To statistically test the sample distance between freshwater and aerosol samples, adonis test in the vegan package for permutational multivariate analysis of variance (PERMANOVA) was conducted. Alpha diversity indices including Chao1 and Simpson were calculated using the microbiome package. To perform statistical tests comparing the indices between freshwater and aerosol groups, the Wilcoxon rank-sum test was conducted. The core microbiome and genes were filtered using microbiome package to elements that were found in more than 50% of each group and enriched by more than 1 and 0.001%, respectively.

3. Results

3.1. Quantification of total MCs and MC-producing *Microcystis*

Total MCs in the water and aerosol samples were measuring (Table 1). The mean concentration of MCs in freshwater samples was approximately 1,158 μg/L. This value was about 48 times higher than that of the world health organization (WHO) recreational guideline (24 μg/L). The highest concentration of MCs was the FW5 sample (5337.39 μg/L). In addition, the mean concentration of MCs in the aerosol samples was 1.22 ng/m^3 (ranging from 0.10 to 3.68 ng/m^3).

TABLE 1 Concentrations of total MCs in the freshwater and aerosol samples.

Freshwater		Aerosols	
Site	MCs concentration (μg/L)	Site	MCs concentration (ng/m^3)
FW1	15.12	AR1	0.20
FW2	5.20	AR2	0.19
FW3	366.44	AR3	3.68
FW4	70.46	AR4	0.28
FW5	5337.39	AR5-1	2.40
		AR5-2	0.10
		AR5-3	1.70

TABLE 2 Concentrations of MC-producing *Microcystis* in the freshwater and aerosol samples.

Freshwater		Aerosols	
Site	*mcyE* concentration (copies/100mL)	Site	*mcyE* concentration (copies/m^3)
FW1	4.0×10^7	AR1	9.4×10^1
FW2	1.8×10^8	AR2	1.4×10^0
FW3	1.0×10^9	AR3	4.2×10^0
FW4	7.8×10^8	AR4	1.7×10^0
FW5	2.8×10^9	AR5-1	7.7×10^0
		AR5-2	1.2×10^0
		AR5-3	5.8×10^0

To reveal concentration of MC-producing *Microcystis* in water and aerosol samples, the levels of *Microcystis* (gene copy/100 mL of freshwater and gene copy/m^3 of aerosol) were measured using the quantification PCR system targeting the *mcyE* gene, which is related with MC-producing genes (Table 2). The *mcyE* gene was detected in all freshwater and aerosol samples. The mean concentration of *Microcystis* (gene copies/100 mL of freshwater) in the water samples was 9.7×10^8. The FW5 sample had the highest concentration of the *mcyE* gene at 2.8×10^9 copies/100 mL. In the aerosol samples, the mean concentration of MC-producing *Microcystis* (gene copies/m^3) was 1.7×10^1. The highest concentration of MCs was detected from the AR1 sample (9.4×10^1 gene copies m^3).

3.2. Microbial compositions of water and aerosol samples during algal bloom

The freshwater microbiome was dominated by *Microcystis*, but in the aerosol microbiome, various organisms, such as eukaryotes and viruses, were detected (Figure 1; Supplementary Figure S1). The freshwater microbiome was composed of 99.79% bacteria, which was composed of 76.65% *Microcystis*, followed by 0.31% *Pseudanabaena*,

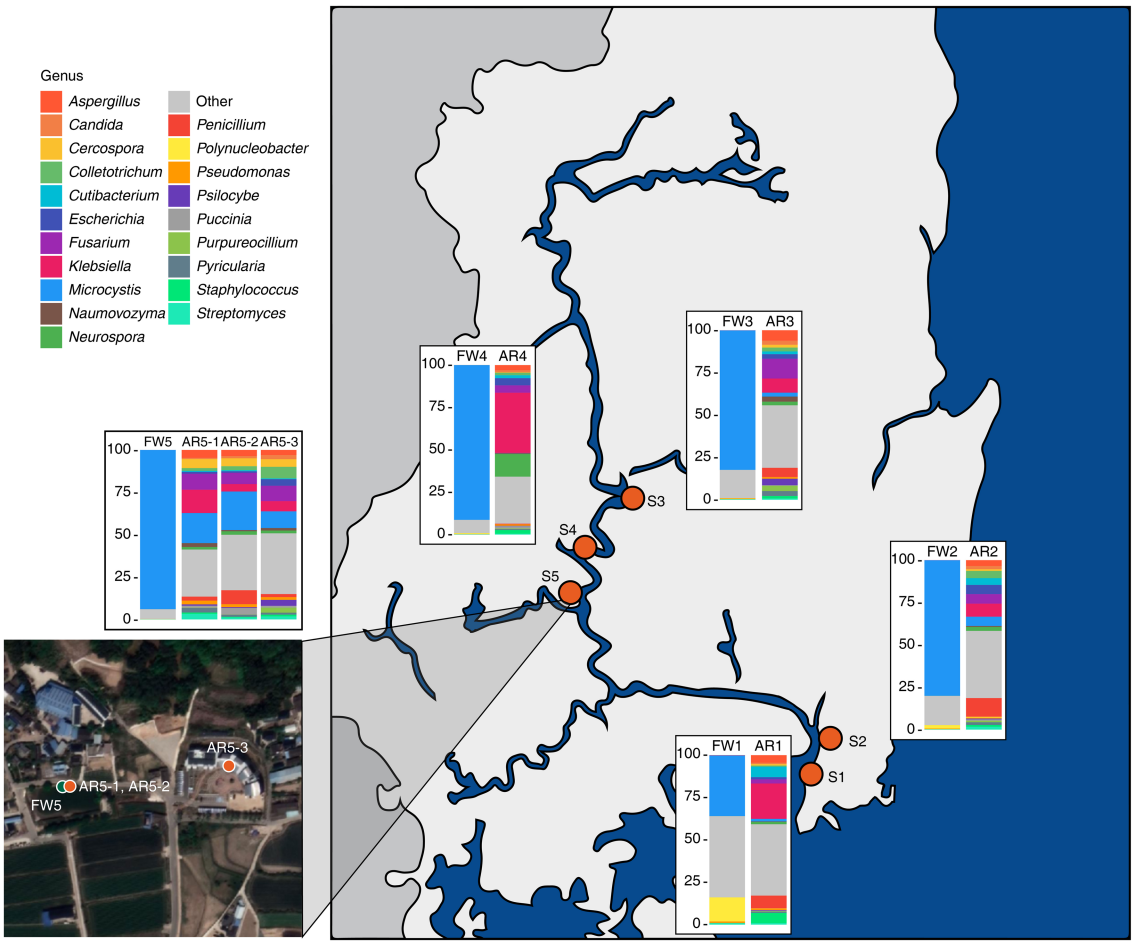

FIGURE 1
Sampling sites and the microbial composition at the genus level in the collected samples. Bar plots depicting the taxonomic composition at the genus level for both freshwater and aerosol samples across different sites.

0.26% *Flavobacterium*, 0.22% *Synechococcus*, and 0.19% *Planktothrix* (Figure 1; Supplementary Table S1). The aerosol microbiome was composed of 56.33% bacteria, 41.88% eukaryotes, and 1.29% viruses (Supplementary Figure S1). Especially, *Klebsiella* (13.8%) and *Microcystis* (8.54%) were dominant in the aerosol microbiome, as were fungi such as *Fusarium* (7.04%) and *Aspergillus* (4.07%) (Figure 1; Supplementary Table S1).

3.3. Microbial diversity and core microbiome of the freshwater and aerosols

PCoA based on Bray–Curtis dissimilarity showed that microbial communities differed significantly between the freshwater and aerosols (Figure 2A). The aerosol microbiome had a greater variety of microbes and a higher level of evenness (Simpson's index) than the freshwater microbiome (Figure 2B). Furthermore, the core microbiome of the each group was explored. The core microbiome refers to a set of microbial taxa that are consistently found across multiple individuals or groups, representing a stable and shared component of the overall microbiome (Neu et al., 2021). Total of five core microbiome genera, including *Aeromonas*, *Microcystis*, *Burkholderia*, *Pseudomonas*, and *Streptomyces*, were identified that were common to each groups (Figure 2C). The stacked bar chart showed the proportion of core microbiomes within each group (orange and blue), with the core microbiome shared between freshwater and aerosol samples shown in yellow. The freshwater samples are dominated by water-aerosol core microbiome (yellow), whereas the aerosol samples were predominantly composed of aerosol-unique core microbiome (orange) (Figure 2D). Biosynthetic genes of microcystin.

3.4. Identifying MC biosynthetic gene cluster (BGC) from freshwater and aerosols

The microcystin BGC, produced by *Microcystis,* was identified in high abundance in both freshwater and aerosol samples (Figure 3A). The biosynthetic genes of microcystin (*mcyA, mcyB, mcyC, mcyD, mcyE, and mcyG*) were found in all freshwater samples, whereas these biosynthetic genes of microcystin were detected in the AR5-1, AR5-2, and AR5-3 samples (Figure 3A). Furthermore, the taxonomy of contigs annotated with each gene was examined and it is found that some contigs were classified as *Planktothrix* and *Nostoc*;

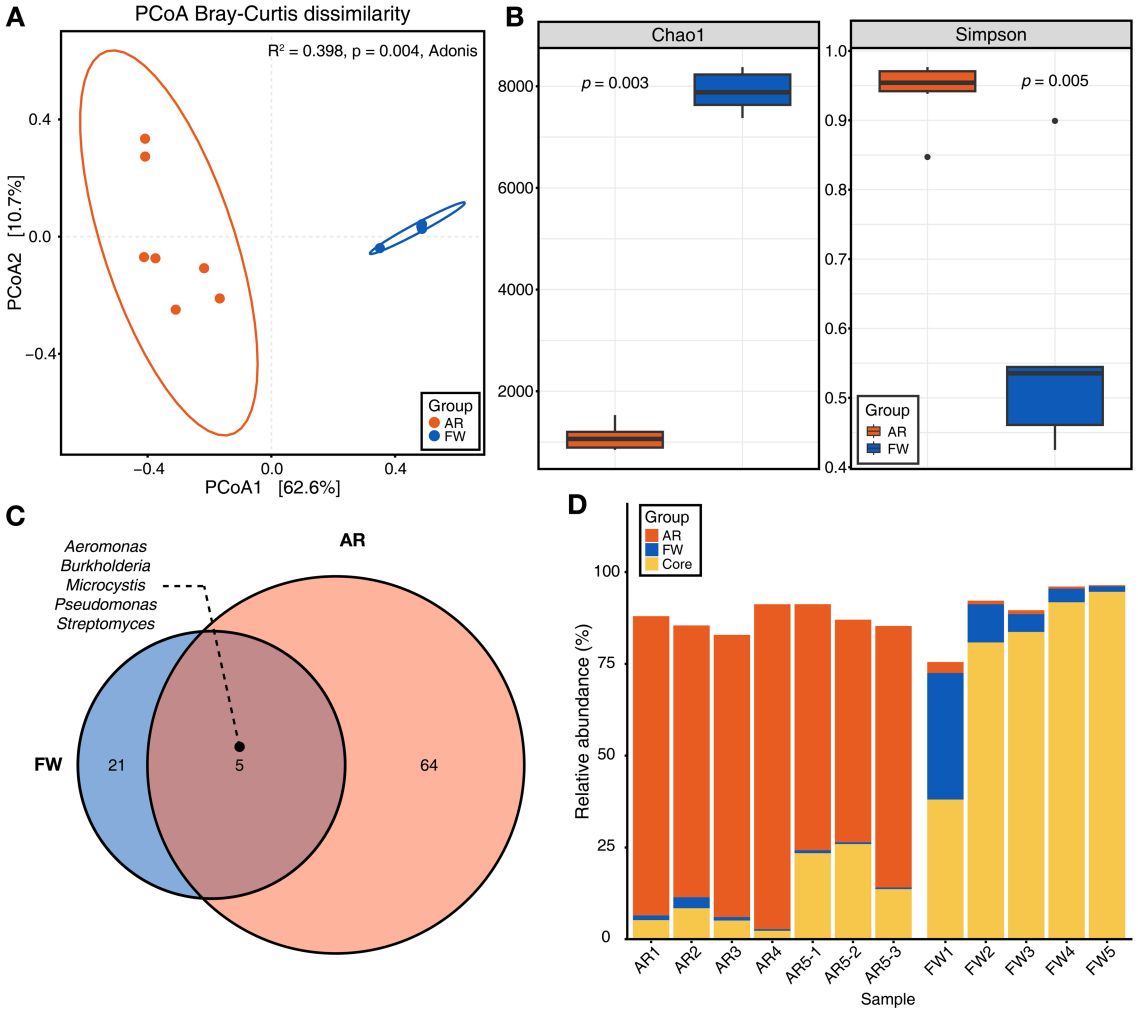

FIGURE 2
Microbial diversity and core microbiome of aerosol and freshwater. **(A)** Beta-diversity of microbiome through principal coordinates analysis (PCoA) based on Bray–Curtis dissimilarity (p=0.004). **(B)** Chao1 and Simpson indices for alpha-diversity was visualized using bar plot (Wilcoxon rank sum test, p=0.003 for Chao1, p=0.005 for Simpson). **(C)** The Venn diagram illustrated the genera commonly found in both aerosol and freshwater samples (Detection=0.1, Prevalence=0.5). **(D)** Stacked bar chart displaying the relative abundance of aerosol, freshwater, and core microbiome constituents for each sample.

however, 95.1% of the contigs were classified as *Microcystis* (Figure 3B).

3.5. Functional profiling of ARGs and virulence factors

Functional diversities were also significantly different between freshwater and aerosol samples in both the resistome and pathobiome (Figures 4A,C). ARGs were also found in the aerosol samples, although at lower concentrations than in the freshwater samples (Figure 4B). In the freshwater samples, ARGs associated with target modification mechanisms constituted the highest percentage, whereas in the aerosol samples, ARGs with efflux pump mechanisms were more prevalent (Figure 4B). Regarding virulence factors (VFs), although they were significantly more abundant in freshwater, both groups were enriched in genes belonging to the adherence type (Figure 4D). Interestingly, the abundance of a specific gene, named *PhoQ*, was notably high in AR2 samples. Upon examining genes with a high proportion of each virulence type, we observed that the *tufA* gene had the highest abundance in the Adherence type, followed by *gmd* in the Immune Modulation type, *katB* in the Stress Survival type, and *hemB* in the Nutritional/Metabolic Factor type. (Supplementary Table 3). To identify commonly found VFs in freshwater and aerosol samples, we defined core genes as detected to 50% in each group sample. A total of ten core VFs were identified in both freshwater and aerosol samples (Figure 5A). Additionally, we analyzed the taxonomic origins of contigs harboring core VF genes and found that contigs encoding *groEL, htpB, pgi, rpoS, and tufA* genes were part of the core microbiome associated with *Aeromonas*, *Microcystis*, *Pseudomonas*, and *Streptomyces* taxa (Figure 5B). For the core ARGs, we compared the freshwater and aerosol samples at each site individually, each site had their unique core ARGs including *aac(6′)-Ie-aph(2″)-Ia, rphB, MexB, ugd, ceoB, lnuA, rpoB2, mdtC, rsmA,* and *sul1* genes (Figures 6A-E). Notably, among the core ARGs, it was confirmed that *ugd, rsmA, rpoB2, and ceoB* were presented in

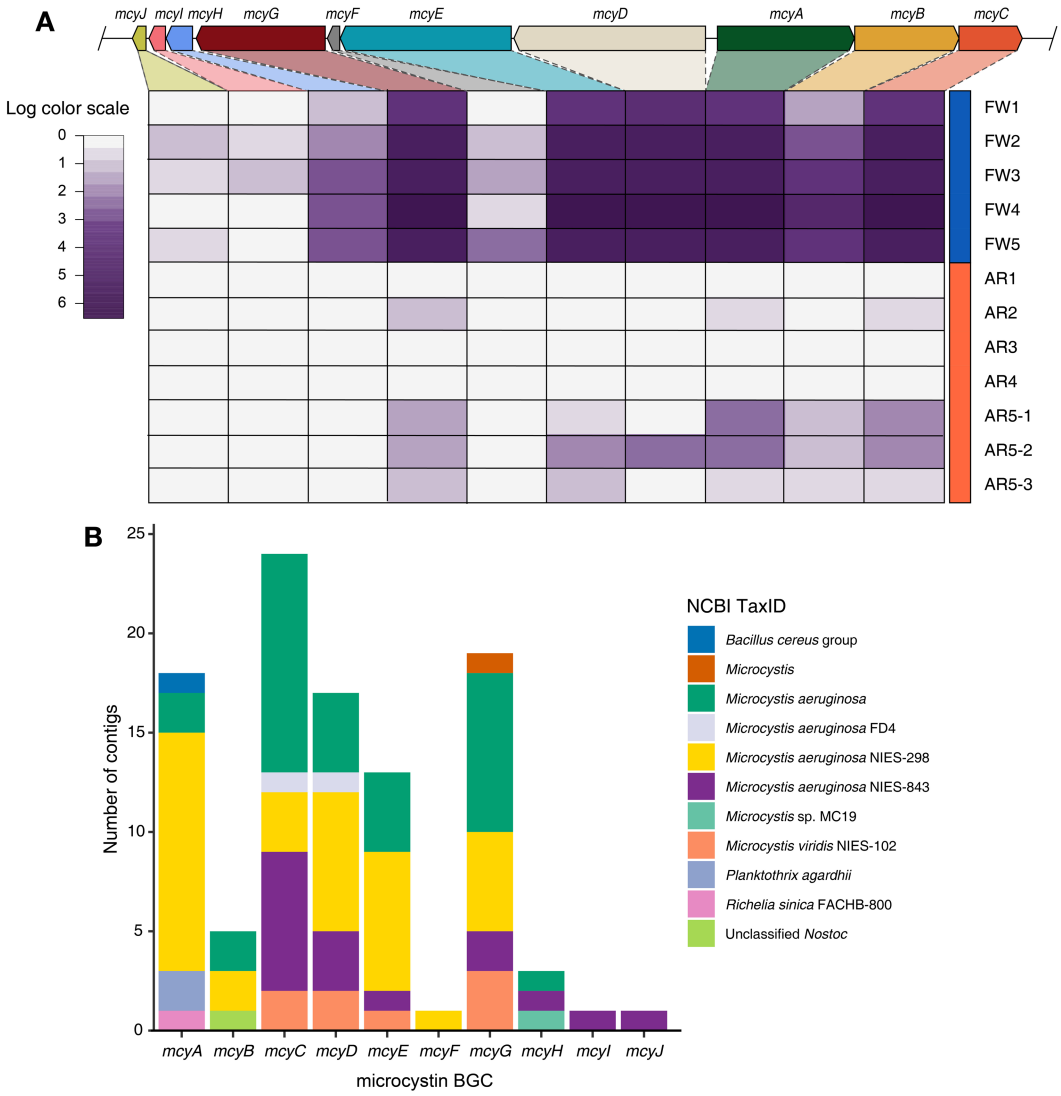

FIGURE 3
Identification of microcystin BGC and taxonomy composition of contigs. **(A)** Heatmap displaying the log-scaled abundance of the *mcy* genes in each sample. **(B)** Stacked bar plot showing the taxonomy information of contigs encoding for each *mcy* genes.

contigs classified as part of the core microbiome, with the exception of *Microcystis* (Supplementary Table 2).

4. Discussion

Due to eutrophication and increased water temperature, the increasing frequency and intensity of HABs in freshwater environments are becoming a global problem (O'Neil et al., 2012). Particularly, in recent years, there has been growing interest in the toxic factors present in aerosols emitted from freshwater bodies. For instance, Wood and Dietrich (2011) detected aerosolized MCs concentrations of up to 1.8 pg./m^3 in two lakes in New Zealand, and Backer et al. (2010) detected an average of 0.052 ng/m^3 of MCs in the air of bloom-affected lakes in California. Numerous studies have extensively explored the composition of microbial communities in aerosols, with a particular emphasis on harmful algae (Madikizela et al., 2018; Olson et al., 2020; Harb et al., 2021; Plaas et al., 2022). Especially, Plaas et al. (2022) identified aerosolized *Dolichospermum*, *Microcystis*, and *Aphanizomenon*. However, limited research has been conducted on the function of microbial communities that are related to pathogenicity factors (Olson et al., 2020). This study investigated the microbial communities in freshwater environments and nearby aerosol samples using metagenomic sequencing, to explore the composition and function of micro-organisms. We aimed to assess the potential hazards of aerosols generated from HAB-affected freshwater bodies with identifying profiles of pathogenic and virulence factors in microbial communities.

Our results demonstrated the taxonomic composition of the freshwater samples: 30–90% of the *Microcystis* genus and MCs were discovered at five sites in the Nakdong River basin. The *Microcystis* genus represents one of the key cyanobacteria and is known for its carcinogenic properties, hepatotoxicity, and reproductive toxicity, among other effects (Svirčev et al., 2010; Lone et al., 2015). Conversely, in the aerosol samples, *Microcystis* was not detected in large quantities across all samples but was found to be present in high proportions at

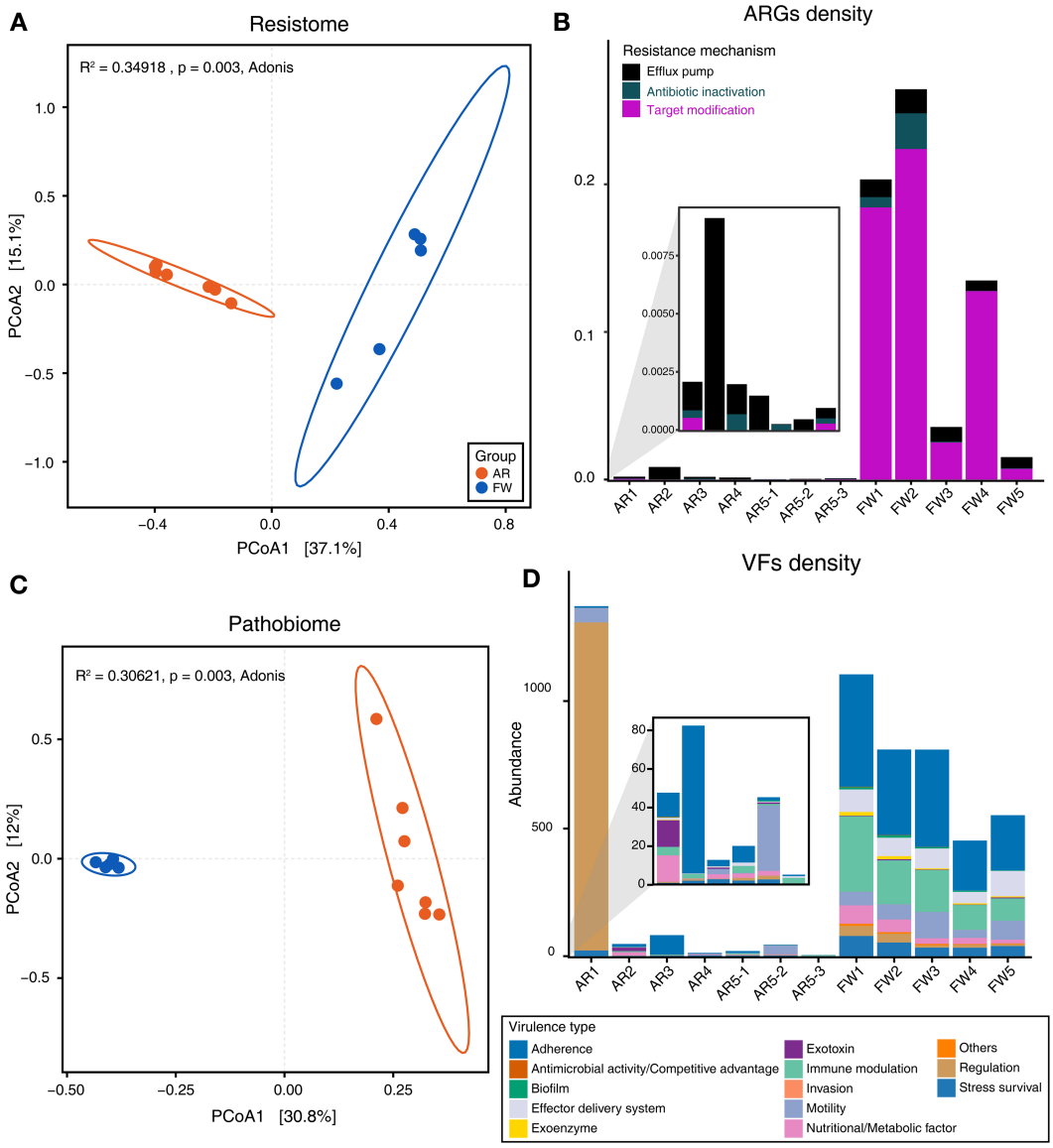

FIGURE 4
Analysis of functional diversity and density of resistome and pathobiome genes identified in AR and FW samples. **(A)** Beta-diversity of ARGs through PCoA based on Bray–Curtis dissimilarity (p=0.003). **(B)** Stacked bar plot representing the density of ARGs and the proportion of each ARG type in the samples. **(C)** Beta-diversity of VFs through PCoA based on Bray–Curtis dissimilarity (p=0.003). **(D)** Stacked bar plot representing the density of VFs and the proportion of each virulence type in the samples.

specific sites (AR5-1 ~ 3). A previous study indicated that microbial diversity of aerosols varies according to climate; this difference is likely influenced by the climate (water temperature, humidity, and wind direction) at the time of sampling (Lone et al., 2015).

The microbial community diversity is markedly distinct between freshwater and aerosol samples, with the freshwater group exhibiting greater bacterial richness but significantly less evenness compared to the aerosol group. This disparity is attributable to the dominance of *Microcystis* in the freshwater group during bloom seasons. However, in the aerosol group, various micro-organisms, including bacteria, fungi, and viruses, are relatively evenly distributed. Collectively, these results indicate that the aerosol environment, which can change rapidly in response to climatic and ambient conditions, is only marginally influenced by the adjacent water microbial community. This observation aligns with the higher proportion of the aerosol-core microbiome than the aerosol-freshwater core microbiome in the taxonomic composition of the aerosol samples. Interestingly, AR5-1 ~ 3 samples exhibited a high proportion of *Microcystis*, which was consistent in neighboring freshwater samples. Among the regions identified in this study, FW5 had the highest abundance of *Microcystis*.

We examined specific genes related with MC biosynthesis (*mcy* gene) produced by toxin-producing cyanobacteria. The core genes *mcyA-E* and *mcyG*, which are responsible for the synthesis, assembly, and modification of MCs (Tillett et al., 2000), were present in high abundance in the freshwater samples. We also observed the *mcy* genes

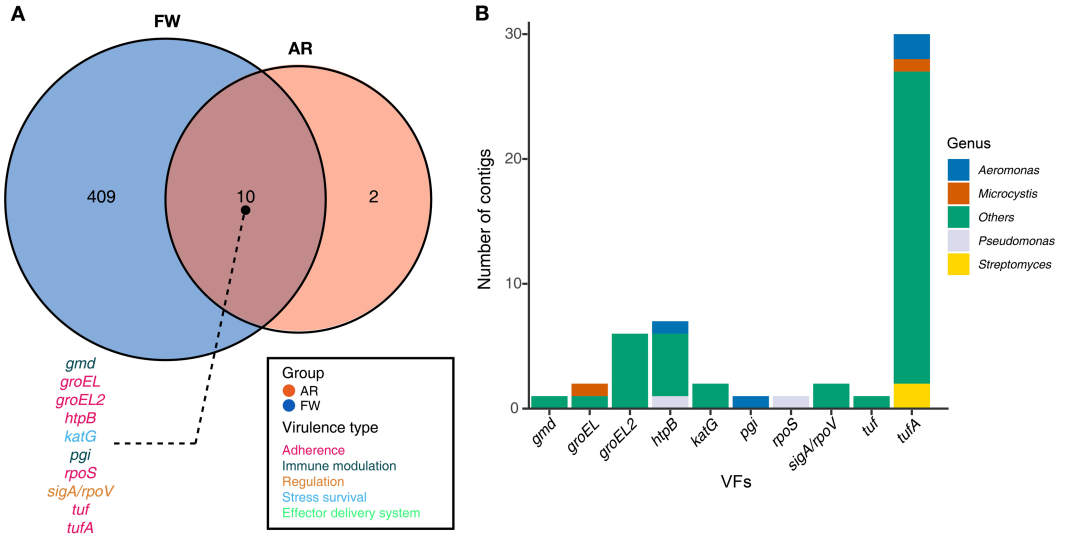

FIGURE 5
Core VFs in both groups and the taxonomic information of the contigs encoding genes. **(A)** The Venn diagram illustrated the number of core VFs found in both aerosol and freshwater samples (Detection=0.001, Prevalence=0.5). For the VFs present in the intersection of the Venn diagrams, the gene names were annotated using distinct colors corresponding to their respective virulence types. **(B)** A stacked bar plot illustrating the distribution of contigs encoding each gene, categorized according to taxonomic information.

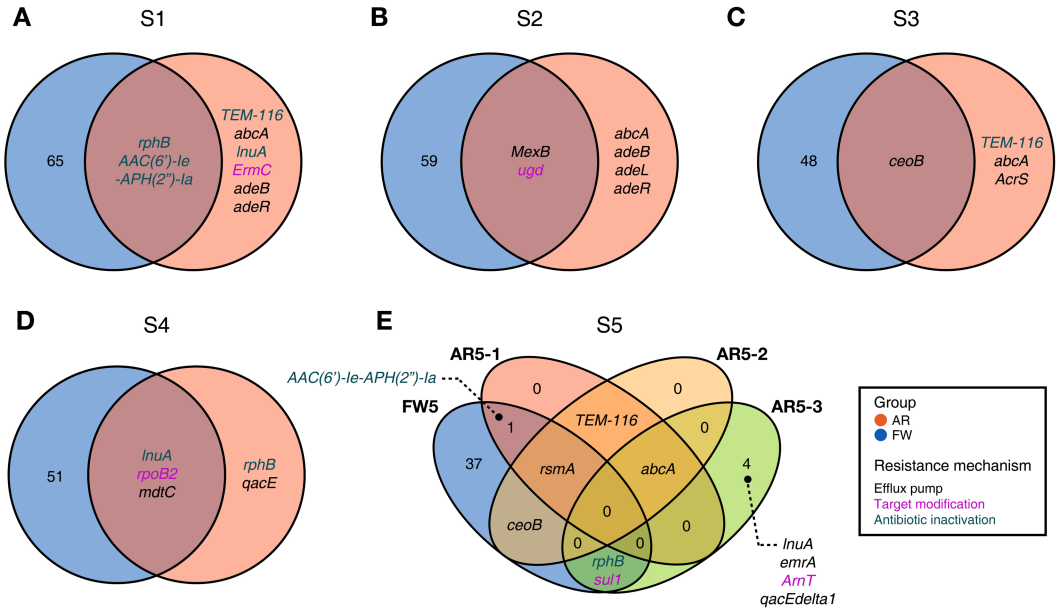

FIGURE 6
Commonly found ARGs in individual FW and AR samples at the same site. **(A-E)** The Venn diagram visualizing common ARGs in each site, colors indicating the resistance mechanism.

in the aerosol samples. The abundance of *mcy* genes was consistently higher in the AR 5–1, 5–2, and 5–3 samples with high *Microcystis* abundance than in other samples (e.g., AR 1–4). Furthermore, most of the contigs encoding MC BGC are classified as *Microcystis*, which suggests that *Microcystis* found in aerosols may indeed have a toxin-producing function and raises the possibility of transporting harmful substances via aerosols.

Furthermore, the genera *Aeromonas*, *Burkholderia*, *Pseudomonas*, and *Streptomyces* were identified as common components of the core microbiome. These Gram-negative bacteria form biofilms and are highly adapted and widespread in various environments due to their remarkable metabolic versatility (Seshadri et al., 2006; Rojo, 2010; Kaltenpoth and Flórez, 2020; Kumar et al., 2023). Consequently, they have the potential to colonize multiple

environments when dispersed through aerosols. Additionally, the presence of these four genera among the contigs encoding ARGs implies the potential existence of ARG carriers within the core microbiome. Indeed, *Aeromonas* and *Burkholderia* are already well established as ARG carriers in river (Esiobu et al., 2002; Piotrowska and Popowska, 2014). Although no direct evidence exists to attribute the presence of these core microbiomes in aerosol samples to freshwater sources, microbes found in freshwater samples are also commonly detected in aerosol samples, and these microbes have pathogenic characteristics that can cause dissemination of harmful agents through aerosols.

In addition, VFs and ARGs were analyzed to determine the distribution of potential harmful factors in the aerosol microbiome. Both types of genes exhibited significant differences between the aerosol and freshwater groups, with freshwater samples displaying higher gene abundance than aerosol samples. However, ARGs and VFs were also detected in the aerosol samples, albeit at low concentrations. Previous studies have demonstrated that aerosol samples can be dispersed over considerable distances, indicating a potential risk of harmful agents in aerosols spreading to humans (Gorbunov, 2020). Benson et al. (2005) suggested that trace amounts of MCs could potentially induce adverse effects when MCs are introduced into the human respiratory tract via aerosols. Moreover, the acute toxicity of MCs may be more potent when exposure occurs via inhalation rather than ingestion (Creasia, 1990). A major contributor to the proliferation and outbreak of ARGs is the misuse of antibiotics (Shallcross and Davies, 2014). Although antibiotics are extensively employed in human, livestock, and agricultural settings (Madikizela et al., 2018; Chang et al., 2019; Tian et al., 2021), to our knowledge, they are not applied to or transported through the air. Nonetheless, the detection of ARGs in aerosols can be attributed to antibiotic-resistant bacteria carrying ARGs. Indeed, prior studies have reported the detection of ARGs in aerosols near livestock barns, where ARGs are frequently found (Li et al., 2019). Given the detection of ARGs in aerosols around freshwater environments, ARGs present in aerosols in areas with minimal human activity are likely to have been transferred from freshwater environments, which are known as ARG reservoirs.

Furthermore, a total of ten VFs were identified as common in both AR and FW samples, among which the *groEL*, *groEL2*, *htpB*, *rpoS*, *tuf*, and *tufA* genes are of the adherence type. If bacteria carrying these functional genes become aerosolized, they may play a crucial role in the subsequent attachment of aerosolized bacteria to host cells or surfaces, a critical step in establishing infections (Hennequin et al., 2001; Srivastava et al., 2008). Moreover, in accordance with previous findings, the presence of VFs in core microbiome taxa suggests that harmful, functional microbes indeed exist in aerosols.

5. Conclusion

In this preliminary study, we employed metagenomic sequencing to explore the microbial communities within aerosols and their associated MC-producing genes, which have not yet been thoroughly investigated. Aerosols have been inadequately studied due to challenges in sample collection and their susceptibility to the surrounding environment. However, recent outbreaks of COVID-19 and pneumonia infections (*Mycobacterium tuberculosis*), both prevalent nosocomial infections, are transmitted via aerosols (Li et al., 2020; Borges et al., 2021). Furthermore, the major limitation of this study is a lack of collecting field blanks, which is for ensuring the quality of aerosol samples, concurrently during the day. However, in this study, collection of blank samples was conducted on a clean bench under controlled laboratory conditions, potentially influencing the results. For a future study, it is necessary to consider measuring the blanks in the field under the same conditions to guarantee the accuracy of the data.

Consequently, monitoring harmful microorganisms and their genes in aerosols is essential. This study underscores the importance of aerosol metagenomics by identifying detrimental microorganisms and genes in aerosols from environments with minimal human interaction. Moreover, because of the limited data on contributing factors and the small sample size in this study, we could not establish a direct link between freshwater environments and aerosols. Therefore, future research is needed to confirm the transfer of harmful microorganisms from freshwater environments to aerosols.

Data availability statement

The datasets presented in this study are deposited in NCBI SRA online repositories under BioProject accession number PRJNA949880 (https://www.ncbi.nlm.nih.gov/bioproject/PRJNA949880).

Author contributions

J-HS and SL designed study, supervised the project, and edited the manuscript. JK and SH collected data and samples. JK, SH, GL, and M-JK analysed data, performed statistical analyses, and wrote the draft. GL and M-JK conducted sequencing. All authors contributed to the article and approved the submitted version.

Funding

This research was supported by a project to train professional personnel in biological materials by the Ministry of Environment and the Korea Basic Science Institute (National Research Facilities and Equipment Center) grant funded by the Ministry of Education (2021R1A6C101A416). This work was also supported by the National Research Foundation of Korea (NRF) grant funded by the Korea government (MSIT) (No. 2022R1C1C1008799). This work was supported by the Pukyong National University Research Fund in 2021(CD20210981).

Acknowledgments

The authors would like to thank the Jiyoung Lee at The Ohio State University for her support. The authors would also like to thank KNU NGS Core Facility for the sequencing using DNBSEQ-G400RS platform.

Conflict of interest

The authors declare that the research was conducted in the absence of any commercial or financial relationships that could be construed as a potential conflict of interest.

Publisher's note

All claims expressed in this article are solely those of the authors and do not necessarily represent those of their affiliated organizations, or those of the publisher, the editors and the reviewers. Any product that may be evaluated in this article, or claim that may be made by its manufacturer, is not guaranteed or endorsed by the publisher.

Supplementary material

The Supplementary material for this article can be found online at: https://www.frontiersin.org/articles/10.3389/fmicb.2023.1203317/full#supplementary-material

References

Alcock, B. P., Raphenya, A. R., Lau, T. T. Y., Tsang, K. K., Bouchard, M., Edalatmand, A., et al. (2019). CARD 2020: antibiotic resistome surveillance with the comprehensive antibiotic resistance database. *Nucleic Acids Res.* 48, D517–D525. doi: 10.1093/nar/gkz935

Backer, L. C., Mcneel, S. V., Barber, T., Kirkpatrick, B., Williams, C., Irvin, M., et al. (2010). Recreational exposure to microcystins during algal blooms in two California lakes. *Toxicon* 55, 909–921. doi: 10.1016/j.toxicon.2009.07.006

Bass, D., Stentiford, G. D., Wang, H. C., Koskella, B., and Tyler, C. R. (2019). The pathobiome in animal and plant diseases. *Trends Ecol. Evol* 43(11), 996–1008. doi: 10.1016/j.tree.2019.07.012

Benson, J. M., Hutt, J. A., Rein, K., Boggs, S. E., Barr, E. B., and Fleming, L. E. (2005). The toxicity of microcystin LR in mice following 7 days of inhalation exposure. *Toxicon* 45, 691–698. doi: 10.1016/j.toxicon.2005.01.004

Bhattacharya, R., Sugendran, K., Dangi, R., and Rao, P. (1997). Toxicity evaluation of freshwater cyanobacterium *Microcystis aeruginosa* PCC 7806: II nephrotoxicity in rats. *Biomed. Environ. Sci.* 10, 93–101.

Bolger, A. M., Lohse, M., and Usadel, B. (2014). Trimmomatic: a flexible trimmer for Illumina sequence data. *Bioinformatics* 30, 2114–2120. doi: 10.1093/bioinformatics/btu170

Borges, J. T., Nakada, L. Y. K., Maniero, M. G., and Guimarães, J. R. (2021). SARS-CoV-2: a systematic review of indoor air sampling for virus detection. *Environ. Sci. Pollut. Res.* 28, 40460–40473. doi: 10.1007/s11356-021-13001-w

Buchfink, B., Xie, C., and Huson, D. H. (2015). Fast and sensitive protein alignment using DIAMOND. *Nat. Methods* 12, 59–60. doi: 10.1038/nmeth.3176

Bushnell, B. (2014). "BBMap: a fast, accurate, splice-aware aligner". In *9th annual genomics of Energy & Environment Meeting*. 17-20 march, University of California. 2014.

Chang, Y., Chusri, S., Sangthong, R., McNeil, E., Hu, J., Du, W., et al. (2019). Clinical pattern of antibiotic overuse and misuse in primary healthcare hospitals in the southwest of China. *PLoS One* 14:e0214779. doi: 10.1371/journal.pone.0214779

Choi, A. -R., Oh, H. -M., and Lee, J. -A. (2002). Ecological study on the toxic *Microcystis* in the lower Nakdong River. *Algae* 17, 171–185. doi: 10.4490/ALGAE.2002.17.3.171

Creasia, D. (1990). Acute inhalation toxicity of microcystin-LR with mice. *Toxicon* 28:605.

Dawson, R. M. (1998). The toxicology of microcystins. *Toxicon* 36, 953–962. doi: 10.1016/S0041-0101(97)00102-5

Esiobu, N., Armenta, L., and Ike, J. (2002). Antibiotic resistance in soil and water environments. *Int. J. Environ. Health Res.* 12, 133–144. doi: 10.1080/09603120220129292

Gonçalves, A. L., Rodrigues, C. M., Pires, J. C. M., and Simões, M. (2016). The effect of increasing CO_2 concentrations on its capture, biomass production and wastewater bioremediation by microalgae and cyanobacteria. *Algal Res.* 14, 127–136. doi: 10.1016/j.algal.2016.01.008

Gorbunov, B. (2020). Aerosol particles laden with viruses that cause COVID-19 travel over 30m distance. *Preprints.org* [preprint] (2020). Available at: doi: 10.20944/preprints202004.0546.v1

Hachicha, R., Elleuch, F., Ben Hlima, H., Dubessay, P., De Baynast, H., Delattre, C., et al. (2022). Biomolecules from microalgae and Cyanobacteria: applications and market survey. *Appl. SciApplied Sciences*. 12:1924. doi: 10.3390/app12041924

Harb, C., Pan, J., DeVilbiss, S., Badgley, B., Marr, L. C., Schmale, D. G., III, Foroutan, H, et al. (2021). Increasing freshwater salinity impacts aerosolized bacteria. Environ. *Sci. Technol* 55(9), 5731–5741. doi: 10.1021/acs.est.0c08558

Hennequin, C., Porcheray, F., Waligora-Dupriet, A. -J., Collignon, A., Barc, M. -C., Bourlioux, P., et al. (2001). GroEL (Hsp60) of *Clostridium difficile* is involved in cell adherence. *Microbiology* 147, 87–96. doi: 10.1099/00221287-147-1-87

Hur, M., Lee, I., Tak, B. -M., Lee, H. J., Yu, J. J., Cheon, S. U., et al. (2013). Temporal shifts in cyanobacterial communities at different sites on the Nakdong River in Korea. *Water Res.* 47, 6973–6982. doi: 10.1016/j.watres.2013.09.058

Ito, E., Kondo, F., Terao, K., and Harada, K. -I. (1997). Neoplastic nodular formation in mouse liver induced by repeated intraperitoneal injections of microcystin-LR. *Toxicon* 35, 1453–1457. doi: 10.1016/S0041-0101(97)00026-3

Kaltenpoth, M., and Flórez, L. V. (2020). Versatile and dynamic symbioses between insects and Burkholderia bacteria. *Annu. Rev. Entomol.* 65, 145–170. doi: 10.1146/annurev-ento-011019-025025

Kim, H. G., Hong, S., Chon, T. -S., and Joo, G. -J. (2021). Spatial patterning of chlorophyll a and water-quality measurements for determining environmental thresholds for local eutrophication in the Nakdong River basin. *Environ. Pollut.* 268:115701. doi: 10.1016/j.envpol.2020.115701

Kim, S., Chung, S., Park, H., Cho, Y., and Lee, H. (2019). Analysis of environmental factors associated with Cyanobacterial dominance after river weir installation. *Water.* 11:1163. doi: 10.3390/w11061163

Kumar, M., Tiwari, P., Zeyad, M. T., Ansari, W. A., Kumar, S. C., Chakdar, H., et al. (2023). Genetic diversity and antifungal activities of the genera *Streptomyces* and *Nocardiopsis* inhabiting agricultural fields of Tamil Nadu India. *J. King Saud Univ. Sci.* 35:102619. doi: 10.1016/j.jksus.2023.102619

Labohá, P., Sychrová, E., Brózman, O., Sovadinová, I., Bláhová, L., Prokeš, R., et al. (2023). Cyanobacteria, cyanotoxins and lipopolysaccharides in aerosols from inland freshwater bodies and their effects on human bronchial cells. *Environ. Toxicol. Pharmacol.* 98:104073. doi: 10.1016/j.etap.2023.104073

Lad, A., Breidenbach, J. D., Su, R. C., Murray, J., Kuang, R., Mascarenhas, A., et al. (2022). As we drink and breathe: adverse health effects of microcystins and other harmful algal bloom toxins in the liver, gut, lungs and beyond. *Life.* 12:418. doi: 10.3390/life12030418

Lee, H. -J., Park, H. -K., and Cheon, S. -U. (2018). Effects of weir construction on phytoplankton assemblages and water quality in a large river system. *Int. J. Environ. Res. Public Health* 15:2348. doi: 10.3390/ijerph15112348

Lee, S., Kim, J., and Lee, J. (2021). Colonization of toxic cyanobacteria on the surface and inside of leafy green: a hidden source of cyanotoxin production and exposure. *Food Microbiol.* 94:103655. doi: 10.1016/j.fm.2020.103655

Li, D., Liu, C. -M., Luo, R., Sadakane, K., and Lam, T. -W. (2015). MEGAHIT: an ultra-fast single-node solution for large and complex metagenomics assembly via succinct de Bruijn graph. *Bioinformatics* 31, 1674–1676. doi: 10.1093/bioinformatics/btv033

Li, J., Zhang, L., Ren, Z., Xing, C., Qiao, P., and Chang, B. (2020). Meteorological factors correlate with transmission of 2019-nCoV: proof of incidence of novel coronavirus pneumonia in Hubei Province, China. *Medrxiv [Preprint] (2020)*. Available at. doi: 10.1101/2020.04.01.20050526

Li, W., and Godzik, A. (2006). Cd-hit: a fast program for clustering and comparing large sets of protein or nucleotide sequences. *Bioinformatics* 22, 1658–1659. doi: 10.1093/bioinformatics/btl158

Li, W., Mao, F., Te, S. H., He, Y., and Gin, K. Y. H. (2021). Impacts of *Microcystis* on the dissemination of the antibiotic resistome in cyanobacterial blooms. *ACS ESe&T Water.* 1, 1263–1273. doi: 10.1021/acsestwater.1c00006

Li, Y., Liao, H., and Yao, H. (2019). Prevalence of antibiotic resistance genes in air-conditioning systems in hospitals, farms, and residences. *Int. J. Environ. Res. Public Health* 16:683. doi: 10.3390/ijerph16050683

Liu, B., Zheng, D., Zhou, S., Chen, L., and Yang, J. (2022). VFDB 2022: a general classification scheme for bacterial virulence factors. *Nucleic Acids Res.* 50, D912–D917. doi: 10.1093/nar/gkab1107

Lone, Y., Koiri, R. K., and Bhide, M. (2015). An overview of the toxic effect of potential human carcinogen microcystin-LR on testis. *Toxicol. Rep.* 2, 289–296. doi: 10.1016/j.toxrep.2015.01.008

Lu, J., Breitwieser, F. P., Thielen, P., and Salzberg, S. L. (2017). Bracken: estimating species abundance in metagenomics data. *PeerJ. Comput. Sci.* 3:e104. doi: 10.7717/peerj-cs.104

Lu, J., Struewing, I., Wymer, L., Tettenhorst, D. R., Shoemaker, J., and Allen, J. (2020). Use of qPCR and RT-qPCR for monitoring variations of microcystin producers and as an early warning system to predict toxin production in an Ohio inland lake. *Water Res.* 170:115262. doi: 10.1016/j.watres.2019.115262

Madikizela, L. M., Ncube, S., and Chimuka, L. (2018). Uptake of pharmaceuticals by plants grown under hydroponic conditions and natural occurring plant species: a review. *Sci. Total Environ.* 636, 477–486. doi: 10.1016/j.scitotenv.2018.04.297

Murby, A. L., and Haney, J. F. (2016). Field and laboratory methods to monitor lake aerosols for cyanobacteria and microcystins. *Aerobiologia*, 32, 395–403.

Neu, A. T., Allen, E. E., and Roy, K. (2021). Defining and quantifying the core microbiome: Challenges and prospects. *Proc. Natl. Acad. Sci.*, 118(51), e2104429118. doi: 10.1073/pnas.2104429118

O'Neil, J. M., Davis, T. W., Burford, M. A., and Gobler, C. J. (2012). The rise of harmful cyanobacteria blooms: the potential roles of eutrophication and climate change. *Harmful Algae* 14, 313–334. doi: 10.1016/j.hal.2011.10.027

Olson, N. E., Cooke, M. E., Shi, J. H., Birbeck, J. A., Westrick, J. A., and Ault, A. P. (2020). Harmful algal bloom toxins in aerosol generated from inland lake water. *Environ. Sci. Technol.* 54, 4769–4780. doi: 10.1021/acs.est.9b07727

Oren, A. (2011). Cyanobacterial systematics and nomenclature as featured in the international bulletin of bacteriological nomenclature and taxonomy/international journal of systematic bacteriology/international journal of systematic and evolutionary microbiology. *Int. J. Syst. Evol. Microbiol.* 61, 10–15. doi: 10.1099/ijs.0.018838-0

Orrell, J. (2022). *Risk analysis of aerosolized algae atmospheric transport in northwestern Ohio from the western basin of Lake Erie*. [master's thesis]. [Columbus (OH)]: The Ohio State University.

Palinska, K. A., and Surosz, W. (2014). Taxonomy of cyanobacteria: a contribution to consensus approach. *Hydrobiologia* 740, 1–11. doi: 10.1007/s10750-014-1971-9

Park, H. -K., Lee, H. -J., Heo, J., Yun, J. -H., Kim, Y. -J., Kim, H. -M., et al. (2021). Deciphering the key factors determining spatio-temporal heterogeneity of cyanobacterial bloom dynamics in the Nakdong River with consecutive large weirs. *Sci. Total Environ.* 755:143079. doi: 10.1016/j.scitotenv.2020.143079

Piotrowska, M., and Popowska, M. (2014). The prevalence of antibiotic resistance genes among Aeromonas species in aquatic environments. *Ann. Microbiol.* 64, 921–934. doi: 10.1007/s13213-014-0911-2

Plaas, H. E., Paerl, R. W., Baumann, K., Karl, C., Popendorf, K. J., Barnard, M. A., et al. (2022). Harmful cyanobacterial aerosolization dynamics in the airshed of a eutrophic estuary. *Sci. Total Environ.* 852:158383. doi: 10.1016/j.scitotenv.2022.158383

Rogers, M. M., and Stanley, R. K. (2023). Airborne algae: a rising public health risk. *Environ. Sci. Technol*, 57, 5501–5503. doi: 10.1021/acs.est.3c01158

Rojo, F. (2010). Carbon catabolite repression in *Pseudomonas*: optimizing metabolic versatility and interactions with the environment. *FEMS Microbiol. Rev.* 34, 658–684. doi: 10.1111/j.1574-6976.2010.00218.x

Ryu, H. -S., Park, H. -K., Lee, H. -J., Shin, R. -Y., and Cheon, S. -U. (2016). Occurrence and succession pattern of Cyanobacteria in the upper region of the Nakdong River: factors influencing Aphanizomenon bloom. *J. Korean Soc. Water Environ.* 32, 52–59. doi: 10.15681/KSWE.2016.32.1.52

Schaefer, A. M., Yrastorza, L., Stockley, N., Harvey, K., Harris, N., Grady, R., et al. (2020). Exposure to microcystin among coastal residents during a cyanobacteria bloom in Florida. *Harmful Algae* 92:101769. doi: 10.1016/j.hal.2020.101769

Seshadri, R., Joseph, S. W., Chopra, A. K., Sha, J., Shaw, J., Graf, J., et al. (2006). Genome sequence of *Aeromonas hydrophila* ATCC 7966^{T}: jack of all trades. *J. Bacteriol.* 188, 8272–8282. doi: 10.1128/JB.00621-06

Shallcross, L. J., and Davies, D. S. C. (2014). Antibiotic overuse: a key driver of antimicrobial resistance. *Br. J. Gen. Pract.* 64, 604–605. doi: 10.3399/bjgp14X682561

Sharma, N. K., Rai, A. K., Singh, S., and Brown, R. M. Jr. (2007). Airborne algae: their present status and relevance[1]. *J. Phycol.* 43, 615–627. doi: 10.1111/j.1529-8817.2007.00373.x

Sipari, H., Rantala-Ylinen, A., Jokela, J., Oksanen, I., and Sivonen, K. (2010). Development of a Chip assay and quantitative PCR for detecting microcystin Synthetase E gene expression. *Appl. Environ. Microbiol.* 76, 3797–3805. doi: 10.1128/AEM.00452-10

Smith, V. H., and Schindler, D. W. (2009). Eutrophication science: where do we go from here? *Trends Ecol*, 24, 201–207. doi: 10.1016/j.tree.2008.11.009

Srivastava, S., Yadav, A., Seem, K., Mishra, S., Chaudhary, V., and Nautiyal, C. (2008). Effect of high temperature on *Pseudomonas putida* NBRI0987 biofilm formation and expression of stress sigma factor RpoS. *Curr. Microbiol.* 56, 453–457. doi: 10.1007/s00284-008-9105-0

Stewart, I., Webb, P. M., Schluter, P. J., and Shaw, G. R. (2006). Recreational and occupational field exposure to freshwater cyanobacteria – a review of anecdotal and case reports, epidemiological studies and the challenges for epidemiologic assessment. *Environ. Health* 5:6. doi: 10.1186/1476-069X-5-6

Svirčev, Z., Baltić, V., Gantar, M., Juković, M., Stojanović, D., and Baltić, M. (2010). Molecular aspects of microcystin-induced hepatotoxicity and hepatocarcinogenesis. *J. Environ. Sci. Health C* 28, 39–59. doi: 10.1080/10590500903585382

Swe, T., Miles, C. O., Cerasino, L., Mjelde, M., Kleiven, S., and Ballot, A. (2021). Microcystis, Raphidiopsis raciborskii and Dolichospermum smithii, toxin producing and non-toxigenic cyanobacteria in Yezin Dam, Myanmar. *Limnologica* 90, 125901. doi: 10.1016/j.limno.2021.125901

Tesson, S. V. M., Skjøth, C. A., Šantl-Temkiv, T., and Löndahl, J. (2016). Airborne microalgae: insights, opportunities, and challenges. *Appl. Environ. Microbiol.* 82, 1978–1991. doi: 10.1128/AEM.03333-15

Tian, M., He, X., Feng, Y., Wang, W., Chen, H., Gong, M., et al. (2021). Pollution by antibiotics and antimicrobial resistance in livestock and poultry manure in China, and countermeasures. *Antibiotics.* 10:539. doi: 10.3390/antibiotics10050539

Tillett, D., Dittmann, E., Erhard, M., Von Döhren, H., Börner, T., and Neilan, B. A. (2000). Structural organization of microcystin biosynthesis in *Microcystis aeruginosa* PCC7806: an integrated peptide–polyketide synthetase system. *Chem. Biol.* 7, 753–764. doi: 10.1016/S1074-5521(00)00021-1

Vigar, M., Thuneibat, M., Jacobi, A., and Roberts, V. A. (2022). Summary report–One Health Harmful Algal Bloom System (OHHABS). *Centers for Disease Control and Prevention. Available at*: https://www.cdc.gov/habs/data/2020-ohhabs-data-summary.html

Wilson, N. (2022). Nutrient and sediment dynamics in two coastal plain rivers in the Bay of Plenty (Master dissertation, The University of Waikato). available at: https://researchcommons.waikato.ac.nz/handle/10289/15218

Wood, D. E., Lu, J., and Langmead, B. (2019). Improved metagenomic analysis with kraken 2. *Genome Biol.* 20, 257–213. doi: 10.1186/s13059-019-1891-0

Wood, S. A., and Dietrich, D. R. (2011). Quantitative assessment of aerosolized cyanobacterial toxins at two New Zealand lakes. *J. Environ. Monitor.* 13, 1617–1624. doi: 10.1039/C1EM10102A

Zhang, Q., Zhang, Z., Lu, T., Peijnenburg, W. J. G. M., Gillings, M., Yang, X., et al. (2020). Cyanobacterial blooms contribute to the diversity of antibiotic-resistance genes in aquatic ecosystems. *Commun. Biol.* 3:737. doi: 10.1038/s42003-020-01468-1

Zhao, C. S., Shao, N. F., Yang, S. T., Ren, H., Ge, Y. R., Feng, P., et al. (2019). Predicting cyanobacteria bloom occurrence in lakes and reservoirs before blooms occur. *Sci. Total Environ.* 670, 837–848. doi: 10.1016/j.scitotenv.2019.03.161

frontiers | Frontiers in Microbiology

TYPE Original Research
PUBLISHED 28 August 2023
DOI 10.3389/fmicb.2023.1233327

OPEN ACCESS

EDITED BY
George S. Bullerjahn,
Bowling Green State University, United States

REVIEWED BY
Cuong Tu Ho,
Vietnam Academy of Science and Technology, Vietnam
Matthew Saxton,
Miami University, United States

*CORRESPONDENCE
Jiyoung Lee
✉ lee.3598@osu.edu

RECEIVED 01 June 2023
ACCEPTED 15 August 2023
PUBLISHED 28 August 2023

CITATION
Lee J, Lee S, Hu C and Marion JW (2023) Beyond cyanotoxins: increased *Legionella*, antibiotic resistance genes in western Lake Erie water and disinfection-byproducts in their finished water.
Front. Microbiol. 14:1233327.
doi: 10.3389/fmicb.2023.1233327

Beyond cyanotoxins: increased *Legionella*, antibiotic resistance genes in western Lake Erie water and disinfection-byproducts in their finished water

Jiyoung Lee[1,2,3]*, Seungjun Lee[4], Chenlin Hu[5] and Jason W. Marion[6]

[1]Division of Environmental Health Sciences, College of Public Health, The Ohio State University, Columbus, OH, United States, [2]Department of Food Science and Technology, The Ohio State University, Columbus, OH, United States, [3]Infectious Diseases Institute, The Ohio State University, Columbus, OH, United States, [4]Department of Food Science and Nutrition, Pukyong National University, Busan, Republic of Korea, [5]College of Pharmacy, University of Houston, Houston, TX, United States, [6]Department of Public Health and Clinical Sciences, Eastern Kentucky University, Richmond, KY, United States

Background: Western Lake Erie is suffering from harmful cyanobacterial blooms, primarily toxic *Microcystis* spp., affecting the ecosystem, water safety, and the regional economy. Continued bloom occurrence has raised concerns about public health implications. However, there has been no investigation regarding the potential increase of *Legionella* and antibiotic resistance genes in source water, and disinfection byproducts in municipal treated drinking water caused by these bloom events.

Methods: Over 2 years, source water (total $n = 118$) and finished water (total $n = 118$) samples were collected from drinking water plants situated in western Lake Erie (bloom site) and central Lake Erie (control site). Bloom-related parameters were determined, such as microcystin (MC), toxic *Microcystis*, total organic carbon, N, and P. Disinfection byproducts (DBPs) [total trihalomethanes (THMs) and haloacetic acids (HAAs)] were assessed in finished water. Genetic markers for *Legionella*, antibiotic resistance genes, and mobile genetic elements were quantified in source and finished waters.

Results: Significantly higher levels of MC-producing *Microcystis* were observed in the western Lake Erie site compared to the control site. Analysis of DBPs revealed significantly elevated THMs concentrations at the bloom site, while HAAs concentrations remained similar between the two sites. *Legionella* spp. levels were significantly higher in the bloom site, showing a significant relationship with total cyanobacteria. Abundance of ARGs (*tet*Q and *sul*1) and mobile genetic elements (MGEs) were also significantly higher at the bloom site.

Discussion: Although overall abundance decreased in finished water, relative abundance of ARGs and MGE among total bacteria increased after treatment, particularly at the bloom site. The findings underscore the need for ongoing efforts to mitigate bloom frequency and intensity in the lake. Moreover, optimizing water treatment processes during bloom episodes is crucial to maintain water quality. The associations observed between bloom conditions, ARGs, and *Legionella*, necessitate future investigations into the potential enhancement of antibiotic-resistant bacteria and *Legionella* spp. due to blooms, both in lake environments and drinking water distribution systems.

KEYWORDS

trihalomethane, Lake Erie, haloacetic acids, microcystin, *Microcystis*, mobile genetic elements, antibiotic resistance, *Legionella*

Introduction

Changes in the global climate have been linked to increasing eutrophication and an increase in frequency, duration and intensity of harmful algae blooms (Glibert, 2020). Among these blooms, freshwater blooms are dominated by cyanobacterial blooms, in which most are associated with the production of cyanotoxins (Loftin et al., 2016). These blooms, pose health risks by compromising drinking water sources, food production, aquatic ecosystems, and recreational waters (Brooks et al., 2016; Lee J. et al., 2017; Mrdjen et al., 2018). Microcystins (MCs), prevalent cyanotoxins, are commonly detected in freshwater used for drinking water supplies, irrigation, recreation, and fish farms (Loftin et al., 2016; Lee S. et al., 2017; Mrdjen et al., 2018). Epidemiological and animal studies have linked exposures to bloom-affected water to an increased frequency of non-alcoholic liver diseases, liver cancer, neurodegenerative diseases, gut microbiome disturbance, and more progressed liver cancer (Zhang et al., 2015; Lee et al., 2019, 2020, 2022; Gorham et al., 2020).

Lake Erie in the United States has witnessed recurring severe cyanobacteria blooms, particularly the massive 2011 event spanning 5,000 km^2 (Stumpf et al., 2016; Zhang et al., 2017; Jankowiak et al., 2019). Elevated MCs exceeding 1 μg/L in finished drinking water in 2013–2014 prompted "Do Not Drink" advisories (Stumpf et al., 2016). Effective drinking water treatment is pivotal for safeguarding public health from cyanotoxins, necessitating robust strategies for MCs and cyanotoxin removal in bloom-impacted source water beyond source protection measures. While MCs are effectively removed using disinfection with free chlorine or ozone followed by additional activated carbon treatment (Cheung et al., 2013; Gonsior et al., 2019) in most cases, little is known about disinfection by-products (DBPs) that can form via chlorination in the Lake Erie region from MCs and other organics associated with blooms. Previous studies have demonstrated that bloom conditions are associated with an increase in DBP pre-cursors and DBPs (Zamyadi et al., 2012; Zong et al., 2015; Foreman et al., 2021). Disinfectants and chlorine react easily with all types of organic matter, including dissolved and algal organic matter to produce genotoxic and carcinogenic DBPs including trihalomethanes (THMs) and haloacetic acids (HAAs) (Liu et al., 2018). Therefore, conventional water treatment using activated carbon can be useful for removing cyanotoxins, and dissolved and algal organic compounds (Ho et al., 2011; U.S. EPA, 2016; Cermakova et al., 2017).

While activated carbon and rest procedures reduce unwanted contaminants, biofilms can become established in the system and contribute to promoting antibiotic resistance genes (ARGs) (Guo et al., 2018). Specifically, activated carbon filtration has been linked to increasing the abundance of antibiotic resistance bacteria (ARB) and antibiotic resistance genes (ARGs) (Xu et al., 2016, 2020a). Furthermore, recent studies report that cyanobacteria, especially *Microcystis*, harbor significant amounts of ARGs and may play a significant role as a reservoir and source for ARGs in bloom seasons whereby cyanobacterial blooms promote conjugative transfer of ARGs (Wang et al., 2020, 2021). More studies recently reported that cyanobacteria may promote the spread of ARGs in bacteria due to the significant contribution of mobile genetic elements (MGEs) located in genera, such as *Microcystis* (Volk and Lee, 2022). The interest in *Legionella* spp. is heightened in bloom-affected source waters as biofilm-loving *Legionella* spp. including *L. pneumophila* have long been known to grow when cyanobacteria densities are great and biofilm masses exist (Tison et al., 1980; Fliermans et al., 1981; Pope et al., 1982; Declerck, 2010; Cai et al., 2014). Additionally, biofilms can support the growth and persistence of *Legionella* spp. in drinking water systems (Berjeaud et al., 2016) including where activated carbon is used (Li et al., 2017).

While drinking water treatment plants (DWTPs) in bloom-affected areas give necessary and considerable attention to removing cyanotoxins and cyanobacteria during bloom seasons, there are emerging issues not yet studied in the Lake Erie region. We hypothesize that water from heavy bloom areas have (1) higher DBP levels in finished water due to increased interactions between bloom-associated organic matter and chlorine during treatment, (2) higher ARG from using activated carbon to absorb toxins as well as from the higher abundance of *Microcystis* in the source water, and (3) bloom-related aggregated biomass provides a niche for promoting *Legionella* in the lake water and is thus positively associated with *Microcystis* in Lake Erie. In the present study, we investigated two water treatment plants in the Lake Erie region (western Lake Erie for greater bloom frequency and intensity, and central Lake Erie for low bloom frequency and intensity) for 2 years. Specifically, we (1) examined the dynamics of *Microcystis* and MCs in the source water, (2) determined the association between cyanobacteria and *Legionella* in the source water, and (3) monitored both DBPs and ARGs in their finished water. The study outcome provides more holistic understanding about the water quality issues beyond bloom toxicity and cyanotoxin where cyanobacterial blooms are chronically prevalent.

Materials and methods

Study sites and water samples

Two drinking water treatment plants in Ohio, United States, were selected based on annual cyanobacterial bloom intensity. The first was the Collins Park Water Treatment Plant in Toledo, which is a historically high-bloom area in western Lake Erie (Ohio Department Health et al., 2020) and the second was the City of Painesville Water Treatment Plant, a low- or no-bloom area in central Lake Erie (Supplementary Figure S1). Water samples were collected once weekly during the summer and fall (May–November) of 2013 and 2014 from the Toledo and Painesville sites, totaling 58 and 60 samples, respectively. Samples were collected from the source water (sampled at the drinking water intakes within Lake Erie) and from the finished

drinking water at each plant. Collections were done in sterile bottles and shipped in a cooler on ice. For toxin measurements, amber glass vials were used. The samples reached The Ohio State University (Columbus, Ohio, United States) for laboratory analysis within 15 h of sample collection. In the lab, the collected source water (200 mL) was filtered using the polycarbonate membrane (0.45 μm pore size, Millipore, Burlington, MA, United States) for molecular analyses, and filters were kept at −20°C and further analyses were performed as soon as possible.

Water quality parameters

Conventional water quality parameters (water temperature, turbidity, hardness, and pH) and total chlorine in finished water were measured routinely on-site according to the Standard Methods (Rice et al., 2012) by the two water treatment plants and the data were obtained. Chlorophyll-*a* and phycocyanin were measured using the AquaFluor® Handheld fluorometer (Turner Designs, California, United States). Total phosphorus (TP) and soluble reactive phosphorus were measured using the USEPA-accepted Method 8190 (Hach PhosVer 3 with Acid Persulfate Digestion). Total nitrogen (TN) in the higher range (0.23–13.50 mg/L NO_3^--N) and the lower range (0.01–0.5 mg/L NO_3^--N) were analyzed using Method 10206 (Hach dimethylphenol method) and Method 8192, respectively. Total organic carbon (TOC) was analyzed at Alloway Laboratory (Marion, Ohio, United States) using the USEPA 451.3 (U.S. EPA, 2005).

MC measurement

Total MCs in water samples were measured using enzyme-linked immunosorbent assay (ELISA) kits (Abraxis, Warminster, PA, United States) with MC-LR (0.15–5 μg/L) as a working standard. The absorbance was read at 450 nm on the Dynex MRX microplate reader (Dynex Technologies. Inc., Chantilly, VA, United States). The detection range of the assay is 0.15–5.0 ng/mL with a detection limit of 0.10 ng/mL. All the ELISA assays were performed in triplicate.

Disinfection by-products

DBPs (TTHMs and HAA5) in finished water were quantified with gas chromatography–mass spectrometry (GC–MS) using the USEPA-524.2 method.[1] TTHMs included bromoform ($CHBr_3$), chloroform ($CHCl_3$), bromodichloromethane ($CHCl_2Br$), chlorodibromomethane ($CHClBr_2$). HAA5 included monchloroacetic acid ($CH_2ClCOOH$, MCAA), dichloroacetic acid ($CHCl_2COOH$, DCAA), trichloracetic acid (CCl_3COOH, TCAA), monobromoacetic acid ($CH_2BrCOOH$, MBAA) and dibromoacetic acid ($CHBr_2COOH$, DBAA). DBPs were quantified at Alloway Laboratory (Marion, Ohio, United States).

1 https://www.epa.gov/esam/epa-method-5242-measurement-purgeable-organic-compounds-water-capillary-column-gas

Quantification of total and toxic *Microcystis* abundance

We quantified concentrations of total and MC-producing *Microcystis* by targeting the *Microcystis* phycocyanin intergenic spacer (PC-IGS) and microcystin synthetase gene B (*mcyB*), using published approaches with slight modifications (Klase et al., 2019). For *Microcystis* PC-IGS, the PCR mixture (20 μL) in duplicate contained TaqMan universal PCR master mix (10 μL) (Life Technologies, United States), each primer (188F/254R, 300 nM), PC-IGS probe (100 nM), additional $MgCl_2$ (1.25 mM) and DNA template (2 μL). The PCR profile followed an initial cycle of 50°C for 2 min, 95°C for 10 min, 50 cycles at 95°C for 30 s, 56°C for 1 min, and 72°C for 30 s. For *Microcystis mcyB*, the PCR protocol was identical to that for PC-IGS, except we used 900 nM of each *mcyB*-specific-primer (30F/108R) and 250 nm of *mcyB* probe. The standard working curve was generated for each assay according to the standard *Microcystis* PC-IGS and *mcyB* DNA standard (pGEMT-PC-IGS and *mcyB*), respectively. The PC-IGS probe had a 5′ end of the fluorescent reporter, 6FAM, and a 3′ end of the non-fluorescent quencher (NFQ) that was attached with a minor groove binder (MGB) moiety (MGB-NFQ). In contrast, the *mcyB* probe contained a 5′ end of the fluorescent reporter, instead. We estimated the proportion of the potentially MC-producing genotype in the *Microcystis* population according to the ratio between *Microcystis mcyB* and PC-IGS in percentage unit (%).

Droplet digital PCR for total bacteria, ARGs and *Legionella*

We targeted three antibiotic resistance genes (*tetQ* for tetracycline resistance, *sul1* for sulfonamide resistance, and bla_{KPC} for carbapenem resistance), total bacteria (targeting 16S rRNA gene), *Legionella* species (targeting the 5S rRNA gene), as well as a mobile genetic element [MGE, class 1 integron-integrase gene (*intI1*)] (Krøjgaard et al., 2011; Jia et al., 2014; Yin et al., 2017; Gupta et al., 2019; Klase et al., 2019) using the QX200 droplet digital PCR system (ddPCR, Bio-Rad, Hercules, CA, United States). For quantification of total bacteria, *tetQ*, *sul1*, and *intI1*, the ddPCR mixture (20 μL) contained 2X EvaGreen supermix (Bio-Rad), 200 nM of each primer, DNA template, and RNase-/DNase frees PCR water. To quantify KPC and *Legionella*, the ddPCR mixture (20 μL) contained 2X supermix for probes, 200 nM of each primer, 200 nM of the probe, DNA template, and RNase-/DNase free PCR water. With 20 μL of PCR mixture, droplets were generated using the Droplet generator (Bio-Rad) with droplet generation oil. PCR was performed using a thermal cycler (C1000 touch thermal cycler, Bio-Rad, Hercules, CA, United States), following previous studies (Yin et al., 2017; Gupta et al., 2019; Klase et al., 2019). After the PCR reaction, concentrations of targeted genes were analyzed using the Droplet Reader and QuantaSoft software (Bio-Rad Hercules, CA, United States).

Statistical analysis

Data were explored using scatterplots, time-series plots, box plots and bar charts. Means and standard deviations (SD) were calculated

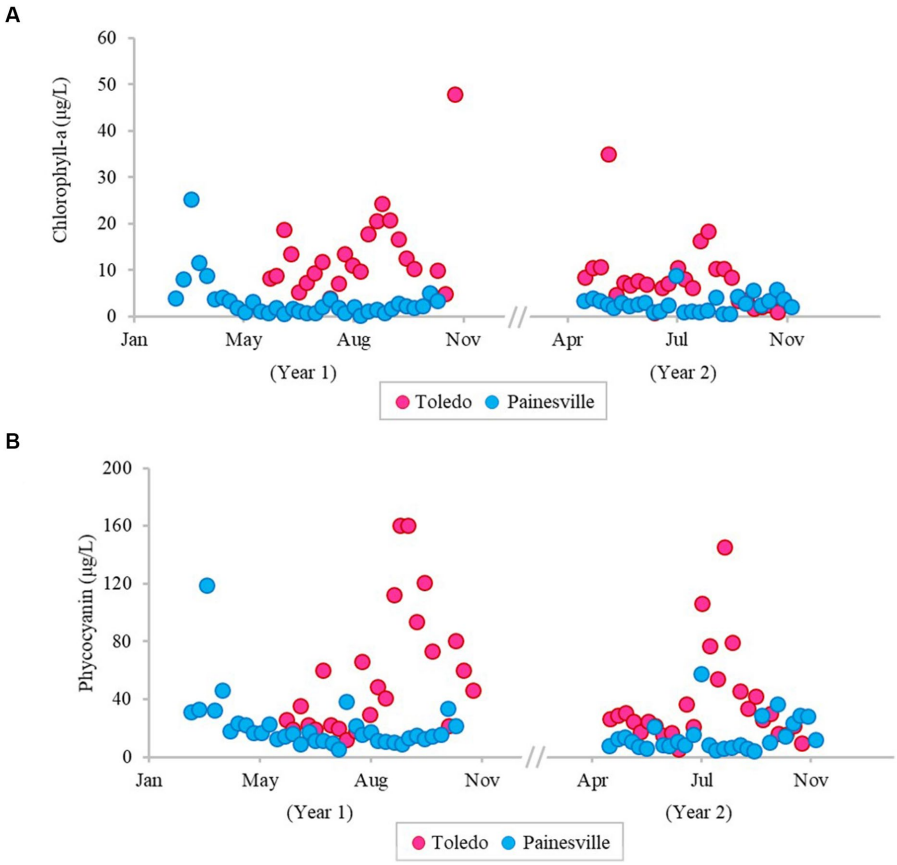

FIGURE 1
Temporal changes of concentration (pg/L) of bloom-related parameters, chlorophyll-a **(A)** and phycocyanin **(B)**, in source water from the bloom site (Toledo) (dark pink) and the control site (Painesville) (blue).

and data are presented as the mean ± SD. A one-way analysis of variance (ANOVA) was used for the spatial difference in the variables with a significance level set at $p < 0.05$. After ANOVA, Tukey Honest Significant Difference tests were used to determine if the means were different ($p < 0.05$) between the groups. All analyses were conducted using SPSS 24.0 (SPSS, Chicago, IL, United States).

Results

Source water

The severity of blooms in the source water from western (Toledo) and central (Painesville) Lake Erie was examined (Figures 1–3) as were source water chemical parameters and water temperatures. The mean concentrations of chlorophyll-*a* and phycocyanin in the source water from western Lake Erie (bloom site) were 8.32 μg/L and 37.4 μg/L, respectively (Figure 1). The mean concentrations of chlorophyll-*a* and phycocyanin in the source water from central Lake Erie (control site) were 2.92 μg/L and 14.8 μg/L, respectively (Figure 1). The mean concentrations of two bloom indicators in the bloom site were significantly higher than that from the control site ($p < 0.05$). Similarly, significantly higher concentrations of total *Microcystis* (PC-IGS gene) and toxin-producing *Microcystis* (*mcy*B gene) were observed in the bloom site source water ($p < 0.05$) (Figure 2). Specifically, the mean concentration of the PC-IGS gene (gene copies/mL) was 5.57×10^4 in Toledo source water (bloom site) vs. 8.79×10^1 in the Painesville source water (control site). The mean concentration of the *mcy*B gene (gene copies/mL) was 1.48×10^4 in the bloom site vs. 1.32×10^1 in the control site. In regard to the cyanotoxin measurement, the mean concentration of microcystin in the bloom site source water was 1.65 μg/L which was also higher than the control site (not detected) (Figure 3). These results show that the intensity and frequency of blooms at the bloom site (Toledo) was obviously higher than the control site (Painesville).

Among water chemistry parameters, concentrations were consistently higher at the bloom sites; whereby mean total phosphorus levels for the two-year study period were 140 μg/L and 90 μg/L for the Toledo and Painesville DWTP source water samples. The mean total organic carbon was 0.36 mg/L (Toledo) and 0.24 mg/L (Painesville) and the mean total nitrate was 0.64 mg/L and 0.33 mg/L in the Toledo and Painesville source water samples, respectively. In addition to chemistry parameters, the mean temperatures of source water samples were 19.6°C and 16.1°C for Toledo and Painesville, respectively.

To evaluate the potential association between cyanobacteria and *Legionella*, the concentrations of *Legionella* were examined in the source water from the western Lake Erie and the control site for 2 years. The concentrations of *Legionella* (gene copies/mL) were 2.49×10^2 (ranging from 5.10×10^0 to 5.09×10^3) in the bloom source water and 1.63×10^2 (ranging from 4.66×10^1 to

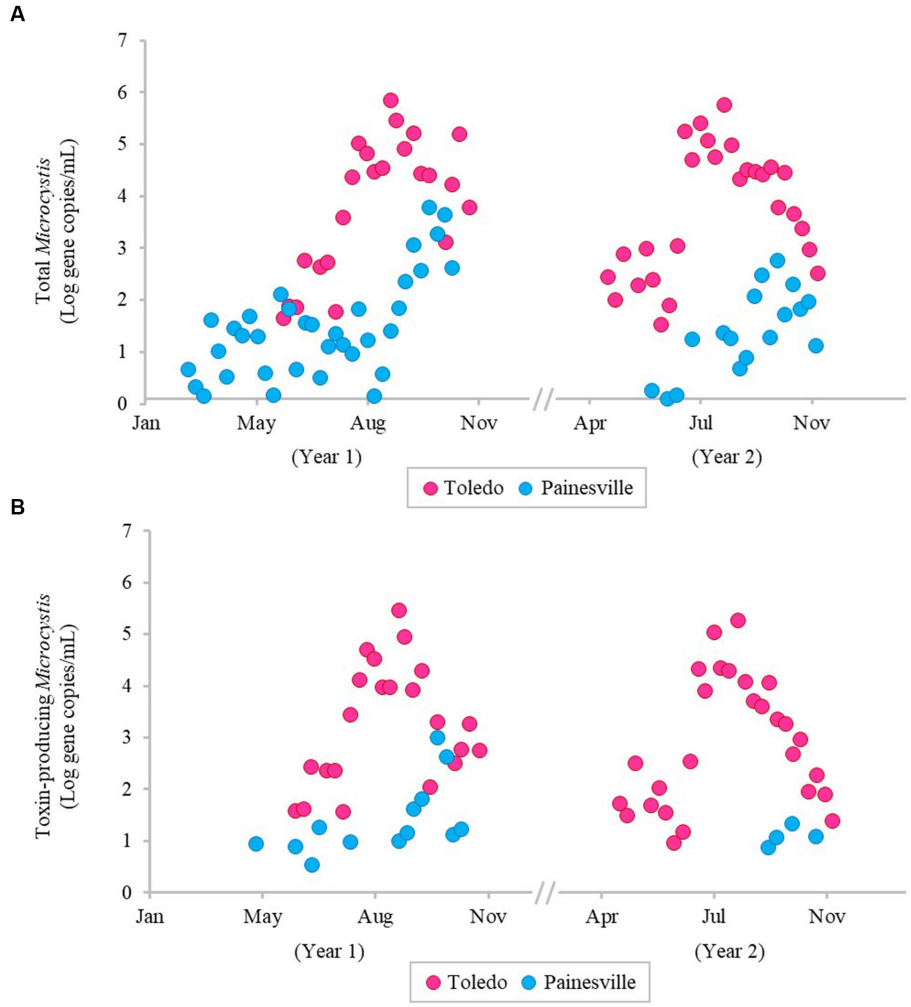

FIGURE 2
Temporal changes of population of total Microcystis **(A)** and toxin-producing Microcystis **(B)** in source water from the bloom site (Toledo) (dark pink) and the control site (Painesville) (blue).

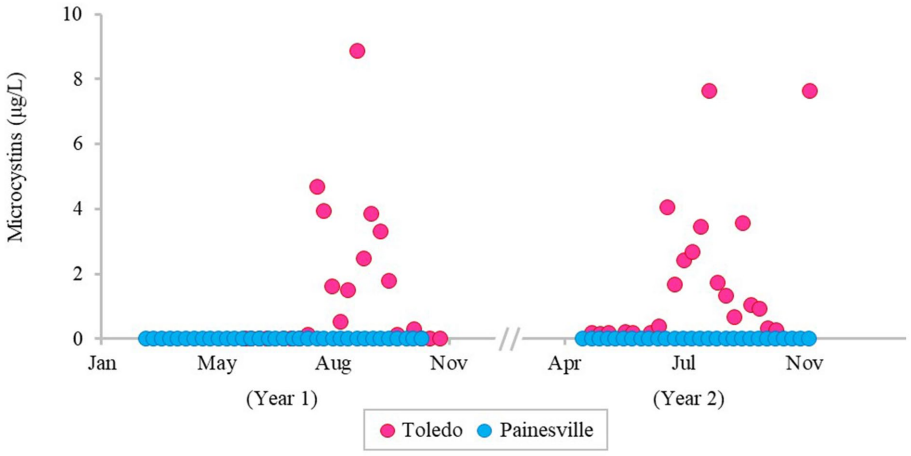

FIGURE 3
Temporal changes of concentration of microcystin in source water from the bloom site (Toledo) (dark pink) and the control site (Painesville) (blue).

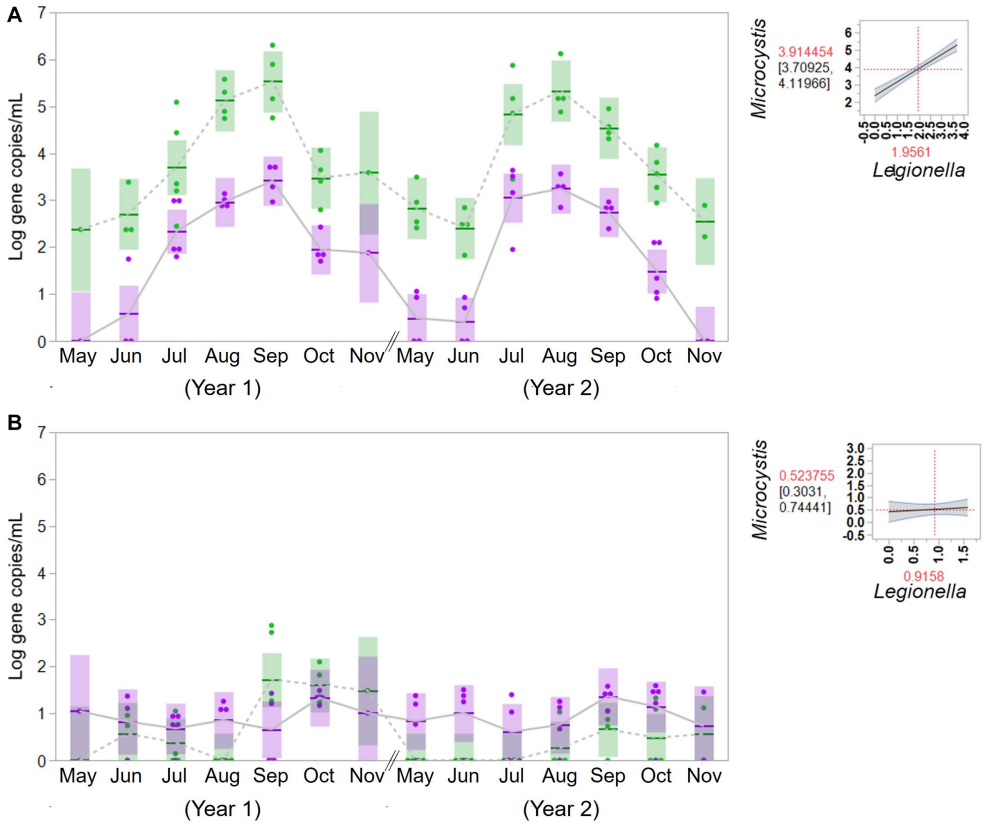

FIGURE 4
Temporal change of concentration of Microcystis (green) and Legionella (purple) in source water from the bloom site (western Lake Erie, Toledo) **(A)** and the control site (central Lake Erie, Painesville) **(B)**. Statistical analysis for relationship between total cyanobacteria and Legionella species in the source water.

3.85×10^2) in the control source water. The associations between cyanobacteria and *Legionella* in the source water are summarized in Figure 4. An apparent significant relationship was observed in western Lake Erie between the concentration of the molecular markers for total cyanobacteria and *Legionella* spp. ($F = 89.82$, $p = 0.001$), but there was no relationship observed between the markers for total cyanobacteria and *Legionella* spp. observed in source water samples from the non-bloom site in Painesville ($F = 0.31$, $p = 0.5814$).

Finished water

The concentrations of DBPs (TTHMs and HAA5) in the finished water from the bloom vs. control sites are summarized in Figure 5. The mean concentrations of TTHMs were 22.43 μg/L from the bloom site and 14.03 μg/L from the control site, and the mean TTHMs concentration from the bloom site was significantly higher than the control site ($p < 0.05$). The mean concentrations of HAA5 were 8.86 μg/L from the bloom site and 9.06 μg/L from the control site, and the mean HAA5 concentrations between the two locations were not significantly different ($p > 0.05$). Figure 6 shows that TOC levels in finished water were not statistically different between the bloom vs. control sites ($p > 0.05$). The mean concentrations of TOC were 1.42 mg/L from the bloom site and 1.72 mg/L from the control site. Furthermore, microcystin was not detected in finished water samples from either location.

Concentrations of ARGs [tetracycline (*tetQ*), sulfonamide (*sul1*), carbapenem (bla_{KPC}) resistance genes] were quantified in source and finished waters. The concentrations of all the ARGs were significantly lower ($p < 0.05$) in the finished water vs. the source water at bloom and control locations (Figure 7). In comparing the mean concentrations (gene copies/100 mL) of ARGs in the finished water, the Toledo finished water mean ARG concentrations were 3.70×10^2 (*tetQ*), 3.26×10^2 (*sul1*), and 1.91×10^2 (bla_{KPC}). The mean concentrations (gene copies/100 mL) of ARGs in the finished water from Painesville WTP were 2.43×10^2 (*tetQ*), 4.31×10^2 (*sul1*), and 4.69×10^2 (bla_{KPC}).

Concentrations of MGE (class 1 integron-integrase gene [*intI1*]) and the total bacteria gene (16S rRNA) were also significantly reduced by drinking water treatment. After water treatment processing, the mean concentrations of the MGE (gene copies/100 mL of *intI1*) in the finished water were 4.19×10^0 in Toledo and 0.82×10^0 in Painesville which represented significant ($p < 0.01$) reductions from their source water (Figure 8). Similarly, concentrations of the total bacterial gene in the finished water of the bloom and control sites (4.56×10^3 in Toledo, 3.55×10^4 in Painesville) were significantly lower ($p < 0.01$) than in their

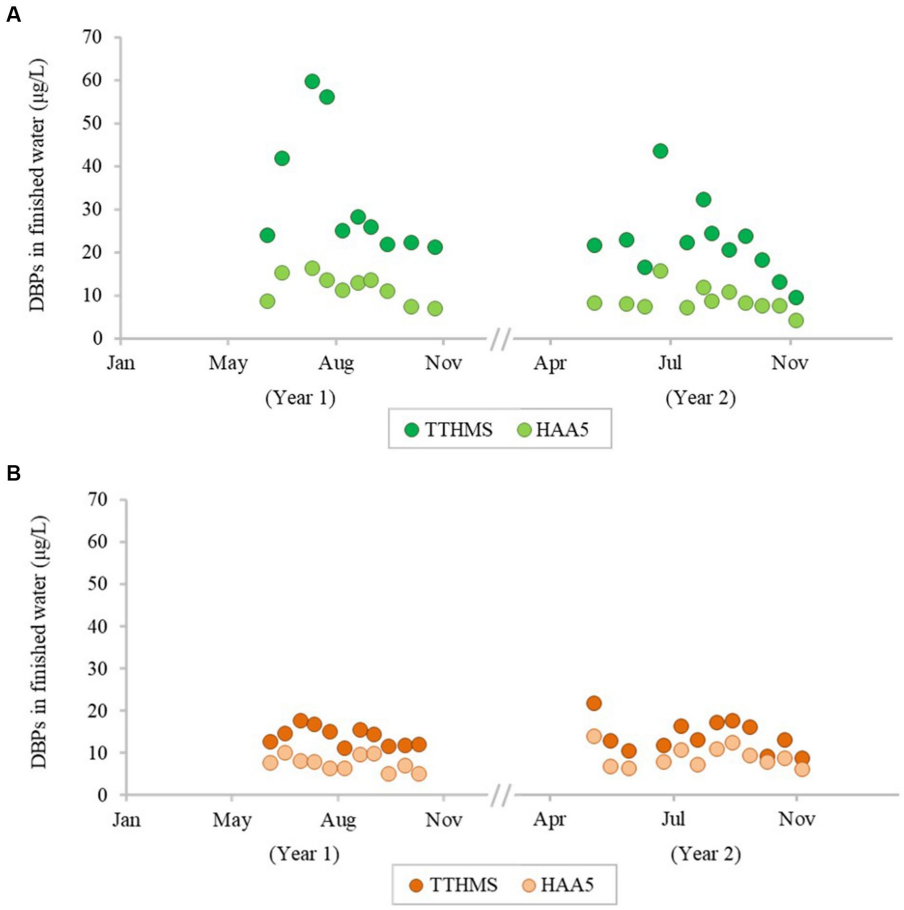

FIGURE 5
Temporal change of concentration of disinfection by-products in finished water from the bloom site **(A)** and the control site **(B)**.

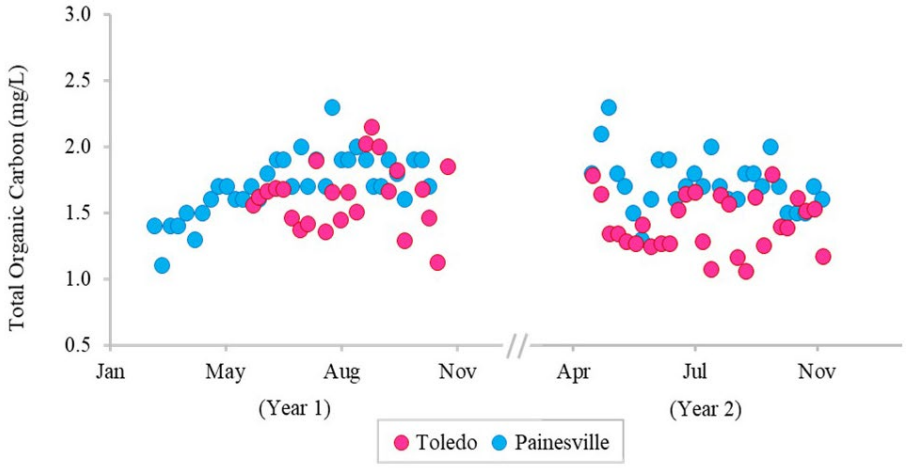

FIGURE 6
Temporal change of concentration of total organic carbon in the finished water of the bloom site (Toledo) (dark pink) and the control site (Painesville) (blue).

source water (6.48×10^8 in Toledo, 9.00×10^9 in Painesville). While drinking water treatment resulted in significantly lower concentrations of total bacteria, ARGs, and MGE, the relative abundance of ARGs among total bacteria (16S rRNA) increased significantly ($p < 0.05$) at both the bloom and control sites (Figure 9).

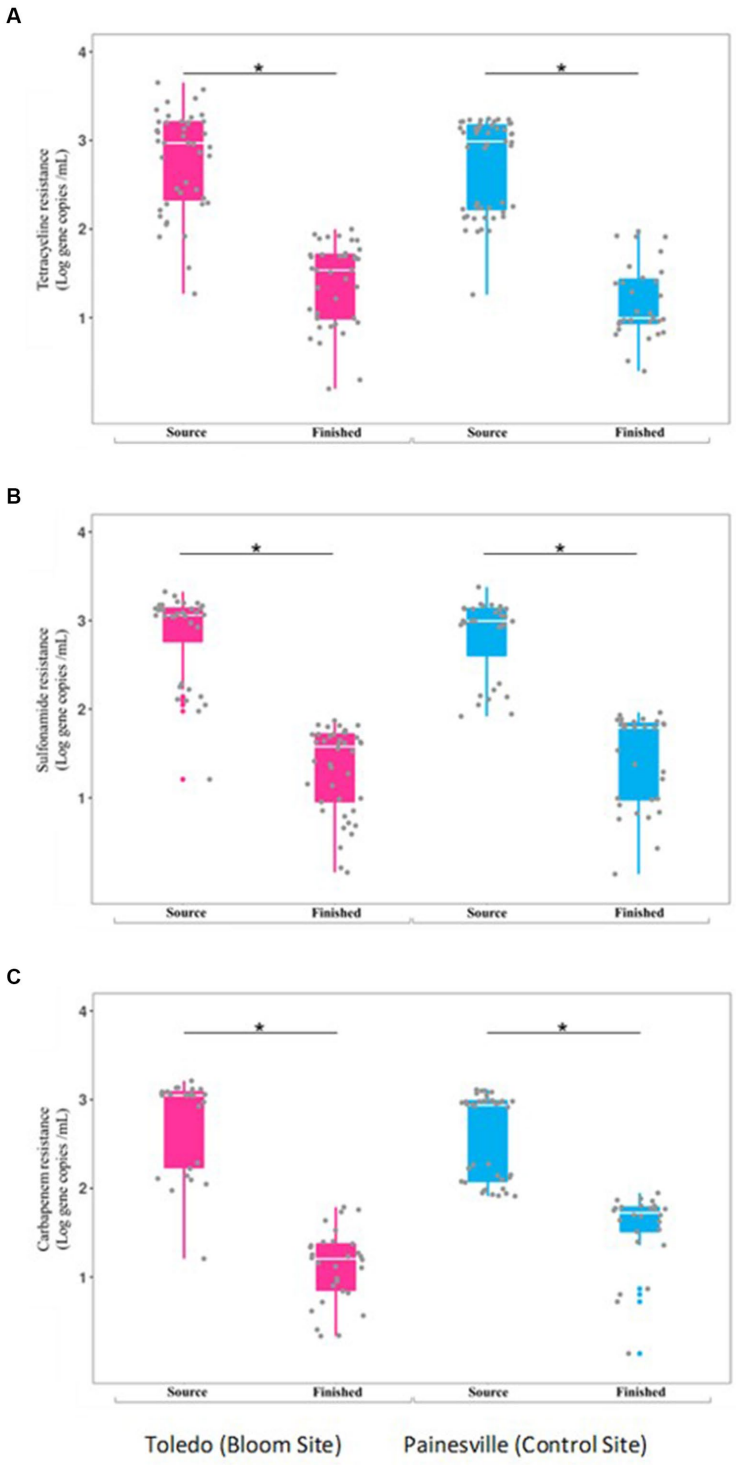

FIGURE 7
Concentrations of antibiotic resistance genes [tetQ **(A)**, sull **(B)**, and blak PC **(C)**] in source and finished waters from the bloom site (Toledo) (dark pink) and the control site (Painesville) (blue). *$p < 0.05$.

Discussion

Bloom conditions at the western Lake Erie site

Two drinking water treatment plants, drawing from Lake Erie as their source water, were chosen in Toledo (a high-bloom region in western Lake Erie) and Painesville (a low- or no-bloom area in central Lake Erie) to examine water quality challenges beyond cyanotoxins when utilizing bloom-impacted source water. In assessing blooms, with an emphasis on cyanobacteria, multiple water quality parameters were employed to evaluate source and finished water quality. Upon characterizing bloom conditions, as expected, there were significant differences in chlorophyll-*a*, phycocyanin, total *Microcystis*,

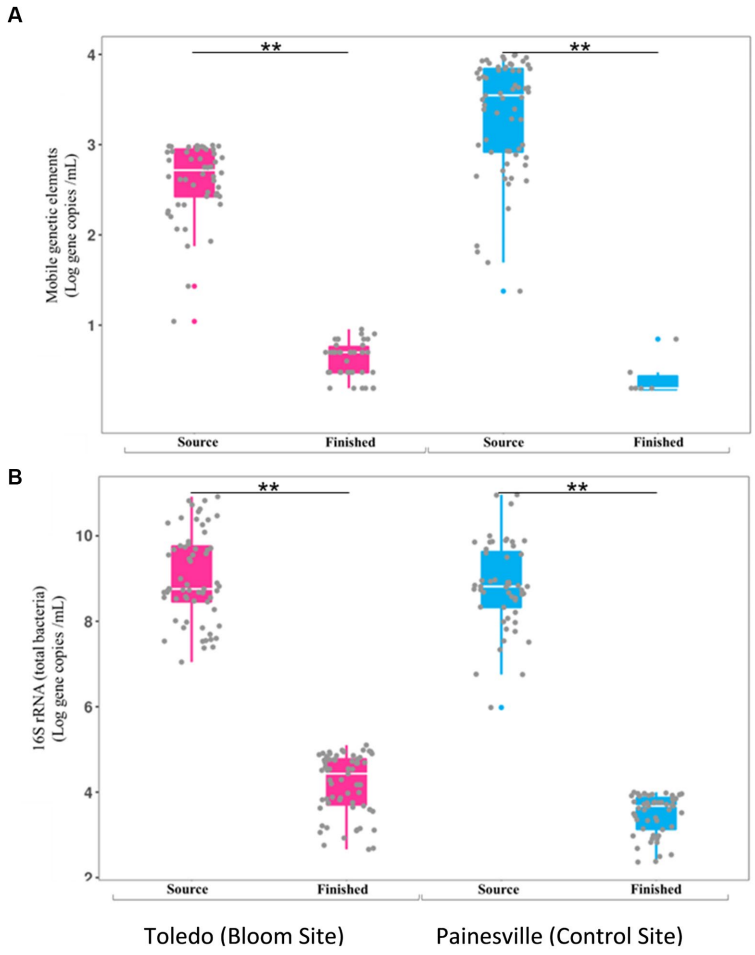

FIGURE 8
Concentrations of mobile genetic elements [MGES **(A)**] and 16S rRNA [total bacteria **(B)**] in source and finished waters from the bloom site (Toledo) (dark pink) and the control site (Painesville) (blue). $^{**}p < 0.01$.

MC-producing *Microcystis*, and MC between the two locations. These differences were supported by the underlying water chemistry and temperatures enabling greater primary productivity by cyanobacteria as warmer water temperatures and higher concentrations of nutrients (P and N) are linked to cyanobacteria bloom formation, particularly when water temperatures approach or exceeds 20°C (Paerl and Huisman, 2008; Stumpf et al., 2012).

As predicted, bloom conditions manifested in source water during the warm months, mainly from July, August and September at the Toledo water intake (bloom site). Figures 1–4 show corroboration between bloom indicators (chlorophyll-*a* and phycocyanin), *Microcystis* densities, and ultimately cyanotoxins. Three of the source water MC results from Toledo exceeded the provisional 2015 Ohio contact recreation advisory threshold (6 μg/L) and one sample exceeded the revised and current (post-2019) Ohio and U.S. EPA contact recreation advisory threshold (8 μg/L standard) (Kasich et al., 2015; U.S. EPA, 2019). Notably, although MC levels were elevated in Toledo's source water, they remained undetectable in finished water samples. Of note, the *Microcystis* concentrations indicated by PC-IGS genetic marker measurement in the source water in Toledo were similar to those in a Japanese Lake Mikata where *Microcystis* blooms occurred (Yoshida et al., 2007).

Elevated DBP formation potential and DBPs from bloom conditions

Once cyanobacterial blooms occur, blooms can impair surface water supplies used for drinking water. Blooms are associated with increases in TOC, turbidity, taste and odor compounds, and precursors for DBP formation (Nguyen et al., 2005). As hypothesized, TOC and turbidity levels were elevated in the bloom site source water relative to the control site (Painesville). Algal-derived organic carbon can be a significant source of DBP precursors for drinking water treatment facilities (Nguyen et al., 2005).

While DBP precursors can be elevated in source water, the presence of DBPs in finished drinking water varies according to the source water characteristics (e.g., temperature, pH, natural organic matter, etc.) and the processes used in water treatment. TOC concentrations are often used to predict DBP formation because TOC is a precursor to DBP formation. In this study, we investigated not only temporal variation in TOC (DBP formation precursor), but also the concentration of two commonly regulated DBPs, TTHMs and HAA5, in drinking water. TTHMs and HAA5, considered potentially carcinogenic, are the most important groups of DBPs (Rodriguez et al., 2004). The primary drinking water regulations for the

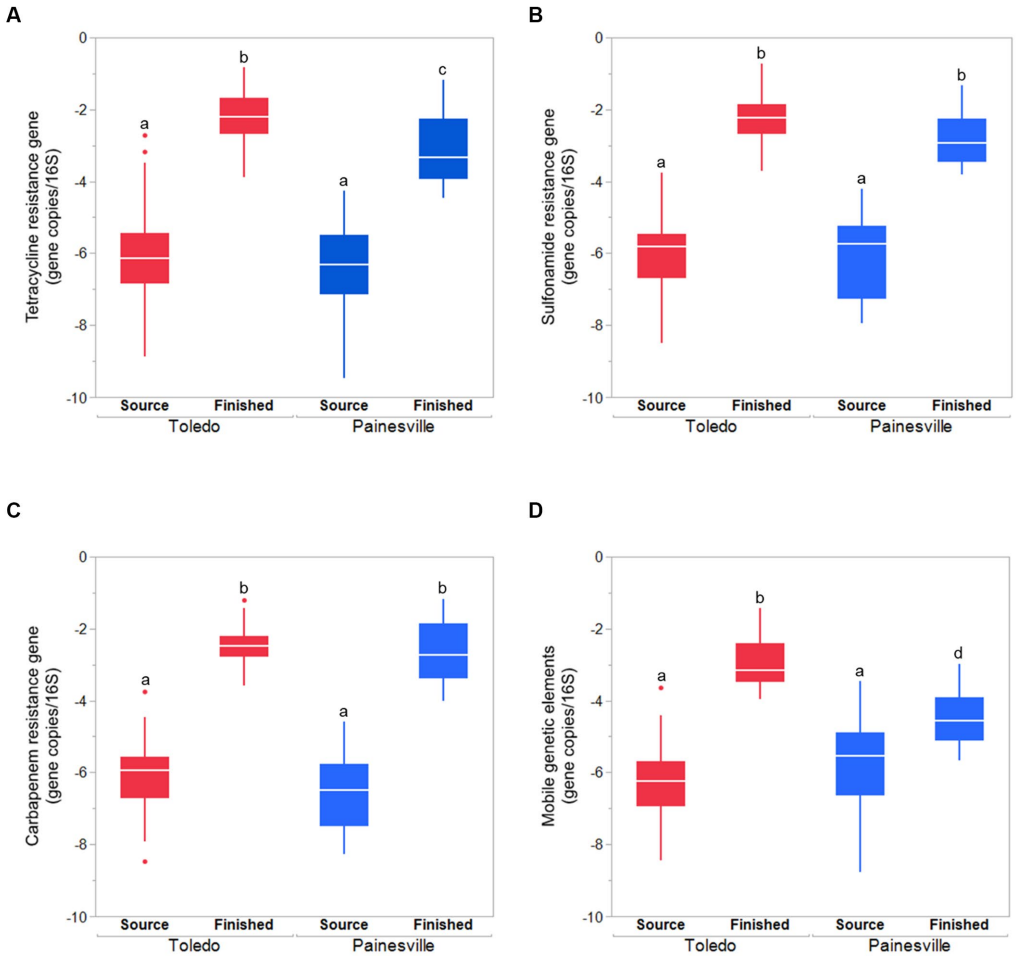

FIGURE 9
The relative abundances (gene copies/16S rRNA gene) of ARGS [tetracycline **(A)**, sulfonamide **(B)**, carbapenem resistance genes **(C)**] and mobile genetic element **(D)** in source water and finished water from the bloom site (Toledo) and the control site (Painesville). [b]Represents a significant difference from "a" ($p < 0.01$). [c]Represents a significant difference from "a" ($p < 0.01$) and from "b" ($p < 0.05$).

U.S. mandates that the maximum acceptable levels of DBPs are 80 µg/L for TTHMs and 60 µg/L for HAA5 (U.S. EPA, 2023). Our results show that TOC concentrations in Toledo source water were higher than Painesville source water, and it is likely that the increase in TOC is related to cyanobacteria densities (Cory et al., 2016). As TOC levels were higher in the source water at Toledo, so were TTHMs and HAA5 in the finished water relative to the Painesville finished water. While DBPs were quantifiable, none of the samples exceeded primary standards set by the U.S. EPA, indicating that the current TOC removal processes at the two DWTPs can effectively control common DBPs.

Relationship between *Legionella* and *Microcystis* in bloom site source water

Beyond altering source and finished water quality, cyanobacteria blooms in western Lake Erie occur in the context of a complex microbial ecosystem and can alter microbial communities.

One type of change was the observed apparent positive relationship between *Legionella* spp. abundance and *Microcystis* in the source water for the Toledo DWTP (bloom site), which was present in both study years, but non-existent in the source water of the Painesville DWTP that served as a control site. Recent research from western Lake Erie (near Toledo [bloom site]) focusing on bacterial diversity from non-cyanobacteria showed clear differential responses among non-cyanobacteria to cyanobacteria abundance (estimated by chlorophyll-*a*) (Berry et al., 2017). Among bacteria that are linked to an increase in abundance during bloom conditions, there is evidence that the density of *Legionella* is correlated with *Microcystis* and eutrophication (Numberger et al., 2022). When looking at similar warm season water samples from three inland Ohio lakes, which like Western Lake Erie exhibit eutrophic conditions, Lee et al. (2016) documented *Legionella* spp. and the Legionellacea as being among the most abundant and ubiquitous bacteria present in Ohio inland lakes.

While *Legionella* species are common in various natural and human-made aquatic environments, some species, mostly *L. pneumophila*, may cause legionellosis, which is a serious pulmonary infection established in persons following the inhalation of particles of contaminated aerosolized water. While there is some evidence that certain cyanobacteria can stimulate the growth of *Legionella* (Świątecki and Zdanowski, 2007; Bergeron et al., 2015), there are few studies primarily focusing on *Legionella* and cyanobacteria densities. Tison

et al. (1980) suggested an intimate association between *Legionella* spp. and cyanobacteria (*Fisherella*). Their observation indicated that *Legionella* could use algal extracellular products as its carbon and energy sources (Tison et al., 1980; Berendt, 1981). A previous study also reported that symbiotic interactions between *Legionella* and cyanobacteria may help the colonization of aquatic environments (Carvalho et al., 2007). Several factors (e.g., temperature, pH, and concentrations of nutrients and ions) and possibly products produced by other non-cyanobacterial bacteria, such as earlier arriving Betaproteobacteriales (van der Kooij et al., 2018), which are also abundant in Lake Erie during blooms (Berry et al., 2017), may all contribute to *Legionella* growth in aquatic environments as part of an ecological succession linked to bloom conditions of certain cyanobacteria species, like *Microcystis*.

While the potential for an ongoing increased global incidence of legionellosis due to a warmer climate has been described (Walker, 2018), the role of environmental waters warrants additional study. In Ohio, the incidence rate of legionellosis has consistently been 1.9 to 2.6 times greater than the U.S. average in recent years (Han, 2021). Recently, aerosols associated with roadway exposures have been considered as part of the increased incidence (Han, 2021), but of particular interest here is how anticipated future increases in eutrophic waters experiencing further eutrophication and warming globally may contribute to increased aerosol-related *Legionella* exposures, which could occur from boat wake (water skiing), fountains, etc. Beyond warmer water, there may be possible synergisms occurring in warming eutrophic waters as high concentrations of phosphates can enable substantial growth of cyanobacteria and increased turbidity and/or aggregated biofilm materials which can prompt or enhance the growth of *Legionella* and other Gammaproteobacteria (Cai et al., 2013; Lee et al., 2016; Srivastava et al., 2016). While the Gammaproteobacteria include many biofilm formers that may benefit from increased turbidity, these bacteria are also associated with an abundance of antibiotic resistance genes (Zhang et al., 2021).

Relative abundance of ARGs increases in finished water from Lake Erie

Adding to the complexity of bloom ecology beyond *Legionella* densities are other broader emergent concerns regarding the establishment, maintenance, or promotion of antibiotic resistance bacteria (ARB) and ARGs in the source water (Volk and Lee, 2022), finished water (Li et al., 2016), and the distribution system (Xi et al., 2009; Xu et al., 2016). When the source water is impacted by bloom conditions, a convergence of numerous selective pressures emerge in the microbial community, including interspecies competition in the source water coupled with impacts from the water treatment processes, such as activated carbon use and disinfection. Xu et al. (2020b) demonstrated that when MCs were present an increase in ARGs was observed in the DWTP.

In this study, while hypothesized there would be differences in the densities of MGEs and ARGs in the source water samples from bloom and control sites, no differences were observed for MGEs or the ARGs for tetracycline, sulfonamide, and carbapenem resistance (Figure 7). At both study locations, the DWTP processes significantly reduced the amount of MGEs and ARGs from source water to finished water. The differences that emerged were specific to relative abundances of ARGs and MGEs. At both DWTPs, while reduced in overall density, the total bacterial density was reduced even more greatly by the treatment processes. In comparison of the two DWTPs, the MGEs increased in relative abundance more in the Toledo DWTP than the Painesville DWTP.

Previous studies have revealed that commonly used disinfection technology can enrich ARB and spread ARGs (Shi et al., 2013). Water processing, including filtration and chlorination, remove most bacteria; however, extracellular stress can promote the replication of plasmids in bacteria. For example, chlorination might increase the copy number of plasmids in the surviving bacteria cells, resulting in the higher relative abundance of ARGs in treated water (Shi et al., 2013). While densities of ARGs and MGE were higher in the source water than the finished water, a limitation of this study was that it did not study the water distribution system, which can have higher levels of bacteria than the finished water due to regrowth potential of bacteria in the distribution system (Xi et al., 2009). If the source water selected for greater survival of biofilm formers preferring higher phosphate levels, corrosion control measures for the distribution system using phosphate may play a role in the regrowth of antibiotic resistant bacteria (Kappell et al., 2019; Kimbell et al., 2020). As expected, the finished water which included corrosion control had higher total P levels than the source water at the bloom site and control site (Supplementary Table S1).

Future research needs

The main scope of the present study was source water and finished water in Lake Erie region, thus tap samples or samples from within the distribution system were not included in this study, but we suggest that future study includes examining the distribution systems of bloom-impacted community water systems since it can contribute great knowledge regarding the public health implications of biofilm formation, ARGs, MGEs, and potential bacterial regrowth. This study adds to the body of evidence that some efforts should be made to monitor ARG concentrations before, during, and after drinking water treatments. As part of monitoring for ARGs and *Legionella*, methods reliant on culturable *Legionella* or other bacteria (e.g., *Pseudomonas* spp., *Mycobacterium* spp.) may provide benefits, but may underreport densities of some bacteria resistant to disinfection when hosted inside free-living Amoeba, which warrants a need to use a PCR-based approach (Calvo et al., 2013).

Complicating future studies on ARGs and MGEs in finished water and distribution systems are not only disinfectants but also disinfection byproducts. While this study illustrated that chlorine-related DBPs (THMs and HAA5) were elevated during bloom conditions, yet meeting regulatory thresholds, we suggest to characterize other DBPs that are likely elevated in cyanobacteria-impacted waters. Since there is considerable evidence that THMs and HAAs are linked to ARGs in the finished water and distribution system (Lv et al., 2014; Li and Gu, 2019; Zhang et al., 2023), we recommend to assess unregulated N-DBPs which likely are less abundant than THMs and HAAs, but are more common in bloom-impacted waters, and able to elicit greater cytotoxicity (Fang et al., 2010; Liu et al., 2020) in a future study. In addition, emerging literature indicates that future studies on DBPs ought to consider a broader range of DBPs for also assessing potential human health risks (Li and Mitch, 2018; Kali et al., 2021). Thus, in bloom-impacted waters there would likely be benefits from assessing N-DBPs which are associated with the chlorination of *Microcystis aeruginosa* (Fang et al., 2010).

These same N-DBPs may also be of interest for improving understanding of antibiotic resistance phenomena in treated waters.

Conclusion

In this study, a compelling and statistically significant correlation emerged between *Legionella* and cyanobacteria within the water of the bloom site. Increasing levels of *Microcystis* were also associated with disinfection byproducts (THMs and HAA5) in the water of the bloom site, but did not exceed primary regulatory standards. At both the bloom site and control site, the DWTPs reduced the density of ARGs and MGEs; however, their relative abundance increased in finished water. This study not only fills existing gaps in the understanding of cyanobacteria and *Legionella* ecology but also underscores several pivotal areas of needed future research for aquatic environments with human exposure potential. Furthermore, our findings indicate a potential health risk of *Legionella*-related disease in proximity to areas impacted by blooms.

Data availability statement

The original contributions presented in the study are included in the article/Supplementary material, further inquiries can be directed to the corresponding author.

Author contributions

JL: conceptualization, funding acquisition, methodology, supervision, and writing-original draft. SL: formal analysis, methodology, visualization, writing—review and editing. CH: formal analysis, methodology, visualization, and writing—review and editing. JM: methodology, writing-review and editing. All authors contributed to the article and approved the submitted version.

Funding

This study was partially funded by US EPA Science to Achieve Results (STAR) grant (RD835192010).

Acknowledgments

The assistance provided by drinking water treatment plants in Toledo and Painesville, Ohio, and their staff members are greatly appreciated. The authors are thankful for Tyler Gorham for his help in processing water samples.

Conflict of interest

The authors declare that the research was conducted in the absence of any commercial or financial relationships that could be construed as a potential conflict of interest.

Publisher's note

All claims expressed in this article are solely those of the authors and do not necessarily represent those of their affiliated organizations, or those of the publisher, the editors and the reviewers. Any product that may be evaluated in this article, or claim that may be made by its manufacturer, is not guaranteed or endorsed by the publisher.

Supplementary material

The Supplementary material for this article can be found online at: https://www.frontiersin.org/articles/10.3389/fmicb.2023.1233327/full#supplementary-material

References

Berendt, R. F. (1981). Influence of blue-green algae (cyanobacteria) on survival of *Legionella pneumophila* in aerosols. *Infect. Immun.* 32, 690–692. doi: 10.1128/iai.32.2.690-692.1981

Bergeron, S., Boopathy, R., Nathaniel, R., Corbin, A., and LaFleur, G. (2015). Presence of antibiotic resistant bacteria and antibiotic resistance genes in raw source water and treated drinking water. *Int. Biodeterior. Biodegrad.* 102, 370–374. doi: 10.1016/j.ibiod.2015.04.017

Berjeaud, J. M., Chevalier, S., Schlusselhuber, M., Portier, E., Loiseau, C., Aucher, W., et al. (2016). *Legionella pneumophila*: the paradox of a highly sensitive opportunistic waterborne pathogen able to persist in the environment. *Front. Microbiol.* 7:486. doi: 10.3389/fmicb.2016.00486

Berry, M. A., Davis, T. W., Cory, R. M., Duhaime, M. B., Johengen, T. H., Kling, G. W., et al. (2017). Cyanobacterial harmful algal blooms are a biological disturbance to Western Lake Erie bacterial communities. *Environ. Microbiol.* 19, 1149–1162. doi: 10.1111/1462-2920.13640

Brooks, B. W., Lazorchak, J. M., Howard, M. D., Johnson, M. V. V., Morton, S. L., Perkins, D. A., et al. (2016). Are harmful algal blooms becoming the greatest inland water quality threat to public health and aquatic ecosystems? *Environ. Toxicol. Chem.* 35, 6–13. doi: 10.1002/etc.3220

Cai, H., Jiang, H., Krumholz, L. R., and Yang, Z. (2014). Bacterial community composition of size-fractioned aggregates within the phycosphere of cyanobacterial blooms in a eutrophic freshwater lake. *PLoS One* 9:e102879. doi: 10.1371/journal.pone.0102879

Cai, H. Y., Yan, Z. S., Wang, A. J., Krumholz, L. R., and Jiang, H. L. (2013). Analysis of the attached microbial community on mucilaginous cyanobacterial aggregates in the eutrophic Lake Taihu reveals the importance of planctomycetes. *Microb. Ecol.* 66, 73–83. doi: 10.1007/s00248-013-0224-1

Calvo, L., Gregorio, I., García, A., Fernández, M. T., Goñi, P., Clavel, A., et al. (2013). A new pentaplex-nested PCR to detect five pathogenic bacteria in free living amoebae. *Wat. Res.* 47, 493–502. doi: 10.1016/j.watres.2012.09.039

Carvalho, F. R., Vazoller, R. F., Foronda, A. S., and Pellizari, V. H. (2007). Phylogenetic study of legionella species in pristine and polluted aquatic samples from a tropical Atlantic forest ecosystem. *Curr. Microbiol.* 55, 288–293. doi: 10.1007/s00284-006-0589-1

Cermakova, L., Kopecka, I., Pivokonsky, M., Pivokonska, L., and Janda, V. (2017). Removal of cyanobacterial amino acids in water treatment by activated carbon adsorption. *Sep. Purif. Technol.* 173, 330–338. doi: 10.1016/j.seppur.2016.09.043

Cheung, M. Y., Liang, S., and Lee, J. (2013). Toxin-producing cyanobacteria in freshwater: a review of their problems, impact on drinking water safety, and efforts for protecting public health. *J. Microbiol.* 51, 1–10. doi: 10.1007/s12275-013-2549-3

Cory, R. M., Davis, T. W., Dick, G. J., Johengen, T., Denef, V. J., Berry, M. A., et al. (2016). Seasonal dynamics in dissolved organic matter, hydrogen peroxide, and cyanobacterial blooms in Lake Erie. *Front. Mar. Sci.* 3:54. doi: 10.3389/fmars.2016.00054

Declerck, P. (2010). Biofilms: the environmental playground of *Legionella pneumophila*. *Environ. Microbiol.* 12, 557–566. doi: 10.1111/j.1462-2920.2009.02025.x

Fang, J., Ma, J., Yang, X., and Shang, C. (2010). Formation of carbonaceous and nitrogenous disinfection by-products from the chlorination of *Microcystis aeruginosa*. *Wat. Res.* 44, 1934–1940. doi: 10.1016/j.watres.2009.11.046

Fliermans, C. B., Cherry, W. B., Orrison, L. H., Smith, S. J., Tison, D. L., and Pope, D. H. (1981). Ecological distribution of *Legionella pneumophila*. *Appl. Environ. Microbiol.* 41, 9–16. doi: 10.1128/aem.41.1.9-16.1981

Foreman, K., Vacs Renwick, D., McCabe, M., Cadwallader, A., Holsinger, H., Kormondy, C., et al. (2021). Effects of harmful algal blooms on regulated disinfection byproducts: findings from five utility case studies. *AWWA Wat. Sci.* 3:e1223. doi: 10.1002/aws2.1223

Glibert, P. M. (2020). Harmful algae at the complex nexus of eutrophication and climate change. *Harmful Algae* 91:101583. doi: 10.1016/j.hal.2019.03.001

Gonsior, M., Powers, L. C., Williams, E., Place, A., Chen, F., Ruf, A., et al. (2019). The chemodiversity of algal dissolved organic matter from lysed *Microcystis aeruginosa* cells and its ability to form disinfection by-products during chlorination. *Wat. Res.* 155, 300–309. doi: 10.1016/j.watres.2019.02.030

Gorham, T., Root, E., Jia, Y., Shum, C. K., and Lee, J. (2020). Relationship between cyanobacterial bloom impacted drinking water sources and hepatocellular carcinoma incidence rates. *Harmful Algae* 95:101801. doi: 10.1016/j.hal.2020.101801

Guo, X. P., Yang, Y., Lu, D. P., Niu, Z. S., Feng, J. N., Chen, Y. R., et al. (2018). Biofilms as a sink for antibiotic resistance genes (ARGs) in the Yangtze estuary. *Wat. Res.* 129, 277–286. doi: 10.1016/j.watres.2017.11.029

Gupta, M., Lee, S., Bisesi, M., and Lee, J. (2019). Indoor microbiome and antibiotic resistance on floor surfaces: an exploratory study in three different building types. *Int. J. Environ. Res. Public Health* 16:4160. doi: 10.3390/ijerph16214160

Han, X. Y. (2021). Effects of climate changes and road exposure on the rapidly rising legionellosis incidence rates in the United States. *Plos one* 16:e0250364. doi: 10.1371/journal.pone.0250364

Ho, L., Lambling, P., Bustamante, H., Duker, P., and Newcombe, G. (2011). Application of powdered activated carbon for the adsorption of cylindrospermopsin and microcystin toxins from drinking water supplies. *Wat. Res.* 45, 2954–2964. doi: 10.1016/j.watres.2011.03.014

Jankowiak, J., Hattenrath-Lehmann, T., Kramer, B. J., Ladds, M., and Gobler, C. J. (2019). Deciphering the effects of nitrogen, phosphorus, and temperature on cyanobacterial bloom intensification, diversity, and toxicity in western Lake Erie. *Limnol. Oceanogr.* 64, 1347–1370. doi: 10.1002/lno.11120

Jia, S., He, X., Bu, Y., Shi, P., Miao, Y., Zhou, H., et al. (2014). Environmental fate of tetracycline resistance genes originating from swine feedlots in river water. *J. Environ. Sci. Health.* 49, 624–631. doi: 10.1080/03601234.2014.911594

Kali, S., Khan, M., Ghaffar, M. S., Rasheed, S., Waseem, A., Iqbal, M. M., et al. (2021). Occurrence, influencing factors, toxicity, regulations, and abatement approaches for disinfection by-products in chlorinated drinking water: a comprehensive review. *Environ. Poll.* 281:116950. doi: 10.1016/j.envpol.2021.116950

Kappell, A. D., Harrison, K. R., and McNamara, P. J. (2019). Effects of zinc orthophosphate on the antibiotic resistant bacterial community of a source water used for drinking water treatment. *Environ. Sci. Water Res. Technol.* 5, 1523–1534. doi: 10.1039/C9EW00374F

Kasich, J. R., Taylor, M., Butler, C. W., Zehringer, J., and Hodges, R. (2015). State of Ohio harmful algal bloom response strategy for recreational waters. Available at: https://www.epa.gov/sites/default/files/2016-12/documents/draft-hh-rec-ambient-water-swimming-document.pdf.

Kimbell, L. K., Wang, Y., and McNamara, P. J. (2020). The impact of metal pipe materials, corrosion products, and corrosion inhibitors on antibiotic resistance in drinking water distribution systems. *Appl. Microbiol. Biotech.* 104, 7673–7688. doi: 10.1007/s00253-020-10777-8

Klase, G., Lee, S., Liang, S., Kim, J., Zo, Y. G., and Lee, J. (2019). The microbiome and antibiotic resistance in integrated fishfarm water: implications of environmental public health. *Sci. Total Environ.* 649, 1491–1501. doi: 10.1016/j.scitotenv.2018.08.288

Krøjgaard, L. H., Krogfelt, K. A., Albrechtsen, H. J., and Uldum, S. A. (2011). Detection of legionella by quantitative-polymerase chain reaction (qPCR) for monitoring and risk assessment. *BMC Microbiol.* 11, 254–257. doi: 10.1186/1471-2180-11-254

Lee, S., Jiang, X., Manubolu, M., Riedl, K., Ludsin, S. A., Martin, J. F., et al. (2017). Fresh produce and their soils accumulate cyanotoxins from irrigation water: implications for public health and food security. *Food Res. Int.* 102, 234–245. doi: 10.1016/j.foodres.2017.09.079

Lee, S., Kim, J., Choi, B., Kim, G., and Lee, J. (2019). Harmful algal blooms and non-alcoholic liver diseases: focusing on the areas near the four major rivers in South Korea. *J. Environ. Sci. Health Part C* 37, 356–370. doi: 10.1080/10590501.2019.1674600

Lee, C. S., Kim, M., Lee, C., Yu, Z., and Lee, J. (2016). The microbiota of recreational freshwaters and the implications for environmental and public health. *Front. Microbiol.* 7:1826. doi: 10.3389/fmicb.2016.01826

Lee, J., Lee, S., and Jiang, X. (2017). Cyanobacterial toxins in freshwater and food: important sources of exposure to humans. *Annu. Re. Food Sci. Technol.* 8, 281–304. doi: 10.1146/annurev-food-030216-030116

Lee, J., Lee, S., Mayta, A., Mrdjen, I., Weghorst, C., and Knobloch, K. (2020). Microcystis toxin-mediated tumor promotion and toxicity Lead to shifts in mouse gut microbiome. *Ecotoxicol. Environ. Saf.* 206:111204. doi: 10.1016/j.ecoenv.2020.111204

Lee, S., Choi, B., Kim, S., Kim, J., Kang, D., and Lee, J. (2022). Relationship Between Freshwater Harmful Algal Blooms and Neurodegenerative Disease Incidence Rates in South Korea. *Environmental Health*. 21, 1–11. doi: 10.1186/s12940-022-00935-y

Li, D., and Gu, A. Z. (2019). Antimicrobial resistance: a new threat from disinfection byproducts and disinfection of drinking water? *Curr. Opin. Environ. Sci. Health* 7, 83–91. doi: 10.1016/j.coesh.2018.12.003

Li, X. F., and Mitch, W. A. (2018). Drinking water disinfection byproducts (DBPs) and human health effects: multidisciplinary challenges and opportunities. *Environ. Sci. Technol.* 52, 1681–1689. doi: 10.1021/acs.est.7b05440

Li, Q., Yu, S., Li, L., Liu, G., Gu, Z., Liu, M., et al. (2017). Microbial communities shaped by treatment processes in a drinking water treatment plant and their contribution and threat to drinking water safety. *Front. Microbiol.* 8:2465. doi: 10.3389/fmicb.2017.02465

Li, D., Zeng, S., He, M., and Gu, A. Z. (2016). Water disinfection byproducts induce antibiotic resistance-role of environmental pollutants in resistance phenomena. *Environ. Sci. Technol.* 50, 3193–3201. doi: 10.1021/acs.est.5b05113

Liu, C., Ersan, M. S., Plewa, M. J., Amy, G., and Karanfil, T. (2018). Formation of regulated and unregulated disinfection byproducts during chlorination of algal organic matter extracted from freshwater and marine algae. *Wat. Res.* 142, 313–324. doi: 10.1016/j.watres.2018.05.051

Liu, C., Ersan, M. S., Wagner, E., Plewa, M. J., Amy, G., and Karanfil, T. (2020). Toxicity of chlorinated algal-impacted waters: formation of disinfection byproducts vs. reduction of cyanotoxins. *Wat. Res.* 184:116145. doi: 10.1016/j.watres.2020.116145

Loftin, K. A., Graham, J. L., Hilborn, E. D., Lehmann, S. C., Meyer, M. T., Dietze, J. E., et al. (2016). Cyanotoxins in inland lakes of the United States: occurrence and potential recreational health risks in the EPA National Lakes Assessment 2007. *Harmful Algae* 56, 77–90. doi: 10.1016/j.hal.2016.04.001

Lv, L., Jiang, T., Zhang, S., and Yu, X. (2014). Exposure to mutagenic disinfection byproducts leads to increase of antibiotic resistance in *Pseudomonas aeruginosa*. *Environ. Sci. Technol.* 48, 8188–8195. doi: 10.1021/es501646n

Mrdjen, I., Fennessy, S., Schaal, A., Dennis, R., Slonczewski, J. L., Lee, S., et al. (2018). Tile drainage and anthropogenic land use contribute to harmful algal blooms and microbiota shifts in inland water bodies. *Environ. Sci. Technol.* 52, 8215–8223. doi: 10.1021/acs.est.8b03269

Nguyen, M. L., Westerhoff, P., Baker, L., Hu, Q., Esparza-Soto, M., and Sommerfeld, M. (2005). Characteristics and reactivity of algae-produced dissolved organic carbon. *J. Environ. Eng.* 131, 1574–1582. doi: 10.1061/(ASCE)0733-9372(2005)131:11(1574)

Numberger, D., Zoccarato, L., Woodhouse, J., Ganzert, L., Sauer, S., Márquez, J. R. G., et al. (2022). Urbanization promotes specific bacteria in freshwater microbiomes including potential pathogens. *Sci. Total Environ.* 845:157321. doi: 10.1016/j.scitotenv.2022.157321

Ohio Department of Health, Ohio Environmental Protection Agency & Ohio Department of Natural Resources. (2020). State of Ohio harmful algal bloom response strategy for recreational waters. Available at: https://epa.ohio.gov/static/Portals/35/hab/HABResponseStrategy.pdf.

Paerl, H. W., and Huisman, J. (2008). Blooms like it hot. *Science* 320, 57–58. doi: 10.1126/science.1155398

Pope, D. H., Soracco, R. J., Gill, H. K., and Fliermans, C. B. (1982). Growth of *Legionella pneumophila* in two-membered cultures with green algae and cyanobacteria. *Curr. Microbiol.* 7, 319–321. doi: 10.1007/BF01566871

Rice, E. W., and Bridgewater, L.American Public Health Association (Eds) (2012). *Standard methods for the examination of water and wastewater (vol. 10)*. Washington, DC: American Public Health Association.

Rodriguez, M. J., Sérodes, J. B., and Levallois, P. (2004). Behavior of trihalomethanes and haloacetic acids in a drinking water distribution system. *Wat. Res.* 38, 4367–4382. doi: 10.1016/j.watres.2004.08.018

Shi, P., Jia, S., Zhang, X. X., Zhang, T., Cheng, S., and Li, A. (2013). Metagenomic insights into chlorination effects on microbial antibiotic resistance in drinking water. *Wat. Res.* 47, 111–120. doi: 10.1016/j.watres.2012.09.046

Srivastava, A., Ko, S. R., Ahn, C. Y., Oh, H. M., Ravi, A. K., and Asthana, R. K. (2016). Microcystin biosynthesis and mcyA expression in geographically distinct Microcystis strains under different nitrogen, phosphorus, and boron regimes. *Biomed. Res. Int.* 2016:5985987. doi: 10.1155/2016/5985987

Stumpf, R. P., Johnson, L. T., Wynne, T. T., and Baker, D. B. (2016). Forecasting annual cyanobacterial bloom biomass to inform management decisions in Lake Erie. *J. Gt. Lakes Res.* 42, 1174–1183. doi: 10.1016/j.jglr.2016.08.006

Stumpf, R. P., Wynne, T. T., Baker, D. B., and Fahnenstiel, G. L. (2012). Interannual variability of cyanobacterial blooms in Lake Erie. *PLoS One* 7:e42444. doi: 10.1371/journal.pone.0042444

Świątecki, A., and Zdanowski, B. (2007). The seasonal dynamics of organic matter remineralization by bacterial consortia in the heated Konin lakes. *Fish. Aquatic Life* 15, 309–320.

Tison, D. L., Pope, D. H., Cherry, W. B., and Fliermans, C. B. (1980). Growth of *Legionella pneumophila* in association with blue-green algae (cyanobacteria). *Appl. Environ. Microbiol.* 39, 456–459. doi: 10.1128/aem.39.2.456-459.1980

U.S. EPA (2005). Method 415.3 - measurement of total organic carbon, dissolved organic carbon and specific UV absorbance at 254nm in source water and drinking water. Available at: https://cfpub.epa.gov/si/si_public_record_report.cfm?Lab=NERL&dirEntryId=103917.

U.S. EPA (2016). Water treatment optimization for cyanotoxins. Available at: https://www.epa.gov/ground-water-and-drinkingwater/water-treatment-optimization-cyanotoxins-document.

U.S. EPA (2019). Recommended human health recreational ambient water quality criteria or swimming advisories for microcystins and cylindrospermopsin. Available at: https://www.epa.gov/sites/default/files/2019-05/documents/hh-rec-criteria-habs-document-2019.pdf.

U.S. EPA (2023). National primary drinking water regulations. Available at: https://www.epa.gov/ground-water-and-drinking-water/national-primary-drinking-water-regulations.

van der Kooij, D., Veenendaal, H. R., Italiaander, R., van der Mark, E. J., and Dignum, M. (2018). Primary colonizing Betaproteobacteriales play a key role in the growth of *Legionella pneumophila* in biofilms on surfaces exposed to drinking water treated by slow sand filtration. *Appl. Environ. Microbiol.* 84, e01732–e01718. doi: 10.1128/AEM.01732-18

Volk, A., Lee, J. (2022). Cyanobacterial blooms: A player in the freshwater environmental resistome with public health relevance?. *Environmental Research* 114612. doi: 10.1016/j.envres.2022.114612

Walker, J. T. (2018). The influence of climate change on waterborne disease and legionella: a review. *Perspect. Public Health* 138, 282–286. doi: 10.1177/1757913918791198

Wang, Z., Chen, Q., Zhang, J., Guan, T., Chen, Y., and Shi, W. (2020). Critical roles of cyanobacteria as reservoir and source for antibiotic resistance genes. *Environ. Int.* 144:106034. doi: 10.1016/j.envint.2020.106034

Wang, Z., Chen, Q., Zhang, J., Yan, H., Chen, Y., Chen, C., et al. (2021). High prevalence of unstable antibiotic heteroresistance in cyanobacteria causes resistance underestimation. *Wat. Res.* 202:117430. doi: 10.1016/j.watres.2021.117430

Xi, C., Zhang, Y., Marrs, C. F., Ye, W., Simon, C., Foxman, B., et al. (2009). Prevalence of antibiotic resistance in drinking water treatment and distribution systems. *Appl. Environ. Microbiol.* 75, 5714–5718. doi: 10.1128/AEM.00382-09

Xu, L., Campos, L. C., Canales, M., and Ciric, L. (2020a). Drinking water biofiltration: behaviour of antibiotic resistance genes and the association with bacterial community. *Wat. Res.* 182:115954. doi: 10.1016/j.watres.2020.115954

Xu, L., Ouyang, W., Qian, Y., Su, C., Su, J., and Chen, H. (2016). High-throughput profiling of antibiotic resistance genes in drinking water treatment plants and distribution systems. *Environ. Poll.* 213, 119–126. doi: 10.1016/j.envpol.2016.02.013

Xu, L., Zhou, Z., Zhu, L., Han, Y., Lin, Z., Feng, W., et al. (2020b). Antibiotic resistance genes and microcystins in a drinking water treatment plant. *Environ. Pollut. B.* 258:113718. doi: 10.1016/j.envpol.2019.113718

Yin, Y., Gu, J., Wang, X., Song, W., Zhang, K., Sun, W., et al. (2017). Effects of copper addition on copper resistance, antibiotic resistance genes, and intl1 during swine manure composting. *Front. Microbiol.* 8:344. doi: 10.3389/fmicb.2017.00344

Yoshida, M. T., Yoshida, T., Takashima, Y., Hosoda, N., and Hiroishi, S. (2007). Dynamics of microcystin-producing and non-microcystin-producing Microcystis populations is correlated with nitrate concentration in a Japanese Lake. *FEMS Microbiol. Lett.* 266, 49–53. doi: 10.1111/j.1574-6968.2006.00496.x

Zamyadi, A., Ho, L., Newcombe, G., Bustamante, H., and Prévost, M. (2012). Fate of toxic cyanobacterial cells and disinfection by-products formation after chlorination. *Wat. Res.* 46, 1524–1535. doi: 10.1016/j.watres.2011.06.029

Zhang, F., Hu, C., Shum, C. K., Liang, S., and Lee, J. (2017). Satellite remote sensing of drinking water intakes in Lake Erie for cyanobacteria population using two MODIS-based indicators as a potential tool for toxin tracking. *Front. Mar. Sci.* 4:124. doi: 10.3389/fmars.2017.00124

Zhang, F., Lee, J., Liang, S., and Shum, C. K. (2015). Cyanobacteria blooms and non-alcoholic liver disease: evidence from a county level ecological study in the United States. *Environ. Health* 14:41. doi: 10.1186/s12940-015-0026-7

Zhang, M., Zhang, L., Lin, K., Wang, Y., Xu, S., Bai, M., et al. (2023). Influence of chlorinated disinfection by-products on transmission of antibiotic resistance genes in biofilms and water of a simulated drinking water distribution system. *Environ. Eng. Res.* 28:210617. doi: 10.4491/eer.2021.617

Zhang, Q., Zhang, Z., Lu, T., Yu, Y., Penuelas, J., Zhu, Y. G., et al. (2021). Gammaproteobacteria, a core taxon in the guts of soil fauna, are potential responders to environmental concentrations of soil pollutants. *Microbiome* 9, 1–17. doi: 10.1186/s40168-021-01150-6

Zong, W., Sun, F., Pei, H., Hu, W., and Pei, R. (2015). Microcystin-associated disinfection by-products: the real and non-negligible risk to drinking water subject to chlorination. *Chem. Eng. J.* 279, 498–506. doi: 10.1016/j.cej.2015.05.048

frontiers | Frontiers in Microbiology

TYPE Original Research
PUBLISHED 30 August 2023
DOI 10.3389/fmicb.2023.1219261

OPEN ACCESS

EDITED BY
Petra M. Visser,
University of Amsterdam, Netherlands

REVIEWED BY
Nico Salmaso,
Fondazione Edmund Mach, Italy
Iwona Dorota Jasser,
University of Warsaw, Poland

*CORRESPONDENCE
H. Dail Laughinghouse
✉ hlaughinghouse@ufl.edu

RECEIVED 08 May 2023
ACCEPTED 14 August 2023
PUBLISHED 30 August 2023

CITATION
Lefler FW, Barbosa M, Zimba PV, Smyth AR, Berthold DE and Laughinghouse HD (2023) Spatiotemporal diversity and community structure of cyanobacteria and associated bacteria in the large shallow subtropical Lake Okeechobee (Florida, United States). *Front. Microbiol.* 14:1219261. doi: 10.3389/fmicb.2023.1219261

Spatiotemporal diversity and community structure of cyanobacteria and associated bacteria in the large shallow subtropical Lake Okeechobee (Florida, United States)

Forrest W. Lefler[1], Maximiliano Barbosa[1], Paul V. Zimba[2], Ashley R. Smyth[3], David E. Berthold[1] and H. Dail Laughinghouse[1]*

[1]Agronomy Department, Fort Lauderdale Research and Education Center, University of Florida—IFAS, Davie, FL, United States, [2]Rice Rivers Center, Virginia Commonwealth University, Charles City, VA, United States, [3]Soil, Water and Ecosystem Sciences Department, Tropical Research and Education Center, University of Florida—IFAS, Homestead, FL, United States

Lake Okeechobee is a large eutrophic, shallow, subtropical lake in south Florida, United States. Due to decades of nutrient loading and phosphorus rich sediments, the lake is eutrophic and frequently experiences cyanobacterial harmful algal blooms (cyanoHABs). In the past, surveys of the phytoplankton community structure in the lake have been conducted by morphological studies, whereas molecular based studies have been seldom employed. With increased frequency of cyanoHABs in Lake Okeechobee (e.g., 2016 and 2018 *Microcystis*-dominated blooms), it is imperative to determine the diversity of cyanobacterial taxa that exist within the lake and the limnological parameters that drive bloom-forming genera. A spatiotemporal study of the lake was conducted over the course of 1 year to characterize the (cyano)bacterial community structure, using 16S rRNA metabarcoding, with coincident collection of limnological parameters (e.g., nutrients, water temperature, major ions), and cyanotoxins. The objectives of this study were to elucidate spatiotemporal trends of community structure, identify drivers of community structure, and examine cyanobacteria-bacterial relationships within the lake. Results indicated that cyanobacterial communities within the lake were significantly different between the wet and dry season, but not between periods of nitrogen limitation and co-nutrient limitation. Throughout the year, the lake was primarily dominated by the picocyanobacterium *Cyanobium*. The bloom-forming genera *Cuspidothrix*, *Dolichospermum*, *Microcystis*, and *Raphidiopsis* were highly abundant throughout the lake and had disparate nutrient requirements and niches within the lake. Anatoxin-a, microcystins, and nodularins were detected throughout the lake across both seasons. There were no correlated (cyano)bacteria shared between the common bloom-forming cyanobacteria *Dolichospermum*, *Microcystis*, and *Raphidiopsis*. This study is the first of its kind to use molecular based methods to assess the cyanobacterial community structure within the lake. These data greatly improve our understanding of the cyanobacterial community structure within the lake and the physiochemical parameters which may drive the bloom-forming taxa within Lake Okeechobee.

KEYWORDS

harmful algal blooms, *Microcystis*, *Dolichospermum*, eutrophication, picocyanobacteria, metabarcoding, microbiome

1. Introduction

Shallow lakes are sensitive to anthropogenic influences (Scheffer, 2004) and cyanobacteria can often dominate the phytoplankton community of eutrophic shallow lakes, especially in warm climates (Reynolds, 1987; Bonilla et al., 2023). Lake Okeechobee is a large shallow subtropical lake in peninsular Florida (United States), that has been undergoing anthropogenic induced eutrophication since the 1970's (Canfield et al., 2021). The accumulation of nutrients has resulted in an increase in cyanobacterial dominance of the phytoplankton community leading to cyanobacterial harmful algal blooms (cyanoHABs). Lake Okeechobee has a humid subtropical climate and experiences wet (May through November) and dry (November through May) seasons. The lake has a mean depth of ~2.7 m (Havens et al., 1994) and a large drainage basin (12,000 km^2), which begins in Orlando running through the Kissimmee Chain of Lakes via the Kissimmee River, flowing south before emptying into the northern region of the lake. This inflow accounts for the majority of the input, with lesser inputs from Lake Istokpoga and Fisheating Creek (Zhang Y. et al., 2020; Canfield et al., 2021). Lake outflow is controlled by the United States Army Corps of Engineers through three main tributaries: south through the Everglades Agricultural Area and ultimately into Florida Bay, west through the Caloosahatchee River into the Gulf of Mexico, and east via the St. Lucie Canal into the St. Lucie Estuary. Land use in the drainage basin is predominantly agricultural (~46%), but urban and suburban areas also exist contributing to the increased nutrient inputs into the lake (Zhang et al., 2011).

Prior to 1974, records show that the phytoplankton community of Lake Okeechobee consisted of <30% cyanobacteria (Marshall, 1977); however, by the 1980's, the community structure had shifted to a cyanobacteria dominated community (>60%) due to increased eutrophication (Cichra et al., 1995; Havens et al., 1998). This shift to a cyanobacterial dominated community corresponded with an increase in cyanoHABs within Lake Okeechobee. In the past (1970's–1980's), cyanoHABs were dominated by diazotrophic cyanobacteria (i.e., *Aphanizomenon*, *Dolichospermum*, *Raphidiopsis*; Joyner, 1974; Marshall, 1977; Jones, 1987), whereas current blooms are often dominated by the non-diazotrophic species *Microcystis aeruginosa* (Kützing) Kützing; although *M. aeruginosa* blooms have been reported as early as 1973 (Davis and Marshall, 1975). Despite this, *Dolichospermum* and *Raphidiopsis* dominated blooms still occur within the lake, though blooms composed of these genera are less frequent and intense than those composed of *Microcystis*. These three notorious genera are known to form cyanoHABs globally and have disparate nutrient requirements where *Dolichospermum* is known to proliferate in low nitrogen conditions, whereas *Microcystis* prefers high nitrogen, low phosphorus concentrations (Werner and Laughinghouse, 2009; Li and Li, 2012; Chia et al., 2018; Werner et al., 2020). These bloom-forming genera can also produce several cyanotoxins (e.g., anatoxins, cylindrospermopsins, microcystins), resulting in deleterious effects to aquatic systems and human health (O'Neil et al., 2012; Huang and Zimba, 2019).

Environmental drivers of cyanoHABs and bloom-forming genera have been studied in detail (e.g., O'Neil et al., 2012; Paerl et al., 2016). Much of the historical focus was on the role of phosphorus (P) on cyanobacteria productivity, known as the P-only paradigm, although there was a recent shift to focus on the role of both nitrogen (N) and P in bloom proliferation (Paerl et al., 2016). External nutrient loading into Lake Okeechobee, primarily as P, has decreased water quality and total phosphorus (TP) concentrations have nearly doubled since the 1970's, while total nitrogen (TN) concentrations have remained relatively stable (James and Pollman, 2011). Additionally, much of the P in the lake is legacy phosphorus bound to sediment which, when resuspended, can further increase P concentrations (i.e., internal loading; Moore et al., 1998; Fisher et al., 2005). Because of this increased P loading, primary productivity within Lake Okeechobee has been considered N-limited (Havens, 1995; Havens et al., 2003; Kramer et al., 2018), and periods of increased N loading into the lake have increased cyanoHABs (Havens et al., 2016; Lapointe et al., 2017; Kramer et al., 2018).

In fresh waters, the bacterioplankton community (including cyanobacteria) play critical roles in biogeochemical cycles (e.g., carbon, N, P; Falkowski et al., 2008). Bacteria can form symbiotic relationships with cyanobacteria, either as epibionts on colonies, known as the phycosphere (Bell and Mitchell, 1972) or as co-existing, free living, taxa (Morris et al., 2011). The associated bacteria are capable of filling in missing genomic functions (e.g., vitamin synthesis, nitrogen cycling; Morris et al., 2011; Garcia et al., 2015) and form mutualistic relationships with cyanobacteria (Cook et al., 2020). Thus, associated bacteria have the potential to increase the fitness of cyanobacteria, such as intensifying their growth rate (Jackrel et al., 2021). Despite their close relationships, the role of bacteria in cyanoHABs and relationships with bloom-forming cyanobacteria are often overlooked (Pound et al., 2021). Furthermore, the majority of the focus on bacterial-cyanobacterial interactions have centered on the phycosphere (i.e., epibionts or particle-associated) bacteria, with less focus on the bacterioplankton (i.e., free-living; Louati et al., 2023).

High-throughput sequencing (HTS) facilitates insights into microbial community via sequencing taxonomically informative regions (i.e., metabarcoding), such as the 16S rRNA, or whole genome sequencing (metagenomics). Metabarcoding is used extensively for bacterial communities, including the characterization of the cyanobacterial community (e.g., Pessi et al., 2016; Huang et al., 2020; Khomutovska et al., 2020) as these methods provide valuable information on the cyanobacterial community structure and provide increased taxonomic resolution compared to traditional morphological evaluations alone (MacKeigan et al., 2022).

Extensive research has investigated the global/general drivers of cyanoHABs, with much of the focus on *Microcystis* and *Dolichospermum* and intergeneric competition (e.g., O'Neil et al., 2012; Paerl and Otten, 2013; Paerl and Otten, 2016; Almanza et al., 2019; Shan et al., 2019). Within Lake Okeechobee, previous research has studied how various limnological parameters affect shifts within the cyanobacterial community (Havens et al., 1998; Ma et al., 2022), the diversity of phytoplankton including bloom forming genera (Cichra et al., 1995; Ma et al., 2022), and the drivers of increased algal abundance (as chlorophyll; Havens et al., 1994; Xu et al., 2022); However, the specific drivers of bloom forming cyanobacterial genera within Lake Okeechobee remain unexplored. Considering the dominance of cyanobacteria within Lake Okeechobee and the increased frequency and intensity of cyanoHABs (e.g., 2016 and 2018 *Microcystis* blooms), it is imperative to characterize the cyanobacterial community to identify spatial and temporal trends of common bloom-forming genera, specifically *Dolichospermum*, *Microcystis* and

Raphidiopsis, and elucidate their respective environmental drivers within this system.

Over the course of 1 year, six sites within Lake Okeechobee were sampled for 16S rRNA metabarcoding analysis and limnological parameters to characterize the cyanobacterial and associated bacterial community. Our objectives were to (1) characterize (temporally and spatially) the cyanobacterial community structure within Lake Okeechobee, (2) elucidate the limnological parameters that potentially drive cyanobacterial abundance, and (3) examine cyanobacterial-bacterial relationships. To our knowledge, a spatiotemporal assessment using molecular methods has yet to be conducted on Lake Okeechobee and this study is the first of its kind.

2. Materials and methods

2.1. Study area and limnological parameters

Sampling on Lake Okeechobee occurred 10 times over the course of 1 year (August 2019–September 2020) at approximately five-week intervals at six locations within the lake, Figure 1. Surface water samples (<0.5 m depth) were collected using acid washed and sterile 1 L Nalgene bottles for environmental DNA extractions and stored on ice until processing. Additional water samples were collected for nutrient analyses (i.e., nitrate, nitrite, ammonium, orthophosphate, and total reactive phosphorus) and major ion analysis (i.e., boron, copper, calcium, potassium, sodium, iron, cobalt, magnesium, manganese, aluminum, and zinc). For orthophosphate and major ion analysis, samples were filtered through a 0.45 µm glass filter (MilliporeSigma, Burlington, MA, United States) in the field and the latter acidified with nitric acid. All samples were kept on ice until processing. Water quality measurements (i.e., dissolved oxygen, water temperature, pH, salinity, conductivity, turbidity, chlorophyll-*a* abundance, and phycocyanin abundance) were gathered using a YSI EXO3 (Xylem Inc., OH, United States) multiparameter sonde on site. Secchi depth was measured using a Secchi disk and used to estimate water transparency and to calculate photic depth (Zeu). Samples for cyanotoxin analysis were collected in 250 mL HDPE amber bottles. A total of 57 samples were collected during this study.

Immediately upon arrival in the laboratory, water samples for eDNA were filtered through 0.7 µm Whatman glass filters (GF/F MilliporeSigma, Burlington, MA, United States) until clogging and stored at −80°C. Water samples for nutrient composition analysis were frozen and stored, except orthophosphate, which was kept at 4°C until processing. Total reactive phosphorus (TRP; i.e., unfiltered),

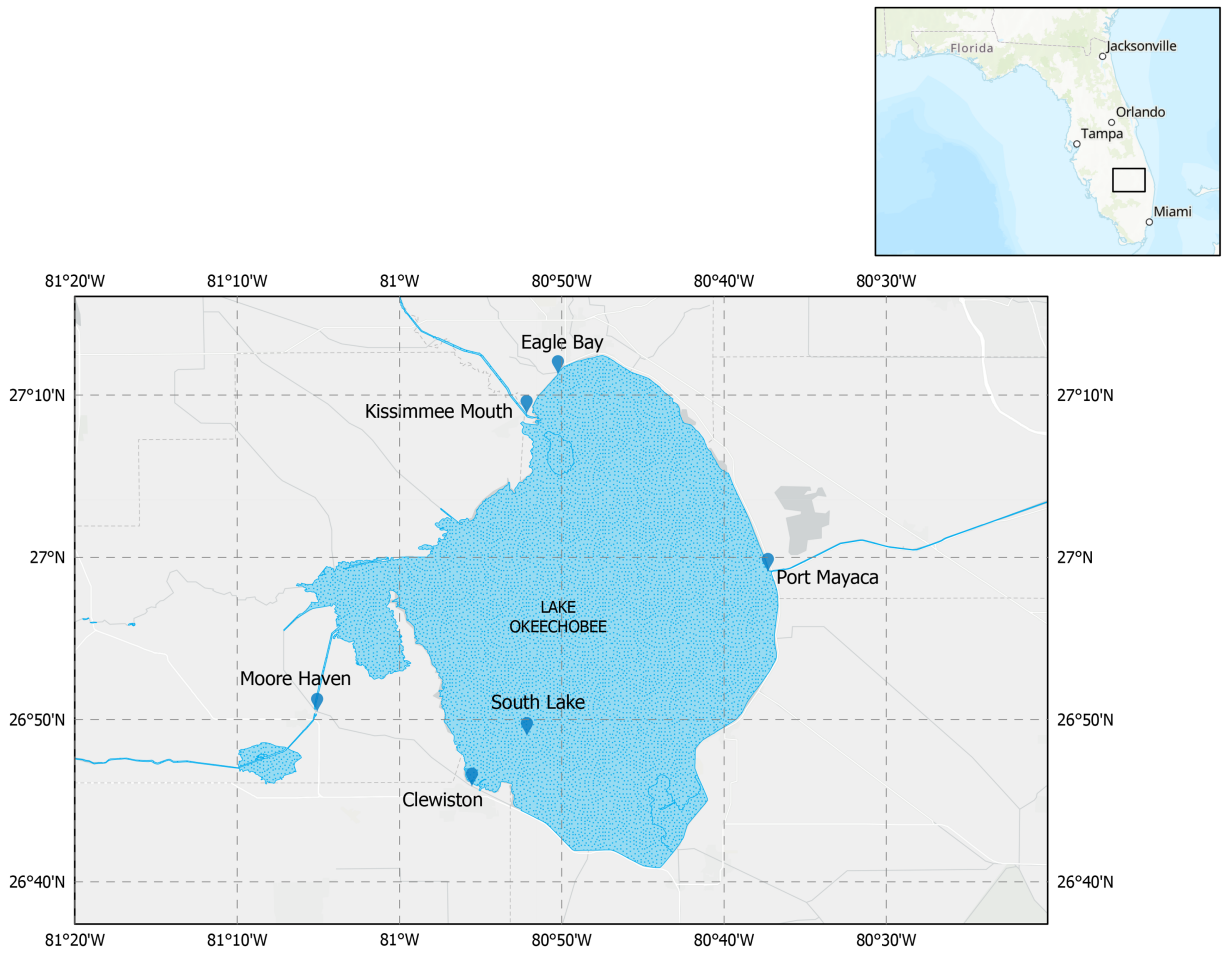

FIGURE 1
Map of Lake Okeechobee with the sampling locations.

nitrate, nitrite, and ammonium were analyzed using Standard Methods 4500 (APHA, 2017) on a Seal AutoAnalyzer (Seal AA500; Seal Analytical, WI, United States). Trace elements were quantified using an Avio 200 ICP-OES (Inductively Coupled Plasma Optical Emission Spectrometer) following Standard Method 3,120 (Baird and Bridgewater, 2017). Additional water chemistry parameters were obtained from the South Florida Water Management Districts DBHydro database.[1]

2.2. Cyanotoxin analysis

Mass spectrometry multiple reaction monitoring (MS-MRM) was used to analyze samples from all collection sites for multiple microcystin (MC) congeners as well as nodularin (NOD), saxitoxin (STX), and cylindrospermopsin (CYN). Water samples were frozen and thawed three times, then concentrated using C18 sorbent (Strata-X, Phenomenex Corporation, Torrance, CA, United States, 60 mg sorbent, 3 mL syringe volume). After elution, samples were placed into autosampler vials for high performance liquid chromatography tandem mass spectrometry (HPLC-MS/MS) analysis on an Agilent 1200 series HPLC in-line with an Agilent 6410b triple quadrupole mass spectrometer (Agilent, Santa Clara, CA, United States) fitted with an electrospray ionization source. The autosampler was maintained at 8°C and injected 40 µL of sample. The analytes were passed through a column shield prefilter (MAC-MOD Analytical, Inc., Chadds Ford, PA, United States) and loaded onto a Luna C18(2), 3-µm particle size, 150 × 3 mm column (Phenomenex Corporation, Torrance, CA, United States) heated to 35°C with 100% mobile phase A (90% water, 10% acetonitrile, 0.1% formic acid) at a flow rate of 0.4 mL min^{-1}. Initial conditions were maintained for 2 min, and analytes were eluted over a six-minute gradient from 0% to 90% mobile phase B (100% acetonitrile, 0.1% formic acid) followed by 3 min at 90% mobile phase B, before returning to initial conditions for 3 min. MS/MS analysis used Agilent MassHunter Data Acquisition software (version B.02.01, Agilent, Santa Clara, CA, United States). Samples were run in positive ion mode by MS-MRM and full scan mode (m/z 100–1,200). Data were analyzed using Agilent MassHunter Qualitative Analysis software (version B.03.01, Agilent, Santa Clara, CA, United States). A standard curve ($1/y^2$ weighting) was established for each toxin (except MC-LW, which was quantified using the MC-LR standard curve) by integrating the peak area of the quantifier ion from duplicate standards (6 concentrations ranging from 0 to 10 ng μL^{-1}), with a limit of detection of 0.5 ng on the Phenomenex column. Standards were prepared in methanol and analyzed in the same manner as the samples. To measure the amount of each toxin in the samples, the peak area of the quantifier ion was compared to the appropriate standard curve. The limit of detection of each toxin in water is 0.0003–0.0009 µg L^{-1} microcystin (varies based on congener), 0.0005 µg L^{-1} cylindrospermopsin, and 0.0009–0.0013 µg L^{-1} saxitoxin. Standards for toxin analysis included various sources for microcystins including Enzo Life Sciences (Farmingdale, NY, United States), Cayman Chemical (Ann Arbor, MI, United States), Greenwater Laboratories (Palatka, FL, United States), and CCS purification. Pure saxitoxin standards were purchased from Cayman Chemical (Ann Arbor, MI, United States) and additional material was isolated from a toxic strain of *Dolichospermum circinale* (obtained from Dr. Brett Neilan). Cylindrospermopsin standards were obtained from Dr. Brett Neilan.

2.3. DNA extraction, amplicon library preparation, and processing

DNA was extracted using a DNeasy Blood and Tissue Kit (Qiagen, Hilden, Germany), modified according to Djurhuus et al. (2017). The V4–V5 hypervariable regions of the 16S rRNA were amplified using 515FY-926R primer pair described in Parada et al. (2016). Samples were amplified in triplicate before pooling. Amplicon libraries were sequenced using paired-end (2 × 250 bp) Illumina Novaseq (Novogene, Beijing, China), sequencing depth varied from 88,722 to 139,935 reads per samples with a mean of 129,647. The V3–V4 variable regions of the 16S rRNA were obtained by using both sets of cyanobacterial specific primer pairs (i.e., CYA359F-781Ra/b) described by Nübel et al. (1997). However, these produced a low number of cyanobacterial ASV's due to amplification of eukaryotic phytoplankton chloroplast 16S rRNA sequences and were thus excluded from analysis (data not shown).

Amplicon sequences were demultiplexed and assigned to specific sample IDs based on their MIDs at Novogene using an in-house bioinformatic pipeline. DADA2 (Callahan et al., 2016) was used to process raw sequences in R v4.0.0 (R Core Team, 2023). Paired-end reads were filtered, trimmed, and merged. Cleaned and merged reads were dereplicated and subsequently analyzed for detection and removal of potential chimeras using DADA2. Non-chimeric sequences were pooled to define amplicon sequence variants (ASVs) and identical ASVs which only varied in length were collapsed using the "collapseNoMismatch" command in DADA2, ASVs ranged in length from 325 to 393 nt.

Taxonomic assignment of ASVs was based on a naïve Bayesian classifying method (Wang et al., 2007) with CyanoSeq V1.2 (Lefler et al., 2023) and SILVA 138.1 (Quast et al., 2012) as the taxonomic databases. The CyanoSeq database was supplemented with 16S rRNA sequences from unialgal cyanobacterial cultures isolated from Lake Okeechobee and surrounding fresh waters housed in the Berthold Laughinghouse Culture Collection (BLCC) at the University of Florida – IFAS, Fort Lauderdale Research and Education Center (Davie, FL, United States). All non-cyanobacterial ASVs, including chloroplasts, were removed prior to downstream analyses. All archaeal, chloroplast, eukaryotic, and mitochondrial ASVs were removed for network analysis. A maximum likelihood phylogenetic tree of the cyanobacterial ASVs was created using RAxML-NG (Kozlov et al., 2019), by determining the sequence evolutionary model (GTR-I-G4) using ModelTestNG (Darriba et al., 2020). A maximum likelihood phylogenetic tree of the bacterial ASVs was created using IQTree with ultrafast bootstrapping (Minh et al., 2020).

ASV's which corresponded to the Aphanizomenonaceae and Microcystaceae were extracted, and phylogenetic trees were constructed for each family. Cyanobacterial ASVs that could not be classified to the genus level (except for Prochlorococcaceae) were extracted and placed in the reference tree from CyanoSeq (v1.2) along with their three closest BLAST hits to provide increased resolution. Sequences were added to the alignment using MAFFT (Katoh and Standley, 2013), full length sequences (i.e., >600 bp) were added with—add and—keeplength parameters, while ASVs and short

1 https://www.sfwmd.gov/science-data/dbhydro

sequences (i.e., <600 bp) were added using—add-fragment and—keeplength parameters. The alignment was trimmed using TrimAl (Capella-Gutiérrez et al., 2009) using -automated1 parameter and the sequence evolutionary model was determined using ModelTestNG (Darriba et al., 2020). The phylogenetic tree was built using RAxML-NG with 1,000 bootstrap replicates (Kozlov et al., 2019).

2.4. Statistical and network analyses

Sequence read abundances were filtered using the phyloseq package (McMurdie and Holmes, 2013). ASVs that occurred in less than 10% of samples or occurred less than 100 times across all samples were removed from all downstream analyses, except alpha diversity. The vegan package (Oksanen et al., 2019) was used for statistical analyses, calculation of richness and diversity indices, and generation of ordinations in combination with ggplot2 (Wickham, 2016) in R v4.0.0 (R Core Team, 2023). Alpha diversity was calculated using Faith's Phylogenetic Distance indices, and Wilcoxon tests were used to compare between groups. Data were not rarefied (McMurdie and Holmes, 2014), prior to analyses, the data were log-transformed (1og10) to avoid biases toward rare species and minimize influence of most abundant groups. Indicator species were determined using the indicspecies package (De Cáceres and Legendre, 2009).

Similarities in cyanobacterial communities among sampling sites and seasons (i.e., wet vs. dry season, nitrogen limitation vs. co-limitation) were explored using the Non-Metric Multidimensional Scaling (NMDS) analysis with generalized Unifrac distances (Chen J. et al., 2012; Chen X. et al., 2012). The "adonis2" function of the vegan package was used to conduct a permutational multivariate analysis of variance (PERMANOVA) on generalized Unifrac distances to test the effect of sampling sites, nutrient limitation, and seasonal impact on cyanobacterial community composition. Partial redundancy analysis (pRDA) was employed using the rda() function in the vegan package to find relationships between significant environmental variables ($p \leq 0.05$) and *Cuspidothrix*, *Cyanobium*, *Dolichospermum*, *Microcystis*, *Raphidiopsis*, and *Vulcanococcus* were selected as these were the five most abundant described genera in our data. Environmental variables were standardized based on square root transformation prior to analysis.

Generalized additive models (GAMs) were used to model the relationship between cyanobacterial genera (as rarefied read abundance) and limnological parameters (e.g., water temperature, nutrients, etc.) with sampling sites and outing as random effects. GAMs were conducted in R using the mgcv package (v1.8-42; Wood, 2011) and drawn with gratia (Simpson, 2023) and ggplot2.

Cyanobacterial-bacterial relationships were explored using the Sparse Inverse Covariance Estimation for Ecological Association Inference (SpiecEasi; v1.1.0) package in R (Kurtz et al., 2015) using the top 500 most abundant genera. Networks were visualized in Cytoscape v3.9.1 (Shannon et al., 2003).

3. Results

3.1. Limnological parameters

Dissolved inorganic nitrogen to dissolved inorganic phosphorus ratio (DIN:DIP) was determined, as was the dissolved inorganic nitrogen (DIN), defined here as the sum of nitrate, nitrite, and ammonia, to soluble reactive phosphate. DIN:DIP ratio ranged from 0.02 to 75, while DIN ranged from 0.05–0.634 mg L^{-1}. These data are reported in Supplementary Data S1. Total nitrogen and phosphorus measurements were obtained from the South Florida Water Management Districts DBHydro database; the TN:TP mass ratio ranged from 11 to 71 with a mean of 28. Total nitrogen concentrations ranged from 0.87–3.14 mg $L^{-1}$and total phosphorus concentrations ranged from 0.056–0.392 mg L^{-1}. Periods of nutrient limitation were determined by collecting TN and TP data from the sites in closest proximity to our sampling sites and plotting the TN:TP ratio as a time series during our sampling events (Supplementary Figure S1). Only one site indicated phosphorus limitation (TN:TP $\geq$ 23) and was thus excluded from further analyses. Nutrient limitation was based on values provided by Paerl et al. (2016) where N:P $\geq$ 23 indicates P-limitation, N:P $\leq$ 9 indicates N-limitation, and 23 > N:P > 9 indicates co-nutrient limitation. Other water quality parameters (e.g., trace elements, conductivity, photic depth) are reported in Supplementary Data S1. Daily mean lake depth was determined from the LZ40 station (lat 26.901815, long −80.789003) and ranged from 3.5–4.7 m.

3.2. Cyanobacterial composition

After filtering, there were an average of 67,826 (min = 44,914, max = 84,259, sd = 8,876) reads across samples assigned to 4,048 ASVs, 274 of which were cyanobacteria with an average of 20,168 (min = 2,429, max = 58,317, sd = 11,403) reads. The cyanobacteria, phylum Cyanobacteriota, frequently made up >25% of the total bacterial community (Supplementary Figure S2A). Based on relative read abundance, the Synechococcales, Nostocales, and Chroococcales were the most abundant cyanobacterial orders (Supplementary Figure S2B), with the Prochlorococcaceae, Aphanizomenonaceae, and Microcystaceae as the most abundant families (Supplementary Figure S2C). The most abundant genus within Lake Okeechobee was *Cyanobium*, a member of the Prochlorococcaceae, followed by *Dolichospermum*, and *Microcystis*. The most abundant toxigenic bloom-forming genera were *Dolichospermum* and *Microcystis* (Figure 2), although several other potentially toxic bloom-forming genera were found throughout the lake at lower relative abundances including *Aphanizomenon*, *Cuspidothrix*, *Raphidiopsis*, and *Sphaerospermopsis*.

Due to the high abundance and bloom potential of the Aphanizomenonaceae and Microcystaceae, phylogenetic inferences of these ASVs were conducted to confirm taxonomic assignment (Supplementary Figures S3, S4). All ASVs assigned to a genus were found to be monophyletic with their respective genus. ASV1987 was assigned as "Aphanizomenonaceae" but phylogenetic inferences revealed this belonged to *Amphiheterocytum* and was manually reassigned (Supplementary Figure S3). ASV176 was only assigned to the rank "Aphanizomenonaceae" and formed a well-supported clade away from known genera within the Aphanizomenonaceae, thus this was reassigned as "Aphanizomenonaceae Cluster 1" (Supplementary Figure S3). ASV1176 was assigned as "Microcystaceae" but phylogenetic inferences revealed this belonged to *Coelosphaerium* and was manually reassigned (Supplementary Figure S4). Three ASVs (ASV339, ASV751, ASV2762) were assigned as Microcystaceae and formed a well-supported clade

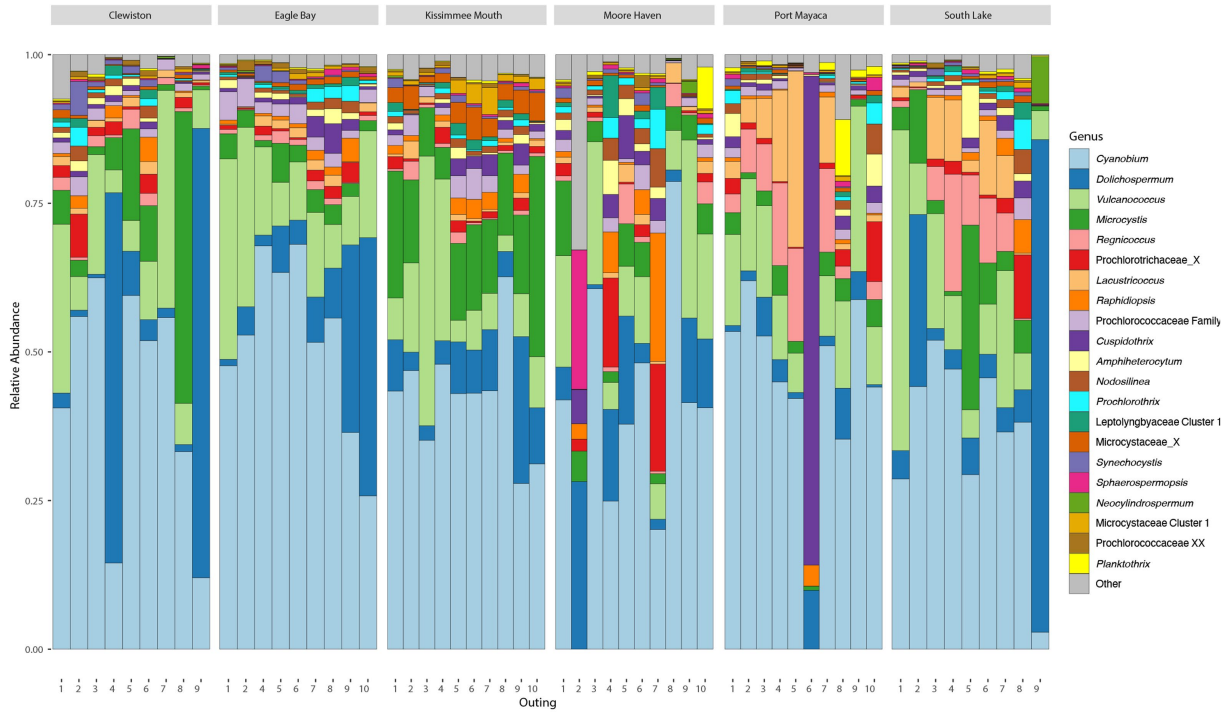

FIGURE 2
Bar plots showing the relative abundance of most abundant cyanobacterial genera found during the study.

away from known genera within the Microcystaceae, thus reassigned as "Microcystaceae Cluster 1" (Supplementary Figure S4). There were several sequences which were classified as Microcystaceae X, an undescribed genus within the Microcystaceae; this genus was within the top 15 most abundance genera (Figure 2). These ASVs formed a clade with no cultured strains (Supplementary Figure S4), only sequences which were collected in a culture-independent manner from other fresh waterbodies (e.g., Reelfoot Lake, Tennessee, United States). A phylogenetic tree of the picocyanobacteria, order Synechococcales, was constructed with 259 sequences, 176 of which were ASVs (Supplementary Figure S5).

Phylogenetic inferences of ASVs which could not be classified past the order level were also conducted. These were found in several clades across the tree (Supplementary Figure S6). Two ASVs (125 and 2,225) were only classified as Cyanophyceae class and manually reassigned as "Leptolyngbyaceae Cluster 1," as these ASVs formed a clade within the Leptolyngbyaceae with sequences from other freshwater lakes. AVS's 378 and 1838 were also only classified at the class level and fell within the Synechococcaceae and reassigned as "Synechococcaceae Cluster 1." These ASV's formed a well-supported clade with other uncultured sequences from freshwater bacterioplankton samples. ASV3311 was found to be *Pseudanabaena*, ASV5289 clustered with *Neocylindrospermum*, and several ASVs (ASV170, ASV437, ASV669, ASV793, ASV5103) clustered with *Nodosilinea*; these were all manually reassigned.

3.3. Cyanobacterial-bacterial correlations

A network was created to observe the correlations between most abundant cyanobacterial genera (Figure 3). There were no correlated taxa, bacterial nor cyanobacterial, shared between *Dolichospermum*, *Microcystis*, and *Raphidiopsis*. *Dolichospermum* was positively correlated with several taxa, and negatively correlated with two bacteria including *Acidibacter*. *Microcystis* was correlated with less taxa than *Dolichospermum*, and negatively correlated with *Rheinheimera*. *Raphidiopsis* was also negatively correlated with *Rheinheimera*, in addition to *Legionella*. *Raphidiopsis* was correlated with several cyanobacterial taxa, in comparison to *Dolichospermum* and *Microcystis*. *Pseudanabaena* was correlated to both *Microcystis* and *Cuspidothrix*, however *Microcystis* and *Cuspidothrix* were not correlated with each other. The Prochlorococcecean taxa (i.e., *Cyanobium*, *Regnicoccus*, *Lacustricoccus*, *Vulcanococcus*) shared several correlated taxa, distinct from the crown cyanobacteria.

3.4. Community composition

There were no significant differences in taxonomic richness between cyanobacterial communities based on either metric at each sampling site (Figures 4A,B). The NMDS revealed overlap between these communities (Figure 4C), and results from the pairwise PERMANOVA showed that there were no significant differences in cyanobacterial communities between sites ($p > 0.05$). The southern region of the lake (i.e., Clewiston and South Lake) had higher relative abundances of *Dolichospermum*, while the northern region near the mouth of the Kissimmee River had a higher relative abundance of *Microcystis*; Moore Haven had the highest relative abundance of *Raphidiopsis* (Figure 4D).

Similar to the cyanobacterial communities, there were no significant differences in taxonomic richness between bacterial communities based on either metric at each sampling site

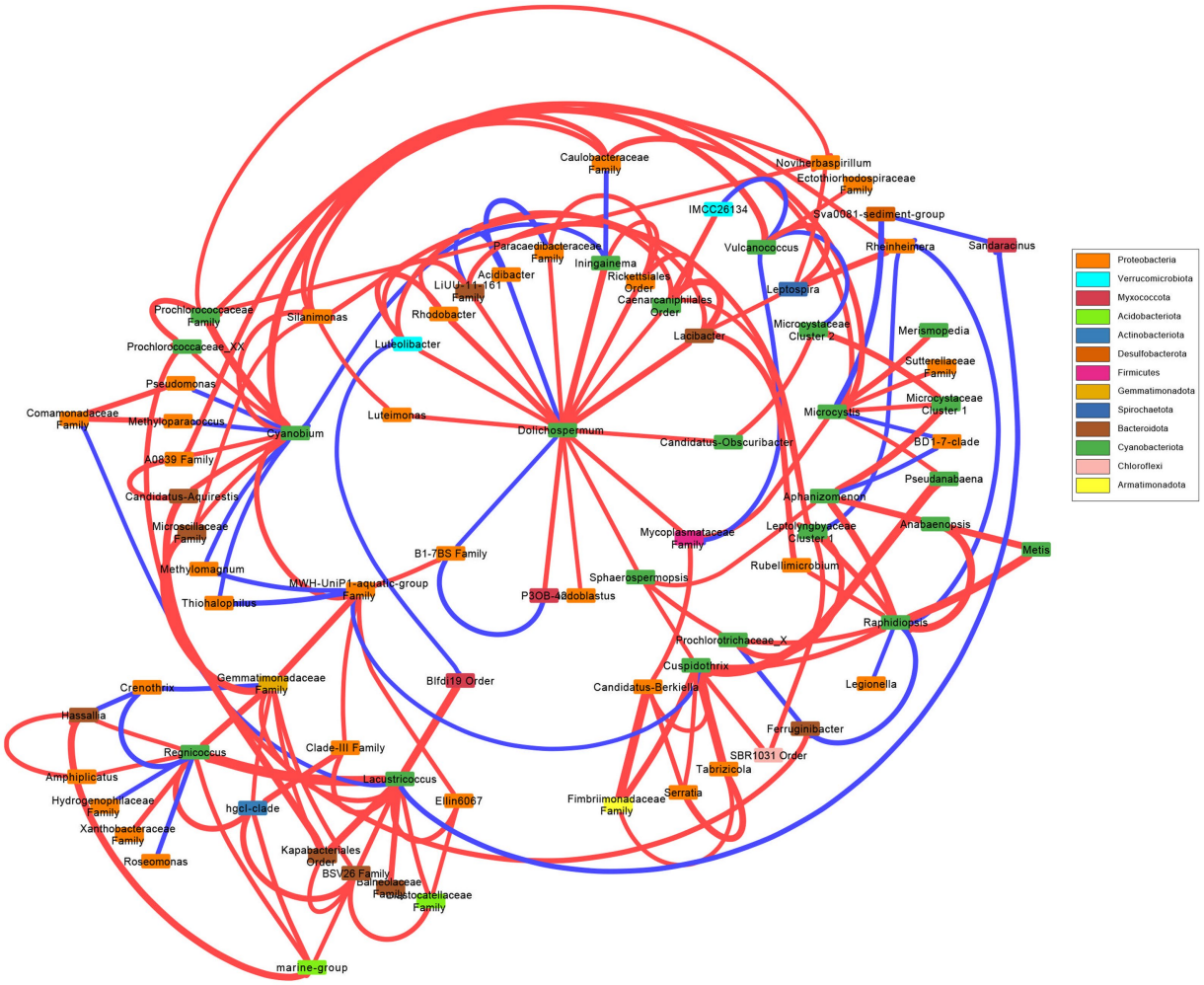

FIGURE 3
Network analysis of the most abundant cyanobacterial genera and the significant cyanobacterial-(cyano)bacterial relations. Edge thickness represent weight and color represent positive (red) or negative (blue) correlations. Box color represent phylum.

(Supplementary Figures S7A,B). The NMDS revealed overlap between these communities (Supplementary Figure S7C), and results from the pairwise PERMANOVA showed that there were significant differences between bacterial communities between Clewiston and Kissimmee Mouth ($R^2 = 0.11$, $p = 0.03$). There were no major differences between relative abundances of bacterial phyla between sites (Supplementary Figure S7D).

There were no significant differences in taxonomic richness in cyanobacterial communities between the wet and dry seasons (Figures 5A,B). The non-metric multidimensional scaling (NMDS) analysis showed an overlap between wet and dry seasons for the cyanobacterial communities (Figure 5C). Results from PERMANOVA showed significant differences between the cyanobacterial communities in the wet and dry seasons, although season accounted for a relatively small proportion of the variation data ($R^2 = 0.06$, $p < 0.01$). The relative abundance of the Prochlorococcaceae was nearly equal between wet and dry seasons, accounting for ~60% of the cyanobacterial relative abundance (Supplementary Figure S8A). *Dolichospermum* relative abundance was nearly double in the wet season compared to the dry season, where it was also the dominant non-Prochlorococcaceae taxon. There also appeared to be an increased relative abundance in *Amphiheterocytum*, *Cuspidothrix*, and *Raphidiopsis* in the dry season; *Microcystis* relative abundance appeared even between the two seasons (Figure 5D). Indicator species, as genera, between seasonal communities were determined and listed in Supplementary Table S1.

There were no significant differences in taxonomic richness in bacterial communities between the wet and dry seasons (Supplementary Figures S9A,B). The non-metric multidimensional scaling (NMDS) analysis showed an overlap between wet and dry seasons for the cyanobacterial communities (Figure 5C). Results from PERMANOVA showed significant differences between the bacterial communities in the wet and dry seasons, although season accounted for a relatively small proportion of the variation data ($R^2 = 0.08$, $p < 0.001$). There was an increased relative abundance of Proteobacteria (=Pseudomonadota) in the wet season, and an increased relative abundance of Actinobacteria (=Actinomycetota) in the dry season (Supplementary Figure S9D).

The relative abundance of the phylum Cyanobacteriota within the lake did not differ between seasons comprising ~30% of the relative abundance (Supplementary Figure S8C). Additionally, there were no significant differences in cyanobacterial communities between seasons

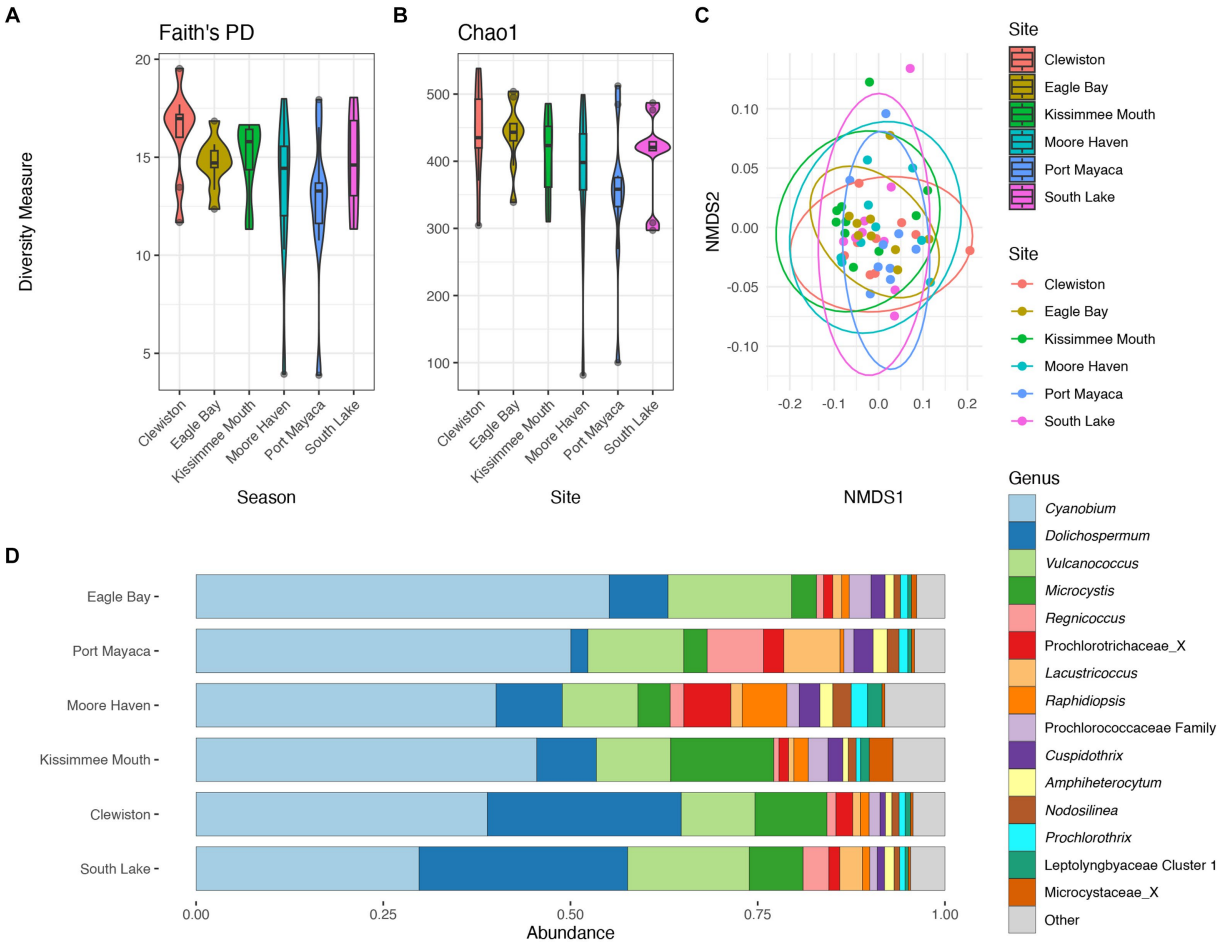

FIGURE 4
Diversity measures of the cyanobacterial communities at the different sampling locations. Faith phylogenetic diversity **(A)** and Chao1 index **(B)** between each sampling location. Non-metric Multidimensional Scaling (NMDS) ordination within two dimensions of the cyanobacterial communities based on generalized-Unifrac distances between sampling locations, colors represent **(C)**. Bar plot of the average relative abundance of the most abundant cyanobacterial genera at each location **(D)**.

based on alpha diversity metrics (Figures 5A,B). Conversely, the cyanobacterial communities differed between seasons based on results from the PERMANOVA.

There were no significant differences in taxonomic richness between cyanobacterial communities during N-limitation and co-limitation (Figures 6A,B). The NMDS analysis showed an overlap between the cyanobacterial communities during N-limitation and co-limitation (Figure 6C). When comparing the N-limited and co-limited cyanobacterial communities, there were no significant differences in community composition (PERMANOVA $R^2 = 0.02$, $p = 0.29$). The relative abundance of the Prochlorococcaceae was nearly equal between N-limited and co-limited communities and accounted for ~55%–60% of the relative abundance, although their relative abundance was slightly higher in N-limited communities (Supplementary Figure S8B). When observing the non-Prochlorococcaceae taxa, there appears to be a non-significant increased relative abundance in *Dolichospermum* in the N-limited communities compared to the co-limited communities (PERMANOVA $R^2 = 0.02$, $p = 0.5$), while *Microcystis* relative abundance showed the opposite trend (PERMANOVA $R^2 = 0.05$, $p = 0.2$; Figure 6D). Indicator species, as genera, between N-limited and co-limited communities were determined; only *Planktothrix* and Synechococcaceae Cluster 1 were determined to be indicator species within N-limited communities. There was an increased relative abundance of cyanobacteria (=Cyanobacteriota) in the co-limited communities compared to the N-limited communities (Supplementary Figure S8D).

There were no significant differences in taxonomic richness between bacterial communities during N-limitation and co-limitation (Supplementary Figures S10A,B). The NMDS analysis showed an overlap between the bacterial communities in the wet and dry seasons (Supplementary Figure S10C). When comparing the N-limitation and co-limited cyanobacterial communities, there were no significant differences in community composition (PERMANOVA $R^2 = 0.01$, $p = 0.42$). There were no major differences between relative abundances of any bacterial phyla between seasons (Supplementary Figure S10D). There was an increased relative abundance of Proteobacteria (=Pseudomonadota) and Actinobacteria (=Actinomycetota) in N-limited communities, and an increased relative abundance of Planctomycetota in the co-limited communities (Supplementary Figure S10D).

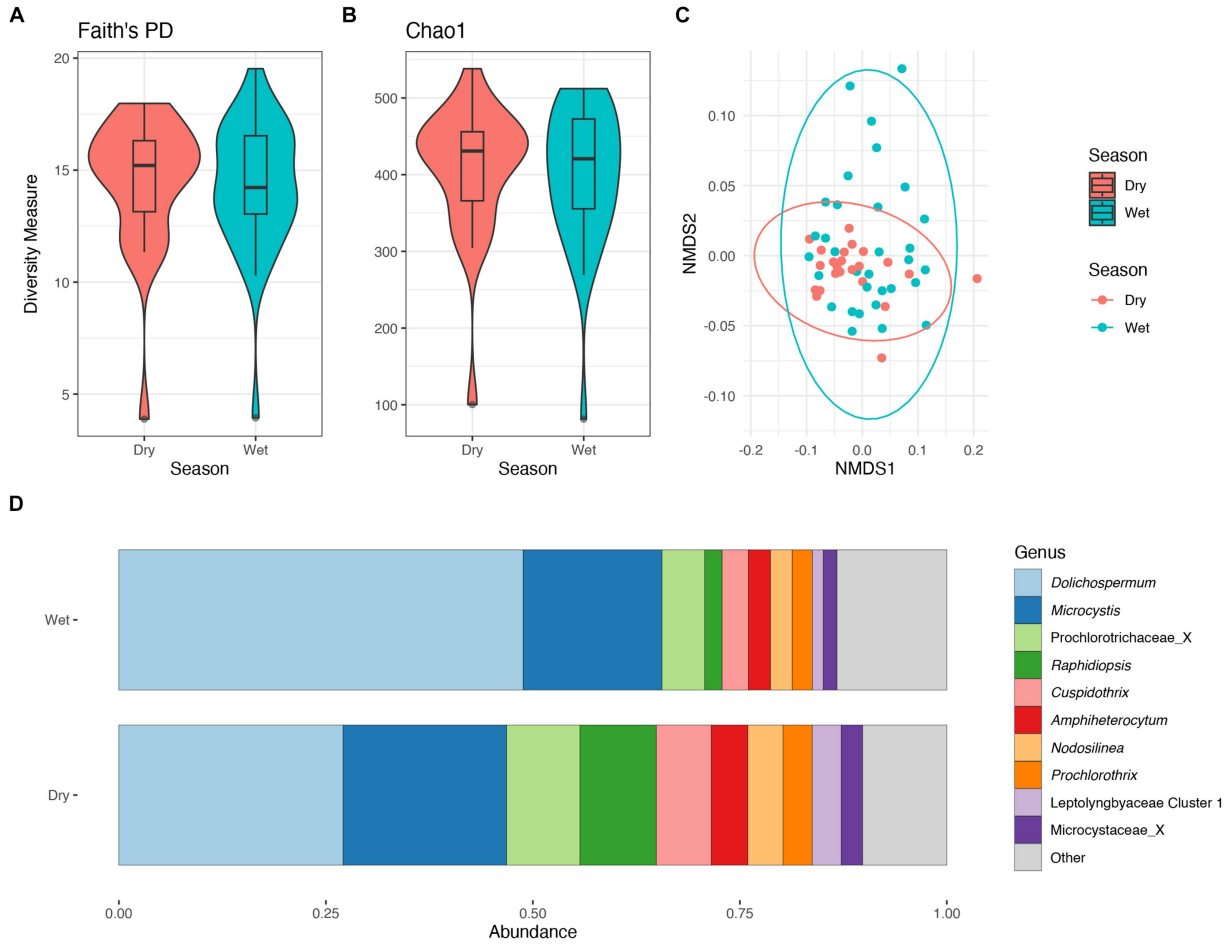

FIGURE 5
Diversity measures of the cyanobacterial communities between wet and dry season. Faith phylogenetic diversity **(A)** and Chao1 index **(B)** between each season. Non-metric Multidimensional Scaling (NMDS) ordination within two dimensions of the cyanobacterial communities based on generalized-Unifrac distances between sampling locations, colors represent season **(C)**. Bar plot of the average relative abundance of the most abundant, non-prochlorococcacean, cyanobacterial genera during each season **(D)**.

3.5. Influences of limnological parameters on common cyanobacteria

Due to the high relative abundance of *Cuspidothrix*, *Cyanobium*, *Dolichospermum*, *Microcystis*, *Raphidiopsis*, and *Vulcanococcus* (Figure 2) the environmental drivers of these taxa were subjected to further investigation via a partial redundancy analysis (pRDA). From the model, the conditioned variables (sample sites and outings) explained 11% of the variation, while water chemistry explained 34.4% of the variation, the remaining 54.6% of the variation was unexplained; the value of p for the model was 0.002. The triplot from the pRDA revealed that *Cuspidothrix, Cyanobium*, *Microcystis*, *Raphidiopsis*, and *Vulcanococcus* were associated with each other, but not *Dolichospermum* (Figure 7). *Cuspidothrix, Cyanobium*, *Microcystis*, and *Vulcanococcus* were positively associated with increased dissolved oxygen, copper, and zinc concentrations, and inversely associated with orthophosphate and iron concentration. *Dolichospermum* was positively associated with photic depth, inversely associated with DIN, and not associated with TRP.

Effects of individual limnological parameters (i.e., water temperature, photic depth, lake depth, DIN, TRP, and DIN:DIP) on *Cuspidothrix*, *Cyanobium*, *Dolichospermum*, *Microcystis*, *Raphidiopsis*, and *Vulcanococcus* relative abundances were investigated using GAMs. In this study, GAMs used the negative binomial distribution assumption; sample outing and site were regarded as random effects. Results are listed in Table 1. The effects of water temperature, photic depth, lake depth, and conductivity on bloom-forming genera (i.e., *Cuspidothrix*, *Dolichospermum*, *Microcystis*, and *Raphidiopsis*) are visualized in Figure 8 and the relationship between nutrients and bloom-forming cyanobacteria are visualized in Figure 9. The diazotrophic bloom-forming genera (i.e., *Cuspidothrix*, *Dolichospermum* and *Raphidiopsis*) were inversely correlated with increases in DIN (Figures 9A,C,D; Table 1), whereas *Microcystis* was positively correlated with DIN (Figure 9B; Table 1). *Dolichospermum* was positively, and significantly, correlated with increased TRP concentrations whereas *Raphidiopsis* relative abundance decreased with increasing TRP concentrations, although this trend was not significant (Figures 9F,H; Table 1). *Cuspidothrix* relative abundance was positively correlated with TRP concentrations up until ~0.5 mgL^{-1} after which it began to decrease (Figure 9E; Table 1). There was no noticeable relationship between *Microcystis* relative abundance and

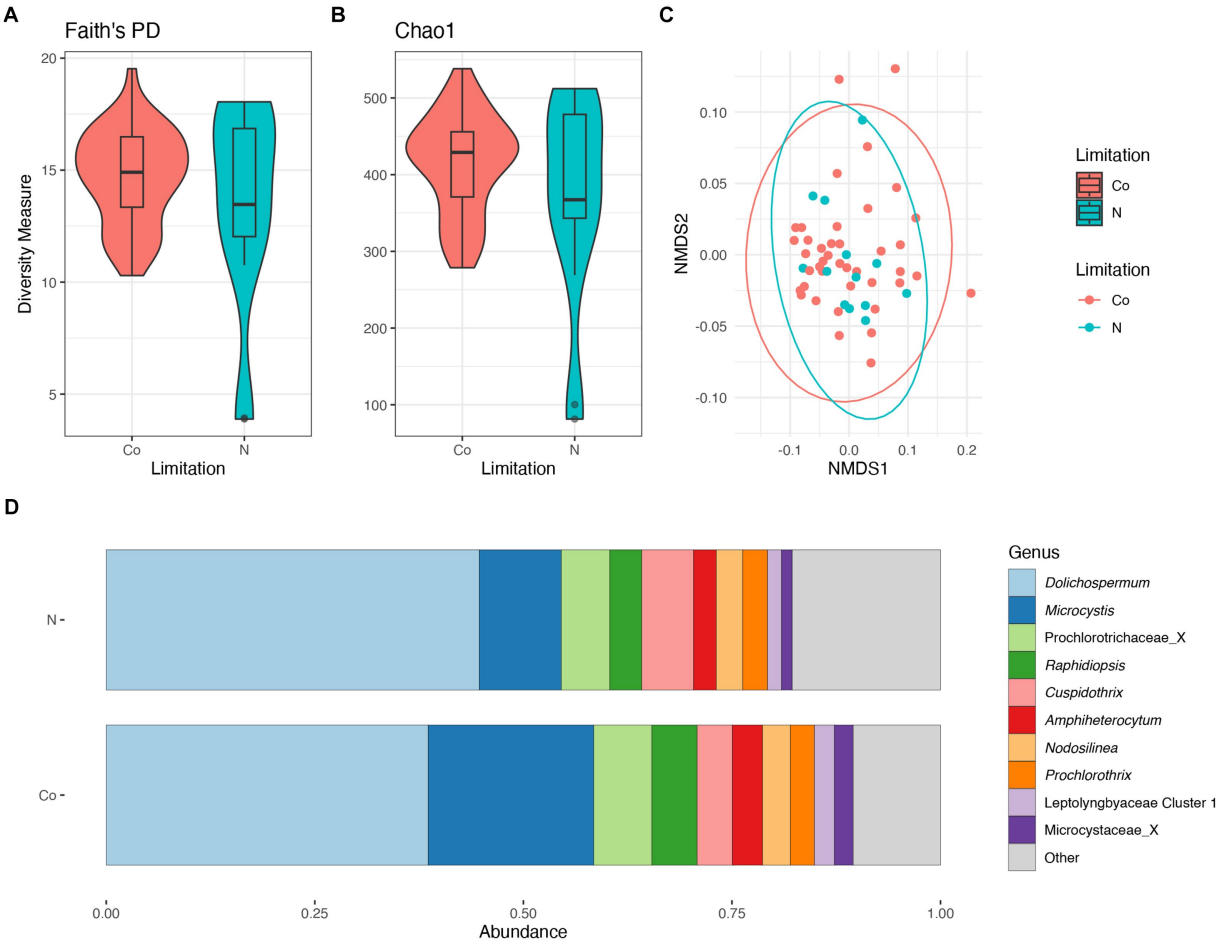

FIGURE 6
Diversity measures of the cyanobacterial communities between nitrogen and co-nutrient limitation. Faith phylogenetic diversity **(A)** and Chao1 index **(B)** between nutrient limitations. Non-metric Multidimensional Scaling (NMDS) ordination within two dimensions of the cyanobacterial communities based on generalized-Unifrac distances between nutrient limitations, colors represent limitation **(C)**. Bar plot of the average relative abundance of the most abundant, non-prochlorococcacean, cyanobacterial genera during nutrient limitations **(D)**.

TRP concentrations (Figure 9F; Table 1), Both *Cuspidothrix* and *Dolichospermum* relative abundances were negatively correlated with DIN:DIP, whereas *Microcystis* and *Raphidiopsis* relative abundances were positively, and linearly, correlated with DIN:DIP (Figures 9I–L; Table 1). Water temperature had a varied response on the bloom-forming genera, with *Cuspidothrix* and *Raphidiopsis* having the highest relative abundances in the cooler waters (~25°C) of the dry season, whereas *Dolichospermum* and *Microcystis* relative abundances increased with increasing water temperatures (Figures 8A–D). Both *Dolichospermum* and *Microcystis* relative abundances peaked around 30°C, in the warmer wet season. *Dolichospermum* and *Microcystis* relative abundances were positively correlated with photic depth (Figures 8E–H; Table 1), whereas there were no trends between *Cuspidothrix* and *Raphidiopsis* relative abundances and photic depth. Furthermore, lake depth had a significant negative linear relationship with *Raphidiopsis* relative abundance (Figure 8L; Table 1).

The effects of water temperature, photic depth, lake depth, and conductivity on *Cyanobium* and *Vulcanococcus* are visualized in Supplementary Figure S11 and the effects of nutrients in Supplementary Figure S12. Water temperature had a positive linear relationship on both *Cyanobium* and *Vulcanococcus* relative abundance, although this relationship was greater on *Vulcanococcus* (Supplementary Figures S11A,D; Table 1). Both *Cyanobium* and *Vulcanococcus* relative abundance had a negative relationship with both photic and lake depth (Supplementary Figures S11B,C,E,F; Table 1). DIN had a negative, although weak, correlation with *Cyanobium* and *Vulcanococcus* relative abundance (Supplementary Figures S12A,D; Table 1). TRP had a strong negative correlation with *Cyanobium* relative abundance (Supplementary Figure S12B; Table 1). DIN:DIP had no relationship with *Cyanobium* relative abundance, but had a negative, and linear, relationship with *Vulcanococcus* relative abundance (Supplementary Figures S12C,F; Table 1).

3.6. Cyanotoxins

Cyanotoxins were detected on 16 occasions over the annual cycle at the six sites sampled. Microcystins, nodularins, and anatoxin-a were detected throughout the lake and through time (Supplementary Table S2). Both microcystin-LR (MC-LR) and microcystin-RR (MC-RR) were detected with MC-LR being the

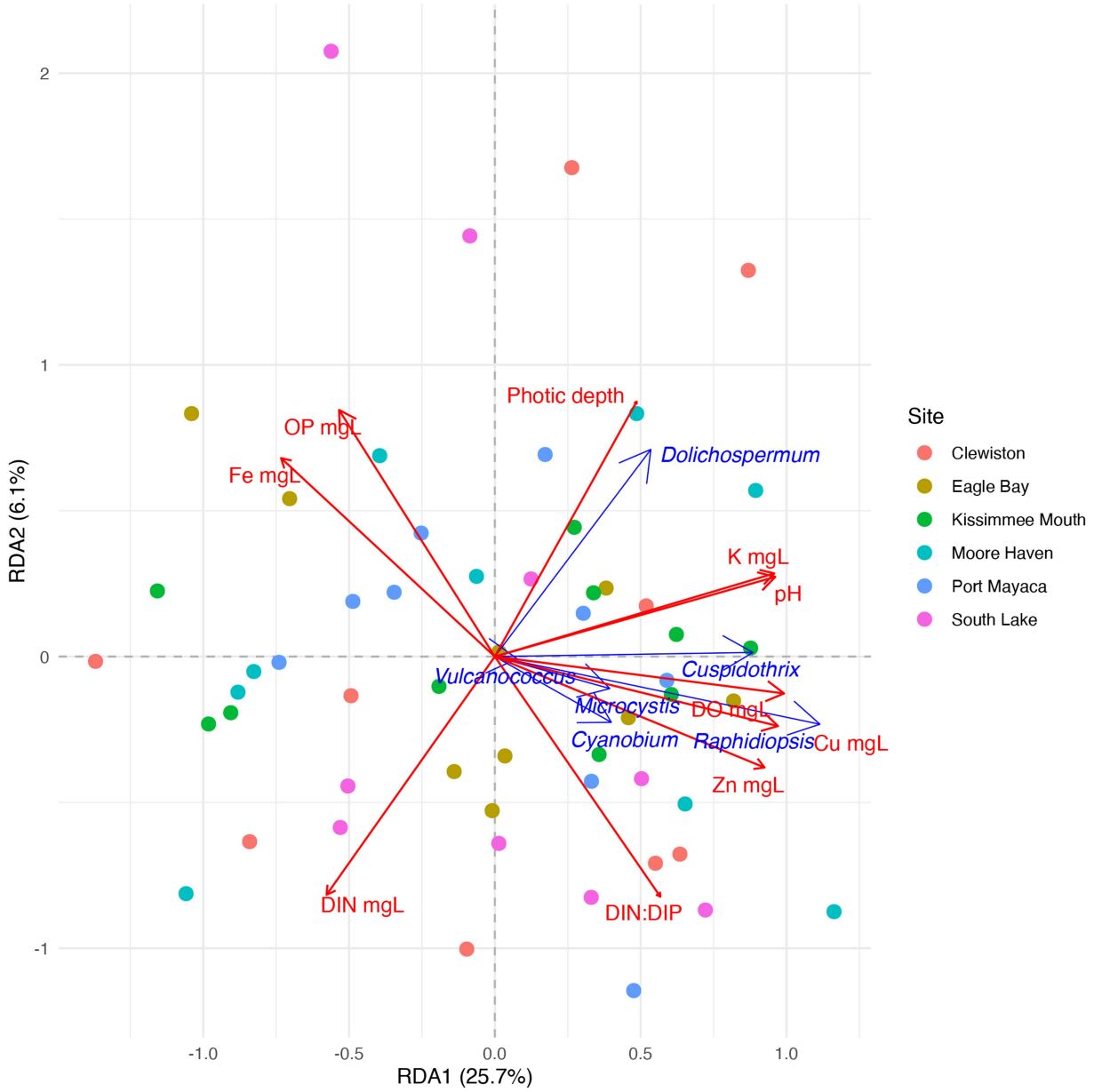

FIGURE 7
Partial redundancy analysis (pRDA) ordination within two dimensions of the cyanobacterial genera *Cuspidothrix*, *Cyanobium*, *Dolichospermum*, *Microcystis*, *Raphidiopsis*, and *Vulcanococcus*. Drivers of taxonomic variation are shown by blue arrows. Significant environmental drivers are shown by red arrows. Circles indicate samples, colors indicate sample site.

most commonly occurring congener; MC-LR was detected 11 times and MC-RR once. Nodularins were detected seven times, and anatoxin-a was detected once. Microcystin-LR co-occurred with nodularins three times. Cyanotoxin concentrations were low, and ranged between 0.04 and 1.4 $\mu g\,L^{-1}$, with nodularin being the toxin with the highest concentration (1.12 $\mu g\,L^{-1}$), while MC-LR reached concentrations of 0.6 $\mu g\,L^{-1}$. Cyanotoxins were detected nine times during the wet season in four out of six sampling events and seven times in the dry season in three out of four sampling events. Anatoxin-a was only detected once, in the wet season. Nodularins occurred more frequently in the dry season than the wet season (five vs. two occurrences) while microcystins were observed six times in the wet season and five times in the dry season. Due to the infrequent occurrence of these toxins, statistical analyses to elucidate drivers of their occurrence proved unsuccessful (data not shown).

Several known toxin producing genera occurred (e.g., *Aphanizomenon*, *Dolichospermum*, *Microcystis*, *Raphidiopsis*). A correlation analyses was applied to identify which genera were correlated with these cyanotoxins (Supplementary Figure S13). There were several genera correlated with MC-LR, with *Microcystis* being the only confirmed microcystin producer in Lake Okeechobee. Several genera were correlated to MC-RR, with *Chrysosporum*, *Microcystis*, and *Planktothricoides* being the known toxin producing genera. *Aphanizomenon*, *Lagosinema*, Microcystaceae Cluster 1, *Parasynechococcus*, *Planktothricoides*,

10.3389/fmicb.2023.1219261

TABLE 1 Results of the generalized linear models (GAMs).

Genus	Explanatory variable	edf	Deviance %	R^2	AIC
Cuspidothrix	s(Water Temperature)	2.1	27.4	0.049	508
	s(Photic Depth m)	2.4	30.6	0.032	505
	s(Lake Depth m)**	6.1	45.5	0.043	497
	s(DIN mg L^{-1})*	1	43.5	0.04	231
	s(TRP mg L^{-1})	4.2	44.6	0.03	436
	s(DIN:DIP)	1	49.5	−0.314	208
Cyanobium	s(Water Temperature)	1	1.42	0.006	831
	s(Photic Depth m)*	2.6	12.2	0.065	828
	s(Lake Depth m)	1	5.97	0.056	829
	s(DIN mg L^{-1})	1	5.04	0.07	389
	s(TRP mg L^{-1})**	1	9.31	0.101	725
	s(DIN:DIP)	1	0.038	−0.044	350
Dolichospermum	s(Water Temperature)	1	21	0.047	685
	s(Photic Depth m)**	3.4	45.1	0.577	667
	s(Lake Depth m)**	4.9	42.4	0.191	671
	s(DIN mg L^{-1})*	1	9.45	−0.011	313
	s(TRP mg L^{-1})***	1.2	41.5	0.479	582
	s(DIN:DIP)	1.7	18.5	0.012	278
Microcystis	s(Water Temperature)	4.6	36.3	0.123	616
	s(Photic Depth m)^	1	14	0.452	627
	s(Lake Depth m)	1	13	0.036	628
	s(DIN mg L^{-1})	4.2	40.8	0.255	304
	s(TRP mg L^{-1})^	1.7	20.4	0.066	552
	s(DIN:DIP)	1	37.9	0.378	269
Raphidiopsis	s(Water Temperature)	2.6	12.8	0.033	439
	s(Photic Depth m)	1	3.21	−0.008	441
	s(Lake Depth m)**	1	14.2	0.072	425
	s(DIN mg L^{-1})	1.4	11.1	−0.08	184
	s(TRP mg L^{-1})	1	5.45	−0.001	394
	s(DIN:DIP)	1	13	−1.5	168
Vulcanococcus	s(Water Temperature)	1	19.9	0.15	689
	s(Photic Depth m)	1	13	0.09	694
	s(Lake Depth m)	1	15.6	0.116	691
	s(DIN mg L^{-1})	1	0.166	−0.038	324
	s(TRP mg L^{-1})	1.6	16.9	0.118	611
	s(DIN:DIP)	1	8.96	0.046	286

Significant explanatory variables are designated by $p < 0.1$ (^), $p < 0.05$ (*), $p < 0.01$ (**), $p < 0.001$ (***).

Prochlorococcaceae_XX, and *Pseudanabaena* were the genera most correlated with nodularins (Supplementary Figure S13).

4. Discussion

This study provides a detailed analysis of Lake Okeechobee's spatiotemporal cyanobacterial and bacterial community structure. Lake Okeechobee has gained notoriety for its *Microcystis*-dominated cyanoHABs in the past decade. Until now, characterizations of the cyanobacterial community structure in Lake Okeechobee have been carried out via microscopy (e.g., Havens et al., 1994; Cichra et al., 1995; Beaver et al., 2013), apart from Kramer et al. (2018) which focused on full metagenomic sequencing of the cyanoHAB that occurred in 2016. Thus, few data exist on molecular characterizations of the bacterial/cyanobacterial community structure within Lake Okeechobee and this study is the first of its kind.

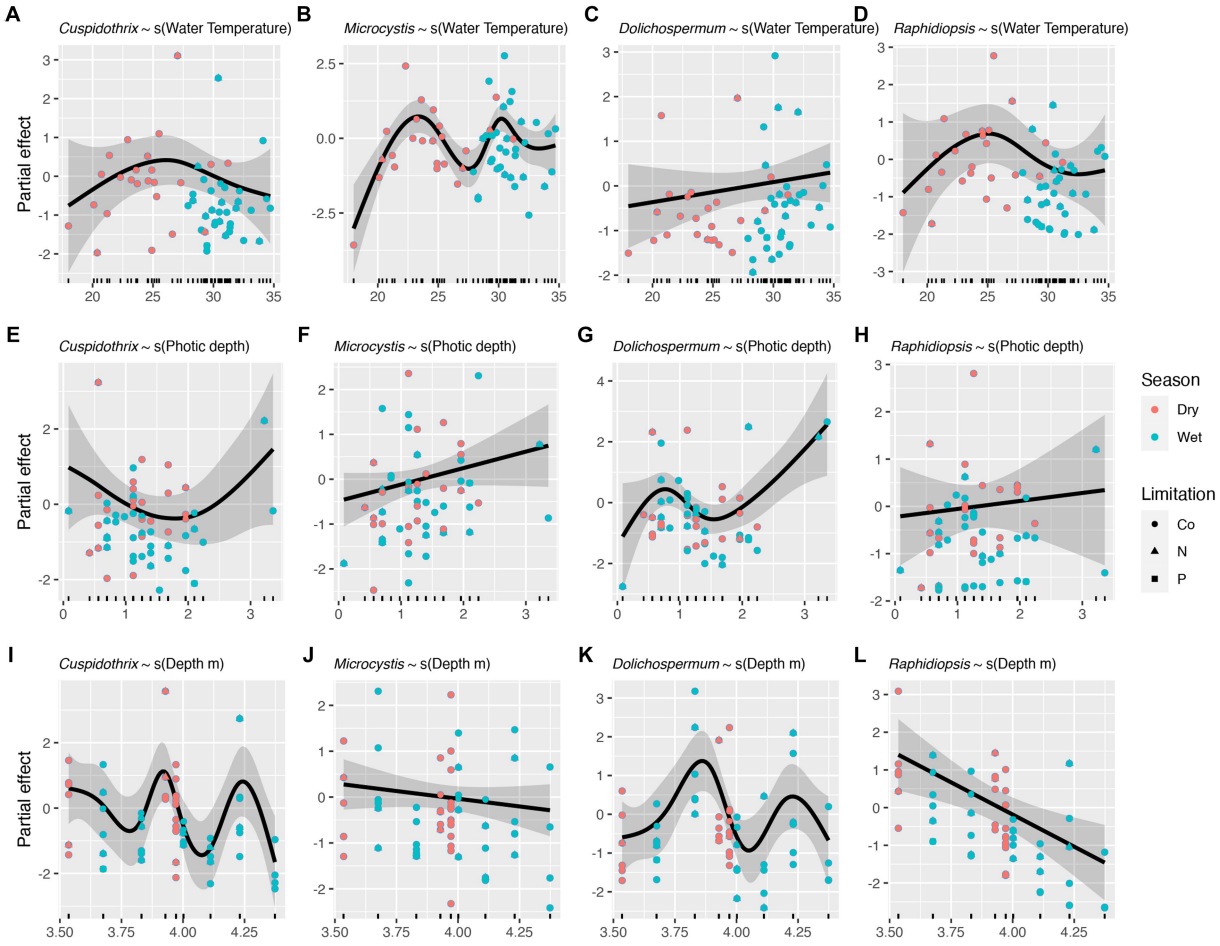

FIGURE 8
Effects of water temperature **(A–D)**, photic depth **(E–H)**, lake depth **(I–L)**, on bloom forming cyanobacteria as identified with generalized additive models (GAMs). Shaded areas indicate 95% confidence intervals, shapes indicate limitation, and colors indicate season.

4.1. Cyanobacterial diversity and cyanotoxins

Many of the cyanobacterial taxa that are well documented in the literature via microscopy (e.g., *Aphanizomenon*, *Dolichospermum* [=*Anabaena*], *Microcystis,* and *Raphidiopsis* [=*Cylindrospermopsis*]) were identified from the molecular methods employed in this study. Surprisingly, the high abundance of Prochlorococcacean cyanobacteria was not expected, as these taxa are not well recorded in Lake Okeechobee, likely due to their small size (< 2 μm). Additionally, the cyanobacterial genus *Planktolyngbya*, whose presence in Lake Okeechobee is well documented (e.g., Beaver et al., 2013), was not observed in the molecular data. However, *Limnolyngbya* was observed which was separated from *Planktolyngbya* (Li and Li, 2016), and may be the correct taxon. Within the Aphanizomenonaceae a single ASV (176) clustered with sequences classified as *Anabaena* and *Dolichospermum* but away from these genera (Supplementary Figure S3). Within the Microcystaceae, the ASVs labeled as Microcystaceae Cluster 1, clustered with sequences from the freshwater lakes, Las Cumbres Lake (Panama) and Reelfoot Lake (Tennessee, United States), and may represent a widespread cyanobacterium (Supplementary Figure S4). Phylogenetic inferences of the ASVs that could not be classified past the class level revealed potentially novel cyanobacterial diversity within the lake. There were two clades of ASV's which clustered within the Leptolyngbyaceae and Synechococcaceae, respectively, which may represent novel diversity (Supplementary Figure S6).

Picocyanobacteria (<2 μm) belonging to the family Prochlorococcaceae dominated the cyanobacterial community throughout the lake, with *Cyanobium* demonstrating the highest relative abundance followed by *Vulcanococcus*. The genera *Dolichospermum*, *Microcystis*, and *Raphidiopsis* are known to cause cyanoHABs within Lake Okeechobee (e.g., Jones, 1987; James et al., 2008; Kramer et al., 2018) and were highly abundant throughout the lake during this study (Figure 2). Other bloom-forming, diazotrophic *Aphanizomenon*-like and *Dolichospermum*-like genera, such as *Cuspidothrix* and *Sphaerospermopsis*, were also observed in the molecular data, although their presence in Lake Okeechobee have not been recorded, likely due to their cryptic morphology (Rajaniemi et al., 2005; Werner et al., 2012).

Notably, *Dolichospermum* was not correlated to microcystins nor to nodularins (Supplementary Figure S13). *Dolichospermum* is known to produce several cyanotoxins (Otten and Paerl, 2015), however toxin production by *Dolichospermum* within Lake Okeechobee remains unknown, although metagenomic analyses suggest it may produce saxitoxin (Kramer et al., 2018). From the correlation analysis, the

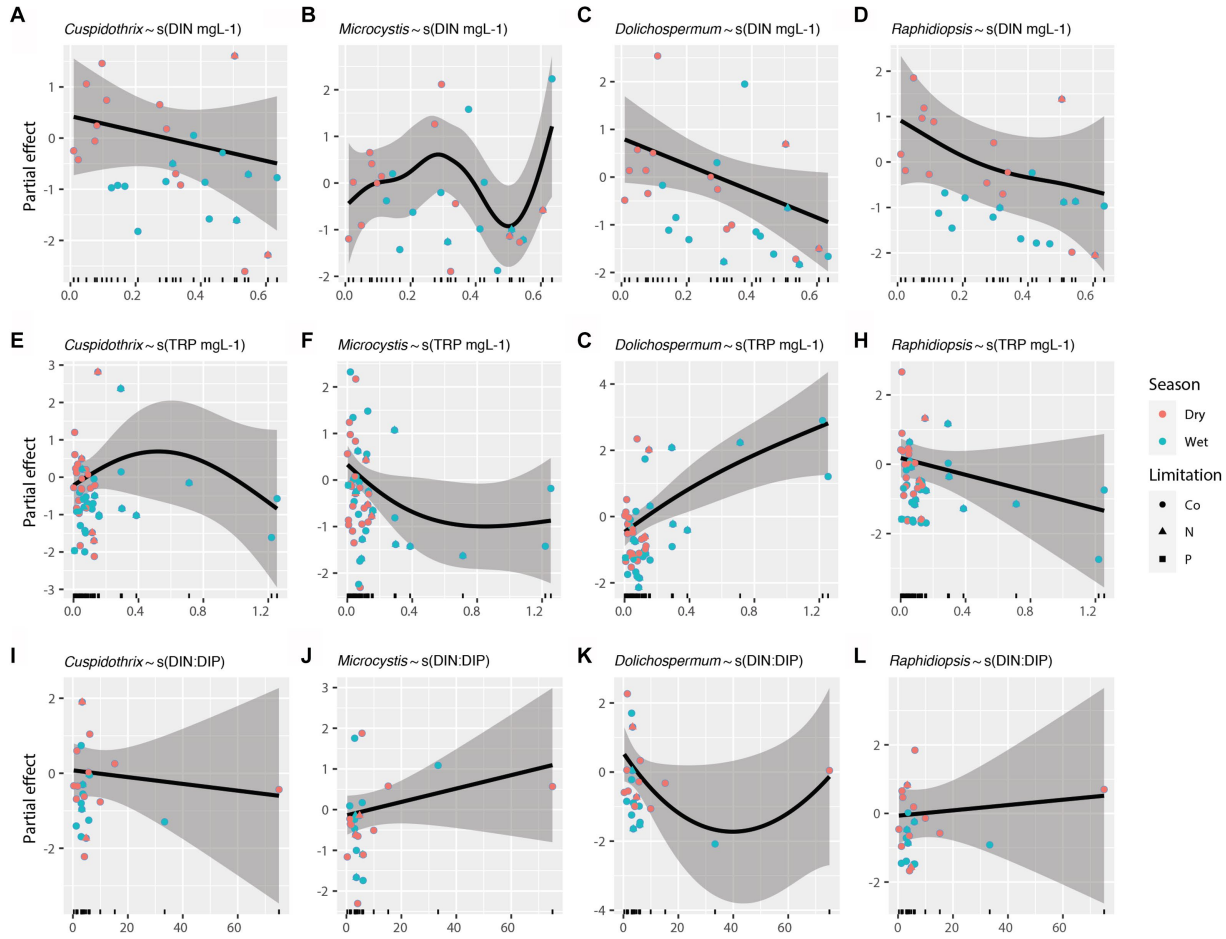

FIGURE 9
Effects of dissolved inorganic nitrogen **(A–D)**, total reactive phosphorus **(E–H)**, and DIN:DIP **(I–L)** on bloom forming cyanobacteria as identified with generalized additive models (GAMs). Shaded areas indicate 95% confidence intervals, shapes indicate limitation, and colors indicate season.

potential producer of nodularins remains obscure as none of the positively correlated genera are known producers of nodularins (Supplementary Figure S13). Conversely, *Iningainema* is an established nodularin producer (McGregor and Sendall, 2017; Berthold et al., 2021) which is known to occur in the lake (Laughinghouse lab, unpublished data), however its abundance was negatively correlated to nodularin concentrations (Supplementary Figure S13). *Microcystis* is a known microcystins producer within Lake Okeechobee (Lefler et al., 2020; Kinley-Baird et al., 2021) and is the likely toxin producer, although other taxa may also be producing these toxins. The correlations between the picocyanobacteria genera and toxins (i.e., *Parasynechococcus* with MC-LR, and Prochlorococcaceae_XX with nodularin) were unexpectedly high considering the diversity of the known toxigenic taxa (Supplementary Figure S13). While this group are not traditionally considered toxigenic, it has been recently found that picocyanobacteria in tropical freshwaters are capable of cylindrospermopsin production (Gin et al., 2021; Sim et al., 2023). Thus, it imperative to further assess the toxigenic potential of these abundant cyanobacteria. The lack of definitive correlations between a genus (or genera) and toxins highlights the unknown toxigenic potential within the lake.

The community structure was more variable during the wet season, while communities from the dry season were more similar (Figure 5C). Communities within both seasons were dominated by picocyanobacteria (e.g., *Cyanobium*) with an non-significant increase in *Dolichospermum* in the wet season (PERMANOVA $R^2 = 0.02$, $p = 0.2$), and significant increase in *Raphidiopsis* in the dry season (PERMANOVA $R^2 = 0.08$, $p = 0.02$; Figure 5D). *Raphidiopsis* relative abundance was higher in the dry season (Figure 5D) and determined to be an indicator species for dry season communities (Supplementary Table S1). Furthermore, *Raphidiopsis* relative abundance was higher at Moore Haven, the headwaters of the Caloosahatchee River, a shallow area of the lake within the rim canal. While *Raphidiopsis* blooms are uncommon in Lake Okeechobee, *Raphidiopsis*-dominated blooms have recently been observed in the shallow areas of the lake (i.e., transition zone) during dry periods (Laughinghouse and Lefler, pers. observ.). The communities at the mouth of the Kissimmee River had a higher relative abundance of *Microcystis* in comparison to other locations (Figure 4D). This region of Lake Okeechobee is known to have increased frequency of *Microcystis*-dominated cyanoHABs, likely due to external nutrient loading from the Kissimmee drainage basin (Havens et al., 1994). Conversely, the southern region of the lake is distant from major inflows and thus external nutrient loadings and was found to possess higher relative abundance of *Dolichospermum* (Figures 2, 4D).

4.2. Drivers of abundant cyanobacterial genera

Increases in both N and P are known to drive the growth of bloom-forming genera, although their concentrations and ratios have disparate effects on these genera (Paerl et al., 2016). Our results highlight the disparate responses in abundances of these bloom-forming genera to N, P, and DIN:DIP. While increasing DIN concentrations had a negative relationship on relative abundance of the bloom-forming diazotrophic genera, as expected, only *Dolichospermum* relative abundance had a positive, and linear, response to increasing TRP concentrations (Figures 9E,G,H). *Cuspidothrix* relative abundance was highest with TRP concentrations around ~0.5 mg L^{-1} (Figure 9E), potentially indicating this genus has lower P requirements, but higher than that of *Raphidiopsis*. These data suggest that P concentrations do not affect all bloom-forming diazotrophic genera similarly. Furthermore, *Raphidiopsis* relative abundance had an increased, although weak, response to DIN:DIP, whereas *Cuspidothrix* and *Dolichospermum* relative abundances were negatively correlated with increasing DIN:DIP (Figures 9I,K,L), suggesting that DIN:DIP, and potentially TN:TP, does not affect all diazotrophs equally. *Dolichospermum* and *Microcystis* relative abundances were positively affected by photic depth (Figures 8F,G; Table 1), supporting previous research on their drivers within Lake Okeechobee (Havens et al., 1998, 2003). *Cuspidothrix* and *Raphidiopsis* relative abundances were both generally unaffected by photic depth, indicating these genera are more adapted to low light conditions, an observation supported by previous research on *Raphidiopsis* within the system (Havens et al., 2003).

Altogether, these genera have overlapping, but distinct niches within Lake Okeechobee. *Dolichospermum* and *Microcystis* favor the warmer wet season, in clear waters with increased photic depth, which align with previous research on the lake (Havens et al., 1998). They differ in their nutrient requirements, with *Dolichospermum* benefitting from waters with low DIN and high TRP concentrations whereas *Microcystis* is ambivalent to TRP concentrations and prefers waters with a high DIN:DIP (Paerl et al., 2016; Chia et al., 2018). *Cuspidothrix* and *Raphidiopsis* were more prevalent during the cooler waters of the dry season with low DIN, where *Cuspidothrix* relative abundance is correlated with higher photic depths and *Raphidiopsis* is correlated with shallow waters.

Spatially, *Dolichospermum* relative abundance was highest in the southern region of the lake (i.e., South Lake and Clewiston), away from sites of significant hydrological, and thus external nutrient, inputs. This genus prefers increased SRP concentrations and likely benefits from the internal legacy P that is continuously resuspended and released from the sediments. Furthermore, the lack of an external N load likely behooves *Dolichospermum* in so far as reducing competition from non-diazotrophic bloom forming genera, specifically *Microcystis*. *Microcystis* relative abundances was highest in the northern part of the lake, at the mouth of the Kissimmee River, which is known to have an increased abundance of *Microcystis* (Havens et al., 1994). Kramer et al. (2018) indicated that increases in N concentrations in Lake Okeechobee promotes non-diazotrophic cyanobacterial abundance in the lake and data from Zhang et al. (2011) show a significant increase in TN concentrations from several point sources in this region of the watershed. The increase in *Microcystis* abundance in the northern region is likely due to the N rich inputs from the Kissimmee drainage basin via the Kissimmee River, which accounts for ~70% of the inputs into Lake Okeechobee (Zhang J. et al., 2020), as well as the surrounding agricultural and urban inputs. This area has a large drainage basin that is affected by both agricultural and urban runoff, contributing to nutrient inputs (e.g., N & P). Modern fertilizers are comprised of ammonium and urea as their source of nitrogen and their increased use is hypothesized to drive harmful algal blooms, known as the HAB-HB (Harmful Algal Bloom-Haber Bosch) connection (Glibert et al., 2014); additional sources of urea include sewage/septic and livestock runoff. Urea can represent >50% of the dissolved organic nitrogen pool and can be high in agriculturally impacted lakes (Bogard et al., 2012). An increase in urea may give *Microcystis* a competitive advantage as it is capable of assimilating urea as a source of carbon and nitrogen (Krausfeldt et al., 2019). However, neither total nitrogen nor organic nitrogen were quantified during this study and, to the authors best knowledge, urea concentrations in Lake Okeechobee are unknown. The effects of urea, and other forms of organic nitrogen, on *Microcystis* abundance in Lake Okeechobee remain unknown and warrants further investigation to better understand bloom drivers in this system.

Considering the lake is an N, or co-nutrient, limited system, nitrogen inputs also likely lead to an increase in N:P. During this study, the northern region was frequently co-nutrient limited, experiencing N-limitation only briefly (Supplementary Figure S1). Together these results, along with results from Kramer et al. (2018), suggest N inputs, both organic and inorganic, from the Kissimmee River can promote increased *Microcystis* abundance in the northern region of the lake, potentially effectuating *Microcystis* blooms throughout Lake Okeechobee. Furthermore, there is a need to understand the role of organic N (e.g., urea) within this system to determine how much is coming into the lake and its effect on *Microcystis* and other bloom forming taxa.

In comparison to the bloom-forming genera, the drivers of the picocyanobacteria are more elusive. Notably, *Vulcanococcus* relative abundance was positively correlated with water temperatures, and decreased with increased DIN:DIP (Supplementary Figures S11A, S12C), whereas the relative abundance of *Cyanobium* decreased with increasing TRP (Supplementary Figure S12B). The picocyanobacteria likely dominate the system due to their large surface-to-volume ratio that facilitates nutrient uptake when nutrients are scarce and reduces their light requirements (Havens et al., 1998).

Since the taxonomic resolution of metabarcoding is limited, the potential drivers are for the genera, and are not species specific. A total of six ASVs corresponded to *Microcystis* (Supplementary Figure S4), which may be several different species of *Microcystis*. *Microcystis* species are known to form microcystin-producing blooms within Lake Okeechobee (Kinley-Baird et al., 2021; Pokrzywinski et al., 2022), however both microcystin and non-microcystin producing *Microcystis* species are known to occur and bloom in Florida (Lefler et al., 2020, 2022, 2023). Furthermore, recent phylogenomic analyses supported several of the morphologically different species of *Microcystis*, each with various toxigenic potential (Cai et al., 2023). Similarly, several species of *Dolichospermum* and *Raphidiopsis* are known to occur in Lake Okeechobee (Cichra et al., 1995; Havens et al., 2003). Due to the diversity of bloom-forming genera within Lake Okeechobee, it is imperative to characterize these taxa and experimentally test how limnological parameters (e.g., N, P, water temperature, etc.) affect their potential to bloom and synthesize various toxins using *in-situ*, *ex-situ*, and strain level approaches (e.g., Kramer et al., 2018; Wagner et al., 2021).

4.3. Cyanobacterial-bacterial relationships

Cyanobacterial-bacterial relationships have garnered large interest in the past years (Morris et al., 2011; Cook et al., 2020; Smith et al., 2021), highlighting the importance of these enigmatic relationships. These relationships can be mutualistic (Woodhouse et al., 2016), cyanoHABs can alter the bacterioplankton communities (Berry et al., 2017), and some cyanobacterial genera (e.g., *Microcystis*) can be dependent on bacteria, and cyanobacteria, within their mucilage (Cook et al., 2020). Relationships between *Microcystis* and bacteria have been the focus of much research (e.g., Cook et al., 2020; Smith et al., 2022). However, these studies have concentrated on the relationships between *Microcystis* and the epibiont bacterial communities (e.g., Cook et al., 2020; Smith et al., 2021) or understanding the distinctions between epibiont and pelagic bacterial communities during bloom conditions (e.g., Parveen et al., 2013; Louati et al., 2023). However, temporal associations between cyanobacterial and co-occurring bacterioplankton during non-bloom conditions are rarely investigated. Previous research on Lake Taihu (China), another shallow subtropical lake, indicated that the bacterial community structure changes with the phytoplankton community (Niu et al., 2011).

Overall, the bacterial and cyanobacterial communities changed concurrently, with significant differences between communities in the wet and dry seasons, with neither cyanobacterial nor bacterial communities differing between N or co-limitation. The majority of the associated bacterial taxa belonged to the Proteobacteria (=Pseudomonadota; Figure 3), which was the dominate bacterial phylum, excluding Cyanobacteriota (Supplementary Figures S8C,D). Of the bloom forming genera *Cuspidothrix*, *Dolichospermum*, *Microcystis*, and *Raphidiopsis*, only *Cuspidothrix* and *Raphidiopsis* were correlated. Furthermore, only a single bacterial taxon, an unknown member of the Firmicutes (=Bacillota) was shared between *Dolichospermum* and *Microcystis*, this lack of correlated bacteria is supported by results from Louati et al. (2015) (Figure 3). *Cuspidothrix* and *Raphidiopsis* both occupied a similar niche within Lake Okeechobee and were correlated with each other but shared no correlated taxa. However, *Cuspidothrix* and *Microcystis* occupied distinct niches within Lake Okeechobee, and were not correlated with each other, but were both positively correlated with the cyanobacterial genus *Pseudanabaena* (Figure 3). This genus is known to occur within the mucilage of *Microcystis* colonies and may occupy the sheath of *Cuspidothrix*. Despite the dominance of *Cyanobium*, this genus was not correlated to the common bloom-forming genera, *Cuspidothrix*, *Dolichospermum*, and *Raphidiopsis*, but was correlated with *Microcystis* (Figure 3).

Dolichospermum shared correlations with several bacteria ($n = 11$) across five phyla, compared to *Microcystis*' two (Figure 3). *Cuspidothrix* was also correlated to several bacteria ($n = 4$) across three phyla. This may indicate that *Cuspidothrix* and *Dolichospermum* have coevolved with these bacteria and/or have a symbiotic relationship. Conversely, *Raphidiopsis* was only positively correlated to a single bacteria genus, *Rubellimicrobium*, a member of the Pseudomonadota, and may not be as reliant on bacterial interactions as *Dolichospermum*. However, more in-depth analyses (e.g., *in situ* metagenomic and metatranscriptomic studies, laboratory experiments) are needed to better understand these relationships (e.g., Vico et al., 2021; Zuo et al., 2022).

In addition to other cyanobacteria, *Microcystis* was only positively correlated to Pseudomonadota, with its sole negative correlation with an unknown member of the Desulfobacterota (Figure 3). Proteobacteria are known to co-occur with *Microcystis* blooms (Parveen et al., 2013; Louati et al., 2023) and are copiotrophic (Simonato et al., 2010). One of the known correlated genera within the Pseudomonadota was *Silanimonas*. *Silanimonas* is known to co-exist with *Microcystis*, and the species *S. algicola* was isolated from a *Microcystis* colony (Chun et al., 2017). This species is known to perform nitrate reduction, part of the denitrification process in aerobic systems. However, it remains to be seen if denitrification was occurring, although denitrification is known to occur during cyanoHABs (Chen et al., 2011; Zhang et al., 2017).

In contrast to the bloom-forming genera, the picocyanobacteria (*Cyanobium*, *Lacustricoccus*, and *Regnicoccus*) were correlated with several bacteria and cyanobacteria (Figure 3). Whereas *Vulcanococcus* possessed few correlated taxa, many of which were negative. Similarly, to the closely related *Prochlorococcus*, these freshwater picocyanobacteria are likely reliant on co-occurring bacterial taxa (Morris et al., 2012).

Understanding the complex relationships between bacteria and cyanobacteria has the potential to provide valuable insights into functional bacterial traits that may assist cyanobacterial bloom proliferations (Louati et al., 2023). Due to the limitations of these data (i.e., 16S rRNA), those potential functional roles of the co-occurring pelagic bacterial taxa cannot be assessed; however, future efforts should be mindful of these relationships. Additionally, due to the shallow depth and polymictic nature of Lake Okeechobee, we cannot rule out if some of these bacterial taxa are particle-associated, and resuspended sediment particles. Furthermore, this study was limited to the bacterial community, and relationships with protists and other microalgae were not studied and may help further elucidate these dynamics. These data do, however, highlight an important observation that within the same water body, disparate bloom-forming cyanobacteria co-occur with dissimilar associated bacterial taxa.

5. Conclusion

These data highlight the cyanobacterial diversity within Lake Okeechobee, confirming the presence of many genera found from previous morphological assessments of the cyanobacteria, as well as highlighting potentially novel cyanobacteria. *Cyanobium* dominates the cyanobacterial communities, with *Cuspidothrix*, *Dolichospermum*, *Microcystis*, *Raphidiopsis*, and *Vulcanococcus* as the most abundant described genera. There were no differences between cyanobacterial nor bacterial communities during N or co-nutrient limitation. The cyanobacterial and bacterial communities significantly differ between wet and dry season, with a significant increase in *Raphidiopsis* in the dry season, although both seasons showed dominance of the picocyanobacteria. *Cuspidothrix*, *Dolichospermum*, *Microcystis*, and *Raphidiopsis* were the most commonly occurring bloom-forming taxa and possessed contrasting environmental drivers and microbial communities. Overall, these three bloom-forming genera have distinct abiotic drivers within Lake Okeechobee. Both *Dolichospermum* and *Microcystis* prefer the warmer wet season, in waters with increased photic depth. Our results, along with others (i.e., Havens et al., 1994; Kramer et al., 2018), suggest N inputs, both organic and inorganic,

from the Kissimmee River can promote *Microcystis* abundance in the northern region of the lake, potentially effectuating *Microcystis* blooms in Lake Okeechobee. Furthermore, there is a need to understand the effects of organic forms of N (e.g., urea) on *Microcystis* in this system to elucidate whether it's a species of nitrogen (e.g., NO_3, urea, etc.) or solely the N:P ratio which may drive these proliferations. *Dolichospermum* increased abundance in the southern region of the lake, away from external nutrient inputs, may indicate that it benefits from resuspension of legacy P from sediments from the increased weather events associated with the wet season. In addition to their disparate abiotic drivers, these two genera were correlated with distinct bacteria, which may facilitate their ability to form blooms and out-compete one another, or other, cyanobacteria when conditions are right. *Cuspidothrix* and *Raphidiopsis* relative abundance increases in the cooler waters of the dry season, with low DIN and TRP concentrations. While these genera are correlated (Figure 3), and have similar nutrient requirements (Figure 9), they differ by lake depth, with *Raphidiopsis* relative abundance higher in shallow waters. Additionally, *Cuspidothrix* and *Raphidiopsis* have distinct correlated bacteria, which may promote dominance of one over the other when abiotic conditions are ideal for both.

These data highlight the variable nutrient requirement and niches these bloom-forming genera occupy within Lake Okeechobee, increasing our understanding of who is blooming when and why. They also highlight the need for dual nutrient control, as increases in both N and P can drive different bloom-forming genera.

Data availability statement

Sequences were deposited at the Sequence Read Archive of the National Center for Biotechnology Information (NCBI) and made publicly available under accession number PRJNA967631. R code used for data analysis, including a full list of R packages, is on GitHub (github.com/flefler/LakeOkeechobee_16SrRNA).

Author contributions

FL, DB, and HL contributed to the conception and design of the study and finalized the manuscript. FL, MB, DB, and HL collected data. FL, MB, DB, and PZ were responsible for the laboratory data analyses. FL analyzed sequencing data, performed statistical analyses, and wrote the first draft of the manuscript. HL supervised the project and secured funding. FL, MB, DB, PZ, AS, and HL critically reviewed the draft and provided feedback. All authors contributed to the article and approved the submitted version.

Funding

The authors acknowledge the University of Florida—IFAS Seed Fund and USDA-NIFA Hatch Project #FLA-FTL-00565697 for financial support.

Acknowledgments

The authors would like to thank the US Army Corps South Florida Operations Office for logistical support in the field. For PZ, this is contribution #99 from the Rice Rivers Center, VCU.

Conflict of interest

The authors declare that the research was conducted in the absence of any commercial or financial relationships that could be construed as a potential conflict of interest.

Publisher's note

Supplementary material

The Supplementary material for this article can be found online at: https://www.frontiersin.org/articles/10.3389/fmicb.2023.1219261/full#supplementary-material

References

Almanza, V., Pedreros, P., Laughinghouse, H. D., Félez, J., Parra, O., Azócar, M., et al. (2019). Association between trophic state, watershed use, and blooms of cyanobacteria in south-Central Chile. *Limnologica* 75, 30–41. doi: 10.1016/j.limno.2018.11.004

APHA (2017). *Standard methods for the examination of water and wastewater*, *23rd* Edn. American Public Health Association; American Water Works Association; Water Environment Federation Washington, DC, USA.

Baird, R., and Bridgewater, L. (2017). *Standard methods for the examination of water and wastewater*, *23rd* Edn. American Water Works Association: Washington, DC, USA.

Beaver, J. R., Casamatta, D. A., East, T. L., Havens, K. E., Rodusky, A. J., James, R. T., et al. (2013). Extreme weather events influence the phytoplankton community structure in a large lowland subtropical lake (Lake Okeechobee, Florida, USA). *Hydrobiologia* 709, 213–226. doi: 10.1007/s10750-013-1451-7

Bell, W., and Mitchell, R. (1972). Chemotactic and growth responses of marine bacteria to algal extracellular products. *Biol. Bull.* 143, 265–277. doi: 10.2307/1540052

Berry, M. A., White, J. D., Davis, T. W., Jain, S., Johengen, T. H., Dick, G. J., et al. (2017). Are Oligotypes meaningful ecological and phylogenetic units? A case study of Microcystis in Freshwater Lakes. *Front. Microbiol.* 8:365. doi: 10.3389/fmicb.2017.00365

Berthold, D. E., Lefler, F. W., Huang, I.-S., Abdulla, H., Zimba, P. V., and Laughinghouse, H. D. (2021). Iningainema tapete sp. nov. (Scytonemataceae, Cyanobacteria) from greenhouses in central Florida (USA) produces two types of nodularin with biosynthetic potential for microcystin-LR and anabaenopeptin production. *Harmful Algae* 101:101969. doi: 10.1016/j.hal.2020.101969

Bogard, M. J., Donald, D. B., Finlay, K., and Leavitt, P. R. (2012). Distribution and regulation of urea in lakes of Central North America: urea in prairie lakes. *Freshw. Biol.* 57, 1277–1292. doi: 10.1111/j.1365-2427.2012.02775.x

Bonilla, S., Aguilera, A., Aubriot, L., Huszar, V., Almanza, V., Haakonsson, S., et al. (2023). Nutrients and not temperature are the key drivers for cyanobacterial biomass in the Americas. *Harmful Algae* 121:102367. doi: 10.1016/j.hal.2022.102367

Cai, H., McLimans, C. J., Beyer, J. E., Krumholz, L. R., and Hambright, K. D. (2023). *Microcystis* pangenome reveals cryptic diversity within and across morphospecies. *Sci. Adv.* 9:eadd3783. doi: 10.1126/sciadv.add3783

Callahan, B. J., McMurdie, P. J., Rosen, M. J., Han, A. W., Johnson, A. J. A., and Holmes, S. P. (2016). DADA2: high-resolution sample inference from Illumina amplicon data. *Nat. Methods* 13, 581–583. doi: 10.1038/nmeth.3869

Canfield, D. E., Bachmann, R. W., and Hoyer, M. V. (2021). Restoration of Lake Okeechobee, Florida: mission impossible? *Lake Reserv Manage* 37, 95–111. doi: 10.1080/10402381.2020.1839607

Capella-Gutiérrez, S., Silla-Martínez, J. M., and Gabaldón, T. (2009). trimAl: a tool for automated alignment trimming in large-scale phylogenetic analyses. *Bioinformatics* 25, 1972–1973. doi: 10.1093/bioinformatics/btp348

Chen, J., Bittinger, K., Charlson, E. S., Hoffmann, C., Lewis, J., Wu, G. D., et al. (2012). Associating microbiome composition with environmental covariates using generalized UniFrac distances. *Bioinformatics* 28, 2106–2113. doi: 10.1093/bioinformatics/bts342

Chen, W., Liu, H., Zhang, Q., and Dai, S. (2011). Effect of nitrite on growth and microcystins production of Microcystis aeruginosa PCC7806. *J. Appl. Phycol.* 23, 665–671. doi: 10.1007/s10811-010-9558-y

Chen, X., Yang, L., Xiao, L., Miao, A., and Xi, B. (2012). Nitrogen removal by denitrification during cyanobacterial bloom in Lake Taihu. *J. Freshwater Ecol.* 27, 243–258. doi: 10.1080/02705060.2011.644405

Chia, M. A., Jankowiak, J. G., Kramer, B. J., Goleski, J. A., Huang, I.-S., Zimba, P. V., et al. (2018). Succession and toxicity of Microcystis and anabaena (Dolichospermum) blooms are controlled by nutrient-dependent allelopathic interactions. *Harmful Algae* 74, 67–77. doi: 10.1016/j.hal.2018.03.002

Chun, S.-J., Cui, Y., Ko, S.-R., Lee, H.-G., Oh, H.-M., and Ahn, C.-Y. (2017). Silanimonas algicola sp. nov., isolated from laboratory culture of a bloom-forming cyanobacterium, Microcystis. *Int. J. Syst. Evol. Microbiol.* 67, 3274–3278. doi: 10.1099/ijsem.0.002102

Cichra, M. F., Badylak, S., Henderson, N., Rueter, B. H., and Phlips, E. J. (1995). Phytoplankon community structure in the open water zone of a shallow subtropical lake (Lake Okeechobee, Florida, USA). *Archiv für Hydrobiologie* 45, 157–175.

Cook, K. V., Li, C., Cai, H., Krumholz, L. R., Hambright, K. D., Paerl, H. W., et al. (2020). The global *Microcystis* interactome. *Limnol. Oceanogr.* 65:11361. doi: 10.1002/lno.11361

Darriba, D., Posada, D., Kozlov, A. M., Stamatakis, A., Morel, B., and Flouri, T. (2020). ModelTest-NG: A new and scalable tool for the selection of DNA and protein evolutionary models. *Mol. Biol. Evol.* 37, 291–294. doi: 10.1093/molbev/msz189

Davis, F. E., and Marshall, M. L. (1975). Chemical and biological investigations of Lake Okeechobee January 1973—June 1974 interim Report.

De Cáceres, M., and Legendre, P. (2009). Associations between species and groups of sites: indices and statistical inference. *Ecology* 90, 3566–3574. doi: 10.1890/08-1823.1

Djurhuus, A., Port, J., Closek, C. J., Yamahara, K. M., Romero-Maraccini, O., Walz, K. R., et al. (2017). Evaluation of filtration and DNA extraction methods for environmental DNA biodiversity assessments across multiple trophic levels. *Front. Mar. Sci.* 4:314. doi: 10.3389/fmars.2017.00314

Falkowski, P. G., Fenchel, T., and Delong, E. F. (2008). The microbial engines that drive Earth's biogeochemical cycles. *Science* 320, 1034–1039. doi: 10.1126/science.1153213

Fisher, M. M., Reddy, K. R., and James, R. T. (2005). Internal nutrient loads from sediments in a shallow, subtropical Lake. *Lake Reserv Manage* 21, 338–349. doi: 10.1080/07438140509354439

Garcia, S. L., Buck, M., McMahon, K. D., Grossart, H. P., Eiler, A., and Warnecke, F. (2015). Auxotrophy and intrapopulation complementary in the 'interactome' of a cultivated freshwater model community. *Mol. Ecol.* 24, 4449–4459. doi: 10.1111/mec.13319

Gin, K. Y. H., Sim, Z. Y., Goh, K. C., Kok, J. W. K., Te, S. H., Tran, N. H., et al. (2021). Novel cyanotoxin-producing Synechococcus in tropical lakes. *Water Res.* 192:116828. doi: 10.1016/j.watres.2021.116828

Glibert, P. M., Maranger, R., Sobota, D. J., and Bouwman, L. (2014). The Haber Bosch–harmful algal bloom (HB–HAB) link. *Environ. Res. Lett.* 9:105001. doi: 10.1088/1748-9326/9/10/105001

Havens, K. E. (1995). Secondary nitrogen limitation in a subtropical lake impacted by non-point source agricultural pollution. *Environ. Pollut.* 89, 241–246. doi: 10.1016/0269-7491(94)00076-P

Havens, K. E., Hanlon, C., and James, R. T. (1994). Seasonal and spatial variation in algal bloom frequencies in Lake Okeechobee, Florida, U.S.A. *Lake Reserv Manage* 10, 139–148. doi: 10.1080/07438149409354185

Havens, K. E., James, R. T., East, T. L., and Smith, V. H. (2003). N:P ratios, light limitation, and cyanobacterial dominance in a subtropical lake impacted by non-point source nutrient pollution. *Environ. Pollut.* 122, 379–390. doi: 10.1016/S0269-7491(02)00304-4

Havens, K. E., Phlips, E. J., Cichra, M. F., and Li, B. (1998). Light availability as a possible regulator of cyanobacteria species composition in a shallow subtropical lake. *Freshw. Biol.* 39, 547–556. doi: 10.1046/j.1365-2427.1998.00308.x

Havens, K., Paerl, H., Phlips, E., Zhu, M., Beaver, J., and Srifa, A. (2016). Extreme weather events and climate variability provide a lens to how Shallow Lakes may respond to climate change. *Water* 8:229. doi: 10.3390/w8060229

Huang, I.-S., Pinnell, L. J., Turner, J. W., Abdulla, H., Boyd, L., Linton, E. W., et al. (2020). Preliminary assessment of microbial community structure of wind-tidal flats in the Laguna Madre, Texas, USA. *Biology* 9:183. doi: 10.3390/biology9080183

Huang, I.-S., and Zimba, P. V. (2019). Cyanobacterial bioactive metabolites—A review of their chemistry and biology. *Harmful Algae* 86, 139–209. doi: 10.1016/j.hal.2019.05.001

Jackrel, S. L., Yang, J. W., Schmidt, K. C., and Denef, V. J. (2021). Host specificity of microbiome assembly and its fitness effects in phytoplankton. *ISME J.* 15, 774–788. doi: 10.1038/s41396-020-00812-x

James, R. T., and Pollman, C. D. (2011). Sediment and nutrient management solutions to improve the water quality of Lake Okeechobee. *Lake Reserv Manage* 27, 28–40. doi: 10.1080/07438141.2010.536618

James, T. R., Chimney, M. J., Sharfstein, B., Engstrom, D. R., Schottler, S. P., East, T., et al. (2008). Hurricane effects on a shallow lake ecosystem, Lake Okeechobee, Florida (USA). *Fundam. Appl. Limnol.* 172, 273–287. doi: 10.1127/1863-9135/2008/0172-0273

Jones, B. (1987). Lake Okeechobee eutrophication research and management. *Aquaculture* 9, 21–26.

Joyner, B. F. (1974). Chemical and biological conditions of Lake Okeechobee, Florida, 1969-72. *Florida Geol Survey*. doi: 10.35256/RI71

Katoh, K., and Standley, D. M. (2013). MAFFT multiple sequence alignment software version 7: improvements in performance and usability. *Mol. Biol. Evol.* 30, 772–780. doi: 10.1093/molbev/mst010

Khomutovska, N., de los Ríos, A., and Jasser, I. (2020). Diversity and colonization strategies of endolithic cyanobacteria in the Cold Mountain desert of Pamir. *Microorganisms* 9:6. doi: 10.3390/microorganisms9010006

Kinley-Baird, C., Calomeni, A., Berthold, D. E., Lefler, F. W., Barbosa, M., Rodgers, J. H., et al. (2021). Laboratory-scale evaluation of algaecide effectiveness for control of microcystin-producing cyanobacteria from Lake Okeechobee, Florida (USA). *Ecotoxicol. Environ. Saf.* 207:111233. doi: 10.1016/j.ecoenv.2020.111233

Kozlov, A. M., Darriba, D., Flouri, T., Morel, B., and Stamatakis, A. (2019). RAxML-NG: a fast, scalable and user-friendly tool for maximum likelihood phylogenetic inference. *Bioinformatics* 35, 4453–4455. doi: 10.1093/bioinformatics/btz305

Kramer, B. J., Davis, T. W., Meyer, K. A., Rosen, B. H., Goleski, J. A., Dick, G. J., et al. (2018). Nitrogen limitation, toxin synthesis potential, and toxicity of cyanobacterial populations in Lake Okeechobee and the St. Lucie River estuary, Florida, during the 2016 state of emergency event. *PLoS One* 13:e0196278. doi: 10.1371/journal.pone.0196278

Krausfeldt, L. E., Farmer, A. T., Castro Gonzalez, H. F., Zepernick, B. N., Campagna, S. R., and Wilhelm, S. W. (2019). Urea is both a carbon and nitrogen source for *Microcystis aeruginosa*: tracking 13C incorporation at bloom pH conditions. *Front. Microbiol.* 10:1064. doi: 10.3389/fmicb.2019.01064

Kurtz, Z. D., Müller, C. L., Miraldi, E. R., Littman, D. R., Blaser, M. J., and Bonneau, R. A. (2015). Sparse and compositionally robust inference of microbial ecological networks. *PLoS Comput. Biol.* 11:e1004226. doi: 10.1371/journal.pcbi.1004226

Lapointe, B. E., Herren, L. W., and Paule, A. L. (2017). Septic systems contribute to nutrient pollution and harmful algal blooms in the St. Lucie estuary, Southeast Florida, USA. *Harmful Algae* 70, 1–22. doi: 10.1016/j.hal.2017.09.005

Lefler, F. W., Barbosa, M., Berthold, D. E., and Laughinghouse, H. D. (2020). Genome Sequences of Two *Microcystis aeruginosa* (*Chroococcales*, *Cyanobacteria*) Strains from Florida (United States) with Disparate Toxigenic Potentials. *Microbiol Resour Announc* 9, e00844–e00820. doi: 10.1128/MRA.00844-20

Lefler, F. W., Berthold, D. E., Barbosa, M., and Laughinghouse, H. D. (2022). The effects of algaecides and herbicides on a nuisance *Microcystis wesenbergii*-dominated bloom. *Water* 14:1739. doi: 10.3390/w14111739

Lefler, F. W., Berthold, D. E., and Laughinghouse, H. D. (2023). CyanoSeq: a database of cyanobacterial 16S rRNA sequences with curated taxonomy. *J. Phycol.* 59, 470–480. doi: 10.1111/jpy.13335

Li, X., and Li, R. (2016). *Limnolyngbya circumcreta gen.* & *comb. nov.* (Synechococcales, Cyanobacteria) with three geographical (provincial) genotypes in China. *Phycologia* 55, 478–491. doi: 10.2216/15-149.1

Li, Y., and Li, D. (2012). Competition between toxic Microcystis aeruginosa and nontoxic Microcystis wesenbergii with anabaena PCC7120. *J. Appl. Phycol.* 24, 69–78. doi: 10.1007/s10811-010-9648-x

Louati, I., Nunan, N., Tambosco, K., Bernard, C., Humbert, J.-F., and Leloup, J. (2023). The phyto-bacterioplankton couple in a shallow freshwater ecosystem: who leads the dance? *Harmful Algae* 126:102436. doi: 10.1016/j.hal.2023.102436

Louati, I., Pascault, N., Debroas, D., Bernard, C., Humbert, J.-F., and Leloup, J. (2015). Structural diversity of bacterial communities associated with bloom-forming freshwater cyanobacteria differs according to the cyanobacterial genus. *PLoS One* 10:e0140614. doi: 10.1371/journal.pone.0140614

MacKeigan, P. W., Garner, R. E., Monchamp, M.-È., Walsh, D. A., Onana, V. E., Kraemer, S. A., et al. (2022). Comparing microscopy and DNA metabarcoding techniques for identifying cyanobacteria assemblages across hundreds of lakes. *Harmful Algae* 113:102187. doi: 10.1016/j.hal.2022.102187

Ma, C., Li, Z., Mwagona, P. C., Rabbany, A., and Bhadha, J. H. (2022). Spatial and seasonal dynamics of phytoplankton groups and its relationship with environmental variables in Lake Okeechobee, USA. *J. Freshwater Ecol.* 37, 173–187. doi: 10.1080/02705060.2022.2032852

Marshall, M. L. (1977). Phytoplankton and Primary Productivity Studies in Lake Okeechobee. South florida water management district.

McGregor, G. B., and Sendall, B. C. (2017). Iningainema pulvinus gen nov., sp nov. (Cyanobacteria, Scytonemataceae) a new nodularin producer from Edgbaston Reserve, north-eastern Australia. *Harmful Algae* 62, 10–19. doi: 10.1016/j.hal.2016.11.021

McMurdie, P. J., and Holmes, S. (2013). Phyloseq: an R package for reproducible interactive analysis and graphics of microbiome census data. *PLoS One* 8:e61217. doi: 10.1371/journal.pone.0061217

McMurdie, P. J., and Holmes, S. (2014). Waste not, want not: why rarefying microbiome data is inadmissible. *PLoS Comput. Biol.* 10:e1003531. doi: 10.1371/journal.pcbi.1003531

Minh, B. Q., Schmidt, H. A., Chernomor, O., Schrempf, D., Woodhams, M. D., von Haeseler, A., et al. (2020). IQ-TREE 2: new models and efficient methods for phylogenetic inference in the genomic era. *Mol. Biol. Evol.* 37, 1530–1534. doi: 10.1093/molbev/msaa015

Moore, P. A., Reddy, K. R., and Fisher, M. M. (1998). Phosphorus flux between sediment and overlying water in Lake Okeechobee, Florida: spatial and temporal variations. *J. Environ. Qual.* 27, 1428–1439. doi: 10.2134/jeq1998.00472425002700060020x

Morris, J. J., Johnson, Z. I., Szul, M. J., Keller, M., and Zinser, E. R. (2011). Dependence of the cyanobacterium Prochlorococcus on hydrogen peroxide scavenging microbes for growth at the Ocean's surface. *PLoS One* 6:e16805. doi: 10.1371/journal.pone.0016805

Morris, J. J., Lenski, R. E., and Zinser, E. R. (2012). The black queen hypothesis: evolution of dependencies through adaptive gene loss. *MBio* 3, e00036–e00012. doi: 10.1128/mBio.00036-12

Niu, Y., Shen, H., Chen, J., Xie, P., Yang, X., Tao, M., et al. (2011). Phytoplankton community succession shaping bacterioplankton community composition in Lake Taihu, China. *Water Res.* 45, 4169–4182. doi: 10.1016/j.watres.2011.05.022

Nübel, U., Garcia-Pichel, F., and Muyzer, G. (1997). PCR primers to amplify 16S rRNA genes from cyanobacteria. *Appl. Environ. Microbiol.* 63, 3327–3332. doi: 10.1128/aem.63.8.3327-3332.1997

O'Neil, J. M., Davis, T. W., Burford, M. A., and Gobler, C. J. (2012). The rise of harmful cyanobacteria blooms: the potential roles of eutrophication and climate change. *Harmful Algae* 14, 313–334. doi: 10.1016/j.hal.2011.10.027

Oksanen, J., Blanchet, F. G., Friendly, M., Kindt, R., Legendre, P., McGlinn, D., et al. (2019). *Vegan: community ecology package. R Package Version 2.5-6*.

Otten, T. G., and Paerl, H. W. (2015). Health effects of toxic cyanobacteria in U.S. drinking and recreational waters: our current understanding and proposed direction. *Curr Envir Health Rpt* 2, 75–84. doi: 10.1007/s40572-014-0041-9

Paerl, H. W., and Otten, T. G. (2013). Harmful cyanobacterial blooms: causes, consequences, and controls. *Microb. Ecol.* 65, 995–1010. doi: 10.1007/s00248-012-0159-y

Paerl, H. W., and Otten, T. G. (2016). Duelling 'CyanoHABs': unravelling the environmental drivers controlling dominance and succession among diazotrophic and non-N_2-fixing harmful cyanobacteria: environmental drivers of CyanoHABs. *Environ. Microbiol.* 18, 316–324. doi: 10.1111/1462-2920.13035

Paerl, H. W., Scott, J. T., McCarthy, M. J., Newell, S. E., Gardner, W. S., Havens, K. E., et al. (2016). It takes two to tango: when and where dual nutrient (N & P) reductions are needed to Protect Lakes and downstream ecosystems. *Environ. Sci. Technol.* 50, 10805–10813. doi: 10.1021/acs.est.6b02575

Parada, A. E., Needham, D. M., and Fuhrman, J. A. (2016). Every base matters: assessing small subunit rRNA primers for marine microbiomes with mock communities, time series and global field samples: primers for marine microbiome studies. *Environ. Microbiol.* 18, 1403–1414. doi: 10.1111/1462-2920.13023

Parveen, B., Ravet, V., Djediat, C., Mary, I., Quiblier, C., Debroas, D., et al. (2013). Bacterial communities associated with *Microcystis* colonies differ from free-living communities living in the same ecosystem: bacterial diversity inside *Microcystis* colonies. *Environ. Microbiol. Rep.* 5:716. doi: 10.1111/1758-2229.12071

Pessi, I. S., Maalouf, P. D. C., Laughinghouse, H. D., Baurain, D., and Wilmotte, A. (2016). On the use of high-throughput sequencing for the study of cyanobacterial diversity in Antarctic aquatic mats. *J. Phycol.* 52, 356–368. doi: 10.1111/jpy.12399

Pokrzywinski, K. L., Bishop, W. M., Grasso, C. R., Fernando, B. M., Sperry, B. P., Berthold, D. E., et al. (2022). Evaluation of a peroxide-based algaecide for cyanobacteria control: A mesocosm trial in Lake Okeechobee, FL, USA. *Water* 14:169. doi: 10.3390/w14020169

Pound, H. L., Martin, R. M., Sheik, C. S., Steffen, M. M., Newell, S. E., Dick, G. J., et al. (2021). Environmental studies of cyanobacterial harmful algal blooms should include interactions with the dynamic microbiome. *Environ. Sci. Technol.* 55:12776. doi: 10.1021/acs.est.1c04207

Quast, C., Pruesse, E., Yilmaz, P., Gerken, J., Schweer, T., Yarza, P., et al. (2012). The SILVA ribosomal RNA gene database project: improved data processing and web-based tools. *Nucleic Acids Res.* 41, D590–D596. doi: 10.1093/nar/gks1219

Rajaniemi, P., Komárek, J., Willame, R., Hrouzek, P., Katovská, K., Hoffmann, L., et al. (2005). Taxonomic consequences from the combined molecular and phenotype evaluation of selected anabaena and Aphanizomenon strains. *Algol Stud* 117, 371–391. doi: 10.1127/1864-1318/2005/0117-0371

R Core Team (2023). *R: A language and environment for statistical computing*. R Foundation for Statistical Computing, Vienna, Austria.

Reynolds, C. S. (1987). Cyanobacterial water-blooms. Editor, callow J.A. *Adv. Bot. Res.* 13, 67–143. doi: 10.1016/S0065-2296(08)60341-9

Scheffer, M. (2004). *Ecology of Shallow Lakes*. Dordrecht: Springer Netherlands.

Shan, K., Song, L., Chen, W., Li, L., Liu, L., Wu, Y., et al. (2019). Analysis of environmental drivers influencing interspecific variations and associations among bloom-forming cyanobacteria in large, shallow eutrophic lakes. *Harmful Algae* 84, 84–94. doi: 10.1016/j.hal.2019.02.002

Shannon, P., Markiel, A., Ozier, O., Baliga, N. S., Wang, J. T., Ramage, D., et al. (2003). Cytoscape: A software environment for integrated models of biomolecular interaction networks. *Genome Res.* 13, 2498–2504. doi: 10.1101/gr.1239303

Simonato, F., Gómez-Pereira, P. R., Fuchs, B. M., and Amann, R. (2010). Bacterioplankton diversity and community composition in the southern lagoon of Venice. *Syst. Appl. Microbiol.* 33, 128–138. doi: 10.1016/j.syapm.2009.12.006

Simpson, G. (2023). Gratia: graceful ggplot-based graphics and other functions for GAMs fitted using mgcv. R package version 0.1. Available at: https://gavinsimpson.github.io/gratia/.

Sim, Z. Y., Goh, K. C., He, Y., and Gin, K. Y. H. (2023). Present and future potential role of toxin-producing Synechococcus in the tropical region. *Sci. Total Environ.* 896:165230. doi: 10.1016/j.scitotenv.2023.165230

Smith, D. J., Berry, M. A., Cory, R. M., Johengen, T. H., Kling, G. W., Davis, T. W., et al. (2022). Heterotrophic bacteria dominate catalase expression during *Microcystis* blooms. *Appl. Environ. Microbiol.* 88, e02544–e02521. doi: 10.1128/aem.02544-21

Smith, D. J., Tan, J. Y., Powers, M. A., Lin, X. N., Davis, T. W., and Dick, G. J. (2021). Individual *Microcystis* colonies harbour distinct bacterial communities that differ by *Microcystis* oligotype and with time. *Environ. Microbiol.* 23, 3020–3036. doi: 10.1111/1462-2920.15514

Vico, P., Iriarte, A., Bonilla, S., and Piccini, C. (2021). Metagenomic analysis of *Raphidiopsisraciborskii* microbiome: beyond the individual. *Biodivers Data J.* 9:514. doi: 10.3897/BDJ.9.e72514

Wagner, N. D., Quach, E., Buscho, S., Ricciardelli, A., Kannan, A., Naung, S. W., et al. (2021). Nitrogen form, concentration, and micronutrient availability affect microcystin production in cyanobacterial blooms. *Harmful Algae* 103:102002. doi: 10.1016/j.hal.2021.102002

Wang, Q., Garrity, G. M., Tiedje, J. M., and Cole, J. R. (2007). Naïve Bayesian classifier for rapid assignment of rRNA sequences into the new bacterial taxonomy. *Appl. Environ. Microbiol.* 73, 5261–5267. doi: 10.1128/AEM.00062-07

Werner, V. R., and Laughinghouse, H. D. (2009). Bloom-forming and other planktonic anabaena (cyanobacteria) morphospecies with twisted trichomes from Rio Grande do Sul state, Brazil. *Nova Hedwigia* 89, 17–47. doi: 10.1127/0029-5035/2009/0089-0017

Werner, V. R., Laughinghouse, H. D., Fiore, M. F., Santanna, C. L., Hoff, C., de Souza Santos, K. R., et al. (2012). Morphological and molecular studies of *Sphaerospermopsis torques-reginae* (cyanobacteria, Nostocales) from south American water blooms. *Phycologia* 51, 228–238. doi: 10.2216/11-32.1

Werner, V. R., Tucci, A., Silva, L. M., Yunes, J. S., Neuhaus, E. B., Berthold, D. E., et al. (2020). Morphological, ecological and toxicological aspects of Raphidiopsis raciborskii (cyanobacteria) in a eutrophic urban subtropical lake in southern Brazil. *Iheringia Ser Bot* 75, –e2020018. doi: 10.21826/2446-82312020v75e2020018

Wickham, H. (2016). *ggplot2: Elegant graphics for data analysis*. New-York: SpringerVerlag.

Woodhouse, J. N., Kinsela, A. S., Collins, R. N., Bowling, L. C., Honeyman, G. L., Holliday, J. K., et al. (2016). Microbial communities reflect temporal changes in cyanobacterial composition in a shallow ephemeral freshwater lake. *ISME J.* 10, 1337–1351. doi: 10.1038/ismej.2015.218

Wood, S. N. (2011). Fast stable restricted maximum likelihood and marginal likelihood estimation of semiparametric generalized linear models. J. R. *Stat. Soc. Series B. Stat. Methodol.* 73, 3–36. doi: 10.1111/j.1467-9868.2010.00749.x

Xu, T., Yang, T., Zheng, X., Li, Z., and Qin, Y. (2022). Growth limitation status and its role in interpreting chlorophyll a response in large and shallow lakes: A case study in Lake Okeechobee. *J. Environ. Manage.* 302:114071. doi: 10.1016/j.jenvman.2021.114071

Zhang, J., Burke, P., Iricanin, N., Hill, S., Gray, S., and Budell, R. (2011). Long-term water quality trends in the Lake Okeechobee watershed, Florida. *Crit. Rev. Environ. Sci. Technol.* 41, 548–575. doi: 10.1080/10643389.2010.530577

Zhang, J., Welch, Z., and Jones, P. (2020) Chapter 8B: Lake Okeechobee watershed annual Report. 2020 South Florida environmental Report volume I 2020;(8B):1–77.

Zhang, W., Gao, Y., Yi, N., Wang, C., Di, P., and Yan, S. (2017). Variations in abundance and community composition of denitrifying bacteria during a cyanobacterial bloom in a eutrophic shallow lake in China. *J. Freshwater Ecol.* 32, 467–476. doi: 10.1080/02705060.2017.1323681

Zhang, Y., Zuo, J., Salimova, A., Li, A., Li, L., and Li, D. (2020). Phytoplankton distribution characteristics and its relationship with bacterioplankton in Dianchi Lake. *Environ. Sci. Pollut. Res.* 27, 40592–40603. doi: 10.1007/s11356-020-10033-6

Zuo, J., Tan, F. J., Zhang, H. T., Xue, Y. Y., Grossart, H. P., Jeppesen, E., et al. (2022). Interaction between *Raphidiopsis raciborskii* and rare bacterial species revealed by dilution-to-extinction experiments. *Harmful Algae* 120:102350. doi: 10.1016/j.hal.2022.102350

frontiers | Frontiers in Microbiology

TYPE Original Research
PUBLISHED 31 August 2023
DOI 10.3389/fmicb.2023.1200816

OPEN ACCESS

EDITED BY
George S. Bullerjahn,
Bowling Green State University, United States

REVIEWED BY
Assaf Sukenik,
University of Haifa, Israel
Robert Michael McKay,
University of Windsor, Canada

*CORRESPONDENCE
Elke Dittmann
✉ editt@uni-potsdam.de

RECEIVED 05 April 2023
ACCEPTED 17 August 2023
PUBLISHED 31 August 2023

CITATION
Roy S, Guljamow A and Dittmann E (2023) Impact of temperature on the temporal dynamics of microcystin in *Microcystis aeruginosa* PCC7806.
Front. Microbiol. 14:1200816.
doi: 10.3389/fmicb.2023.1200816

Impact of temperature on the temporal dynamics of microcystin in *Microcystis aeruginosa* PCC7806

Souvik Roy, Arthur Guljamow and Elke Dittmann*

Department of Microbiology, Institute for Biochemistry and Biology, University of Potsdam, Potsdam, Germany

Cyanobacterial blooms pose a serious threat to water quality and human health due to the production of the potent hepatotoxin microcystin. In microcystin-producing strains of the widespread genus *Microcystis*, the toxin is largely constitutively produced, but there are fluctuations between the cellular and extracellular pool and between free microcystin and protein-bound microcystin. Here we addressed the question of how different temperatures affect the growth and temporal dynamics of secondary metabolite production in the strain *Microcystis aeruginosa* PCC7806 and its microcystin-deficient Δ*mcyB* mutant. While the wild-type strain showed pronounced growth advantages at 20°C, 30°C, and 35°C, respectively, the Δ*mcyB* mutant was superior at 25°C. We further show that short-term incubations at 25°C–35°C result in lower amounts of freely soluble microcystin than incubations at 20°C and that microcystin congener ratios differ at the different temperatures. Subsequent assessment of the protein-bound microcystin pool by dot blot analysis and subcellular localization of microcystin using immunofluorescence microscopy showed re-localization of microcystin into the protein-bound pool combined with an enhanced condensation at the cytoplasmic membrane at temperatures above 25°C. This temperature threshold also applies to the condensate formation of the carbon-fixing enzyme RubisCO thereby likely contributing to reciprocal growth advantages of wild type and Δ*mcyB* mutant at 20°C and 25°C. We discuss these findings in the context of the environmental success of *Microcystis* at higher temperatures.

KEYWORDS

cyanobacteria, *Microcystis*, temperature, microcystin, RubisCO, biocondensates

Introduction

In the summer months, many freshwater lakes are dominated by bloom-forming cyanobacteria, which cause severe environmental and socio-economic consequences (Havens, 2008; Steffensen, 2008). Global bloom formation is expected to further rise in the Anthropocene with higher temperatures and increasing atmospheric CO_2 concentrations (Visser et al., 2016). A particularly widespread genus is the unicellular, colony-forming cyanobacterium *Microcystis* which is infamous for the production of the potent hepatotoxin microcystin (MC) of which a large number of structurally related congeners have been described. *Microcystis* blooms commonly comprise a mixture of toxic and non-toxic genotypes that either possess or lack biosynthetic genes for the nonribosomal peptide MC (Pancrace et al., 2019). The variation in

the amounts of toxin produced is mainly attributed to the varying portion of MC-producing strains in blooms during the season (Briand et al., 2009).

The impact of environmental stimuli on MC production, on the other hand, is comparatively low. MC production has been intensively investigated in *Microcystis* laboratory strains. The toxins are produced from the beginning of the logarithmic phase with variations in their production rates typically not exceeding a factor of two to three (Neilan et al., 2013). Several studies have observed a linear relationship between the MC content of cells and their specific growth rate (Orr and Jones, 1998; Long et al., 2001). MC is primarily a cell-bound toxin, but the low levels of extracellular MC show pronounced temporal variations and are particularly observed at higher cell densities (Wiedner et al., 2003; Guljamow et al., 2021). Comparison of mRNA transcript levels of the MC gene clusters revealed, among other conditions, a stimulating impact of high light, iron-limiting conditions, cell density and low temperature on MC biosynthesis (Kaebernick et al., 2000; Sevilla et al., 2008; Martin et al., 2020). The increase in *mcy* gene transcription, however, was not necessarily reflected at the metabolite level. This discrepancy was recently solved by the discovery of a protein-bound pool of MC that is not extracted by methanol and accumulates primarily under conditions with increased *mcy* transcription (Meissner et al., 2013).

The analysis of protein binding partners of MC revealed a frequent affiliation of proteins to the Calvin Benson cycle including the small and large subunit of the CO_2-fixing enzyme RubisCO (Zilliges et al., 2011; Wei et al., 2016). This finding was particularly interesting because major differences in the inorganic carbon adaptation were observed in parallel between the wild-type and the Δ*mcy*B mutant strain, with an inverse advantage at low and high CO_2 conditions, respectively (Jähnichen et al., 2007; Van de Waal et al., 2011). RubisCO is a bifunctional enzyme whose carboxylation activity is compromised by the alternative substrate O_2. To promote the carboxylation reaction, cyanobacteria have evolved a carbon concentrating mechanism based on two sub-components: (1) the presence and activation of a complement of bicarbonate and CO_2 uptake transporters and (2) the encapsulation of RubisCO in carboxysomes (Burnap et al., 2015). In the context of this mechanism, which is ubiquitous in cyanobacteria, it is extremely interesting that *Microcystis*, of all cyanobacteria, exhibits a plasticity in the content of bicarbonate uptake transporter genes (Sandrini et al., 2014). Moreover, a detailed analysis of the subcellular localization of RubisCO in *Microcystis aeruginosa* PCC7806 revealed a frequent localization of RubisCO underneath the cytoplasmic membrane rather than within carboxysomes, especially under high cell density and high light conditions that were also shown to promote MC expression and condensate formation of MC (Barchewitz et al., 2019). Localization of RubisCO at the cytoplasmic membrane was connected with a high accumulation of the RubisCO product 3-phospho-glycerate and was consistent with a growth advantage of the toxin-producing wild type (Barchewitz et al., 2019). RubisCO has a tendency for liquid–liquid phase separation (LLPS) during the formation of carboxysomes in cyanobacteria as well as pyrenoids in the green alga *Chlamydomonas reinhardtii* (Wang et al., 2019; He et al., 2020). The formation of biocondensates via LLPS may be stimulated by intrinsically unstructured proteins but also by ligands and is generally promoted at the membranes (Alberti et al., 2019). In a recent study, we could demonstrate that RubisCO condensate formation in *Microcystis* is dynamic and may be stimulated by extracellular MC (Guljamow et al., 2021). Hence, there is increasing evidence that *Microcystis* strains employ a multi-level strategy in their inorganic carbon adaptation, which is not only reflected in their genotypic and phenotypic plasticity, but also involves non-canonical regulation at the protein level, presumably dependent on MC and other secondary metabolites.

Here, we have analyzed the impact of different temperatures on MC dynamics and RubisCO condensate formation. Presence or absence of MC leads to opposing effects on growth at different temperatures ranging from 20°C to 35°C. Short-term temperature shift experiments lead to pronounced differences in the intracellular and extracellular dynamics of MC and other secondary metabolites in *M. aeruginosa* PCC7806. Our data suggest that temperature is one of the critical factors for MC and RubisCO condensate formation and thereby significantly influences dynamics of soluble MC as well as growth of *M. aeruginosa* PCC7806.

Materials and methods

Cultivation conditions

Microcystis aeruginosa PCC7806 was cultivated in BG-11 medium. Chloramphenicol in a final concentration of 5 μg mL^{-1} was added for cultivation of the Δ*mcyB* mutant (Dittmann et al., 1997). For the growth curve experiments, the cultures were diluted with fresh medium to OD_{750} of 0.1 once logarithmic growth was achieved and split into three triplicates that were analyzed in parallel throughout the experiment. Diluted triplicates of *M. aeruginosa* cultures were then cultured simultaneously in an AlgaeTron AG130 growth chamber (Photo Systems Instruments, Drasov, Czech Republic) under continuous low-light condition (16 μmol photons m^{-2} s^{-1}) at temperatures ranging from 20°C to 35°C, each temperature at a time. To estimate the growth, optical density at 750 nm of each replicate was determined photometrically (Novaspec III, Amersham Biosciences, United Kingdom) once a day for 14 days. For the temperature shift experiments, cells were pre-cultured at 23°C on a benchtop under a natural day and night cycle without external aeration or agitation until cultures reached a medium cell density of 0.6 ± 0.02 OD_{750}. Cells were harvested by centrifugation, washed twice with growth medium, resuspended in fresh medium and then equally distributed into three conical flasks. Cell cultures were grown in an AlgaeTron AG130 for 48 h in continuous low-light condition (16 μmol photons m^{-2} s^{-1}) at 20°C with continuous agitation on an orbital shaker at 72 rpm (acclimatization period) followed by a 24-h test period during which only the temperature was modified to 20°C (control condition, no change), 25°C, 30°C or 35°C. During the test period, samples were collected on the 16th, 20th & 24th hour after the temperature shift.

To determine the maximum growth rates, slope (m) was calculated between optical density measurements at 750 nm, from the 9th to the 14th day. The analysis was performed for both strains, encompassing the entire range of temperatures under investigation.

To assess the potential temperature-induced effects on the morphology of *M. aeruginosa*, cell diameters were determined. Diameters of multiple cells ($n = 18$) were measured across diverse micrographs. The measurement procedure was performed by the Zeiss ZEN Lite software tool (version 3.8), and calculations were based on the assumption of a circular cellular morphology.

Cell counts were conducted to examine the correlation between cell quantities and optical density values at 750 nm, measured at a temperature of 25°C. Three biological replicates of both wild-type *M. aeruginosa* and the Δ*mcyB* mutant were prepared identically to previously performed growth curve experiments and incubated at 25°C in an AlgaeTron AG130. Culture samples were collected daily for 14 days from each replicate and subsequently, cells were counted under—microscope at 40× magnification in Neubauer's hemocytometer chamber with 0.02 mm chamber depth. Simultaneously, cell densities were photometrically measured at 750 nm (Novaspec III, Amersham Biosciences, United Kingdom).

Protein extraction

Cell pellets from 25 mL liquid cell culture were resuspended in 1.5 mL of native extraction buffer (50 mM HEPES; 5 mM $MgCl_2 \times 6H_2O$; 25 mM $CaCl_2 \times 2H_2O$; 10% glycerol; pH 7). Phenylmethylsulfonyl fluoride (PMSF) was added at a final concentration of 1 mM. Samples were disrupted using a cell disruptor (Constant Cell Disruption Systems, Constant System Ltd., England) at 40 Kpsi (2,757.9 bar). Samples obtained from the cell disruptor were first centrifuged at 2,000 × g for 3 min, 4°C to pellet unbroken cells. Supernatants were further centrifuged at 13,000 × g for 10 min, 4°C, thus separating the cytoplasmic protein fraction (supernatant) from the membrane-associated protein fraction (pellet).

SDS-PAGE & immunoblotting

For SDS-PAGE, the Bis-Tris buffer system was used along with variable (8%–15%) polyacrylamide concentrations for gels (BiteSize Bio based on NuPAGE Invitrogen, Carlsbad, CA, United States). The protein samples were added with loading dye (5x concentrated): 250 mM Tris pH 6.8, 0.1% bromophenol blue, 50% glycerol, 10% SDS, 500 mM 2-mercaptoethanol) and dithiothreitol (DTT) at a final concentration of 200 mM. All protein samples were heated at 95°C for 10 min and centrifuged for 1 min at 13,000 × g to remove possible cell debris before loading on the gel. Protein concentrations were measured using Bradford assay and samples were later normalized to equal concentrations, resulting in equal amounts of protein loaded in each lane. The protein ladder was PageRuler Plus Pre-stained (Thermo Fisher Scientific, Waltham, MA, United States). The gel was run at a voltage of 80 V for an initial 15 min followed by a constant 160 V in a MOPS running buffer (10.46 g L^{-1} MOPS, 6.06 g L^{-1} Tris, 1 g L^{-1} SDS, 0.3 g L^{-1} EDTA). Images were taken in ChemiDoc MP Imaging System (Bio-Rad, Germany). For Native-PAGE, a similar setup was used except cells were added with Native-PAGE 5× loading dye (without SDS) and samples were not heated before loading into Bis-Tris gel. Also, Native-PAGE MOPS running buffer (not containing SDS) was used for electrophoresing the samples.

For immunoblot analysis, protein gels were blotted with a wet blot electrophoresis apparatus (Mini-Protean, Bio-Rad, Hercules, CA, United States) onto nitrocellulose membranes (Amersham Protein Premium 0.45 µm MC; GE Healthcare, Chicago, IL, United States). The transfer buffer (14.42 g L^{-1} glycine, 3.03 g L^{-1} Tris) contained 20% methanol (*v*/*v*). Membranes were blocked with 1% polyvinylpyrrolidone (PVP) K-30 in TBS-T (6.06 g L^{-1} Tris, 8.77 g L^{-1} NaCl, pH 7.4, 0.1% (*v*/*v*) Tween-20, Sigma-Aldrich, St. Louis, MO, United States) and washed once for 5 min, 4°C with TBS-T. Primary antibodies were incubated in TBS-T overnight at 4°C with the following concentrations: RbcL 1:10,000 (anti-RbcL, RubisCO large subunit, form I (affinity purified), AS03037A, Rabbit, Agrisera AB, Sweden); RbcS 1:5000; CcmK 1:5000; MC 1:5000, (anti-MC-LR MC10E7, mouse; Enzo Life Sciences, Lörrach, Germany). The antibodies against *Microcystis* RbcS and CcmK were produced in our laboratory as previously described (Barchewitz et al., 2019). Membranes were washed with TBS-T and secondary antibodies (anti-mouse-IgG HRP-conjugate for MC and anti-rabbit-IgG HRP-conjugate for all other antibodies) were applied in TBS-T and incubated for at least 1 h at 4°C. Membranes were washed 4 times for 5 min, 4°C, chemiluminescence was detected with the ChemiDoc MP Imaging System (Bio-Rad, Germany). Multiple western blot experiments from different replicate experiments were performed to obtain concurrent outcomes representing the influence of temperature on target protein within the protein pool. Images shown are representatives of such observations.

Dot-blot analysis was performed to assess the influence of temperature on protein-bound MC within *M. aeruginosa* samples. To perform dot-blot analysis, equal concentrations of 4 µL protein extracts, diluted to a concentration of 10^{-1} were directly deposited onto a nitrocellulose membrane (Amersham Protein Premium 0.45 µm MC; GE Healthcare, Chicago, IL, United States). Subsequently, membranes were treated similarly to western blots and added with 1:5000 anti-MC-LR primary antibody (MC10E7, mouse; Enzo Life Sciences, Lörrach, Germany) and a secondary anti-mouse-IgG HRP-conjugate antibody. Membranes were washed 4 times, 5 min each at 4°C and chemiluminescence was detected with the ChemiDoc MP Imaging System (Bio-Rad, Germany).

Chemical analytics

To analyze both intracellular & extracellular peptides, cell pellets from 25 mL liquid culture and 50 mL supernatant (culture medium) were taken in separate tubes. For metabolite extraction, cell pellets were resuspended in 2 mL of 100% methanol and subsequently shaken for 5 min at 3200 rpm (Vortex Genie 2; Scientific Industries, Bohemia, NY, United States). After sonication (GM 3100, Bandelin electronic, Berlin, Germany) for 10 min at 50% amplitude, 3 s on/off pulse, the sample was centrifuged for 20 min (4,700 × g, 20 min, 4°C). Supernatant collected was transferred to a fresh tube and allowed to be dried in a vacuum concentrator (RVC 2-25 CDplus; Christ, Osterode am Harz, Germany). The dried samples were resuspended in 200 µL of equal portions (1:1) 100% Methanol:MilliQ Water, and filtered using Acrodisc 4 mm with 0.45 µm membrane (Pall Life Sciences, Port Washington, NY, United States) before 20 µL of it was loaded on the high-performance liquid chromatograph Prominence LC-20 AD (Shimadzu, Kyoto, Japan) to analyze the peptides. The extracts were separated on a Symmetry Shield RP18 Column (100 Å, 3.5 µm, 4.6 mm × 100 mm) (Shimadzu Europe, Duisburg, Germany) with a mobile phase containing 0.05% Trifluoroacetic acid along with variable concentration of acetonitrile used as the organic solvent (30, 36, 100, 100, 30, 30% at 0, 12, 13, 14, 15, 17 min respectively). The quantification of peaks and examination of the chromatograms were done with LabSolutions software package (Shimadzu, Kyoto, Japan). MC and cyanopeptolins were identified based on their retention times and using MALDI-TOF MS (Bruker, Billerica, United States). Prior to

MALDI-TOF measurement, sampled HPLC peak fractions were vacuum dried and resuspended in 10 µL of 20% acetonitrile −0.05% TFA. A 0.3 µL portion of the sample solution was mixed with an equal volume of an α-cyano-4-hydroxycinnamic acid matrix (3 mg/mL in 84% acetonitrile,13% ethanol, 3% water, and 0.1% TFA), spotted, and analyzed with a Bruker Microflex LRF apparatus (λ = 337 nm nitrogen laser) (Bruker, Billerica, United States) in positive-ion reflectron mode. Data were analyzed using the mMass software tool.

MC and cyanopeptolin were quantified based on quantitative standards. MC-LR [Microcystin-LR (Analytical Standard), Product ALX-350-431-C010, Enzo Life Sciences, Inc.] and (D-Asp^3)-MC-LR [(D-Asp^3)microcystin-LR, Product ALX-350-173-C025, Enzo Life Sciences, Inc.]. The cyanopeptolin standard was purified and weighed in our laboratory as described previously (Barchewitz et al., 2019).

Immunofluorescence microscopy

Five mL of *M. aeruginosa* PCC7806 culture were pelleted for 1 min at 10,000 × g and washed twice with 1 mL of PBS (8.18 g L^{-1} NaCl, 0.2 g L^{-1} KCl, 1.42 g L^{-1} Na_2HPO_4, 0.25 g L^{-1} KH_2HPO_4, pH 8.3). Cell pellets were resuspended with 1 mL of 4% formaldehyde in PBS and incubated for 30 min at room temperature for the fixation process. Fixed cells were then washed twice with PBS and resuspended in 100 µL PBS. Meanwhile, 12 mm thick microscope coverslips (R. Langenbrinck GmbH, coverslips round 12 mm) were washed with 100% ethanol using ultra-sonication cleanser (Bandelin Sonorex TK52; Ultraschall-Welt, Germany) for 30 min. Twenty µL of resuspended cells were spread evenly on a microscope coverslip, slips were air-dried and stored at −20°C for later use. For antibody hybridization, coverslips with fixed samples were equilibrated in PBS for 5 min at room temperature. Afterwards, the slips were incubated with 2 mg mL^{-1} lysozyme in PBS-TX (PBS with 0.3% (*v*/*v*) Triton X-100, Sigma-Aldrich, Darmstadt, Germany) for 30 min at room temperature and washed twice with PBS-TX for 3 min. The slips were then blocked with 1% PVP K-30 in PBS-T (PBS with 0.3% *v*/*v* Tween-20, Sigma-Aldrich, Darmstadt, Germany) for at least 1 h at 4°C followed by a double washing step with PBS-T. Primary antibody dilutions in PBS-T were as follows: RbcS 1:200 RubisCO small subunit (rabbit antiserum); CcmK 1:200 (rabbit antiserum); MC 1:250 (MC-LR MC10E7, mouse; Enzo Life Sciences, Lörrach, Germany). Post-incubation of at least 1 h at room temperature, the slides were again washed twice with PBS-T and the secondary antibodies used (depending on the primary antibodies) were as follows; Alexa Fluor 488 goat anti-rabbit (1:200), Alexa Fluor 488 goat anti-mouse (1:100) and Alexa Fluor 546 goat anti-chicken (1:200); (all from ThermoFisher Scientific. Waltham, MA, United States). Subsequently, the slides were washed twice and air-dried until most of the PBS-T evaporated. A drop of ProLong™ Glass Antifade Mountant (Invitrogen™; ThermoFisher Scientific, Germany) was added to the glass slide and the dried coverslip was placed on top. The slides were allowed to cure for 24 h in the dark and were stored at −20°C until use. Laser scanning confocal micrographs were obtained using a Zeiss LSM 780 (Carl Zeiss, Oberkochen, Germany) with a Plan-Apochromat 63×/1.40 oil immersion objective. Alexa Fluor 488 was excited at 488 nm (detection spectrum 493–556 nm), Alexa Fluor 546 (570–632 nm), and autofluorescence at 633 nm (647–721 nm). The excitation was performed simultaneously.

For enhanced visualization of MC localization, immunofluorescence pixel intensities were plotted against cell diameter by analyzing multiple cells ($n > 8$) from various immunographs using the Zeiss ZEN lite software tool (version 3.8). To better visualize the temperature-induced bio-condensates among the two strains, we used the built-in 2.5D function of Zeiss ZEN lite software. In this analysis, we plotted RbcS immunofluorescence intensities as the *z*-axis parameter, while the *y*-axis and *x*-axis corresponded to the pixel coordinates.

Statistical analysis

Analysis of variance (ANOVA) was carried out to test for statistical significance of differences in mean values using the *aov* function of R (version 4.3.0). For the growth rate determination experiment, a two-way ANOVA was carried out to test for the interaction of the parameters "strain" (i.e., either wild type or mutant) and "temperature" (i.e., the experimental temperature conditions) on the influence of the mean growth rate. Pairwise statistical significance in mean differences was determined with the *TukeyHSD* function in R using a 95% confidence interval. Compact letter display grouping was performed with the *multcompLetters4* function of the multcompView package of R.

Results

Effects of temperature on growth and MC production in *Microcystis aeruginosa* PCC7806 and its Δ*mcyB* mutant

To investigate the effects of different temperatures on the growth of MC-producing wild-type strain PCC7806 (WT) and its Δ*mcyB* mutant, three replicates of both strains were cultivated in batch cultures for 14 days at 20°C, 25°C, 30°C and 35°C, respectively (Figure 1). Growth was monitored by measuring the optical density of the cultures at 750 nm (OD_{750}, Figure 1A) as we found the OD_{750} to be a reliable and robust proxy for cell count (Supplementary Figure S1). Statistical analyses revealed that both the genetic background (WT vs. mutant) and the cultivation temperature have a significant effect on the maximum growth rate of *M. aeruginosa* (Figure 1B and Supplementary Tables S1, S2). While the Δ*mcyB* mutant strain showed maximal growth rates at 25°C, where it clearly outperformed the WT, the MC-producing strain PCC7806 grew fastest at 30°C. Moreover, the WT strain still showed robust growth at 35°C whereas the Δ*mcyB* mutant showed virtually no growth at all. Strikingly, the Δ*mcyB* mutant strain also grew poorly at 20°C where the WT strain already showed significant proliferation. Overall, growth rates of the Δ*mcyB* mutant were less robust against changes in cultivation temperature. While the growth advantages of the WT at high temperatures are in agreement with previous observations (Dziallas and Grossart, 2011), the significant growth differences at 20°C were unexpected and suggested a critical breakpoint for growth of the strain *M. aeruginosa* PCC7806 between 20°C and 25°C at the given light conditions.

To better understand possible temperature-dependent MC-effects we next studied the impact of temperature on MC production itself. For this purpose, we designed a temperature shift experiment where

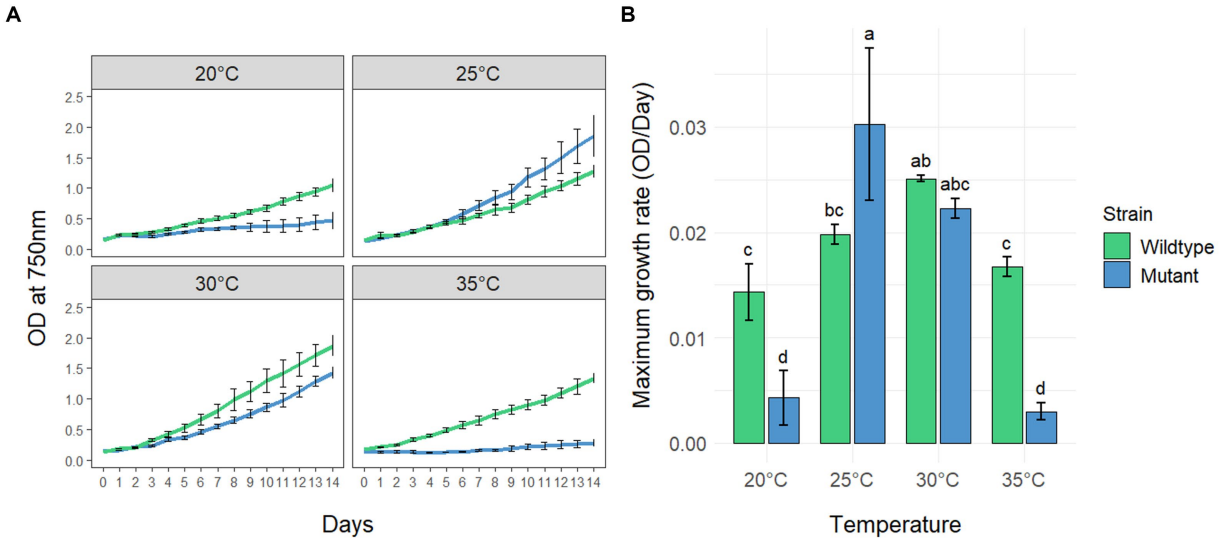

FIGURE 1
Growth of *Microcystis aeruginosa* PCC7806 (wildtype) and its MC-deficient *ΔmcyB* mutant. **(A)** Growth curves of batch cultures under continuous low light conditions. Shown are the mean OD_{750} values with standard deviations of three replicate cultures. **(B)** Maximum growth rates of the same cultures as in **(A)**. Statistically significant differences of the means across all conditions are indicated with compact letter display (CLD) after two-way ANOVA and TukeyHSD test with a 95% family-wise confidence level. CLD groups not sharing a letter differ significantly. The maximum growth rates, standard deviations and results of statistical analyses are presented in the supplementary section as Supplementary Tables S1, S2.

replicates of a culture of the WT strain were acclimated to 20°C, grown to medium cell density and either maintained at these conditions or exposed to 25°C, 30°C and 35°C for 24 h, respectively. To take possible dynamics of intra- and extracellular MC into account, we took samples at three different time points at 16, 20 and 24 h after the temperature shift. MC was quantified by HPLC based on a quantitative standard for MC-LR. The two major congeners produced by *M. aeruginosa* PCC7806, MC-LR and (D-Asp^3)-MC-LR were quantified as MC-LR equivalents (Figure 2). As expected, higher amounts of MC were detected in the intracellular pool at all temperatures. While the cell-bound amount of MC was similar at 25°C, 30°C and 35°C, it was almost twice as high in cultures kept at 20°C (Figures 2A,B). Moreover, the proportion of the two congeners differed at 20°C and 25°C–35°C, respectively. While the proportion of (D-Asp^3)-MC-LR was fluctuating around 20% at the three higher temperatures, it made up to 39% of the total intracellular MC pool at 20°C (Figures 2A,B). The extracellular MC was also strikingly different at 20°C compared to the other three temperatures. Here, too, the proportion of the (D-Asp^3)-MC variant with up to 66% of the total MC was higher than at the other temperatures. Temporal fluctuations of extracellular MC were also most pronounced at 20°C. It is of note, that the extracellular proportion of (D-Asp^3)-MC-LR was generally higher at all temperatures compared to the intracellular pool. The amount of extracellular MC was relatively stable at 25°C, 30°C and 35°C, but at an overall higher level at 35°C.

To better interpret the specificity of the dynamic MC effects, we additionally quantified cyanopeptolin A at the four different temperatures using a quantitative standard. In this case, we also included extracts of the Δ*mcyB* mutant that was subjected to an identical temperature shift experiment (Supplementary Figure S2). In the wild-type strain, slightly higher intracellular values were detected for cyanopeptolin A at 20°C, but the difference between 20°C and 25°C–35°C was not as significant as it was for MC (Supplementary Figure S2A). In the Δ*mcyB* mutant, no obvious difference was observed between 20°C and 25°C–35°C. While cyanopeptolin quotas were rather similar in WT and Δ*mcyB* mutant at 20°C they deviated at 25°C–35°C where the cyanopeptolin A levels remained high in the mutant but decreased in the WT, similar to MC. Generally, fewer fluctuations were detected for cyanopeptolin A in both the wild-type strain and the Δ*mcyB* mutant compared to MC, with the exception of the 35°C samples in the mutant. The lower intracellular values at 35°C in the mutant are partly correlated with higher extracellular values, so that the intracellular dynamics can probably be attributed in part to release of cyanopeptolin A (Supplementary Figure S2B).

Temperature has an impact on MC and RubisCO condensate formation

In addition to the samples for chemical analysis, parallel samples for immunofluorescence microscopy (IFM) and protein analysis were taken at all time points at the four different temperatures. To assess the degree of MC condensate formation and the subcellular localization of protein-bound MC, samples were analyzed by immunofluorescence microscopy using an anti-MC antibody (Figure 3A). No specific signals were obtained in control experiments, either without primary antibody (for WT) or with a combination of primary and secondary antibodies (for Δ*mcyB*, Supplementary Figure S3). Averaging the fluorescence intensity profiles across a random sample of cells (Supplementary Figure S4) we found that at 20°C, MC signals were very evenly distributed throughout the cells with an occasional enrichment at the cell's periphery, presumably at the cell membrane. In contrast, at each of the higher temperatures, the localization of the MC signals showed a clear tendency towards increased condensation at the cell membrane compared to the 20°C samples. The extent of the

10.3389/fmicb.2023.1200816

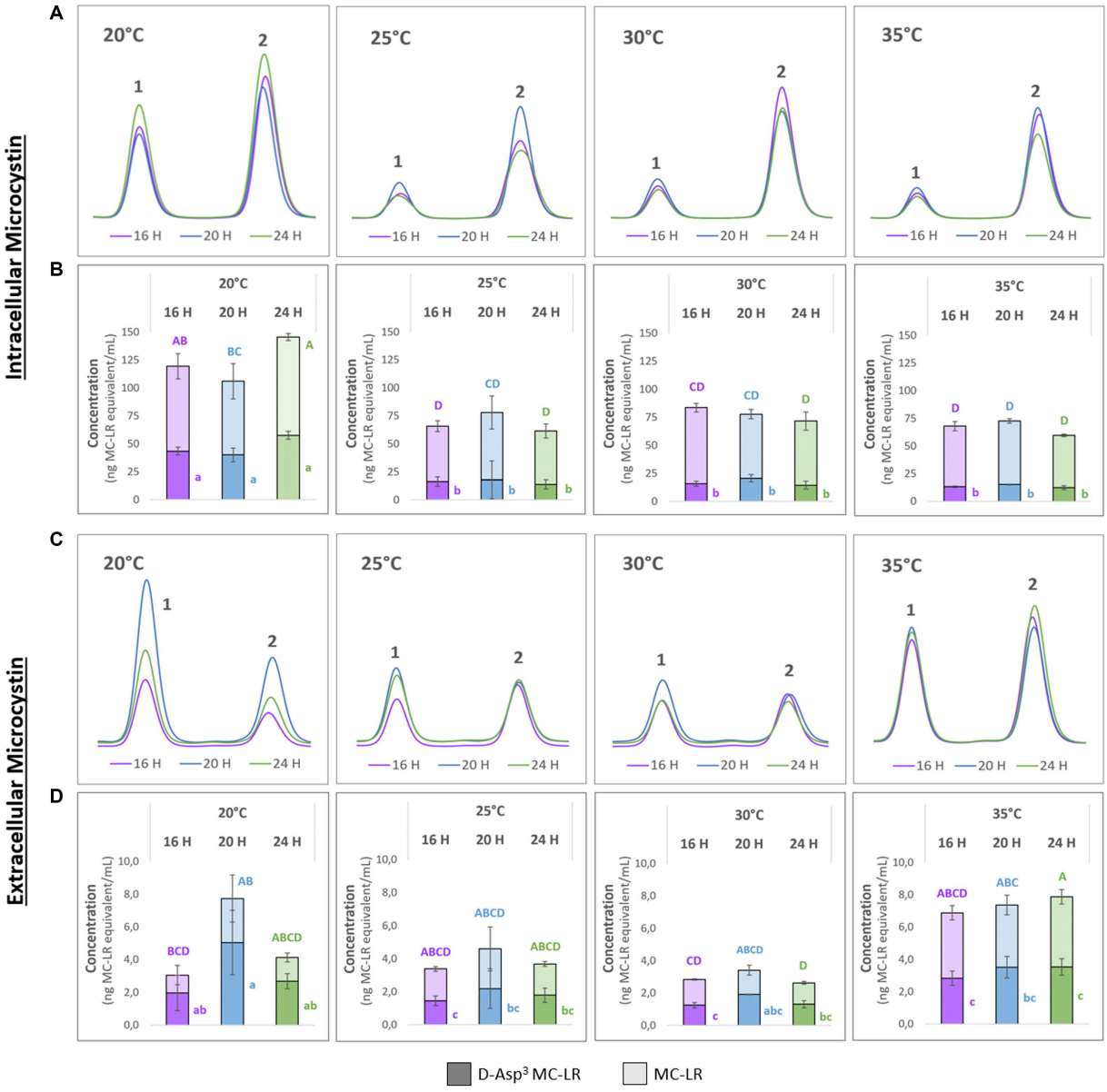

FIGURE 2
Temporal dynamics of (D-Asp[3])-MC-LR (**1**) and MC-LR (**2**) after acclimation of precultures to 20°C and subsequent temperature shift to 20°C, 25°C, 30°C and 35°C. Samples were taken after 16, 20 and 24 h. **(A,C)** Representative HPLC profiles; **(B)** intracellular and **(D)** extracellular amounts of **1** and **2** as means with standard deviations based on three biological replicates. Statistically significant differences are indicated with compact letter display (CLD) after one-way ANOVA and TukeyHSD test with a 95% family-wise confidence level. Upper case letters are for total MC content, lower case letters are for **1** only. CLD groups not sharing a letter differ significantly.

condensation changed dynamically between the different time points (Figure 3A). The comparison of the soluble protein profiles showed very pronounced differences between samples exposed to 20°C and those exposed to higher temperatures (Figure 3B). While protein profiles were highly similar at 25°C–35°C, soluble protein patterns looked significantly different at 20°C, even though all samples were derived from the same pre-culture and were only exposed to the gradually different temperatures for 16–24 h. Similarly, significant differences were noted between 20°C and 25° in the MC immuno-dot-blot analysis conducted to assess the overall quantity of protein-bound MC (Figure 3C). MC protein binding amounts were similar at 25°C–35°C but fundamentally different at 20°C. Here, an overall lower tendency for MC binding was observed. Protein condensate formation at 25°C–35°C was even more apparent in Native PAGE analysis where MC was predominantly detected in large aggregates not entering the gels (Supplementary Figure S5). Both MC immunofluorescence analysis and MC immunoblot analysis therefore indicated very clear differences in MC-protein binding at 20°C, both quantitatively and qualitatively. The increased tendency to form condensates at higher temperatures could also explain the marked differences in soluble intracellular MC content at 20°C and the differences in proportions for MC congeners (Figure 2).

Next, we also compared the subcellular localization of the MC-binding partner RubisCO by IFM (Figure 4). In these

10.3389/fmicb.2023.1200816

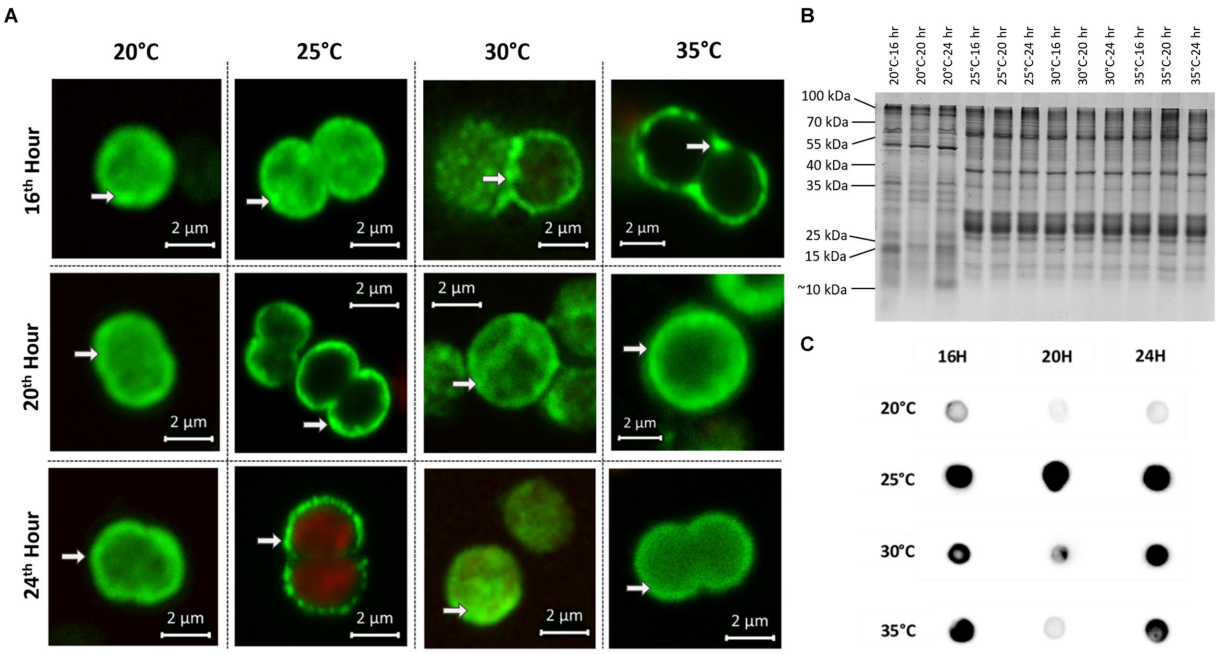

FIGURE 3
Subcellular localization and protein-binding of MC after temperature shift to 20°C, 25°C, 30°C and 35°C for 16, 20 and 24 h. **(A)** Representative MC immunofluorescence micrographs show a plasticity in the subcellular localization of MC and increased condensation of the signals at the periphery of cells at 25°C–35°C. White arrows point to peripheral MC signals. MC signals are depicted in green and autofluorescence is shown in red. **(B)** SDS-PAGE analysis of soluble protein samples displays distinct protein pattern at 20°C and 25°C–35°C. **(C)** MC immuno-dot-blot analysis shows a lower level of MC-binding to proteins at 20°C.

experiments, we also included the MC-deficient Δ*mcyB* mutant. Analysis of the wild type samples revealed a predominant localization of RubisCO below the cytoplasmic membrane at 25°C–35°C. Again, the subcellular localization at 20°C was strikingly different (Figure 4A). At the lower temperature, RubisCO was predominantly evenly distributed in the cell and only occasionally appeared below the membrane. A similar trend was observed in samples of the Δ*mcyB* deficient mutant. The mutant cells, however, showed a lower degree of RubisCO condensate formation also at higher temperatures (Figure 4B; Supplementary Figure S7). At 25°C to 35°C plasticity was observed with cells either showing cytosolic localization or localization underneath the membrane. This effect is more clearly visible on intensity landscape plots of the IFM images (Figure 4C; Supplementary Figure S7). RubisCO condensates appear as local foci of fluorescence that are visualized as spikes protruding from the background level of fluorescence. Both the number and the "height" of the RubisCO-derived fluorescence foci were much lower in the Δ*mcyB* mutant, indicating an overall lower degree of RubisCO condensation (Figure 4C; Supplementary Figure S7). In agreement with this, we did not observe major differences in the soluble protein profiles of the Δ*mcyB* mutant at the four different temperatures (Supplementary Figure S6, compared with the WT, Figure 3B). To check to what extent the membrane localization also affects carboxysomal proteins, we additionally compared the localization of CcmK. Here, the typical cytosolic carboxysome structures were visible at all temperatures. Only occasionally were additional signals also visible at membranes. Wild type and mutant did not differ significantly in carboxysome localization and also showed few dynamic differences at different time points (Supplementary Figure S8). These observations indicate a clear influence of the factor temperature on the condensate formation of MC and RubisCO, but not carboxysomes. Under the selected conditions, a condensation threshold was observed between 20°C and 25°C, especially in the MC-producing WT.

Discussion

In this study, we were able to show that production or lack of MC has a pivotal influence on the growth rate of the strain *M. aeruginosa* PCC7806 at different temperatures and that cultivation temperature, in turn, has a significant effect on the amount of freely soluble MC. We could consistently show that MC quantity, MC congener proportions, MC subcellular localization and MC binding to proteins differ markedly after short-term exposure to either 20°C or 25°C–35°C. The co-occurrence of these observations indicates that the temperature dependence and dynamics of MC depend on the condensation processes *in vivo* and that the temperature threshold for condensation is between 20°C and 25°C.

We have shown previously that MC protein condensates are not taken into account in the analysis of methanol-soluble extracts of *Microcystis* and that the amount of these condensates can change dynamically, e.g., under the influence of extracellular MC (Meissner et al., 2013; Guljamow et al., 2021). We assume that the condensation effects observed by immunofluorescence microscopy reflect the formation of MC-containing droplets by LLPS. There is mounting evidence that LLPS is a major factor in the formation of membrane-less compartments in bacterial cells and that it can have different consequences including subcellular enrichment, inactivation or

10.3389/fmicb.2023.1200816

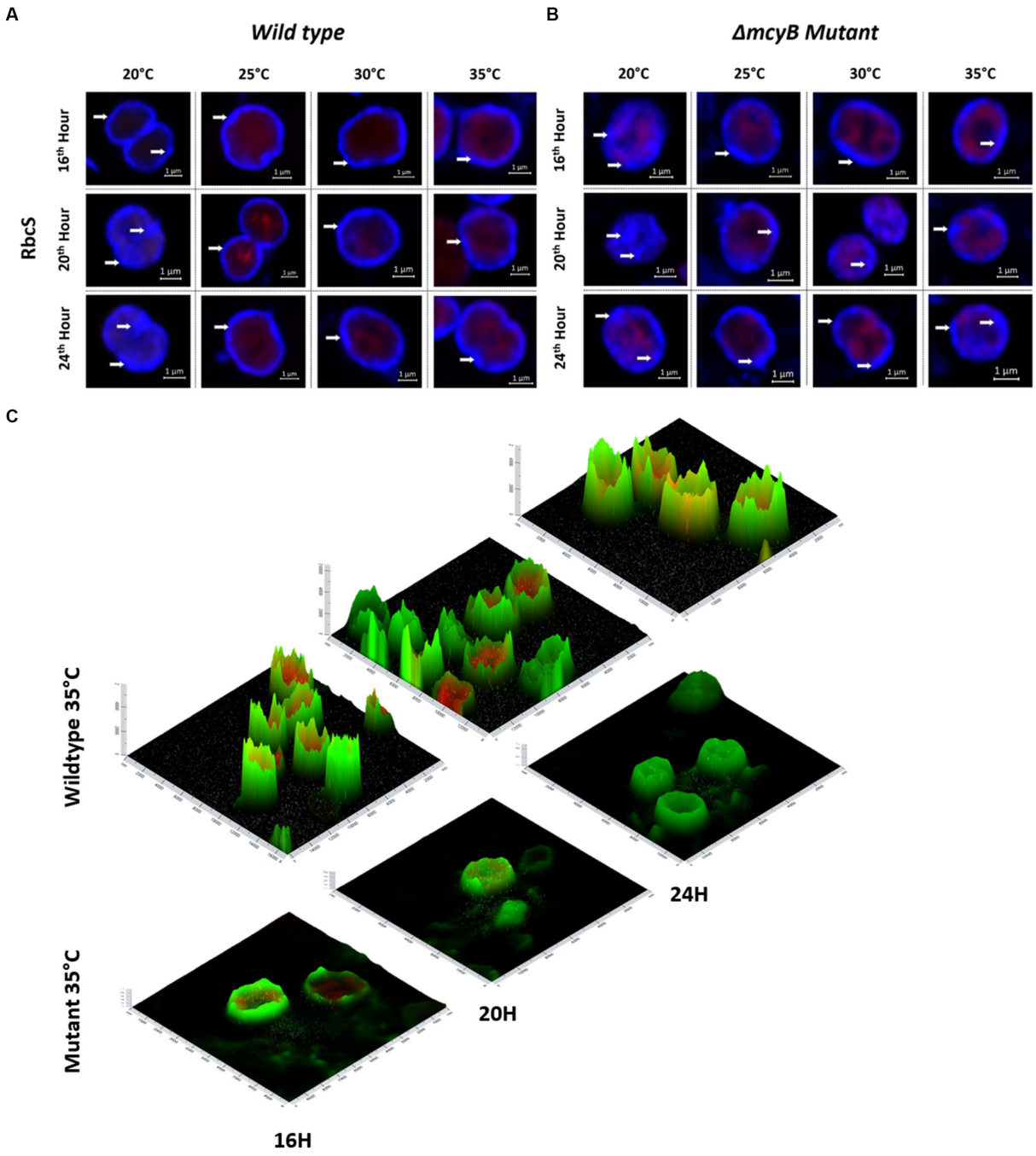

FIGURE 4
Subcellular localization of RubisCO after temperature shift to 20°C, 25°C, 30°C and 35°C for 16, 20 and 24 h. Representative RbcS immunofluorescence micrographs from **(A)** WT PCC7806 indicate a predominant cytosolic localization of RubisCO at 20°C and a membrane-associated localization at 25°C–35°C. **(B)** The Δ*mcyB* mutant displays a predominant membrane association of RubisCO at 25°C–35°C, but a lower degree of condensation than in the WT. **(C)** Spatial fluorescence intensity distribution of RbcS-derived signals at 35°C. Foci of high fluorescence intensities, appearing as "spikes" are more prevalent in the WT. RbcS signals are shown in blue **(A,B)** and green **(C)**, autofluorescence is shown in red. White arrows point to peripheral RbcS signals.

activation of proteins (Alberti et al., 2019). Through protein compartmentalization, microbial cells can achieve enhanced metabolic efficiency whilst still maintaining free communication with the external environment (Gao et al., 2021). Whether or not proteins and ligands undergo phase separation depends on the nature of the proteins, their concentration and the physicochemical parameters, not least the temperature (Alberti et al., 2019). Heat-labile proteins can be protected by condensation (Gao et al., 2021). We have already described recently that MC condensation occurs almost exclusively at higher cell densities ($OD_{750} > 0.5$) (Wei et al., 2016; Barchewitz et al., 2019). This effect is probably triggered by higher MC and protein concentrations. Building upon these observations, the present study was designed to evaluate whether the physicochemical parameter temperature has additive or opposite effects on MC condensate formation. Indeed, we could observe that temperature has a significant influence, however, not gradually, but rather depending on a distinct

threshold. In our experiment, this threshold value was between 20°C and 25°C. Given these results, the inconsistency of reports on the effects of temperature on MC production is particularly striking (Buley et al., 2022). Since many of the studies use growth temperatures between 20°C–25°C, part of the observed discrepancies may be due to the condensation processes *in vivo* and the resulting effects on MC quantifications. Stephen Wilhelm and coworkers have observed an increase in MC production after episodic temperature decrease from optimal growth temperatures at 26°C to 18°C (Martin et al., 2020). The increase in MC production was correlated with an increased MC transcription. Considering the short-term nature of the experiments tested in our study and the observed differences in MC congener proportions we believe that a lower degree of condensate formation is largely responsible for the higher amount of MC detected at 20°C. Vice versa, higher temperatures promote condensate formation leading to an apparent decrease in MC accumulation. Differences in the congener ratios may be due to differences in the propensity of different MC variants to form condensates. To be able to exactly quantify the protein-bound pool of MC would be helpful to verify this hypothesis. However, this turns out to be difficult because of the formation of large insoluble aggregates that do not enter SDS-PAGE gels and the at least partially covalent nature of MC binding to proteins (Supplementary Figure S5). We have therefore refrained from quantifying the condensates in this study and focused on demonstrating conditions favoring condensation.

While the influence of condensate formation on detectable MC quota is rather evident, the reasons for the reciprocal differences in the growth of wild-type and MC-free mutant are not well understood. Reversal of the growth advantages of the MC-producing WT strain and the Δ*mcyB* mutant has been observed repeatedly (Van de Waal et al., 2011). The mutant appears to have an advantage especially under optimal growth conditions such as elevated CO_2 levels (Van de Waal et al., 2011). In this study, too, the mutant seems to be superior to the WT especially at optimal temperatures around 25°C while the wild type grows better under limiting growth conditions. Yet, the reasons for the growth advantage of the WT strain at 35°C and 20°C are not necessarily the same. We suspect that the differences in growth at 35°C may be due to the better stress adaptation of the wild type strain. This hypothesis is in agreement with observations of Dziallas and Grossart (2011) who compared the accumulation of stress markers in *M. aeruginosa* PCC7806 and the Δ*mcyB* mutant at higher temperatures. However, the fundamental differences in the subcellular localization of RubisCO and the global protein profiles observed between 20°C and 25°C (but *not* between 25°C and 30/35°C) could also indicate a condensation-dependent switch of metabolic states between the two temperatures. Different metabolic states could in turn explain temperature-dependent differences in growth. Metabolomic studies of *Microcystis* have shown an astounding metabolic plasticity and suggested a metabolic switch, e.g., in low-light high-light shift experiments and a possible involvement of MC (Meissner et al., 2015). Whether or not a metabolic switch occurs in temperature shift experiments has to be tested in future metabolomic studies.

Although the experiments in our study only provide a limited insight into the influence of temperature on MC production and cannot reflect the complex situation in the field, they further highlight the impact of MC on the phenotypic plasticity and environmental adaptability of *M. aeruginosa* PCC7806. *Microcystis* belongs to the cyanobacteria with a high temperature optimum of growth. Notably, the temperature optima are highly strain specific (Paerl and Huisman, 2008; Huisman et al., 2018). Our study suggests that MC and other secondary metabolites may contribute to both short and long-term adaptation of *Microcystis* to changing temperatures. Thereby, even small temperature differences can possibly lead to rapid metabolic changes. Although the condensed MC fraction is not easily quantifiable, future studies should consider temperature-dependent condensation processes when interpreting MC quota, especially in the case of sudden changes in MC amounts.

Data availability statement

The original contributions presented in the study are included in the article/Supplementary material, further inquiries can be directed to the corresponding author.

Author contributions

ED, AG, and SR designed research and analyzed data. SR performed experiments. SR and ED wrote the paper with contributions from all authors. All authors contributed to the article and approved the submitted version.

Funding

This study was supported by Deutsche Forschungsgemeinschaft (DFG, German Research Foundation)—Project-ID 239748522-SFB 1127 to ED.

Acknowledgments

The authors are grateful to Markus Heuser for technical assistance.

Conflict of interest

The authors declare that the research was conducted in the absence of any commercial or financial relationships that could be construed as a potential conflict of interest.

Publisher's note

Supplementary material

The Supplementary material for this article can be found online at: https://www.frontiersin.org/articles/10.3389/fmicb.2023.1200816/full#supplementary-material

References

Alberti, S., Gladfelter, A., and Mittag, T. (2019). Considerations and challenges in studying liquid–liquid phase separation and biomolecular condensates. *Cells* 176, 419–434. doi: 10.1016/j.cell.2018.12.035

Barchewitz, T., Guljamow, A., Meissner, S., Timm, S., Henneberg, M., Baumann, O., et al. (2019). Non-canonical localization of RubisCO under high-light conditions in the toxic cyanobacterium *Microcystis aeruginosa* PCC7806. *Environ. Microbiol.* 21, 4836–4851. doi: 10.1111/1462-2920.14837

Briand, E., Escoffier, N., Straub, C., Sabart, M., Quiblier, C., and Humbert, J. F. (2009). Spatiotemporal changes in the genetic diversity of a bloom-forming *Microcystis aeruginosa* (cyanobacteria) population. *ISME J.* 3, 419–429. doi: 10.1038/ismej.2008.121

Buley, R. P., Gladfelter, M. F., Fernandez-Figueroa, E. G., and Wilson, A. E. (2022). Can correlational analyses help determine the drivers of microcystin occurrence in freshwater ecosystems? A meta-analysis of microcystin and associated water quality parameters. *Environ. Monit. Assess.* 194:493. doi: 10.1007/s10661-022-10114-8

Burnap, R. L., Hagemann, M., and Kaplan, A. (2015). Regulation of CO_2 concentrating mechanism in cyanobacteria. *Life* 5, 348–371. doi: 10.3390/life5010348

Dittmann, E., Neilan, B. A., Erhard, M., von Döhren, H., and Börner, T. (1997). Insertional mutagenesis of a peptide synthetase gene that is responsible for hepatotoxin production in microcystis aeruginosa PCC 7806. *Mol. Microbiol.* 26, 779–784. doi: 10.1046/j.1365-2958.1997.6131982.x

Dziallas, C., and Grossart, H. P. (2011). Increasing oxygen radicals and water temperature select for toxic *Microcystis* sp. *PLoS One* 6:e25569. doi: 10.1371/journal.pone.0025569

Gao, Z., Zhang, W., Chang, R., Zhang, S., Yang, G., and Zhao, G. (2021). Liquid–liquid phase separation: unraveling the enigma of biomolecular condensates in microbial cells. *Front. Microbiol.* 12:751880. doi: 10.3389/fmicb.2021.751880

Guljamow, A., Barchewitz, T., Große, R., Timm, S., Hagemann, M., and Dittmann, E. (2021). Diel variations of extracellular microcystin influence the subcellular dynamics of RubisCO in *Microcystis aeruginosa* PCC7806. *Microorganisms* 9:1265. doi: 10.3390/microorganisms9061265

Havens, K. E. (2008). "Cyanobacteria blooms: effects on aquatic ecosystems" in *Cyanobacterial harmful algal blooms: state of the science and research needs. Advances in experimental medicine and biology*. ed. H. K. Hudnell, vol. *619* (New York, NY: Springer), 733–747.

He, S., Chou, H. T., Matthies, D., Wunder, T., Meyer, M. T., Atkinson, N., et al. (2020). The structural basis of RubisCO phase separation in the pyrenoid. *Nat. Plants* 6, 1480–1490. doi: 10.1038/s41477-020-00811-y

Huisman, J., Codd, G. A., Paerl, H. W., Ibelings, B. W., Verspagen, J. M. H., and Visser, P. M. (2018). Cyanobacterial blooms. *Nat. Rev. Microbiol.* 16, 471–483. doi: 10.1038/s41579-018-0040-1

Jähnichen, S., Ihle, T., Petzoldt, T., and Benndorf, J. (2007). Impact of inorganic carbon availability on microcystin production by *Microcystis aeruginosa* PCC7806. *Appl. Environ. Microbiol.* 73, 6994–7002. doi: 10.1128/AEM.01253-07

Kaebernick, M., Neilan, B. A., Börner, T., and Dittmann, E. (2000). Light and the transcriptional response of the microcystin biosynthesis gene cluster. *Appl. Environ. Microbiol.* 66, 3387–3392. doi: 10.1128/AEM.66.8.3387-3392.2000

Long, B. M., Jones, G. J., and Orr, P. T. (2001). Cellular microcystin content in N-limited *Microcystis aeruginosa* can be predicted from growth rate. *Appl. Environ. Microbiol.* 67, 278–283. doi: 10.1128/AEM.67.1.278-283.2001

Martin, R. M., Moniruzzaman, M., Stark, G. F., Gann, E. R., Derminio, D. S., Wei, B., et al. (2020). Episodic decrease in temperature increases *mcy* gene transcription and cellular microcystin in continuous cultures of *Microcystis aeruginosa* PCC7806. *Front. Microbiol.* 11:601864. doi: 10.3389/fmicb.2020.601864

Meissner, S., Fastner, J., and Dittmann, E. (2013). Microcystin production revisited: conjugate formation makes a major contribution. *Environ. Microbiol.* 15, 1810–1820. doi: 10.1111/1462-2920.12072

Meissner, S., Steinhauser, D., and Dittmann, E. (2015). Metabolomic analysis indicates a pivotal role of the hepatotoxin microcystin in high light adaptation of *Microcystis*. *Environ. Microbiol.* 17, 1497–1509. doi: 10.1111/1462-2920.12565

Neilan, B. A., Pearson, L. A., Muenchhoff, J., Moffitt, M. C., and Dittmann, E. (2013). Environmental conditions that influence toxin biosynthesis in cyanobacteria. *Environ. Microbiol.* 15, 1239–1253. doi: 10.1111/j.1462-2920.2012.02729.x

Orr, P. T., and Jones, G. J. (1998). Relationship between microcystin production and cell division rates in nitrogen-limited *Microcystis aeruginosa* cultures. *Limnol. Oceanogr.* 43, 1604–1614. doi: 10.4319/lo.1998.43.7.1604

Paerl, H. W., and Huisman, J. (2008). Climate. Blooms like it hot. *Science* 320, 57–58. doi: 10.1126/science.1155398

Pancrace, C., Ishida, K., Briand, E., Pichi, D. G., Weiz, A. R., Guljamow, A., et al. (2019). Unique biosynthetic pathway in bloom-forming cyanobacterial genus *Microcystis* jointly assembles cytotoxic aeruginoguanidines and microguanidines. *ACS Chem. Biol.* 14, 67–75. doi: 10.1021/acschembio.8b00918

Sandrini, G., Matthijs, H. C. P., Verspagen, J. M. H., Muyzer, G., and Huisman, J. (2014). Genetic diversity of inorganic carbon uptake systems causes variation in CO_2 response of the cyanobacterium *Microcystis*. *ISME J.* 8, 589–600. doi: 10.1038/ismej.2013.179

Sevilla, E., Martin-Luna, B., Vela, L., Bes, M. T., Fillat, M. F., and Peleato, M. L. (2008). Iron availability affects *mcyD* expression and microcystin-LR synthesis in *Microcystis aeruginosa* PCC7806. *Environ. Microbiol.* 10, 2476–2483. doi: 10.1111/j.1462-2920.2008.01663.x

Steffensen, D. A. (2008). "Economic cost of cyanobacterial blooms" in *Cyanobacterial harmful algal blooms: state of the science and research needs. Advances in experimental medicine and biology*. ed. H. K. Hudnell, vol. *619* (New York, NY: Springer), 855–865.

Van de Waal, D. B., Verspagen, J. M., Finke, J. F., Vournazou, V., Immers, A. K., Kardinaal, W. E., et al. (2011). Reversal in competitive dominance of a toxic versus non-toxic cyanobacterium in response to rising CO_2. *ISME J.* 5, 1438–1450. doi: 10.1038/ismej.2011.28

Visser, P. M., Verspagen, J. M. H., Sandrini, G., Stal, L. J., Matthijs, H. C. P., Davis, T. W., et al. (2016). How rising CO_2 and global warming may stimulate harmful cyanobacterial blooms. *Harmful Algae* 54, 145–159. doi: 10.1016/j.hal.2015.12.006

Wang, H., Yan, X., Aigner, H., Bracher, A., Nguyen, N. D., Hee, W. Y., et al. (2019). RubisCO condensate formation by CcmM in β-carboxysome biogenesis. *Nature* 566, 131–135. doi: 10.1038/s41586-019-0880-5

Wei, N., Hu, L., Song, L., and Gan, N. (2016). Microcystin-bound protein patterns in different cultures of *Microcystis aeruginosa* and field samples. *Toxins* 8:293. doi: 10.3390/toxins8100293

Wiedner, C., Visser, P. M., Fastner, J., Metcalf, J. S., Codd, G. A., and Mur, L. R. (2003). Effects of light on the microcystin content of *Microcystis* strain PCC7806. *Appl. Environ. Microbiol.* 69, 1475–1481. doi: 10.1128/AEM.69.3.1475-1481.2003

Zilliges, Y., Kehr, J. C., Meissner, S., Ishida, K., Mikkat, S., Hagemann, M., et al. (2011). The cyanobacterial hepatotoxin microcystin binds to proteins and increases the fitness of *Microcystis* under oxidative stress conditions. *PLoS One* 6:e17615. doi: 10.1371/journal.pone.0017615

Frontiers in Microbiology

Explores the habitable world and the potential of microbial life

The largest and most cited microbiology journal which advances our understanding of the role microbes play in addressing global challenges such as healthcare, food security, and climate change.

Discover the latest Research Topics

See more →

Frontiers

Avenue du Tribunal-Fédéral 34
1005 Lausanne, Switzerland
frontiersin.org

Contact us

+41 (0)21 510 17 00
frontiersin.org/about/contact